Basudev Sahoo

Visible Light Photocatalyzed Redox-Neutral Organic Reactions and Synthesis of Novel Metal-Organic Frameworks

Springer Theses

Recognizing Outstanding Ph.D. Research

Aims and Scope

The series "Springer Theses" brings together a selection of the very best Ph.D. theses from around the world and across the physical sciences. Nominated and endorsed by two recognized specialists, each published volume has been selected for its scientific excellence and the high impact of its contents for the pertinent field of research. For greater accessibility to non-specialists, the published versions include an extended introduction, as well as a foreword by the student's supervisor explaining the special relevance of the work for the field. As a whole, the series will provide a valuable resource both for newcomers to the research fields described, and for other scientists seeking detailed background information on special questions. Finally, it provides an accredited documentation of the valuable contributions made by today's younger generation of scientists.

Theses are accepted into the series by invited nomination only and must fulfill all of the following criteria

- They must be written in good English.
- The topic should fall within the confines of Chemistry, Physics, Earth Sciences, Engineering and related interdisciplinary fields such as Materials, Nanoscience, Chemical Engineering, Complex Systems and Biophysics.
- The work reported in the thesis must represent a significant scientific advance.
- If the thesis includes previously published material, permission to reproduce this must be gained from the respective copyright holder.
- They must have been examined and passed during the 12 months prior to nomination.
- Each thesis should include a foreword by the supervisor outlining the significance of its content.
- The theses should have a clearly defined structure including an introduction accessible to scientists not expert in that particular field.

More information about this series at http://www.springer.com/series/8790

Basudev Sahoo

Visible Light Photocatalyzed Redox-Neutral Organic Reactions and Synthesis of Novel Metal-Organic Frameworks

🕊 Springer

Author
Dr. Basudev Sahoo
Angewandte Homogenkatalyse
LIKAT Rostock
Rostock
Germany

Supervisor
Prof. Frank Glorius
Organisch Chemisches Institut Westfälische
  Wilhelms-Universität Münster
Münster
Germany

To my beloved parents, brothers and sisters-in-law

Supervisor's Foreword

In Dr. Basudev Sahoo's thesis work, conceptually novel and synthetically valuable methods were developed using visible light photocatalysis. This emerging field has become an indispensable tool for organic synthesis and employs environmentally benign and abundant visible light in the presence of a photosensitizer as an attractive alternative to harmful UV light in photo-mediated reactions. During his doctoral studies, Dr. Sahoo merged the concept of gold catalysis with visible light photocatalysis in a dual catalytic fashion, demonstrating the compatibility of these two important and challenging catalytic modes for the first time. This novel dual catalytic system allowed for the development of mild protocols for the difunctionalization of non-activated alkenes and has since been expanded upon and employed in further reactions by us and other groups. Moreover, his knowledge and expertise in photocatalysis helped him to develop a novel trifluoromethylation method which combined radical addition chemistry with a polar rearrangement to synthesize valuable fluorinated compounds. The incorporation of fluorinated groups onto organic molecules is attracting increasing attention as these compounds feature heavily in pharmaceuticals, agrochemicals, and material research. Since nitrogen-based heterocycles make a large class of bioactive compounds, a mild method for the synthesis of indolizine heterocycles was also developed using a photochemical approach, which has been seldom explored for this class of compound. During this study, the product of the reaction was found to mediate its own formation under photochemical conditions. This rarely observed phenomenon obviated the need for an external photocatalyst and could inspire the future development of autocatalytic photochemical reactions. In addition to his work on photocatalysis, he has also been engaged in synthetic work focused on the preparation of highly porous metal-organic framework (MOF) materials. The scientific

contributions made by Dr. Sahoo, presented in this thesis, have significantly accelerated the development of the fields he has worked on, and have inspired many new projects in my group.

Münster, Germany   Prof. Frank Glorius
April 2016

Abstract

Visible light-mediated photocatalysis has emerged as an environmental friendly elegant approach for streamlined organic synthesis. Recently, many conceptually novel and challenging advancements have been accomplished in this growing research area. The content of this thesis is about the developments of novel methodologies for synthesis of valuable organic compounds using visible light photocatalysis as toolbox and also synthesis of novel metal-organic frameworks (MOFs) as characteristic porous materials.

In initial phase of my Ph.D. work, a novel dual catalytic system combining gold with visible light photoredox catalysis has been developed for selective intra- and intermolecular heteroarylation of non-activated alkenes under mild reaction conditions (Scheme 1.1). In this work, the compatibility of gold catalysis with photoredox catalysis was demonstrated for the first time. Furthermore, this methodology benefits from mild reaction conditions and readily available light sources and avoids the use of strong external oxidants in contrast to previous methods.

The second part of my Ph.D. work was concentrated on the visible light photoredox-catalyzed semipinacol rearrangement for trifluoromethylation of cycloalkanols (Scheme 1.2). This protocol gives access to a novel class of densely
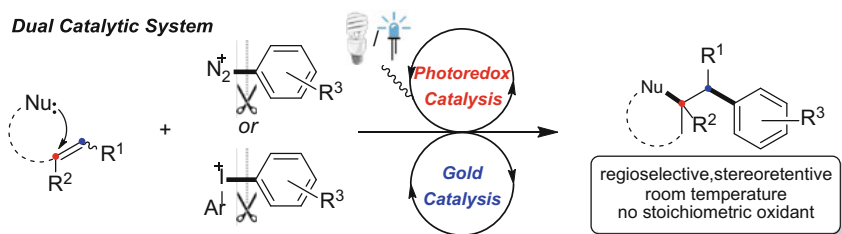
Scheme 1.1 Dual gold and visible light photoredox-catalyzed heteroarylation of non-activated alkenes

Semipinacol Rearrangement
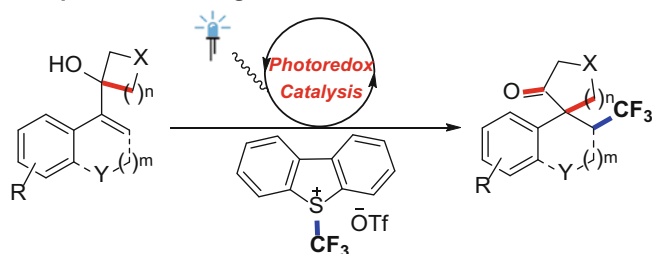
Scheme 1.2 Visible light photoredox-catalyzed trifluoromethylation via semipinacol rearrangement

Scheme 1.3 Visible light photocatalytic synthesis of polycyclic indolizines

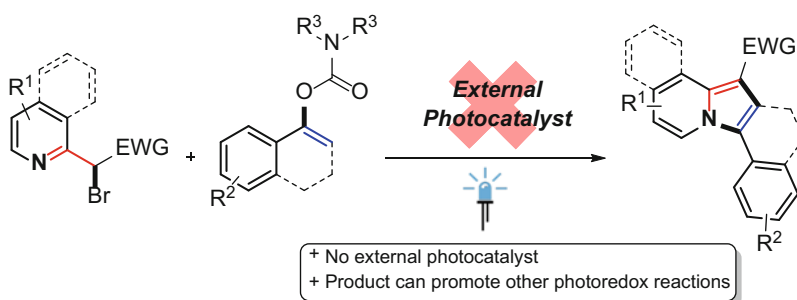functionalized trifluoromethylated cycloalkanones with all carbon quaternary centers. Interestingly, these reactions proceed via radical–polar crossover followed by 1,2-alkyl migration. To the best of our knowledge, this methodology represents the first report of 1,2-alkyl migration in visible light-mediated photoredox catalysis.

In third part of my Ph.D. work, we have developed a novel methodology for the synthesis of valuable polycyclic indolizines under visible light-mediated reaction conditions (Scheme 1.3). To our delight, these reactions do not need any external photosensitizing agents in contrast to conventional photocatalysis, but do need visible light irradiation. Various analytical and laboratory experiments indicate that indolizine products are responsible in some way for their own formation, although further insightful investigations required for complete elucidation of mechanism. Furthermore, gratifyingly, this indolizine product can promote other photocatalyzed reactions in lieu of standard photocatalyst.

In final phase of my Ph.D. work, a triarylborane linker with three carboxylic acid anchoring groups, (4,4′,4″-boranetriyltris(3,5-dimethylbenzoic acid) (H_3TPB)), has been successfully developed and incorporated into the metal-organic frameworks along with a linear BDC co-linker to give mixed MOFs, DUT-6 (Boron) (Scheme 1.4). This new DUT-6 (Boron) showed fluorescent activity and exhibited
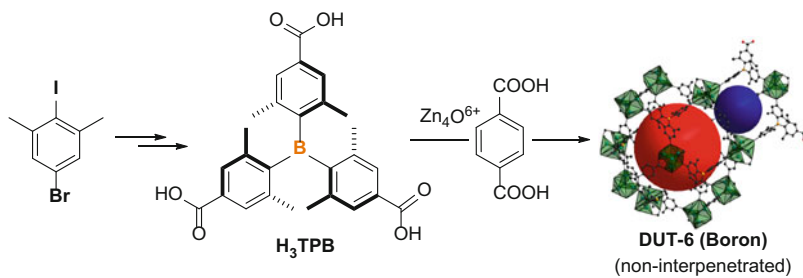
Scheme 1.4 Synthesis of triarylborane linker (H₃TPB) and incorporation into DUT-6

higher isosteric heat of adsorption for CO_2 in contrast to the DUT-6. However, this microporous DUT-6 (Boron) represents the first example of a highly porous non-interpenetrated MOF containing a triarylborane linker.

Parts of this thesis have been published in the following journal articles:

6. "External Photocatalyst-Free Visible Light-Mediated Synthesis of Indolizines" Basudev Sahoo,[†] Matthew N. Hopkinson,[†] Frank Glorius,* *Angew. Chem. Int. Ed.* **2015**, *54*, 15545-15549. ([†]These authors contributed equally to this work).

5. "Visible-Light Photoredox-Catalyzed Semipinacol-Type Rearrangement: Trifluoro-methylation/Ring Expansion via a Radical-Polar Mechanism" Basudev Sahoo, Jun-Long Li, Frank Glorius,* *Angew. Chem. Int. Ed.* **2015**, *54*, 11577–11580.

4. "Copolymerisation at work: the first example of a highly porous MOF comprising a triarylborane-based linker" Stella Helten,[†] Basudev Sahoo,[†] Volodymyr Bon, Irena Senkovska, Stefan Kaskel,* Frank Glorius,* *CrystEngComm.* **2015**, *17*, 307–312. ([†]These authors contributed equally).

3. "Dual Photoredox and Gold Catalysis: Intermolecular Multicomponent Oxyarylation of Alkenes" Matthew N. Hopkinson, Basudev Sahoo, Frank Glorius,* *Adv. Synth. Catal.* **2014***, 356*, 2794–2800.

2. "Dual Catalysis sees the Light: Combining Photoredox with Organo-, Acid and Transition Metal Catalysis" Matthew N. Hopkinson,[†] Basudev Sahoo,[†] Jun-Long Li, Frank Glorius,* *Chem. Eur. J.* **2014**, *20*, 3874–3886. ([†]These authors contributed equally).

1. "Combining Gold and Photoredox Catalysis: Visible Light-Mediated Oxy- and Aminoarylation of Alkenes" Basudev Sahoo, Matthew N. Hopkinson, Frank Glorius,* *J. Am. Chem. Soc.* **2013***, 135,* 5505–5508.

Acknowledgements

Contents

Abbreviations

Ac	Acetyl
^{i}Am	*Iso*-amyl
^{n}Bu	*Normal*-butyl
^{n}BuLi	*Normal*-butyllithium
^{t}Bu	*Tertiary*-butyl
^{t}BuLi	*Tertiary*-butyllithium
Bn	Benzyl
Bz	Benzoyl
CCDC	Cambridge Crystallographic Data Centre
CFL	Compact fluorescent lamp
Cp	Cyclopentadienyl
Cy	Cyclohexyl
d	Doublet
dap	2,9-dianisyl-1,10-phenanthroline
DBU	1,8-diazabycyclo[5.4.0]-undec-7-ene
DCE	1,2-dichloroethane
DCM	Dichloromethane
DEF	*N,N*-diethylformamide
DFT	Density functional theory
DIPA	Diisopropylamine
DIPEA	diisopropylethylamine
DMA	*N,N*-dimethylacetamide
DMAP	*N,N*-dimethylaminopyridine
DMF	*N,N*-dimethylformamide
DMSO	Dimethylsulphoxide
D$_2$O	Deuterated water
d.r.	Diastereoisomeric ratio
EI	Electron impact mass spectrometry
ESI-MS	Electrospray ionization mass spectrometry
EWG	Electron-withdrawing group

EDG	Electron-donating group
Et	Ethyl
Et$_2$O	Diethyl ether
EtOAc	Ethylacetate
EtOH	Ethanol
ee	Enantiomeric excess
equiv.	Equivalent
GC	Gas chromatography
HRMS	High-resolution mass spectrometry
Hz	Hertz
h	Hour(s)
IR	Infrared spectroscopy
IRMOF	Isoreticular metal-organic framework
J	NMR: coupling constant
LA	Lewis acid
LiCl	Lithium chloride
LED	Light-emitting diode
M	Molar
m	Multiplet
Mg	Magnesium
mg	Milligram
min	Minute(s)
m	Meta
*m*CPBA	*Meta*-chloroperoxybenzoic acid
mL	Milliliter
μL	Microliter
MS	Molecular sieves
MsOH	Methanesulphonic acid
MTBE	Methyl-*tert*-butyl ether
Me	Methyl
MeOH	Methanol
NBS	*N*-bromosuccinimide
NMR	Nuclear magnetic resonance
NTf$_2$	Ditrifluoromethanesulfonyl amine
o	Ortho
OTf	Trifluomethanesulfonate
OTs	*p*-toluenesulfonate
p	Para
PG	Protective group
Ph	Phenyl
Piv	Pivlolyl
P(^{t}Bu)$_3$	tri-*tert*-butylphosphine
PEt$_3$	Triethylphosphine
PPh$_3$	Triphenylphosphine
PMe$_3$	Trimethylphosphine

^{i}Pr	Isopropyl
^{n}Pr	*Normal*-propyl
ppb	Parts per billion
ppm	Parts per million
Py	Pyridyl
PC	Photocatalyst
q	Quartet
Q_{st}	Isosteric heat of adsorption
R_F	Retention factor in chromatography
R_t	Retention time
rt	Room temperature
s	Singlet
SET	Single electron transfer
SHE	Standard hydrogen electrode
SCE	Standard calomel electrode
S_N	Nucleophilic substitution
TBHP	*Tert*-Butyl hydroperoxide
THF	Tetrahydrofuran
TFA	Trifluoroacetic acid
TsOH	*p*-toluenesulfonic acid
TMS	Trimethylsilyl
TLC	Thin layer chromatography
TMEDA	Tetramethylethylenediamine
t	Triplet
UV	Ultraviolet
V	Volt
VIS	Visible
χ	Electronegativity

Chapter 1
Introduction to Photocatalysis

1.1 Historical Background

> On the arid lands there will spring up industrial colonies without smoke and without smokestacks; forests of glass tubes will extend over the plains and glass buildings will rise everywhere; inside of these will take place the photochemical processes that hitherto have been the guarded secret of the plants, but that will have been mastered by human industry which will know how to make them bear even more abundant fruit than nature, for nature is not in a hurry and mankind is. And if in a distinct future the supply of coal becomes completely exhausted, civilization will not be checked by that, for life and civilization will continue as long as the sun shines! [1]

— G. Ciamician (1912)

The year 2012 was the centenary of the famous article "The photochemistry of the future" [1]. In this inspiring article, the Italian photochemist G. Ciamician presented his great vision of the future aspects of solar energy imagining a chemical industry where chemicals could be manufactured in a similar way to photosynthesis as used by plants in the presence of sunlight [1]. Although sunlight is considered to be a clean, safe, inexpensive and abundant natural energy source, the vast majority of organic compounds do not absorb photons in the visible region of the solar spectrum but rather absorb in the UV range [1–5]. This limitation has narrowed the scope of organic compounds able to be activated under visible light irradiation, restricting the progress of photochemical synthesis in industry until the recent development of energy-efficient UV photo-reactors. Photochemical synthesis (e.g. photo-induced pericyclic reactions) is considered to be much cleaner and sustainable in contrast to conventional synthetic routes. According to the principles of green chemistry, this is assumed as a green method since direct activation of the substrate by light reduces or eliminates the use of additional hazardous reagents for conventional activations [4, 6, 7]. However, since UV photons possess considerably high energy (in the order of the C–C bond cleavage energy) [8], reactions conducted under UV light irradiation often lead to decomposition when the molecules

contain strained ring systems or relatively weak bonds. Although there are inter-
esting reports on multistep syntheses of some complex molecules using photo-
chemical key steps, interest in the photochemical synthesis of molecules has
remained confined to a small part of the scientific community [9, 10].

In order to attenuate these limitations, photosensitizing compounds, which are
capable of absorbing photons in the visible spectrum and subsequently passing on
the energy to organic compounds, have exhibited great utility in visible light
induced organic synthesis. Moreover, conducting reactions in the presence of cat-
alytic photosensitizers under visible light irradiation from commercially available
household light sources may obviate the expense inherent to the special set up of
UV photo-reactors as well as avoiding the safety precautions needed for UV light
mediated reactions. Over the last few decades, attention has been focused on the use
of visible light photosensitizing compounds to convert solar energy into electricity
in solar cells [11–16] and water splitting for the production of chemical fuels [17,
18]. However, visible light active photocatalysts did not receive the wide attention
of synthetic organic chemists beyond few reports from Kellogg [19, 20] Pac [21]
Deronzier [22, 23] Willner [24, 25] and Tanaka [26]. In 2008, MacMillan [27]
Yoon [28] and Stephenson [29] disclosed elegant and groundbreaking reports on
highly efficient visible light photoredox catalysis, reinventing this field in organic
synthesis.

1.2 Classifications of Photocatalyst

Photocatalysts can be classified into two different major classes based on the cat-
alytic nature of the materials: (a) homogeneous photocatalysts and (b) heteroge-
neous photocatalysts. Organometallic polypyridyl metal complexes (e.g. $[Ru(bpy)_3]$
$Cl_2 \cdot 6H_2O$) [30, 31] and organic dyes (e.g. eosin Y) [32–35] belong to the homo-
geneous group of photocatalysts, while inorganic semiconductors comprising of
metal oxides [36–43] or sulfides [39] (e.g. TiO_2 [36, 37, 39, 40], ZnO [40],
$PbBiO_2Br$ [39], CeO_2 [38], and CdS [39]), polyoxometalates [44] and graphitic
carbon nitride (g-C_3N_4) polymers, [45, 46] and photoactive metal-organic frame-
works (MOFs) [47–50] make up the heterogeneous group. Organometallic poly-
pyridyl transition metal complexes and organic dyes are the most common and most
efficient photocatalysts and are nowadays widely applied in organic synthesis [4, 5,
31, 33–35, 51–65]. In some cases, polypyridyl metal complexes or organic dyes
have been immobilized on photo-active solid supports (e.g. TiO_2) [39] or
photo-inactive solid supports (e.g. silica particle) [66] or solvated in ionic liquids
[67] for recyclability.

1.3 Characteristics of Homogeneous Photocatalysts

Due to their rich photophysical and electrochemical properties, organometallic polypyridyl transition metal complexes and organic dyes exhibit high photocatalytic activity under visible light irradiation [11, 30, 38–74]. The photo-activity of the photocatalysts (organometallic metal complexes or organic dyes) can be visualized in a Jablonski diagram (Fig. 1.1) [75, 76]. Absorbing a photon, the photocatalyst $PC(S_0)$ in its singlet ground state is excited to one of the higher energy vibrational levels of the first singlet excited state $*PC(S_1^n)$ which then relaxes to the lowest vibrational level of the first singlet excited state $*PC(S_1^0)$ via internal conversion (vibrational relaxation). This singlet excited state $*PC(S_1^0)$ can regenerate the singlet ground state $PC(S_0)$ via a spin-allowed radiative pathway (fluorescence, k_f) or a non-radiative pathway (k_{nr}). Another deactivation pathway of $*PC(S_1^0)$ involves its conversion to the lowest energy triplet excited state $*PC(T_1^0)$ via successive fast intersystem crossing (ISC) (spin-orbital coupling) and internal conversion (vibrational relaxation). Since the transition of the triplet excited state to the singlet ground state is spin forbidden, the triplet excited state $*PC(T_1^0)$ is reasonably long lived (e.g. τ = 1100 ns for $Ru(bpy)_3^{2+}$). This triplet excited state $*PC(T_1^0)$ can undergo radiative deactivation (phosphorescence, k_p) or non-radiative deactivation (k_{nr}) to regenerate the singlet ground state $PC(S_0)$, completing the cycle.

Photo-excited singlet states of organic dyes having heavy atoms (Br or I) and organometallic complexes of heavy metals (e.g. Cu, Ru, Ir, Au) undergo rapid intersystem crossing to the lower energy triplet excited states. In the presence of substrates possessing quenching ability, the triplet excited state $*PC(T_1^0)$ can then be quenched to the singlet ground state $PC(S_0)$, diminishing the phosphorescence intensity [76]. In photocatalysis, the photo-excited catalyst can be quenched by the substrates via outer-sphere single electron transfer (SET) or energy transfer (ET) processes leading to productive downstream reactivity (Fig. 1.2) [5].
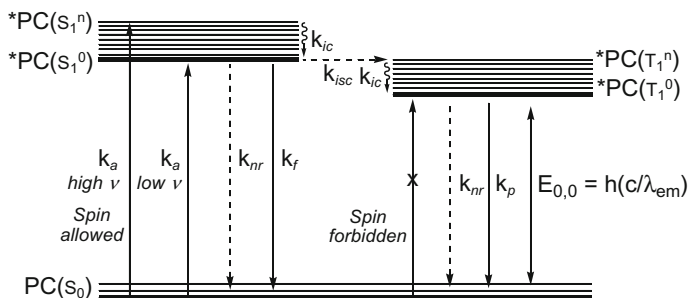
Fig. 1.1 Jablonski diagram. *PC* photocatalyst, k_a rate of absorption, k_{ic} rate of internal conversion, k_{isc} rate of intersystem crosssing, k_{nr} rate of non-radiative deactivation, k_f fluorescence, k_p phosphorescence, $E_{0,0}$ = energy of emission from the triplet state
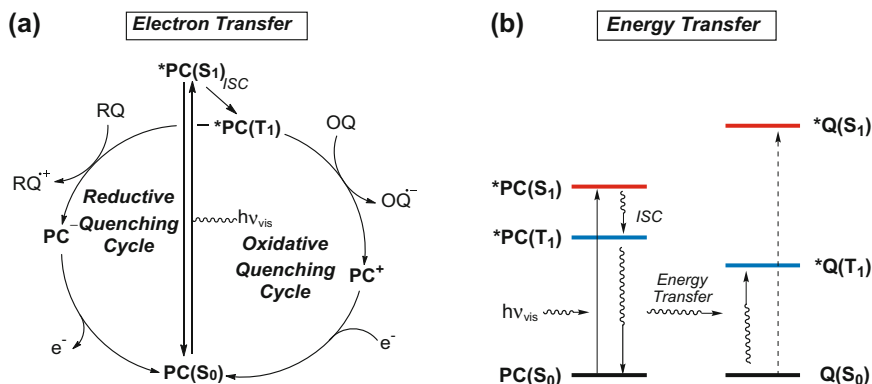
Fig. 1.2 Visible light photocatalysis: **a** photoredox catalytic cycle via single electron transfer (SET); **b** photocatalytic cycle via energy transfer (ET). *PC* photocatalyst, *Q* quencher (e.g. substrate), *RQ* reductive quencher, *OQ* oxidative quencher, *ISC* intersystem crossing. S_O singlet ground state, S_1 first singlet excited state and T_1 first triplet excited state

In an outer sphere electron transfer process, the photo-excited triplet state *PC (T_1) can be quenched by two different mechanisms: reductive quenching and oxidative quenching (Fig. 1.2a) [5, 30, 31, 52, 60, 77]. In a reductive quenching process, the excited photocatalyst in the *PC(T_1) state accepts an electron from an electron-rich substrate (RQ), affording the reduced photocatalyst (PC$^-$) and a radical-cation (RQ$^{•+}$). The reduced photocatalyst (PC$^-$) then donates electron to an electron-deficient species in a subsequent step to regenerate the ground state photocatalyst (PC). The radical-cation (RQ$^{•+}$) releases radical or cationic intermediate, which can engage in a subsequent step. In a similar manner, in oxidative quenching, the photocatalyst in the *PC(T_1) state donates an electron to an electron-deficient substrate (OQ), delivering the oxidized photocatalyst (PC$^+$) and a radical-anion (OQ$^{•-}$). The oxidized photocatalyst (PC$^+$) then accepts an electron from an electron-rich species present in the reaction mixture to regenerate the ground state photocatalyst (PC) and the radical-anion releases a radical upon mesolysis capable of reacting via a number of different pathways in subsequent steps. This process largely depends on the redox potentials of the species involved.

In an energy transfer process, the photo-excited triplet state *PC(T_1) interacts with the substrate, which has an accessible low energy triplet state (comparable to the photo-excited triplet state energy, Fig. 1.2b) [5]. In this interaction, triplet-triplet energy transfer results in a photo-excited triplet state of the substrate and regenerates the ground state of the photocatalyst. The photo-excited substrate can then engage in photochemical reactions. Stern-Volmer luminescence quenching experiments are generally performed to find out the actual quencher from a set of reagents present in the reaction mixture [31].

In visible light photocatalysis, coordinately saturated organometallic-based photocatalysts are chemically and conformationally stable under the reaction conditions and do not generally bind to the substrates. As a result, no other types of activations are generally observed except outer sphere electron transfer or energy transfer. Furthermore, the long-lived excited states of the photocatalysts provide sufficient time for effective interactions with the substrates in their proximity. In addition, an appropriate redox potential window of the photoredox catalyst is highly desirable for the reaction design.

In the photoredox catalyst toolbox, well investigated organometallic photocatalysts are either homoleptic (one type of ligand) or heteroleptic (two or more different types of ligands) polypyridyl metal complexes. The most common homoleptic photocatalysts are [Ru(bpy)$_3$](PF$_6$)$_2$ (bpy = 2,2′-bipyridine) and *fac*-Ir (ppy)$_3$ (ppy = 2-phenylpyridine) [31]. On the other hand, the most common heteroleptic photocatalysts are [Ir(ppy)$_2$(dtbbpy)](PF$_6$) (dtbbpy = 4,4′-di-*tert*-butyl-2,2′-bipyridine) and [Ir(dF(CF$_3$)ppy)$_2$(dtbbpy)](PF$_6$) (dF(CF$_3$)ppy = 2-(2,4-difluorophenyl)-5-trifluoromethylpyridine) [31]. For organometallic photocatalysts, various sets of redox potentials can be accessed by tuning the electronic properties of the ligands and metal ions and thus changing the HOMO-LUMO energy gap for metal to ligand charge transfer (MLCT) [30]. Electron-rich ligands (e.g. ppy) increases the reductive power of the ground state metal complex while electron-poor ligands (e.g. bpz, bpz = 2,2′-bipyrazine) increases the oxidative power of the metal complex in ground state [30]. The redox potential of the excited photoredox catalyst cannot be directly determined. These values are instead calculated with the help of cyclic voltammetry and spectroscopic data following the Rehm-Weller equation [78].
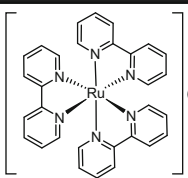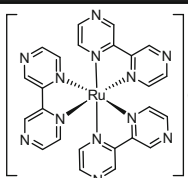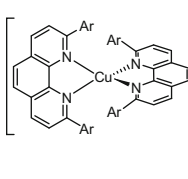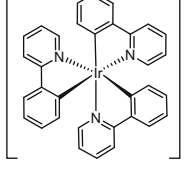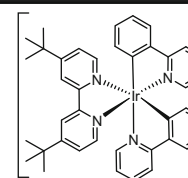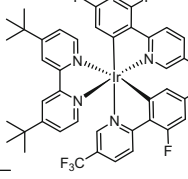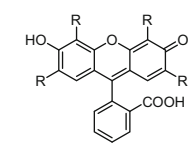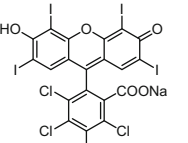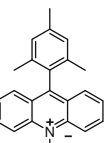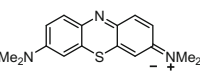
A list of organometallic photocatalysts and organic dyes is shown in Table 1.1. The photoelectronic properties of selected photoredox catalysts are outlined in Table 1.2. A list of selected reductive and oxidative quenchers is given in Table 1.3.

1.4   Visible Light Photocatalysis in Organic Synthesis

1.4.1   Photoredox Catalyzed Organic Transformations via Electron Transfer

Since photo-excited photoredox catalysts have higher oxidizing and reducing abilities compared to their ground states, giving access to two different sets of redox potentials with reasonably long life-times (Table 1.2), over the last three decades, and in particular over last seven years, there has been tremendous progress in the

Table 1.1 List of selected homoleptic and heteroleptic organometallic photocatalysts and organic dyes

field of photoredox catalysis in organic synthesis [4, 5, 31, 35, 51–59, 62, 64]. From a redox point of view, visible light photoredox-catalyzed reactions can be classified into three different categories: redox-neutral, net oxidative and net reductive reactions [31]. In redox-neutral processes, both the oxidation and reduction steps are involved in the same reaction mechanism maintaining overall redox neutrality. In net oxidative reactions, the products possess higher oxidation levels than the starting materials, while in net reductive processes the products are in lower oxidation levels compared to the starting materials. In this chapter, only redox-neutral visible light photo-redox-catalyzed processes are discussed in three sections, although many interesting organic transformations have been reported based on net redox processes over the last decades [31].

Table 1.2 Photoelectronic properties of selected photoredox catalysts [31, 34]

Photocatalyst	$E_{1/2}(M^+/M^*)$ (V)	$E_{1/2}(M^*/M^-)$ (V)	$E_{1/2}(M^+/M)^a$ (V)	$E_{1/2}(M/M^-)^a$ (V)	Absorption λ_{abs} (nm)	Emission λ_{em} (nm)	Excited-state life time (τ, ns)
$Ru(bpy)_3^{2+}$	−0.81	+0.77	+1.29	−1.33	452	615	1100
$Ru(bpz)_3^{2+}$	−0.26	+1.45	+1.86	−0.80	443	591	740
fac-$Ir(ppy)_3$	−1.73	+0.31	+0.77	−2.19	375	494[b]	1900
$Ir(ppy)_2(dtbbpy)^+$	−0.96	+0.66	+1.21	−1.51	–	581	557
$Ir(dF(CF_3)ppy)_2(dtbbpy)^+$	−0.89	+1.21	+1.69	−1.37	380	470	2300
$Cu(dap)_2^+$	−1.43	–	+0.62	–	–	670[c]	270
Eosin Y	−1.11	+0.83	+0.78	−1.06	539	–	24,000
Acridinium perchlorate	–	+2.06	–	−0.57	430	–	–

[a]Redox potential measured against SCE
[b]Measured in EtOH:MeOH (1:1)
[c]Measured in DCM

Table 1.3 List of selected reductive and oxidative quenchers [31, 34, 52, 73, 127, 128]
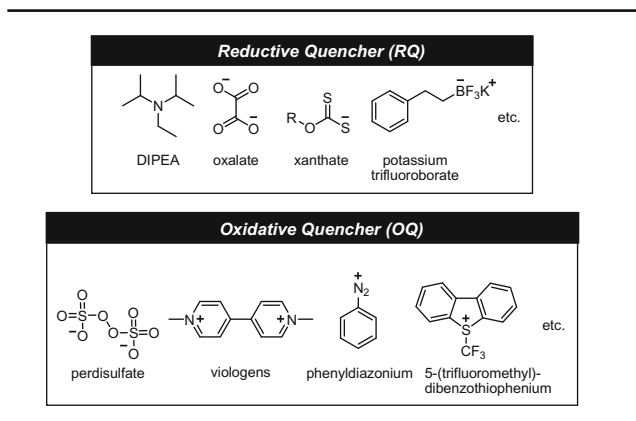
1.4.1.1 Redox-Neutral Photoredox Catalysis: Single Catalysis

Oxidative quenching cycle

Since photoredox catalysts are single electron transfer agents, most photoredox-catalyzed reactions involve radical or radical-ionic intermediates during the process and many of these reactions proceed via a key step: Radical-Polar Crossover.[1] In an oxidative quenching cycle, the photo-excited photocatalyst behaves as a strong reductant being itself oxidized. In 1984, Deronzier et al. [23] disclosed an overall redox-neutral visible light-mediated Pschorr synthesis of phenanthrene derivatives **1**, in the presence of [Ru(bpy)$_3$](BF$_4$)$_2$ (5 mol%). This method obviates the formation of the undesired byproduct **2** under direct photolysis (>360 nm) and benefits from milder reaction conditions compared to previously reported electro-chemical processes [79] or thermal methods (Scheme 1.1) [23, 80, 81].

In a mechanistic hypothesis, single electron reduction of aryldiazonium sub-strates **3** by the photo-excited *[Ru(bpy)$_3$]$^{2+}$ generates the higher-valent [Ru(bpy)$_3$]$^{3+}$ and an aryl radical **4**, which undergoes homoaromatic substitution (HAS) to deliver another cyclized radical intermediate **5**. In the next step, oxidation of this radical intermediate **5** to the cationic intermediate **6** by [Ru(bpy)$_3$]$^{3+}$, regenerating the photocatalyst [Ru(bpy)$_3$]$^{2+}$ via a radical-polar crossover, gives rise to the phenanthrene derivative **1** upon deprotonation (Scheme 1.2) [23].

After a long time in 2012, König et al. [82] reported an elegant method for the arylation of heteroarenes with aryldiazonium salts in the presence of the organic dye eosin Y and green light (Scheme 1.3). This reaction proceeds via oxidative quenching of photo-excited eosin Y with aryldiazonium salts **7** delivering aryl radicals **8** and oxidized eosin Y. Aryl radical addition to the electron-rich

---

[1]Radical-Polar Crossover process will be described in brief in Chap. 3.

Deronzier and co-workers (1984)
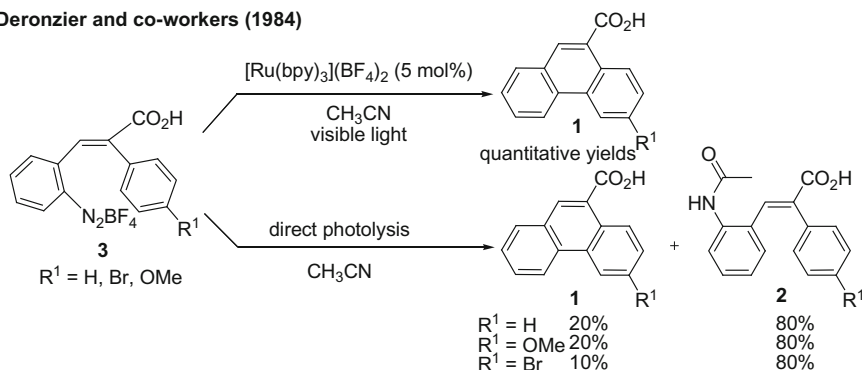
Scheme 1.1 Pschorr synthesis of phenanthrene derivatives under photoredox catalysis and direct photolysis [23]
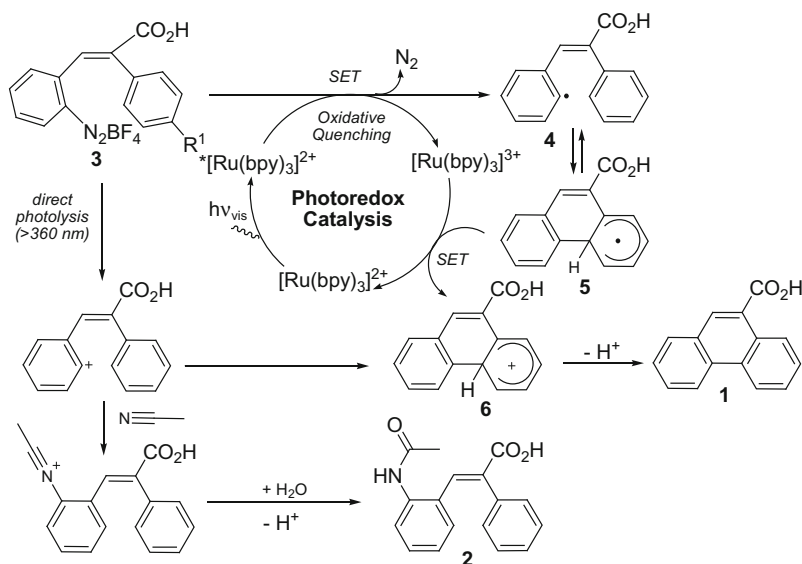
Scheme 1.2 Proposed mechanism for the Pschorr synthesis of phenanthrene derivatives under photoredox catalysis and direct photolysis [23]

heteroarene **9** followed by radical-polar crossover with the oxidized eosin Y leads to cationic intermediates **10**, which afford the final products **11**, upon aromatizing deprotonation (Scheme 1.3) [82].

This type of photoredox catalysis has been applied to generate other radicals such as the trifluoromethyl ($^{\bullet}CF_3$) and cyanomethyl ($^{\bullet}CH_2CN$) radical. In 2011, MacMillan et al. [83] developed an efficient protocol for the trifluoromethylation of a wide range of arenes and heteroarenes including some highly important drug

König and co-workers (2012)

R^1 + N$_2$BF$_4$ (from 7) → Eosin Y (1 mol%), DMSO, 20 °C, green LEDs → 11

9 (1 equiv.)   7 R^2 (5-10 equiv.)   11 (40-86%)

X = O, S, NBoc; R^1, R^2 = EWG, EDG

Mechanism cycle:

7 → SET → N$_2$ → 8

*Eosin Y ← hν$_{vis}$ ← Eosin Y

Oxidative Quenching

Eosin Y$^{•+}$

8 + 9 → 10 (H) → chain → 7 → 8

10 → -H$^+$ (deprotonation) → 11
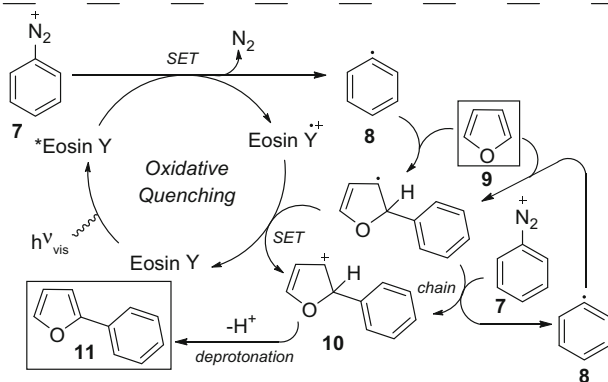
Scheme 1.3 Transition metal free arylation of heteroarenes by visible light photoredox catalysis and proposed reaction mechanism [82]

MacMillan and co-workers(2011)

[Ru(phen)$_3$]Cl$_2$ (1-2 mol%), CF$_3$SO$_2$Cl (1-4 equiv.), K$_2$HPO$_4$, CH$_3$CN, 23 °C, 26 W CFL

A, B = O, S, N; X, Y, Z = O, N; R = EWG, EDG   70-94%

Scheme 1.4 Visible light photoredox-catalyzed trifluoromethylation of (hetero)arenes [83]

molecules, highlighting the practical applicability of this mild method using [Ru (phen)$_3$]Cl$_2$ (1–2 mol%, phen = 1,10-phenanthroline) and relatively inexpensive CF$_3$SO$_2$Cl (1–4 equiv.) as the $^•$CF$_3$ source and K$_2$HPO$_4$ as base (Scheme 1.4).

In this line of research, alkene motifs have also become successful partners with other π-congeners. In late 2013, Greaney et al. [84] reported a visible light photoredox-catalyzed three component oxy- and aminoarylation of activated alkenes using strongly reducing *fac*-Ir(ppy)$_3$ (5 mol%), Zn(OAc)$_2$ (20 mol%) as an additive and air and moisture stable diaryliodonium salts (2.0 equiv.) as aryl

(a) **Greaney and co-workers (2013) & König and co-workers (2014)**
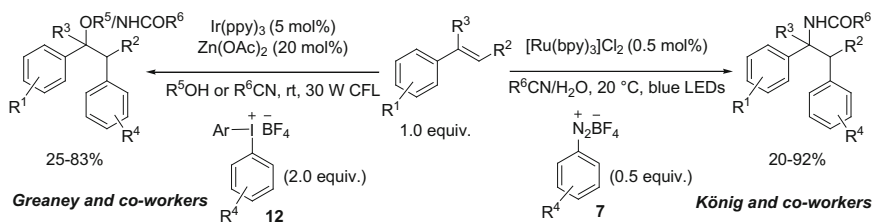
R^1, R^4 = EWG, EDG; R^2, R^3 = H, alkyl, aryl, EWG; R^5, R^6 = H, alkyl

(b) **Lei and co-workers (2014)**

R^1 = EWG, EDG; R^2 = H, aryl; R^3 = alkyl
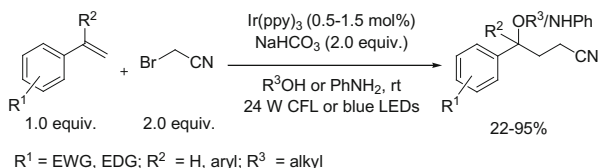
Scheme 1.5 **a** Oxy- and aminoarylations of styrenes by visible light photoredox catalysis [84, 85]; **b** visible light photoredox-catalyzed oxy- and aminocyanomethylation of styrenes [87]

precursors under visible light irradiation from a 30 W CFL (Scheme 1.5a). Earlier in 2014, König et al. [85] also reported the same visible light photoredox-catalyzed aminoarylation of activated alkenes (2.0 equiv.) using a different set of reaction conditions: [Ru(bpy)$_3$]Cl$_2$ (0.5 mol%) with a lower loading of the aryldiazonium salt (1.0 equiv.) as aryl precursors under visible light irradiation from blue LEDs (Scheme 1.5a). In both cases, this redox neutral Meerwein-type reaction proceeds via oxidative quenching and radical-polar crossover similar to the mechanism depicted in Scheme 4.2 in Chap. 4 for oxytrifluoromethylation. The same reactivity was extended to the trifluoromethyl ($^•$CF$_3$) radical by Koike et al. [86] and the cyanomethyl ($^•$CH$_2$CN) radical by Lei et al. [87] (Scheme 4.4a in Chap. 4 and Scheme 1.5b respectively). In addition to these reports, many impressive organic transformations based on this concept have enriched the literature [88–91].

Another important class of redox-neutral photoredox reactions proceeding via an oxidative quenching cycle is atom transfer radical addition (ATRA) to alkenes (see Chap. 3, Sect. 3.1.4.3) [92].

Reductive quenching cycle

In a reductive quenching cycle, the photo-excited photoredox catalyst acts as a strong oxidant being itself reduced. Over the last 7 years, there has been a significant amount of development of redox-neutral reactions, which proceed via a reductive quenching cycle. In 2010, Stephenson and co-workers described the direct functionalization of heteroarenes with activated alkyl bromides in the

Stephenson and co-workers (2010)
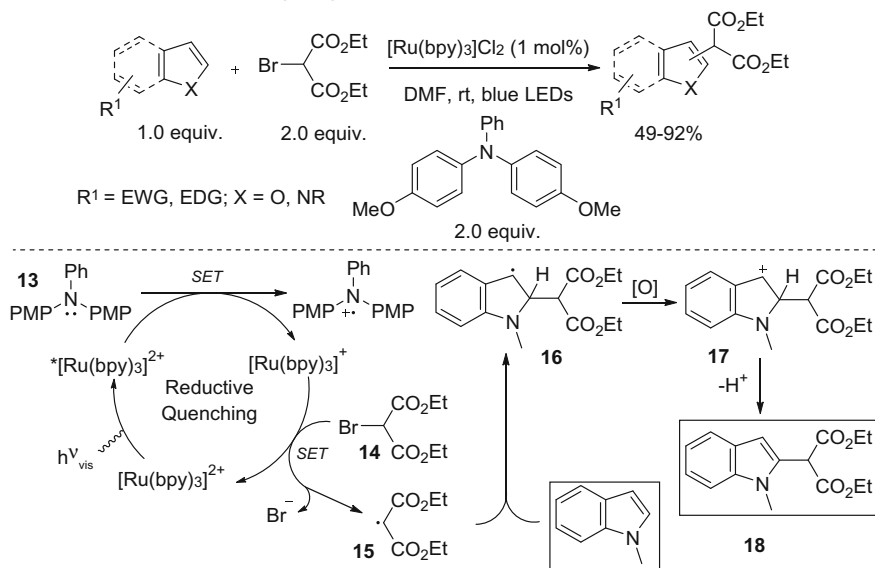
Scheme 1.6 Visible light photoredox-catalyzed direct functionalization of heteroarenes with diethyl 2-bromomalonate and the mechanistic hypothesis [93]

presence of a combination of $[Ru(bpy)_3]Cl_2$ as photocatalyst, a triaryl amine quencher and blue LEDs under mild conditions (Scheme 1.6) [93]. In their mechanistic proposal, the photo-excited $*[Ru(bpy)_3]^{2+}$ is quenched to the reductant $[Ru(bpy)_3]^+$ by the electron rich triaryl amine **13**. The reduction of diethyl 2-bromomalonate (**14**) to the C-centered radical **15** by the reductant $[Ru(bpy)_3]^+$ regenerates $[Ru(bpy)_3]^{2+}$. In the next step, selective radical addition to heteroarenes results in a stabilized benzylic radical **16**, which further oxidizes to give the benzylic cation **17** via radical-polar crossover. In the final step, aromatizing deprotonation of benzylic cation **17** delivers the functionalized heteroarene **18** (Scheme 1.6) [93].

In 2012, Zheng et al. [94] reported an overall redox-neutral elegant method for the visible light photoredox-catalyzed [2+3] cycloaddition reaction between cyclopropyl amines and activated alkenes in the presence of $[Ru(bpz)_3](PF_6)_2$ (2 mol%) to afford cyclopentyl amines (**19**) (Scheme 1.7). Mechanistically, in a reductive quenching cycle, photo-excited $*[Ru(bpz)_3]^{2+}$ is quenched by the N-aryl protected cyclopropyl amine generating the N-centered radical-cation **20** with a pendant cyclopropyl ring and the reduced species $[Ru(bpz)_3]^+$. Ring opening of the cyclopropyl ring of the N-centered radical-cation **20** leads to an intermediate **21**, which undergoes [2+3] cycloaddition to generate the N-centered radical-cation **22** with a pendant cyclopentyl ring. Single electron reduction of this radical-cation **22** results in final product **19** and regenerates the photocatalyst $[Ru(bpz)_3]^{2+}$ (Scheme 1.7) [94].

Zheng and coworkers (2012)
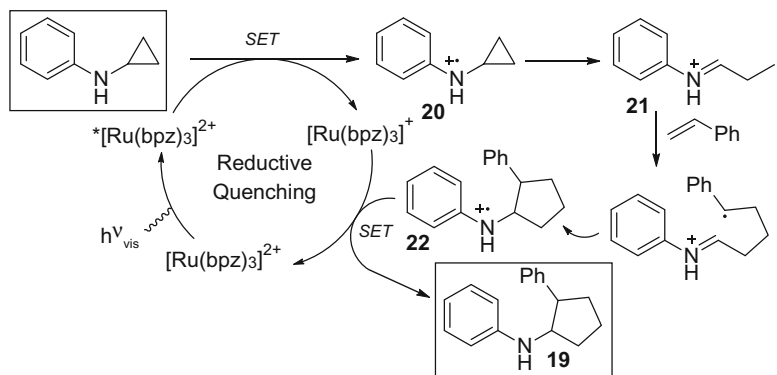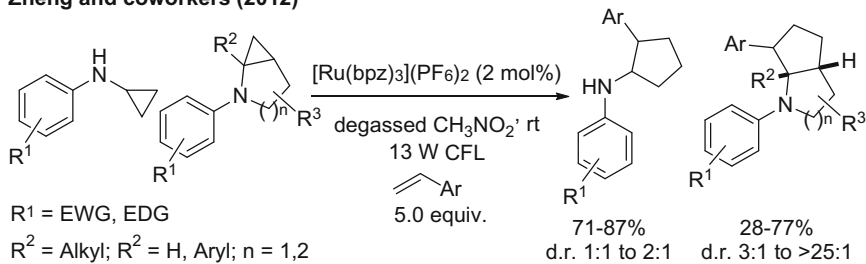
Scheme 1.7 Visible light photoredox-catalyzed [2+3] cycloaddition between *N*-aryl cyclopropyl amines and activated alkenes and a possible mechanistic proposal [94]

1.4.1.2 Photoredox Catalysis: Dual Catalysis (Transition Metal)

The concept of combining two privileged catalytic activation modes together to promote a single transformation, which is not possible in the presence of either catalyst alone, has recently captured the attention of synthetic chemists to develop novel transformations [95–97]. Over the last few years, a significant effort has been made to combine visible light photoredox catalysis with other catalytic modes such as organo-, transition metal and acid catalysis to develop novel dual catalytic systems [60, 61, 63, 65]. In a dual catalytic system, the photoredox catalyst interacts with either the substrate or the other catalyst or both to generate substrate-derived reactive intermediates or active forms of the other catalyst via electron transfer.

Over the last few decades, the exploration of transition metal catalysis emphasizing on understanding the reactivity modes and exploiting these in an enormous number of applications in organic synthesis for both academic and industrial purposes has been acknowledged by the award of three times Nobel Prizes (in 2001, 2005 and 2010) to the pioneering leaders of this esteemed field of research. Various innovative and novel concepts been developed over the last few decades. One of the novel concepts employed in transition metal catalysis is the cooperative effect of two or more catalysts together to promote unprecedented transformations [96, 97].

In 2007, Osawa and co-workers successfully developed the first palladium/photoredox dual catalytic system to promote the Sonogashira coupling of aryl bromides and terminal alkynes (Scheme 1.8) [98]. The combination of the photocatalyst [Ru(bpy)$_3$](PF$_6$)$_2$ and visible light enhanced the efficiency of this copper-free Sonogashira coupling [98]. However, the role of the photocatalyst was not clear.

Later in 2011, Sanford and co-workers described another efficient palladium/photoredox dual catalytic system for the directed ortho-selective C–H functionalization of unactivated arenes combining a palladium(II/IV) catalytic cycle and visible light photoredox catalytic cycle under mild conditions (Scheme 1.9) [99]. Inspired by the seminal report from Deronzier et al. [23] they anticipated that the aryl radical generated from aryldiazonium salts under photoredox conditions might be oxidizing enough to promote palladium-catalyzed C–H arylation of non-activated arenes under mild reaction conditions [99]. When they treated aryl-diazonium salts **7** with non-activated arenes **23** in the presence of palladium acetate (10 mol%) and [Ru(bpy)$_3$]Cl$_2$·6H$_2$O (2.5 mol%) under visible light irradiation from a 26 W CFL, the desired C–H arylation products **24** were obtained in good to moderate yields (Scheme 1.9).

Osawa and co-workers (2007)
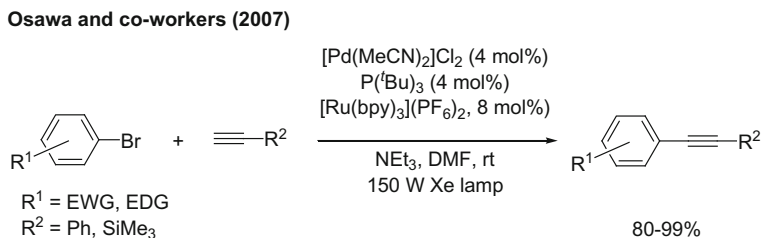
Scheme 1.8   Dual palladium/photoredox-catalyzed Sonogashira coupling [98]

Sanford and co-workers (2011)

DG = Directing Group; R^1 = H, EDG; R^2 = H, EWG, EDG
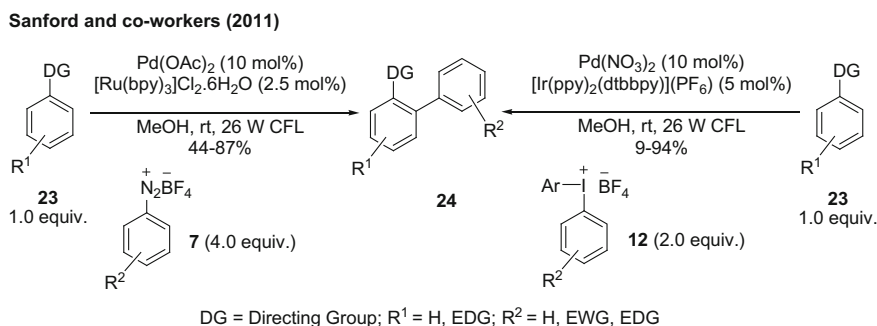
Scheme 1.9 Dual palladium and visible light photoredox-catalyzed C–H arylation of non-activated arenes [99, 100]

In order to expand the scope of the arylating reagent, Sanford and co-workers successfully employed air and moisture stable diaryliodonium salts **12** in the presence of the stronger reducing photocatalyst [Ir(ppy)$_2$(dtbbpy)](PF$_6$) (5 mol%) and Pd(NO$_3$)$_2$ (10 mol%) to carry out the C–H arylation reaction of non-activated arenes (Scheme 1.9) [100].

A mechanistic hypothesis for this reaction is depicted in Scheme 1.10. In an initial step, single electron reduction of the aryldiazonium salts **7** by the photo-excited *[Ru(bpy)$_3$]$^{2+}$ generates highly oxidizing nucleophilic aryl radicals **8** and the oxidized photocatalyst [Ru(bpy)$_3$]$^{3+}$. In a concurrent catalytic cycle, a five-membered palladacycle **25** is obtained via C–H activation. At this stage, the formed aryl radical would possibly oxidize Pd(II) in the palladacycle **25** to give a Pd(III) intermediate **26**, which is further oxidized to a Pd(IV) intermediate **27** by [Ru(bpy)$_3$]$^{3+}$, regenerating the photocatalyst [Ru(bpy)$_3$]$^{2+}$. In the final step, reductive elimination of both coupling fragments from the high valent palladium (IV) center results in the C–H arylated product **24** and regenerates the palladium(II) catalyst. In a high level theoretical calculation, Maestro, Derat and co-workers showed that the last two steps may occur in the reverse order, where reductive elimination from a Pd(III) intermediate precedes single electron oxidation of a Pd(I) catalyst to Pd(II) [101].

As a continuation of their interest in dual catalysis in 2012, Sanford and co-workers successfully employed a copper/photoredox dual catalytic system for the perfluoroalkylation of arylboronic acids (**28**) with perfluoroalkyl iodides as inexpensive perfluoroalkyl sources under mild reaction conditions (60 °C, no base
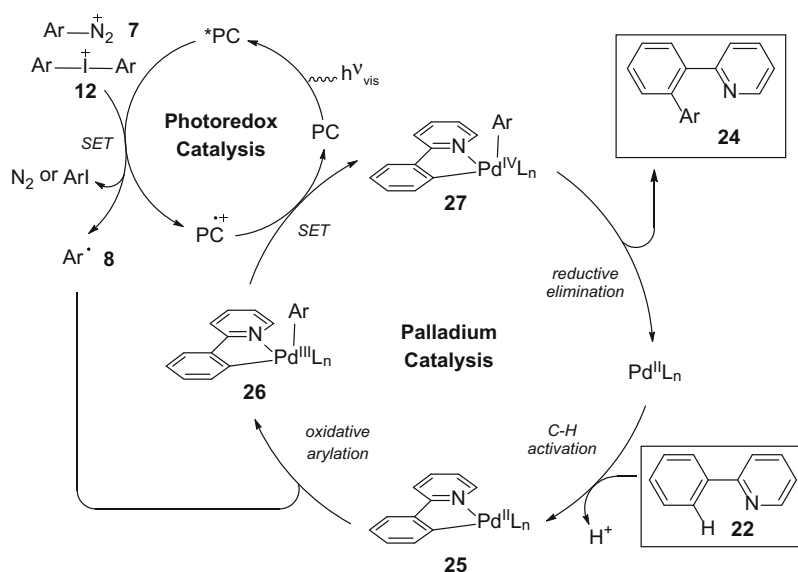
Scheme 1.10 Mechanistic hypothesis for the dual palladium and visible light photoredox-catalyzed C–H arylation of non-activated arenes [99, 101]

or acid) to give access to perfluoroalkyl-substituted arenes **29** (Scheme 1.11) [102]. A tentative mechanism for this trifluoromethylation of arylboronic acids is shown in Scheme 1.12 [102]. In an initial step, the photo-excited *$[Ru(bpy)_3]^{2+}$ is quenched by the copper(I) catalyst in a reductive quenching pathway generating a copper(II) intermediate and $[Ru(bpy)_3]^+$. Single electron transfer from $[Ru(bpy)_3]^+$ to CF_3I produces a $^•CF_3$ radical and regenerates $[Ru(bpy)_3]^{2+}$. This $^•CF_3$ radical then oxidizes the copper(II) intermediate to the copper(III) intermediate **30** bearing the CF_3 group. Finally, transmetalation of an aryl group followed by reductive elimination furnishes the trifluoromethylated products **29** and regenerates the copper catalyst.

Very recently, dual catalysis combining transition metal catalysis (Ni [103–108], Rh [109], Ru [110], Pd [111–113] and Cu [114–116]) and visible light photoredox catalysis has extensively been explored. Some of them also belong to net redox proceses.
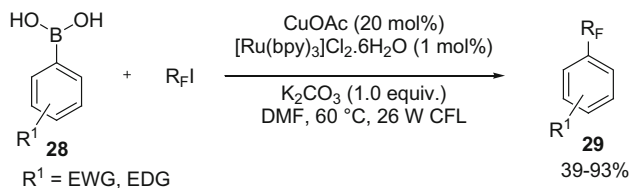
Scheme 1.11 Dual copper and visible light photoredox-catalyzed perfluoroalkylation of arylboronic acids [102]
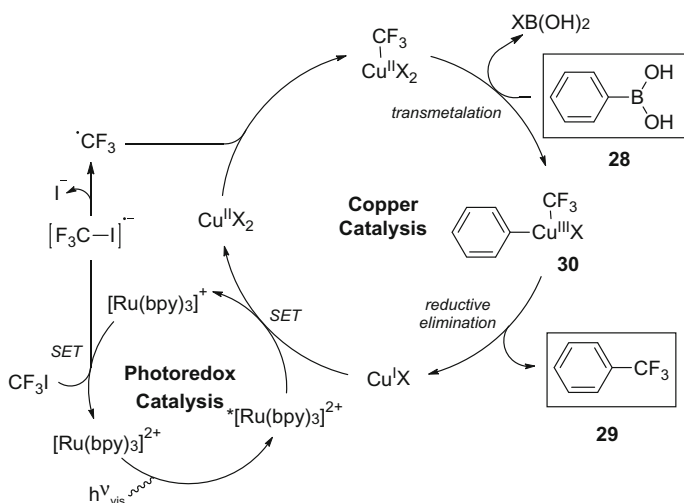
Scheme 1.12 Mechanistic proposal for dual copper and visible light photoredox-catalyzed trifluoromethylation of arylboronic acids [102]

1.4.1.3 Redox-Neutral Photoredox Catalysis: EDA Complex Formation

In visible light photoredox catalysis, an external photosensitizer is generally used to carry out the reactions [31]. In contrast to reactions of this type, in 2013, Melchiorre and co-workers uncovered a novel concept, where two components in association with one another absorbs visible light leading to inner sphere charge transfer in a solvent cage and giving rise to downstream reactivity [117].

They reported the visible light-driven chiral amine-catalyzed asymmetric α-alkylation of aldehydes and cyclic ketones with high yield and selectivity (Scheme 1.13) [117, 118]. In these reactions, none of the reaction components: aldehyde/ketone, amine catalyst and alkyl bromide in isolation absorbs light in the visible range. When these components are mixed together, a colored solution is obtained which absorbs light significantly in the visible range. The origin of visible light absorption is attributed to the electron donor-acceptor (EDA) complex formed between the electron donor enamine intermediate, in situ generated from the aldehyde/ketone and the amine catalyst by condensation, and the electron acceptor alkyl bromide (Scheme 1.14). The formed complex absorbs light and undergoes effective electron transfer from the enamine to the alkyl bromide in the solvent cage. Once the alkyl bromide radical-anion **33** leaves the cage, an alkyl radical intermediate **34** is generated upon mesolysis of the radical-anion. This alkyl radical **34** then adds to the electron rich enamine intermediate delivering another radical intermediate **35**. Subsequent electron transfer from intermediate **35** to another

Scheme 1.13 Chiral amine-catalyzed asymmetric α-alkylation of aldehydes and cyclic ketones via visible light-driven exciplex formation [117, 118]
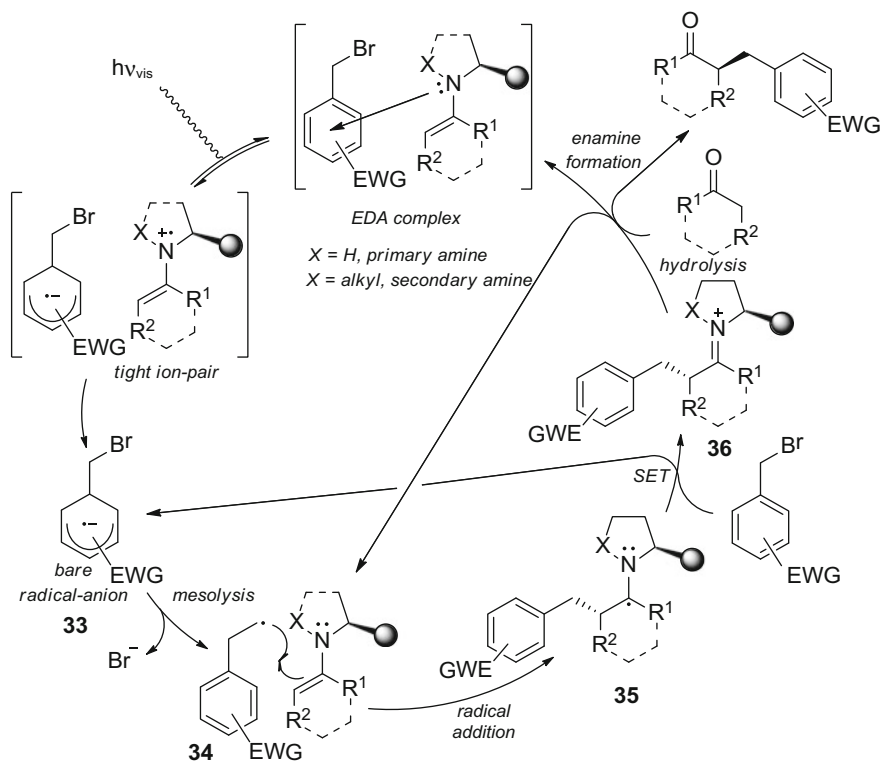
Scheme 1.14 Plausible reaction mechanism for the amine-catalyzed asymmetric α-alkylation of carbonyl compounds via visible light-driven exciplex formation [117, 118]

equivalent of the alkyl bromide in a chain process leads to iminium ion **36** formation, which delivers the final product upon hydrolysis and regenerates the amine catalyst.

Since the reaction is performed in the presence of catalytic amounts of the amine catalyst resulting in a catalytic amount of the enamine intermediate, this reaction can be considered as a catalytic method in an analogy to standard photoredox catalysis.

1.4.2 Photocatalyzed Organic Transformations via Triplet Energy Transfer

Although over the last few years visible light photoredox catalysis involving electron transfer has been widely exploited [31], visible light photocatalysis involving energy transfer still remains less explored [119–126]. In visible light photoredox-catalyzed cycloaddition reactions, only electron rich and electron poor alkenes can be employed as substrates. These substrates are capable of donating or

Yoon and co-workers (2012)

R^1 = EWG, EDG; R^2 = H, alkyl, aryl;
R^3, R^4 = H, alkyl, aryl, EDG, EWG; X = O, NTs, CH$_2$, n = 1,2

64-90%
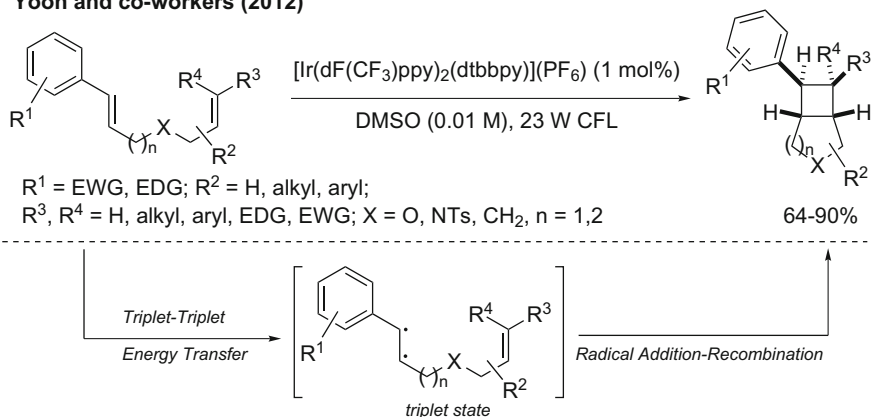
Scheme 1.15 Visible light photocatalyzed [2+2] cycloaddition of styrenes via triplet–triplet energy transfer [121]

accepting an electron to generate radical-cations or radical-anions for downstream reactivity. To overcome these limitations in substrate scope, Yoon and co-workers have made significant advances in the development of cycloaddition reactions proceeding via energy transfer. Until 2012, there were only two reports of carbon-carbon bond-forming reactions proceeding via triplet sensitization with transition metal complexes under visible light irradiation [119, 120]. Yoon et al. [121] then reported an elegant method for [2+2] cross cycloadditions of styrenes with pendant substituted alkenes in an intramolecular fashion (Scheme 1.15).

They carried presence of [Ir(dF(CF$_3$)ppy)$_2$(dtbbpy)](PF$_6$) (1 mol%) in DMSO and visible light from a 23 W CFL. This reaction seemed to be independent of solvent polarity, indicating the feasibility of energy transfer in contrast to the preference of polar solvents typically required for electron transfer processes to stabilize the charged radical-ionic intermediates. In general, the redox potentials of styrenes are out of the range accessible with the photo-excited [Ir(dF(CF$_3$)ppy)$_2$(dtbbpy)]$^+$. However, the calculated triplet state energy of styrenes is in the same range or even lower than that of the photo-excited [Ir(dF(CF$_3$)ppy)$_2$(dtbbpy)]$^+$. The authors believed that these reactions proceed via triplet–triplet energy transfer generating a triplet excited state of the substrate, which can engage in a [2+2] cycloaddition as depicted in Scheme 1.15.

1.5 Summary

In summary, this chapter provides an overview of emerging visible light induced photocatalysis encompassing a brief historical background of this field, the general features of the photocatalysts and the different types of reactivity exhibited by these

photocatalysts. Selected examples of overall redox-neutral photoredox-catalyzed organic transformations covering different reactivity modes have been described. Some of the redox-neutral photocatalytic reactions intentionally presented in this chapter are directly or indirectly related to our own contributions described in Chaps. 2–4.

References

1. G. Ciamician, Science **36**, 385–394 (1912)
2. N.S. Lewis, Science **315**, 798–801 (2007)
3. M. Oelgemöller, C. Jung, J. Mattay, Pure Appl. Chem. **79**, 1939–1947 (2007)
4. T.P. Yoon, M.A. Ischay, J. Du, Nat. Chem. **2**, 527–532 (2010)
5. D.M. Schultz, T.P. Yoon, Science **343**, 1239176 (2014)
6. M. Fagnoni, D. Dondi, D. Ravelli, A. Albini, Chem. Rev. **107**, 2725–2756 (2007)
7. S. Protti, M. Fagnoni, Photochem. Photobiol. Sci. **8**, 1499–1516 (2009)
8. S.J. Blanksby, G.B. Ellison, Acc. Chem. Res. **36**, 255–263 (2003)
9. N. Hoffmann, Chem. Rev. **108**, 1052–1103 (2008)
10. T. Bach, J.P. Hehn, Angew. Chem. Int. Ed. **50**, 1000–1045 (2011)
11. K. Kalyanasundaram, Coord. Chem. Rev. **46**, 159–244 (1982)
12. M.K. Nazeeruddin, A. Kay, I. Rodicio, R. Humphry-Baker, E. Mueller, P. Liska, N. Vlachopoulos, M. Graetzel, J. Am. Chem. Soc. **115**, 6382–6390 (1993)
13. M.K. Nazeeruddin, S.M. Zakeeruddin, R. Humphry-Baker, M. Jirousek, P. Liska, N. Vlachopoulos, V. Shklover, C.-H. Fischer, M. Grätzel, Inorg. Chem. **38**, 6298–6305 (1999)
14. S.H. Wadman, J.M. Kroon, K. Bakker, R.W.A. Havenith, G.P.M. van Klink, G. van Koten, Organometallics **29**, 1569–1579 (2010)
15. Y. Qin, Q. Peng, Int. J. Photoenergy **2012**, 21 (2012)
16. D.W. Ayele, W.-N. Su, J. Rick, H.-M. Chen, C.-J. Pan, N.G. Akalework, B.-J. Hwang, *Advances in Organometallic Chemistry and Catalysis* (Wiley, NY, 2013), pp. 501–511
17. A. Kudo, Y. Miseki, Chem. Soc. Rev. **38**, 253–278 (2009)
18. R.M. Navarro Yerga, M.C. Álvarez Galván, F. del Valle, J.A. Villoria de la Mano, J.L.G. Fierro. ChemSusChem **2**, 471–485 (2009)
19. D.M. Hedstrand, W.H. Kruizinga, R.M. Kellogg, Tetrahedron Lett. **19**, 1255–1258 (1978)
20. T.J. Van Bergen, D.M. Hedstrand, W.H. Kruizinga, R.M. Kellogg, J. Org. Chem. **44**, 4953–4962 (1979)
21. C. Pac, M. Ihama, M. Yasuda, Y. Miyauchi, H. Sakurai, J. Am. Chem. Soc. **103**, 6495–6497 (1981)
22. H. Cano-Yelo, A. Deronzier, Tetrahedron Lett. **25**, 5517–5520 (1984)
23. H. Cano-Yelo, A. Deronzier, J. Chem. Soc. Perkin Trans. **2**, 1093–1098 (1984)
24. Z. Goren, I. Willner, J. Am. Chem. Soc. **105**, 7764–7765 (1983)
25. R. Maidan, Z. Goren, J.Y. Becker, I. Willner, J. Am. Chem. Soc. **106**, 6217–6222 (1984)
26. K. Hironaka, S. Fukuzumi, T. Tanaka, J. Chem. Soc. Perkin Trans. **2**, 1705–1709 (1984)
27. D.A. Nicewicz, D.W.C. MacMillan, Science **322**, 77–80 (2008)
28. M.A. Ischay, M.E. Anzovino, J. Du, T.P. Yoon, J. Am. Chem. Soc. **130**, 12886–12887 (2008)
29. J.M.R. Narayanam, J.W. Tucker, C.R.J. Stephenson, J. Am. Chem. Soc. **131**, 8756–8757 (2009)
30. J.W. Tucker, C.R.J. Stephenson, J. Org. Chem. **77**, 1617–1622 (2012)
31. C.K. Prier, D.A. Rankic, D.W.C. MacMillan, Chem. Rev. **113**, 5322–5363 (2013)
32. D. Ravelli, M. Fagnoni, ChemCatChem **4**, 169–171 (2012)
33. D. Ravelli, M. Fagnoni, A. Albini, Chem. Soc. Rev. **42**, 97–113 (2013)

34. D.P. Hari, B. Konig, Chem. Commun. **50**, 6688–6699 (2014)
35. D.A. Nicewicz, T.M. Nguyen, ACS Catal. **4**, 355–360 (2014)
36. A.L. Linsebigler, G. Lu, J.T. Yates, Chem. Rev. **95**, 735–758 (1995)
37. N. Wu, J. Wang, D.N. Tafen, H. Wang, J.-G. Zheng, J.P. Lewis, X. Liu, S.S. Leonard, A. Manivannan, J. Am. Chem. Soc. **132**, 6679–6685 (2010)
38. N. Zhang, X. Fu, Y.-J. Xu, J. Mater. Chem. **21**, 8152–8158 (2011)
39. M. Cherevatskaya, M. Neumann, S. Füldner, C. Harlander, S. Kümmel, S. Dankesreiter, A. Pfitzner, K. Zeitler, B. König, Angew. Chem. Int. Ed. **51**, 4062–4066 (2012)
40. M. Rueping, J. Zoller, D.C. Fabry, K. Poscharny, R.M. Koenigs, T.E. Weirich, J. Mayer, Chem. Eur. J. **18**, 3478–3481 (2012)
41. P. Riente, A. Matas Adams, J. Albero, E. Palomares, M.A. Pericàs, Angew. Chem. Int. Ed. **53**, 9613–9616 (2014)
42. C. Liu, W. Zhao, Y. Huang, H. Wang, B. Zhang, Tetrahedron **71**, 4344–4351 (2015)
43. P. Riente, M.A. Pericàs, ChemSusChem **8**, 1841–1844 (2015)
44. Y. Guo, C. Hu, J. Mol. Catal. A Chem. **262**, 136–148 (2007)
45. F. Su, S.C. Mathew, G. Lipner, X. Fu, M. Antonietti, S. Blechert, X. Wang, J. Am. Chem. Soc. **132**, 16299–16301 (2010)
46. Y. Wang, X. Wang, M. Antonietti, Angew. Chem. Int. Ed. **51**, 68–89 (2012)
47. J. Long, S. Wang, Z. Ding, S. Wang, Y. Zhou, L. Huang, X. Wang, Chem. Commun. **48**, 11656–11658 (2012)
48. P. Wu, C. He, J. Wang, X. Peng, X. Li, Y. An, C. Duan, J. Am. Chem. Soc. **134**, 14991–14999 (2012)
49. D. Shi, C. He, B. Qi, C. Chen, J. Niu, C. Duan, Chem. Sci. **6**, 1035–1042 (2015)
50. X. Yu, S.M. Cohen, Chem. Commun. **51**, 9880–9883 (2015)
51. K. Zeitler, Angew. Chem. Int. Ed. **48**, 9785–9789 (2009)
52. J.M.R. Narayanam, C.R.J. Stephenson, Chem. Soc. Rev. **40**, 102–113 (2011)
53. F. Teplý, Collect. Czech. Chem. Commun. **76**, 859–917 (2011)
54. L. Shi, W. Xia, Chem. Soc. Rev. **41**, 7687–7697 (2012)
55. J. Xuan, W.-J. Xiao, Angew. Chem. Int. Ed. **51**, 6828–6838 (2012)
56. D.P. Hari, B. König, Angew. Chem. Int. Ed. **52**, 4734–4743 (2013)
57. M. Reckenthäler, A.G. Griesbeck, Adv. Synth. Catal. **355**, 2727–2744 (2013)
58. Y. Xi, H. Yi, A. Lei, Org. Biomol. Chem. **11**, 2387–2403 (2013)
59. J. Xuan, L.-Q. Lu, J.-R. Chen, W.-J. Xiao, Eur. J. Org. Chem. **2013**, 6755–6770 (2013)
60. M.N. Hopkinson, B. Sahoo, J.-L. Li, F. Glorius, Chem. Eur. J. **20**, 3874–3886 (2014)
61. E. Jahn, U. Jahn, Angew. Chem. Int. Ed. **53**, 13326–13328 (2014)
62. T. Koike, M. Akita, Top. Catal. **57**, 967–974 (2014)
63. N. Hoffmann, ChemCatChem **7**, 393–394 (2015)
64. E. Meggers, Chem. Commun. **51**, 3290–3301 (2015)
65. M. Peña-López, A. Rosas-Hernández, M. Beller, Angew. Chem. Int. Ed. **54**, 5006–5008 (2015)
66. G.J. Barbante, T.D. Ashton, E.H. Doeven, F.M. Pfeffer, D.J.D. Wilson, L.C. Henderson, P. S. Francis, ChemCatChem **7**, 1655–1658 (2015)
67. D.C. Fabry, M.A. Ronge, M. Rueping, Chem. Eur. J. **21**, 5350–5354 (2015)
68. A. Juris, V. Balzani, F. Barigelletti, S. Campagna, P. Belser, A. von Zelewsky, Coord. Chem. Rev. **84**, 85–277 (1988)
69. A. Penzkofer, A. Beidoun, M. Daiber, J. Lumin. **51**, 297–314 (1992)
70. A. Penzkofer, A. Beidoun, Chem. Phys. **177**, 203–216 (1993)
71. A. Penzkofer, A. Beidoun, S. Speiser, Chem. Phys. **170**, 139–148 (1993)
72. M.A. Miranda, H. Garcia, Chem. Rev. **94**, 1063–1089 (1994)
73. S. Fukuzumi, H. Kotani, K. Ohkubo, S. Ogo, N.V. Tkachenko, H. Lemmetyinen, J. Am. Chem. Soc. **126**, 1600–1601 (2004)
74. L. Flamigni, A. Barbieri, C. Sabatini, B. Ventura, F. Barigelletti, Top. Curr. Chem. **281**, 143–203 (2007)
75. A. Jabłoński, Nature **131**, 839–840 (1933)

76. J.R. Lakowicz, *Principles of Fluorescence Spectroscopy*, 3rd edn. (Springer, New York, 2006)
77. J. Du, K.L. Skubi, D.M. Schultz, T.P. Yoon, Science **344**, 392–396 (2014)
78. D. Rehm, A. Weller, Isr. J. Chem. **8**, 259–271 (1970)
79. R.M. Elofson, F.F. Gadallah, J. Org. Chem. **36**, 1769–1771 (1971)
80. A.N. Nesmeyanov, L.G. Makarova, T.P. Tolstaya, Tetrahedron **1**, 145–157 (1957)
81. B. Maggio, D. Raffa, M.V. Raimondi, S. Cascioferro, S. Plescia, M.A. Sabatino, G. Bombieri, F. Meneghetti, G. Daidone, ARKIVOC **16**, 130–143 (2008)
82. D.P. Hari, P. Schroll, B. König, J. Am. Chem. Soc. **134**, 2958–2961 (2012)
83. D.A. Nagib, D.W.C. MacMillan, Nature **480**, 224–228 (2011)
84. G. Fumagalli, S. Boyd, M.F. Greaney, Org. Lett. **15**, 4398–4401 (2013)
85. D. Prasad Hari, T. Hering, B. König, Angew. Chem. Int. Ed. **53**, 725–728 (2014)
86. Y. Yasu, T. Koike, M. Akita, Angew. Chem. Int. Ed. **51**, 9567–9571 (2012)
87. H. Yi, X. Zhang, C. Qin, Z. Liao, J. Liu, A. Lei, Adv. Synth. Catal. **356**, 2873–2877 (2014)
88. Y. Yasu, T. Koike, M. Akita, Org. Lett. **15**, 2136–2139 (2013)
89. Y. Yasu, T. Koike, M. Akita, Chem. Commun. **49**, 2037–2039 (2013)
90. R. Tomita, Y. Yasu, T. Koike, M. Akita, Beilstein J. Org. Chem. **10**, 1099–1106 (2014)
91. Y. Yasu, Y. Arai, R. Tomita, T. Koike, M. Akita, Org. Lett. **16**, 780–783 (2014)
92. J.D. Nguyen, J.W. Tucker, M.D. Konieczynska, C.R.J. Stephenson, J. Am. Chem. Soc. **133**, 4160–4163 (2011)
93. L. Furst, B.S. Matsuura, J.M.R. Narayanam, J.W. Tucker, C.R.J. Stephenson, Org. Lett. **12**, 3104–3107 (2010)
94. S. Maity, M. Zhu, R.S. Shinabery, N. Zheng, Angew. Chem. Int. Ed. **51**, 222–226 (2012)
95. Z. Shao, H. Zhang, Chem. Soc. Rev. **38**, 2745–2755 (2009)
96. M. Rueping, R.M. Koenigs, I. Atodiresei, Chem. Eur. J. **16**, 9350–9365 (2010)
97. A.E. Allen, D.W.C. MacMillan, Chem. Sci. **3**, 633–658 (2012)
98. M. Osawa, H. Nagai, M. Akita, *Dalton Transactions* (2007), 827–829
99. D. Kalyani, K.B. McMurtrey, S.R. Neufeldt, M.S. Sanford, J. Am. Chem. Soc. **133**, 18566–18569 (2011)
100. S.R. Neufeldt, M.S. Sanford, Adv. Synth. Catal. **354**, 3517–3522 (2012)
101. G. Maestri, M. Malacria, E. Derat, Chem. Commun. **49**, 10424–10426 (2013)
102. Y. Ye, M.S. Sanford, J. Am. Chem. Soc. **134**, 9034–9037 (2012)
103. A. Noble, S.J. McCarver, D.W.C. MacMillan, J. Am. Chem. Soc. **137**, 624–627 (2014)
104. J.C. Tellis, D.N. Primer, G.A. Molander, Science **345**, 433–436 (2014)
105. Z. Zuo, D.T. Ahneman, L. Chu, J.A. Terrett, A.G. Doyle, D.W.C. MacMillan, Science **345**, 437–440 (2014)
106. O. Gutierrez, J.C. Tellis, D.N. Primer, G.A. Molander, M.C. Kozlowski, J. Am. Chem. Soc. **137**, 4896–4899 (2015)
107. D.N. Primer, I. Karakaya, J.C. Tellis, G.A. Molander, J. Am. Chem. Soc. **137**, 2195–2198 (2015)
108. J. Xuan, T.-T. Zeng, J.-R. Chen, L.-Q. Lu, W.-J. Xiao, Chem. Eur. J. n/a–n/a (2015)
109. D.C. Fabry, J. Zoller, S. Raja, M. Rueping, Angew. Chem. Int. Ed. **53**, 10228–10231 (2014)
110. D.C. Fabry, M.A. Ronge, J. Zoller, M. Rueping, Angew. Chem. Int. Ed. **54**, 2801–2805 (2015)
111. S.B. Lang, K.M. O'Nele, J.A. Tunge, J. Am. Chem. Soc. **136**, 13606–13609 (2014)
112. J. Zoller, D.C. Fabry, M.A. Ronge, M. Rueping, Angew. Chem. Int. Ed. **53**, 13264–13268 (2014)
113. J. Xuan, T.-T. Zeng, Z.-J. Feng, Q.-H. Deng, J.-R. Chen, L.-Q. Lu, W.-J. Xiao, H. Alper, Angew. Chem. Int. Ed. **54**, 1625–1628 (2015)
114. M. Rueping, R.M. Koenigs, K. Poscharny, D.C. Fabry, D. Leonori, C. Vila, Chem. Eur. J. **18**, 5170–5174 (2012)
115. W.-J. Yoo, T. Tsukamoto, S. Kobayashi, Angew. Chem. **127**, 6687–6690 (2015)
116. W.-J. Yoo, T. Tsukamoto, S. Kobayashi, Angew. Chem. Int. Ed. **54**, 6587–6590 (2015)
117. E. Arceo, I.D. Jurberg, A. Álvarez-Fernández, P. Melchiorre, Nat. Chem. **5**, 750–756 (2013)

118. E. Arceo, A. Bahamonde, G. Bergonzini, P. Melchiorre, Chem. Sci. **5**, 2438–2442 (2014)
119. H. Ikezawa, C. Kutal, K. Yasufuku, H. Yamazaki, J. Am. Chem. Soc. **108**, 1589–1594 (1986)
120. R.R. Islangulov, F.N. Castellano, Angew. Chem. Int. Ed. **45**, 5957–5959 (2006)
121. Z. Lu, T.P. Yoon, Angew. Chem. Int. Ed. **51**, 10329–10332 (2012)
122. Y.-Q. Zou, S.-W. Duan, X.-G. Meng, X.-Q. Hu, S. Gao, J.-R. Chen, W.-J. Xiao, Tetrahedron **68**, 6914–6919 (2012)
123. E. Arceo, E. Montroni, P. Melchiorre, Angew. Chem. Int. Ed. **53**, 12064–12068 (2014)
124. E.P. Farney, T.P. Yoon, Angew. Chem. Int. Ed. **53**, 793–797 (2014)
125. A.E. Hurtley, Z. Lu, T.P. Yoon, Angew. Chem. Int. Ed. **53**, 8991–8994 (2014)
126. X.-D. Xia, J. Xuan, Q. Wang, L.-Q. Lu, J.-R. Chen, W.-J. Xiao, Adv. Synth. Catal. **356**, 2807–2812 (2014)
127. K. Ohkubo, K. Mizushima, R. Iwata, K. Souma, N. Suzuki, S. Fukuzumi, Chem. Commun. **46**, 601–603 (2010)
128. Y. Yasu, T. Koike, M. Akita, Adv. Synth. Catal. **354**, 3414–3420 (2012)

Chapter 2
Dual Gold and Visible Light Photoredox-Catalyzed Heteroarylations of Non-activated Alkenes

2.1 Introduction

2.1.1 General Properties of Homogeneous Gold Catalysts

Gold (Au) is a third row noble transition metal belonging to group 11 of the periodic table and is situated below silver in the coinage metal series. Gold with the ground state electronic configuration $[Xe]4f^{14}5d^{10}6s^1$ has highest first ionization potential ($E^0_{Au(I)/Au(0)}$ = +1.69 V vs. SHE) among d-block elements, due to the relativistic contraction of 6s atomic orbital [1]. As a consequence, elemental gold is very stable in the presence of air and moisture and was long thought to be inactive to perform chemical reactions. Among possible oxidation states (−I to +V), Au(I) and Au(III) species are stable, existing as salts or complexes, while Au(II) is generally unstable and easily undergoes disproportionation to Au(I) and Au(III). In the presence of a strong oxidant, Au(I) can be oxidized to Au(III) ($E^0_{Au(III)/Au(I)}$ = +1.41 V vs. SHE) [1]. Some commercially available Au(I) and Au (III) precursors are listed in Fig. 2.1. In general for catalysis, gold(I) complexes are often employed along with a co-catalyst silver(I) salt with an appropriate, non-coordinating counter-anion is added to the reaction mixture to abstract a halide from the gold center, creating a vacant coordination site accessible to the substrates for binding. In 2005, Gagosz and co-workers developed air stable cationic (phosphine)gold(I) complexes with a loosely bound NTf_2 anion which easily dissociates in solution [2].

The cationic gold(I) complex $[LAu]^+$ (i.e. L = neutral, ligand e.g. a phosphine or NHC) thus generated is most often employed as a highly efficient carbophilic π-Lewis acid catalyst capable of activating carbon-carbon multiple bonds. The π-activation of multiple bonds can be attributed to the strong in-plane σ-donation
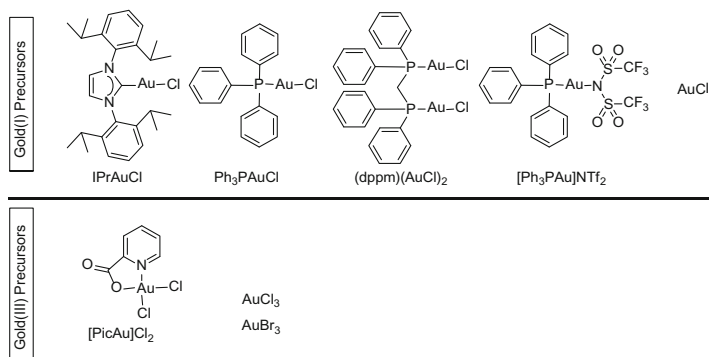
Fig. 2.1 Some common commercially-available Au(I) and Au(III) precursors

from the substrate π-orbital onto the metal [π(alkyne) → d(Au)] with a comparatively weak back-bonding interaction from the gold to the substrate π*-orbital [π*(alkyne) ← d(Au)]. With alkyne substrates, which have an additional out-of-plane double bond, further weak π(alkyne) → d(Au) bonding and π*(alkyne) ← d(Au) back-bonding interactions are possible [3, 4]. Due to the stronger σ-acceptance compared to π-back donation [3, 4], overall charge density in the ligated alkyne/alkene is reduced and electrophilicity is enhanced. The predominance of carbophilic behavior observed with soft LAu^+ species can be rationalized by the fact that it forms kinetically more labile complexes with hard basic heteroatoms (e.g. O and N) [5]. Due to the high redox potential of the Au(I)/Au(III) couple $(E_{1/2}[Au(III)/Au(I)] = +1.41$ V vs. SHE) [1], LAu^+-catalyzed reactions can be conducted under aerobic conditions and no undesired redox processes hamper the desired reactivity. As a result, a wide spectrum of functional groups are tolerated in these types of reactions [5]. Alongside alkynes, this activation approach can be extended to organic substrates containing π-system such as allenes and alkenes [5].

Since the last decade of the twentieth century, a significant amount of interest has been devoted to the development of highly emissive luminescent gold(III) complexes [6, 7], which can absorb photons in visible range of spectrum, and recently some polypyridyl gold(III) complexes have been shown to participate in visible light photoredox catalysis [8]. However, the vast majority of organic reactions are catalyzed by gold(I) complexes rather than gold(III) complexes and the absorption abilities of mononuclear gold(I) complexes (e.g. Ph_3PAuCl, Et_3PAuCl or Me_3PAuCl), and coordinatively-saturated bimetallic gold(I) complexes [e.g. $(dppm)_2(AuCl)_2$, dppm = 1,1-bis(diphenylphosphino)methane] are usually confined to the UV range of the spectrum [9–12]. This phenomenon limits their applications in visible light induced gold-catalyzed organic transformations [11, 13, 14].

2.1.2 Gold-Catalyzed Organic Transformations

2.1.2.1 Historical Background

Over the last several years, gold catalysis has played an outstanding role in various areas of chemistry [4, 5, 15–32]. AuCl$_3$-catalyzed hydration of alkynes to ketones reported by Thomas and co-workers in 1976 was one of the earliest reports on gold catalysis (Scheme 2.1) [33]. However, the real breakthrough in gold(I) catalysis was made by a group of scientists in BASF in 1998, who developed a highly efficient (phosphine)gold(I)-catalyzed method for the addition of alcohols onto alkynes with very high TON and TOF replacing toxic mercury(II) catalysts (Scheme 2.1) [34].

Since then, this field has been explored enormously with highly efficient and stable gold(I) (pre)catalysts being applied [17, 35, 36] to access synthetically important reactivity and mechanistic insight [18, 21, 28, 30, 31]. The compatibility of gold catalysis with other reagents has also been extensively explored and studies devoted to extending the scope of these reactions beyond their current limitations, such as overcoming protodeauration, have been conducted [23, 24, 27, 37]. Novel methodologies exploring many aspects of the chemistry of gold continue to be reported at a fast rate [5, 25, 26, 38], including applications in asymmetric catalysis [20, 32, 39, 40] and natural product synthesis [29].

2.1.2.2 Difunctionalizations of Carbon–Carbon Multiple Bonds: Mechanistic Hypothesis

Gold(I)-catalyzed nucleophilic addition type reactions have emerged as an enabling technology for selective difunctionalizations of alkynes, allenes and alkene substrates. A general mechanistic scenario for these transformations exemplified for alkynes is shown in Scheme 2.2 [16]. In an initial step, commercially available or self-prepared gold(I) complexes of the form [LAuX] (**37**) (L = neutral ligand, e.g. phosphine, NHC and X = charged ligand, e.g. Cl, Br) loses its charged ligand (X) in the presence of a scavenger (e.g. Ag$^+$) to generate the catalytically-active cationic species [LAu]$^+$ (**38**). This cationic species [LAu]$^+$ (**38**) then enters the catalytic cycle and coordinates to an alkyne (**39**), generating the alkyne-ligated gold (I) intermediate **40** and activating it towards an internal or external nucleophile. The

Scheme 2.1 Early examples of gold catalysis: hydration of alkynes and addition of alcohols onto alkynes [33, 34]
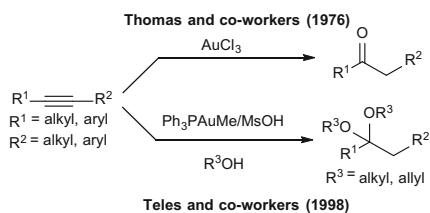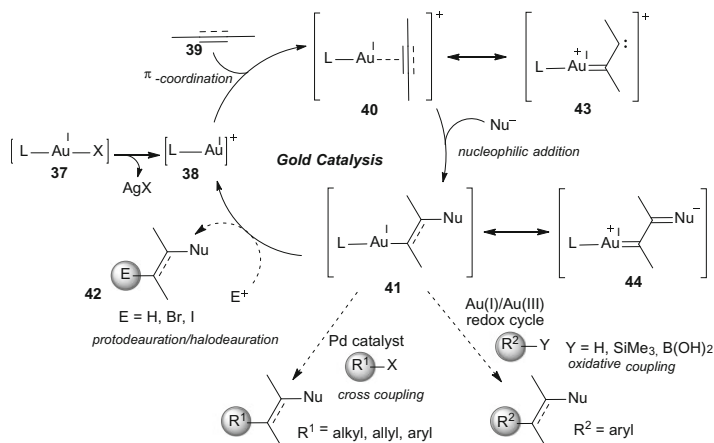
Scheme 2.2 General mechanistic cycle of Au(I)-catalyzed difunctionalization of carbon-carbon multiple bonds [5]

addition of the nucleophile results in the alkenylgold intermediate **41**, which is then quenched in the presence of an electrophile releasing the product **42** and regenerating the cationic species [LAu]$^+$ (**38**). In a different scenario, the alkyne bound to Au(I) in the coordination sphere of intermediates **40** and **41** could behave as *vic*-dicarbene synthons **43** and **44,** respectively, and their great potential in synthesis has been explored over the last few years [5]. It is worth mentioning that allenes and alkenes can be activated in a similar manner, resulting in vinylgold(I) and alkylgold (I) intermediates respectively.

In the vast majority of the cases, the alkenylgold intermediate **41** undergoes protodeauration releasing hydrofunctionalized products, while in a few cases, halonium ions (I$^+$, Br$^+$) have been used to quench the alkenylgold intermediate **41** delivering halofuntionalized products [41–43].

Hydrofunctionalizations of alkynes, allenes and to some extent alkenes, undoubtedly, deserve an important position among gold-catalyzed organic transformations and many impressive reactions based on these processes have enriched the library of synthetic organic chemistry [4, 5, 15, 16, 18, 22, 25, 31]. However, in many cases, rapid protodeauration limits the synthetic potential of gold catalysis. In this regard, organic chemists have invested significant efforts to develop alternative routes for the decomplexation of organogold intermediates which can compete with the protodeauration pathway.

One inspiring approach was the use of dual metal catalytic systems where organogold intermediates obtained under redox-neutral gold catalysis hand over organic fragments to other metals through transmetallation process (see Section "Organogold Reactivity in Dual Metal Catalysis") [23].

Another approach that has captured the attention of researchers is oxidative coupling strategy, where organogold intermediates obtained under redox-neutral gold catalysis conditions take part in an oxidative coupling step delivering

complex products (see Section "Nucleophilic Addition/Rearrangement-Oxidative Coupling") [24, 27, 37].

Organogold Reactivity in Dual Metal Catalysis

Over the past decades, dual catalysis has become a powerful tool in organic synthesis. The concept of combining two privileged catalytic activation modes together to promote a single transformation, which is not possible in the presence of either catalyst alone, has recently captured the attention of synthetic chemists [44, 45]. In the field of transition metal catalysis, transmetallation is a common step involved in most cross-coupling reactions. There has been a huge progress of developing efficient transmetallating reagents such as organo-magnesium, tin, boron, zinc, silicon, lithium, etc., which have been applied in many famous metal-catalyzed cross-coupling and other reactions (Table 2.1).

In gold catalysis, most of the reactions proceed via alkenylgold intermediates (for alkynes and allenes) or alkylgold intermediates (alkenes), being involved in one of the steps in catalytic cycle. To extend the scope of gold catalysis beyond protodeauration, a group of scientists, including Blum, Hashmi and others have been interested in using in situ generated organogold intermediates in other transition metal-catalyzed processes, mostly in cross-coupling type reactions, as potential transmetallating agents in either a stoichiometric or catalytic manner [23, 46–49]. A seminal report [41] on stable alkenylgold intermediate isolation from Hammond and co-workers in 2008 has enhanced the interest of organic chemists more in this line of research.

In 2009, Blum and co-workers reported the method for the carboauration of alkynes **45** catalyzed by palladium to generate alkenylgold intermediates **46**, which could be subsequently used in palladium-catalyzed cross-coupling chemistry (Scheme 2.3a) [47]. In the same year, Hashmi and co-workers also developed a protocol for cross-coupling reactions with a catalytic amount of palladium and stoichiometric amounts of stable alkenylgold intermediates (Scheme 2.3b) [46]. One set of organogold intermediates **47** used in this study were prepared according to the procedure previously developed by Hammond and co-workers in 2008 [41]. Moreover, Blum and co-workers also reported a carboauration with palladium

Table 2.1 Organometallic reagents used in related cross-coupling reactions

Organometallic reagent	Cross-coupling reaction
R–MgX	Kumada coupling
R–**Sn**	Migita-Kosugi-Stille coupling
R–**B**	Suzuki-Miyaura coupling
R–**Zn**	Negishi coupling
R–**Si**	Hiyama coupling
R–**Cu**	Sonogashira-Hagihara coupling
R–**Au**	??

(a) Blum and co-workers (2009)
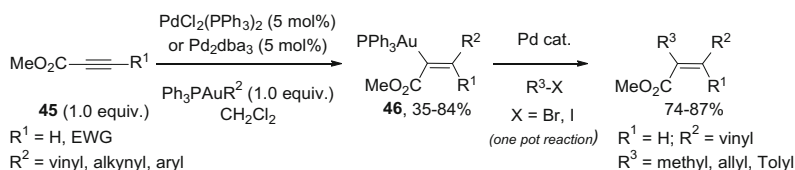
(b) Hashmi and co-workers (2009)
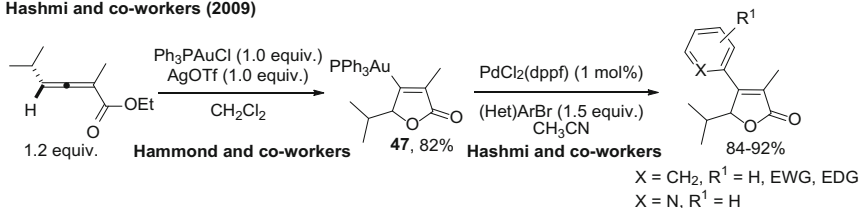
Scheme 2.3 Palladium-catalyzed cross-coupling reactions of organogold reagents [46, 47]

catalysis [47]. In addition to palladium catalysis, organogold intermediates have also been applied in nickel-catalyzed cross-coupling reactions as transmetallating reagents [49].

Although significant contributions have been made to the development of novel organic transformations using dual metal systems with gold and other transition metals, the vast majority of them reported to date are limited to the use of stoichiometric amount of gold [23]. Another limitation is that, in the cases where the other transition metal catalysts (e.g. Ni and Pd) can react via single electron transfer, the substrate scope of the reaction is somewhat limited to compounds, which undergo fast oxidative addition as alternative competing deactivation pathways resulting in the reduction of organogold(I) intermediates to inactive gold(0) can otherwise occur [23]. Another serious concern is the choice of an appropriate ligand, which is crucial to avoid the poisoning of the gold catalysts via the formation of coordinatively-saturated gold complexes (e.g. $[Ph_3P\text{-}Au\text{-}PPh_3]^+$) through ligand exchange between gold and another metal catalyst [23].

Nucleophilic Addition/Rearrangement-Oxidative Coupling

Cascade difunctionalization processes constitute a new class of gold-catalyzed organic transformations, where a carbon–carbon or heteroatom-carbon bond formation generated upon nucleophilic addition onto a carbon–carbon multiple bond activated by gold is accompanied by the formation of a new carbon–carbon or heteroatom-carbon bond under oxidative conditions [24, 27, 37].

An interesting observation by Hashmi and co-workers in early 2008 of a Au(III)-mediated oxidative coupling of vinyl gold intermediates derived from allenyl carbinols upon cyclization disclosed the concept of gold mediated cascade nucleophilic addition oxidative coupling for the first time (Scheme 2.4a) [50]. In late

(a) Hashmi and co-workers (2008)

47%   10%
minor product

(b) Wegner and co-workers (2008)

48

R^1 = H, alkyl

49, 13–67%
major product

50, 8–40%

Via

53

Reductive Elimination

→ Au(I)

c) Zhang and co-workers (2009)

51

R^1, R^2 = alkyl

(2-biphenyl)Cy$_2$PAuNTf$_2$ (5 mol%)

Selectfluor (2.0 equiv.)
CH$_3$CN/H$_2$O = 500:1
60 °C, 25–40 min

52, 80–93%
sole product

Selectfluor
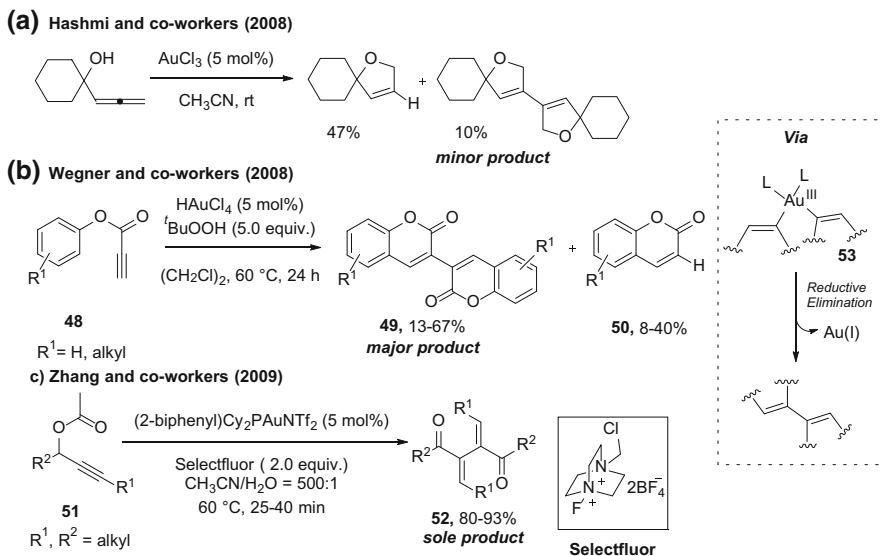
Scheme 2.4 Au-mediated/catalyzed oxidative coupling reactions of allenes and alkynes [50–52]

2008, Wegner and co-workers reported the first catalytic version of this type of oxidative coupling reaction, where cyclization-oxidative dimerization of arylpropionic esters **48** with HAuCl$_4$ (5 mol%) afforded dicoumarin derivatives **49** (13–67 %) in the presence of the oxidant ^{t}BuOOH (5.0 equiv.) (Scheme 2.4b) [51]. Unfortunately, they could not suppress the competitive protodeauration pathway leading to coumarin **50** formation. Thereby, gold-catalyzed oxidative coupling reactions remained challenging to the scientific community until 2009 when Zhang and co-workers successfully developed a catalytic cascade method for the rearrangement-oxidative homocoupling of propargylic acetates **51** to (E,E)-dienones **52** in the presence of (2-biphenyl)Cy$_2$PAuNTf$_2$ (5 mol%) and 2.0 equiv. of Selectfluor as an oxidant at 60 °C in a mixture of acetonitrile and water (500:1, Scheme 2.4c) [52]. In all the above cases, the homocoupled products are generated upon reductive elimination from a gold(III) intermediate **53**. In 2009 prior to homocouling report, Zhang and co-workers described an exciting oxidative gold catalyzed cross coupling of propargylic acetates with arylboronic acids furnishing α-arylated enones [53].

Since then, over the last six years, the versatility of this novel approach has been exploited in many impressive organic transformations, particularly cascade nucleophilic addition-oxidative cross-coupling processes for the difunctionalization of multiple bonds. Although alkynes and allenes have been used in most of these transformations, alkenes have also been successfully employed [24, 27, 37].

Oxidative gold catalysis is an indispensable tool for the difunctionalization of alkenes where nucleophilic addition-carboauration of C=C bond results in an alkylgold intermediate forming a C(sp^3)–Au bond which then reacts with an aryl

precursor (arylboronic acid, arylsilane or simple arene) under oxidative conditions to release an alkylated arene product via $C(sp^3)$–$C(sp^2)$ bond formation. It is worth mentioning that alternative well-established palladium-catalyzed reactions of this type typically suffer from side-reactions involving competitive β-hydride elimination of an alkylpalladium intermediate. This elementary step is not favoured with gold catalysts.

In 2010, Zhang and co-workers reported heteroarylations of non-activated alkenes in an intramolecular fashion, where 4-penten-1-ol **54** was treated with phenylboronic acid **28** (2.0 equiv.) as an aryl precursor in the presence of a privileged gold catalyst (triphenylphosphine)gold(I) chloride (Ph₃PAuCl, 10 mol%) and an exogenous oxidant, Selectfluor (2.0 equiv.) in acetonitrile at 70 °C to deliver the oxyarylated product, 2-benzyl tetrahydrofuran **57** (Scheme 2.5a) [54]. In order to show the broad scope of the developed method, the reactions were performed with different alkene substrates **54–56** with γ-hydroxy, γ-tosyl amine and β-carboxylic acid groups as nucleophiles and also longer tethers between the nucleophile and the alkene to afford the desired 2-benzyl substituted tetrahydrofurans **57**, pyrrolidines **58**, lactones **59** and six membered 2-benzyl substituted tetrahydropyrans **60** and pyrimidines **61** respectively in moderate to excellent yields (Scheme 2.5).

In the same year, Toste and co-workers also reported similar aminoarylations of non-activated alkenes under slightly different reaction conditions (Scheme 2.5b).

In contrast to Zhang's reaction conditions, they employed a lower amount of oxidant (1.5 equiv.), lower temperature (rt-40 °C) and a slightly lower catalyst loading of a bimetallic phosphinegold complex (dppm)(AuBr)₂ (3 mol%, dppm = 1,1-bis(diphenylphosphino-methane)), which was found to be the best catalyst for these studies [55]. The preference for bimetallic gold catalysts was thought to be based on beneficial aurophilic stabilization of Au(III) through Au^{III}–Au^{I} interactions [56].

For the mechanistic illustration of the developed gold-catalyzed intramolecular aminoarylation of alkene, Toste and co-workers and other research groups performed some theoretical calculations and control experiments to identify the intermediates and also the sequence of steps involved in the catalytic cycle [55–57]. In a study focused on elucidating the stereochemical arrangement of the amino and aryl groups in the final products **58**, the deuterium labelled γ-aminoalkene substrate **62** was reacted under the standard conditions. This reaction delivered the expected pyrrolidine product **63** in high diastereoselectivity with conformational analysis of the ¹H NMR spectrum revealing that the amino and aryl groups were in an *anti*-orientation (Scheme 2.6) [54].

Based on the mechanistic studies by means of theoretical calculations and control experiments, a general plausible reaction mechanism is shown in Scheme 2.7 [54–57]. In an initial step, the neutral linear gold catalyst [LAuX] gets oxidized to the square planner gold(III) intermediate **A** by the F⁺ oxidant, selectfluor. At this point, coordination of the gold(III) metal center to the alkene is followed by a nucleophilic attack onto the activated alkene **55** to obtain intermediate **B**. In next step, aryl group transfer from the arylboronic acid to the

(a) **Zhang and co-workers (2010)**

54   **28** (2.0 equiv.)

R^1 = H, alkyl, aryl
n = 1, 2

57 n = 1 56-73%
60 n = 2, R^1 = H, 35%
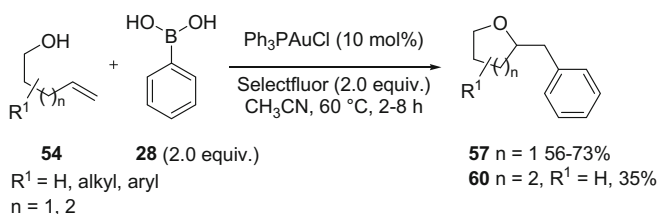
(b) **Zhang and co-workers (2010) & Toste and co-workers (2010)**

55   **28** (2.0 equiv.)

58 n = 1 44-94%
61 n = 2 63-82%

R^1 = H, alkyl, aryl; R^2 = EDG and EWG
n = 1, 2

(c) **Zhang and co-workers (2010)**

56   **28** (2.0 equiv.)   **59** 78-79%

R^1 = H, alkyl
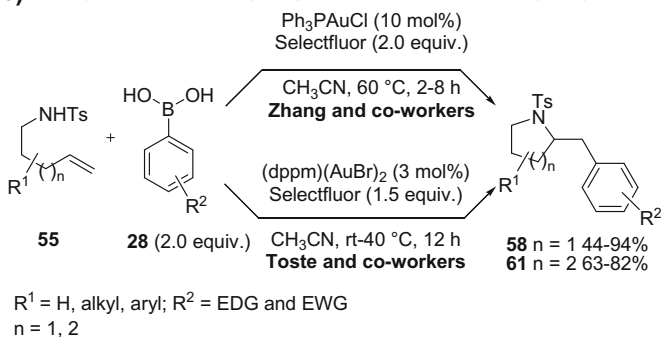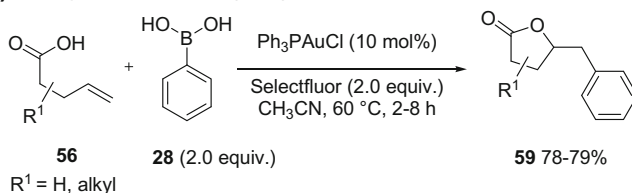
Scheme 2.5 Oxidative gold-catalyzed intramolecular heteroarylation of non-activated alkenes [54, 55]

62   **28** (2.0 equiv.)

63 83%
d.r. = 22:1
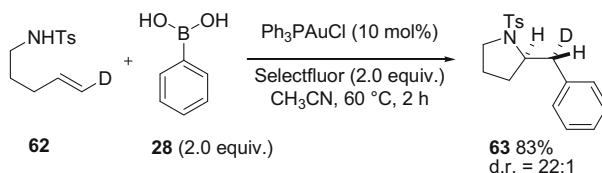
Scheme 2.6 Aminoarylation of deuterium labelled γ-aminoalkene under Zhang's reaction conditions [54]

sp^3-hybridized carbon attached to Au(III) in a concerted five membered transition state assisted by the fluoride ion bound to Au(III) in intermediate **C** gives rise to the heteroarylation product **58**. The *anti*-relationship of nucleophile and aryl groups could be explained by *syn*-nucleophilic-auration of the C=C bond followed by S_N2
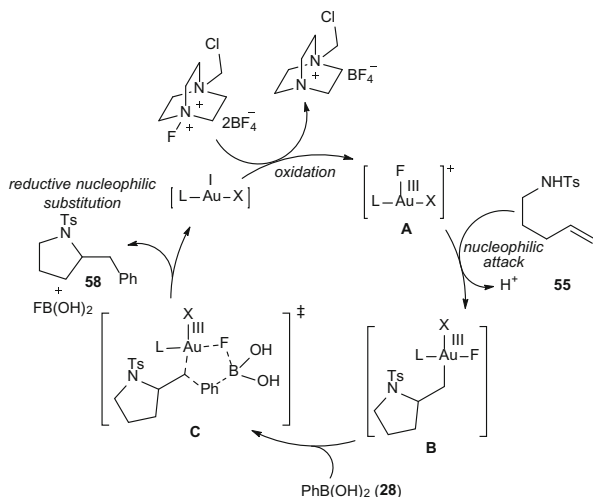
type aryl transfer with inversion of configuration assisted by the fluoride ligand
bound to the Au(III) activating the boron center of the boronic acid. An alternative
possibility is *anti*-aminoauration of the alkene followed by transmetallation-
reductive elimination or a S$_N$i-type substitution mechanism.

To show the versatility of this approach, Toste and co-workers extended this
reactivity to relatively more difficult selective three component intermolecular
oxyarylations of terminal alkenes using arylboronic acids as aryl precursors
(Scheme 2.8) [58]. However, all these methods where arylboronic acids were used
as aryl precursors suffer from oxygen and nitrogen based functional groups toler-
ance on the aryl rings. To solve this problem, Toste and co-workers and Russell and
co-workers independently developed methods where easily synthesized arylsilanes
were successfully employed in place of arylboronic acids (Scheme 2.8) [59, 60].
The next advancement in this strategy was accomplished by Gouverneur and
co-workers and Nevado and co-workers using simple arenes as potential aryl
precursors in intramolecular processes [61, 62].

This strategy for difunctionalizations of alkenes suffers from some serious
limitations such as a lack of substrate scope. For example, electron rich alkene
substrates (e.g. styrenes) and boronic acids featuring electron rich substituents (e.g.
oxygen, nitrogen substituents) on the aryl ring are not well tolerated under the harsh
oxidative reaction conditions implicit to the use of the very strong oxidant,
Selectfluor. Moreover, these methods have been so far limited to mono-substituted
terminal alkenes.
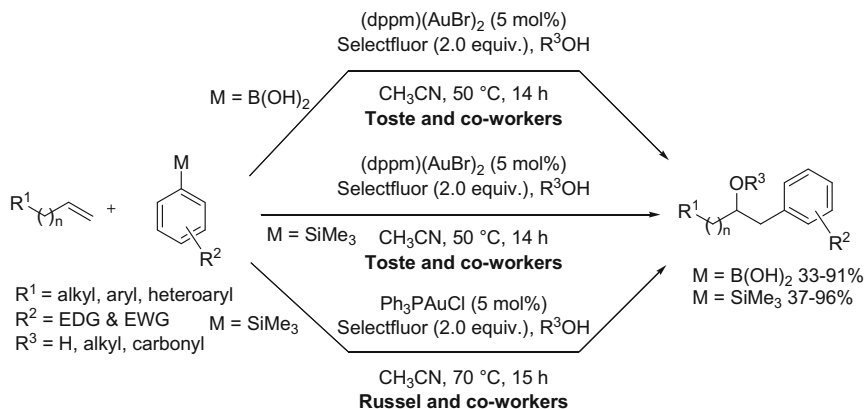
Scheme 2.8 Oxidative gold-catalyzed intermolecular oxyarylation of non-activated alkenes [58–60]

2.1.3 Aryldiazonium Salts: Synthesis and Reactivity

Aryldiazonium salts are attractive reactants used in different fields of chemistry, such as nucleophilic aromatic substitution reactions [63], transition metal catalysis as alternatives to aryl halides and aryl triflates [64], material chemistry for surface modification [65] and most importantly, radical chemistry [66] as excellent aryl radical sources. The chemistry of diazonium salts benefits from (a) very easy preparation, even in large scale, (b) typically high chemoselectivity in cross-coupling reactions due to their superior reactivity compared to aryl halides, (c) ambient reaction conditions and (d) easy removal of a gaseous leaving group (nitrogen gas) without interfering reaction components [67].

Aryldiazonium salts **7** can be prepared from commercially available anilines **64** in an aqueous medium with sodium nitrite and a strong acid (e.g. HBF_4) (Scheme 2.9) [68]. In organic solvents (Et_2O, DME or THF), aryldiazonium salts are prepared using organic nitrites (^tBuONO or ^iAmONO) and BF_3-Et_2O (Scheme 2.9) [69]. The stability of the aryldiazonium salts can be tuned by choosing an appropriate counteranion, such as the *o*-benzenedisulphonimide anion, which results in a high degree of stabilization and can be reused [70]. In many recent studies, aryldiazonium salts are generated in situ using organic nitrites (^tBuONO or ^iAmONO) in organic solvents (e.g. CH_3CN) and directly used in the next step [71–74].

Depending on the reaction conditions (counteranion, nucleophilic additive, solvent, reducing agent and wavelength of light), aryldiazonium salts can undergo homolytic cleavage or heterolytic cleavage to obtain aryl radicals or cations respectively (Scheme 2.10) [66]. Single electron reduction of aryldiazonium salts with subsequent loss of dinitrogen delivers aryl radicals, which participate in classical name reactions: (a) the Sandmayer reaction [75–77], (b) the Pschorr
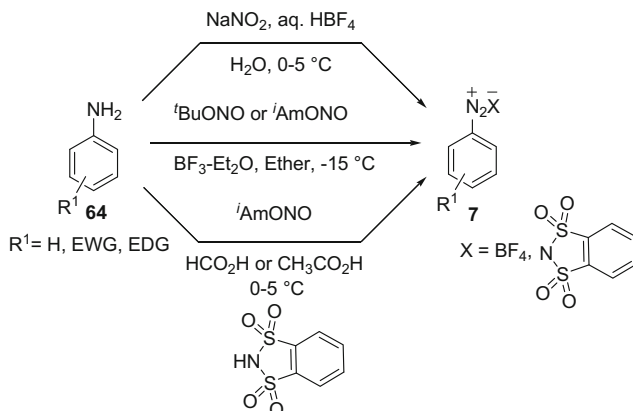
Scheme 2.9 Synthesis of aryldiazonium salts [68, 69]
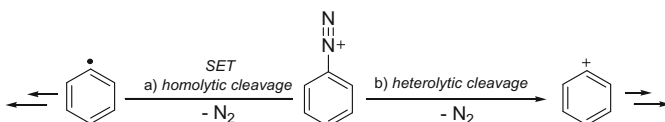
Scheme 2.10 Reactivity of diazonium salts: (a) homolytic cleavage; (b) heterolytic cleavage

cyclization [78], (c) the Gomberg-Bachmann reaction [79–81] and (d) the Meerwein arylation [82, 83] and also many conceptually novel and synthetically important organic transformations [66, 67, 71, 84]. There are many single electron reductants known such as Cu(I) salts [75, 76, 85, 86], $FeSO_4$ [87], ferrocene [87], ascorbic acid [72, 87], $TiCl_3$ [88–90], Bu_4NI [73, 74] and TEMPONa [91] to generate aryl radicals from aryldiazonium salts at ambient temperature [81]. In this direction of research, under visible light irradiation, polypyridyl metal complexes (e.g. $[Ru(bpy)_3]Cl_2$) and organic dyes (e.g. eosin Y or fluorescein) are highly efficient at generating aryl radicals from aryldiazonium salts allowing for milder conditions for subsequent reactions [67, 92–94].

2.1.4 Diaryliodonium Salts: Synthesis and Reactivity

Since the seminal report on diaryliodonium salts was published by Hartmann and Meyer [95] in 1894, diaryliodonium salts, IUPAC nomenclature "diaryl-λ^3-iodi-nanes", constitute a synthetically highly important class of hypervalent iodine compounds, which are widely applied in many different fields of chemistry such as in synthetic organic chemistry as arylating agents [96, 97], in polymer chemistry as

cationic photoinitiators [98, 99] and as precursors to ^{18}F-labelled compounds used in Positron Emission Tomography (PET) imaging [100].

Some important features of diaryliodonium compounds, which highlight its importance in practical applications are listed below: (a) these reagents are non-toxic, mild and moisture and air stable; (b) symmetrical diaryliodoniums have no issue of selectivity, whereas unsymmetrical examples typically selectively transfer one aryl group over another one depending on electronic factors, sterics (e.g. the use of a bulkier dummy aryl group generally favours transfer of the other aryl moeity) [101] and also the reaction conditions; (c) diaryliodonium salts have very high electrophilicity and possess a strong aryl iodide leaving group [102]; (d) easy counteranion exchange has given access to a wide variety of these compounds, which allows for judicious selections to be made to avoid potential nucleophilic attack by the counteranion under the reaction conditions or to improve solubility. Typically diaryliodonium salts with halide counteranions are sparingly soluble in organic solvents while non-coordinating BF_4 and OTf lead to improved solubility in many widely-employed solvents [96, 97].

There are many synthetic routes already developed giving access to diaryliodonium salts for practical applications in organic synthesis [96, 97]. Some selected routes starting from different arene precursors are shown in Scheme 2.11 [103–108].

These compounds are highly electrophilic in nature at the iodine center due to the presence of a node of a non-bonding orbital that resides on iodine. Thereby diaryliodoniums react with many different nucleophiles at the iodine center. The reaction occurs through initial Nu–I bond formation followed by reductive elimination of one aryl group and nucleophile from the iodine center (Scheme 2.12a) [96]. Moreover, oxidative addition of these compounds to transition metals (e.g. copper, palladium, etc.) results in aryl–metal intermediates, which can take part in subsequent steps of the transformation such as in cross-coupling (Scheme 2.12b) [96]. In the presence of single electron reductants, diaryliodonium salts can afford aryl radicals (Scheme 2.12c) [66]. Very recently, diaryliodonium salts have been used by the scientific community in photoredox catalysis as aryl precursors to generate aryl radicals for arylation of alkenes and arenes under mild conditions (Scheme 2.12c) [109, 110].

2.2 Results and Discussion

2.2.1 Inspiration

In one of the earlier reports of photoredox catalysis in 1984, Deronzier and co-workers described the Pschorr reaction for the synthesis of phenanthrene derivatives **1** from aryldiazonium salts **3** in the presence of $[Ru(bpy)_3](BF_4)_2$ (5 mol %) in acetonitrile under visible light irradiation (>410 nm) from a 250 W Hg lamp
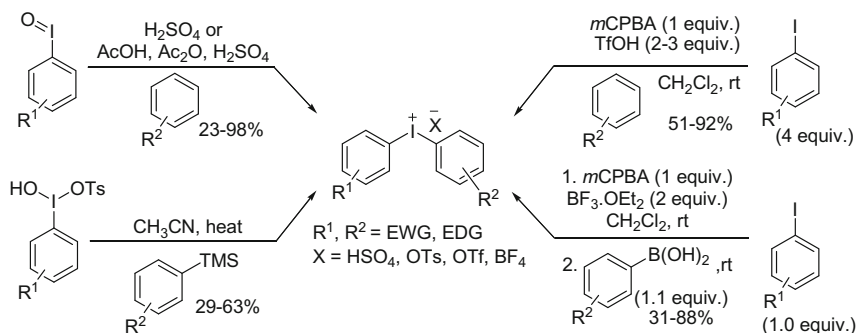
Scheme 2.11 Synthesis of diaryliodonium salts [103–108]
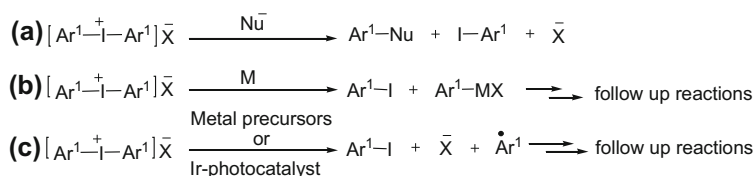
Scheme 2.12 Reactivity of diaryliodonium salts: **a** nucleophilic substitution; **b** oxidative addition to metals; **c** aryl radical formation under visible light photoredox catalysis
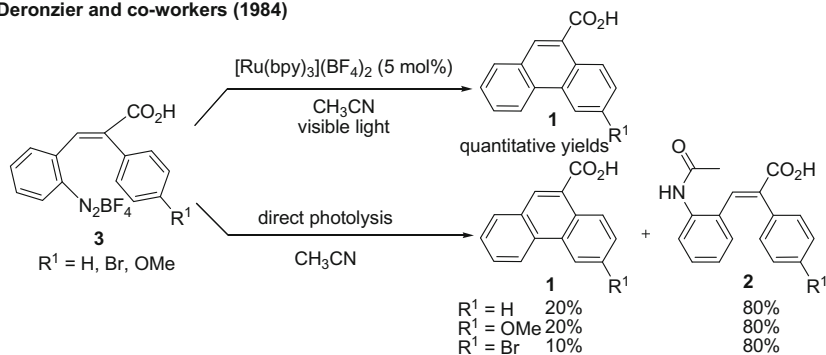
Scheme 2.13 Pschorr reaction under photoredox catalysis and direct photolysis [111]

(Scheme 2.13 and see Sect. 1.4.1.1) [111]. This method avoids the formation of the undesired byproduct **2** under direct photolysis (>360 nm) and benefits from milder reaction conditions compared to previously reported electrochemical processes [112] or thermal methods (Scheme 2.13) [113, 114].

After several intervening years, in 2011, Sanford and co-workers realized the potential of Deronzier's system and successfully applied it to their well-established

Sanford and co-workers (2011)
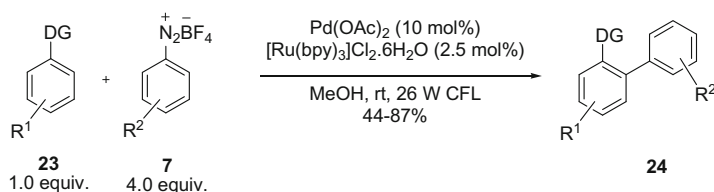
DG = Directing Group; R^1 = H, EDG; R^2 = H, EWG, EDG

Scheme 2.14 Dual palladium and visible light-mediated photoredox-catalyzed directed C–H arylation [115]

directed *ortho*-selective C–H arylation process, combining photoredox with palladium catalysis to access Pd(II)/Pd(IV) catalytic cycles (Scheme 2.14 and see Sect. 1.4.1.2) [115].

Inspired by these two seminal reports, we were interested in developing a dual catalytic system combining photoredox catalysis and gold catalysis and anticipated that in analogy to Pd(II)/Pd(IV) cycles, photoredox-generated aryl radicals from aryldiazonium salts may facilitate Au(I)/Au(III) catalytic cycles and enable the oxyarylation of alkenes while avoiding strong external oxidants and benefiting from milder reaction conditions.

2.2.2   Intramolecular Oxy- and Aminoarylation of Alkenes

2.2.2.1   Preliminary Tests and Optimization Studies

In a preliminary test, 4-penten-1-ol (**54**) was treated with 4.0 equiv. of phenyldiazonium tetrafluoroborate (**65**) in the presence of 10 mol% of the gold(I) precatalyst (triphenylphosphine)gold(I) chloride (Ph_3PAuCl) and 5 mol% of [Ru (bpy)$_3$](PF$_6$)$_2$ in degassed methanol (0.1 M) under visible light irradiation from a 23 W compact fluorescent light (CFL) bulb for 6 h. To our delight, we observed the 5-*exo-trig* cyclization-arylation product 2-benzyl tetrahydrofuran (**57**) in 51 % NMR yield as the major product (Table 2.2, entry 1).

As the next step, we performed exhaustive optimization studies of this cascade cyclization-arylation reaction (Table 2.2). Our first attempt to improve the yield involved the screening of different gold catalysts with various ligands and counteranions. The reaction efficiency was highly dependent on the gold catalysts used for these studies. Neutral (dimethylsulfide)gold(I) chloride (Me_2SAuCl) delivered the product **57** in only 20 % NMR yield, while the electron-rich NHC-gold complex IPrAuCl (IPr = 1,3-bis(2,6-diisopropyl-phenyl)imidazol-2-ylidene) was an inefficient catalyst for this process, delivering only a trace amount of product **57**

Table 2.2 Optimization studies[a]

Entry	[M] catalyst (mol%)	mol% [Ru (bpy)$_3$]$^{2+}$	Equiv. of 65	Solvent	Time (h)	Yield (%)[b]
1	Ph$_3$PAuCl (10)	5.0	4	MeOH	6	51
2	(Me$_2$S)AuCl (10)	5.0	4	MeOH	12	26
3	IPrAuCl (10)	5.0	4	MeOH	12	Trace
4	[dppm(AuCl)$_2$] (10)	5.0	4	MeOH	12	22
5	AuCl (10)	5.0	4	MeOH	12	Trace
6	AuCl$_3$ (10)	5.0	4	MeOH	12	Trace
7	[(Pic)AuCl$_2$] (10)	5.0	4	MeOH	12	Trace
8	[Ph$_3$PAu]NTf$_2$ (10)	5.0	4	MeOH	4	84
9	[Ph^{t}Bu$_2$PAu(CH$_3$CN)]SbF$_6$ (10)	5.0	4	MeOH	12	–
10	[(Ph$_3$P)$_2$Au]OTf (10)	5.0	4	MeOH	12	50
11	[IPrAu]NTf$_2$ (10)	5.0	4	MeOH	12	Trace
12	[Ph$_3$PAu]NTf$_2$ (10)	5.0	4	CH$_3$CN	12	20
13	[Ph$_3$PAu]NTf$_2$ (10)	5.0	4	1,4-Dioxane	12	20
14	[Ph$_3$PAu]NTf$_2$ (10)	5.0	4	Acetone	12	14
15	[Ph$_3$PAu]NTf$_2$ (10)	5.0	4	CH$_2$Cl$_2$	12	3
16	[Ph$_3$PAu]NTf$_2$ (10)	5.0	4	DMA	12	17
17	[Ph$_3$PAu]NTf$_2$ (10)	5.0	4	EtOH	12	66
18	**[Ph$_3$PAu]NTf$_2$ (10)**	**2.5**	**4**	**MeOH**	**4**	**88(79)**
19	[Ph$_3$PAu]NTf$_2$ (10)	1.0	4	MeOH	12	61
20	[Ph$_3$PAu]NTf$_2$ (5)	2.5	4	MeOH	12	50
21	[Ph$_3$PAu]NTf$_2$ (1)	2.5	4	MeOH	7.5	22
22	[Ph$_3$PAu]NTf$_2$ (5)	1.2	4	MeOH	12	70
23	[Ph$_3$PAu]NTf$_2$ (5)	1.2	3	MeOH	12	60
24	Pd(OAc)$_2$ (10)	2.5	4	MeOH	6	–
25	Cu(OAc)$_2$ (10)	2.5	4	MeOH	8	–
26	PtCl$_2$ (10)	2.5	4	MeOH	8	–
27	[Ph$_3$PAu]NTf$_2$ (10)	–	4	MeOH	4	4
28	–	2.5	4	MeOH	4	–
29[c]	[Ph$_3$PAu]NTf$_2$ (10)	4	4	MeOH	4	6

[a]Alkenol **54** (0.2 mmol), phenyldiazonium salt **65**, [Ru(bpy)$_3$](PF$_6$)$_2$, the transition metal catalyst and the solvent were added to a flame-dried Schlenk flask in the absence of light. The mixture was degassed with three freeze-pump-thaw cycles, flushed with argon, sealed and stirred at rt under visible light irradiation (23 W CFL bulb) for the designated time
[b]NMR yield using diethyl phthalate as an internal reference. Isolated yields in parentheses
[c]The reaction was conducted in the dark. *dppm* diphenylphosphinomethane; *IPr* 1,3-bis (2,6-diisopropylphenyl)imidazol-2-ylidene); *Pic* picolinato

(Table 2.2, entry 2–3). The bimetallic gold complex (dppm)(AuCl)$_2$, (dppm = diphenylphosphinylmethane), which is known to be a good catalyst in oxidative Au(I)/Au(III) catalysis [55], was less efficient in our study, affording product **57** in 22 % NMR yield (Table 2.2, entry 4). Simple gold chloride (AuCl) without any ligand was unsuitable for the reaction (Table 2.2, entry 5). In a similar way, gold(III) precatalysts AuCl$_3$ and (Pic)AuCl$_2$ (Pic = picolinato) were also inefficient catalysts for this reaction (Table 2.2, entry 6–7). Changing the counteranions from tightly bound chloride to loosely bound NTf$_2$ led to a dramatic change in the reaction efficiency. The Gagosz catalyst [Ph$_3$PAu]NTf$_2$, which is considered to generate cationic [Ph$_3$PAu]$^+$ upon solvation, furnished product **57** in 84 % NMR yield (Table 2.2, entry 8). In a screen of cationic gold catalysts, [Ph^{t}Bu$_2$PAu(CH$_3$CN)]SbF$_6$ showed no reactivity, whereas coordinatively saturated [(Ph$_3$P)$_2$Au]OTf, which is considered to be inactive in redox neutral gold catalysis, catalyzed this reaction in moderate efficiency, delivering product **57** in 50 % NMR yield (Table 2.2, entry 9–10). Again, the cationic NHC-gold complex IPrAuNTf$_2$ remained ineffective to promote this reaction (Table 2.2, entry 11). After screening of 11 different gold catalysts, the Gagosz catalyst [Ph$_3$PAu]NTf$_2$ was found to be the best for this transformation. In a solvent screen, methanol remained the best solvent for this process. On moving from methanol to other non-alcoholic solvents such as CH$_3$CN, 1,4-dioxane, acetone, CH$_2$Cl$_2$ and DMA, the efficiency of the reaction dropped dramatically (Table 2.2, entry 12–16). In another alcoholic solvent, ethanol, a significant drop of reaction efficiency was also observed with the product **57** being afforded in 66 % NMR yield (Table 2.2, entry 17). Lowering the loading of the photocatalyst [Ru(bpy)$_3$](PF$_6$)$_2$ from 5 to 2.5 mol% furnished the product **57** in 88 % NMR yield enhancing the reaction efficiency, however further lowering the loading to 1 mol% reduced the reaction efficiency again (Table 2.2, entry 18–19). Lowering the gold catalyst loading from 10 to 5 and 1 mol% had an adverse effect on the efficiency of the reaction (Table 2.2, entry 20–21). When loadings of gold and photocatalyst were reduced to 5 and 1.2 mol% respectively keeping the ratio between the gold catalyst and photocatalyst same, the efficiency of the reaction decreased (Table 2.2, entry 22). A similar effect was also observed when the stoichiometry of the phenyldiazonium salt **65** was reduced to 3.0 equiv. (Table 2.2, entry 23). On the other hand, the other transition metal catalysts Pd(OAc)$_2$, CuOAc and PtCl$_2$ did not catalyze the reaction at all (Table 2.2, entry 24–26). As a result of these studies, the combination of 10 mol% [Ph$_3$PAu]NTf$_2$, 2.5 mol% [Ru(bpy)$_3$](PF$_6$)$_2$ and 4.0 equiv. of the phenyldiazonium salt in methanol (0.1 M) as the solvent was identified as the optimized conditions for this transformation.

Control reactionss confirmed the necessities of all three components: the photoredox catalyst [Ru(bpy)$_3$](PF$_6$)$_2$, the gold catalyst [Ph$_3$PAu]NTf$_2$ and light (Table 2.2, entry 27–29). Without [Ru(bpy)$_3$](PF$_6$)$_2$, the reaction gave only 4 % yield of the product while without [Ph$_3$PAu]NTf$_2$ no reactivity was observed (Table 2.2, entry 27–28). In the absence of light, a trace amount of product **57** (6 %) was observed (Table 2.2, entry 29).

2.2.2.2   Substrate Scope and Limitations[1]

With these optimal reaction conditions in hand, we next investigated the scope and limitations of the developed dual catalytic method for the oxyarylation of alkenes, which are summarized in Tables 2.3 and 2.4.

Varying the alkene substrates

At the beginning, the scope and limitations of the process with respect to the alkene substrates was explored by treating 4-methylphenyldiazonium tetrafluoroborate (**86**) with various substituted alkenol substrates **66–75**. The reaction conducted with (±) 3-phenylpent-4-en-1-ol **66,** a primary alcohol, afforded the cyclization-arylation product (±) 2-(4-methylbenzyl)-3-phenyltetrahydro-furan **76** in 70 % yield and 1.6:1 d.r., while (±) *trans*-2-allylcyclohexenol **67**, a secondary alcohol, delivered (±) 2-(4-methylbenzyl)octahydro-benzofuran **77** in 66 % yield and 2.8:1 d.r. showing the tolerance of the process towards substituents on the alkyl tether (Table 2.3, entry 1–2). Under the same reaction conditions, a tertiary alcohol, 3-ethylhept-6-en-3-ol **68**, was reacted with 4-methylphenyldiazonium salt **86** to obtain the corresponding oxyarylation product 2,2-diethyl-5-(4-methylbenzyl) tetrahydro-furan **78** in 56 % yield (Table 2.3, entry 3). The reactions of 1,1-disubstituted alkenes **69** and **70**, which are unsuitable substrates for previously reported gold-catalyzed heteroarylations of alkenes under oxidative conditions [54, 55], were successful coupling partners in this study affording the desired oxyarylation products **79** (39 %) and **80** (63 %) respectively (Table 2.3, entry 4–5). In contrast to previously-reported oxidative gold-catalyzed heteroarylations of alkenes [54, 55], internal alkenes (*E*)-**71** and (*Z*)-**72** were successfully employed in this oxyarylation process under dual catalytic conditions to furnish the expected oxyarylation products (±) (*R,R*)-**81** (59 %) and (±) (*R,S*)-**82** (56 %) with excellent diastereoselectivities (in both cases d.r. > 25:1) respectively (Table 2.3, entry 6–7). This high diastereoselectivity supports the involvement of the gold catalyst in the stereochemistry-determining steps and provides mechanistic evidence for the process (vide infra). The alkenol **75** with an extra CH$_2$ tether was suited for this process affording the product **85** in 34 % yield (Table 2.3, entry 10). Alkene substrates with nitrogen nucleophiles were also successfully employed in this process. Substrates **73** and **74** with pendant protected amine nucleophiles delivered the corresponding pyrrolidine products **83** (84 %) and **84** (54 %) respectively (Table 2.3, entry 8–9).

Varying the aryldiazonium salts

Aryldiazonium salts **86–92**, with diverse substitution patterns, were investigated in this study using 4-penten-1-ol as the alkene under the optimized reaction conditions (Table 2.4). Aryldiazonium salts **86** and **87**, bearing electron-neutral methyl and phenyl substituents respectively, were well suited for this transformation giving rise to the corresponding products **93** (78 %) and **94** (64 %) (Table 2.4, entry 2–3).

---

[1]A part of the substrate scope studies was carried out by Dr. Matthew N. Hopkinson (WWU).

Table 2.3 Scope of alkene substrates[a]

Entry	Alkenols	Product	Yield(d.r.)[%][b]
1	**66** Ph	**76** Ph	70 (1.6:1)
2	**67**	**77**	66 (2.8:1)
3	**68**	**78**	56
4 5	R = Me **69** R = Ph **70**	**79** **80**	39% 63%
6	**71**	**81**	59 (>25:1)
7[c]	**72**	**82**	56 (>25:1)
8[d] 9[d]	R = H **73** R = Me **74**	**83** **84**	84 54
10	**75**	**85**	34

[a]General conditions: **66–75** (0.2 mmol, 1 equiv.), [Ph₃PAu]NTf₂ (0.02 mmol), [Ru(bpy)₃](PF₆)₂ (0.005 mmol), **86** (4.0 equiv.), degassed MeOH (0.1 M), rt, 4–16 h, 23 W fluorescent light bulb

[b]Isolated yields. *d.r.* determined by ^{1}H NMR

[c]Reaction performed on a 0.4 mmol scale

[d]5.0 equiv. of **74** used

The aryldiazonium salt **88**, with an electron-withdrawing ester functionality was the most efficient coupling partner among the tested aryldiazonium salts furnishing the desired product **95** in 83 % yield (Table 2.4, entry 4). Aryldiazonium salts **89–91**, featuring electron-withdrawing halogen functional groups such as fluoride, bromide and also bromide and chloride together, were successfully employed in this process to obtain the oxyarylation products **96–98**, in which chloride and bromide functionalities are available for further functionalization (Table 2.4, entry 5–7). Aryldiazonium salt **92**, bearing both an electron-withdrawing trifluoromethyl group and an electron-donating methoxy group was tolerated under the reaction conditions giving rise to the desired product **99** in 32 % yield (Table 2.4, entry 8). In none of the cases was the protodeauration product detected in the reaction mixture.

2.2.3   Intermolecular Oxyarylation of Alkenes

Since a multicomponent intermolecular process is more difficult than its intramolecular version, it is highly encouraging to develop methodologies for the intermolecular difunctionalization of alkenes for constructing important complex building blocks. One of the common methods for the arylation of alkenes in an intermolecular fashion is the palladium-catalyzed Mizoroki-Heck reaction involving aryl halides and alkenes as coupling components to deliver styrene derivatives. However, there has been a significant research attention paid to the development of methodologies for the addition of two functional groups across the C=C double bond, instead of maintaining the alkene functionality. In this regard, we extended our previously developed dual catalytic methodology to the selective three component oxyarylation of terminal alkenes under milder reaction conditions compared to previously-reported methods [58–60].

2.2.3.1   Preliminary Tests and Optimization Studies

In a preliminary test, we employed our previously-developed standard reaction conditions where a terminal alkene, 1-octene (**100**), was reacted with 4.0 equiv. of phenyldiazonium tetrafluoroborate (**65**) in the presence of 10 mol% of [Ph$_3$PAu] NTf$_2$ and 2.5 mol% of [Ru(bpy)$_3$](PF$_6$)$_2$ in degassed methanol (0.1 M) under visible light irradiation from a 23 W CFL bulb for 16 h. We were delighted to observe selective formation of the oxyarylation product, (2-methoxyoctyl)benzene (**102**) in 90 % NMR yield and 84 % isolated yield as the major product.

   In order to optimize this reaction,[2] various gold catalysts with electron-rich phosphines (tricyclohexylphosphine and tris(4-methoxyphenyl)phosphine) and an electron-poor phosphine (tris(4-trifluoromethylphenyl)phosphine) were screened

---

[2]The optimization studies were carried out by Dr. Matthew N. Hopkinson (WWU Münster).

Table 2.4 Scope of aryldiazonium salts for the Au/Ru-catalyzed oxyarylation of alkenes[a]

Reaction scheme:

Alkenol (with OH and terminal alkene) + Ar-N$_2$BF$_4$ (R^1 substituted, 4.0 equiv)

Conditions: 10 mol % [Ph$_3$PAu]NTf$_2$, 2.5 mol % [Ru(bpy)$_3$](PF$_6$)$_2$, 23 W CFL bulb, degassed MeOH, rt → tetrahydrofuran product with benzyl-R^1 group

Entry	[Ar-N$_2$]BF$_4$	Product	Yield (%)[b]
1	phenyl **65**	**57**	79
2	4-methylphenyl **86**	**93**	78
3	4-Ph-phenyl **87**	**94**	64
4	4-EtO$_2$C-phenyl **88**	**95**	83
5	4-F-phenyl **89**	**96**	75
6	4-Br-phenyl **90**	**97**	60
7	4-Cl-2-Br-phenyl **91**	**98**	42
8	3-F$_3$C-5-OMe-phenyl **92**	**99**	32

[a]Alkenol **54** (0.2 mmol), aryldiazonium salt **65**, **86-92** (0.8 mmol), [Ph$_3$PAu]NTf$_2$ (0.02 mmol), [Ru(bpy)$_3$](PF$_6$)$_2$ (0.005 mmol) and MeOH (2 mL) were added to a flame-dried Schlenk flask in the absence of light. The mixture was degassed with three freeze-pump-thaw cycles, flushed with argon, sealed and stirred at rt under visible light irradiation (23 W compact fluorescent light bulb) 4–12 h

[b]Isolated yield

because our previous intramolecular oxyarylation reactions were highly ligand dependant, favouring phosphine ligands. In the survey of different photoredox catalysts such as the polypyridyl metal complexes ($[Ru(bpy)_3](PF_6)_2$ and [Ir $(ppy)_2(dtbbpy)](PF_6)$) and organic dyes (eosin Y, fluorescein, rhodamine B and rose bengal) and light sources (23 W CFL, blue LEDs, green LEDs), we found that a combination of 10 mol% of $[Ph_3PAu]NTf_2$ and 5 mol% of fluorescein in degassed methanol (0.1 M) under visible light irradiation from a 23 W CFL bulb could catalyze the reaction of 1-octene (**100**) with 4.0 equiv. of the phenyldiazonium salt with the highest efficiency, delivering (2-methoxyoctyl)benzene (**102**) in 88 % NMR yield and 86 % isolated yield (Scheme 2.15a). The use of an inexpensive photoredox catalyst, fluorescein dye (404 times cheaper than previously used $[Ru(bpy)_3](PF_6)_2$, according to the prices offered by Sigma Aldrich in June, 2014) made this protocol more attractive. In order to replace comparatively less stable aryldiazonium salts, air and moisture stable diaryliodonium salts were tested in the same reaction. After an exhaustive screening of many different gold catalysts with a variety of ligands, various photoredox catalysts, light sources, mixture of solvents and diaryliodonium salts with different counteranions, we were delighted to find optimized reaction conditions for this process where treating 1-octene (**100**) with 4.0 equiv. of diphenyliodonium tetrafluoroborate (**101**) in the presence of 10 mol% of $[Ph_3PAu]NTf_2$ and 5 mol% of $[Ir(ppy)_2(dtbbpy)](PF_6)$ in degassed methanol (0.1 M) under visible light irradiation from 5 W blue LEDs furnished (2-methoxyoctyl)benzene (**102**) in 91 % NMR yield and 82 % isolated yield as the major product (Scheme 2.15b). It is worth mentioning that organic dyes did not catalyze this reaction with diaryliodonium salts and that a more strongly reducing iridium photocatalyst was required.
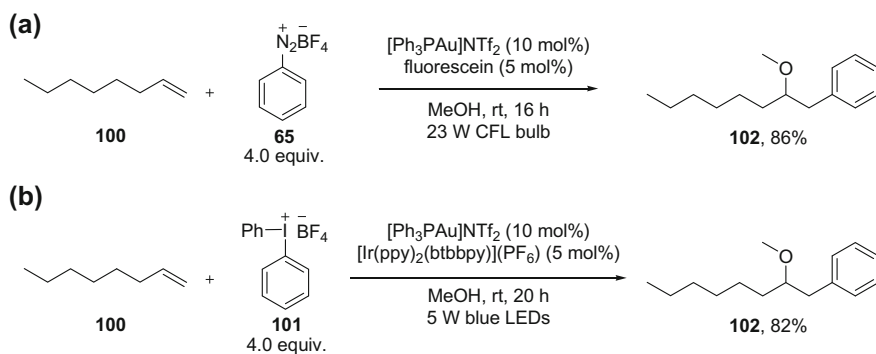
Scheme 2.15 Intermolecular oxyarylation of alkenes: **a** Oxyarylation with aryldiazonium tetrafluoroborate; **b** oxyarylation with diaryliodonium tetrafluoroborate

2.2.3.2   Substrate Scope and Limitations[3]

Having optimized reaction conditions for both the methods in hand, we explored the scope and limitations of both protocols for intermolecular oxyarylation in terms of alkene substrates and arylprecursors (conditions A: with aryldiazonium and conditions B: with diaryliodonium salts) (Table 2.5).

In contrast to previously reported oxyarylations of activated alkenes which proceed via radical-addition [91, 110, 116, 117], we could successfully employ unactivated alkenes without requiring any radical stabilizing groups in these dual catalytic methods. In none of the cases were styrene-type products resulting from Mizoriki-Heck coupling or hydroetherification could be detected under the optimized reaction conditions. Electron-withdrawing and electron-donating functional groups on the aryl ring in the aryldiazonium and diaryliodonium salts were well tolerated. Substrates bearing a methyl substituent at the *ortho*-, *meta*- or *para*-positions of the aryl ring were all suitable for this process under both reaction conditions employing aryldiazonium and diaryliodonium salts, but a different trend of tolerance was observed in these studies. The *para*-methyl-substituted aryldiazonium salt reacted efficiently delivering the desired ether product **103** in 62 % yield, while the corresponding diaryliodonium salt afforded same product **103** in a poor yield (26 %). An opposite trend of reactivity was observed for *ortho*-methyl-substituted substrates, with the aryldiazonium salt producing the desired ether product **104** in 28 % yield (conditions A) and the diarylaiodonium salt leading to **104** in 75 % yield (conditions B). A *meta*-methyl substituent in both the cases was well tolerated under both sets of reaction conditions. Electron-withdrawing bromide functionality was also well tolerated under both reaction conditions furnishing the expected ether product **106**, susceptible for further functionalization, in good yield (conditions A: 69 % and conditions B: 65 %). Diaryliodonium salts featuring electron-withdrawing fluorine and trifluoromethyl functional groups were successfully applied for this process only under the reaction conditions B, affording the ether products **107** (82 %) and **108** (36 %), respectively. Ethyl ester functionality at the *para*-position on the aryl ring of the aryldiazonium salt and at the *meta*-position on the aryl ring of the diaryliodonium salt was tolerated in these oxyarylation processes delivering the corresponding products **109** (64 %) and **110** (50 %), respectively, in good to moderate yields. Both compounds were isolated with contamination with small amounts of the corresponding methyl esters resulting from transesterification with the methanol solvent. Diverse functional groups on the alkenes were tolerated in these dual-catalyzed oxyarylation reactions under both sets of reaction conditions, affording the ether products **111**–**114** in moderate to good yields. Alkene substrates having pendant 4-methoxyphenol and a protected amine *N*-phthalimide group were also successful in this process under reaction conditions B, giving products **115** (26 %) and **116** (52 %), respectively, in low to moderate yields. Apart from methanol, other oxygen nucleophiles such as ethanol

---

[3]A part of the substrate scope was carried out by Dr. Matthew N. Hopkinson (WWU Münster).

Table 2.5 Scope of intermolecular oxyarylation of alkenes with aryldiazonium salts and diaryliodonium salts[a]

102 (R² = H) **A:** 86%, **B:** 82%
   (**B:** 2.0 mmol scale, 91%)
103 (R² = p-Me) **A:** 62%, **B:** 26%
105 (R² = m-Me) **A:** 70%, **B:** 60%
104 (R² = o-Me) **A:** 28%, **B:** 75%
106 (R² = p-Br) **A:** 69%, **B:** 65%
107 (R² = p-F) **B:** 82%
108 (R² = p-CF₃) **B:** 36%
109 (R² = p-CO₂Et) **A:** 50% [a]
110 (R² = m-CO₂Et) **B:** 50% [b]

114
A: 76%, **B:** 67%

117 (R³ = Et) **B:** 75%
118 (R³ = iPr) **B:** 26%

119
B: 26%

111
A: 75%, **B:** 78%

112
A: 60%, **B:** 66%

113
A: 84%, **B:** 82%

115
B: 26%

116
B: 52%

57 (Y = O) **B:** 68%
120 (Y = NTs) **B:** 79%
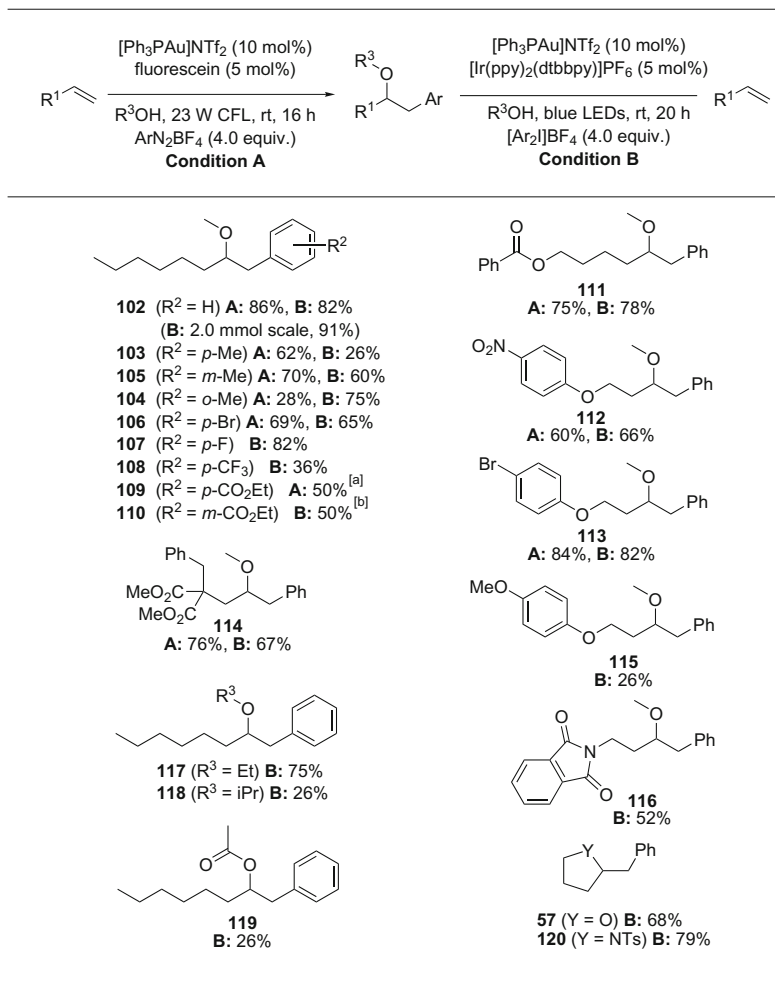
Reaction conditions A Alkene (0.2 mmol), aryldiazonium salt (0.8 mmol), [Ph₃PAu]NTf₂ (10 mol %) and fluorescein (5 mol%) in degassed MeOH (0.1 M) reacted in the presence of visible light from a 23 W CFL for 16 h at rt. Isolated yields

[a]Isolated as a 92:8 mixture with the corresponding methyl ester
Reaction conditions B Alkene (0.2 mmol), diaryliodonium salt (0.8 mmol), [Ph₃PAu]NTf₂ (10 mol%) and [Ir(ppy)₂(dtbbpy)]PF₆ (5 mol%) in degassed MeOH (0.1 M) reacted in the presence of visible light from blue LEDs at rt for 20 h. Isolated yields
[b]Isolated as a 81:19 mixture with the corresponding methyl ester

and isopropanol and even acetic acid were successfully employed in these studies to give access to ether **117–118** and ester **119** compounds, although these nucleophiles were used as solvent. We repeated the intramolecular oxy- and aminoarylation of alkenes **54** and **73** under reaction conditions B using diaryliodonium salts. These reactions delivered the corresponding tetrahydrofuran and pyrrolidine products **57** and **120,** showing that diaryliodonium salts are suitable aryl sources for our previously-developed intramolecular heteroarylations of alkenes. Finally, we repeated the parent reaction with 1-octene, diphenyliodonium tetrafluoroborate (**101**) and methanol on a 2.0 mmol scale, which produced the expected product **102** in 91 % yield. This showed that the reaction efficiency does not drop upon scaling-up the reaction.

In order to investigate the selectivity of aryl transfer from diaryliodonium salts, we employed an unsymmetrical diaryliodonium salt (**121**) having electronically slightly different phenyl and *para*-bromophenyl groups (Scheme 2.16). Interestingly, the electron-deficient *para*-bromophenyl group was transferred in a slight preference over the electron-neutral phenyl group furnishing product **106** and **102** in a ratio of 1.3:1 and in 90 % combined NMR yield.

2.2.4 Mechanistic Studies on Heteroarylations of Alkenes[4]

In order to gain insight into the reaction mechanism, we conducted a literature survey and performed control experiments. The results obtained from control experiments confirmed that all the components (the gold catalyst, photoredox catalyst and visible light) are essential for this process (Table 2.2, entry 27–29). In the absence of one of these three components, either the reaction shut down or the reaction efficiency dropped dramatically.

In order to investigate whether visible light irradiation is required throughout the reaction or only to initiate the process, a light off-on experiment was conducted. In this test, the reaction between 4-penten-1-ol (**54**) and phenyldiazonium tetrafluoroborate (**65**) was performed under the optimized reaction conditions on a 0.2 mmol scale in degassed deuterated methanol (Scheme 2.17). The reaction mixture was subjected to stirring for sequential periods of time under visible light irradiation from a 23 W CFL bulb followed by stirring in the dark. At each time point, an aliquot (200 μL) of the reaction mixture was taken out under argon atmosphere, which was then quenched with D_2O (50 μL) and diluted with a $CDCl_3$ solution (500 μL) containing the internal standard diethyl phthalate. The measured NMR yields of tetrahydrofuran **57** are displayed in Fig. 2.2.

The outcome of this experiment indicated that the reaction proceeds smoothly under visible light irradiation. The reaction shut down when irradiation of the reaction mixture was stopped and the reactivity could be recovered upon switching

---

[4]A part of the mechanistic studies was carried by Dr. Matthew N. Hopkinson (WWU Münster).
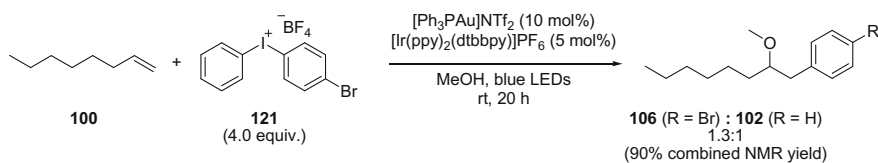
Scheme 2.16 Oxyarylation of 1-octene with an unsymmetrical diaryliodonium salt **121**
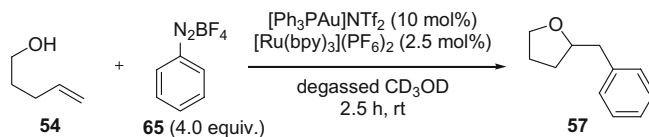
Scheme 2.17 Dual gold and photoredox-catalyzed oxyarylation of 4-penten-1-ol (**54**) with phenyldiazonium salt **65** in deuterated methanol (MeOH-d$_4$)

Time (min)	NMR Yield (%)[a]
0	0
20	40
60	41
90	68
120	68
150	81

[a] Diethyl phthalate used as internal standard
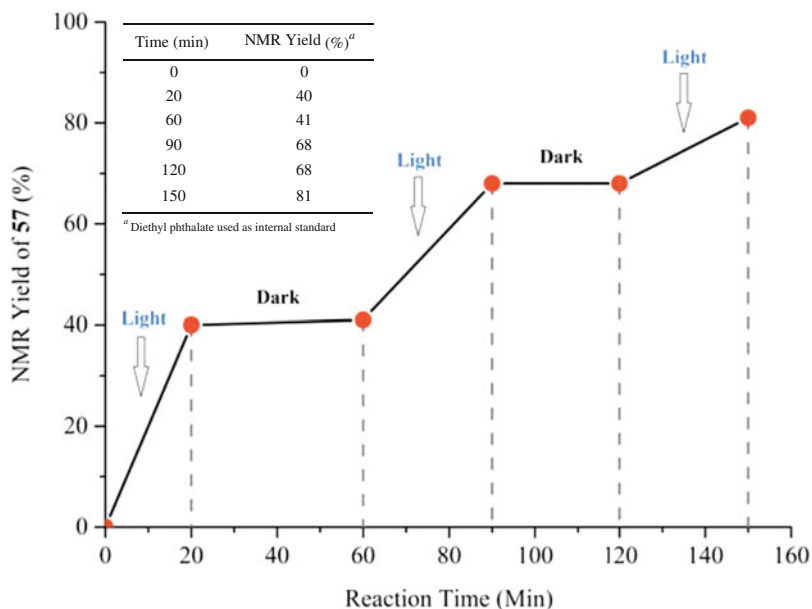
Fig. 2.2 Effect of visible light irradiation on the reaction efficiency

on the light again. This experiment confirmed that continuous visible light irradiation is mandatory for the completion of this process.

The reaction with the activated styrene substrate **70**, which could potentially react with aryl radicals directly in a Meerwein-type arylation process, with aryldiazonium salt **86** under the standard reaction conditions afforded the corresponding
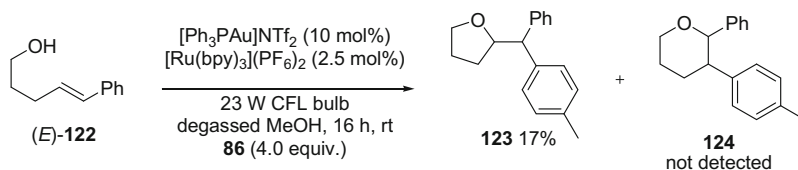
Scheme 2.18 Dual gold and photoredox-catalyzed oxyarylation of styrene-type alkenol *E*-**122** with aryldiazonium salt **86**

product **80** in 63 % yield, whereas only 14 % yield of the product **80** was obtained omitting the gold catalyst (Table 2.3, entry 5). These results suggested that while the Meerwein-type aryl radical addition to this activated alkene is possible, this process is less favorable than the gold-catalyzed process. As shown by a control reaction with 4-penten-1-ol **54** and from previous-studies on aryl radical addition reactions, unactivated alkenes are poor substrates for this type of process, implying that such a radical addition pathway is unlikely to be operating in this dual-catalyzed reaction [84, 91, 118]. In an analogous test, employing another activated styrene **122**, where Meerwein-type addition would preferentially give rise to a 6-membered ring product (**124**), resulted in the exclusive formation of the 5-membered ring oxyarylation product **123** albeit in a low yield of 17 % with no products resulting from Meerwein-type radical addition being detected. In a control reaction without the gold catalyst, no reactivity was observed with this substrate. From the above two results it seemed that the gold-catalyzed process does not involve a Meerwein-type radical addition and even predominates over this pathway with activated alkenes (Scheme 2.18).

Although during the substrate scope study, no protodeauration products [e.g. 2-methyltetrahydrofuran (**125**)] were detected in any of the reaction mixtures, still the possibility remained that products resulting from protodeauration might be formed under these acidic conditions and become arylated in a subsequent step. In that situation we would not be able to detect protodeauration products. In order to rule out this possibility, we treated 2-methyltetrahydrofuran (**125**) with phenyl-diazonium salt **65** under the standard reaction conditions and no formation of the oxyarylated product **57** was observed (Scheme 2.19). The lack of 2-methyltetrahydrofuran or pyrrolidine products observed throughout this study suggests that protodeauration of the alkylgold intermediate formed in this trans-formation is not an efficient process. In a relevant mechanistic study, Toste and co-workers isolated various alkylgold(I) complexes and tested their stability upon treatment with *p*-toluenesulfonic acid and, in analogy to our experminental obser-vations, obtained no protodeauration product [57].

In a study focused on elucidating the stereochemical relationship between the nucleophile and the aryl group in the final products, the deuterium-labelled γ-aminoalkene substrates (D)-(*E*)-**126** and (D)-(*Z*)-**127** were reacted under the standard conditions, delivering the expected pyrrolidine products **128** and **129** with high diastereoselectivities, respectively, with the amino and aryl group being in an
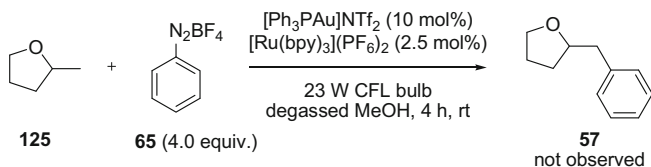
Scheme 2.19 Control experiment of 2-methyltetrahydrofuran **125** with phenyldiazonium salt **65** under the standard reaction conditions
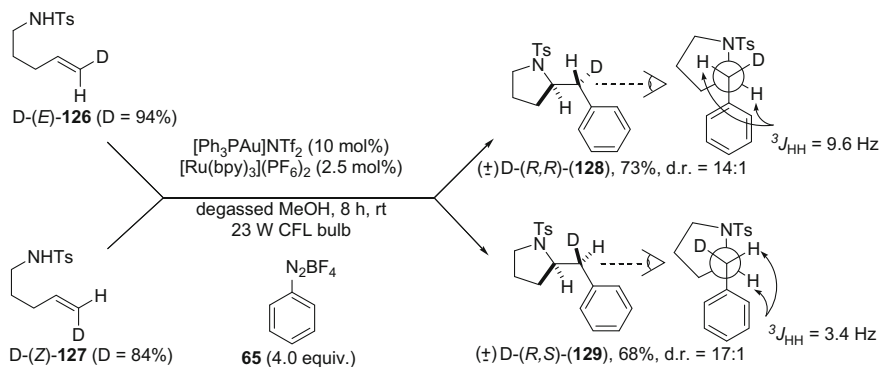
Scheme 2.20 Dual gold and photoredox-catalyzed aminoarylation of deuterated γ-amino-alkenes (**126–127**) with phenyldiazonium salt **65**

anti-relationship in both cases (Scheme 2.20) [54]. This fact was determined by comparing the ^{1}H NMR spectra for these compounds with those reported by Zhang et al. [54] who in turn determined the stereochemistry by an analysis of the differences in the vicinal $^3J_{HH}$ coupling constants resulting from restricted rotation around the formerly olefinic C–C bond. Similar results were also obtained when internal γ-hydroxyalkenes (*E*)-**71** and (*Z*)-**72** were employed in the intramolecular oxyarylation process under the standard conditions, where the expected oxyarylation products (±) (*R,R*)-**81** (59 %) and (±) (*R,S*)-**82** (56 %) were furnished with excellent diastereoselectivities (d.r. > 25:1 in the both cases) respectively (Table 2.3, entry 6–7). The above stereochemical observations imply that the nucleophile and the aryl group add in a *trans*-fashion across the C=C double bond of the alkenes. This stereochemical event can be rationalized by an initial *anti*-aminoauration or oxyauration of the alkenes followed by an arylation event occurring with retention of stereochemistry [e.g. via reductive elimination from gold(III)].

Based on previous literature reports [109, 115] and our mechanistic experiment studies, we hypothesized a reaction mechanism of the type shown in Scheme 2.21. According to the previously reported studies on alkene activation with cationic gold (I), [57] we propose that a cationic gold(I) species derived from Gagosz's catalyst
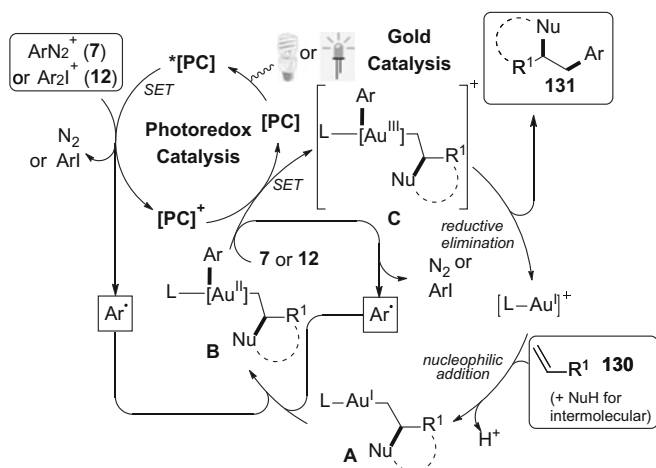
[PC] = photoredox catalyst (i.e. fluorescein, $[Ru(bpy)_3]^{2+}$ or $[Ir(ppy)_2(dtbbpy)]^+$), Nu = O or NTs.

Scheme 2.21 A plausible reaction mechanism for intra- and intermolecular oxyarylation of alkenes with aryldiazonium and diaryliodonium salts

could coordinate to the alkene **130** and activate it towards *anti*-attack of an internal or external hydroxy or amine nucleophile leading to the formation of the alkylgold intermediate **A**. In a parallel photoredox catalytic cycle, single electron reduction of the aryldiazonium salt or diaryliodonium salt with the photo-excited photoredox catalyst (*PC) would release a nucleophilic aryl radical upon extrusion of dinitrogen or an aryl iodide molecule and generate the oxidized photoredox catalyst (PC$^+$). At this stage, the aryl radical could oxidize the alkylgold(I) intermediate **A** to obtain the highly reactive gold(II) intermediate **B** bearing both coupling fragments. Spectroscopic and theoretical studies on the trapping of nucleophilic phenyl radicals by gold(I) species to generate phenylgold(II) intermediates by Corma, Garcia and co-workers strengthened this speculation [119]. In the next step, the unstable gold (II) intermediate **B** is expected to transfer an electron to the oxidized photoredox catalyst (PC$^+$) via SET to regenerate the photoredox catalyst (PC) and deliver the gold(III) intermediate **C**. Alternatively SET could occur with another molecule of the aryldiazonium or diaryliodonium salt in a radical chain process. Fast reductive elimination from gold(III) intermediate **C** at this point would furnish the oxy- or aminoarylation product **131** and regenerate the gold(I) catalyst.

2.3   Summary

In conclusion, we have successfully combined two different catalytic modes, gold catalysis and photoredox catalysis, in a novel dual catalytic system, demonstrating their compatibility. This novel dual catalytic system catalyzes oxyarylation and aminoarylation reactions of non-activated γ-hydroxyalkenes, γ-aminoalkenes and also a δ-hydroxyalkene with aryldiazonium salts to give access to substituted saturated heterocyclic compounds (tetrahydrofurans, pyrrolidines and a tetrahydropyran). In contrast to previous reports on oxidative gold-catalyzed heteroarylations of alkenes [54, 55], internal alkenes could successfully be employed using this system. This method avoids the use of strong external oxidizing agents such as Selectfluor, hypervalent iodine reagent or ^{t}BuOOH, which limit the substrate scope of previously-reported related processes. Moreover, this transformation benefits from milder reaction conditions and the use of readily available visible light sources. This concept can be extended to multicomponent intermolecular oxyarylation of non-activated alkenes, simple alcohols and aryl-diazonium salts using inexpensive fluorescein dye as the photocatalyst in place of expensive transition metal-based photocatalysts such as $[Ru(bpy)_3](PF_6)_2$. The combination of the more oxidizing photocatalyst $[Ir(ppy)_2(dtbbpy)](PF_6)$ and a gold catalyst in the presence of visible light irradiation from blue LEDs enabled diaryliodonium salts, which are readily prepared and air and moisture stable, to be applied in both intra- and intermolecular oxyarylation processes, extending the scope of these reactions. In this later method, acetic acid could also be applied as a nucleophile in addition to various alcohols.

References

1. S.G. Bratsch, J. Phys. Chem. Ref. Data **18**, 1–21 (1989)
2. N. Mézailles, L. Ricard, F. Gagosz, Org. Lett. **7**, 4133–4136 (2005)
3. M.S. Nechaev, V.M. Rayón, G. Frenking, J. Phys. Chem. A **108**, 3134–3142 (2004)
4. A. Fürstner, P.W. Davies, Angew. Chem. Int. Ed. **46**, 3410–3449 (2007)
5. A. Furstner, Chem. Soc. Rev. **38**, 3208–3221 (2009)
6. C.-W. Chan, W.-T. Wong, C.-M. Che, Inorg. Chem. **33**, 1266–1272 (1994)
7. W.-P. To, G.S.-M. Tong, W. Lu, C. Ma, J. Liu, A.L.-F. Chow, C.-M. Che, Angew. Chem. Int. Ed. **51**, 2654–2657 (2012)
8. Q. Xue, J. Xie, H. Jin, Y. Cheng, C. Zhu, Org. Biomol. Chem. **11**, 1606–1609 (2013)
9. M.M. Savas, W.R. Mason, Inorg. Chem. **26**, 301–307 (1987)
10. A. Vogler, H. Kunkely, Coord. Chem. Rev. **219–221**, 489–507 (2001)
11. G. Revol, T. McCallum, M. Morin, F. Gagosz, L. Barriault, Angew. Chem. Int. Ed. **52**, 13342–13345 (2013)
12. M. Tonelli, S. Turrell, O. Cristini-Robbe, H. El Hamzaoui, B. Capoen, M. Bouazaoui, M. Gazzano, M.C. Cassani, RSC Adv. **4**, 26038–26045 (2014)
13. S.J. Kaldas, A. Cannillo, T. McCallum, L. Barriault, Org. Lett. **17**, 2864–2866 (2015)
14. T. McCallum, E. Slavko, M. Morin, L. Barriault, Eur. J. Org. Chem. **2015**, 81–85 (2015)
15. D.J. Gorin, F.D. Toste, Nature **446**, 395–403 (2007)

16. A.S.K. Hashmi, Chem. Rev. **107**, 3180–3211 (2007)
17. D.J. Gorin, B.D. Sherry, F.D. Toste, Chem. Rev. **108**, 3351–3378 (2008)
18. E. Jiménez-Núñez, A.M. Echavarren, Chem. Rev. **108**, 3326–3350 (2008)
19. Z. Li, C. Brouwer, C. He, Chem. Rev. **108**, 3239–3265 (2008)
20. R.A. Widenhoefer, Chem. Eur. J. **14**, 5382–5391 (2008)
21. A.S.K. Hashmi, Angew. Chem. Int. Ed. **49**, 5232–5241 (2010)
22. N.D. Shapiro, F.D. Toste, Synlett **2010**, 675–691 (2010)
23. J.J. Hirner, Y. Shi, S.A. Blum, Acc. Chem. Res. **44**, 603–613 (2011)
24. M.N. Hopkinson, A.D. Gee, V. Gouverneur, Chem. Eur. J. **17**, 8248–8262 (2011)
25. N. Krause, C. Winter, Chem. Rev. **111**, 1994–2009 (2011)
26. M. Rudolph, A.S.K. Hashmi, Chem. Commun. **47**, 6536–6544 (2011)
27. H.A. Wegner, M. Auzias, Angew. Chem. Int. Ed. **50**, 8236–8247 (2011)
28. L.-P. Liu, G.B. Hammond, Chem. Soc. Rev. **41**, 3129–3139 (2012)
29. M. Rudolph, A.S.K. Hashmi, Chem. Soc. Rev. **41**, 2448–2462 (2012)
30. I. Braun, A.M. Asiri, A.S.K. Hashmi, ACS Catal. **3**, 1902–1907 (2013)
31. C. Obradors, A.M. Echavarren, Chem. Commun. **50**, 16–28 (2014)
32. Y.-M. Wang, A.D. Lackner, F.D. Toste, Acc. Chem. Res. **47**, 889–901 (2014)
33. R.O.C. Norman, W.J.E. Parr, C.B. Thomas, J. Chem. Soc. Perkin Trans. **1**, 1983–1987 (1976)
34. J.H. Teles, S. Brode, M. Chabanas, Angew. Chem. Int. Ed. **37**, 1415–1418 (1998)
35. N. Marion, S.P. Nolan, Chem. Soc. Rev. **37**, 1776–1782 (2008)
36. C.-Y. Wu, T. Horibe, C.B. Jacobsen, F.D. Toste, Nature **517**, 449–454 (2015)
37. K.M. Engle, T.-S. Mei, X. Wang, J.-Q. Yu, Angew. Chem. Int. Ed. **50**, 1478–1491 (2011)
38. M. Bandini, Chem. Soc. Rev. **40**, 1358–1367 (2011)
39. S. Sengupta, X. Shi, ChemCatChem **2**, 609–619 (2010)
40. A. Pradal, P.Y. Toullec, V. Michelet, Synthesis **2011**, 1501–1514 (2011)
41. L.-P. Liu, B. Xu, M.S. Mashuta, G.B. Hammond, J. Am. Chem. Soc. **130**, 17642–17643 (2008)
42. L. Ye, L. Zhang, Org. Lett. **11**, 3646–3649 (2009)
43. M.N. Hopkinson, G.T. Giuffredi, A.D. Gee, V. Gouverneur, Synlett **2010**, 2737–2742 (2010)
44. A.E. Allen, D.W.C. MacMillan, Chem. Sci. **3**, 633–658 (2012)
45. Z. Du, Z. Shao, Chem. Soc. Rev. **42**, 1337–1378 (2013)
46. A.S.K. Hashmi, C. Lothschütz, R. Döpp, M. Rudolph, T.D. Ramamurthi, F. Rominger, Angew. Chem. Int. Ed. **48**, 8243–8246 (2009)
47. Y. Shi, S.D. Ramgren, S.A. Blum, Organometallics **28**, 1275–1277 (2009)
48. Y. Shi, K.E. Roth, S.D. Ramgren, S.A. Blum, J. Am. Chem. Soc. **131**, 18022–18023 (2009)
49. J.J. Hirner, S.A. Blum, Organometallics **30**, 1299–1302 (2011)
50. A.S.K. Hashmi, M.C. Blanco, D. Fischer, J.W. Bats, Eur. J. Org. Chem. **2006**, 1387–1389 (2006)
51. H.A. Wegner, S. Ahles, M. Neuburger, Chem. Eur. J. **14**, 11310–11313 (2008)
52. L. Cui, G. Zhang, L. Zhang, Bioorg. Med. Chem. Lett. **19**, 3884–3887 (2009)
53. G. Zhang, Y. Peng, L. Cui, L. Zhang, Angew. Chem. Int. Ed. **48**, 3112–3115 (2009)
54. G. Zhang, L. Cui, Y. Wang, L. Zhang, J. Am. Chem. Soc. **132**, 1474–1475 (2010)
55. W.E. Brenzovich, D. Benitez, A.D. Lackner, H.P. Shunatona, E. Tkatchouk, W.A. Goddard, F.D. Toste, Angew. Chem. Int. Ed. **49**, 5519–5522 (2010)
56. E. Tkatchouk, N.P. Mankad, D. Benitez, W.A. Goddard, F.D. Toste, J. Am. Chem. Soc. **133**, 14293–14300 (2011)
57. R.L. LaLonde, J.W.E. Brenzovich, D. Benitez, E. Tkatchouk, K. Kelley, I.I.I.W.A. Goddard, F.D. Toste, Chem. Sci. **1**, 226–233 (2010)
58. A.D. Melhado, W.E. Brenzovich, A.D. Lackner, F.D. Toste, J. Am. Chem. Soc. **132**, 8885–8887 (2010)
59. L.T. Ball, M. Green, G.C. Lloyd-Jones, C.A. Russell, Org. Lett. **12**, 4724–4727 (2010)
60. W.E. Brenzovich, J.-F. Brazeau, F.D. Toste, Org. Lett. **12**, 4728–4731 (2010)

61. M.N. Hopkinson, A. Tessier, A. Salisbury, G.T. Giuffredi, L.E. Combettes, A.D. Gee, V. Gouverneur, Chem. Eur. J. **16**, 4739–4743 (2010)
62. T. de Haro, C. Nevado, Angew. Chem. Int. Ed. **50**, 906–910 (2011)
63. H. Zollinger, Acc. Chem. Res. **6**, 335–341 (1973)
64. A. Roglans, A. Pla-Quintana, M. Moreno-Mañas, Chem. Rev. **106**, 4622–4643 (2006)
65. S. Mahouche-Chergui, S. Gam-Derouich, C. Mangeney, M.M. Chehimi, Chem. Soc. Rev. **40**, 4143–4166 (2011)
66. C. Galli, Chem. Rev. **88**, 765–792 (1988)
67. D.P. Hari, B. König, Angew. Chem. Int. Ed. **52**, 4734–4743 (2013)
68. P. Hanson, J.R. Jones, A.B. Taylor, P.H. Walton, A.W. Timms, J. Chem. Soc. Perkin Trans. **2**, 1135–1150 (2002)
69. M.P. Doyle, W.J. Bryker, J. Org. Chem. **44**, 1572–1574 (1979)
70. M. Barbero, M. Crisma, I. Degani, R. Fochi, P. Perracino, Synthesis **1998**, 1171–1175 (1998)
71. F. Mo, G. Dong, Y. Zhang, J. Wang, Org. Biomol. Chem. **11**, 1582–1593 (2013)
72. F.P. Crisóstomo, T. Martín, R. Carrillo, Angew. Chem. Int. Ed. **53**, 2181–2185 (2014)
73. M. Hartmann, A. Studer, Angew. Chem. Int. Ed. **53**, 8180–8183 (2014)
74. M. Hartmann, C.G. Daniliuc, A. Studer, Chem. Commun. **51**, 3121–3123 (2015)
75. T. Sandmeyer, Ber. Dtsch. Chem. Ges. **17**, 1633 (1884)
76. T. Sandmeyer, Ber. Dtsch. Chem. Ges. **17**, 2650 (1884)
77. H.H. Hodgson, Chem. Rev. **40**, 251–277 (1947)
78. R. Pschorr, Ber. Dtsch. Chem. Ges. **29**, 496 (1896)
79. M. Gomberg, W.E. Bachmann, J. Am. Chem. Soc. **46**, 2339–2343 (1924)
80. O.C. Dermer, M.T. Edmison, Chem. Rev. **57**, 77–122 (1957)
81. A. Wetzel, G. Pratsch, R. Kolb, M.R. Heinrich, Chem. Eur. J. **16**, 2547–2556 (2010)
82. H. Meerwein, E. Buchner, K. v. Emsterk. J. Prakt. Chem. **152**, 237 (1939)
83. G.Pratsch, M. Heinrich, in *Radicals in Synthesis III*, ed. by M. Heinrich, A. Gansäuer, Vol. 320. (Springer, Berlin, 2012), pp. 33–59
84. M.R. Heinrich, Chem. Eur. J. **15**, 820–833 (2009)
85. H. Brunner, C. Blüchel, M.P. Doyle, J. Organomet. Chem. **541**, 89–95 (1997)
86. P. Mastrorilli, C.F. Nobile, N. Taccardi, Tetrahedron Lett. **47**, 4759–4762 (2006)
87. C. Galli, J. Chem. Soc. Perkin Trans. **2**, 1459–1461 (1981)
88. A.L.J. Beckwith, R.O.C. Norman, J. Chem. Soc. B, 403–412 (1969)
89. A. Citterio, F. Minisci, A. Albinati, S. Bruckner, Tetrahedron Lett. **21**, 2909–2910 (1980)
90. R. Cannella, A. Clerici, N. Pastori, E. Regolini, O. Porta, Org. Lett. **7**, 645–648 (2005)
91. M. Hartmann, Y. Li, A. Studer, J. Am. Chem. Soc. **134**, 16516–16519 (2012)
92. J. Xuan, W.-J. Xiao, Angew. Chem. Int. Ed. **51**, 6828–6838 (2012)
93. C.K. Prier, D.A. Rankic, D.W.C. MacMillan, Chem. Rev. **113**, 5322–5363 (2013)
94. D.P. Hari, B. Konig, Chem. Commun. **50**, 6688–6699 (2014)
95. C. Hartmann, V. Meyer, Ber. Dtsch. Chem. Ges. **27**, 426 (1894)
96. E.A. Merritt, B. Olofsson, Angew. Chem. Int. Ed. **48**, 9052–9070 (2009)
97. M.S. Yusubov, A.V. Maskaev, V.V. Zhdankin, ARKIVOC **1**, 370–409 (2011)
98. Y. Toba, J. Photopolym. Sci. Technol. **16**, 115–118 (2003)
99. J.V. Crivello, J. Polym. Sci. Part A Polym. Chem. **47**, 866–875 (2009)
100. M.S. Yusubov, D.Y. Svitich, M.S. Larkina, V.V. Zhdankin, ARKIVOC **1**, 364–395 (2013)
101. K.M. Lancer, G.H. Wiegand, J. Org. Chem. **41**, 3360–3364 (1976)
102. T. Okuyama, T. Takino, T. Sueda, M. Ochiai, J. Am. Chem. Soc. **117**, 3360–3367 (1995)
103. F.M. Beringer, M. Drexler, E.M. Gindler, C.C. Lumpkin, J. Am. Chem. Soc. **75**, 2705–2708 (1953)
104. F.M. Beringer, R.A. Falk, M. Karniol, I. Lillien, G. Masullo, M. Mausner, E. Sommer, J. Am. Chem. Soc. **81**, 342–351 (1959)
105. G.F. Koser, R.H. Wettach, C.S. Smith, J. Org. Chem. **45**, 1543–1544 (1980)
106. C.S. Carman, G.F. Koser, J. Org. Chem. **48**, 2534–2539 (1983)
107. M. Bielawski, M. Zhu, B. Olofsson, Adv. Synth. Catal. **349**, 2610–2618 (2007)

108. M. Bielawski, D. Aili, B. Olofsson, J. Org. Chem. **73**, 4602–4607 (2008)
109. S.R. Neufeldt, M.S. Sanford, Adv. Synth. Catal. **354**, 3517–3522 (2012)
110. G. Fumagalli, S. Boyd, M.F. Greaney, Org. Lett. **15**, 4398–4401 (2013)
111. H. Cano-Yelo, A. Deronzier, J. Chem. Soc. Perkin Trans. **2**, 1093–1098 (1984)
112. R.M. Elofson, F.F. Gadallah, J. Org. Chem. **36**, 1769–1771 (1971)
113. A.N. Nesmeyanov, L.G. Makarova, T.P. Tolstaya, Tetrahedron **1**, 145–157 (1957)
114. B. Maggio, D. Raffa, M.V. Raimondi, S. Cascioferro, S. Plescia, M.A. Sabatino, G. Bombieri, F. Meneghetti, G. Daidone, ARKIVOC **16**, 130–143 (2008)
115. D. Kalyani, K.B. McMurtrey, S.R. Neufeldt, M.S. Sanford, J. Am. Chem. Soc. **133**, 18566–18569 (2011)
116. T. Taniguchi, H. Zaimoku, H. Ishibashi, Chem. Eur. J. **17**, 4307–4312 (2011)
117. Y. Su, X. Sun, G. Wu, N. Jiao, Angew. Chem. Int. Ed. **52**, 9808–9812 (2013)
118. M.R. Heinrich, A. Wetzel, M. Kirschstein, Org. Lett. **9**, 3833–3835 (2007)
119. C. Aprile, M. Boronat, B. Ferrer, A. Corma, H. García, J. Am. Chem. Soc. **128**, 8388–8389 (2006)

Chapter 3
Visible Light Photoredox Catalyzed Trifluoromethylation-Ring Expansion via Semipinacol Rearrangement

3.1 Introduction

3.1.1 General Features of Fluorinated Compounds

Fluorine, with ground state electronic configuration $[He]2s^2 2p^5$, is the first member of the halogen series (Group 9) in the periodic table. It also has the second smallest atomic radius after hydrogen (r_w = 1.47 and 1.20 Å, respectively) and it is the most electronegative element in the periodic table; electronically, fluorine is more similar to its neighbor oxygen (Pauling scale: χ(F): 4.0 and χ(O): 3.5) than other halogens [1, 2]. The C–F bond (d = 1.35 Å) is 1.24 times longer than the C–H bond (d = 1.09 Å), yet the C–F bond (C–F bond: 105.4 kcal/mol) is stronger than the C–H bond (C–H bond: 98.8 kcal/mol) [2]. A trifluoromethyl (CF_3) group is constituted when three fluorine atoms and one carbon atom are assembled forming three $C(sp^3)$-F bonds. From structural point of view, although a trifluoromethyl (CF_3) group is usually compared to a methyl (CH_3) group, its size resembles an isopropyl group ($CH(CH_3)_2$). Due to the high electronegativity of fluorine, electronically, the trifluoromethyl (CF_3) group is highly electron-withdrawing and exerts a significant impact on pKa values, thus influencing the acidity or basicity of the functional groups neighbor to it.

3.1.2 Importances of Fluorinated Compounds

Fluorine was long thought to be an abiotic element limiting its application to military and some special material demands. Moreover, only a handful of organo-fluorine compounds, not more than a dozen, exist in nature. However, ∼20 % of all drugs and ∼30 % of all agrochemicals in markets contain fluorinated compounds [3–8]. A selection of fluorine containing drugs and agrochemicals, with their respective

activities, is shown in Fig. 3.1 [3, 5, 8, 9]. The unique physicochemical properties of fluorinated compounds have captured the attention of scientists in different fields of research such as medicinal, agrochemical, polymer and material [3–5, 7–11]. Due to the high bond energy, the installment of fluorine or trifluoromethyl groups in drug molecules reduces the susceptibility of oxidizing functionality to cytochrome P450 enzyme, thereby increasing metabolic stability [4]. The high lipophilicity of fluori-nated drugs increases its membrane permeability. The bioavailability and high lipophilicity of fluorinated agrochemicals increase their in vivo uptake and facilitate transportation [3, 5]. For these reasons, research in fluorine chemistry helps to design drugs and improve the therapeutic efficacy and pharmacological properties of bio-molecules [5, 8]. In addition, Teflon, a perfluorinated polymer, is used as a non-stick coating in the production of cooking utensils due to its low friction coefficient [7]. Moreover, fluorinated solvents are used in catalyst recovery and purification forming an immiscible 'fluorous phase' when these solvents are mixed with water or organic solvents [12].
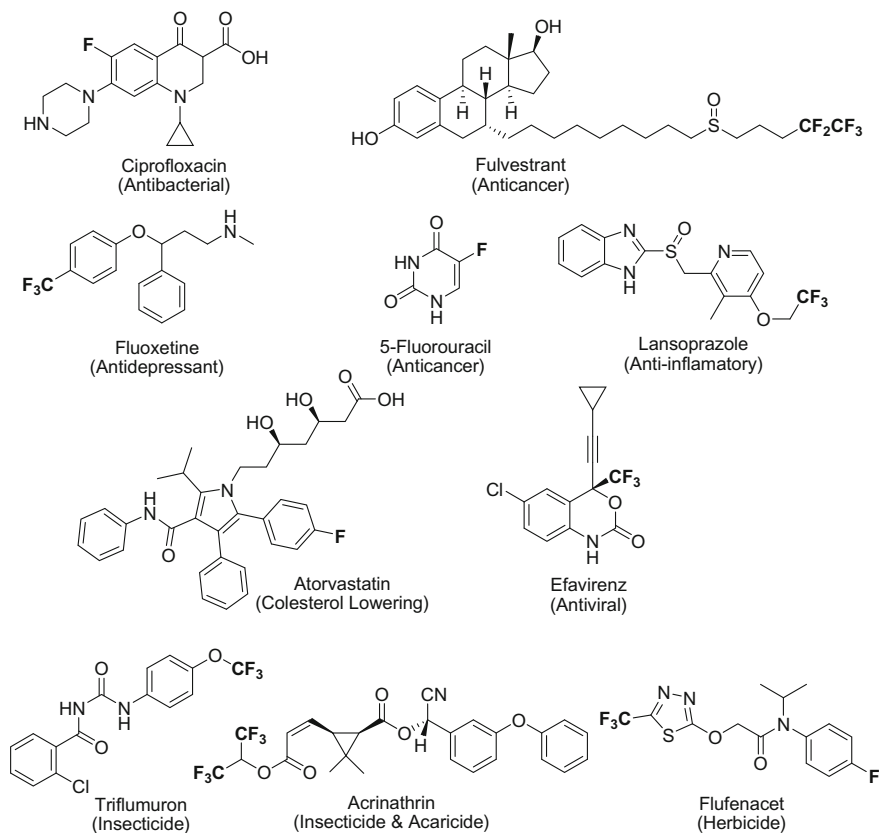
Fig. 3.1 Selected fluorine containing drugs and agrochemicals

3.1.3 Radical-Polar Crossover Process

'Radical-polar crossover', a term first introduced by John Murphy in 1993 [13], is an interesting concept applied in synthetic organic chemistry [14, 15]. In this process, a radical and a polar mechanisms are involved in the same reaction pot [14]. In this type of reactions, reactive intermediates involved in the radical process remain inert during the ionic process and vice versa, therefore maintaining the orthogonality of radical and polar steps [14]. One of the earlier reports on this process is the tetrathiafulvalene (TTF) catalyzed cyclization-nucleophilic addition reaction of aryldiazonium salts (**132**) to obtain dihydrobenzofuran derivatives (**133**), reported by John Murphy and co-workers in 1993 (Scheme 3.1) [13]. In this process, an electron transfer from TTF to an aryldiazonium salt (**132**) via SET results in an aryl radical (**134**) and a radical-cation TTF$^{+\cdot}$. The aryl radical (**134**) then adds onto the pendent alkene, in a *5-exo-trig* fashion, leading to a secondary alkyl radical **135**. The radical **135** undergoes a radical-radical recombination with the radical-cation TTF$^{+\cdot}$ involving a radical-polar crossover event and affording the sulphonium intermediate **136** at the radical-polar step. The nucleophilic substitution reaction with water present in moist acetone affords the product **133**.

In multicomponent radical-polar crossover reactions, a metal species is generally used to selectively oxidize or reduce one of the radicals, thus turning a radical intermediate into ionic one [15].

3.1.4 Trifluoromethylation of Alkenes

Due to the high demand of fluorinated and trifluoromethyl substituted drugs, agrochemicals and materials in the market, the development of environmental friendly, cost effective, operationally simple and highly efficient methods for
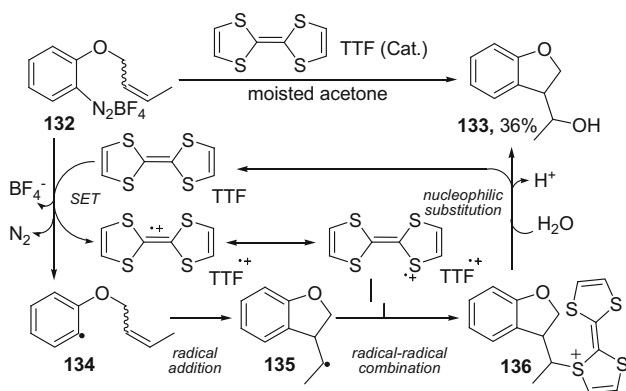
Scheme 3.1 Radical-polar crossover reaction and mechanism [13]

trifluoromethyl group incorporation in simple and complex molecular architectures has become highly interesting to the chemists and biologists across a wide range of fields in academia and industry [7, 16–22].

3.1.4.1 Trifluoromethylating Reagents

In 1984, Ruppert et al. [23] reported for the first time the synthesis of a nucleophilic CF_3 reagent, (Me_3SiCF_3) which was later simplified by Prakash et al. [24]. In the same year, Yagupolskii et al. [25] reported the synthesis of an electrophilic CF_3 reagent, diaryl(trifluoromethyl)sulphonium salt **137** (Fig. 3.2). Since then, various groups of scientists around the world have devoted their attention to the development of air and moisture stable, easily accessible and efficient trifluoromethylating reagents, either electrophilic [21, 22, 26] or nucleophilic [27–29] in nature. According to the electronic nature of in situ released CF_3 group in the reaction, trifluoromethylating reagents can be classified into three different categories: (a) Nucleophilic (CF_3^-) (b) Electrophilic (CF_3^+) and (c) Radical ($CF_3^\cdot$) [30]. A list of nucleophilic, radical and electrophilic CF_3 sources is outlined in Fig. 3.2. Most of these reagents are commercially available. Some of the nucleophilic and most of electrophilic reagents could also be used in radical trifluoromethylation processes.
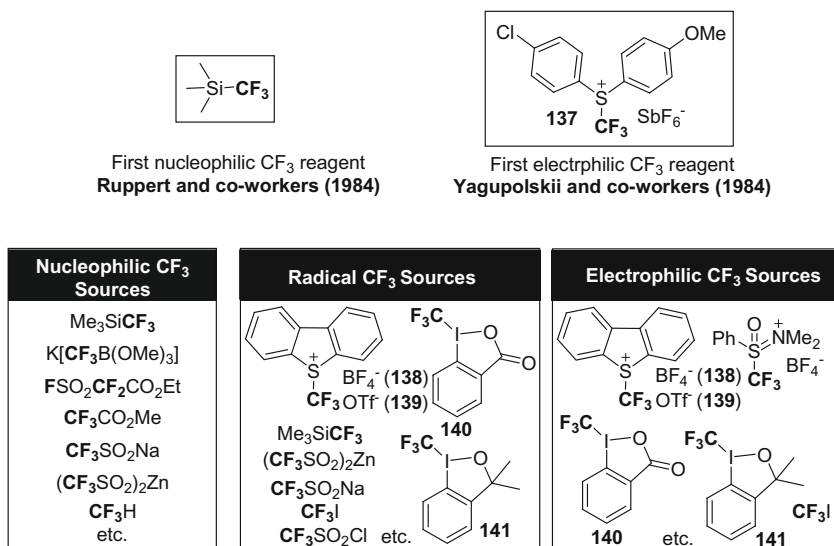
Fig. 3.2 Selected trifluoromethylating reagents

3.1.4.2 Classifications of Trifluoromethylated Compounds and Trifluoromethylation

In most of the trifluoromethylated compounds, the CF_3 functionality is attached to a carbon atom either directly with a $C–CF_3$ bond or via hetero atom tethers (O, S, Se, etc.), e.g. $C–O–CF_3$, $C–S–CF_3$, $C–Se–CF_3$, etc. Based on the hybridization states of the carbon atom attached to the CF_3 group, trifluoromethylated compounds can be classified into three different categories: (a) alkynyl compounds containing $C(sp)–CF_3$ bonds, (b) vinyl or aryl compounds possessing $C(sp^2)–CF_3$ bonds, and (c) aliphatic compounds having $C(sp^3)–CF_3$ bonds. For the synthesis of vinylic compounds containing $C(sp^2)–CF_3$ and aliphatic compounds possessing $C(sp^3)–CF_3$, readily available alkene motifs could be used in a direct functionalization process with trifluoromethylating reagents [18, 20, 31]. In contrast to electrophilic and nucleophilic trifluoromethylation of alkenes, transition metal catalyzed/mediated or transition metal free trifluoromethylation of alkenes via radical or radical-polar crossover processes have been explored in large extent to enrich the library of trifluoromethylated compounds [17, 18, 32]. For the trifluoromethylation of alkenes, copper(I) salts, with or without ligand, have become the most efficient and widely used catalysts [18]. However, this process can also be efficiently catalyzed by other transition metals, such as iron(II) [33, 34] and silver salts [35], $Ru(PPh_3)_2Cl_2$ [36] and other metal precursors in some cases. There has also been a significant development of transition metal free approaches for this purpose [37–41].

3.1.4.3 Visible Light Photoredox-Catalyzed Trifluoromethylations via Radical-Polar Crossover

With the rapid progress of visible light photocatalysis in organic synthesis over the last few years, many impressive trifluoromethylation processes have been developed. Polypyridyl transition metal complexes, enabling single-electron transfer (SET) under visible light irradiation from commercially available and cheap light sources, have been used to catalyze a wide range of trifluoromethylation processes in an operationally simple and efficient manner [18, 42]. Electrophilic trifluoromethylating reagents are the most often used CF_3 source in the trifluoromethylation of alkenes. However, nucleophilic trifluoromethylating agents are also competent for this reaction. In general, a photoredox catalyst acts as a single electron transferring agent [43]. In a single electron reduction process of an electrophilic trifluoromethylating reagent (e.g. Umimoto's and Togni's reagents, CF_3SO_2Cl and CF_3I) with a photo-excited polypyridyl transition metal complex ($[Ru(bpy)_3](PF_6)_2$, $Ir(ppy)_3$ etc.) (*oxidative quenching*), an electrophilic CF_3 radical is generated in situ. This CF_3 radical will participate in a radical addition to an alkene generating a reactive alkyl radical intermediate (Scheme 3.2) [44]. This alkyl radical species can then engage in various radical processes, such as atom-transfer radical addition, hydrogen atom abstraction, or radical-polar crossover processes,
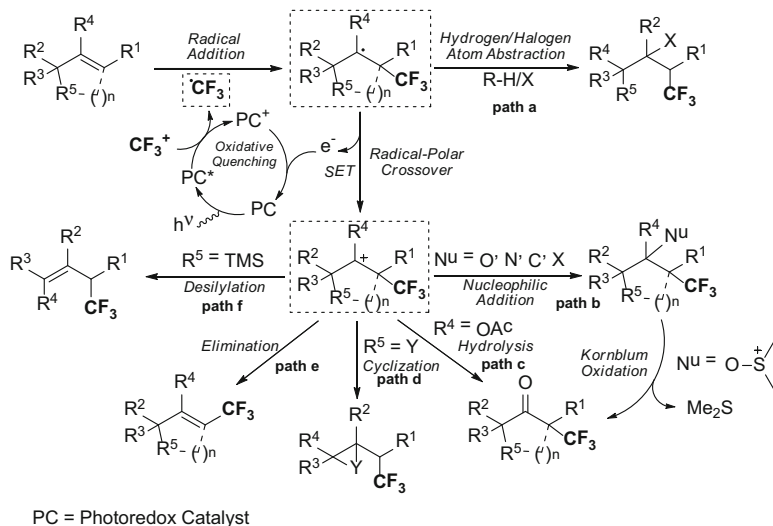
Scheme 3.2 Visible light photoredox catalyzed trifluoromethylation of alkenes via radical and radical-polar crossover process

involving ionic intermediates (carbocation) and further functionalization like intra- and intermolecular nucleophilic trapping, elimination (Scheme 3.2).

In 2011, Stephenson and co-workers described the visible light induced photoredox catalyzed atom transfer radical addition (ATRA) of CF_3I across C=C bond of non-activated alkenes in the presence of the photocatalyst $[Ir(dF(CF_3)ppy)_2(dtbbpy)](PF_6)$ (1 mol%) (Scheme 3.3a) [45]. According to the authors' proposal, this reaction is believed to proceed via a similar mechanism to pathways (a) or (b) in Scheme 3.2. Later, Stephenson and co-workers reported the same reaction with a different set of conditions under a reductive quenching pathway [46]. In 2013, Gouverneur and co-workers reported a methodology for the hydrotrifluoromethylation of non-activated alkenes in the presence of $[Ru(bpy)_3]Cl_2 \cdot 6H_2O$ (5 mol%), 5-(trifluoromethyl)dibenzothiophenium trifluoromethanesulfonate (Umemoto's reagent, **139**) and methanol as hydrogen atom source (Scheme 3.3b) [47]. The authors believed that this reaction proceeds via a mechanistic route similar to pathway (a) in Scheme 3.2.

In the meantime in 2012, Koike, Akita and co-workers described the oxytrifluoromethylation of activated alkenes using Umemoto's reagent **138** and oxygen nucleophiles, such as alcohols, acids and even water, in the presence of a highly reducing photoredox catalyst, *fac*-Ir(ppy)$_3$ (1 mol%), under visible light irradiation from blue LEDs (Scheme 3.4a) [44, 48]. This reaction occurs involving a key step, a radical-polar crossover followed by nucleophilic trapping as shown in Scheme 3.2 (pathway b). This concept of radical-polar crossover and nucleophilic trapping has been extended to nitrogen [49], carbon [50] and halogen [45, 51] based nucleophiles recently by same group, Masson and co-workers and Han and

(a) **Stephenson and co-workers (2011)**

(b) **Gouverneur and co-workers (2013)**
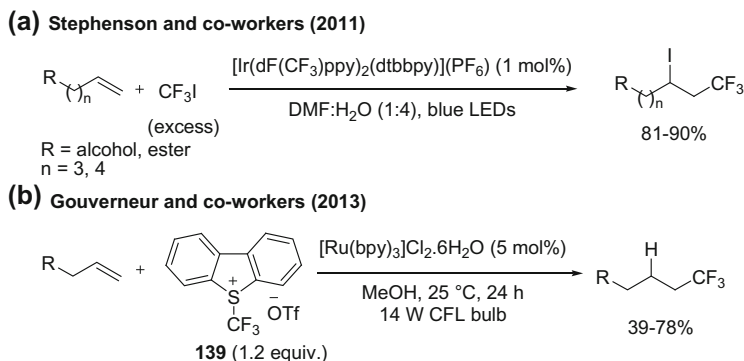
Scheme 3.3 Visible light photoredox catalyzed difunctionalizations of alkenes: **a** iodotrifluoromethylation of alkenes; **b** hydrotrifluoromethylation of alkenes [45, 47]

co-workers respectively. In 2014, Koike, Akita and co-workers merged this novel reactivity with Kornblum oxidation, employing DMSO as nucleophile, to obtain α-trifluoromethylated aryl ketone upon dimethylsulfide elimination (Scheme 3.4b) [52]. The same α-trifluoromethylated aryl ketone could be accessed from vinyl acetates in the presence of a different CF_3-source, CF_3SO_2Cl, and photoredox catalyst $[Ir(ppy)_2(dtbbpy)](PF_6)$ following a mechanism similar to pathway (c) depicted in Scheme 3.2 (Scheme 3.4c) [53]. In continuation of this progress, Cho and co-workers developed in 2013 a methodology for the preparation of trifluoromethylated epoxides and aziridines employing allylic alcohols and amines. The reaction conditions were: $[Ru(bpy)_3]Cl_2$ (0.5 mol%), DBU (2.0 equiv., for epoxide) or TMEDA (2.0 equiv., for aziridine), and CF_3I (3.0 equiv.) with visible light irradiation from a 14 W CFL bulb (Scheme 3.4d). This reactions followed a mechanistic route similar to the intramolecular nucleophilic trapping illustrated in Scheme 3.2 (path d) [54].

Later in 2014, Qing and co-workers developed an elegant method for the regioselective synthesis of β-trifluoromethylstyrenes, where the regioselectivity was controlled by a combination of the photoredox catalyst, an electrophilic trifluoromethylating reagent and the solvent (Scheme 3.5a) [55]. The photoredox catalyst *fac*-$[Ir(ppy)_3]$ and Umemoto's reagent **138** in DMA delivered β-trifluoromethylstyrenes in moderate to good yields and *Z:E* ratios, while $[Ru(bpy)_3]$ $Cl_2 \cdot 6H_2O$ and Togni's reagent **141** in DMF afforded (*E*)-β-trifluoromethylstyrenes as sole products in moderate to good yields (Scheme 3.5a). The latter protocol occurs via a conventional SET-elimination pathway, as depicted in Scheme 3.2 (pathway e), whereas in the former, the SET-elimination pathway is accompanied by an additional triplet-triplet energy transfer (TTET), thus leading to the isomerization of the alkene double bond.

(a) Koike, Akita and co-workers (2012)

R^1, R^2 = H, alkyl, aryl
R^3 = alkyl, aryl

138 (1.1 equiv.)

fac-[Ir(ppy)$_3$] (1 mol%)

CH$_2$Cl$_2$:R^{4}OH (9:1)
or acetone:H$_2$O (9:1)
3 W blue LEDs (425 nm)

R^4 = alkyl, acyl

41-96%

(b) Koike, Akita and co-workers (2014)

R^1, R^2 = H, alkyl, aryl
R^3 = H, alkyl

140 (1.2 equiv.)

fac-[Ir(ppy)$_3$] (2 mol%)

DMSO, rt, 2 h,
3 W blue LEDs (425 nm)

28-87%

(c) Zhang, Yu and co-workers (2013)

R^1 = H, alkyl, aryl
R^2 = H, alkyl

CF$_3$SO$_2$Cl

(2.5 equiv.)

[Ir(ppy)$_2$(dtbbpy)](PF$_6$) (1 mol%)

CH$_3$CN, rt, 5-24 h,
13 W White LEDs

63-93%

(d) Cho and co-workers (2013)

+ CF$_3$I

(3.0 equiv.)

[Ru(bpy)$_3$]Cl$_2$ (0.5 mol%)
DBU (2.0 equiv.) or TMEDA (2.0 equiv.)

CH$_3$CN, rt,
14 W CFL bulb

R^1 = alkyl, aryl; 80-91%

R^2 = alkyl; 60-65%

Scheme 3.4 Visible light photoredox catalyzed difunctionalizations of alkenes: **a** oxy-trifluoromethylation of activated alkene; **b** trifluoromethylation-Kornblum oxidation of alkene; **c** trifluoromethylation of vinylacetate; **d** trifluoromethylation-cyclization of allylic alcohols and amines [44, 52–54]

In 2014, Gouverneur and co-workers reported a novel methodology for the allylic trifluoromethylation of allylsilanes under two different sets of reaction conditions (Scheme 3.5b) [56]. They were able to obtain enantioenriched products starting from enantiopure allylsilanes following a chiral pool strategy. The authors proposed that this reaction proceeds via desilylation of the starting material, rather than deprotonation, in a similar way to the mechanism shown in Scheme 3.2 (pathway f).

In addition to the reports here discussed, many other impressive visible light mediated photoredox catalyzed trifluoromethylation of alkenes, which are out of the scope of our discussion, have been developed during the last five years [57–59].

(a) Qing and co-workers (2014)

138 (1.1 equiv.)

[Ir(ppy)$_3$] (3 mol%)

DMA, rt, 10 h, blue LED
55–86% (Z:E = 3.6:1 to10:1)

[Ru(bpy)$_3$]Cl$_2$.6H$_2$O (2 mol%)

DMF, rt, 20 h, blue LEDs
50–78%, *E-selective*

141 (1.2 equiv.)

(b) Gouverneur and co-workers (2014)

139 (1.8 equiv.)

[Ru(bpy)$_3$]Cl$_2$.6H$_2$O (5 mol%)
EtOH, rt, 24 h, 14 W CFL bulb

R^1 = H, alkyl, R^2 = H, alkyl, 22–76%
E/Z: 3.3 to >20
Condition A

[Ru(bpy)$_3$]Cl$_2$.6H$_2$O (5 mol%)
MeOH, rt, 24 h, 14 W CFL bulb

R^1 = H, alkyl, R^2 = H, alkyl, 41–83%
E/Z: 1.6 to >20
R^1 = alkyl, R^2 = aryl, e.r.(E) >99:1
41–59%, *E/Z*: 3.2 to 7.2
e.r.(E) 85:15 to 88:12
Condition B

140 (1.8 equiv.)
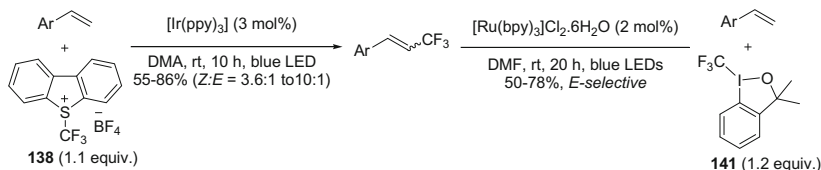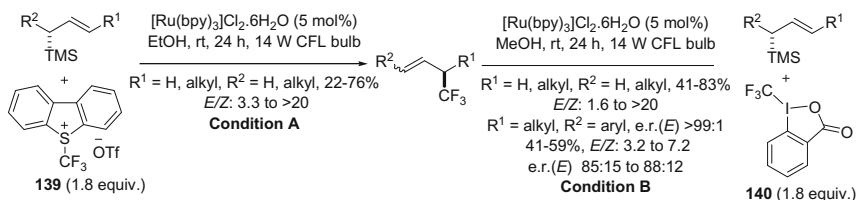
Scheme 3.5 Visible light photoredox catalyzed difunctionalizations of alkenes: **a** vinylic trifluoromethylation of alkenes; **b** allylic trifluoromethylation of alkenes [55, 56]

3.1.5 Semipinacol Rearrangements

The semipinacol rearrangement is a long known chemical process in organic chemistry which helps to address synthetic challenges, such as the construction of quaternary carbon centers with subsequent formation of a carbonyl functional group [60–62]. This rearrangement benefits from a broad substrate scope, as there are many known methodologies to generate a carbocation adjacent to a carbinol carbon. In addition, it is compatible with various reaction conditions (acidic, basic and even neutral), has high regioselectivity and it is also stereospecific nature in some cases. In contrast, pinacol rearrangement of diols suffer from serious regio- and stereo-electivity issues [61]. Organic chemists have often appreciated the potential of the semipinacol rearrangement in organic synthesis. This process has resulted in wide applications in natural product synthesis to introduce structural complexity in molecular architectures [61, 63]. This process involves the generation of a carbo-cation adjacent to a carbinol carbon and a subsequent 1,2-alkyl/aryl carbon shift with simultaneous formation of a C–O π-bond (Scheme 3.6). Allylic alcohols could successfully be applied in this transformation as the addition of an electrophile to

Scheme 3.6 General mechanistic hypothesis of electrophile induced semipinacol rearrangement of allylic alcohols
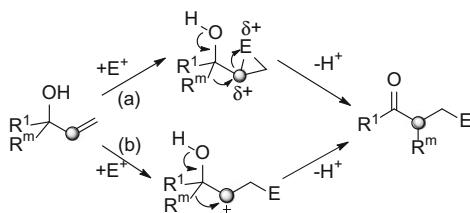
the C=C bond could give access to an electrophilic center vicinal to the carbon atom attached to the hydroxyl group.

Recently, Alexakis and co-workers reported an enantioselective semipinacol rearrangement with a ring expansion of a cycloalkanol in the presence of F^+, from selectfluor, as electrophile and enantiopure BINOL-phosphoric acid for chirality induction (Scheme 3.7a) [64]. According to the authors' proposal, the reaction proceeds via a mechanism similar to pathway (a) shown in Scheme 3.6, where the phosphate anion forms a tight chiral ion-pair. This methodology has been extended to bromination (Br^+) [65] and iodination (I^+) [66] by Alexakis and co-workers, and chlorination (Cl^+) by Yin and You [67].

In 2003, Tu and co-workers disclosed an elegant process of halogenation (chlorination, bromination and iodination) followed by 1,2-alkyl or aryl migration of a different class of allylic alcohols with stoichiometric mixture of Chloramine T and zinc halides (Scheme 3.7b) [68]. Later, they expanded the scope to an asymmetric protonation-1,2-alkyl shift catalyzed by a chiral phosphoric acid [69] and also asymmetric fluorination-semipinacol rearrangement catalyzed by chiral quinine
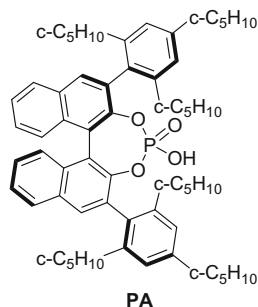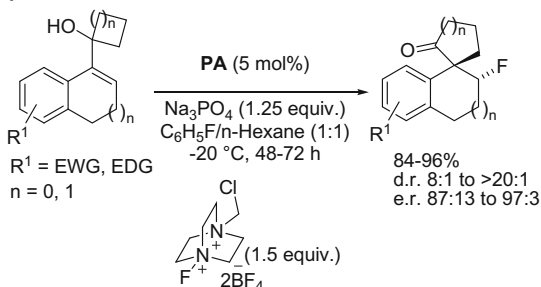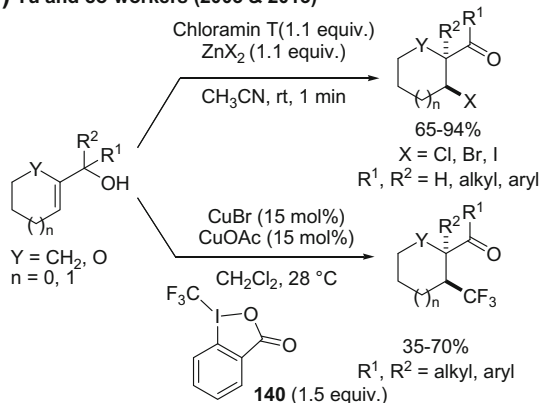
Scheme 3.7 Electrophile induced semipinacol rearrangements of allylic alcohols: **a** Asymmetric fluorination-ring expansion; **b** halogenation or trifluoromethylation followed by 1,2-alkyl/aryl migration [64, 68, 71]

[70]. Recently, they have also described a copper catalyzed trifluoromethylation-semipinacol rearrangement, of the same class of allylic alcohols used in their previous studies, with Togni's reagent **140** as trifluoromethyl (CF_3) source where the migration step could proceed via either radical or cationic reaction pathways (Scheme 3.7b) [71].

3.2   Results and Discussion

3.2.1   *Inspiration*

We have already described earlier in this chapter the term 'radical-polar crossover', which is one of the key steps involved in the visible light photoredox catalysis to access carbocation intermediate (Scheme 3.2). Although many impressive transformations based on this process, including trifluoromethylation reactions, have been reported, these transformations are mostly limited to nucleophilic trapping or elimination reactions. Therefore, there is still enough scope for further development of new reaction pathways, which are characteristic of carbocations. As mentioned earlier in the chapter, the key steps in the semipinacol rearrangement are the formation of a carbocation vicinal to a carbinol carbon, and concomitant or subsequent 1,2-alkyl/aryl migration with a simultaneous C–O π-bond formation. Therefore, we were interested in exploiting the carbocation formation and further develop the semipinacol rearrangement [60–62]. We were inspired by the recent elegant reports on halogenation driven semipinacol rearrangements from Alexakis et al. and You et al. [64–67]. However, these reports were limited to halogenations involving highly electrophilic haloniums (F^+, Cl^+, Br^+ and I^+) from electrophilic halogen sources. Motivated by the previously mentioned beneficial influence of fluorine in pharmaceutical, agrochemical and material chemistry, we were interested in trifluoromethylation reactions with electrophilic trifluoromethylating reagents [4, 5, 7–9]. Since the trifluoromethylation of an alkene with an electrophilic trifluoromethylating reagent requires a one-electron reducing agent [17, 18, 42] and following our research interest in photocatalysis, we considered that a photoredox catalyst would be a suitable candidate for this purpose. We designed our reaction starting from α-cycloalkanol-substituted styrenes as depicted in Scheme 3.8. The addition of the CF_3 radical and subsequent oxidation via SET would lead to the formation of a carbocation, which would undergo a 1,2-alkyl migration for the expansion of the cycloalkanol group. In this designed reaction scheme, two undesired side reactions need to be overcome to validate our desired process: (1) the intramolecular trapping of the carbocation with a vicinal hydroxyl group, delivering an epoxide derivative, and (2) deprotonation of the intermediate carbocation species furnishing an alkene derivative (Scheme 3.8).
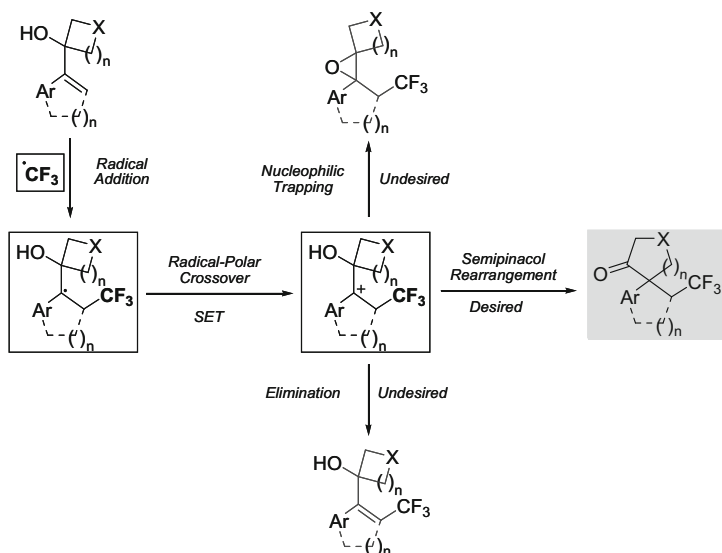
Scheme 3.8 Reaction design for the trifluoromethylation-semipinacol rearrangement

3.2.2 Preliminary Experiments and Optimization Studies

In an initial experiment, a mixture of 1-(1-phenylvinyl)cyclobutanol (**142**) and 5-(trifluoromethyl)dibenzothiophenium trifluoromethanesulfonate (**139**, 1.4 equiv.) in DMF (0.1 M) was irradiated with 5 W blue LEDs (λ_{max} = 465 nm) in the presence of the photocatalyst [Ru(bpy)$_3$](PF$_6$)$_2$ (2 mol%). To our delight, we observed the ring expanded product, 2-phenyl-2-(2,2,2-trifluoroethyl)cyclopentanone (**143**) in 60 % GC yield as the major product, along with the formation of the undesired nucleophilic trapping byproduct 2-phenyl-2-(2,2,2-trifluoroethyl)-1-oxaspiro[2.3] hexane (**144**) in a ratio of **143**:**144** = 2.3:1, which was determined by ^{19}F NMR analysis (Table 3.1, entry 1).
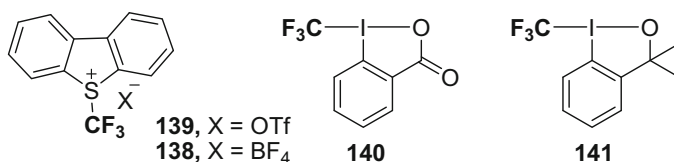
The reaction was conducted in the presence of a little excess of TMSOTf (1.2 equiv.), thus protecting the hydroxyl functional group in situ, and reducing its nucleophilicity, to suppress byproduct **144** formation. Delightfully, the expected product **143** was obtained exclusively in 98 % GC yield under these reaction

Table 3.1 Optimization studies[a]
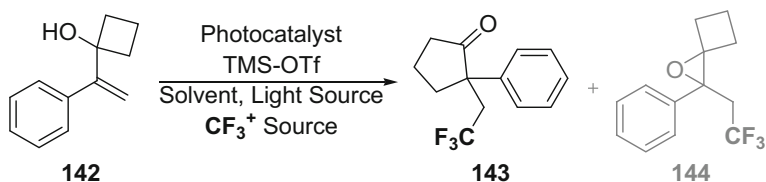
Entry	[PC cat.] (mol%)	Solvent	CF₃⁺) source (equiv.)	Additive (equiv.)	Light	Yield (%)[b]
1[c]	[Ru(bpy)₃](PF₆)₂ (2)	DMF (0.1)	**139** (1.4)	–	Blue LEDs	60
2	[Ru(bpy)₃](PF₆)₂ (2)	DMF (0.1)	**139** (1.4)	TMSOTf (1.2)	Blue LEDs	98
3	[Ru(bpy)₃](PF₆)₂ (2)	DMF (0.1)	**138** (1.4)	TMSOTf (1.2)	Blue LEDs	81
4	[Ru(bpy)₃](PF₆)₂ (2)	DMF (0.1)	**140** (1.4)	TMSOTf (1.2)	Blue LEDs	9
5	[Ru(bpy)₃](PF₆)₂ (2)	DMF (0.1)	**141** (1.4)	TMSOTf (1.2)	Blue LEDs	–
6	[Ru(bpy)₃](PF₆)₂ (2)	DMSO (0.1)	**139** (1.4)	TMSOTf (1.2)	Blue LEDs	90
7	[Ru(bpy)₃](PF₆)₂ (2)	CH₃CN (0.1)	**139** (1.4)	TMSOTf (1.2)	Blue LEDs	–
8	[Ru(bpy)₃](PF₆)₂ (2)	MeOH (0.1)	**139** (1.4)	TMSOTf (1.2)	Blue LEDs	78
9	[Ru(bpy)₃](PF₆)₂ (2)	THF (0.1)	**139** (1.4)	TMSOTf (1.2)	Blue LEDs	3
10	[Ru(bpy)₃](PF₆)₂ (2)	1,2-DCE (0.1)	**139** (1.4)	TMSOTf (1.2)	Blue LEDs	–
11	[Ir(ppy)₂(dtbbpy)] (PF₆) (2)	DMF (0.1)	**139** (1.4)	TMSOTf (1.2)	Blue LEDs	97
12	[Ir(ppy)₃] (2)	DMF (0.1)	**139** (1.4)	TMSOTf (1.2)	Blue LEDs	96
13	Fluorescein (2)	DMF (0.1)	**139** (1.4)	TMSOTf (1.2)	Blue LEDs	–
14	[Ru(bpy)₃](PF₆)₂ (2)	DMF (0.1)	**139** (1.4)	TMSOTf (1.2)	23 W CFL	92
15	[Ru(bpy)₃](PF₆)₂ (2)	DMF (0.1)	**139** (1.2)	TMSOTf (1.2)	Blue LEDs	95
16	[Ru(bpy)₃](PF₆)₂ (2)	DMF (0.1)	**139** (1.2)	TMSOTf (0.5)	Blue LEDs	70
17	**[Ru(bpy)₃](PF₆)₂ (1)**	**DMF (0.1)**	**139 (1.2)**	**TMSOTf (1.2)**	**Blue LEDs**	**94 (74)**
18	–	DMF (0.1)	**139** (1.2)	TMSOTf (1.2)	Blue LEDs	–
19	[Ru(bpy)₃](PF₆)₂ (1)	DMF (0.1)	**139** (1.2)	TMSOTf (1.2)	–	–

[a]1-(1-Phenylvinyl)cyclobutanol (**142**, 0.1 mmol), trimethylsilyl trifluoromethanesulfonate (TMSOTf) and the solvent were added to a Schlenk tube under argon. The mixture was stirred at rt for 2 h. Then [**CF₃⁺**] reagent and photoredox catalyst were added to the reaction mixture and stirred at rt for 6 h under visible light irradiation

[b]GC yield of **143** using mesitylene as an internal reference. Isolated yields in *parentheses*

[c]In the absence of TMSOTf, **143** was obtained along with **144** in a ratio of **143**:**144** = 2.3:1, which was determined by ¹⁹F NMR analysis

conditions without formation of **144** in detectable amounts (Table 3.1, entry 2). In a survey of different electrophilic trifluoromethylating reagents, another Umemoto's reagent, with BF_4 counteranion (**138**, 1.4 equiv.), afforded the product **143** in 81 % GC yield reducing the reaction efficiency due to ineffective protection of the hydroxyl group, whereas Togni's reagent **140** (1.4 equiv.) and **141** (1.4 equiv.) were unsuitable (only 9 % GC yield and no product respectively, Table 3.1, entries 3–5). The superiority of Umemoto's reagents compared to Togni's reagents can be rationalized by their redox potentials Umemoto's reagents (**138–139**) (−0.75 V vs. Cp_2Fe in CH_3CN), Togni's reagent **140** (−1.34 V vs. Cp_2Fe in CH_3CN) and Togni's reagent **141** (−1.49 V vs. Cp_2Fe in CH_3CN) [44]. Due to its higher redox potential, Umemoto's reagents were more easily reduced compared to Togni's reagents. Next we screened different solvents. The reaction proceeded smoothly in DMSO with slightly lower efficiency, while no reactivity was observed in acetonitrile (Table 3.1, entries 6–7). When the reaction was run in a nucleophilic solvent, such as methanol, the desired product **143** was formed in 78 % GC yield along with the methanol trapped byproduct **145** (Table 3.1, entry 8 and Scheme 3.10b). In THF, only trace amounts of product were obtained and no reaction occurred in 1,2-dichloroethane (Table 3.1, entries 9–10). After the solvent screening, DMF resulted as the best solvent for this reaction. In a screening of various photoredox catalysts, [Ir(ppy)$_2$(dtbbpy)] (PF$_6$) (dtbbpy = 4,4′-di-*tert*-butyl-2,2′-bipyridine) and [Ir(ppy)$_3$] furnished the product **143** in 97 and 96 % GC yields, respectively (Table 3.1, entries 11–12). Unfortunately, the organic fluorescein dye remained inefficient for this transformation (Table 3.1, entry 13). In order to find a more user-friendly light source, a commercially available 23 W CFL bulb was also tested. This visible light source was able to promote the reaction delivering **143** in 92 % GC yield (Table 3.1, entry 14). Further optimization revealed that the stoichiometry of the Umemoto's reagent **139** could be reduced from 1.4 equiv. to 1.2 equiv. without significant loss of product **143** (Table 3.1, entry 15). Since according to the proposed catalytic cycle TMSOTf would be regenerated at the end, we attempted to reduce the amount of TMSOTf to 0.5 equiv. unfortunately, an adverse effect on the reaction efficiency was observed (Table 3.1, entry 16). Finally, the loading of [Ru(bpy)$_3$](PF$_6$)$_2$ could be reduced to 1 mol% without hampering the reaction efficiency (Table 3.1, entry 17). Under these optimized conditions, the product **143** was obtained in 94 % GC yield and 74 % isolated yield (Table 3.1, entry 17). Control experiments conducting the reaction in the absence of a photocatalyst and in dark confirmed that both the photocatalyst [Ru(bpy)$_3$](PF$_6$)$_2$ and visible light were essential for this process (Table 3.1, entries 18–19).

3.2.3 Substrate Scope and Limitations

With the optimized reaction conditions in hand, we sought to explore the substrate scope and limitations for this transformation. The outcome of this evaluation has been summarized in Table 3.2. First we studied the influence of the substituents on

Table 3.2 Substrate scope of trifluoromethylation-semipinacol rearrangement[a]

Substrate	Product	Yield(d.r.)	Substrate	Product	Yield(d.r.)
142	143	74%	149	167	51%
146	164	73%	150	168	39%
147	165	60%	155	173	52% (1:1)
148	166	78%	158	176	41% (10:1)

Substrate	Product	Yield(d.r.)	Substrate	Product	Yield(d.r.)

(continued)

Table 3.2 (continued)

the aromatic ring of 1-(1-arylvinyl)cyclobutanol (**142**, **146–163**) on the outcome of the reaction. Electron-withdrawing halogen substituents (**146–147**) at the *para* position of the benzene ring were well tolerated. The corresponding ring expansion products **164** and **165**, which features a chloro group susceptible for further functionalization via cross coupling, could be obtained in good yields (73 and 60 % respectively). The electron-rich *para*-methyl substituted substrate **148** delivered the expected product **166** in 78 % yield, while shifting the methyl group to the *meta* and *ortho* positions decreased the reaction efficiency and yielded the desired products **167** (51 %) and **168** (39 %) in 51 and 39 % yield, respectively. Substrate **151,** featuring a *para*-phenyl substituent on the benzene ring, afforded the corresponding product **169** in 82 % yield. Strongly electron-donating *para*-methoxy and acetal groups in substrates **152** and **153** promoted the reactions efficiently leading to the expected products **170** (90 %) and **171** (86 %) in excellent yields. The 2-naphthyl substituted substrate **154** was also well suited for this transformation delivering the product **172** in 80 % yield. Substrates **155–159,** derived from 1-tetralones, 4-chromanone and 1-indanone, were also well tolerated. Substrates **155** and **156** afforded the ring expansion products **173** and **174**, respectively, as a mixture of diastereomers in moderate to low yields. Surprisingly highly electron-rich 4-chromanone and 5-methoxy-1-tetralone derived substrates, **158** and **159,** furnished the desired products **176** (41 %) and **175** (47 %) in very good to excellent diastereoselectivities (dr. 10:1 and >25:1 respectively). When the 1-indanone derived cycloalkanol **159** was reacted under the optimal reaction conditions, product **177** was obtained in 53 % yield and 1.5:1 d.r. with the recovery of **159** (22 %). However, increasing the amount of **139** (2.0 equiv.) led to complete conversion affording **177** in 65 % yield and 1.5:1 d.r. 1-(1-phenylvinyl) cyclopentanol (**160**) was a suitable substrate in spite of low ring strain delivering the expected product **178** in an acceptable yield 33 %. The oxa-cyclobutanol substrates (**161–162**) also exhibited reactivity, affording the desired products **179** and **180** in lower yields. Substrate **163**, lacking aryl ring that is in conjugation with an alkene double bond, was not a suitable substrate and the formation of **181** could only be detected by GC-MS analysis. Overall, this novel methodology affords a class of densely functionalized fluorinated cycloalkanones with quaternary carbon center.

3.2.4   *Follow up Transformations of Products*

Since the densely functionalized trifluoromethylated cycloalkanones possess a carbonyl functional group, we further investigated the versatility of the developed methodology. We performed some follow-up reactions of the parent product **143** (Scheme 3.9). When the product **143** was treated with sodium borohydride in methanol, the corresponding alcohol **182** was obtained in excellent yield (91 %)
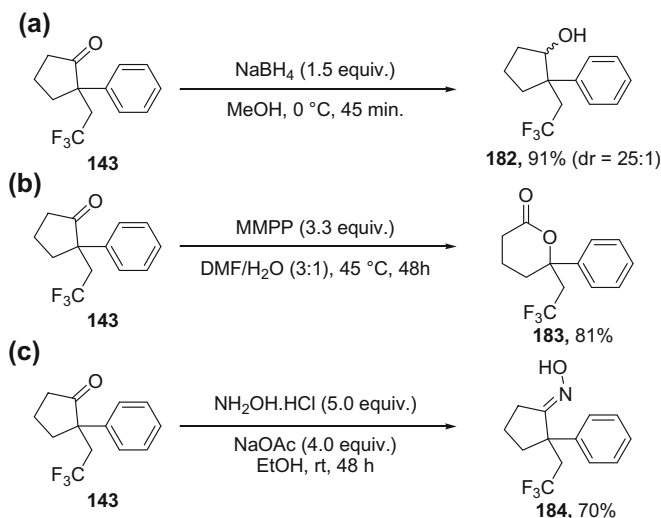
Scheme 3.9 Follow up reactions of product 143: **a** reduction of 183; **b** Baeyer-Villiger oxidation of 143; **c** oxime formation. *MMPP* magnesium monoperoxyphthalate

and diastereoselectivity (25:1) (Scheme 3.9a). In a Baeyer-Villiger oxidation, product **143** was oxidized to the lactone **183** in 81 % yield, while the reaction of the product **143** with hydroxylamine hydrochloride in the presence of sodium acetate delivered the oxime derivative **184** in good yield (71 %) (Scheme 3.9b, c).

3.2.5 Mechanistic Studies

In order to have some mechanistic insights, we did a literature survey [44, 47–49] and conducted some preliminary control experiments. When the reaction was performed in the absence of either photoredox catalyst or visible light, no product was formed (Table 3.1, entries 18–19). These experiments suggested that both components are essential for the reaction. The presence of a radical trapping reagent, 2,2,6,6-tetramethyl-1-piperidinyloxyl (TEMPO) inhibited the reaction forming the TEMPO trapped CF_3 adduct **185**, which was detected by GM-MS analysis (Scheme 3.10a). A methanol trapped intermediate **145** (detected by GCMS analysis) was formed along with the desired product **143** (78 %) when methanol was employed as solvent during the reaction optimization studies. The results of these two reactions support that both radical and ionic intermediates are involved in
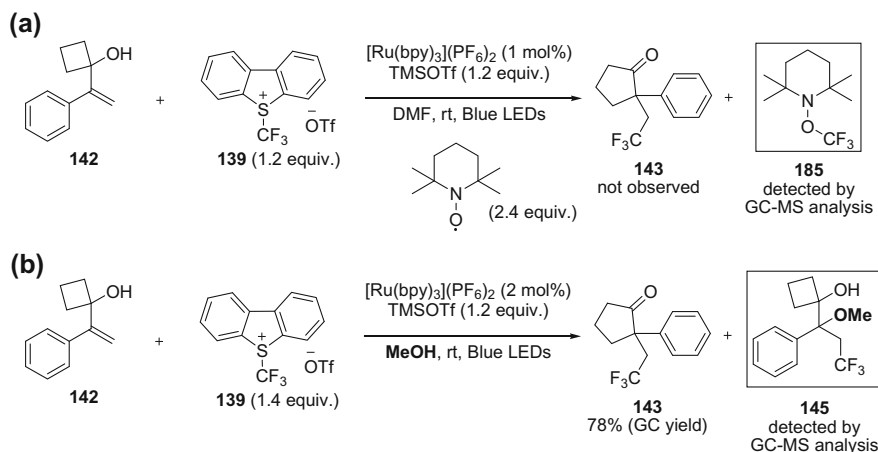
Scheme 3.10 Preliminary mechanistic experiments: **a** radical inhibition experiment with TEMPO; **b** carbocation trapping experiment with methanol

this process. According to a recent report by Koike, Akita and co-workers the Umemoto's reagent **138** could be a quencher of the photo-excited polypyridyl-metal photoredox catalyst (oxidative quenching), while styrene derivative remained innocent in those Stern-Volmer quenching studies [44, 48].

Following literature reports and the control experiments performed, we propose the following reaction mechanism for the visible light mediated photoredox catalyzed trifluoromethylation-ring expansion in scheme 3.11. In the presence of visible light from 5 W blue LEDs (λ_{max} = 465 nm), the photoredox catalyst [Ru(bpy)$_3$](PF$_6$)$_2$ gets excited to the strongly reducing photo-excited state [Ru(bpy)$_3$](PF$_6$)$_2$ ($E_{1/2}$ [Ru^{3+}/*Ru^{2+}] = −0.81 V vs. SCE in CH$_3$CN) [47, 72]. Single electron reduction of the Umemoto's reagent **139** ($E_{1/2}$ = −0.25 V vs. SCE in CH$_3$CN) [47] via SET from the photo-excited *[Ru(bpy)$_3$]$^{2+}$ species would generate an electrophilic radical CF$_3$ and the higher valent [Ru(bpy)$_3$]$^{3+}$. The addition of this electrophilic CF$_3$ radical onto the C=C bond of the silyl protected intermediate **A**, obtained in situ by silyl protection of hydroxyl group from substrate **142** in the presence of TMSOTf, would deliver the stabilized benzylic radical intermediate **B.** At this stage, a radical-polar crossover can occur as the key step to switch the radical pathway to an ionic one. Single electron oxidation of intermediate **B** by the higher valent [Ru(bpy)$_3$]$^{3+}$ ($E_{1/2}$ [Ru^{3+}/Ru^{2+}] = +1.29 V vs. SCE in CH$_3$CN) [47, 72] via SET would lead to the cationic intermediate **C** and regenerate the photoredox catalyst [Ru(bpy)$_3$]$^{2+}$. An alternative pathway might involve oxidizing the intermediate **B** with direct electron transfer to another equivalent of Umemoto's reagent **139** via SET in a chain process to obtain intermediate **C**. The measured quantum yield value (Φ = 3.8) of this photochemical process supports the involvement of a chain process in this transformation. In the next step, 1,2-alkyl
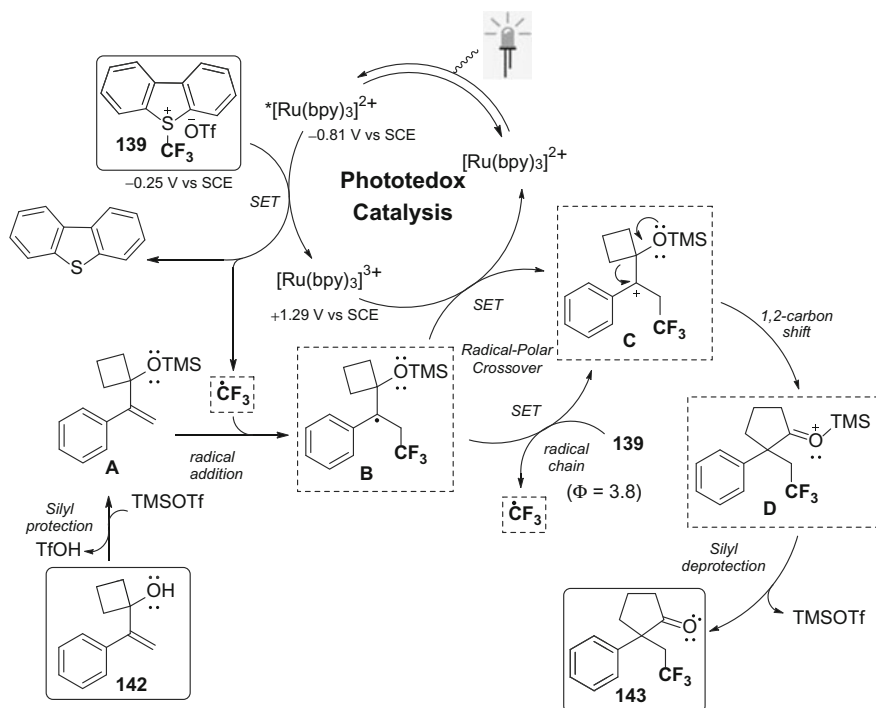
Scheme 3.11 Mechanistic proposal for the visible light photoredox catalyzed trifluoromethyl-semipinacol rearrangement

migration with a C–O π-bond formation would furnish the ring expanded product **143** upon loosing the silyl protecting group.

3.3 Summary

In summary, we have successfully disclosed the first visible light mediated photoredox catalyzed semipinacol rearrangement involving an ionic 1,2-alkyl migration. The photoredox catalyzed radical-polar crossover process enabled this reaction to occur. These transformations constitute a novel class of densely functionalized trifluoromethylated cycloalkanone derivatives possessing quaternary carbon center. Moreover, these compounds could be easily converted to other important functional motifs. This process benefits from milder reaction conditions, such as room temperature, no use of harsh and hazardous reagents, and cheap readily available light sources.

References

1. A. Bondi, J. Phys. Chem. **68**, 441–451 (1964)
2. D. O'Hagan, Chem. Soc. Rev. **37**, 308–319 (2008)
3. P. Jeschke, ChemBioChem **5**, 570–589 (2004)
4. K. Müller, C. Faeh, F. Diederich, Science **317**, 1881–1886 (2007)
5. S. Purser, P.R. Moore, S. Swallow, V. Gouverneur, Chem. Soc. Rev. **37**, 320–330 (2008)
6. T. Yamazaki, T. Taguchi, I. Ojima, in *Fluorine in Medicinal Chemistry and Chemical Biology,* ed. by I. Ojima (Wiley-Blackwell, UK, 2009)
7. T. Furuya, A.S. Kamlet, T. Ritter, Nature **473**, 470–477 (2011)
8. J. Wang, M. Sánchez-Roselló, J.L. Aceña, C. del Pozo, A.E. Sorochinsky, S. Fustero, V.A. Soloshonok, H. Liu, Chem. Rev. **114**, 2432–2506 (2014)
9. V. Gouverneur, K. Müller, *Fluorine in Pharmaceutical and Medicinal Chemistry: Frombiophysical Aspects to Clinical Applications* (Imperial CollegePress, London, 2012)
10. T. Hiyama, *Organofluorine Compounds: Chemistry and Applications* (Springer, Berlin, 2000)
11. W.K. Hagmann, J. Med. Chem. **51**, 4359–4369 (2008)
12. D.P. Curran, Angew. Chem. Int. Ed. **37**, 1174–1196 (1998)
13. C. Lampard, J.A. Murphy, N. Lewis, J. Chem. Soc. Chem. Commun. 295–297 (1993)
14. J.A. Murphy, in *Radicals in Organic Synthesis,* eds. by P. Renaud, M.P. Sibi. The Radical–Polar Crossover Reaction (Wiley-VCH, Weinheim, 2001)
15. E. Godineau, Y. Landais, Chem. Eur. J. **15**, 3044–3055 (2009)
16. O.A. Tomashenko, V.V. Grushin, Chem. Rev. **111**, 4475–4521 (2011)
17. A. Studer, Angew. Chem. Int. Ed. **51**, 8950–8958 (2012)
18. H. Egami, M. Sodeoka, Angew. Chem. Int. Ed. **53**, 8294–8308 (2014)
19. E. Merino, C. Nevado, Chem. Soc. Rev. **43**, 6598–6608 (2014)
20. C. Alonso, E. Martínez de Marigorta, G. Rubiales, F. Palacios, Chem. Rev. **115**, 1847–1935 (2015)
21. J. Charpentier, N. Früh, A. Togni, Chem. Rev. **115**, 650–682 (2015)
22. C. Ni, M. Hu, J. Hu, Chem. Rev. **115**, 765–825 (2015)
23. I. Ruppert, K. Schlich, W. Volbach, Tetrahedron Lett. **25**, 2195–2198 (1984)
24. P. Ramaiah, R. Krishnamurti, G.K.S. Prakash, Org. Synth. **72**, 232 (1995)
25. L.M. Yagupolskii, N.V. Kondratenko, G.N. Timofeeva, J. Org. Chem. USSR **20**, 103–106 (1984)
26. N. Shibata, A. Matsnev, D. Cahard, Beilstein J. Org. Chem. **6**, 65 (2010)
27. M. Tordeux, B. Langlois, C. Wakselman, J. Org. Chem. **54**, 2452–2453 (1989)
28. B.R. Langlois, E. Laurent, N. Roidot, Tetrahedron Lett. **32**, 7525–7528 (1991)
29. G.K.S. Prakash, A.K. Yudin, Chem. Rev. **97**, 757–786 (1997)
30. G. Danoun, B. Bayarmagnai, M.F. Grünberg, L.J. Gooßen, Angew. Chem. Int. Ed. **52**, 7972–7975 (2013)
31. M.-Y. Cao, X. Ren, Z. Lu, Tetrahedron Lett. **56**, 3732–3742 (2015)
32. W.R. Dolbier, Chem. Rev. **96**, 1557–1584 (1996)
33. H. Egami, R. Shimizu, Y. Usui, M. Sodeoka, Chem. Commun. **49**, 7346–7348 (2013)
34. T. Patra, A. Deb, S. Manna, U. Sharma, D. Maiti, Eur. J. Org. Chem. **2013**, 5247–5250 (2013)
35. A. Deb, S. Manna, A. Modak, T. Patra, S. Maity, D. Maiti, Angew. Chem. Int. Ed. **52**, 9747–9750 (2013)
36. N. Kamigata, T. Fukushima, M. Yoshida, J. Chem. Soc., Chem. Commun. 1989, 1559–1560
37. Y. Li, A. Studer, Angew. Chem. Int. Ed. **51**, 8221–8224 (2012)
38. Q. Wang, X. Dong, T. Xiao, L. Zhou, Org. Lett. **15**, 4846–4849 (2013)
39. B. Zhang, C. Mück-Lichtenfeld, C.G. Daniliuc, A. Studer, Angew. Chem. Int. Ed. **52**, 10792–10795 (2013)
40. B. Zhang, A. Studer, Org. Lett. **16**, 1216–1219 (2014)
41. B. Zhang, A. Studer, Org. Biomol. Chem. **12**, 9895–9898 (2014)
42. T. Koike, M. Akita, J. Fluorine Chem. **167**, 30–36 (2014)

43. J.W. Tucker, C.R.J. Stephenson, J. Org. Chem. **77**, 1617–1622 (2012)
44. Y. Yasu, T. Koike, M. Akita, Angew. Chem. Int. Ed. **51**, 9567–9571 (2012)
45. J.D. Nguyen, J.W. Tucker, M.D. Konieczynska, C.R.J. Stephenson, J. Am. Chem. Soc. **133**, 4160–4163 (2011)
46. C.-J. Wallentin, J.D. Nguyen, P. Finkbeiner, C.R.J. Stephenson, J. Am. Chem. Soc. **134**, 8875–8884 (2012)
47. S. Mizuta, S. Verhoog, K.M. Engle, T. Khotavivattana, M. O'Duill, K. Wheelhouse, G. Rassias, M. Médebielle, V. Gouverneur, J. Am. Chem. Soc. **135**, 2505–2508 (2013)
48. Y. Yasu, Y. Arai, R. Tomita, T. Koike, M. Akita, Org. Lett. **16**, 780–783 (2014)
49. Y. Yasu, T. Koike, M. Akita, Org. Lett. **15**, 2136–2139 (2013)
50. A. Carboni, G. Dagousset, E. Magnier, G. Masson, Chem. Commun. **50**, 14197–14200 (2014)
51. S.H. Oh, Y.R. Malpani, N. Ha, Y.-S. Jung, S.B. Han, Org. Lett. **16**, 1310–1313 (2014)
52. R. Tomita, Y. Yasu, T. Koike, M. Akita, Angew. Chem. Int. Ed. **53**, 7144–7148 (2014)
53. H. Jiang, Y. Cheng, Y. Zhang, S. Yu, Eur. J. Org. Chem. **2013**, 5485–5492 (2013)
54. E. Kim, S. Choi, H. Kim, E.J. Cho, Chem. Eur. J. **19**, 6209–6212 (2013)
55. Q.-Y. Lin, X.-H. Xu, F.-L. Qing, J. Org. Chem. **79**, 10434–10446 (2014)
56. S. Mizuta, K.M. Engle, S. Verhoog, O. Galicia-López, M. O'Duill, M. Médebielle, K. Wheelhouse, G. Rassias, A.L. Thompson, V. Gouverneur, Org. Lett. **15**, 1250–1253 (2013)
57. Q.-H. Deng, J.-R. Chen, Q. Wei, Q.-Q. Zhao, L.-Q. Lu, W.-J. Xiao, Chem. Commun. **51**, 3537–3540 (2015)
58. P. Xu, K. Hu, Z. Gu, Y. Cheng, C. Zhu, Chem. Commun. **51**, 7222–7225 (2015)
59. L. Zheng, C. Yang, Z. Xu, F. Gao, W. Xia, J. Org. Chem. **80**, 5730–5736 (2015)
60. T.J. Snape, Chem. Soc. Rev. **36**, 1823–1842 (2007)
61. Z.-L. Song, C.-A. Fan, Y.-Q. Tu, Chem. Rev. **111**, 7523–7556 (2011)
62. K.-D. Umland, S.F. Kirsch, Synlett **24**, 1471–1484 (2013)
63. B. Wang, Y.Q. Tu, Acc. Chem. Res. **44**, 1207–1222 (2011)
64. F. Romanov-Michailidis, L. Guénée, A. Alexakis, Angew. Chem. Int. Ed. **52**, 9266–9270 (2013)
65. F. Romanov-Michailidis, M. Pupier, L. Guenee, A. Alexakis, Chem. Commun. **50**, 13461–13464 (2014)
66. F. Romanov-Michailidis, L. Guénée, A. Alexakis, Org. Lett. **15**, 5890–5893 (2013)
67. Q. Yin, S.-L. You, Org. Lett. **16**, 1810–1813 (2014)
68. B.M. Wang, Z.L. Song, C.A. Fan, Y.Q. Tu, W.M. Chen, Synlett **2003**, 1497–1499 (2003)
69. Q.-W. Zhang, C.-A. Fan, H.-J. Zhang, Y.-Q. Tu, Y.-M. Zhao, P. Gu, Z.-M. Chen, Angew. Chem. Int. Ed. **48**, 8572–8574 (2009)
70. M. Wang, B.M. Wang, L. Shi, Y.Q. Tu, C.-A. Fan, S.H. Wang, X.D. Hu, S.Y. Zhang, Chem. Commun. 5580–5582 (2005)
71. Z.-M. Chen, W. Bai, S.-H. Wang, B.-M. Yang, Y.-Q. Tu, F.-M. Zhang, Angew. Chem. Int. Ed. **52**, 9781–9785 (2013)
72. M. Haga, E.S. Dodsworth, G. Eryavec, P. Seymour, A.B.P. Lever, Inorg. Chem. **24**, 1901–1906 (1985)

Chapter 4
Transition Metal Free Visible Light-Mediated Synthesis of Polycyclic Indolizines

4.1 Introduction

4.1.1 General Properties of Indolizines

Indolizine is a heterocyclic aromatic compound bearing a bridging nitrogen atom. In this heterocyclic compound, a five membered π-electron-rich pyrrole ring is fused to a six membered π-electron-deficient pyridine ring. According to Hückel's (4n + 2) rule, this aromatic compound has 10π electrons with 2 π-electrons arising from the bridging nitrogen atom and 8 π-electrons arising from four C=C π-bonds. The resonance energy and first ionization potential (IP_1) of the parent indolizine are 2.28 and 7.24 eV respectively [1]. This heterocycle is isoelectronic with indole and isoindole. Indolizine acts as a weak base (pKa = 3.94) and is more basic than indole (pKa = −2.4) [2]. The parent indolizine and alkyl-substituted indolizines are usually air and light sensitive liquids or sometimes low-melting solids, while aryl-substituted indolizines are typically relatively stable solids [3]. High level DFT calculations have shown that an extended HOMO of the parent indolizine exclusively resides on the pyrrole ring, while the LUMO is mostly located at the pyridine ring (Fig. 4.1) [4]. Thus, indolizine undergoes aromatic electrophilic substitution reactions (S_EAr) at the C-1 and C-3 positions of the π-excessive pyrrole ring, while aromatic nucleophilic substitutions (S_NAr) are rare [5]. However, introduction of an electron-withdrawing nitro group at the C-6 or C-8 positions makes this indolizine derivative prone to nucleophilic substitutions without loss of the pyrrole-like reactivity. Thus this nitro substituted indolizine is expected to show π-amphoteric behavior [5].

Fig. 4.1 Chemical abstracts
numbering, HOMO and
LUMO of indolizine [4]
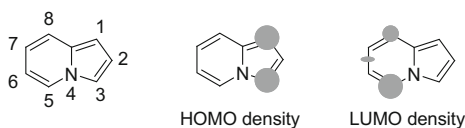
4.1.2 Importances of Indolizines

Indolizine exists as an important core in many naturally-occurring compounds and
synthetic pharmaceuticals possessing biological activity [6–8]. Natural and syn-
thetic substituted indolizine derivatives exhibit central nervous system (CNS) de-
pressant activity [9], anticancer activity [10–12], analgesic activity [13],
anti-inflammatory activity [13], antibacterial activity [14] and antioxidant activity
[15]. The indolizine scaffold is present in calcium channel blockers [16],
sodium-glucose linked transporter Type I (SGL T1) antagonists [17], phosphodi-
esterase IV (PDE4) inhibitors [18], microtubule inhibitors [19] and 15-lipoxygenase
inhibitors [20, 21]. Moreover, indolizidines, derived from indolizines upon com-
plete hydrogenation, exist as an invaluable motif in many natural products and
bioactive compounds [22, 23].

During the combinatorial synthetic study of novel polycyclic drug-like com-
pounds, Park and co-workers discovered an exciting fluorescent material,
9-aryl-dihydropyrrolo[3,4-b]indolizin-3-one (Fig. 4.2) [24]. These types of com-
pounds were later explored as part of a library of fluorescent materials, which were
named Seoul Fluorophores [25, 26]. Afterwards, You, Lan and co-workers
demonstrated that 3-aryl-substituted indolizines also constitute a series of fluores-
cent compounds [27]. Tunable substitution patterns on the indole and pyridine
substructures, and on the aryl rings of 3-aryl indolizines result in electronic per-
turbation of the whole π-system. As a consequence, a wide range of emission
wavelengths covering from 405 to 616 nm become accessible from these color
tunable fluorescent materials. This class of heterocyclic compounds has been used
as photosensors for the detection of volatile organic compounds [28] and as organic
sensitizers in dye-sensitized solar cells [29]. Moreover, indolizines serve as
excellent synthons for the synthesis of invaluable cycl[3.2.2]azines [30].

4.1.3 Synthesis of Indolizines

After the discovery of the parent indolizine by Angeli in 1890 [31, 32], the first
synthesis of this compound was performed by Scholtz in 1912, although unam-
biguous identification of the product was unsuccessful at that time [33]. The
reaction of 2-picoline with acetic anhydride at high temperature (200–220 °C) in a
sealed steel bomb resulting in indolizine is now called the Scholtz reaction
(Scheme 4.1) [33].
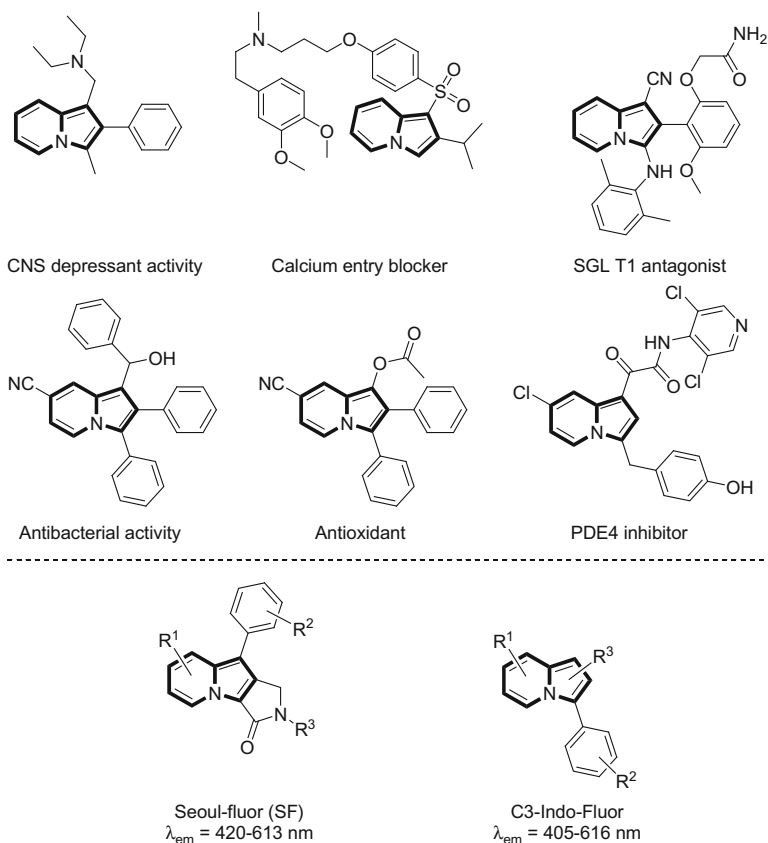
Fig. 4.2 Selected natural and synthetic biologically-active compounds and fluorophores possessing the indolizine core

In 1929, Tschitschibabin and Stepanow gave a mechanistic proposal for the Scholtz reaction, which is depicted in Scheme 4.1 [34]. Condensation of 2-methylpyridine and acetic anhydride at 200–220 °C results in 2-(2-pyridyl) acetylacetone (**186**) which tautomerizes to an enol intermediate **187** under the reaction conditions. In the next steps, cyclization of intermediate **187** followed by dehydration delivers 1-acetylindolizine (**189**). In the presence of acetic anhydride, 1-acetylindolizine (**189**) further undergoes electrophilic acylation at the C-3 position furnishing 1,3-diacetylindolizine. This disubstituted indolizine can be converted into the non-substituted parent indolizine upon hydrolysis.

In common with many other nitrogen heterocycles, diversely-substituted indolizines and their hydrogenated analogs have immense importance because of their biological and photophysical activities and, over the last century, a substantial amount of interest has grown to develop methods for the synthesis of indolizines with diverse functionality.
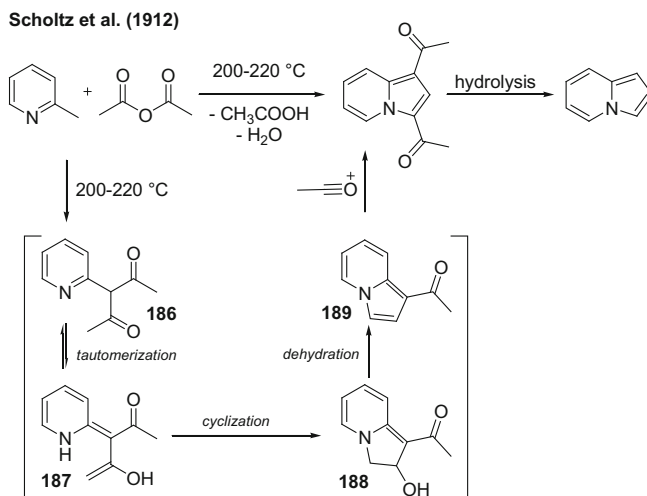
Scheme 4.1 Scholtz reaction and its mechanistic hypothesis [33, 34]

4.1.3.1   Synthesis of Indolizines via Methine Formation

In 1927, Tschitschibabin developed an elegant method to synthesize indolizines from quaternary pyridinium salts upon treatment with a base, which has since been popularized as the Tschitschibabin reaction (Scheme 4.2, where R^1, R^3 = H) [35]. However, this reaction was unsuccessful for those indolizines featuring no substituents on the pyrrole core. Over the last century, a significant number of methods have been reported modifying the Tschitschibabin reaction [36]. In 1960s and 1970s, various research groups have synthesized indolizines starting from pyridine substrates and α-bromocarbonyl compounds in two steps under thermal conditions in the presence of various bases (Scheme 4.2) [37–40]. The principal characteristic of these reactions is the involvement of a methine intermediate generated from a quaternary pyridinium salt upon deprotonation.

4.1.3.2   Synthesis of Indolizines via a 1,3-Dipolar Cycloaddition

Since 1,3-dipolar cycloaddition reactions constitute a powerful method for the synthesis of five-membered heterocyclic compounds, in 1961, Boekelheide and co-workers applied this elegant approach to the synthesis of an indolizine from 1-phenacylpyridinium methylid and dimethyl acetylenedicarboxylate under dehydrogenative conditions using Pd/C in toluene (Scheme 4.3) [41]. Moreover, there have been many impressive transformations devised for the synthesis of diversely-substituted indolizines based on 1,3-dipolar cycloadditions [42, 43].
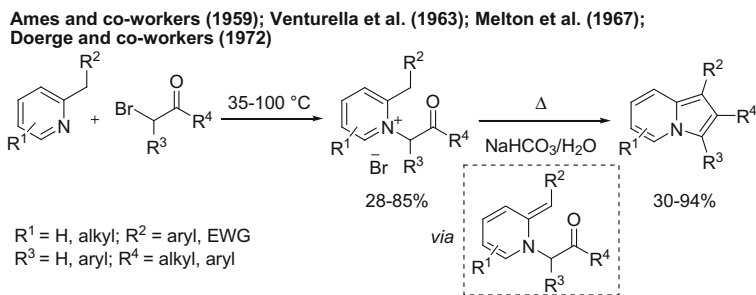
Scheme 4.2 Synthesis of indolizines via methine formation (Tschitschibabin reaction) [37–40]
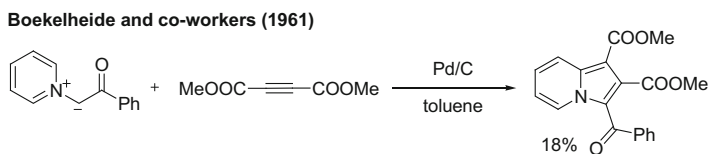
Scheme 4.3 Synthesis of indolizines via a 1,3-dipolar cycloaddition reaction [41]

4.1.3.3 Synthesis of Indolizines via a 1,5-Dipolar Cyclization

1,5-Dipolar cyclization is one of the more popular electrocyclic reactions applied in organic chemistry. Inspired by these reactions, in a seminal report in 1962, Kröhnke and co-workers disclosed an exciting method for synthesizing indolizines [44]. Afterwards, many interesting 1,5-dipolar cyclization-centric synthetic routes have been reported for indolizine synthesis [36]. One of these reports, developed by two research groups independently, was the 1,5-dipolar cyclization of isolated or in situ generated *N*-allylpyridinium ylids upon treatment with K_2CO_3 (Scheme 4.4) [45, 46].

4.1.3.4 Synthesis of Indolizines via Carbene/Metal-Carbenoid Formation

Addition of a sextet carbene onto carbon-carbon multiple bonds is a classical reactions in carbene chemistry. In 1994, Liu and co-workers employed carbene chemistry for the synthesis of indolizine. In this process, arylchlorocarbenes derived from arylchlorodiazirines upon photolysis under UVA irradiation react with 2-vinylpyridine to afford 3-substituted indolizines (Scheme 4.5a) [47]. However, this method is very poor yielding (10–12 %) and has a highly limited substrate scope (only three substrates were successfully employed). Importantly, thermal treatment or ultrasound (US) irradiation gave comparatively better yields (13–52 %) and a relatively larger scope (seven substrates) compared to UV light

Barrett and co-workers (1958); Pratt, Keresztesy, Jr. and co-workers (1967)

R^1 = alkyl; R^2 = alkyl, aryl; R^3 = aryl, OR
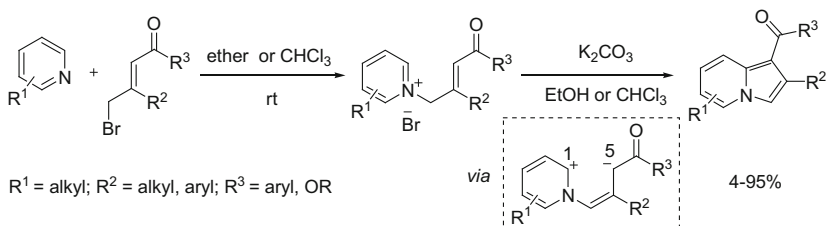
Scheme 4.4 Synthesis of indolizines via a 1,5-dipolar cycloaddition reaction [45, 46]

(a) Liu and co-workers(1994)

5.0 equiv.

R^1 = EWG, EDG   10–12%   via carbene

(b) Gevorgyan and co-workers (2007)

R^1 = EWG, EDG   57–85%   5–10%
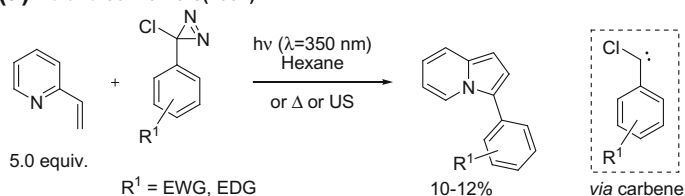
via metal carbenoid
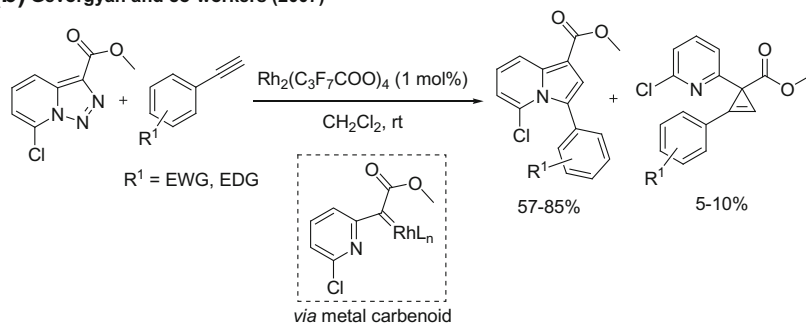
Scheme 4.5 Synthesis of indolizines via carbene/metal-carbenoid formation [47, 48]

irradiation. Later in 2007, Gevorgyan and co-workers reported an exciting route for the synthesis of indolizines from pyridotriazole and terminal alkynes proceeding via a metal-carbenoid intermediate (Scheme 4.5b) [48]. In this annulation reaction, the desired indolizine formation was accompanied by the formation of a cyclopropene byproduct. However, careful selection of an appropriate catalyst counteranion, Rh$_2$(C$_3$F$_7$COO)$_4$ allowed for control over the selectivity.

4.1.3.5   Synthesis of Indolizines via Oxidative Coupling-Cyclization

Transition Metal-Mediated Dehydrogenative Coupling Approach

Very recently, Aggarwal and co-workers uncovered a silver-mediated method for the synthesis of 3-arylindolizines starting from 2-pyridylacetates and terminal alkynes (Scheme 4.6) [49]. This reaction proceeds via a stoichiometric silver-mediated oxidative dehydrogenative $C(sp^3)$–$C(sp)$ coupling of a methylene $C(sp^3)$–H bond and an acetylene $C(sp)$–H bond and a subsequent 5-*endo-dig* cyclization. This protocol benefits from a broad substrate scope of the alkyne and a high atom economy, while the Ag_2CO_3 oxidant could be recovered from reaction residue and recycled.

Iodine-Mediated/Catalyzed Transition Metal-Free Approach

Since the pharmaceutical industry generally prefers metal-free synthetic routes for the synthesis of biomolecules to avoid contamination by metal impurities even at ppb level, a part of scientific community has devoted their attention to this line of research. In this context, Yan and co-workers reported an iodine-mediated oxidative cyclization method for the synthesis of functionalized indolizines from enolizable aldehydes and 2-pyridylacetates (Scheme 4.7a) [50]. Moreover, very recently, Lei and co-workers disclosed a route for the synthesis of substituted indolizines under oxidative conditions using a combination of I_2 and *tert*-butyl hydrogen peroxide (TBHP, Scheme 4.7b) [51]. This reaction is believed to proceed via a radical pathway. It is worth mentioning that the same reaction can be achieved with stoichiometric amounts of $Cu(OAc)_2$ instead of TBHP [52].

4.1.4   Functionalization of Indolizines via Transition Metal Catalysis

In contrast to direct synthetic methods, another strategy to obtain highly-substituted indolizines involves the direct functionalization of a pre-formed indolizine core
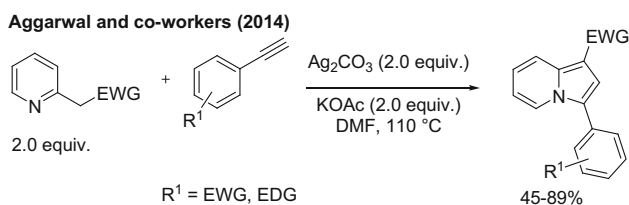
Scheme 4.6 Synthesis of indolizines via oxidative dehydrogenative coupling-cyclization [49]
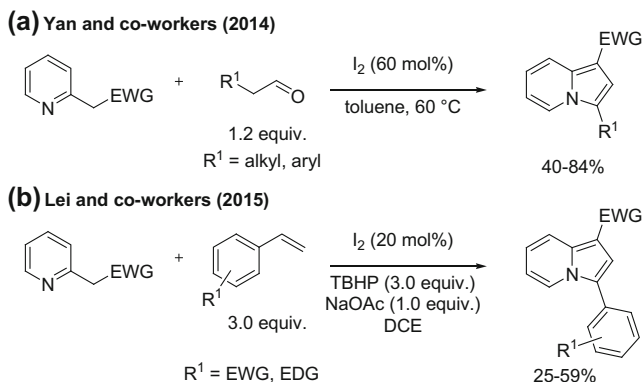
Scheme 4.7 Iodine mediated/catalyzed synthesis of indolizines [50, 51]

structure. Over the last few decades, transition metal catalysis has become a promising tool in this regard.

4.1.4.1 Transition Metal-Catalyzed Redox-Neutral Cross-Coupling

In 2004, Gevorgyan and co-workers and Fagnou and co-workers in 2009 independently disclosed the palladium-catalyzed selective C–H functionalization of indolizines at the C-3 position with aryl bromides [4, 53]. The selectivity for the C-3 position was attributed to the higher HOMO density at C-3. Later, You, Lan and co-workers reported an elegant and versatile method for the selective C–H functionalization of indolizines with less reactive aryl chlorides (Scheme 4.8) [27]. In this reaction, palladium-catalyzed C-3 selective arylation of the indolizine motif gives access to a broader spectrum of fluorescent arylated indolizine derivatives.

4.1.4.2 Transition Metal-Catalyzed Oxidative Cross-Coupling

In addition to conventional cross-coupling methods with aryl halides, a considerable amount of research interest has been devoted to the development of synthetic methods proceeding under oxidative conditions. In 2012, Zhao et al. uncovered an efficient and versatile protocol for the palladium-catalyzed selective C–H functionalization of indolizines under oxidative conditions using stoichiometric amounts of silver acetate (Scheme 4.9a) [54]. In this method, aryltrifluoroborates were used as aryl precursors. In 2014, Hu, Wang, Ji and co-workers reported a milder method for the palladium-catalyzed selective C–H functionalization of indolizines under oxidative conditions [55]. In a later procedure, expensive stoichiometric metal oxidants were replaced with oxygen gas as the terminal oxidant and arylboronic acids were used in place of aryltrifluoroborates (Scheme 4.9b).

You, Lan and co-workers (2012)
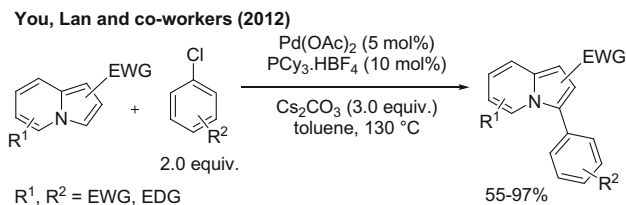
Scheme 4.8 Palladium-catalyzed selective redox neutral C–H arylation of indolizines [27]

(a) Zhao et al. (2012)

(b) Hu, Wang, Ji and co-workers (2014)
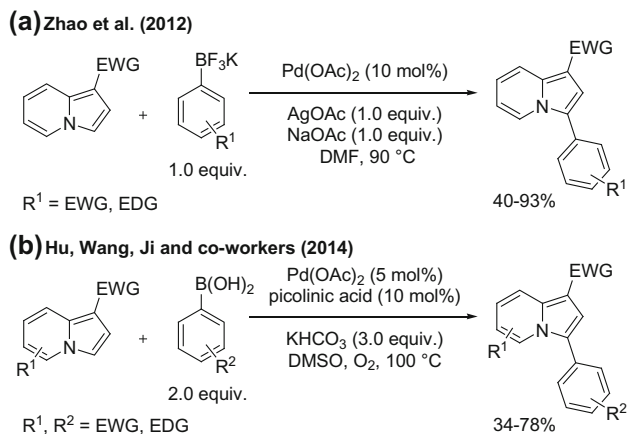
Scheme 4.9 Palladium-catalyzed selective oxidative C–H arylation of indolizines [54, 55]

4.2 Results and Discussion

4.2.1 Inspiration

Although over the last century, many synthetic protocols have been developed for the synthesis of indolizines with diverse substitution patterns, most of these reactions are carried out under thermal conditions with stoichiometric reagents. With the extensive progress of catalysis research, a variety of elegant and efficient methods have been disclosed for the synthesis of densely-substituted indolizines. However, photochemical synthesis of this class of heterocyclic compounds has rarely been explored. Since many substituted indolizines themselves can absorb light in the UVA and UVB range with some even absorbing lower energy visible light, intelligent design of the substitution pattern of the indolizine is important to minimize the photoactivity of the products, which could have adverse effects on the reaction rates. Moreover, some substitution patterns of indolizines make them prone to decompose under light irradiation in the presence of air. These could be the possible reasons why chemists have somewhat neglected synthetic investigations of

indolizines using photochemical reaction conditions. However, following our research interest in visible light photocatalysis, we were interested in designing a system for the synthesis of invaluable C-3 aryl-substituted indolizines using an external photocatalyst which absorbs photons in the visible range.

4.2.2 Reaction Design

Our reaction design starts with a bromopyridine substrate (**190**) and an electron-rich enol carbamate (**191**) in the presence of a photoredox catalyst and a visible light source (Scheme 4.10).

According to our mechanistic hypothesis, we envisaged that 2-bromo-2-(2-pyridyl)acetate (**190**) would quench the photo-excited photoredox catalyst (PC*) in an oxidative quenching pathway to generate a radical-anionic intermediate **A** and the oxidized photoredox catalyst (PC$^{•+}$) (Scheme 4.11). In a mesolysis process, the radical-anionic intermediate **A** would then deliver an alkyl intermediate **B**, which would undergo radical addition to an electron-rich enol carbamate **191** generating another radical intermediate **C**. At this stage, radical intermediate **C** would transfer an electron to the oxidized photoredox catalyst (PC$^{•+}$) via SET, regenerating the ground state photoredox catalyst (PC) and affording a carbocationic intermediate **D**. An alternative pathway could be possible via direct electron transfer from radical intermediate **C** to another molecule of 2-bromo-2-(2-pyridyl)acetate (**190**) in a radical chain process through SET. In a series of follow-up steps, nucleophilic trapping of the carbocationic intermediate **D** by pyridine in intramolecular fashion would deliver another cationic intermediate **E**, which would then afford the indolizine product **192** upon successive deprotonation and elimination of an *N,N'*-dialkyl carbamic acid.

4.2.3 Preliminary Experiments and Optimization Studies

To validate our hypothesis, we performed a preliminary test by treating methyl 2-bromo-2-(2-pyridyl)acetate (**193**) with 3,4-dihydronaphthalen-1-yl
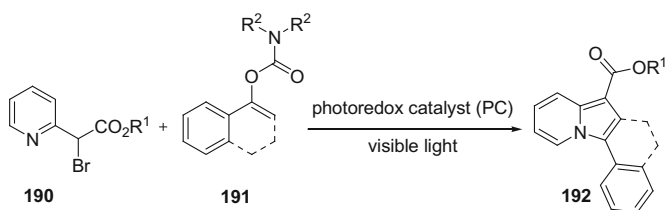
Scheme 4.10 Visible light photoredox-catalyzed synthesis of indolizines
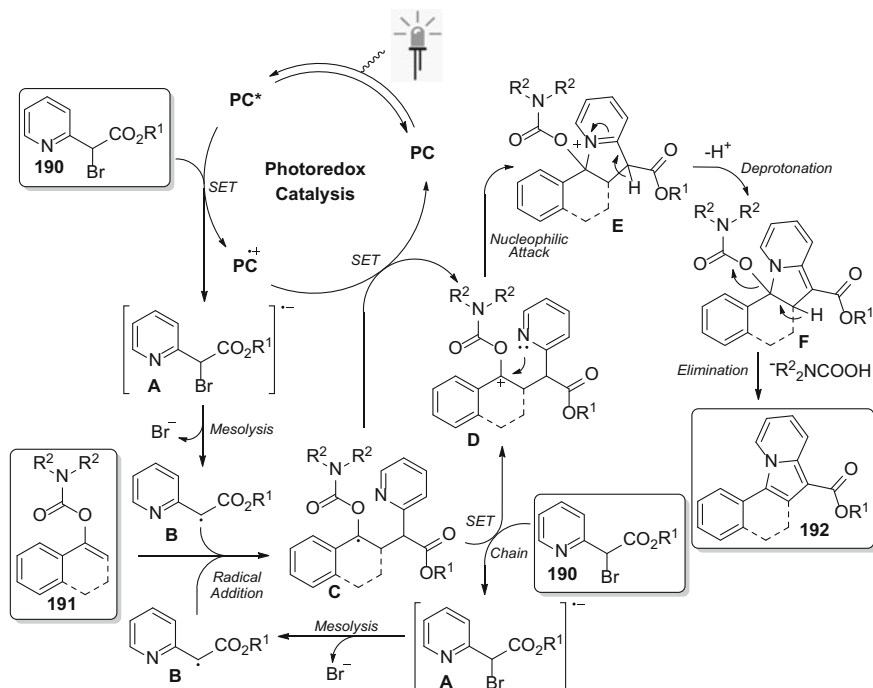
Scheme 4.11 Mechanistic hypothesis for the proposed visible light photoredox-catalyzed indolizine synthesis

dimethylcarbamate (**194**, 5.0 equiv.) in DMF solvent in the presence of the organometallic photoredox catalyst [Ir(ppy)$_2$(dtbbpy)](PF$_6$) (2 mol%) and the inorganic base Na$_2$HPO$_4$ (2.0 equiv.) under visible light irradiation from 5 W blue LEDs (λ_{max} = 465 nm) for 12 h. We were delighted to observe the desired indolizine product **195** in 62 % GC yield, while running the reaction in the dark did not deliver the product **195**, confirming the necessity of light (Scheme 4.12a, b). An interesting observation was made when this reaction was carried out in absence of the photoredox catalyst [Ir(ppy)$_2$(dtbbpy)](PF$_6$). Rather than shutting down the expected reactivity, the indolizine product **195** was delivered in comparable yield 52 % GC yield under these conditions (Scheme 4.12c).

In order to optimize the reaction conditions, we performed an exhaustive screening of different parameters (solvent, leaving group, base, light source, stoichiometry). In a survey of solvents, we observed that the performance of this reaction was almost independent of solvent polarity (Table 4.1, entry 2–12). In nucleophilic solvents such as methanol and acetonitrile, the reaction efficiency dropped significantly, while no reactivity was observed using pyridine as solvent (Table 4.1, entry 3–4, 12). Trifluorotoluene remained the best among the screened solvents (Table 4.1, entry 10). In a screening of different leaving groups, a 1-tetralone derived carbonate, acetate, trifluoromethanesulfonate and secondary
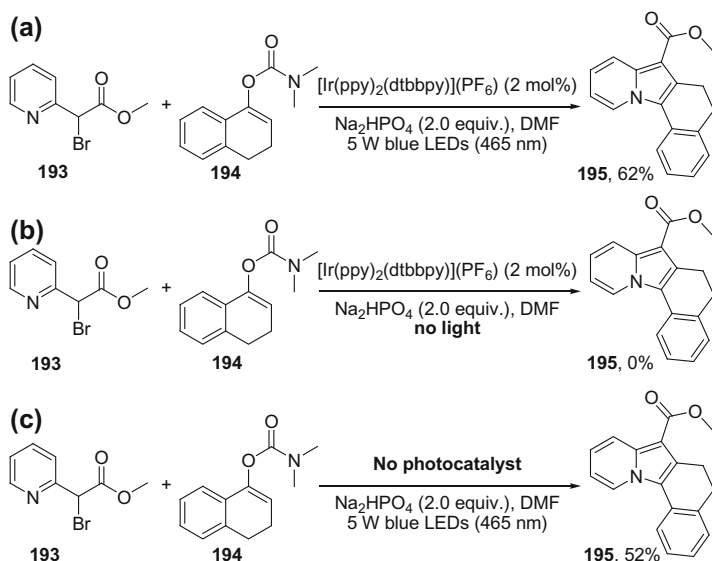
Scheme 4.12 Visible light photoredox-catalyzed indolizine synthesis and control experiments (GC yields)

enamine performed very poorly, while a significant drop of reactivity was observed with a diisopropyl carbamate derivative (Table 4.1, entry 13–17). Since HBr and carbamic acid are obtained as byproducts in this reaction, we surveyed various strong and weak bases to neutralize in situ-generated acids (Table 4.1, entry 18–32). We found that weak bases are better for this reaction with a trend of increasing reaction efficiency upon moving from a strong base to a weak base (Table 4.1, entry 22–25). The weak base HMDS (HMDS = hexamethyldisilazane, pKa = 7.55) [56] was found to be the optimal among the screened bases (Table 4.1, entry 32). Changing the light source to green LEDs (λ_{max} = 525 nm), a 23 W CFL or a 20 W blacklight did not improve the reaction efficiency (Table 4.1, entry 33–35). Next, we varied the stoichiometry of both reacting partners. Reduction of the equivalents of the enol carbamate (from 8 to 3) with respect to pyridine substrate had a detrimental effect on reaction efficiency (Table 4.1, entry 32, 36–38). However, employing the pyridine substrate and the carbamate in the opposite ratio did not improve the reaction efficiency (Table 4.1, entry 39). Degassing of the reaction mixture was very crucial for the reaction outcome (Table 4.1, entry 40). In another test, dilution of the reaction mixture had an adverse effect on the reaction efficiency (Table 4.1, entry 41). Upon enhancing the equivalents of HMDS, the reaction yield remained same, while reducing the amount of HMDS to 1.0 equivalent increased the reaction efficiency slightly (Table 4.1, entry 42–43). The reaction efficiency slightly dropped in the absence of HMDS (Table 4.1, entry 42). Finally, control reactions using the optimized conditions showed again that visible light is essential for the reaction (Table 4.1, entry 45–46). At the end of the optimization studies, we found diethyl

and morpholine carbamates to be suitable replacements for the 1-tetralone derived dimethyl carbamate, while pyrrolidine carbamate and pivalate analogs exhibited moderate efficiency (Table 4.1, entry 47–50).
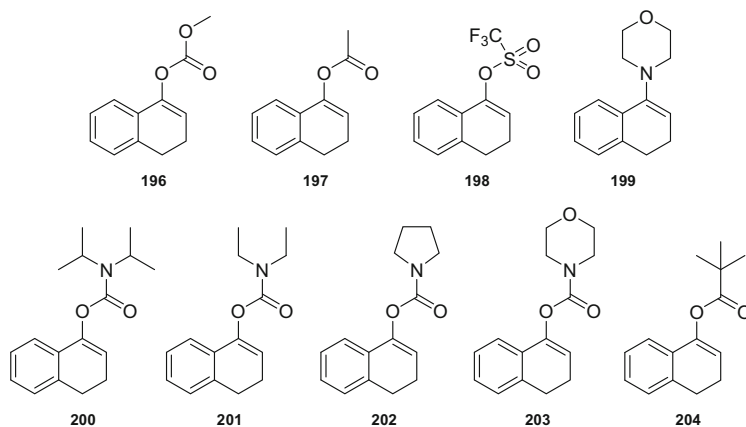
4.2.4   Scope and Limitations[1]

With the optimized reaction conditions in hand, we explored the scope and limitations of the developed transformation. The outcome of our investigations is summarized in Table 4.2.

In the first set of investigations, different ester-substituted indolizine derivatives were obtained in moderate to good yields, while a nitrile-substituted analog was also produced albeit in a poor yield (Table 4.2, **195**, **205**–**208**).

In a second set of investigations, we studied the effect of substituents on the 3-aryl ring of the indolizines, a sub-unit derived from the enol carbamate starting material. Substrates with both electron-rich and electron-deficient substituents were suitable for this transformation, but electron-rich substituents such as methyl and methoxy groups were better tolerated than electron-poor one (e.g. fluorine) (Table 4.2, **209**–**212**).

In a third set of investigations, we set out to explore the effect of substituents on the pyridyl ring of the indolizines. In previous reports, these substitution patterns have rarely been explored. To our delight, both electron-rich and electron-poor functional groups at the C-6 and C-7 positions of the indolizines were well tolerated

---

[1]A part of the substrate scope was carried out by Dr. Matthew N. Hopkinson (WWU Münster).

Table 4.1 Optimization studies[a]

Entry	Base (equiv.)	Solvent	Substrate 193 (equiv.)	Substrate (equiv.)	Light Source	Yield (%)[b]
1[c]	Na$_2$HPO$_4$ (2)	DMF	1	**194** (5)	Blue LEDs	62
2	Na$_2$HPO$_4$ (2)	DMF	1	**194** (5)	Blue LEDs	52
3	Na$_2$HPO$_4$ (2)	CH$_3$CN	1	**194** (5)	Blue LEDs	43
4	Na$_2$HPO$_4$ (2)	MeOH	1	**194** (5)	Blue LEDs	31
5	Na$_2$HPO$_4$ (2)	EtOAc	1	**194** (5)	Blue LEDs	50
6	Na$_2$HPO$_4$ (2)	DCE	1	**194** (5)	Blue LEDs	69
7	Na$_2$HPO$_4$ (2)	1,4-dioxane	1	**194** (5)	Blue LEDs	69
8	Na$_2$HPO$_4$ (2)	THF	1	**194** (5)	Blue LEDs	54
9	Na$_2$HPO$_4$ (2)	toluene	1	**194** (5)	Blue LEDs	50
10	Na$_2$HPO$_4$ (2)	PhCF$_3$	1	**194** (5)	Blue LEDs	74
11	Na$_2$HPO$_4$ (2)	PhCl	1	**194** (5)	Blue LEDs	62
12	Na$_2$HPO$_4$ (2)	pyridine	1	**194** (5)	Blue LEDs	–
13	Na$_2$HPO$_4$ (2)	PhCF$_3$	1	**196** (5)	Blue LEDs	20
14	Na$_2$HPO$_4$ (2)	PhCF$_3$	1	**197** (5)	Blue LEDs	6
15	Na$_2$HPO$_4$ (2)	PhCF$_3$	1	**198** (5)	Blue LEDs	–
16	Na$_2$HPO$_4$ (2)	PhCF$_3$	1	**199** (5)	Blue LEDs	4
17	Na$_2$HPO$_4$ (2)	PhCF$_3$	1	**200** (5)	Blue LEDs	56
18	K$_2$HPO$_4$ (2)	PhCF$_3$	1	**194** (5)	Blue LEDs	67
19	K$_3$PO$_4$ (2)	PhCF$_3$	1	**194** (5)	Blue LEDs	15
20	KOAc (2)	PhCF$_3$	1	**194** (5)	Blue LEDs	28
21	NaOAc (2)	PhCF$_3$	1	**194** (5)	Blue LEDs	46
22	Cs$_2$CO$_3$ (2)	PhCF$_3$	1	**194** (5)	Blue LEDs	35
23	K$_2$CO$_3$ (2)	PhCF$_3$	1	**194** (5)	Blue LEDs	39
24	Na$_2$CO$_3$ (2)	PhCF$_3$	1	**194** (5)	Blue LEDs	49
25	Li$_2$CO$_3$ (2)	PhCF$_3$	1	**194** (5)	Blue LEDs	54
26	KHCO$_3$ (2)	PhCF$_3$	1	**194** (5)	Blue LEDs	40
27	LiNTf$_2$ (2)	PhCF$_3$	1	**194** (5)	Blue LEDs	57
28	TEA (2)	PhCF$_3$	1	**194** (5)	Blue LEDs	29
29	DIPEA (2)	PhCF$_3$	1	**194** (5)	Blue LEDs	31
30	DIPA (2)	PhCF$_3$	1	**194** (5)	Blue LEDs	23
31	DBU (2)	PhCF$_3$	1	**194** (5)	Blue LEDs	–

(continued)

Table 4.1 (continued)

Entry	Base (equiv.)	Solvent	Substrate 193 (equiv.)	Substrate (equiv.)	Light Source	Yield (%)[b]
32	HMDS (2)	PhCF$_3$	1	**194** (5)	Blue LEDs	78
33	HMDS (2)	PhCF$_3$	1	**194** (5)	Green LEDs	–
34	HMDS (2)	PhCF$_3$	1	**194** (5)	23 W CFL	24
35	HMDS (2)	PhCF$_3$	1	**194** (5)	Black CFL	22
36	HMDS (2)	PhCF$_3$	1	**194** (3)	Blue LEDs	67
37	HMDS (2)	PhCF$_3$	1	**194** (4)	Blue LEDs	70
38	HMDS (2)	PhCF$_3$	1	**194** (8)	Blue LEDs	81
39	HMDS (2)	PhCF$_3$	3	**194** (1)	Blue LEDs	37
40[d]	HMDS (2)	PhCF$_3$	1	**194** (5)	Blue LEDs	52
41[e]	HMDS (2)	PhCF$_3$	1	**194** (5)	Blue LEDs	73
42	HMDS (3)	PhCF$_3$	1	**194** (5)	Blue LEDs	73
43	**HMDS (1)**	**PhCF$_3$**	**1**	**194 (5)**	**Blue LEDs**	**77**, 63[f]
44	–	PhCF$_3$	1	**194** (5)	Blue LEDs	60
45	HMDS (1)	PhCF$_3$	1	**194** (5)	–	1
46[g]	HMDS (1)	PhCF$_3$	1	**194** (5)	–	3
47	HMDS (1)	PhCF$_3$	1	**201** (5)	Blue LEDs	65[h]
48	HMDS (1)	PhCF$_3$	1	**202** (5)	Blue LEDs	49[h]
49	HMDS (1)	PhCF$_3$	1	**203** (5)	Blue LEDs	61[h]
50	HMDS (1)	PhCF$_3$	1	**204** (5)	Blue LEDs	36[h]

[a]Methyl 2-bromo-2-(pyridin-2-yl)acetate (**193**, 0.10 mmol), 3,4-dihydronaphthalen-1-yl dimethylcarbamate or other protected tetralone enol (**199** or **196–198** and **200–204**), the base and the solvent (1 mL) were added to a flame-dried Schlenk tube in the absence of light. The mixture was degassed with three freeze-pump-thaw cycles, flushed with argon, sealed and stirred at rt under visible light irradiation for 12 h

[b]GC yield using mesitylene as an internal reference

[c]The reaction was performed in the presence of [Ir(ppy)$_2$(dtbbpy)](PF$_6$) (2 mol%)

[d]The reaction was performed without degassing the solvent

[e]Solvent (2 mL, 0.05 M) was used

[f]Isolated yield on a 0.30 mmol scale

[g]The reaction mixture was heated at 80 °C in the dark

[h]Isolated yield on a 0.20 mmol scale

under the standard reaction conditions (Table 4.2, **213–220**). In products **218** and **214**, bromide and chloride functionalities would be potentially amenable for subsequent cross-coupling reactions. The product **214** was unambiguously characterized by single crystal X-ray structure analysis by Dr. Constantin G. Daniliuc (WWU Münster, Fig. 4.3). The indolizine product **221**, with an aryl substituent on the tether and product **222**, without any tether were both obtained in reasonable yields (Table 4.2, **221–222**). The dimethylcarbamate substrate derived from 1-indanone did not show any reactivity while the diethylcarbamate derived from 1-benzosuberone afforded only trace amounts of the corresponding product.

Table 4.2 Substrate scope of visible light-mediated indolizine synthesis[a]

195 (R[5] = Me) 63%
205 (R[5] = Et) 61%
206 (R[5] = [t]Bu) 45%
207 (R[5] = CH₂Ph) 48%

208
16%[b]

209
67%

210
61%[b]

211
67%[b]

212
38%[b]

213
68%

214
75%

215
42%

216
61%

217
65%

218 (R[6] = Br) 74%
219 (R[6] = F) 55%

220
65%

221
33%[b]

222
28%

223
0% (0%)[c]
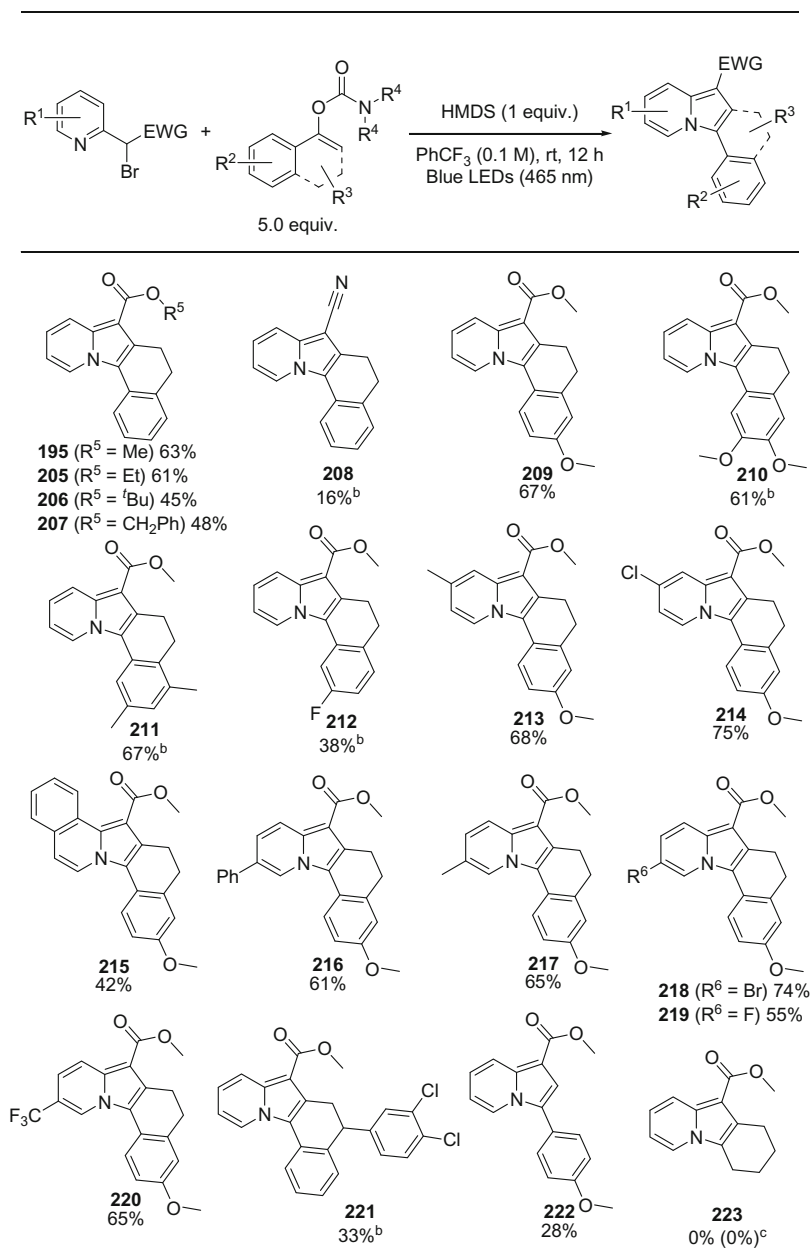
[a]Pyridine substrate (0.20 mmol), enol carbamate (1.00 mmol, 5.0 equiv.) and HMDS (0.20 mmol, 1.0 equiv.) were added to α,α,α-trifluorotoluene (0.1 M) in a flame-dried Schlenk tube under argon atmosphere. The reaction mixture was degassed three freeze-pump-thaw cycles. Then resulted mixture was irradiated with visible light from 5 W blue LEDs (λ_{max} = 465 nm) at rt for 12 h. R[4] = methyl unless otherwise stated

[b]R[4] = ethyl

[c]Reaction conducted in the presence of indolizine **195** (10 mol%)
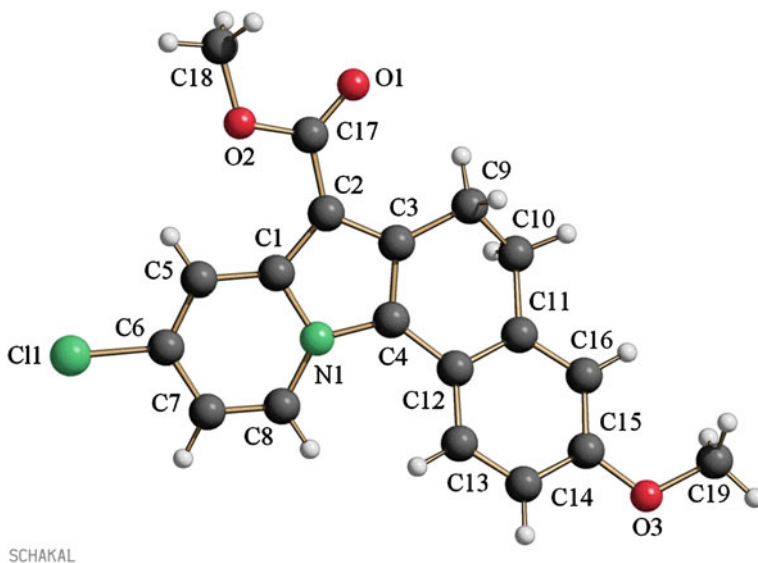
Fig. 4.3 Crystal structure of indolizine **214**

However, the dimethyl carbamate substrate without a stabilizing aryl group in conjugation with the C=C double bond did not show any desired reactivity, even in the presence of the pre-formed indolizine **195** (10 mol%), which may aid the progress of this reaction *(vide infra). In this method, unreacted excess carbamate substrates can be recovered.

4.2.5 Structural Manipulations of the Indolizine Product

To explore further the potential of the developed methodology, we carried out some structural modifications of the parent indolizine **195**. Since the indolizine **195** possesses an alkyl tether (–CH$_2$CH$_2$–), we sought to oxidize this tether to afford the corresponding alkene, thus delivering a fully aromatic derivative. When indolizine **195** was reacted with 1.0 equiv. of 2,3-dichloro-5,6-dicyano-1,4-benzoquinone (DDQ) in anhydrous toluene at 110 °C for 7 h, the expected fully oxidized unsaturated tetracyclic compound **224** was obtained in 71 % yield (Scheme 4.13a). In another follow-up reaction, the partially reduced tetra-substituted fused pyrrole derivative **225** was obtained in 96 %, when indolizine **195** was treated with Adams' catalyst (PtO$_2$) in glacial acetic acid under a hydrogen atmosphere (20 bar) at 25 °C for 40 h (Scheme 4.13b).
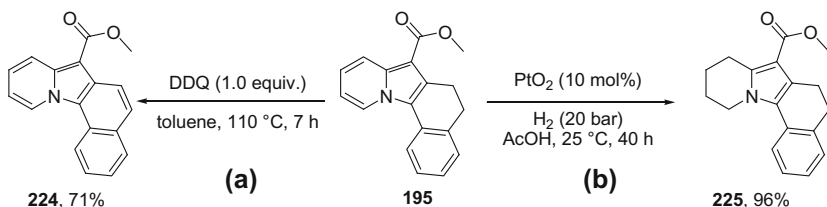
Scheme 4.13 Follow-up reactions of indolizine **195**: **a** Oxidation with DDQ and **b** PtO$_2$-catalyzed partial hydrogenation

4.2.6 Mechanistic Investigations[2]

In order to shed light on the mechanism of this reaction, we carried out various control experiments and spectroscopic and kinetics studies. In order to identify the photoactive species responsible for mediating the visible light-dependent process, absorption spectra were recorded for all the reaction components both in isolation and in combination. While the spectra for the substrates **193** (200 μM) and **194** (200 μM) and for the base HMDS (200 μM) did not reveal any notable visible light absorption, indolizine **195** (100 μM) was found to absorb significantly at the borderline of the UV and visible region with a maxima in the near UV at 340 nm and shoulders at 328 and 372 nm (Fig. 4.4a). Irradiating at either wavelength resulted in a detectable fluorescence emission at 442 nm (excited state lifetime, τ = 4 ns, recorded by L. Stegemann, WWU Münster, Figs. 4.4b and 6.11). In order to investigate whether an excited donor-acceptor complex (EDA complex or exciplex) may be being formed under the reaction conditions, the absorption spectra for a mixture of substrates **193** (100 mM), **201** (500 mM) and HMDS (100 mM) in PhCF$_3$ mimicking the concentration of the actual reaction were recorded (Fig. 4.5a). However, we did not observe the appearance of any new peak or note any shift of the peak position, suggesting that no exciplex is formed between these species. Moreover, we did not observe any significant coloration upon mixing all the reaction components together under degassed condition, which is an indicative feature of reactions proceeding via EDA formation (Fig. 4.5b) [57].

At this stage, we considered the possibility that the indolizine products themselves could act as photoactive mediators for their own formation. Stern-Volmer luminescence quenching experiments were performed with indolizine **195** at $\lambda_{em,max}$ = 442 nm (λ_{ex} = 372 nm). In these studies, significant quenching of the luminescence was observed with the brominated pyridine substrate **193**, while the enol carbamate substrate **194** and base HMDS remained innocent (Fig. 4.6). According to these experiments, if the indolizine product **195** serves as a photocatalyst, substrate **193** would quench the photo-excited photocatalyst to initiate the catalytic cycle.

[2]A part of the mechanistic studies was carried out by Dr. Matthew N. Hopkinson (WWU Münster).
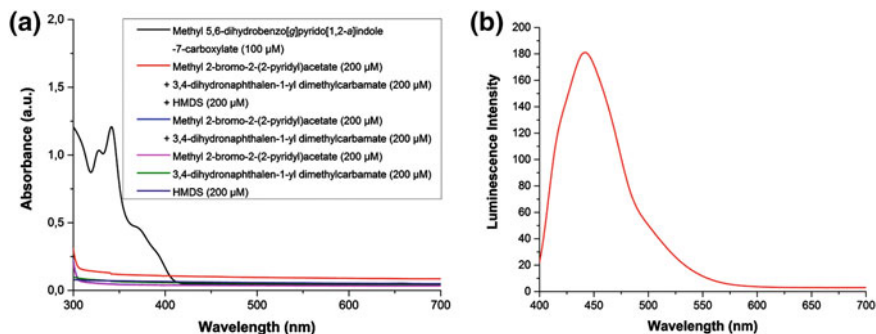
Fig. 4.4 a Absorption spectra of **195** (100 μM in PhCF$_3$), **193** (200 μM in PhCF$_3$), **194** (200 μM in PhCF$_3$), HMDS (200 μM in PhCF$_3$) and a mixture of all three compounds (200 μM in PhCF$_3$); **b** luminescence spectrum of **195** (100 μM in PhCF$_3$) at λ_{ex} = 372 nm. Absorbance is measured in arbitrary units (a.u.). Sahoo et al. [65]. Copyright Wiley-VCH Verlag GmbH & Co. KGaA. Reproduced with permission
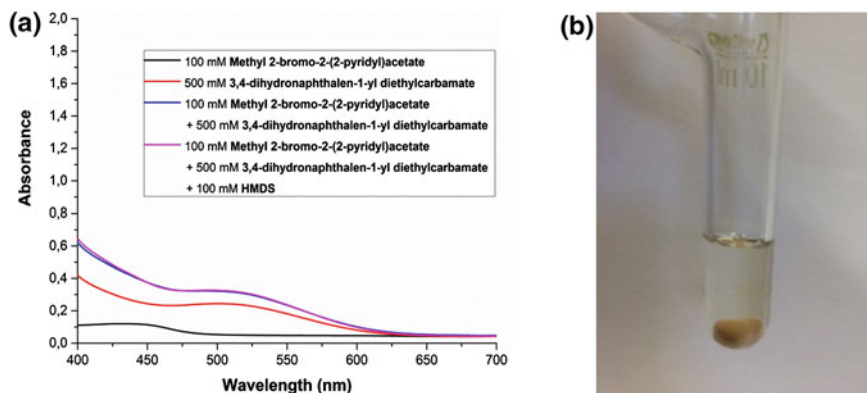
Fig. 4.5 a Absorption spectra of **193** (100 mM in PhCF$_3$), **201** (500 mM in PhCF$_3$), and a mixture of all three compounds (**193** (100 mM) + **201** (500 mM) + HMDS (100 mM) in PhCF$_3$); **b** visualization of the reaction mixture after stirring for 10 min under ambient light (*right*). Absorbance is measured in arbitrary units (a.u.)

Furthermore, a kinetic profile of the reaction, plotting of the yield of **195** as a function of the reaction time, revealed a parabolic curve consistent with the acceleration of the reaction rate as the product concentration increases over time (Fig. 4.7a). Furthermore, spiking the mixture with increasing amounts of pre-formed **195** led to a corresponding increase in the initial reaction rate (Fig. 4.7b, c). These sets of experiments suggest possible autocatalytic or autoinitiative behavior of the indolizine product.

The involvement of an autoinitiated or autocatalytic mechanism is an intriguing possibility. Autocatalytic reactions are of fundamental importance in chemistry as
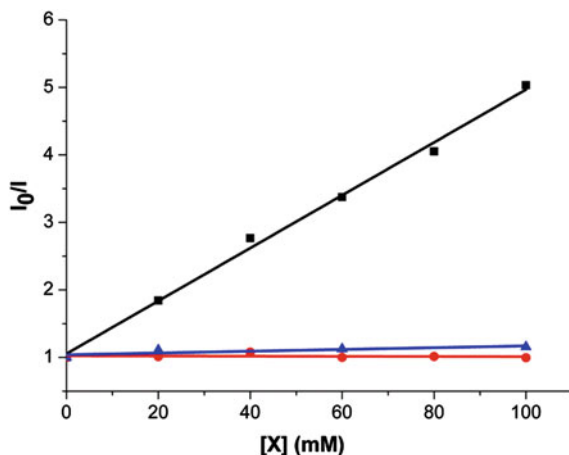
Fig. 4.6 Stern-Volmer luminescence quenching plots examining the 442 nm emission of indolizine **195** in PhCF$_3$ (1 mM), where **193** (*black square*), **194** (*blue triangle*) and HMDS (*red circle*). Sahoo et al. [65]. Copyright Wiley-VCH Verlag GmbH & Co. KGaA. Reproduced with permission
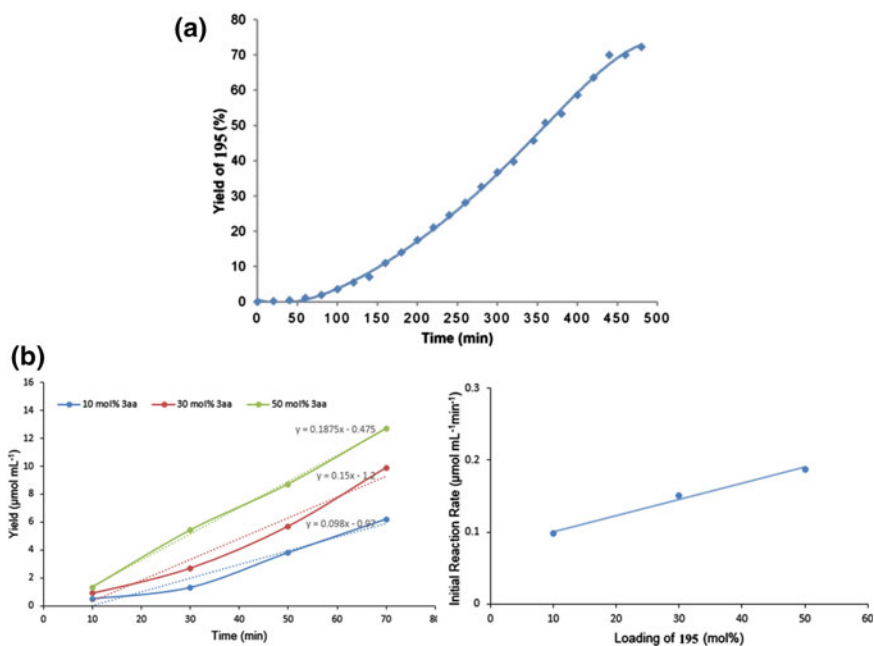
Fig. 4.7 a Kinetic profile of the reaction showing the yield of **195** as a function of time. **b** Effect of spiking the reaction with 10, 30 or 50 mol% of **195** on the initial reaction rate. The *left* graph shows the yield expressed as the concentration of **195** minus the initial added amount as a function of time over the first 70 min for each reaction. The graph on the *right* is a plot of the initial rate of each reaction against the loading of **195**. Sahoo et al. [65]. Copyright Wiley-VCH Verlag GmbH & Co. KGaA. Reproduced with permission

Fig. 4.8 Cyclic
voltammogram of **195** in
0.1 M TBA.BF$_4$/CH$_3$CN.
Scan rate = 0.05 V/s and
voltage range = 0.0–1.5 V.
Sahoo et al. [65]. Copyright
Wiley-VCH Verlag GmbH &
Co. KGaA. Reproduced with
permission
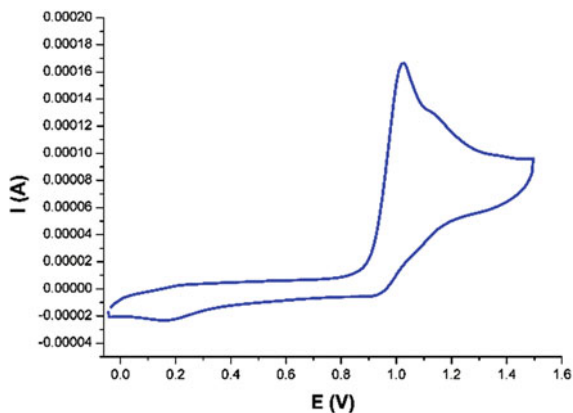
they enable compounds to self-replicate and multiply [58]. Accordingly, auto-catalysis is widely believed to have been instrumental in the emergence of life on earth, with the autocatalytic amplification of enantiomeric excess as demonstrated experimentally by Soai and co-workers explaining the origin of biological homochirality [59, 60]. Photochemical autocatalytic reactions are, however, scarce with only a few examples having been reported notably in the context of signal amplification [61–63].

In order to gain insight into the redox activity of the indolizine **195**, a cyclic voltammetric measurement (CV) was conducted in 0.1 M TBA.BF$_4$/CH$_3$CN revealed the presence of an oxidation wave at around 0.9 V versus Ag/AgCl (Fig. 4.8). However, the irreversible nature of the wave implies that the indolizine probably decomposes once oxidized. Oxidative quenching of the indolizine by the brominated pyridine **193** would presumably lead therefore to the concurrent decomposition of a molecule of the indolizine. However, if an efficient chain mechanism is operating, the amount of indolizine product generated would exceed the amount consumed as a result of initiation.

Inspired by above Stern-Volmer luminescence quenching and kinetic studies, we were curious to test the potential of the indolizine product as photocatalyst/photoinitiator to promote other reactions. As a proof of concept, we conducted the visible light photoredox-catalyzed alkylation of indoles, originally reported by Stephenson and co-workers using [Ru(bpy)$_3$]$^{2+}$ with indolizine **195** [64]. When diethyl 2-bromomalonate was reacted with *N*-methyl indole in the presence of indolizine **195** (10 mol%) under visible light irradiation from 5 W blue LEDs (λ_{max} = 465 nm), the desired alkylated product **18** was obtained in 45 % isolated yield (Scheme 4.14). Control experiments confirmed the necessity of indolizine **195** as well as light (Scheme 4.14).

Although from all these experiments it appears that indolizine **195** is itself involved in this process, we did not observe any significant absorption by the indolizine product at wavelengths consistent with the emission range of the 5 W blue LEDs (λ_{max} = 465 nm) used in these studies (for comparison see Fig. 4.4a
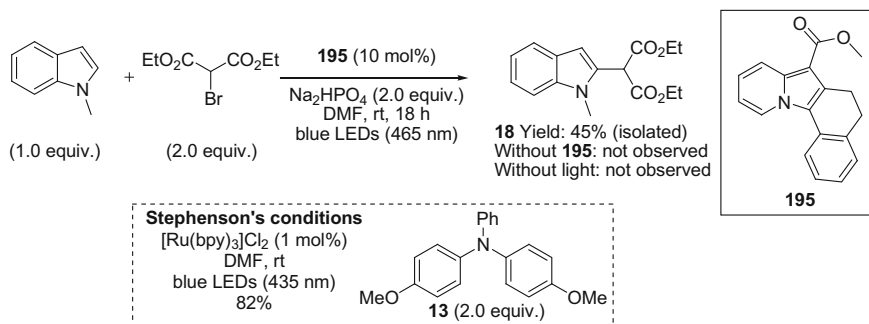
Scheme 4.14 Application of indolizine **195** as a photocatalyst in the visible light-mediated alkylation of *N*-methylindole
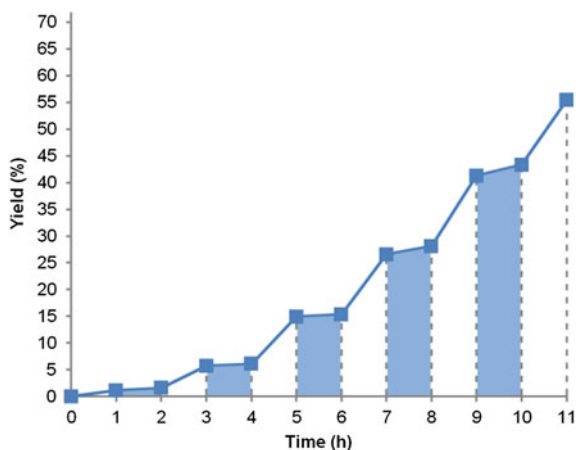
Fig. 4.9 Yield of **195** measured at different times after periods of visible light irradiation and periods of darkness. The *blue shaded* areas represent periods in the dark while the *unshaded* regions show periods under light irradiation. Sahoo et al. [65]. Copyright Wiley-VCH Verlag GmbH & Co. KGaA. Reproduced with permission

and 6.3). In fact, the luminescence of indolizine **195** (λ_{em} = 442 nm) occurs at a shorter wavelength than the emission maximum of the employed light source. As such, we speculate that an as yet unidentified photoactive species derived from the indolizine product might be responsible for catalyzing or initiating this visible light-mediated process.

In order to verify the requirement for continuous light irradiation, a light off-on experiment was conducted (Fig. 4.9). Switching off the light source during the light-mediated synthesis of **195** results in a significant dropping off of the reaction efficiency, which can then be readily restarted by turning the light back on. As

represented in Fig. 4.9, simple regulation of the light irradiation allows for control over the reaction progress. It is important to note, however, that the requirement for continuous light irradiation does not mean that no radical chain mechanism is operating. The timescale of radical chain processes is very short and, as such a similar reaction profile would be observed during a light off-on experiment as no new chains would be initiated in the absence of light.

Since most visible light photoredox-catalyzed reactions proceed via a radical pathway, we performed our reaction in the presence of the radical scavengers 2,2,6,6-tetramethyl-1-piperidinyloxy (TEMPO) and 2,6-di-*tert*-butyl-α-(3,5-di-*tert*-butyl-4-oxo-2,5-cyclohexadien-1-ylidene)-*p*-tolyloxy (galvinoxyl). These additives resulted in the complete shutdown of reactivity, indicating the involvement of radical intermediates. During the reaction with TEMPO, peaks consistent with adducts (**226** and **227**) between the radical scavenger and two different proposed radical intermediates **B** and **C** were detected by ESI mass analysis (Fig. 4.10) (Scheme 4.15).

The full mechanism of this reaction remains ambiguous and further studies would be required to gain complete insight into the nature of the photoactive species and its method of operation. At this stage, a radical chain process involving the key intermediates **B** and **C** seems to be the major pathway with subsequent aromatization leading to the indolizine products (Scheme 4.11). The key question still to be answered concerns the initiation of this cycle with all the data obtained to date indicating that the indolizine product is in some way involved. The absorption spectrum of the product itself, however, would seem to rule out the direct excitation of the indolizine and an as yet identified derivative of it may instead be acting as a photoinitiator.

4.3   Summary

In summary, we have developed a novel methodology for the synthesis of valuable polycyclic indolizines under visible light-mediated reaction conditions. In this methodology, no additional reagents are required to activate the substrates. Diverse substitution patterns on the pyridine, pyrrole and aryl rings are tolerated under these mild reaction conditions, which highlights the synthetic potential of this method. In addition, this reaction represents transition metal-free approach to access indolizines and thus avoids practical complications in the context of pharmaceutical or industrial applications arising from metal contamination. Furthermore, structural manipulations of the indolizines to afford other *N*-heterocyclic compounds increase the value of these products. In order to shed light on the mechanism, various analytical and laboratory experiments were carried out with the kinetic profile of the reaction, a photochemical analysis of the reaction components and the apparent photocatalytic ability of the indolizine in an unrelated visible light-mediated

226
$[M+Na]^+$: $C_{17}H_{26}N_2O_3Na^+$
calculated m/z: 329,18356
measured m/z: 329,18272

227
$[M+Na]^+$: $C_{30}H_{41}N_3O_5Na^+$
calculated m/z: 546.29384
Measured m/z: 546.29314
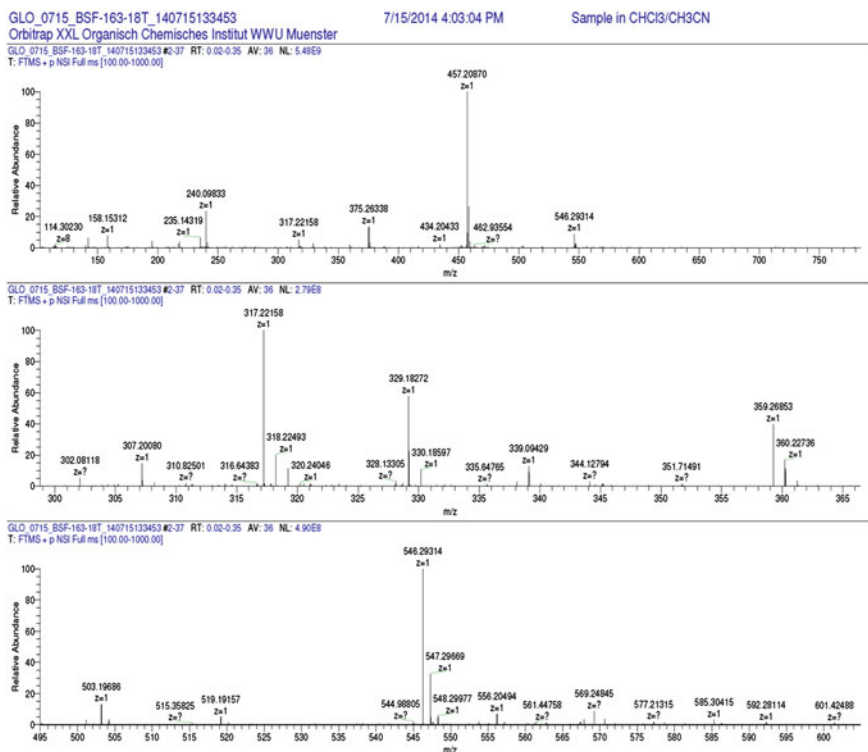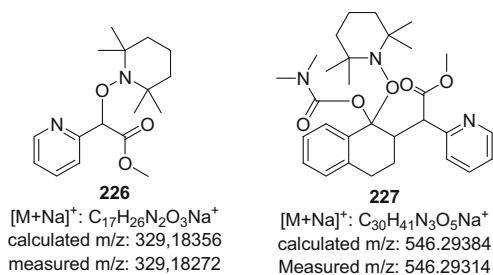
Fig. 4.10 Nanospray ESI mass spectrometry analysis of the reaction conducted in the presence of TEMPO. Two peaks consistent with adducts (**226** and **227**) between TEMPO and proposed radical intermediates **B** and **C** were detected. Sahoo et al. [65]. Copyright Wiley-VCH Verlag GmbH & Co. KGaA. Reproduced with permission

reaction indicating the involvement of the indolizine products as being in some way responsible for their own formation. Further insightful studies will be required, however, to fully elucidate the reaction mechanism. Overall, this procedure benefits from mild reaction conditions such as the use of cost effective, energy-efficient commercial visible light sources without additional reagents. Moreover, its
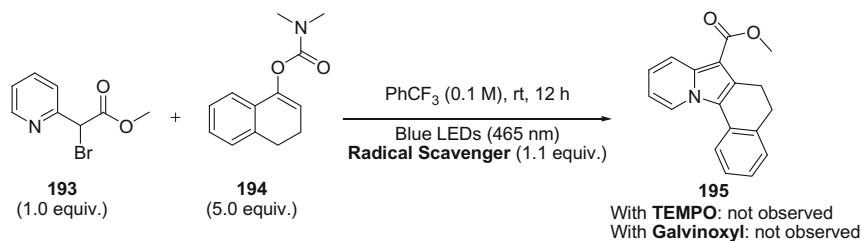
Scheme 4.15 Radical trapping experiments: reactions performed in the presence of TEMPO and galvinoxyl

intriguing mechanism with the suggestion of autocatalytic behavior could open up new areas of photocatalysis research.

References

1. M.H. Palmer, D. Leaver, J.D. Nisbet, R.W. Millar, R. Egdell, J. Mol. Struct. **42**, 85–101 (1977)
2. M. Shipman, Sci. Synth. **10**, 745–787 (2000)
3. W.L. Mosby, *Heterocyclic Systems with Bridgehead Nitrogen Atoms: Part One* (Interscience, New York, 1961), p. 239
4. C.-H. Park, V. Ryabova, I.V. Seregin, A.W. Sromek, V. Gevorgyan, Org. Lett. **6**, 1159–1162 (2004)
5. V.V. Simonyan, A.I. Zinin, E.V. Babaev, K. Jug, J. Phys. Org. Chem. **11**, 201–208 (1998)
6. G.S. Singh, E.E. Mmatli, Eur. J. Med. Chem. **46**, 5237–5257 (2011)
7. V.R. Vemula, S. Vurukonda, C.K. Bairi, Int. J. Pharm. Sci. Rev. Res. **11**, 159–163 (2011)
8. V. Sharma, V. Kumar, Med. Chem. Res. **23**, 3593–3606 (2014)
9. W.B. Harrell, R.F. Doerge, J. Pharm. Sci. **56**, 225–228 (1967)
10. D.A. James, K. Koya, H. Li, G. Liang, Z. Xia, W. Ying, Y. Wu, L. Sun, Bioorg. Med. Chem. Lett. **18**, 1784–1787 (2008)
11. Y.-M. Shen, P.-C. Lv, W. Chen, P.-G. Liu, M.-Z. Zhang, H.-L. Zhu, Eur. J. Med. Chem. **45**, 3184–3190 (2010)
12. A. Boot, A. Brito, T. van Wezel, H. Morreau, M. Costa, F. Proença, Anticancer Res. **34**, 1673–1677 (2014)
13. J.H.C. Nayler, Chem. Abstr. **72**, 55285 (1970)
14. L.-L. Gundersen, C. Charnock, A.H. Negussie, F. Rise, S. Teklu, Eur. J. Pharm. Sci. **30**, 26–35 (2007)
15. O.B. Østby, B. Dalhus, L.-L. Gundersen, F. Rise, A. Bast, R.M. Guido, M. Haenen, Eur. J. Org. Chem. **2000**, 3763–3770 (2000)
16. J. Gubin, J. Lucchetti, J. Mahaux, D. Nisato, G. Rosseels, M. Clinet, P. Polster, P. Chatelain, J. Med. Chem. **35**, 981–988 (1992)
17. W. Mederski, N. Beier, L.T. Burgdorf, R. Gericke, M. Klein, C. Tsaklakidis, Google Patents (2012)
18. S. Chen, Z. Xia, M. Nagai, R. Lu, E. Kostik, T. Przewloka, M. Song, D. Chimmanamada, D. James, S. Zhang, J. Jiang, M. Ono, K. Koya, L. Sun, MedChemComm **2**, 176–180 (2011)
19. H. Li, Z. Xia, S. Chen, K. Koya, M. Ono, L. Sun, Org. Process Res. Dev. **11**, 246–250 (2007)

20. L.-L. Gundersen, K.E. Malterud, A.H. Negussie, F. Rise, S. Teklu, O.B. Østby, Biorg. Med. Chem. **11**, 5409–5415 (2003)
21. S. Teklu, L.-L. Gundersen, T. Larsen, K.E. Malterud, F. Rise, Biorg. Med. Chem. **13**, 3127–3139 (2005)
22. J.P. Michael, Nat. Prod. Rep. **24**, 191–222 (2007)
23. J.P. Michael, Nat. Prod. Rep. **25**, 139–165 (2008)
24. E. Kim, M. Koh, J. Ryu, S.B. Park, J. Am. Chem. Soc. **130**, 12206–12207 (2008)
25. E. Kim, M. Koh, B.J. Lim, S.B. Park, J. Am. Chem. Soc. **133**, 6642–6649 (2011)
26. E. Kim, Y. Lee, S. Lee, S.B. Park, Acc. Chem. Res. **48**, 538–547 (2015)
27. B. Liu, Z. Wang, N. Wu, M. Li, J. You, J. Lan, Chem. Eur. J. **18**, 1599–1603 (2012)
28. M. Becuwe, D. Landy, F. Delattre, F. Cazier, S. Fourmentin, Sensors **8**, 3689 (2008)
29. J. Huckaba, F. Giordano, L.E. McNamara, K.M. Dreux, N.I. Hammer, G.S. Tschumper, S.M. Zakeeruddin, M. Grätzel, M.K. Nazeeruddin, J.H. Delcamp, Adv. Energy Mater. (2015). doi:10.1002/aenm.201401629
30. Y. Tominaga, Y. Shiroshita, T. Kurokawa, H. Gotou, Y. Matsuda, A. Hosomi, J. Heterocycl. Chem. **26**, 477–487 (1989)
31. Ber Angeli, Dtsch. Chem. Ges. **23**, 1793–1797 (1890)
32. Ber Angeli, Dtsch. Chem. Ges. **23**, 2154–2160 (1890)
33. M. Scholtz, Ber. Dtsch. Chem. Ges. **45**, 734–746 (1912)
34. E. Tschitschibabin, F.N. Stepanow, Ber. Dtsch. Chem. Ges. **62**, 1068–1075 (1929)
35. E. Tschitschibabin, Ber. Dtsch. Chem. Ges. **60**, 1607–1617 (1927)
36. T. Uchida, K. Matsumoto, Synthesis **1976**, 209–236 (1976)
37. D.E. Ames, T.F. Grey, W.A. Jones, J. Chem. Soc. 620–622 (1959)
38. V.S. Venturella, J. Pharm. Sci. **52**, 868–871 (1963)
39. T. Melton, D G. Wibberley, J. Chem. Soc. C. 983–988 (1967)
40. K.R. Kallay, R.F. Doerge, J. Pharm. Sci. **61**, 949–951 (1972)
41. V. Boekelheide, K. Fahrenholtz, J. Am. Chem. Soc. **83**, 458–462 (1961)
42. E. Henrick, W. Ritchie, Taylor. Aust. J. Chem. **20**, 2467–2477 (1967)
43. Y. Kobayashi, I. Kumadaki, Y. Sekine, T. Kutsuma, Chem. Pharm. Bull. **21**, 1118–1123 (1973)
44. F. Kröhnke, W. Zecher, Chem. Ber. **95**, 1128–1137 (1962)
45. W. Adamson, P.A. Barrett, J.W. Billinghurst, T.S.G. Jones, J. Chem. Soc. 312–324 (1958)
46. F. Pratt, J.C. Keresztesy, J. Org. Chem. **32**, 49–53 (1967)
47. R. Bonneau, Y.N. Romashin, M.T.H. Liu, S.E. MacPherson, J. Chem. Soc. Chem. Commun. 509–510 (1994)
48. S. Chuprakov, F.W. Hwang, V. Gevorgyan, Angew. Chem. Int. Ed. **46**, 4757–4759 (2007)
49. N. Pandya, J.T. Fletcher, E.M. Villa, D.K. Agrawal, Tetrahedron Lett. **55**, 6922–6924 (2014)
50. L. Xiang, Y. Yang, X. Zhou, X. Liu, X. Li, X. Kang, R. Yan, G. Huang, J. Org. Chem. **79**, 10641–10647 (2014)
51. S. Tang, K. Liu, Y. Long, X. Gao, M. Gao, A. Lei, Org. Lett. **17**, 2404–2407 (2015)
52. R.-R. Liu, J.-J. Hong, C.-J. Lu, M. Xu, J.-R. Gao, Y.-X. Jia, Org. Lett. **17**, 3050–3053 (2015)
53. D. Liégault, L. Lapointe, A. Caron, K.Fagnou Vlassova, J. Org. Chem. **74**, 1826–1834 (2009)
54. Org Zhao, Org. Biomol. Chem. **10**, 7108–7119 (2012)
55. H. Hu, Y. Liu, J. Xu, Y. Kan, C. Wang, M. Ji, RSC Adv. **4**, 24389–24393 (2014)
56. M. J. O'Neil (ed.), *The Merck Index—An Encyclopedia of Chemicals, Drugs, and Biologicals*, 13 ed. (Whitehouse Station, NJ, Merck and Co., Inc., 2001), p. 837
57. E. Arceo, I.D. Jurberg, A. Álvarez-Fernández, P. Melchiorre, Nat. Chem. **5**, 750–756 (2013)
58. J. Bissette, S.P. Fletcher, Angew. Chem. Int. Ed. **52**, 12800–12826 (2013)
59. K. Soai, T. Shibata, H. Morioka, K. Choji, Nature **378**, 767–768 (1995)
60. G. Blackmond, Proc. Natl. Acad. Sci. **101**, 5732–5736 (2004)
61. J.-I. Hong, Q. Feng, V. Rotello, J. Rebek, Science **255**, 848–850 (1992)
62. R. Kottani, J.R.R. Majjigapu, A. Kurchan, K. Majjigapu, T.P. Gustafson, A.G. Kutateladze, J. Am. Chem. Soc. **128**, 14794–14795 (2006)

63. R. Thapaliya, S. Swaminathan, B. Captain, F.M. Raymo, J. Am. Chem. Soc. **136**, 13798–13804 (2014)
64. L. Furst, B.S. Matsuura, J.M.R. Narayanam, J.W. Tucker, C.R.J. Stephenson, Org. Lett. **12**, 3104–3107 (2010)
65. B. Sahoo, M. N. Hopkinson, F. Glorius, External-photocatalyst-free visible-light-mediated synthesis of indolizines. Angew. Chem. Int. Ed. **54**, 15545–15549 (2015)

Chapter 5
Synthesis and Characterizations of Novel Metal-Organic Frameworks (MOFs)

5.1 Intoduction

5.1.1 Historical Background

Metal-organic frameworks (MOFs) are an exciting class of porous crystalline materials. Although crystalline materials have received the attention of scientists since 1960s [1], the concept of metal-organic frameworks (MOFs) began to be popularized in 1990s [2, 3]. Metal-organic frameworks (MOFs) are highly crystalline, porous inorganic and organic hybrid materials with a giant network structure in contrast to purely inorganic zeolites, molecular sieves and purely organic activated carbons. These hybrid materials are composed of inorganic metal ions or clusters and organic spacer molecules. An inorganic metal ion or cluster is called a 'node', while an organic spacer molecule is known as a 'linker or rod'. Although the syntheses of MOFs were initiated in the early 1990s [2, 3], it was not until 1999 that the first highly porous and remarkably stable MOF (assigned as MOF-5) was synthesized by Yaghi et al. [4]. According to this report, MOF-5, with the chemical composition Zn_4O $(BDC)_3 \cdot (DMF)_8 (C_6H_5Cl)$ (BDC = benzene-1,4-dicarboxylate), was prepared by treating zinc nitrate $(Zn(NO_3)_2)$ with H_2BDC in DMF/chlorobenzene (Fig. 5.1) [4, 5]. Since then this field has grown extensively, capturing the attention of many scientists. Outstanding performances of these porous materials in various applications highlight the need to further develop this emerging field [6, 7].

5.1.2 General Characteristic Features of Metal-Organic Frameworks (MOFs)

In general, metal-organic frameworks (MOFs) are highly porous (up to 90 % free volume), crystalline and thermally stable materials with a large internal surface area
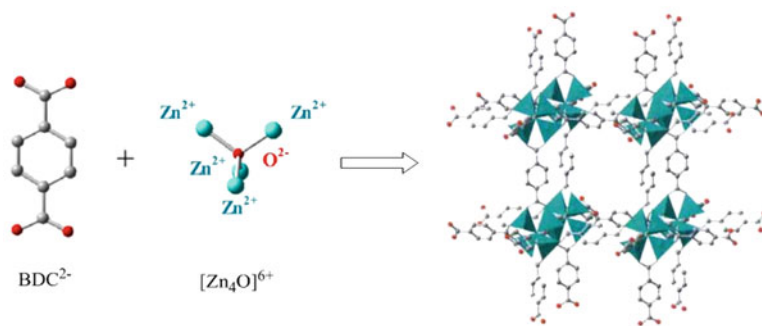
Fig. 5.1 Synthesis of MOF-5 from benzene-1,4-dicarboxylate (BDC) (linker) and tetra-zinc oxo cluster (Zn_4O) (node), generated in situ from $Zn(NO_3)_2$. Adapted from Ref. [5] with the permission of Gesellschaft Deutscher Chemiker (GDCh)

(up to 6000 m^2/g) [8]. Since MOFs are hybrid materials consisting of inorganic nodes and organic linkers, rational design could be used to predict the possibilities for their construction. Reticular chemistry, which involves the principles of precise design and successful synthesis of materials derived from secondary building units connected by stronger chemical bonds is applied to the construction of metal-organic frameworks [9]. These materials can be synthesized using various metal ions (e.g. Al, Zr, Cr, Fe, Ni, Cu, Zn, etc.) and organic linkers (i.e. polycar-boxylates, sulfonates, phosphonates, imidazolates, pyridines, etc.) by tailor made syntheses [8]. Various secondary building units (SBUs) (e.g. tetrahedral, octahe-dral, cubic, rhombic dodecahedron, etc.) can be built up in situ by choosing the proper metal ion and reaction conditions [9, 10]. In addition, careful selection of organic linkers with the ideal spacer length and donor group provides a platform for modular synthesis of a wide spectrum of isoreticular MOFs with large pores for accommodation of guest molecules and large window for their inclusion process. Longer linkers sometimes result in interpenetration of one unit cell into others and result in blocking of the cavity (Fig. 5.2c). However, the use of a mixture of linkers in a certain ratio represents useful approach to tune the cavity and window size. The mixed linker strategy provides access to MOF materials with cavities of different shapes and sizes existing in same 3D network structure, which is beneficial for tuning selectivity. In this context, one of the interesting features of MOF materials is that a minor change in the metal precursor, organic linker or synthesis conditions can result in a dramatic change in structural properties such as topology, cavity size, etc. and sometimes prevents interpenetration. In application perspective, larger cavities with void space are highly desirable for application in storage of gases and liquids, separation and catalysis through host-guest interactions. In addition, ther-mal and chemical stabilities of these materials are crucial to their performance in reactions conducted inside the cavity and recyclability. Apart from these features, one of the serious concerns regarding MOF chemistry is the stability of the frameworks upon activation prior to their use it is necessary to remove solvent
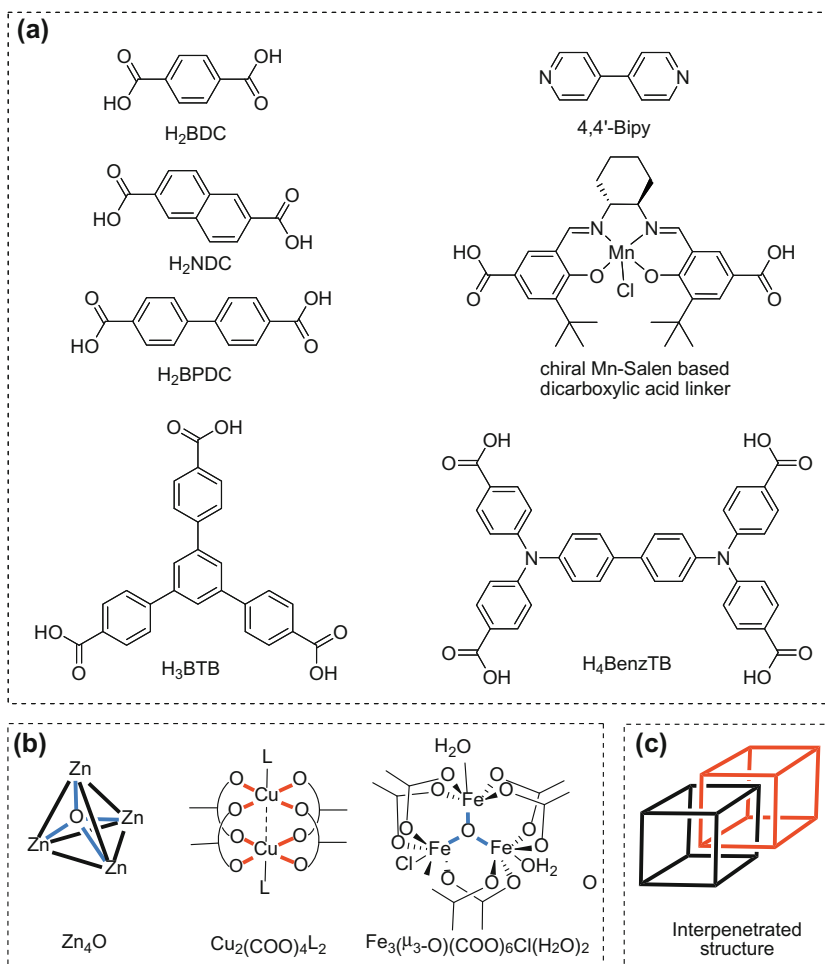
Fig. 5.2 a Selected examples of ditopic, tritopic and tetratopic organic linkers; **b** selected examples of nodes with different geometries; **c** representation of unit cells of an interpenetrated MOF

molecules or reagents under vacuum from the cavity of the MOFs as synthesized and sometimes leads to undesired decomposition. Therefore, special techniques such as supercritical drying must be applied in MOF activation in these situations. In some MOFs, this form of activation allows for the retention of the framework geometry and results in vacant coordination sites for the activation of substrates towards catalysis.

5.1.3 Applications of Metal-Organic Frameworks (MOFs)

MOFs have fascinated scientists from academia to industry due to their characteristic ultraporosity, high crystallinity, exceptionally large internal surface area (up to 6000 m^2/g) and thermal and chemical stabilities [6–8]. Effective activation of MOFs removes all the blockages (mostly solvents) from the cavities and channels to obtain a large amount of void space, up to 90 % [8]. These materials can be used as portable storage devices for fuel gases such as hydrogen [11, 12], methane [13, 14] and acetylene [15]. In addition, MOFs can be used for gas capture (e.g. carbon dioxide) [16] as well as purifications and separations of chemical mixtures in gaseous phase, vapor phase or liquid phase. Even structural isomers such as xylenes [17, 18], and hexanes [19], which are very hard to separate by other means, as well as stereoisomers (e.g. enantiomers and cis-trans isomers) can be separated with the MOFs [20, 21]. The absorption capacity of MOFs can be improved by tuning the physicochemical properties of the internal surface. In this purpose, molecular simulations are very helpful in understanding the interactions between absorbed species and MOF interiors on a molecular level, which can not be observed experimentally [22].

In addition, MOF materials are being explored as chemical sensors to detect gases and volatile analytes with high sensitivity and selectivity [23]. Due to the tunability of MOF structures as well as their properties, the use of these materials is advantageous compared to the known classes of chemosensors. Metal-organic frameworks, especially MOF films, can be used as chemical sensors in chemical threat detection, industrial process management, food quality determination, and medical diagnostics [23].

Recently, significant advances have been made in the field of luminescent MOF chemistry. Hundreds of luminescent MOFs have been reported in the literature [24, 25]. Direct excitation of highly conjugated organic linkers, metal-centered emission via antenna effect (mostly lanthanide based MOFs), charge transfer via metal to ligand charge transfer (MLCT) or ligand to metal charge transfer are mostly responsible for the luminescence behavior of the metal-organic frameworks and sometimes guest induced luminescence of MOFs is also possible [24, 25]. These luminescent MOFs are generally used in chemical sensing as luminescence sensors, electroluminescent devices, nonlinear optics, biomedical imaging and photocatalysis [24, 25]. Recently, noncentrosymmetric MOF synthesis has received the attention of scientists for their second-order nonlinear optics (NLO) [26].

MOFs can be used as drug delivery systems by carrying and releasing drug molecules the destination cells [27]. For this purpose, therefore, MOFs and their individual components should be non-toxic. Moreover, these bioactive MOFs have to be mechanically and chemically stable to both acidic (stomach) and basic (intestine) conditions [27]. Oral administration of MOFs in the form of tablets [e.g. tablet of ibuprofen containing MIL-53(Fe) and MIL-100(Fe) (MIL = Materials of Institut Lavoisier)], powders, pellets or gels have been successful [27].

In another major application, metal-organic frameworks have recently been employed in heterogeneous catalysis [28–31]. Catalytically active MOFs serve as shape and size selective catalysts. In these materials, catalytic centers are immobilized by the organic linkers or nodes. The stability of the framework and accessibility of the large cavity define the MOF reactivity. In this context, to access the cavity, window size should be wide enough and channels should be free for transport of substrates and products. With the increasing demand for enantiopure chiral compounds, asymmetric catalysis has captured the interest of scientists for few decades. Since MOF catalysis reactions take place inside the cavity, chiral modification of the MOF cavity would provide a chiral environment for asymmetric induction [29, 30].

Thanks to these exciting applications, in recent days, MOF materials are extensively being used in industry in various purposes [6, 7].

5.1.4 Synthesis of Metal-Organic Frameworks (MOFs)

Due to the great applications over the last 20 years, MOF synthesis has received the attention of synthetic and material chemists [3]. During the MOF synthesis, many parameters must be taken into consideration such as molar ratio of the starting materials (in particular for mixed MOF synthesis), solvent, temperature, pressure, reaction time and also pH of the reaction medium. Although it is said that MOF materials can be rationally designed, practical rational designs do not always give the expected results experimentally, but rather move inspire the research. The conventional synthesis, including solvothermal and nonsolvothermal procedures, of MOFs is conducted under thermal conditions without any parallelization. In solvothermal synthesis, reactions are performed at high temperatures (higher than the boiling point of solvent) and under high pressure in closed vessels. In nonsolvothermal synthesis, on the other hand, reactions are carried out at solvent's boiling point or even lower temperatures at ambient pressure. There has been a trend to develop synthetic protocols for the synthesis of different MOFs starting from same reaction ingredients. Although the MOF starting materials are the same, different protocols provide MOFs with different yields, structural morphologies and particle sizes. In addition to conventional synthesis, many impressive alternative synthetic routes have been developed with the progress of this growing field. Alternative routes are divided into four different categories based on the energy applied in the synthesis: (a) microwave-assisted synthesis [32], (b) electrochemical synthesis [33], (c) mechanochemical synthesis [34], and (d) sonochemical synthesis [3, 35]. To accelerate the discovery of MOFs, high-throughput screening methods are used in parallel to systematic study [3]. Up-scaling of the synthesis, for large scale production, can be achieved. However, obtaining phase pure crystalline materials is difficult in MOF research. Use of modulators sometimes helps in obtaining better crystals.

In solvothermal synthesis of MOFs, sensitive functional groups do not survive under harsh reaction conditions, thus limiting the scope of functional groups that can be incorporated into the MOF. Instead, these sensitive functional groups can be incorporated into MOFs via postsynthetic modifications under relatively mild conditions through single crystal to single crystal transformations (Fig. 5.3) [36–38]. Postsynthetic modifications via a change in host-guest interaction have become an enabling technology for the fine tuning of the physicochemical properties of metal-organic frameworks.

Many research groups around the world including Cohen and co-workers as leading group have devoted substantial amount of time researching the postsynthetic modification of MOFs. Although Cohen and co-workers reinitiated the study of this field and explored extensively, our group recently disclosed an elegant method for palladium catalyzed efficient, selective and mild C–H bond functionalization of an indole-based linker in a MOF via postsynthetic modification (Scheme 5.1) [39].

Since organic linkers are an essential counterpart of MOF skeletons and many important outcomes arise from the modifications of these linkers, the rational design and synthesis of organic linkers is one of the most important aspects of MOF research. In this line of research, it is important to consider the steric, electronic and stereoelectronic properties of the organic linker in order to modify physicochemical
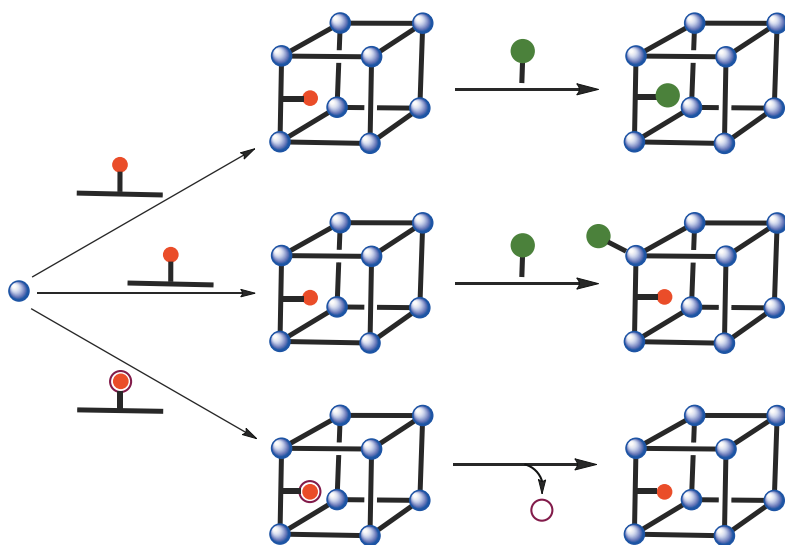
Fig. 5.3 Representations of three different types of postsynthetic modifications with cartoons [38]. All the linkers in each simplified MOF unit are same
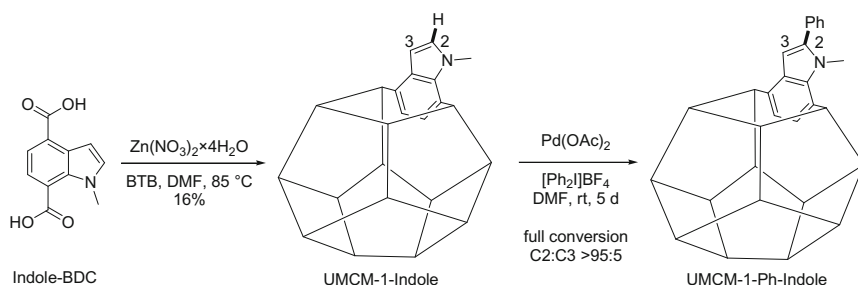
Scheme 5.1 UMCM-1-indole synthesis and its postsynthetic modification via C–H functionalization [39]. *BTB* benzene-1,3,5-tribenzoate; *UMCM* University of Michigan crystalline material

properties of MOFs (interior of the MOF cavity, the strength of adsorption of MOF, the thermal and chemical stability, etc.). Benzene-1,3,5-tribenzoic acid (BTB) is a tritopic organic linker which has been incorporated into many MOFs. BTB is versatile as it can be used alone or in a combination with other linkers. The BTB unit in pure and substituted forms exists in 411 crystal structures [40]. However, in many of these cases, BTB molecule is a co-linker used in combination with other functionalized linkers, giving rise to mixed linker MOFs with tunable structural properties. There have been a substantial number of reports describing the successful modifications of BTB by incorporation of various functional group [41–43], replacement of the middle benzene ring with other elements (e.g. N) [44], with other aromatic motifs (e.g. 1,3,5-triazene) [45–47].

Recently, 4,4′,4″-tricarboxylatetriphenylamine (TPA) linker with a BDC co-linker as well as 4,4′,4″-s-triazene-2,4,6-triyl-tribenzoate (TATB) with no co-linker have been incorporated into UMCM-4 (UMCM = University of Michigan Crystalline Material) [44] and lanthanide based MOFs [45] respectively. Although triarylboranes possess interesting properties like fluorescence [48], co-catalytic activity for polymerization [49] or dihydrogen activation [50], anion sensing (e.g. fluoride and cyanide) [51, 52] and can be used in organic light-emitting diodes (OLEDs) [53], these compounds have not been extensively explored in MOF chemistry [54–56]. Very recently, Kleitz, Wang and co-workers reported an eight-fold interpenetrated MOF (B-MOF) with limited porosity and accessibility using a triarylborane linker having carboxylate coordinating groups (Scheme 5.2) [54].

Over the last decade for asymmetric catalysis, many enantiopure chiral linkers have also been developed and incorporated into MOFs [28–30]. In 2011, our group reported the successful synthesis and incorporation of chiral BTB linkers, functionalized with chiral enantiopure oxazolidinone motifs into MOF (Zn$_3$(chirBTB)$_2$) for asymmetric catalysis [41].

Kleitz, Wang and co-workers (2013)
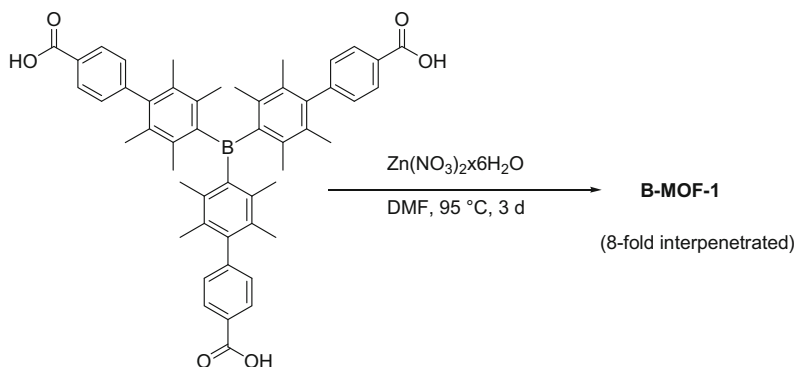
Scheme 5.2 Synthesis of interpenetrated B-MOF [54]

5.2   Results and Discussion

5.2.1   Inspiration

Minor changes made to the organic linkers, metal ions or reaction conditions can lead to a major change in the properties and structural topologies of MOFs. As was discussed earlier in this chapter, H_3BTB is one of the widely used organic linkers in MOF synthesis, giving rise to highly accessible, porous MOFs with large cavity sizes and high pore volumes. We were interested in the development of novel substituted H_3BTB linkers and their application in the construction of metal-organic frameworks for use as asymmetric catalysts, in chiral separations or for screening their viability for postsynthetic modification. Since functionalized BTB linker syntheses involve laborious multistep protocols, synthetic studies on functionalized BTB linker based MOFs are limited. Fascinated by the fluorescent properties [48], cocatalytic activity for polymerization [49] or dihydrogen activation [50] and anion sensing abilities [51, 52] of triarylboranes, we were interested in non-interpenetrated B-MOF synthesis and the development of the rarely explored triarylborane based linkers as alternates to BTB featuring different steric and electronic properties as well as spacer lengths.

5.2.2   Synthesis of Novel Metal-Organic Frameworks (MOFs)

Having this goal in mind, the novel 4,4′,4″-boranetriyltris(3,5-dimethylbenzoic acid) (H_3TPB) linker (**228**) was synthesized in a three steps (procedure shown in Scheme 5.3). Modifying the procedure reported by Zhang, Zhang and co-workers, tris(4-bromo-2,6-dimethylphenyl)borane (**230**) was synthesized in improved yield
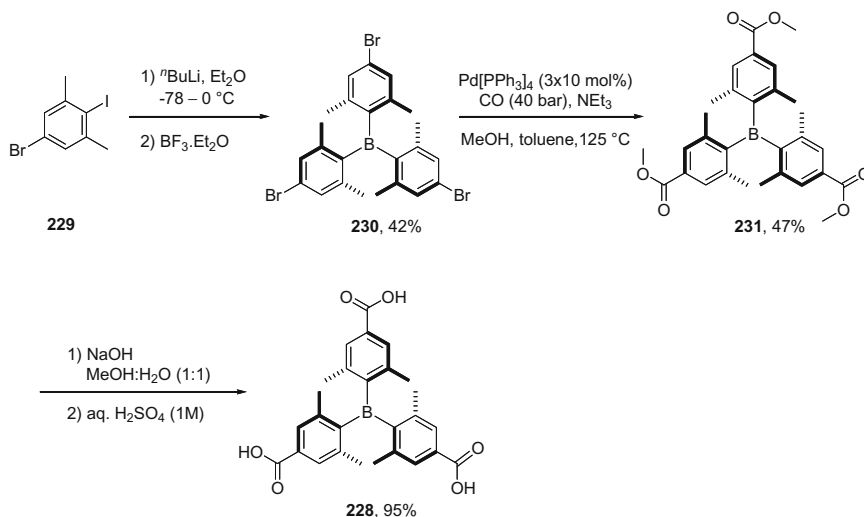
Scheme 5.3 Synthesis of 4,4′,4″-boranetriyltris(3,5-dimethylbenzoic acid) (H$_3$TPB) (**228**)

(42 %) in one pot starting from 5-bromo-2-iodo-1,3-dimethylbenzene. In the next step, tris(4-bromo-2,6-dimethylphenyl)borane (**229**) was treated with ^{t}BuLi and dry CO$_2$ to afford 4,4′,4″-boranetriyltris(3,5-dimethylbenzoic acid) (H$_3$TPB) (**228**) via a lithium-halogen exchange followed by nucleophilic attack to CO$_2$. This product was formed as an inseparable mixture with the corresponding mono- and dicar-boxylic acid derivatives as byproducts. We then changed our plan accordingly and in the second step, a palladium catalyzed esterification of tris (4-bromo-2,6-dimethylphenyl)borane (**230**) in the presence of carbon monoxide (the carbonyl synthon) and methanol (the nucleophile) was conducted in the autoclave at 125 °C and at 40 bars of pressure was developed to furnish corre-sponding ester derivative **231** in moderate yield (47 %). Finally the hydrolysis of this ester derivative **231** under aqueous basic conditions, followed by neutralization with dil. mineral acid delivered the desired product 4,4′,4″-boranetriyltris (3,5-dimethylbenzoic acid) (H$_3$TPB) (**228**) as a white solid in 95 % yield.

Having pure H$_3$TPB material in hand, we set out to synthesize Boron-MOFs in collaboration with Kaskel and co-workers from the Technical University Dresden.[1] Since triarylborane and triarylamine have similar propeller like structures, the pro-cedure to synthesize UMCM-4 with benzene-1,4-dicarboxylic acid (H$_2$BDC) and 4,4′,4″-nitrilotribenzoic acid (H$_3$TPA, TPA = 4,4′,4″-tricarboxylatetriphenylamine) linkers in a 3:3 ratio was followed [44]. H$_3$TPA was replaced with H$_3$TPB to give a new Boron-MOF. However, none of the attempted syntheses led to UMCM analog formation. After an exhaustive screening, an optimized protocol was developed to synthesize a non-interpenetrated DUT-6 (boron) (Zn$_4$O(TPB)$_{4/3}$(BDC) (**234**)

---

[1]The synthesis of MOFs was performed by Stella Helten (collaborator from TU Dresden).
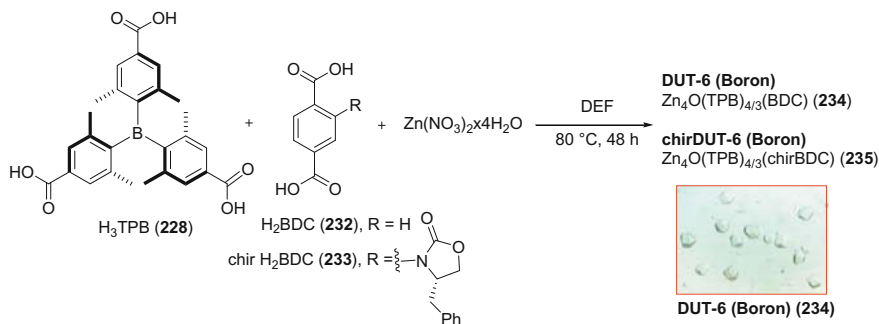
Scheme 5.4 Synthesis of DUT-6 (Boron) (Zn$_4$O(TPB)$_{4/3}$(BDC)) (**234**) and chiral DUT-6 (Boron) (Zn$_4$O(TPB)$_{4/3}$(chirBDC)) (**235**)

in phase pure form (DUT = Dresden University of Technology). Zinc nitrate, H$_2$BDC (**232**) and H$_3$TPB (**228**) were mixed in 4.0:1.0:0.3 ratio in DEF and heated at 80 °C for 48 h (Scheme 5.4). Following the developed protocol, a chiral DUT-6 (Boron) (Zn$_4$O(TPB)$_{4/3}$(chirBDC) (**235**) was also prepared using our previously developed chiral (S)-2-(4-benzyl-2-oxazolidin-2-yl) substituted BDC linker(**233**) [57] with H$_3$TPB (**228**) (Scheme 5.4).

5.2.3 Structural Analysis of Novel Metal-Organic Frameworks (MOFs)[2]

5.2.3.1 PXRD Analysis

Since crystallinity is a crucial feature of MOF materials, preliminary experiments to determine the crystallinity and phase purity of the synthesized materials were conducted using powder X-ray diffraction (PXRD). The PXRD patterns for DUT-6 (Boron) (Zn$_4$O(TPB)$_{4/3}$(BDC)), chiral DUT-6 (Boron) (Zn$_4$O(TPB)$_{4/3}$(chirBDC)) show their crystalline texture (Fig. 5.4).

5.2.3.2 Single Crystal X-ray Analysis

From the single crystal analysis of the B-MOF (Zn$_4$O(TPB)$_{4/3}$(BDC)) (**234**) shown in Fig. 5.5a, it is clear that Zn$_4$O is present as SBU and both the linkers, TPB and BDC, are incorporated into the structure. Four TPB linkers at equatorial positions and two BDC linkers at axial positions connect to one Zn$_4$O cluster center in an

---

[2]Structural analysis of novel metal-organic frameworks (MOFs) has been done by Stella Helten and Dr. Volodymyr Bon (collaborators from TU Dresden).
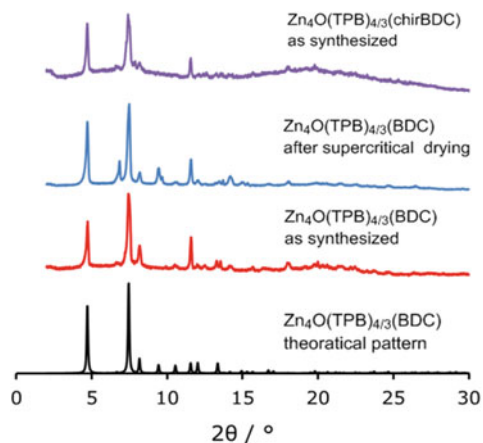
Fig. 5.4 Powder X-ray diffraction patterns of DUT-6 (Boron) (**234**) and chiral DUT-6 (Boron) (**235**) [61]. Theoretical patterns were calculated from the crystal structures (*black*). Ref. [61] reproduced by permission of The Royal Society of Chemistry
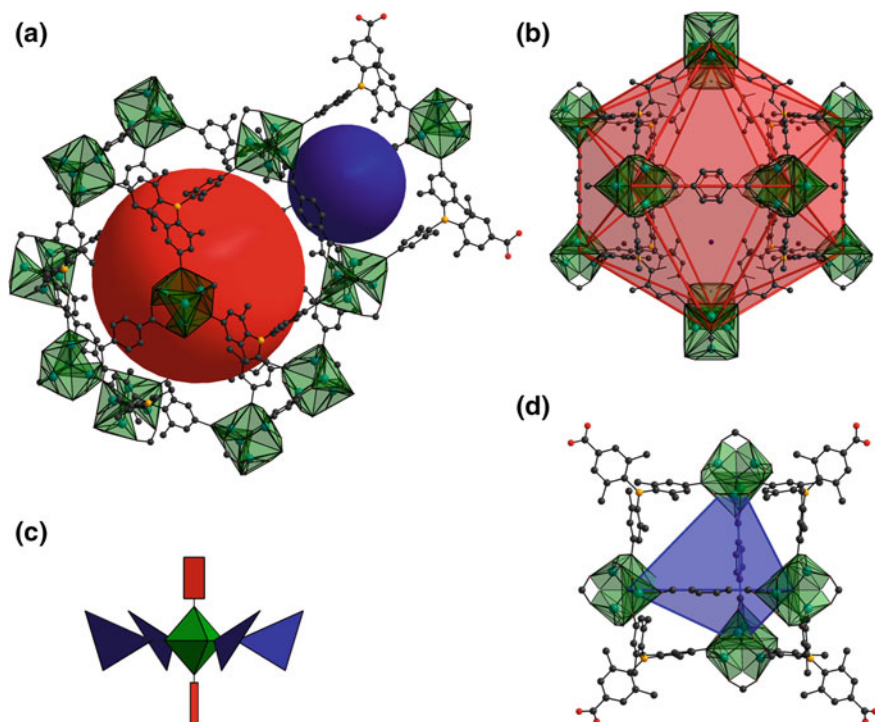
Fig. 5.5 **a** Single X-ray crystal structure of DUT-6 (Boron) ($Zn_4O(TPB)_{4/3}(BDC)$) (**234**) with dodecahedral pores (*red*) and tetrahedral pores (*blue*); **b** dodecahedral pores (*red*); **c** topological representation of SBU; **d** tetrahedral pores (*blue*). Hydrogen atoms are omitted for clarity. Ref. [61]—reproduced by permission of The Royal Society of Chemistry

octahedral arrangement (DUT-6 (Boron) (**234**), Fig. 5.5c). There are two different types of pore, dodecahedral and tetrahedral, present in this mixed linker DUT-6 (Boron) (**234**) (Fig. 5.5b, d). In this microporous DUT-6 (Boron) (**234**), dodecahedral, tetrahedral and window pores have diameters 15, 10 and 5 Å respectively (considering van der Waals radii) in contrast to mesoporous DUT-6 with the corresponding pore diameters of 22, 8 and 7 Å. In DUT-6 (Boron) (**234**), one dodecahedral pore is constructed with twelve Zn_4O units interconnected by eight trigonal and four linear linkers, while a tetrahedral pore is constructed by four trigonal and two linear linkers interconnecting four Zn_4O units (Fig. 5.5b, d). The window is formed by interconnections of two trigonal and one linear linker with three Zn_4O clusters. In the frozen state, the angle between the planes on which aryl ring are lied is 88.4°, which is relatively higher than the angles (72.5°, 65.4° and 68.5°) observed in UMCM-4 due to the steric effects of the methyl substituents on the phenyl ring of the TPB inker.

5.2.3.3   TGA Analysis

Thermogravimetric analysis (TGA) of DUT-6 (Boron) (**234**) was performed on a STA 409 (Netzsch) with synthetic air as a carrier gas, a heating rate of 5 K min^{-1}, and a flow of 100 mL min^{-1}. Synthetic air was used for complete oxidation of the framework. According to the DTA analysis of DUT-6 (Boron) (**234**), linkers start to decompose at 368°C. The experimental residual mass of ZnO (33.97 %) is consistent with the calculated residual mass of 31.05 % (Fig. 5.6).

Fig. 5.6 TGA analysis of DUT-6 (Boron) (**234**). Ref. [61]—reproduced by permission of The Royal Society of Chemistry
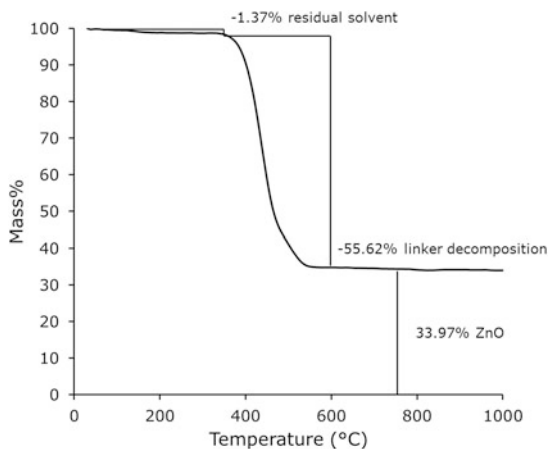
Fig. 5.7 Nitrogen physisorption isotherm of DUT-6 (Boron) (**234**) at 77 K. *Solid circles* represent adsorption and hollow circles represent desorption. Ref. [61]—reproduced by permission of The Royal Society of Chemistry
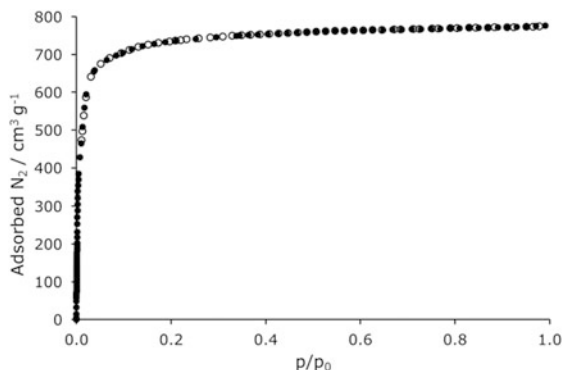
5.2.3.4   Physisorption Experiments

N_2 adsorption study

Nitrogen physisorption measurements were performed on a BELSORP Max (BEL, Japan) at 77 K with up to 1 bar of pressure. The saturation uptake of nitrogen by DUT-6 (Boron) (**234**) is 776 cm^3 g^{-1}, which gives a pore volume of 1.20 cm^3 g^{-1} ($p/p_0 = 0.99$). The Brunauer-Emmett-Teller (BET) surface area of DUT-6 (Boron) (**234**) was calculated based on the adsorption branch in pressure range of $7.7 \times 10^{-4} \leq p/p_0 \geq 9.8 \times 10^{-2}$. The three consistency criteria proposed by Rouquerol et al. [58] were maintained. A value of 2874 m^2 g^{-1} was obtained. DUT-6 (Boron) (**234**) represents the first member of the family of highly porous non-interpenetrated MOFs containing a triarylborane based-linker (Fig. 5.7).

CO_2 adsorption study

In order to better understand the interactions between carbon dioxide molecule and the DUT-6 (Boron) (**234**) surface, carbon dioxide adsorption experiments were performed. At 194.5 K, saturation uptake of CO_2 by the DUT-6 (Boron) (**234**) amounted to 630.58 cm^3 g^{-1}. This value decreased to 40.327 cm^3 g^{-1} at 273 K and 1 bar pressure. The received data permit to calculate the isosteric heat of adsorption (Q_{st}) by the coverage in the range of 0.036–1.8 mmol g^{-1}. The isosteric heat of adsorption at lowest and higher coverage are 21.5 and 18.3 kJ mol^{-1} respectively. This isosteric heat of adsorption at low coverage is relatively higher than that for other MOFs having a Zn_4O cluster at near zero or low coverage (16.7 kJ mol^{-1} for DUT-6 (see Chap. 6, Sect. 6.6.7), 15.65 kJ mol^{-1} for IRMOF-1, [59] 14 kJ mol^{-1} for MOF-177 [60] and 11.9 kJ mol^{-1} for UMCM-1) (Fig. 5.8) [60]. This higher value of DUT-6 (Boron) (**234**) indicates the presence of a specific interaction arising from special sites in the frameworks. This is usually observed with MOFs having open metal sites (21–47 kJ mol^{-1}) (Fig. 5.9).

Fig. 5.8 Carbon dioxide physisorption isotherm of DUT-6 (Boron) (**234**) at 194.5 K. Carbon dioxide physisorption isotherm at 273 K (*inset*). Ref. [61]—reproduced by permission of The Royal Society of Chemistry
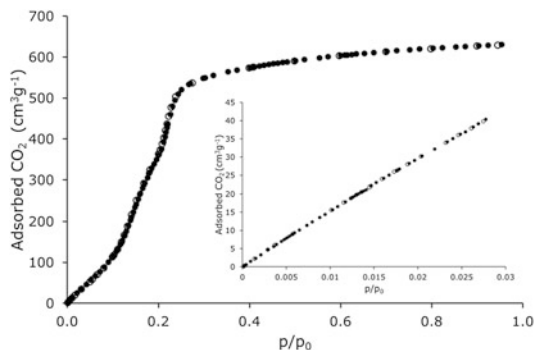
Fig. 5.9 Comparison of isosteric heats of CO_2 adsorption (Q_{st}) for DUT-6 (Boron) (**234**) (*solid bubble*) and DUT-6 (*solid diamonds*). Ref. [61]—reproduced by permission of The Royal Society of Chemistry
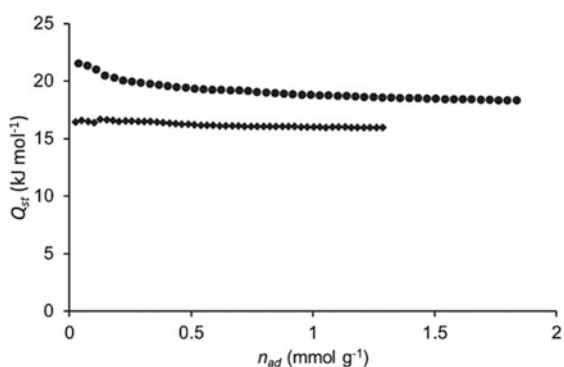
5.2.4   Dye Absorption Studies of Novel Metal-Organic Frameworks (MOFs)[3]

The texture of MOF ($Zn_4O(TPB)_{4/3}(BDC)$) as synthesized is shown in Fig. 5.10.

Since the accessibility of the MOF cavity is a crucial factor for the application of MOFs in catalysis or separations (e.g. enantiomeric separation with the use of chiral MOFs). In order to further validate this concept, dye absorption studies were performed with both DUT-6 (Boron) (**234**) and chiral DUT-6 (Boron) (**235**). Both of these MOFs were able to absorb organic dyes: methylene blue, brilliant green and rhodamine B upon dipping the crystals into the solution to furnish colored crystals (Fig. 5.11). Reichardt's dye could not be absorbed by these Boron-MOFs.

---

[3]Dye absorption studies were carried out by Stella Helten (collaborator from TU Dresden).

Fig. 5.10 Crystals of DUT-6 (Boron) (**234**) as synthesized. Ref. [61]—reproduced by permission of The Royal Society of Chemistry

Fig. 5.11 Crystals of DUT-6 (Boron) (**234**) (middle row) and chiral DUT-6 (Boron) (**235**) (bottom row) coloured by organic dyes. Ref. [61]—reproduced by permission of The Royal Society of Chemistry

5.2.5   *Photophysical Studies of Novel Metal-Organic Frameworks (MOFs)[4]*

In a photophysical study, H_3TPB in DMF absorbs light at λ_{max} = 324 nm and emits at λ_{max} = 402 nm (λ_{ex} = 324 nm), while the DUT-6 (Boron) ($Zn_4O(TPB)_{4/3}(BDC)$) absorbs at λ_{max} = 364 with a broadening of spectra and emits at λ_{max} = 443 nm (λ_{ex} = 364 nm) (Fig. 5.12a, b). The observed bathochromic shift (41 nm) of emission maximum seemingly reflects the energy change between the electronic states of H_3TPB upon incorporation into the MOF (Fig. 5.12c).

---

[4]Photophysical studies were performed by Stella Helten (collaborator from TU Dresden).
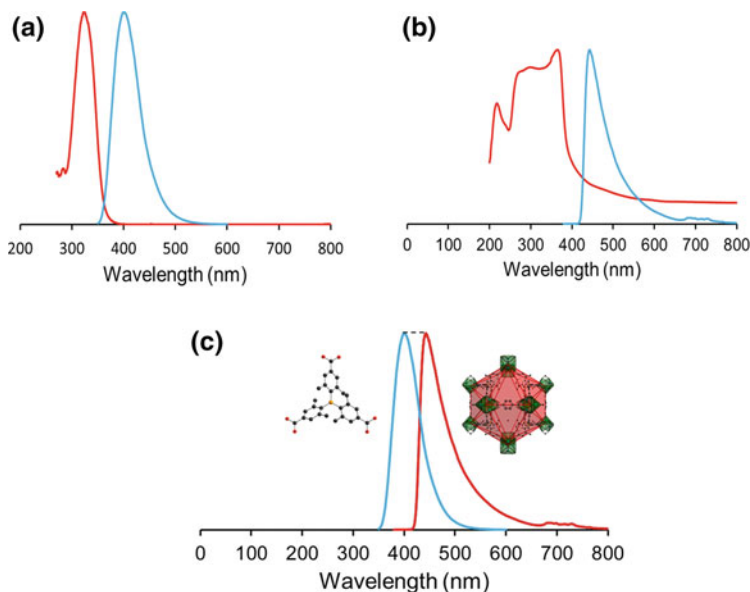
Fig. 5.12 **a** Normalized absorption spectrum of H$_3$TPB (**228**) in DMF (λ_{max} = 324 nm) (*red*) and normalized emission spectrum of H$_3$TPB (**228**) in DMF (λ_{ex} = 324 nm; λ_{max} = 402 nm) (*blue*); **b** normalized solid state absorption spectrum of DUT-6 (Boron) (**234**) (λ_{max} = 364 nm) (*red*) and normalized solid state emission spectrum of DUT-6 (Boron) (**234**) (λ_{ex} = 364 nm, λ_{max} = 443 nm) (*blue*); **c** comparison of normalized emission spectra of H$_3$TPB (**228**) (*blue*) and DUT-6 (Boron) (**234**) (*red*) showing bathochromic shift in emission wavelength. Ref. [61]—reproduced by permission of The Royal Society of Chemistry

5.3   Summary

In summary, we have successfully developed a triarylborane linker with three carboxylic acid anchoring groups (4,4′,4″-boranetriyltris(3,5-dimethylbenzoic acid) (H$_3$TPB)) and incorporated it along with a linear co-linker benzene-1, 4-dicarboxylic acid (H$_2$BDC) into the metal-organic framework to give a novel mixed linker Boron-MOF, DUT-6 (Boron). This DUT-6 (Boron) is highly porous with pore volume 1.2 cm^3 g^{-1} and BET surface area of 2874 m^2 g^{-1}. This microporous DUT-6 (Boron) represents the first example of a highly porous non-interpenetrated MOF containing a triarylborane linker. In parallel, following the same protocol, a chiral DUT-6 (Boron) was also built by replacing normal BDC linker with a chiral (*S*)-2-(4-benzyl-2-oxazolidin-2-yl) substituted BDC linker, thus giving rise to chiral cavity. Organic dye absorption studies showed pore accessibility in two newly synthesized Boron-MOFs. In addition, this new DUT-6 (Boron) showed fluorescent activity and exhibited a higher isosteric heat of adsorption for carbon dioxide in contrast to the DUT-6, which has a similar structural topology.

References

1. E.A. Tomic, J. Appl. Polym. Sci. **9**, 3745–3752 (1965)
2. M. O'Keeffe, Chem. Soc. Rev. **38**, 1215–1217 (2009)
3. N. Stock, S. Biswas, Chem. Rev. **112**, 933–969 (2012)
4. H. Li, M. Eddaoudi, M. O'Keeffe, O.M. Yaghi, Nature **402**, 276–279 (1999)
5. S. Kaskel, Nachr. Chem. **53**, 394–399 (2005)
6. U. Mueller, M. Schubert, F. Teich, H. Puetter, K. Schierle-Arndt, J. Pastre, J. Mater. Chem. **16**, 626–636 (2006)
7. A.U. Czaja, N. Trukhan, U. Muller, Chem. Soc. Rev. **38**, 1284–1293 (2009)
8. H.-C. Zhou, J.R. Long, O.M. Yaghi, Chem. Rev. **112**, 673–674 (2012)
9. D.J. Tranchemontagne, Z. Ni, M. O'Keeffe, O.M. Yaghi, Angew. Chem. Int. Ed. **47**, 5136–5147 (2008)
10. D.J. Tranchemontagne, J.L. Mendoza-Cortes, M. O'Keeffe, O.M. Yaghi, Chem. Soc. Rev. **38**, 1257–1283 (2009)
11. L.J. Murray, M. Dinca, J.R. Long, Chem. Soc. Rev. **38**, 1294–1314 (2009)
12. M.P. Suh, H.J. Park, T.K. Prasad, D.-W. Lim, Chem. Rev. **112**, 782–835 (2012)
13. W. Zhou, Chem. Rec. **10**, 200–204 (2010)
14. Y. Peng, V. Krungleviciute, I. Eryazici, J.T. Hupp, O.K. Farha, T. Yildirim, J. Am. Chem. Soc. **135**, 11887–11894 (2013)
15. Y. Hu, S. Xiang, W. Zhang, Z. Zhang, L. Wang, J. Bai, B. Chen, Chem. Commun. 7551–7553 (2009)
16. K. Sumida, D.L. Rogow, J.A. Mason, T.M. McDonald, E.D. Bloch, Z.R. Herm, T.-H. Bae, J. R. Long, Chem. Rev. **112**, 724–781 (2012)
17. R. El Osta, A. Carlin-Sinclair, N. Guillou, R.I. Walton, F. Vermoortele, M. Maes, D. de Vos, F. Millange, Chem. Mater. **24**, 2781–2791 (2012)
18. D. Peralta, K. Barthelet, J. Pérez-Pellitero, C. Chizallet, G. Chaplais, A. Simon-Masseron, G. D. Pirngruber, J. Phys. Chem. C **116**, 21844–21855 (2012)
19. Z.R. Herm, B.M. Wiers, J.A. Mason, J.M. van Baten, M.R. Hudson, P. Zajdel, C.M. Brown, N. Masciocchi, R. Krishna, J.R. Long, Science **340**, 960–964 (2013)
20. J.-R. Li, R.J. Kuppler, H.-C. Zhou, Chem. Soc. Rev. **38**, 1477–1504 (2009)
21. J.-R. Li, J. Sculley, H.-C. Zhou, Chem. Rev. **112**, 869–932 (2012)
22. R.B. Getman, Y.-S. Bae, C.E. Wilmer, R.Q. Snurr, Chem. Rev. **112**, 703–723 (2012)
23. L.E. Kreno, K. Leong, O.K. Farha, M. Allendorf, R.P. Van Duyne, J.T. Hupp, Chem. Rev. **112**, 1105–1125 (2012)
24. M.D. Allendorf, C.A. Bauer, R.K. Bhakta, R.J.T. Houk, Chem. Soc. Rev. **38**, 1330–1352 (2009)
25. Y. Cui, Y. Yue, G. Qian, B. Chen, Chem. Rev. **112**, 1126–1162 (2012)
26. C. Wang, T. Zhang, W. Lin, Chem. Rev. **112**, 1084–1104 (2012)
27. P. Horcajada, R. Gref, T. Baati, P.K. Allan, G. Maurin, P. Couvreur, G. Férey, R.E. Morris, C. Serre, Chem. Rev. **112**, 1232–1268 (2012)
28. J. Lee, O.K. Farha, J. Roberts, K.A. Scheidt, S.T. Nguyen, J.T. Hupp, Chem. Soc. Rev. **38**, 1450–1459 (2009)
29. L. Ma, C. Abney, W. Lin, Chem. Soc. Rev. **38**, 1248–1256 (2009)
30. M. Yoon, R. Srirambalaji, K. Kim, Chem. Rev. **112**, 1196–1231 (2012)
31. A. Dhakshinamoorthy, A.M. Asiri, H. Garcia, Chem. Commun. **50**, 12800–12814 (2014)
32. J. Klinowski, F.A. Almeida Paz, P. Silva, J. Rocha, Dalton Trans. **40**, 321–330 (2011)
33. U. Mueller, H. Puetter, M. Hesse, H. Wessel, in US patent, Vol. WO2005/049892, 2005
34. A. Pichon, A. Lazuen-Garay, S.L. James, CrystEngComm **8**, 211–214 (2006)
35. J.H. Bang, K.S. Suslick, Adv. Mater. **22**, 1039–1059 (2010)
36. Z. Wang, S.M. Cohen, Chem. Soc. Rev. **38**, 1315–1329 (2009)
37. K.K. Tanabe, S.M. Cohen, Chem. Soc. Rev. **40**, 498–519 (2011)
38. S.M. Cohen, Chem. Rev. **112**, 970–1000 (2012)

39. T. Dröge, A. Notzon, R. Fröhlich, F. Glorius, Chem. Eur. J. **17**, 11974–11977 (2011)
40. F. Allen, Acta Crystallogr. Sect. B Struct. Sci. **58**, 380–388 (2002)
41. K. Gedrich, M. Heitbaum, A. Notzon, I. Senkovska, R. Fröhlich, J. Getzschmann, U. Mueller, F. Glorius, S. Kaskel, Chem. Eur. J. **17**, 2099–2106 (2011)
42. P.V. Dau, K.K. Tanabe, S.M. Cohen, Chem. Commun. **48**, 9370–9372 (2012)
43. H.-R. Fu, F. Wang, J. Zhang, Dalton Trans. **43**, 4668–4673 (2014)
44. A. Dutta, A.G. Wong-Foy, A.J. Matzger, Chem. Sci. **5**, 3729–3734 (2014)
45. S. Ma, X.-S. Wang, D. Yuan, H.-C. Zhou, Angew. Chem. Int. Ed. **47**, 4130–4133 (2008)
46. S. Ma, D. Yuan, X.-S. Wang, H.-C. Zhou, Inorg. Chem. **48**, 2072–2077 (2009)
47. J. Park, D. Feng, H.-C. Zhou, J. Am. Chem. Soc. **137**, 1663–1672 (2015)
48. P.C.A. Swamy, P. Thilagar, Inorg. Chem. **53**, 2776–2786 (2014)
49. E.Y.-X. Chen, T.J. Marks, Chem. Rev. **100**, 1391–1434 (2000)
50. G.C. Welch, R.R.S. Juan, J.D. Masuda, D.W. Stephan, Science **314**, 1124–1126 (2006)
51. E. Galbraith, T.D. James, Chem. Soc. Rev. **39**, 3831–3842 (2010)
52. C.R. Wade, A.E.J. Broomsgrove, S. Aldridge, F.P. Gabbaï, Chem. Rev. **110**, 3958–3984 (2010)
53. M.-S. Lin, L.-C. Chi, H.-W. Chang, Y.-H. Huang, K.-C. Tien, C.-C. Chen, C.-H. Chang, C.-C. Wu, A. Chaskar, S.-H. Chou, H.-C. Ting, K.-T. Wong, Y.-H. Liu, Y. Chi, J. Mater. Chem. **22**, 870–876 (2012)
54. B.A. Blight, R. Guillet-Nicolas, F. Kleitz, R.-Y. Wang, S. Wang, Inorg. Chem. **52**, 1673–1675 (2013)
55. Y. Liu, K. Mo, Y. Cui, Inorg. Chem. **52**, 10286–10291 (2013)
56. X. Wang, J. Yang, L. Zhang, F. Liu, F. Dai, D. Sun, Inorg. Chem. **53**, 11206–11212 (2014)
57. M. Padmanaban, P. Muller, C. Lieder, K. Gedrich, R. Grunker, V. Bon, I. Senkovska, S. Baumgartner, S. Opelt, S. Paasch, E. Brunner, F. Glorius, E. Klemm, S. Kaskel, Chem. Commun. **47**, 12089–12091 (2011)
58. J. Rouquerol, P. Llewellyn, F. Rouquerol, in *Characterization of Porous Solids VII Proceedings of the 7th International Symposium on the Characterization of Porous Solids (COPS-VII)*, Aix-en-Provence, France, 26–28 May 2005, vol. 160, eds. by J.R.P.L. Llewellyn, F. Rodriquez-Reinoso, N. Seaton (Elsevier, 2007), pp. 49–56
59. B. Mu, P.M. Schoenecker, K.S. Walton, J. Phys. Chem. C **114**, 6464–6471 (2010)
60. J.A. Mason, K. Sumida, Z.R. Herm, R. Krishna, J.R. Long, Energy Environ. Sci. **4**, 3030–3040 (2011)
61. S. Helten, B. Sahoo, V. Bon, I. Senkovska, S. Kaskel, F. Glorius, CrystEngComm **17**, 307–312 (2015)

Chapter 6
Experimental Section

6.1 General Considerations

Procedures

Complete characterisation (R_f, NMR, IR, MS) was carried out for compounds without literature precedence. Unless otherwise noted, all reactions were carried out in flame-dried glassware under argon atmosphere. Air and moisture sensitive compounds were stored and weighed into reaction vessels under argon in a glove box (M. Braun). The oxygen level within the glove box was typically below 1 ppm. Light sensitive compounds were stored in freezer at −20 °C in dark. Reaction temperatures are reported as the temperature of the oil bath surrounding the vessel or the temperature inside the custom-made light box. No attempts were made to optimize the yield for the synthesis of starting substrates.

Solvents and chemicals

The following solvents were purified by distillation over the drying agents indicated in parentheses: THF (Na/benzophenone), Et_2O (Na/benzophenone), toluene (CaH_2), CH_2Cl_2 (CaH_2), $n$hexane (CaH_2), tAmylOH (CaH_2), Et_3N (CaH_2). Additional anhydrous solvents (<50 ppm H_2O) were purchased from Acros Organics, Sigma-Aldrich or Carl Roth and stored over molecular sieves under argon atmosphere. Commercially available chemicals were obtained from ABCR, Acros Organics, Alfa Aesar, Combi-Blocks, Fisher Scientific, Fluorochem, Heraeus, Johnson-Matthey, Maybridge, Merck, Sigma-Aldrich, Strem Chemicals, TCI Europe or VWR and used as received unless otherwise stated.

Thin layer chromatography (TLC)

Analytical TLC was performed on either silica gel 60 F_{254} aluminum plates (Merck) or Polygram SIL G/UV_{254} Alox B plates. They were visualized by exposure to short wave UV light (254 or 366 nm), or using a $KMnO_4$ staining solution followed by heating.

Flash column chromatography (FCC)

FCC was performed on Merck silica gel (−40 to 63 μm) or alox B (EcoChrom™, MP alumina N, Act. I). Solvents (CH_2Cl_2, EtOAc, ^{n}pentane, diethyl ether, toluene) were distilled prior to use. MeOH was used in *p.a.* grade.

Nuclear magnetic resonance spectroscopy (NMR)

NMR spectra were recorded at room temperature on a Bruker DPX300, AV300, AV400 or an Agilent DD2 600 or VNMRS 500. Chemical shifts (δ) are given in ppm. For ^{1}H- and ^{13}C-NMR spectra, the residual solvent signals were used as references and the chemical shifts converted to the TMS scale ($CDCl_3$: δ_H = 7.26 ppm, δ_C = 77.16 ppm; CD_2Cl_2: δ_H = 5.32 ppm, δ_C = 53.84 ppm; C_6D_6: δ_H = 7.16 ppm, δ_C = 128.06 ppm; DMSO-d_6: δ_H = 2.50 ppm, δ_C = 39.52 ppm; CD_3OD: δ_H = 3.31 ppm, δ_C = 49.00 ppm) [1]. ^{19}F- and ^{19}F-NMR [2] spectra are not calibrated and δ (ppm) is given relative to CCl_3F. ^{31}P-NMR spectra are not calibrated and δ (ppm) is given relative to H_3PO_4. NMR data was analysed with MNova software from Mestrelab Research S. L. Multiplicities of signals are abbreviated as s (singlet), d (doublet), t (triplet), q (quartet), quint (quintet), sext (sextet), sept (septet), m (multiplet), bs (broad singlet) or a combination of these. Coupling constants (J) are quoted in Hz.

Fourier transform infrared spectroscopy (FT-IR)

FT-IR spectra were recorded on a Varian Associated FT-IR 3100 Excalibur Series with a Specac Golden Gate Single Reflection ATR unit and analysed with a resolution program from Varian Associated. The wave numbers (v) of recorded signals are quoted in cm^{-1}.

Gas chromatography-mass spectrometry (GC-MS)

GC-MS spectra were recorded on an Agilent Technologies 7890A GC system with an Agilent 5975 inert mass selective detector or a triple-axis detector (EI) and a HP-5MS column (0.25 mm × 30 m, film: 0.25 μm) from J&W Scientific. A constant flow of helium (99.999 %) as the carrier gas was used. The methods used start with the initial temperature T_0. After holding this temperature for 3 min, the column is heated to temperature T_1 with a linear temperature gradient and this temperature is held for an additional time t (*e. g.* method 50_40: T_0 = 50 °C, T_1 = 290 °C, gradient = 40 °C/min, t = 3 min). The total ion count was recorded and evaluated with an Agilent ChemStation Enhanced Data Analysis programme. The major signals are quoted in *m/z* with the relative intensity in % given in parentheses. Exact EI mass spectra were recorded on a Waters-Micromass GC-Tof.

Electrospray ionisation-mass spectrometry (ESI-MS)

Exact mass spectra were recorded on a Bruker Daltonics MicroTof. High resolution mass spectra were recorded on a Thermo-Fisher Scientific Orbitrap LTQ XL. Major signals are quoted in *m/z*.

Electrospray ionisation-mass spectrometry (ESI-MS)

CHN elemental analyses were performed on a CHNS 932 analyser (LECO).

Polarimetry

The specific optical rotation $[\alpha]_D^{24}$ of chiral compounds was measured using a Perkin Elmer Polarimeter 341 (T = 24 °C, λ = 589 nm) using a quartz cuvette (10 cm path length).

Single Crystal X-ray crystalography

Data sets were collected with a Nonius KappaCCD diffractometer. Programs used: data collection, COLLECT; data reduction, Denzo-SMN [3]; absorption correction, Denzo [4]; structure solution SHELXS-97 [5]; structure refinement SHELXL-97 [6] and graphics, XP (BrukerAXS, 2000). R-values are given for observed reflections, and wR^2 values are given for all reflections. A pale yellow plate-like specimen of $C_{19}H_{16}C_lNO_3$, approximate dimensions 0.040 mm × 0.140 mm × 0.200 mm, was used for the X-ray crystallographic analysis. The X-ray intensity data were measured. A total of 3257 frames were collected. The total exposure time was 17.39 h. The frames were integrated with the Bruker SAINT Software package using a wide-frame algorithm. The integration of the data using a monoclinic unit cell yielded a total of 32,320 reflections to a maximum θ angle of 68.32° (0.83 Å resolution), of which 2801 were independent (average redundancy 11.539, completeness = 99.8 %, Rint = 5.32 %, Rsig = 2.21 %) and 2480 (88.54 %) were greater than 2σ(F^2). The final cell constants of a = 9.2567(2) Å, b = 7.6968(2) Å, c = 21.6732(5) Å, β = 98.1490(10)°, volume = 1528.56(6) Å^3, are based upon the refinement of the XYZ-centroids of 9934 reflections above 20 σ(I) with 8.242° < 2θ < 136.5°. Data were corrected for absorption effects using the multi-scan method (SADABS). The ratio of minimum to maximum apparent transmission was 0.732. The calculated minimum and maximum transmission coefficients (based on crystal size) are 0.6490 and 0.9110. The final anisotropic full-matrix least-squares refinement on F^2 with 219 variables converged at R1 = 3.17 %, for the observed data and wR2 = 8.61 % for all data. The CCDC-1038989 contains the supplementary crystallographic data for the compound 214. This data can be obtained free of charge from the Cambridge Crystallographic Data Centre via www.ccdc.cam.ac.uk/data_request/cif.

The dataset from the single crystal of DUT-6 (boron) $Zn_4O(TPB)_{4/3}(BDC)$ (**234**), prepared in a glass capillary, was collected at beamline BL14.2, Joint Berlin-MX Laboratory of Helmholtz Zentrum Berlin, equipped with a MX-225 CCD detector (Rayonics, Illinois) and 1-circle goniometer [7]. The data collection was performed at room temperature using monochromatic radiation with λ = 0.88,561 Å. A plethora of single crystals from different batches with various linear dimensions (up to 0.5 mm in all dimensions) were used for single crystal diffraction experiments at room temperature and at 100 K. In spite of sufficient size of single crystals and highly intensive synchrotron radiation, the sufficient intensities could be observed up until a resolution of 1.0–1.1 Å. The indexing of the image frames suggests a primitive cubic lattice for the crystal structure. The image

frames were integrated and scaled using XDSAPP 1.0 [8] graphic shell for the XDS program [9]. The obtained set of intensities was carefully analyzed on extinction. As a result, systematic absences were found for the glide plane, perpendicular to the face diagonal, suggesting the *Pm-3n* space group for the crystal structure solution and refinement. The structure was solved by direct methods and refined by full-matrix least square on F^2 using SHELXS and SHELXL [10] programs respectively. All non-hydrogen atoms were refined in the anisotropic approximation. Hydrogen atoms were generated geometrically regarding the hybridization of the parent atom and refined using the "riding model" with $U_{iso}(H) = 1.5\ U_{iso}(C)$ for CH_3 and $U_{iso}(H) = 1.2\ U_{iso}(C)$ for CH groups. The anisotropic refinement decreased the data to parameter ratio for the observed reflections that had a strong influence on the refinement stability from the dataset with mean $I/\sigma(I) = 2.36$. This prompted us to use 11 distance restraints to fix the geometry of the organic ligands. Besides that, lattice solvent molecules could not be located from the difference Fourier map due to disorder in the highly symmetrical space group. Thus, the SQUEEZE procedure in PLATON was performed to correct the intensities, corresponding to the disordered part of the structure [11]. This results in 5202 electrons squeezed from 13,642 $Å^3$ that corresponds to 15.5 molecules of DEF per formula unit. CCDC-1009603 contains the supplementary crystallographic data for the compound **234**. This data can be obtained free of charge from the Cambridge Crystallographic Data Centre via www.ccdc.cam.ac.uk/data_request/cif.

Powder X-ray diffraction measurement

Powder X-Ray Diffraction data were collected on a STADI P diffractometer with Cu-Kα1 radiation ($\lambda = 1.5405$ Å) at room temperature.

Photospectrometry

Liquid UV-Vis measurements were carried out on a JASCO V-650 spectrophotometer and UV-1650PC spectrophotometer (Shimadzu). Solid state UV-Vis measurements were performed on a Cary 4000 UV-Vis Spectrophotometer with praying mantis geometry using PTFE as white standard. Liquid state fluorescence measurements were conducted on a Cary Eclipse fluorescence spectrophotometer and a JASCO FP6500 spectrofluorometer. Solid state fluorescence measurements were conducted on a Cary Eclipse fluorescence spectrophoto-meter.

The luminescence lifetime of indolizine **195** was recorded on a FluoTime300 spectrometer from PicoQuant equipped with a 300 W ozone-free Xe lamp (250–900 nm), a 10 W Xe flash-lamp (250–900 nm, pulse width < 10 μs) with repetition rates of 0.1–300 Hz, an excitation monochromator (Czerny-Turner 2.7 nm/mm dispersion, 1200 grooves/mm, blazed at 300 nm), diode lasers (pulse width < 80 ps) operated by a computer-controlled laser driver PDL-820 (repetition rate up to 80 MHz, burst mode for slow and weak decays), two emission monochromators (Czerny-Turner, selectable gratings blazed at 500 nm with 2.7 nm/mm dispersion and 1200 grooves/mm, or blazed at 1250 nm with 5.4 nm/mm dispersion and 600 grooves/mm), Glan-Thompson polarizers for excitation (Xe-lamps) and emission,

a Peltier-thermostatized sample holder from Quantum Northwest (−40 to 105 °C), and two detectors, namely a PMA Hybrid 40 (transit time spread FWHM < 120 ps, 300–720 nm) and a R5509-42 NIR-photomultiplier tube (transit time spread FWHM 1.5 ns, 300–1400 nm) with external cooling (−80 °C) from Hamamatsu. Steady-state and fluorescence lifetime was recorded in TCSPC mode by a PicoHarp 300 (minimum base resolution 4 ps). Lifetime analysis was performed using the commercial FluoFit software. The quality of the fit was assessed by minimizing the reduced chi squared function (χ^2) and visual inspection of the weighted residuals and their autocorrelation (see the Fig. 6.11).

TGA analysis

Thermogravimetric Analysis was carried out on a STA 409 (Netzsch) with a heating rate of 5 K min^{-1} and synthetic air as carrier gas with a flow rate of 100 mL min^{-1}.

Physisorption measurement

Nitrogen physisorption experiments were performed on a BELSORP-max (Bel, Japan) at 77 K up to 1 bar. CO_2 physisorption measurements were performed on a BELSORP-max (Bel, Japan) at 195 and 273 K up to 1 bar.

Visible light sources

Visible light from compact fluorescent light bulbs (CFL) was provided by a standard household desk lamp purchased from Massive fitted with the appropriate light bulb (14, 23 or 32 W) (see Fig. 6.1). Blue LEDs (5 W, λ = 465 nm) and green LEDs (5 W, λ = 525 nm) were used for blue and green light irradiation, respectively. In each case, the light source was placed ∼5 cm from the reaction vessel. In the case of the blue and green LED irradiation, a custom made "light box" was used with 6 blue and green LEDs arranged around the reaction vessels (see Fig. 6.2 and 6.4). A fan attached to the apparatus was used to maintain the temperature inside the "box" at no more than 9 °C above room temperature.

Fig. 6.1 Photograph for reactions conducted under 23 W CFL bulb irradiation
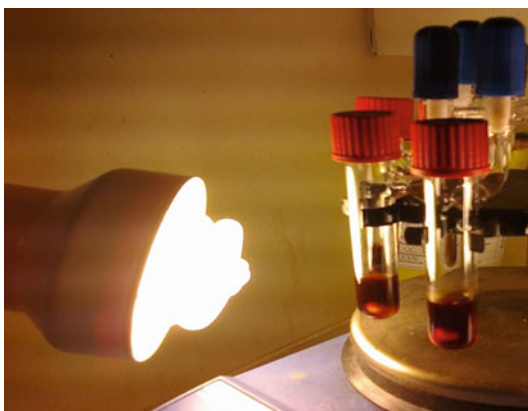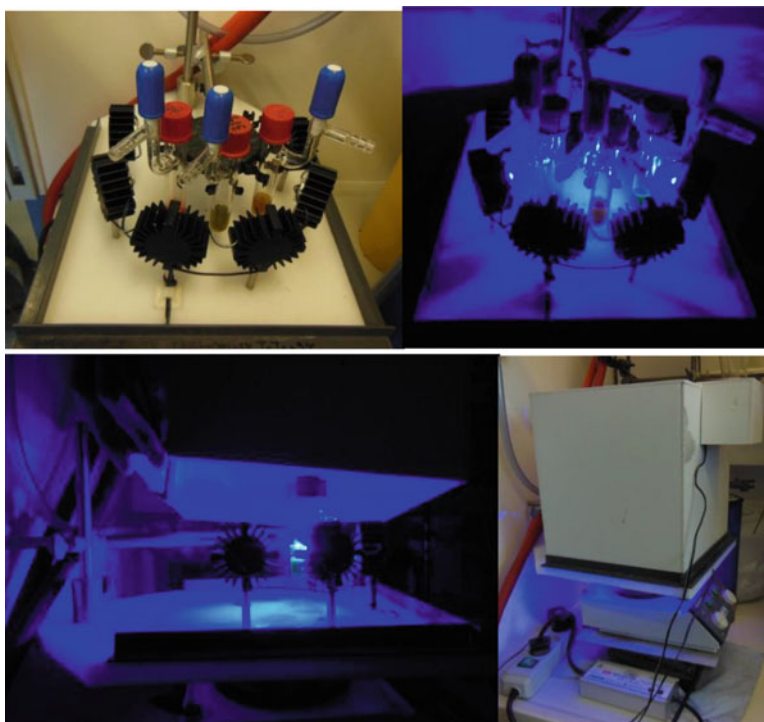
Fig. 6.2 Photographs of the custom-made "light box" used for reactions conducted under blue LED irradiation

Fig. 6.3 Emission spectrum of commercial blue LED (5 W, λ_{max} = 465 nm). Recorded by L. Stegemann, WWU Münster
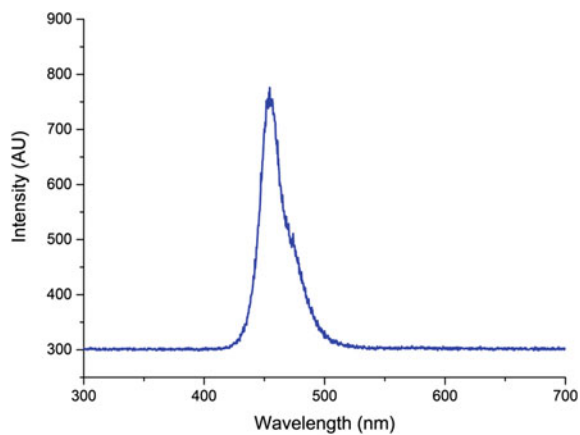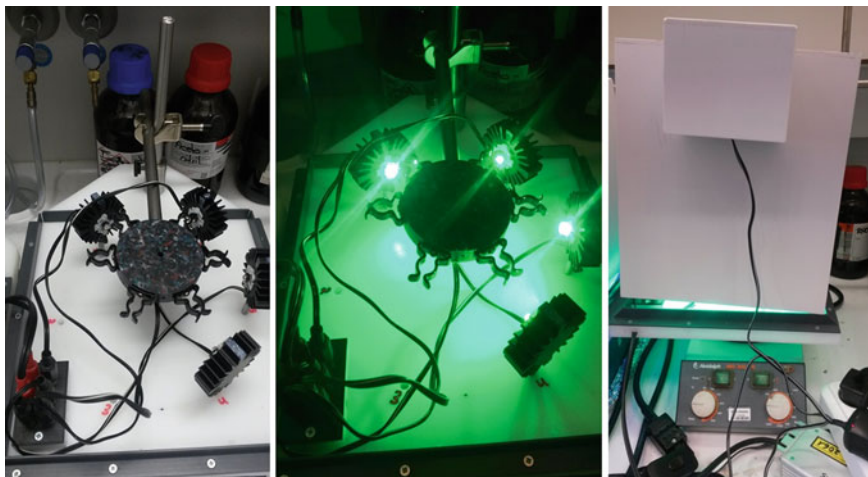
Fig. 6.4 Photographs of the custom-made "light box" used for reactions conducted under green LED irradiation

Fig. 6.5 Emission spectrum of commercial green LED (5 W, $\lambda_{max} = 525$ nm). Recorded by L. Stegemann, WWU Münster
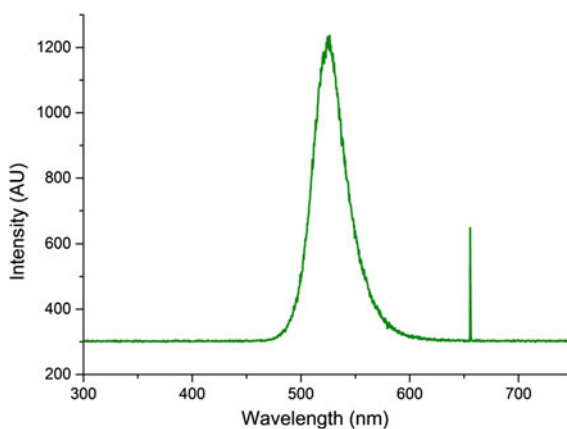
6.2   Synthesis of Photocatalysts

All the organic dyes (Eosin Y, Fluorescein dye, Rhodamine B and Rose Bengal) were commercially available.

Synthesis of Tris(2,2′-bipyridyl)ruthenium(II) bis(hexafluorophosphate) [Ru(bpy)₃](PF₆)₂
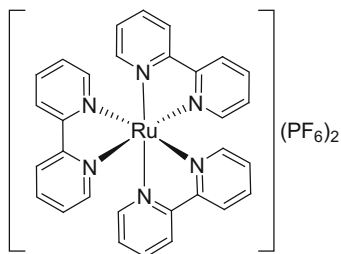
Following a modified procedure reported by Yoon et al. [12] in a round bottomed flask equipped with a magnetic stir bar and connected with a reflux condenser under argon, ruthenium(III) chloride (RuCl$_3$·xH$_2$O, 207 mg, 1.00 mmol, 1.00 equiv.) and 2,2′-bipyridine (960 mg, 6.15 mmol, 6.15 equiv.) were dissolved in dry ethanol (38 mL). The reaction mixture was refluxed at 80 °C for 12 h under argon. After cooling to rt, potassium hexafluorophosphate (KPF$_6$, 709 mg, 3.85 mmol, 3.85 equiv.) was added to the reaction mixture and stirred for another 1 h. The solid precipitate was collected by vacuum filtration and purified by column chromatography through silica (eluent: acetone:satd. aq. KPF$_6$ 19:1) to furnish pure [Ru (bpy)$_3$](PF$_6$)$_2$ (330 mg, 0.384 mmol, 38 %).

^{1}H NMR (300 MHz, acetone-d$_6$): δ (ppm): 8.82 (dt, J = 8.2, 1.1 Hz, 6H), 8.21 (td, J = 7.9, 1.5 Hz, 6H), 8.06 (ddd, J = 5.6, 1.5, 0.7 Hz, 6H), 7.58 (ddd, J = 7.7, 5.6, 1.3 Hz, 6H); **^{13}C NMR (75.5 MHz, acetone-d$_6$)**: δ (ppm): 158.1, 152.7, 138.9, 128.8, 125.3; **^{19}F NMR (100 MHz, acetone-d$_6$)**: δ (ppm): −72.52 (d, J = 707.9 Hz); **^{31}P NMR (100 MHz, acetone-d$_6$)**: δ (ppm) −139.10 (sept, J = 707.5 Hz); **HR-MS (ESI)**: m/z calculated for [C$_{30}$H$_{24}$N$_6$F$_6$PIr]$^+$ ([M-PF$_6$]$^+$): 715.0748, measured: 715.0773.

Synthesis of Tris(2,2′-bipyrazyl)ruthenium(II) bis(hexafluorophosphate) [Ru(bpz)₃](PF₆)₂

2,2′-Bipyrazine (bpz)
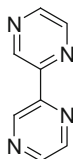
Following a modified procedure reported by Rillema et al. [13] 2-(tributylstannyl) pyrazine (630 μL, 2 mmol, 1.00 equiv.) was added to a solution of 2-chloropyrazine (182 μL, 2.04 mmol, 1.02 equiv.) in m-xylene (8 mL). The reaction mixture was degassed by sparging argon for 30 min. Then Pd(PPh$_3$)$_4$ (116 mg, 0.1 mmol, 0.05 equiv.) was added to the reaction mixture and degassed again sparging argon for 15 min. The resulting reaction mixture was refluxed for

3 d. After cooling to rt, solvent was removed under reduced pressure and purified by flash column chromatography through silica (eluent: ethyl acetate) to afford pure 2,2′-bipyrazine (225 mg, 1.42 mmol, 71 %) as a white solid.

^{1}H NMR (300 MHz, acetonitrile-d₃): δ (ppm): 9.61 (d, J = 1.2 Hz, 1H), 8.67 (s, 2H); **HR-MS (ESI)**: m/z calculated for $[C_8H_7N_4]^+$ ($[M + H]^+$): 159.0665, measured: 159.0672.

Tris2,2′-bipyrazyl)ruthenium(II) bis(hexafluorophosphate) [Ru(bpz)₃](PF₆)₂
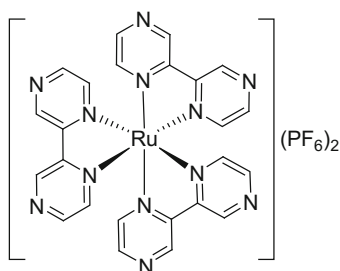
Following a modified procedure reported by Rillema et al. [14], in a round bottomed flask equipped with a magnetic stir bar and connected with a reflux condenser under argon, ruthenium(III) chloride (RuCl₃·xH₂O, 21 mg, 0.10 mmol, 1.00 equiv.) and 2,2′-bipyrazine (50 mg, 0.32 mmol, 3.2 equiv.) were dissolved in ethylene glycol (2 mL). The reaction flask was evacuated and flushed with argon (three times). The reaction mixture was refluxed at 200 °C for 1 h under argon. After cooling to rt, potassium hexafluorophosphate (KPF₆, 74 mg, 0.40 mmol, 4.00 equiv.) was added to the reaction mixture and stirred for another 15 min. The solid precipitate was filtered off and washed with water. Then the product was dissolved in acetonitrile to remove solid residue. Solvent was removed under reduced pressure to furnish pure [Ru(bpz)₃](PF₆)₂ (38 mg, 0.044 mmol, 44 %).

^{1}H NMR (300 MHz, acetonitrile-d₃): δ (ppm): 9.78 (d, J = 0.9 Hz, 6H), 8.65 (d, J = 3.2 Hz, 6H), 7.83 (dd, J = 3.0, 0.9 Hz, 6H); **^{13}C NMR (75.5 MHz, acetonitrile-d₃)**: δ (ppm): 151.3, 149.8, 148.1, 146.5; **^{19}F NMR (100 MHz, acetonitrile-d₃)**: δ (ppm): −72.84 (d, J = 706.8 Hz); **^{31}P NMR (100 MHz, acetonitrile-d₃)**: δ (ppm): −144.65 (sept, J = 706.7 Hz); **HR-MS (ESI)**: m/z calculated for $[C_{24}H_{18}N_6F_6PIr]^+$ ($[M-PF_6]^+$): 721.0457, measured: 721.0461.

Synthesis of *fac*-Tris(2-phenylpyridinato-C^2,N)iridium(III) [Ir(ppy)$_3$]
Tetrakis(2-phenylpyridinato-C^2,N′)(µ-dichloro)diiridium(III) [Ir(ppy)$_2$Cl]$_2$
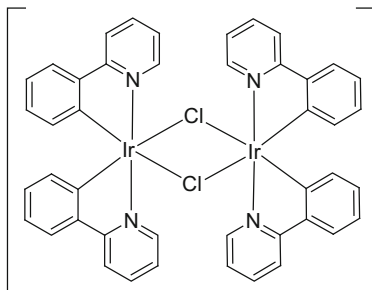
Following a modified procedure from Watts et al. [15], in a two necked round bottomed flask equipped with a magnetic stir bar and connected with a reflux condenser, iridium(III) chloride (IrCl$_3$.3H$_2$O, 429 mg, 1.22 mmol, 1.00 equiv.) and 2-phenyl pyridine (783 mg, 770 µL, 5.05 mmol, 6.15 equiv.) were dissolved in 2-methoxyethanol (33 mL) and water (11 mL). The reaction mixture was refluxed at 110 °C for 24 h. After cooling the reaction mixture to rt, yellow precipitate was collected on a Büchner funnel under vacuum filtration and washed with ethanol and acetone. Finally, the complex was dissolved in dichloromethane to separate from the iridium residue. Removal of the solvent afforded [Ir(ppy)$_2$Cl]$_2$ (531 mg, 0.493 mmol, 81 %) as yellow solid, which was used directly in next step.

^{1}H NMR (300 MHz, DMSO-d$_6$): δ (ppm): 9.66 (dd, J = 80.0, 5.6 Hz, 4H), 8.21 (dd, J = 24.3, 8.2 Hz, 4H), 8.05 (dtd, J = 25.1, 7.8, 1.6 Hz, 4H), 7.75 (dd, J = 16.2, 7.8 Hz, 4H), 7.51 (dt, J = 36.2, 6.4 Hz, 4H), 6.80–6.94 (m, 4H), 6.73 (dt, J = 21.7, 7.5 Hz, 4H), 5.96 (dd, J = 176.5, 7.6 Hz, 4H); **HR-MS (ESI):** *m/z* calculated for [C$_{22}$H$_{16}$N$_2$Ir]$^+$ ([$^1/_2$M-Cl]$^+$): 501.0937, measured: 501.0947.

***fac*-Tris(2-phenylpyridinato-C^2,N)iridium(III) [Ir(ppy)$_3$]**
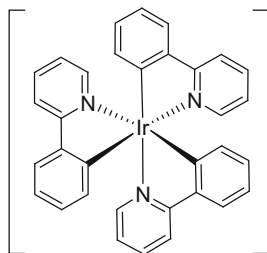
Following a modified procedure reported by Thompson et al. [16], in a heat gun dried round bottomed flask equipped with a magnetic stir bar and connected with a reflux condenser under argon, [Ir(ppy)$_2$Cl]$_2$ (200 mg, 0.187 mmol), 2-phenyl pyridine (72.6 mg, 67 µL, 0.468 mmol, 2.50 equiv.) and dry K$_2$CO$_3$ (258 mg, 1.87 mmol, 10.0 equiv.) were dissolved in ethylene glycol (10 mL). The reaction mixture was degassed using three freeze-pump-thaw cycles. The flask was then

flushed with argon. The reaction mixture was refluxed at 200 °C for 40 h. After cooling to rt, the reaction mixture was diluted with water. The brownish gelatinous solid precipitate was filtered off on a Büchner funnel under vacuum filtration and washed with two portions of methanol and diethyl ether followed by hexane, until a powdered yellow solid obtained. Finally, the crude mixture was purified by flash column chromatography through silica (eluent: dichloromethane) to deliver *fac*-[Ir (ppy)$_3$] (120 mg, 0.183 mmol, 49 %) as pure yellow solid.

^{1}H NMR (300 MHz, CD$_2$Cl$_2$): δ (ppm): 7.92 (dt, *J* = 8.3, 1.1 Hz, 3H), 7.60–7.71 (m, 6H), 7.57 (ddd, *J* = 5.6, 1.7, 0.9 Hz, 3H), 6.84–6.97 (m, 6H), 7.69–7.82 (m, 6H); **^{13}C NMR (75.5 MHz, CD$_2$Cl$_2$)**: δ (ppm): 166.8 (C$_q$), 161.4 (C$_q$), 147.5 (CH), 144.2 (C$_q$), 137.1 (CH), 136.6 (CH), 130.0 (CH), 124.4 (CH), 122.5 (CH), 120.2 (CH), 119.2 (CH); **HR-MS (ESI)**: *m/z* calculated for [C$_{33}$H$_{24}$N$_3$IrNa]$^+$ ([M + Na]$^+$): 678.1493, measured: 678.1481.

Synthesis of Bis(2-phenylpyridinato-C^2,N)(4,4′-Di-*tert*-butyl-4,4′-bipyridyl)iridium(III) hexafluorophosphate [Ir(ppy)$_2$(dtbbpy)]PF$_6$
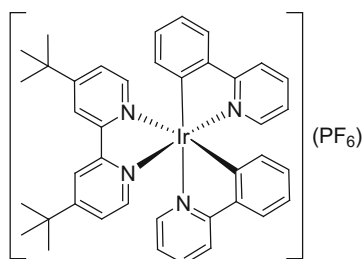
Following a modified procedure reported by Bernhard and Malliaras and co-workers, [17] in a heat gun dried round bottomed flask equipped with a magnetic stir bar and connected with a reflux condenser under argon, previously synthesized [Ir(ppy)$_2$Cl]$_2$ (400 mg, 0.370 mmol, 1.00 equiv.) and 4,4′-di-*tert*-butyl-2,2′-bipyridine (dtbbpy, 217 mg, 0.810 mmol, 2.20 equiv.) were dissolved in ethylene glycol (19 mL). The reaction mixture was refluxed at 150 °C for 15 h. After cooling to rt, the reaction mixture was diluted with water (280 mL). Excess of 4,4′-di-*tert*-butyl-2,2′-bipyridine was removed through three times extractions with diethyl ether (3 × 150 mL). The aqueous phase was heated at 70 °C. After 10 min heating, NH$_4$PF$_6$ (1.87 g, 11.5 mmol, 31 equiv.) in water (19 mL) was added to the aqueous phase and a yellow solid started to precipitate out immediately. This aqueous phase was cooled to 0 °C to complete the precipitation. The yellow solid was filtered off on a Büchner funnel under vacuum filtration and washed with water. After drying under vacuum overnight, pure [Ir(ppy)$_2$(dtbbpy)]PF$_6$ (649 mg, 0.71 mmol, 96 %) was obtained as a yellow powder.

^{1}H NMR (300 MHz, acetone-d$_6$): δ (ppm): 8.88 (d, *J* = 2.0 Hz, 2H), 8.23 (d, *J* = 8.1 Hz, 2H), 7.85–8.03 (m, 6H), 7.79 (ddd, *J* = 5.8, 1.6, 0.8 Hz, 2H), 7.71 (dd, *J* = 5.9, 2.0 Hz, 2H), 7.13 (ddd, *J* = 7.4, 5.8, 1.4 Hz, 2H), 7.03 (td, *J* = 7.5, 1.3 Hz, 2H), 6.91 (td, *J* = 7.4, 1.4 Hz, 2H), 6.34 (dd, *J* = 7.6, 1.2 Hz, 2H), 1.41 (s, 18H);

^{13}C NMR (100 MHz, acetone-d$_6$): δ (ppm): 168.8, 169.9, 156.8, 151.9, 151.1, 149.9, 145.0, 139.5, 132.5, 131.2, 126.4, 125.8, 124.4, 123.3, 120.8, 36.4, 30.4; **^{19}F NMR (300 MHz, acetone-d$_6$)**: δ (ppm): −72.65 (d, J = 707.5 Hz); **^{31}P NMR (300 MHz, acetone-d$_6$)**: δ (ppm): −144.29 (sept, J = 707.5 Hz); **HR-MS (ESI)**: m/z calculated for [C$_{40}$H$_{40}$N$_4$Ir]$^+$ ([M-PF$_6$]$^+$): 769.2879, measured: 769.2900.

Synthesis of Bis(2-(2,4-difluorophenyl)-5-(trifluoromethyl)pyridinato-C^2,N′) (4,4′-di-*tert*-butyl-4,4′-bipyridyl)iridium(III) hexafluorophosphate [Ir(dF(CF$_3$) ppy)$_2$(dtbbpy)](PF$_6$)

This iridium photocatalyst was synthesized by Dr. Matthew N. Hopkinson (WWU Münster) [18].

6.3   Oxy- and Aminoarylations of Alkenes

6.3.1   *Synthesis of Gold Catalysts*

The gold complexes (tht)AuCl (tht = tetrahydrothiophene), Me$_2$SAuCl, Ph$_3$PAuCl, [Ph^{t}Bu$_2$PAu(CH$_3$CN)]SbF$_6$, [dppm(AuCl)$_2$] (dppm = diphenylphosphinomethane), AuCl, [(pic)AuCl$_2$] (pic = picolinato) and AuCl$_3$ were commercially available. IPrAuCl (IPr = 1,3-bis(2,6-diisopropylphenyl)imidazol-2-ylidene) was prepared following a literature procedure reported by Nolan and co-workers [19] The gold(I) chloride complexes ((4-OMe)C$_6$H$_4$)$_3$PAuCl, ((2-Me)C$_6$H$_4$)$_3$PAuCl, ((4-CF$_3$) C$_6$H$_4$)$_3$PAuCl and Cy$_3$PAuCl were prepared by reacting an equimolar ratio of the appropriate phosphine with (tht)AuCl (tht = tetrahydrothiophene) or Me$_2$SAuCl in dichloromethane in a method analogous to that of Hashmi et al. [20] [IPrAu]NTf$_2$, [((4-OMe)C$_6$H$_4$)$_3$PAu]NTf$_2$, [((4-CF$_3$)C$_6$H$_4$)$_3$PAu]NTf$_2$ and [Cy$_3$PAu]NTf$_2$ were prepared by reacting the corresponding gold(I) chloride complex with an equimolar amount of AgNTf$_2$ in dichloromethane in a procedure analogous to that of Gagosz et al. [21]. [(Ph$_3$P)$_2$Au]OTf [22] was prepared by reacting Ph$_3$PAuCl with AgOTf and PPh$_3$ in a method analogous to that of Williams et al. [23]. All above mentioned gold catalysts were synthesized by Dr. Matthew N. Hopkinson (WWU Münster). The following gold complex was synthesized by self according to the procedures given in the cited reference.

[1,1,1-Trifluoro-*N*-[(trifluoromethyl)sulfonyl]methanesulfonamidato-κ*N*] (triphenylphos phine)gold(I) [Ph$_3$PAu]NTf$_2$

Following a literature report from Gagosz et al. [21] Ph$_3$PAuCl (198 mg, 0.40 mmol) and AgNTf$_2$ (172 mg, 0.40 mmol) were weighed in a round bottomed flask and then dichloromethane (2.8 mL) was added to the mixture. After stirring at rt for 15 min, the crude suspension was filtered through Celite. Volume of the filtrate was reduced to 1/3 and the complex [Ph$_3$PAu]NTf$_2$ (250 mg, 0.34 mmol, 85 %) was recrystallized as a white crystalline solid by adding pentane slowly.

¹H NMR (300 MHz, CDCl₃): δ (ppm): 7.45–7.59 (m, 15H); **¹⁹F NMR (300 MHz, CDCl₃)**: δ (ppm): −75.16; **³¹P NMR (300 MHz, CDCl₃)**: δ (ppm): −30.45 (sept, *J* = 707.5 Hz).

6.3.2 Synthesis of Alkene Substrates

Some substrates were commercially available. A part of the substrate synthesis and scope were carried out by Dr. Matthew N. Hopkinson (WWU Münster). A part of substrates was also synthesized by Kristina Oldiges and M. Wünsche (all WWU Münster). The following substrates were synthesized by self according to the procedures given in the cited references. No attempts were made to optimize yields for the synthesis of substrates.

(±)-(*R*,*S*)-2-Allylcyclohexan-1-ol (67) [24]
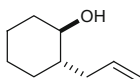
Following a literature report from Waser et al. [24], in a heat gun dried two necked round bottomed flask equipped with a magnetic stir bar and connected with a reflux condenser under argon, cyclohexene oxide (294 mg, 304 μL, 3.00 mmol, 1.00 equiv.) was added dropewise to a solution of allyl magnesium bromide (9.1 mL, 9.1 mmol, 1 M in Et₂O, 3.0 equiv.) diluted with Et₂O (7.3 mL). The reaction mixture was refluxed for 4 h at 40 °C. After cooling to rt, the reaction was quenched with satd. aq. NH₄Cl and extracted with diethyl ether. The combined organic layers were washed with brine and dried over MgSO₄. The crude reaction mixture was purified by flash column chromatography through silica (eluent: dichloromethane:mathanol 99:1 to 96:4) to afford pure (±)-(*R*,*S*)-2-allylcyclohexan-1-ol (**67**, 353 mg, 2.52 mmol, 84 %) as a colourless oil.

¹H NMR (300 MHz, CDCl₃): δ (ppm): 5.86 (ddt, *J* = 17.3, 10.1, 7.3 Hz, 1H), 4.93–5.15 (m, 2H), 3.14–3.37 (m, 1H), 2.33–2.55 (m, 1H), 1.88–2.08 (m, 2H), 1.57–1.83 (m, 4H), 1.07–1.42 (m, 4H), 0.86–1.04 (m, 1H); **HR-MS (ESI)**: *m/z* calculated for [C₉H₁₆ONa]⁺ ([M + Na]⁺): 163.1093, measured: 163.1090.

(±)-3-Phenylpent-4-en-1-ol (66) [25]
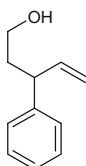
Following a procedure reported by Zhang et al. [25], in a Schlenk tube, a solution of triethyl orthoacetate (1.38 mL, 7.5 mmol, 1.00 equiv.), (*E*) cinnamyl alcohol

(1.29 mL, 10 mmol, 1.33 equiv.) and butyric acid (100 μL, 1.00 mmol, 0.13 equiv.) in toluene (40 mL) was refluxed at 150 °C for 12 h. The reaction mixture was concentrated and purified by flash column chromatography (eluent: pentane:ethyl acetate 17:3) to produce ethyl 3-phenylpent-4-enoate (1.19 g, 5.83 mmol, 78 %) as colourless oil. This ester was directly used in next step.

Ethyl 3-phenylpent-4-enoate (1.18 g, 5.78 mmol, 1.00 equiv.) was dissolved in THF (22 mL) and LiAlH$_4$ (526 mg, 13.9 mmol, 2.4 equiv.) was added at 0 °C. The resulting reaction mixture was allowed to warm and stirred at rt for 6 h. The reaction mixture was poured into aq. 1 M NaOH solution (55 mL) and ice with vigorous stiring. A suspension of aluminium hydroxide was formed. The suspension was filtered through Celite and then aqueous phase was extracted with diethyl ether (3 × 50 mL). The combined organic layers were washed with aq. 1 N HCl solution (45 mL), brine (45 mL), dried over MgSO$_4$ and concentrated under reduced pressure. The crude product was purified by flash column chromatography through silica (eluent:pentane:ethyl acetate 5:1) to deliver pure (±)-3-phenylpent-4-en-1-ol (**66**, 600 mg, 3.70 mmol, 64 %) as a colourless oil.

^{1}H NMR (300 MHz, CDCl$_3$): δ (ppm): 7.11–7.41 (m, 5H), 5.98 (ddd, J = 17.6, 10.2, 7.6 Hz, 1H), 4.99–5.20 (m, 2H), 3.54–3.73 (m, 2H), 3.47 (q, J = 7.6 Hz, 1H), 1.82–2.10 (m, 2H), 1.21–1.39 (m, 1H); **HR-MS (ESI)**: *m/z* calculated for [C$_{11}$H$_{14}$ONa]$^+$ ([M + Na]$^+$): 185.0937, measured: 185.0935.

3-Ethylhept-6-en-3-ol (68) [26]
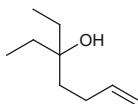
Following a similar procedure reported by Zhang et al. [25], in a heat gun dried two necked round bottomed flask equipped with a magnetic stir bar and connected with a reflux condenser under argon, homoallyl bromide (1.16 mL, 11.4 mmol, 1.14 equiv.) in THF (2.4 mL) was added to a heterogeneous mixture of Mg turnings (288 mg, 12.0 mmol, 1.20 equiv.) in THF (2.4 mL). The reaction mixture was refluxed for 2 h. After cooling to rt, the Grignard solution was diluted with THF (5 mL) and then added to a solution of 3-pentanone (1.06 mL, 10 mmol, 1.00 equiv.) in THF (10 mL) at −78 °C. The resulting reaction mixture was allowed to stir for another 1 h. The reaction was quenched with satd aq. NH$_4$Cl and extracted with diethyl ether. The combined organic layers were washed with brine, dried over MgSO$_4$ and concentrated under reduced pressure. The crude product was purified by flash column chromatography through silica (eluent:pentane:ethyl acetate 9:1) to deliver pure 3-ethylhept-6-en-3-ol (**68**, 611 mg, 4.30 mmol, 43 %) as a colourless oil.

^{1}H NMR (300 MHz, CDCl$_3$): δ (ppm): 5.85 (ddt, J = 16.8, 10.2, 6.6 Hz, 1H), 4.55–5.15 (m, 2H), 2.08 (dtt, J = 9.5, 6.4, 1.5 Hz, 2H), 1.40–1.56 (m, 6H), 1.14 (s, 1H), 0.86 (t, J = 7.5 Hz, 6H); **HR-MS (ESI)**: *m/z* calculated for [C$_9$H$_{18}$ONa]$^+$ ([M + Na]$^+$): 165.1250, measured: 165.1244.

4-Methylpent-4-en-1-ol (69) [27]

Following a procedure reported by Harmata et al. [28], The solution of methallyl alcohol (420 μL, 5 mmol, 1.00 equiv.) and propionic acid (210 μL, 0.560 equiv.) in triethyl orthoacetate (10.5 mL, 57.3 mmol, 11.5 equiv.) was refluxed at 120 °C for 8 h. After cooling to rt, the reaction mixture was diluted with diethyl ether, extracted with 10 % HCl, satd. aq. NaHCO$_3$. The combined organic layers were washed with brine, dried over MgSO$_4$ and concentrated under reduced pressure. The crude ester (668 mg, 4.7 mmol) was obtained as an oil and directly used in next step.

The crude ester (650 mg, 4.57 mmol, 1.00 equiv.) in THF (2.6 mL) was added to a suspension of LiAlH$_4$ (520 mg, 13.7 mmol, 3.00 equiv.) in THF (10 mL) at 0 °C. The reaction mixture was stirred for 30 min and then quenched with water (4 mL). The suspension was filtered through Celite, extracted with diethyl ether (3 × 20 mL), washed with brine, dried over MgSO$_4$ and concentrated under reduced pressure. The crude reaction mixture was purified by flash column chromatography through silica (eluent:pentane:ethyl acetate 9:1) to affoed pure 4-methylpent-4-en-1-ol (**69**, 256 mg, 2.56 mmol, 56 %) as a colourless oil.

^{1}H NMR (300 MHz, CDCl$_3$): δ (ppm): 4.69–4.72 (m, 2H), 3.64 (t, J = 6.5 Hz, 2H), 2.08 (t, J = 7.6 Hz, 2H), 1.71 (s, 3H), 1.63–1.75 (m, 2H).

4-Methyl-*N*-(pent-4-en-1-yl)benzenesulfonamide (73) [29]
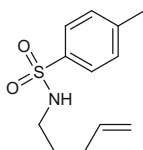
Following a procedure reported by Marcotullio et al. [29], in heat gun dried round bottomed flask, triethylamine (7.0 mL, 50 mmol, 5.0 equiv.) was added slowly to a solution of pent-4-en-1-ol (1.1 mL, 10.0 mmol, 1.00 equiv.) and methanesulphonyl chloride (543 μL, 12.0 mmol, 1.20 equiv.) in dichloromethane (50 mL) at 0 °C. The reaction mixture was sirred at 0 °C for 1 h. The reaction was quenched with water, extracted with dichloromethane, washed with brine and concentrated under reduced pressure to give pent-4-en-1-yl 4-methylbenzenesulfonate (1.75 g, 7.30 mmol). This reaction was repeated. The mesyl protected alcohol was directly used in the next step without further purification.

KOH (1.8 g, 32 mmol, 1.5 equiv.) was dissolved in DMF (30 mL) at 120 °C and *p*-tolylsulphonyl amide (5.47 g, 32.0 mmol, 1.50 equiv.) was then added to the reaction mixture. After 30 min stirring, a solution of pent-4-en-1-yl 4-methylbenzenesulfonate (3.50 g, 14.6 mmol) in DMF (12 mL) was added to the reaction mixture. The resulting reaction mixture was stirred for another 1.5 h at

120 °C. After cooling to rt, the reaction was quenched with water, extracted with diethyl ether, washed with brine, dried over MgSO$_4$ and then concentrated under reduced pressure. The crude reaction mixture was purified by flash column chromatography through silica (eluent:pentane:ethyl acetate 9:1) to affoed pure 4-methyl-*N*-(pent-4-en-1-yl)benzenesulfonamide (**73**, 3.18 g, 13.3 mmol, 66 %) as a colourless oil.

^{1}H NMR (300 MHz, CDCl$_3$): δ (ppm): 7.74 (dt, *J* = 8.4, 1.7 Hz, 2H), 7.31 (d, *J* = 8.4 Hz, 2H), 5.70 (ddt, *J* = 17.0, 10.3, 6.7 Hz, 1H), 4.81–5.20 (m, 2H), 4.31–4.54 (m, 1H), 2.94 (q, *J* = 6.8 Hz, 2H), 2.43 (s, 3H), 2.04 (dtt, *J* = 7.9, 6.6, 1.5 Hz, 2H), 1.51–1.65 (m, 2H); **HR-MS (ESI)**: *m/z* calculated for [C$_{12}$H$_{17}$NO$_2$SNa]$^+$ ([M + Na]$^+$): 262.0872, measured: 262.0869.

N-(2,2-Dimethylpent-4-en-1-yl)-4-methylbenzenesulfonamide (74) [25]
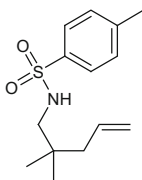
Following a procedure reported by Zhang et al. [25], in heat gun dried round bottomed flask, n-butyllithium (15.0 mL, 24 mmol, 1.6 M in hexane, 1.2 equiv.) was added slowly to a solution of diisopropylamine (3.36 mL, 24.0 mmol, 1.20 equiv.) in THF (50 mL) at 0 °C and stirred for 20 min at same temperature. Isobutyronitrile (1.8 mL, 20 mmol, 1.0 equiv.) was then added to the generated LDA solution at 0 °C and stirred for 2 h. Allyl bromide (2.08 mL, 24 mmol, 1.20 equiv.) was then added to the reaction mixture. After 3 h stirring, the reaction was quenched with water (10 mL) and extracted with diethyl ether (3 × 30 mL). The combined organic layers were washed with brine, dried over MgSO$_4$ and concentrated under reduced pressure to give 2,2-dimethylpent-4-enenitrile (790 mg, 7.23 mmol), which was directly used for next step.

2,2-dimethylpent-4-enenitrile (790 mg, 7.23 mmol, 1.0 equiv.) in diethyl ether (16 mL) was then treated with LiAlH$_4$ (1.10 g, 28.9 mmol, 4.0 equiv.) at rt. The reaction mixture was refluxed for 2 h. After cooling to 0 °C in ice bath, the reaction was quenched with water and aq. 15 % NaOH solution. The suspension was filtered through Celite and extracted with diethyl ether. The filtrate was extracted with diethyl ether, washed with brine, dried over MgSO$_4$ and then concentrated under reduced pressure to give 2,2-dimethylpent-4-en-1-amine (278 mg, 2.46 mmol, 12 % over two steps).

Triethyl amine (670 µL, 4,80 mmol, 2.07 equiv.) was added to a mixture of 2,2-dimethylpent-4-en-1-amine (278 mg, 2.46 mmol, 1.06 equiv.) and *p*-tolylsulphonyl chloride (442 mg, 2.32 mmol, 1.00 equiv.) in dichloromathae (7.7 mL) at 0 °C. The mixture was stirred at rt for 12 h.

The reaction mixture was washed with aq 10 % NaHCO$_3$ solution and brine, dried over MgSO$_4$ and concentrated under reduced pressure. The crude reaction

mixture was purified by flash column chromatography through silica (eluent:pentane:ethyl acetate 17:3) to afford pure *N*-(2,2-dimethylpent-4-en-1-yl)-4-methylbenzenesulfonamide (**74**, 502 mg, 1.88 mmol, 81 %) as a light greenish solid.

^{1}H NMR (300 MHz, CDCl$_3$): δ (ppm): 7.73 (d, *J* = 8.3 Hz, 2H), 7.31 (d, *J* = 8.0 Hz, 2H), 5.73 (ddt, *J* = 17.8, 10.3, 7.4 Hz, 1H), 4.93–5.10 (m, 2H), 4.40 (bs, 1H), 2.68 (d, *J* = 6.9 Hz, 2H), 2.43 (s, 3H), 1.96 (d, *J* = 7.4 Hz, 2H), 0.86 (s, 6H); **HR-MS (ESI)**: *m/z* calculated for [C$_{14}$H$_{21}$NO$_2$SNa]$^+$ ([M + Na]$^+$): 290.1185, measured: 290.1189.

(Z)-4-Methyl-*N*-(pent-4-en-1-yl-5-*d*)benzenesulfonamide (127) [25]
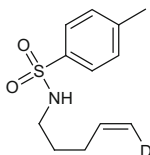
Following a procedure reported by Zhang et al. [25], DIAD (1.18 mL, 6.00 mmol, 1.20 equiv.) was added to a solution of pent-4-yn-1-ol (465 μL, 5.00 mmol, 1.00 equiv.), *N*-(*tert*-butoxycarbonyl)-*p*-toluenesulfonamide (1.49 g, 5.50 mmol, 1.10 equiv.) and triphenylphosphine (1.57 g, 6.00 mmol, 1.20 equiv.) in THF (10 mL) at 0 °C. The reaction mixture was stirred at rt for 12 h. After concentrating the reaction mixture, crude product was purified by flash column chromatography through silica (eluent:pentane:ethyl acetate 5:1) to afford pure *tert*-butyl pent-4-yn-1-yl(tosyl)carbamate (1.61 g, 4.77 mmol, 95 %) as a white solid.

In a heat gun dried round bottomed flask, n-butyllithium (2.44 mL, 3.91 mmol, 1.6 M 1.20 equiv.) was added slowly to a solution of *tert*-butyl pent-4-yn-1-yl (tosyl)carbamate (1.10 g, 3.26 mmol, 1.00 equiv.) in THF (33 mL) at −78 °C. After stirring at −78 °C for 20 min, the reaction mixture was quenched with D$_2$O (600 μL, 32.6 mmol, 10 equiv.) and stirred at 0 °C for 2 h. The reaction mixture was extracted with dichloromethane and purified by flash column chromatography through silica (eluent:pentane:ethyl acetate 6:1) to afford *tert*-butyl (pent-4-yn-1-yl-5-*d*)(tosyl)carbamate (730 mg, 2.16 mmol, 67 %) as a white waxy solid.

A solution of DIBAL-H (3.23 mL, 3.88 mmol, 1.2 M in toluene, 2.00 equiv.) was added slowly to a solution of ZrCp$_2$Cl$_2$ (1.13 g, 3.87 mmol, 2.00 equiv.) in THF (26 mL) at 0 °C. The suspension was stirred at rt for 1 h. *tert*-Butyl (pent-4-yn-1-yl-5-*d*)(tosyl)carbamate (655 mg, 1.94 mmol, 1.00 equiv.) in THF (26 mL) was added to the reaction mixture. After stirring for 1 h, the reaction mixture was quenched with water (2.5 mL) and continued stirring for another 1 h. The reaction mixture was poured into a solution of saturated aqueous NaHCO$_3$ solution (150 mL), extracted with diethyl ether (3 × 60 mL). The combined organic layers were washed with brine, dried over MgSO$_4$, filtered through Celite and then concentrated under reduced pressure. Purification by flash column

chromatography through silica (eluent:pentane:ethyl acetate 9:1) afforded pure *tert*-butyl (*Z*)-(pent-4-en-1-yl-5-*d*)(tosyl)carbamate (270 mg, 0.79 mmol, 41 %).

A solution of *tert*-Butyl (*Z*)-(pent-4-en-1-yl-5-*d*)(tosyl)carbamate (250 mg, 0.73 mmol, 1.00 equiv.) and K_2CO_3 (660 mg, 4.77 mmol, 6.50 equiv.) in methanol (15.8 mL) was refluxed for 2 h. The reaction mixture was diluted with water (15 mL) and extracted with diethyl ether (3 × 40 mL). The combined organic layers were washed with brine, dried over $MgSO_4$, and then concentrated under reduced pressure. Purification by flash column chromatography through silica (eluent:pentane:ethyl acetate 5:1) afforded pure (*Z*)-4-methyl-*N*-(pent-4-en-1-yl-5-*d*)benzenesulfonamide (**126**, 118 mg, 0.49 mmol, 67 %) as a viscous oil.

^{1}H NMR (300 MHz, CDCl₃): δ (ppm): 7.74 (d, *J* = 8.3 Hz, 2H), 7.31 (d, *J* = 8.0 Hz, 2H), 5.55–5.81 (m, 1H), 4.94 (dt, *J* = 10.2, 1.2 Hz, 1H), 4.39 (bs, 1H), 2.96 (q, *J* = 6.9 Hz, 2H), 2.43 (s, 3H), 2.04 (q, *J* = 7.2, 6.6 Hz, 2H), 1.57 (quint, *J* = 7.0 Hz, 2H); **HR-MS (ESI)**: *m/z* calculated for $[C_{12}H_{16}DNO_2SNa]^+$ ($[M + Na]^+$): 263.0935, measured: 263.0932.

Dimethyl 2-allyl-2-benzylmalonate [30]
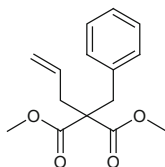
Following a procedure reported by Fürstner et al. [30], dimethyl malonate (2.87 mL, 25.0 mmol, 1.25 equiv.) was added dropwise to a suspension NaH (800 mg, 20.0 mmol, 1.00 equiv.) in THF (100 mL) at 0 °C and stirred for 30 min. Allyl bromide (1.69 mL, 20.0 mmol, 1.00 equiv.) was then added to the reaction mixture and allowed to stir at rt for 14 h. The reaction mixture was quenched with saturated aq. NH_4Cl, extracted with methyl *tert*-butyl ether, washed with brine, dried over $MgSO_4$ and concentrated under reduced pressure. The crude reaction mixture was purified by flash column chromatography through silica (eluent:pentane:ethyl acetate 9:1) to affoed pure dimethyl 2-allylmalonate (2.31 g, 13.4 mmol, 67 %) as a colourless oil.

According to the literature procedure by Curran et al. [31], dimethyl 2-allylmalonate (500 mg, 2.90 mmol, 1.00 equiv.) in THF (2 mL) was added to a suspension of NaH (130 mg, 3.25 mmol, 60 % in mineral oil, 1.12 equiv.) in THF (8 mL). After stirring for 30 min, benzyl bromide (386 μL, 3.25 mmol, 1.12 equiv.) was added dropwise to the reaction mixture. The resulting reaction mixture was stirred for 12 h and then quenched with water (5 mL). The aqueous layer was extracted with diethyl ether. The combined organic layers were washed with brine, dried over $MgSO_4$ and concentrated under reduced pressure. The crude reaction mixture was purified by flash column chromatography through silica (eluent:

pentane:diethyl ether 9:1) to affoed pure dimethyl 2-allyl-2-benzylmalonate (310 mg, 1.18 mmol, 41 %) as a colourless oil.

^{1}H NMR (400 MHz, CD$_2$Cl$_2$): δ (ppm): 7.19–7.31 (m, 3H), 7.04–7.12 (m, 2H), 5.76 (ddt, J = 15.9, 11.3, 7.3 Hz, 1H), 4.96–5.24 (m, 2H), 3.71 (s, 6H), 3.24 (s, 2H), 2.56 (dt, J = 7.2, 1.3 Hz, 2H); **GC-MS**: **t$_R$ (50_40)**: 8.4 min; **EI-MS**: m/z (%): 221 (55), 202 (15), 199 (13), 190 (11), 189 (100), 171 (19), 143 (51), 142 (18), 141 (16), 139 (30), 129 (16), 128 (33), 121 (26), 115 (32), 91 (79), 65 (17), 59 (11), 41 (10).

6.3.3   Synthesis of Aryldiazonium Salts

General Procedure 1:

Following a modified procedure reported by Hanson et al. [32], aniline (1 equiv.) was added to a mixture of 50 % aq. HBF$_4$ (340 μL/mmol) and water (400 μL/mmol). After cooling to 0 °C, NaNO$_2$ (1 equiv.) in water (150 μL/mmol) was added portionwise to the reaction mixture. After stirring at 0 °C for 30 min, the precipitate was filtered and washed with a little amount of chilled water. The solid precipitate was dissolved in acetone and precipitated by adding diethyl ether. The solid product was collected by filtration and dried overnight.

All the aryldiazonium salts (**65, 86–92**) were synthesized following the **GP1** and used directly for the reaction.

6.3.4   Synthesis of Diaryliodonium Salts

General Procedure 2:

Following a modified procedure reported by Olofsson et al. [33], in a round bottomed flask, m-CPBA (1.1 equiv., ∼77 %) was dried under vacuum for 1 h. Dichloromethane (3.4 mL/mmol) was then added to the flask to dissolve m-CPBA under argon. Aryl iodide (1.0 equiv.) followed by BF$_3$·OEt$_2$ (2.5 equiv.) was added to the solution at rt. The resulting reaction mixture was stirred at rt for 1 h. After cooling to 0 °C, arylboronic acid (1.1 equiv.) was added to the reaction mixture. After stirring at rt for another 15–30 min, the crude mixture was poured on silica plug (3 g/mmol) in column chromatogram and eluted with dichloromethane to remove aryl iodide and m-CPBA followed by eluting with an eluent (dichloromethane:methanol = 20:1) to deliver pure diaryliodonium tetrafluoroborate.

All the diaryliodonium salts were synthesized following the **GP2** and used directly for the reaction.

6.3.5 Synthesis and Characterization
of Oxy- and Aminoarylated Products

General Procedure 3:

$X = O, N$
$n = 1, 2$
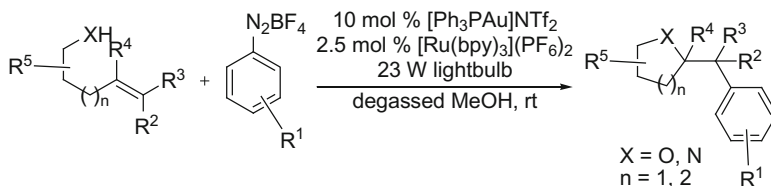
[Ru(bpy)$_3$](PF$_6$)$_2$ (4.3 mg, 5.0 µmol, 2.5 mol%), [Ph$_3$PAu]NTf$_2$ (14.8 mg, 20.0 µmol, 10 mol%), the diazonium salt (0.8 mmol, 4 equiv.) and the alkene substrate (0.2 mmol, 1.0 equiv.) were added to a flame-dried Schlenk flask containing a stirring bar. In the absence of light, anhydrous methanol (2.0 mL, 0.1 M) was added and the mixture was degassed using three freeze-pump-thaw cycles under argon. The flask was then flushed with argon, sealed and the mixture was stirred under irradiation from a desk lamp fitted with a 23 W fluorescent light bulb. After evolution of nitrogen ceased (4–16 h), the mixture was stirred for a further 30 min before being quenched with water (2 mL) and saturated aqueous K$_2$CO$_3$ solution (1 mL). The crude reaction mixture was then extracted with diethyl ether (4 × 5 mL) and the combined organic fractions were dried over anhydrous sodium sulfate, filtered and concentrated in vacuo. The crude products were purified by column chromatography over silica gel (eluent = pentane:sdichloromethane 1:1 or pentane:diethyl ether 4:1 to 9:1).

General Procedure 4:
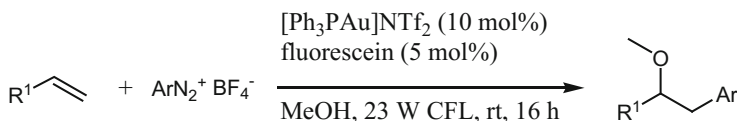
Fluorescein (3.3 mg, 10 µmol, 5 mol%), [Ph$_3$PAu]NTf$_2$ (14.8 mg, 20.0 µmol, 10 mol%), the aryldiazonium salt (0.80 mmol, 4.0 equiv.) and the alkene substrate (0.20 mmol, 1.0 equiv.) were added to a flame-dried Schlenk flask containing a stirring bar. In the absence of light, anhydrous methanol (2.0 mL, 0.10 M) was added and the mixture was degassed using three freeze-pump-thaw cycles. The flask was then flushed with argon, sealed and the mixture was stirred under irradiation from a desk lamp fitted with a 23 W fluorescent light bulb (situated ∼5 cm away from the reaction vessel). After evolution of nitrogen ceased (16 h), the mixture was stirred for a further 30 min before being filtered through a short pad of

silica gel (eluent = EtOAc) and the solvent was removed *in vacuo*. The crude products were purified by column chromatography over silica gel (eluent: pentane/dichloromethane or pentane/ethyl acetate).

General Procedure 5:
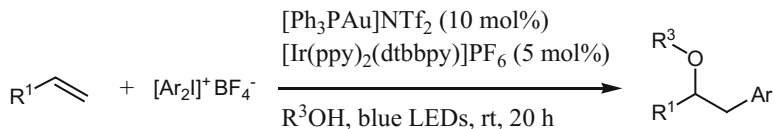
[Ir(ppy)$_2$(dtbbpy)](PF$_6$) (9.1 mg, 10 µmol, 5 mol%), [Ph$_3$PAu]NTf$_2$ (14.8 mg, 20.0 µmol, 10 mol%), the diaryliodonium salt (0.80 mmol, 4.0 equiv.) and the alkene substrate (0.20 mmol, 1.0 equiv.) were added to a flame-dried Schlenk flask containing a stirring bar. In the absence of light, anhydrous methanol (or other alcohol or acid, 2.0 mL, 0.10 M) was added and the mixture was degassed using three freeze-pump-thaw cycles. The flask was then flushed with argon, sealed and the mixture was stirred under irradiation from blue LEDs (situated ∼ 5 cm away from the reaction vessel in a custom-made "light box", see Fig. 6.2). After 20 h of irradiation, the mixture was filtered through a short pad of silica gel (eluent = EtOAc) and the solvent was removed *in vacuo*. The crude products were purified by column chromatography over silica gel (eluent:pentane/ dichloromethane or pentane/ethyl acetate).

2-Benzyltetrahydrofuran (57)
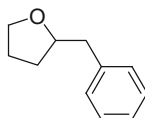
GP3: Prepared from 4-penten-1-ol (**54**) and benzenediazonium tetrafluoroborate (**65**). Colorless oil (26 mg, 0.16 mmol, 79 %).

GP5: Prepared from 4-penten-1-ol (**54**) and diphenyliodonium tetrafluoroborate (**101**). Colorless oil (22 mg, 0.14 mmol, 68 %).

R$_f$ (pentane:diethyl ether 9:1): 0.26; **^{1}H NMR (300 MHz, CDCl$_3$)**: δ (ppm): 7.17–7.31 (m, 5H), 4.06 (m, 1H), 3.90 (m, 1H), 3.74 (m, 1H), 2.92 (dd, *J* = 13.6, 6.4 Hz, 1H), 2.74 (dd, *J* = 13.6, 6.5 Hz, 1H), 1.80–1.97 (m, 3H), 1.56 (m, 1H); **^{13}C NMR (75.5 MHz, CDCl$_3$)**: δ (ppm): 138.9 (C$_q$), 129.1 (CH), 128.2 (CH), 126.1 (CH), 80. (CH), 67.8 (CH$_2$), 41.9 (CH$_2$), 30.9 (CH$_2$), 25.5 (CH$_2$); **GC-MS: t$_R$ (50_40)**: 7.2 min; **EI-MS**: *m/z* (%): 91 (42), 71 (100), 65 (13), 43 (31), 41 (12); **HR-MS (ESI)**: *m/z* calculated for [C$_{11}$H$_{14}$ONa]$^+$ ([M + Na]$^+$): 185.0937, measured: 185.0944; **IR (ATR)**: ν (cm^{-1}): 3027, 2968, 2926, 2859, 1604, 1497, 1454, 1372, 1067, 1011, 919, 874, 745, 700, 625.

2-(4-Methylbenzyl)tetrahydrofuran (93)
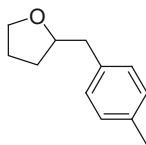
GP3: Prepared from 4-penten-1-ol (**54**) and 4-methylbenzenediazonium tetrafluoroborate (**86**). Colorless oil (28 mg, 0.16 mmol, 78 %).

R$_f$ (pentane:dichloromethane 1:1): 0.17; **^{1}H NMR (300 MHz, CDCl$_3$)**: δ (ppm): 7.09–7.15 (m, 4H), 4.05 (apparent dq, J = 8.1, 6.4 Hz, 1H), 3.90 (m, 1H), 3.74 (m, 1H), 2.90 (dd, J = 13.6, 6.4 Hz, 1H), 2.71 (dd, J = 13.6, 6.6 Hz, 1H), 2.33 (s, 3H), 1.77–1.98 (m, 3H), 1.55 (m, 1H); **^{13}C NMR (75.5 MHz, CDCl$_3$)**: δ (ppm): 135.9 (C$_q$), 135.6 (C$_q$), 129.1 (CH), 129.0 (CH), 80.2 (CH), 67.9 (CH$_2$), 41.5 (CH$_2$), 30.1 (CH$_2$), 25.6 (CH$_2$), 21.1 (CH$_3$); **GC-MS: t$_R$ (50_40)**: 7.6 min; **EI-MS**: *m/z* (%): 105 (27), 77 (12), 71 (100), 70 (11), 43 (28); **HR-MS (ESI)**: *m/z* calculated for [C$_{12}$H$_{16}$ONa]$^+$ ([M + Na]$^+$): 199.1093, measured: 199.1093; **IR (ATR)**: ν (cm^{-1}): 2971, 2922, 2861, 1516, 1458, 1446, 1370, 1183, 1061, 799, 656.

(±)-(3a*R*,7a*S*)-2-(4-Methylbenzyl)octahydrobenzofuran ((±)-(*R*,*S*)-77)

(±)
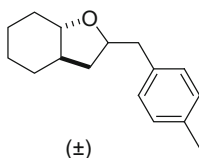
GP3: Prepared from (±)-(1*S*,2*R*)-2-allylcyclohexanol ((±)-(*S*,*R*)- **67**) and 4-methylbenzenediazonium tetrafluoroborate (**86**). GCMS analysis indicated a crude dr of 2.9:1. Pale yellow oil (30 mg, 0.13 mmol, 66 %, partially separable mixture of diastereoisomers, dr = 2.8:1). [Characterization data for major diastereoisomer.]

R$_f$ (pentane:dichloromethane 1:1): 0.39; **^{1}H NMR (300 MHz, CDCl$_3$)**: δ (ppm): 7.07–7.14 (m, 4H), 4.23 (m, 1H), 3.03 (apparent td, J = 10.2, 3.4 Hz, 1H), 2.91 (dd, J = 13.5, 5.5 Hz, 1H), 2.64 (dd, J = 13.5, 7.8 Hz, 1H), 2.31 (s, 3H), 2.11 (m, 1H), 1.63–1.94 (m, 4H), 1.53 (td, J = 12.0, 9.0 Hz, 1H), 1.14–1.40 (m, 4H), 0.96–1.14 (m, 1H); **^{13}C NMR (75.5 MHz, CDCl$_3$)**: δ (ppm): 135.6 (C$_q$), 135.6 (C$_q$), 129.3 (CH), 128.9 (CH), 83.8 (CH), 78.4 (CH), 44.0 (CH), 42.6 (CH$_2$), 35.2 (CH$_2$), 34.1 (CH$_2$), 29.1 (CH$_2$), 25.9 (CH$_2$), 24.3 (CH$_2$), 21.0 (CH$_3$); **GC-MS: t$_R$ (50_40)**: 8.8 min; **EI-MS**: *m/z* (%): 230 (5), 125 (89), 107 (52), 106 (10), 105 (48), 91 (17), 81 (100), 79 (36), 77 (15), 55 (12); **HR-MS (ESI)**: *m/z* calculated for [C$_{16}$H$_{22}$ONa]$^+$ ([M + Na]$^+$): 253.1563, measured: 253.1567; **IR (ATR)**: ν (cm^{-1}): 2931, 2857, 1516, 1456, 1447, 1351, 1142, 1073, 799, 633.

2-(4-Methylbenzyl)-3-phenyltetrahydrofuran (76)

(±)
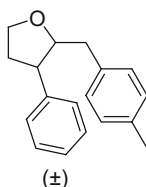
GP3: Prepared from 3-phenyl-4-penten-1-ol (**66**) and 4-methylbenzenediazonium tetrafluoroborate (**86**). Colorless oil (35 mg, 0.14 mmol, 70 %, inseparable mixture of diastereoisomers, dr = 1.6:1). Major diastereoisomer assigned as (±)-(*R*,*R*)-**76** by comparison of literature data for this isomer [34].

R_f (pentane:dichloromethane 1:1): 0.39; **^{1}H NMR (300 MHz, CDCl$_3$)**: δ (ppm): **Major Diastereoisomer**: 7.31–7.36 (m, 2H), 7.20–7.29 (m, 3H), 7.11 (d, *J* = 8.4 Hz, 2H), 7.08 (d, *J* = 8.4 Hz, 2H), 3.96–4.10 (m, 3H), 2.97 (apparent q, *J* = 8.6 Hz, 1H), 2.89 (dd, *J* = 14.2, 3.6 Hz, 1H), 2.71 (dd, *J* = 14.2, 7.8 Hz, 1H), 2.28–2.50 (m, 2H), 2.31 (s, 3H), 2.12 (m, 1H); **Minor Diastereoisomer**: 7.31–7.36 (m, 2H), 7.20–7.29 (m, 3H), 7.05 (d, *J* = 8.0 Hz, 2H), 6.95 (d, *J* = 8.0 Hz, 2H), 4.16–4.25 (m, 2H), 3.88 (td, *J* = 8.8, 6.9 Hz, 1H), 3.36 (m, 1H), 2.28–2.50 (m, 4H), 2.30 (s, 3H), 2.12 (m, 1H); *Note: Several peaks for the diastereoisomers overlap*; **^{13}C NMR (75.5 MHz, CDCl$_3$)**: δ (ppm): **Major and Minor Diastereoisomers**: 142.2 (C$_q$), 141.9 (C$_q$), 136.2 (C$_q$), 135.7 (C$_q$), 135.5 (C$_q$), 135.4 (C$_q$), 129.2 (CH), 128.9 (CH), 128.8 (CH), 128.8 (CH), 128.6 (CH), 128.6 (CH) 128.2 (CH), 127.7 (CH), 126.6 (CH), 126.4 (CH), 86.6 (CH), 83.7 (CH), 67.6 (CH$_2$), 66.9 (CH$_2$), 50.3 (CH), 47.8 (CH), 39.2 (CH$_2$), 37.2 (CH$_2$), 35.5 (CH$_2$), 33.5 (CH$_2$), 21.0 (CH$_3$), 21.0 (CH$_3$); **GC-MS**: t_R (50_40): **Major Diastereoisomer**: 9.2 min; **EI-MS**: *m/z* (%): 148 (11), 147 (100), 146 (16), 117 (26), 115 (11), 105 (21), 91 (52); **Minor Diastereoisomer**: 9.2 min; **EI-MS**: *m/z* (%): 148 (12), 147 (100), 146 (14), 118 (14), 117 (37), 115 (13), 105 (21), 91 (43), 73 (15); **HR-MS (ESI)**: *m/z* calculated for [C$_{18}$H$_{20}$ONa]$^+$ ([M + Na]$^+$): 275.1406, measured: 275.1411; **IR (ATR)**: ν (cm^{-1}): 3027, 2921, 2867, 1515, 1494, 1454, 1358, 1101, 1073, 702, 632.

2,2-Diethyl-5-(4-Methylbenzyl)tetrahydrofuran (78)
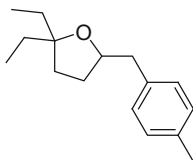
GP3: Prepared from 3-ethyl-6-hepten-3-ol (**68**) and 4-methylbenzenediazonium tetrafluoroborate (**86**). Pale yellow oil (26 mg, 0.11 mmol, 56 %).

R_f (pentane:dichloromethane 1:1): 0.5; **^{1}H NMR (300 MHz, CDCl$_3$)**: δ (ppm): 7.07–7.13 (m, 4H), 4.10 (tt, *J* = 7.7, 5.3 Hz, 1H), 3.00 (dd, *J* = 13.3, 5.1 Hz, 1H), 2.62 (dd, *J* = 13.3, 8.0 Hz, 1H), 2.98 (s, 3H), 1.83 (m, 1H), 1.41–1.71

(m, 7H), 0.87 (td, J = 7.4, 4.8 Hz, 6H); **^{13}C NMR (75.5 MHz, CDCl$_3$)**: δ (ppm): 135.8 (C$_q$), 135.5 (C$_q$), 129.2 (CH), 128.9 (CH), 85.8 (C$_q$), 79.7 (CH), 42.1 (CH$_2$), 34.0 (CH$_2$), 31.5 (CH$_2$), 31.3 (CH$_2$), 31.0 (CH$_2$), 21.0 (CH$_3$), 8.7 (CH$_3$), 8.6 (CH$_3$); **GC-MS: t$_R$ (50_40)**: 8.3 min; **EI-MS**: m/z (%): 203 (11), 131 (59), 128 (12), 127 (80), 118 (10), 115 (11), 110 (9), 109 (100), 106 (10), 105 (62), 91 (16), 83 (21), 77 (13), 67 (12), 57 (29), 55 (19), 41 (11); **HR-MS (ESI)**: m/z calculated for [C$_{16}$H$_{24}$ONa]$^+$ ([M + Na]$^+$): 255.1719, measured: 255.1733; **IR (ATR)**: ν (cm^{-1}): 2964, 2935, 2877, 1515, 1462, 1376, 1124, 1056, 946, 631.

2-Methyl-2-(4-methylbenzyl)tetrahydrofuran (79)
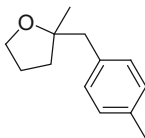
GP3: Prepared from 4-methyl-4-penten-1-ol (**69**) and 4-methylbenzenediazonium tetrafluoroborate (**86**). Pale yellow oil (15 mg, 78 μmol, 39 %).

R$_f$ (pentane:dichloromethane 1:1): 0.19; **^{1}H NMR (300 MHz, CDCl$_3$)**: δ (ppm): 7.06–7.14 (m, 4H), 3.73–3.89 (m, 2H), 2.76 (s, 2H), 2.33 (s, 3H), 1.69–1.94 (m, 3H), 1.60 (m, 1H), 1.17 (s, 3H); **^{13}C NMR (75.5 MHz, CDCl$_3$)**: δ (ppm): 135.5 (C$_q$), 135.4 (C$_q$), 130.3 (CH), 128.6 (CH), 82.9 (C$_q$), 67.4 (CH$_2$), 46.4 (CH$_2$), 36.1 (CH$_2$), 26.3 (CH$_3$), 26.0 (CH$_2$), 21.0 (CH$_3$); **GC-MS: t$_R$ (50_40)**: 7.6 min; **EI-MS**: m/z (%): 105 (27), 85 (100), 43 (49); **HR-MS (ESI)**: m/z calculated for [C$_{13}$H$_{18}$ONa]$^+$ ([M + Na]$^+$): 213.1250, measured: 213.1251; **IR (ATR)**: ν (cm^{-1}): 2966, 2924, 2866, 1514, 1452, 1373, 1112, 1086, 1045, 813, 751, 625.

(±)-(R)-2-((R)-1-(p-Tolyl)ethyl)tetrahydrofuran ((±)-(R,R)-81)

(±)
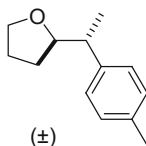
GP3: Prepared from (*E*)-4-hexen-1-ol ((*E*)-**71**) and 4-methylbenzenediazonium tetrafluoroborate (**86**). ^{1}H NMR of the crude reaction mixture showed crude diastereoselectivity of >20:1. Pale yellow oil (22 mg, 0.12 mmol, 59 %, dr > 25:1).

R$_f$ (pentane:dichloromethane 1:1): 0.20; **^{1}H NMR (300 MHz, CDCl$_3$)**: δ (ppm): 7.10 (s, 4H), 3.73–3.93 (m, 3H), 2.69 (dq, J = 8.3, 6.9 Hz, 1H), 2.32 (s, 3H), 1.74–1.84 (m, 2H), 1.67 (m, 1H), 1.45 (m, 1H), 1.34 (d, J = 6.9 Hz, 3H); **^{13}C NMR (75.5 MHz, CDCl$_3$)**: δ (ppm): 141.6 (C$_q$), 135.7 (C$_q$), 129.0 (CH), 127.6 (CH), 84.2 (CH), 68.1 (CH$_2$), 44.9 (CH), 30.0 (CH$_2$), 25.7 (CH$_2$), 21.0 (CH$_3$), 18.9 (CH$_3$); **GC-MS: t$_R$ (50_40)**: 7.5 min; **EI-MS**: m/z (%): 190 (6), 120 (10), 119 (25), 117 (11), 91 (13), 71 (100), 43 (19); **HR-MS (ESI)**: m/z calculated for

$[C_{13}H_{18}ONa]^+$ ([M + Na]$^+$): 213.1250, measured: 213.1252; **IR (ATR)**: ν (cm^{-1}): 2963, 2926, 2870, 1515, 1457, 1376, 1068, 815, 631.

The stereochemistry is assigned based on mechanistic rationale (see assignment for the aminoarylation of deuterated substrates D-(E)-**126** and D-(Z)-**127**) [25]. These assignments are also consistent with literature ^{1}H and ^{13}C NMR data for closely related compounds [35, 36].

(±)-(R)-2-((S)-1-(p-Tolyl)ethyl)tetrahydrofuran ((±)-(R,S)-82)

(±)
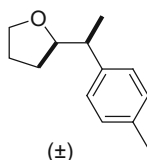
GP3: Prepared from (Z)-4-hexen-1-ol ((Z)-**72**) and 4-methylbenzenediazonium tetrafluoroborate (**86**) on a 0.4 mmol scale. ^{1}H NMR of the crude reaction mixture showed crude diastereoselectivity of >20:1. Pale yellow oil (43 mg, 0.22 mmol, 56 %, dr > 25:1).

R$_f$ (pentane:dichloromethane 1:1): 0.27; **^{1}H NMR (300 MHz, CDCl$_3$)**: δ (ppm): 7.10–7.19 (m, 4H), 3.95 (dt, J = 7.2, 6.9 Hz, 1H), 3.81 (dt, J = 8.3, 6.8 Hz, 1H), 3.70 (m, 1H), 2.78 (apparent quin, J = 7.2 Hz, 1H), 2.33 (s, 3H), 1.92–2.03 (m, 1H), 1.77–1.88 (m, 2H), 1.58 (m, 1H), 1.26 (d, J = 7.1 Hz, 3H); **^{13}C NMR (75.5 MHz, CDCl$_3$)**: δ (ppm): 141.6 (C$_q$), 135.6 (C$_q$), 128.9 (CH), 127.5 (CH), 83.8 (CH), 68.1 (CH$_2$), 44.4 (CH), 29.5 (CH$_2$), 25.8 (CH$_2$), 21.0 (CH$_3$), 18.2 (CH$_3$); **GC-MS: t$_R$ (50_40)**: 7.7 min; **EI-MS**: m/z (%): 190 (5), 119 (23), 117 (10), 91 (12), 71 (100), 43 (21); **HR-MS (ESI)**: m/z calculated for $[C_{13}H_{18}ONa]^+$ ([M + Na]$^+$): 213.1250, measured: 213.1259; **IR (ATR)**: ν (cm^{-1}): 2968, 2872,1515, 1417, 1378, 1365, 1184, 1108, 1066, 1038, 922, 818, 732, 720, 658, 623.

The stereochemistry is assigned based on mechanistic rationale (see assignment for the aminoarylation of deuterated substrates D-(E)-**126** and D-(Z)-**127**) [25]. These assignments are also consistent with literature ^{1}H and ^{13}C NMR data for closely related compounds [35, 36].

2-(4-Methylbenzyl)tetrahydro-2H-pyran (85)
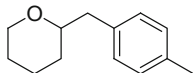
GP3: Prepared from 5-hexen-1-ol (**75**) and 4-methylbenzenediazonium tetrafluoroborate (**86**). Colorless oil (13 mg, 68 μmol, 34 %).

R$_f$ (pentane:dichloromethane 1:1): 0.42; **^{1}H NMR (600 MHz, CDCl$_3$)**: δ (ppm): 7.09–7.12 (s, 4H), 3.96 (m, 1H), 3.47 (dtd, J = 10.8, 6.6, 2.0 Hz, 1H), 3.42 (td, J = 11.8, 2.4 Hz, 1H), 2.85 (dd, J = 13.7, 6.6 Hz, 1H), 2.62 (dd, J = 13.7, 6.6 Hz, 1H), 2.33 (s, 3H), 1.81 (m, 1H), 1.55–1.63 (m, 2H), 1.49 (m, 1H), 1.43 (m, 1H),

1.28 (m, 1H); **^{13}C NMR (151 MHz, CDCl$_3$)**: δ (ppm): 135.7 (C$_q$), 135.5 (C$_q$), 129.2 (CH), 128.9 (CH), 78.9 (CH), 68.6 (CH$_2$), 42.8 (CH$_2$), 31.4 (CH$_2$), 26.1 (CH$_2$), 23.5 (CH$_2$), 21.0 (CH$_3$); **GC-MS**: **t$_R$ (50_40)**: 7.8 min; **EI-MS**: *m/z* (%): 190 (5), 105 (24), 85 (100), 84 (17), 77 (10), 67 (16), 57 (14), 43 (12), 41 (12); **HR-MS (ESI)**: *m/z* calculated for [C$_{13}$H$_{18}$ONa]$^+$ ([M + Na]$^+$): 213.1250, measured: 213.1251; **IR (ATR)**: ν (cm^{-1}): 2933, 2842, 1515, 1462, 1439, 1377, 1351, 1261, 1195, 1173, 1090, 1042, 903, 816, 667, 623. 1142, 1073, 799, 633.

2-(4-Methylbenzyl)-1-tosylpyrrolidine (83)
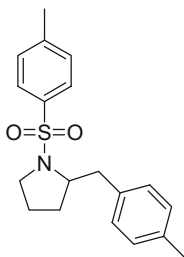
GP3: Prepared from 4-methyl-*N*-(pent-4-en-1-yl)benzenesulfonamide (**73**) and 4-methylbenzenediazonium tetrafluoroborate (**86**). Viscous oil that solidified upon standing (55 mg, 0.17 mmol, 84 %).

   R$_f$ (pentane:diethyl ether 4:1): 0.18; **^{1}H NMR (300 MHz, CDCl$_3$)**: δ (ppm): 7.77 (d, *J* = 8.3 Hz, 2H), 7.32 (d, *J* = 8.0 Hz, 2H), 7.14 (m, 4H), 3.81 (m, 1H), 3.41 (m, 1H), 3.09–3.25 (m, 2H), 2.72 (dd, *J* = 13.3, 9.7 Hz, 1H), 2.43 (s, 3H), 2.34 (s, 3H), 1.59–1.74 (m, 2H), 1.35–1.53 (m, 2H); **^{13}C NMR (75.5 MHz, CDCl$_3$)**: δ (ppm): 143.3 (C$_q$), 135.9 (C$_q$), 135.4 (C$_q$), 134.6 (C$_q$), 129.6 (CH), 129.5 (CH), 129.1 (CH), 127.5 (CH), 61.7 (CH), 49.2 (CH$_2$), 42.2 (CH$_2$), 29.8 (CH$_2$), 23.7 (CH$_2$), 21.5 (CH$_3$), 21.0 (CH$_3$); **GC-MS**: **t$_R$ (50_40)**: 11.9 min; **EI-MS**: *m/z* (%): 226 (6), 225 (14), 124 (100), 155 (34), 105 (16), 91 (47); **HR-MS (ESI)**: *m/z* calculated for [C$_{19}$H$_{23}$NO$_2$SNa]$^+$ ([M + Na]$^+$): 352.1342, measured: 352.1339; **IR (ATR)**: ν (cm^{-1}): 2974, 2951, 2925, 2872, 1598, 1515, 1494, 1449, 1342, 1197, 1158, 1110, 1093, 1034, 987, 816, 734, 666, 589.

(±)-D-(*R*,*R*)-(2-(4-Methylbenzyl-1-tosylpyrrolidine (±)-D-(*R*,*R*)-(128) [25]
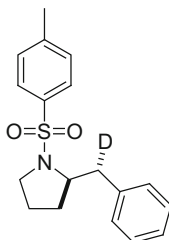
GP3: Prepared from D-(*E*)-4-methyl-*N*-(pent-4-en-1-yl)benzenesulfon-amide (D-(*E*)-**126**, D = 94 %) and benzenediazonium tetrafluoroborate (**65**). Pale yellow viscous oil that solidified upon standing (46 mg, 0.15 mmol, 73 %, dr = 14:1, D = 96 %).

R_f **(pentane:dichloromethane 1:1)**: 0.18; **^{1}H NMR (400 MHz, CDCl$_3$)**: δ (ppm): 7.76 (d, *J* = 8.3 Hz, 2H), 7.28–7.34 (m, 4H), 7.20–7.26 (m, 3H), 3.81 (ddd, *J* = 9.6, 7.7, 3.2 Hz, 1H), 3.40 (m, 1H), 3.13 (dt, *J* = 10.2, 7.1 Hz, 1H), 2.74 (d, *J* = 9.6 Hz, 1H), 2.42 (s, 3H), 2.34 (s, 3H), 1.59–1.71 (m, 2H), 1.36–1.51 (m, 2H); **^{13}C NMR (75.5 MHz, CDCl$_3$)**: δ (ppm): 143.3 (C$_q$), 138.4 (C$_q$), 134.6 (C$_q$), 129.6 (CH), 129.6 (CH), 128.4 (CH), 127.5 (CH), 126.4 (CH), 61.5 (CH), 49.2 (CH$_2$), 42.4 (t, *J* = 20 Hz, CDH), 29.8 (CH$_2$), 23.8 (CH$_2$), 21.5 (CH$_3$); **GC-MS: t_R (50_40)**: 11.4 min; **EI-MS**: *m/z* (%): 225 (17), 224 (100), 124 (100), 155 (40), 92 (22), 91 (58), 65 (12); **HR-MS (ESI)**: *m/z* calculated for [C$_{18}$H$_{20}$DNO$_2$SNa]$^+$ ([M + Na]$^+$): 339.1248, measured: 339.1250; **IR (ATR)**: ν (cm^{-1}): 3027, 2975, 2924, 1598, 1494, 1450, 1334, 1195, 1153, 1108, 1091, 1030, 988, 820, 731, 700, 661, 607.

(±)-D-(*R*,*S*)-(2-(4-Methylbenzyl)-1-tosylpyrrolidine (±)-D-(*R*,*S*)-(129) [25]
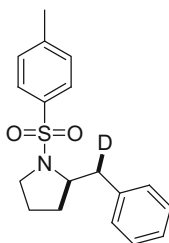
GP3: Prepared from D-(*Z*)-4-methyl-*N*-(pent-4-en-1-yl)benzenesulfon-amide (D-(*Z*)-**127**, D = 99 %) and benzenediazonium tetrafluoroborate (**65**). Pale yellow viscous oil that solidified upon standing (43 mg, 0.14 mmol, 68 %, dr = 17:1, D = 99 %).

R_f **(pentane:diethyl ether 4:1)**: 0.15; **^{1}H NMR (300 MHz, CDCl$_3$)**: δ (ppm): 7.76 (d, *J* = 8.2 Hz, 2H), 7.22–7.33 (m, 7H), 3.79–3.84 (m, 1H), 3.36–3.43 (m, 1H), 3.23 (d, *J* = 3.4 Hz, 1H), 3.09–3.17 (m, 1H), 2.42 (s, 3H), 1.57–1.72 (m, 2H), 1.35–1.51 (m, 2H); **^{13}C NMR (75.5 MHz, CDCl$_3$)**: δ (ppm): 143.3 (C$_q$), 138.4 (C$_q$), 134.8 (C$_q$), 129.6 (CH), 129.6 (CH), 128.4 (CH), 127.5 (CH), 126.4 (CH), 61.5 (CH), 49.2 (CH$_2$), 42.3 (t, *J* = 19.6 Hz, CDH), 29.8 (CH$_2$), 23.8 (CH$_2$), 21.5 (CH$_3$); **GC-MS: t_R (50_40)**: 11.5 min; **EI-MS**: *m/z* (%): 225 (14), 224 (100), 155 (36), 92 (16), 91 (41); **HR-MS (ESI)**: *m/z* calculated for [C$_{18}$H$_{20}$DNO$_2$SNa]$^+$ ([M + Na]$^+$): 339.1248, measured: 339.1253; **IR (ATR)**: ν (cm^{-1}): 3026, 2974, 2874 1598, 1495, 1450, 1343, 1196, 1155, 1091, 1036, 989, 816, 733, 702, 662, 600.

4,4-Dimethyl-2-(4-methylbenzyl)-1-tosylpyrrolidine (84)
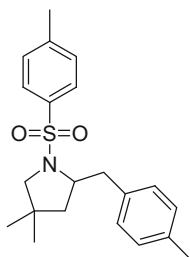
GP3: Prepared from *N*-(2,2-dimethylpent-4-en-1-yl)-4-methylbenzene sulfonamide (**74**) and 4-methylbenzenediazonium tetrafluoroborate (**86**). Pale yellow oil (39 mg, 0.11 mmol, 54 %).

R_f **(pentane:dichloromethane 1:1)**: 0.24; **GC-MS: t_R (50_40)**: 12 min; **^{1}H NMR (300 MHz, CDCl$_3$)**: δ (ppm): 7.78 (d, *J* = 8.3 Hz, 2H), 7.32 (d, *J* = 8.0 Hz, 2H), 7.11 (s, 3H), 3.76 (m, 1H), 3.54 (dd, *J* = 13.1, 3.5 Hz, 1H), 3.12 (s, 2H), 2.72 (dd, *J* = 13.1, 9.9 Hz, 1H), 2.43 (s, 3H), 2.32 (s, 3H), 1.39–1.55 (m, 2H), 0.99 (s, 3H), 0.44 (s, 3H); **^{13}C NMR (75.5 MHz, CDCl$_3$)**: δ (ppm): 143.3 (C$_q$), 135.8 (C$_q$), 135.4 (C$_q$), 135.2 (C$_q$), 129.6 (CH), 129.4 (CH), 129.1 (CH), 127.5 (CH), 61.6 (CH), 61.6 (CH$_2$), 45.7 (CH$_2$), 42.4 (CH$_2$), 37.2 (C$_q$), 26.4 (CH$_3$), 25.8 (CH$_3$), 21.5 (CH$_3$), 21.0 (CH$_3$); **EI-MS**: *m/z* (%): 253 (16), 252 (100), 155 (25), 105 (13), 91 (45); **HR-MS (ESI)**: *m/z* calculated for $[C_{21}H_{27}NO_2SNa]^+$ ([M + Na]$^+$): 380.1655, measured: 380.1653; **IR (ATR)**: ν (cm^{-1}): 2959, 2926, 2873, 1598, 1515, 1452, 1344, 1156, 1092, 1048, 815, 709, 661.

2-([1,1′-Biphenyl]-4-ylmethyl)tetrahydrofuran (94)
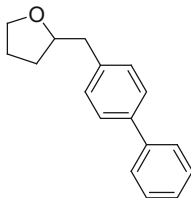
GP3: Prepared from 4-penten-1-ol (**54**) and 4-phenylbenzenediazonium tetrafluoroborate (**87**). Pale yellow oil (31 mg, 0.13 mmol, 64 %).

R_f **(pentane:dichloromethane 1:1)**: 0.17; **^{1}H NMR (300 MHz, CDCl$_3$)**: δ (ppm): 7.50–7.61 (m, 4H), 7.40–7.47 (m, 2H), 7.29–7.36 (m, 3H), 4.11 (m, 1H), 3.93 (m, 1H), 3.76 (td, *J* = 7.8, 6.3 Hz, 1H), 2.95 (dd, *J* = 13.6, 6.7 Hz, 1H), 2.81 (dd, *J* = 13.6, 6.2 Hz, 1H), 1.80–2.03 (m, 3H), 1.58 (m, 1H); **^{13}C NMR (75.5 MHz, CDCl$_3$)**: δ (ppm): 141.1 (C$_q$), 139.1 (C$_q$), 138.1 (C$_q$), 129.6 (CH), 128.7 (CH), 127.1 (CH), 127.0 (CH), 127.0 (CH), 80.0 (CH), 68.0 (CH$_2$), 41.6 (CH$_2$), 31.1 (CH$_2$), 25.6 (CH$_2$); **GC-MS**: t_R **(50_40)**: 9.6 min; **EI-MS**: *m/z* (%):

238 (13), 168 (13), 167 (24), 165 (26), 152 (12), 71 (100), 43 (21); **HR-MS (ESI)**: *m/z* calculated for $[C_{17}H_{18}ONa]^+$ ($[M + Na]^+$): 261.1250, measured: 261.1256; **IR (ATR)**: ν (cm^{-1}): 3028, 2970, 2861, 1602, 1520, 1487, 1448, 1409, 1370, 1060, 1008, 843, 761, 697, 632.

2-(4-Fluorobenzyl)tetrahydrofuran (96)
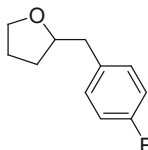
GP3: Prepared from 4-penten-1-ol (**54**) and 4-fluorobenzenediazonium tetra-fluoroborate (**89**). Pale yellow oil (27 mg, 0.15 mmol, 75 %).

R_f **(pentane:dichloromethane 1:1)**: 0.31; **^{1}H NMR (300 MHz, CDCl$_3$)**: δ (ppm): 7.19 (dd, *J* = 8.4, 5.6 Hz, 2H), 6.98 (apparent t, *J* = 8.7 Hz, 1H), 4.04 (m, 1H), 3.88 (m, 1H), 3.74 (dd, *J* = 14.3, 7.7 Hz, 1H), 2.87 (dd, *J* = 13.8, 6.7 Hz, 1H), 2.74 (dd, *J* = 13.8, 6.0 Hz, 1H), 1.81–1.99 (m, 3H), 1.59 (m, 1H); **^{13}C NMR (75.5 MHz, CDCl$_3$)**: δ (ppm): 161.5 (d, *J* = 244 Hz, CF), 134.6 (d, *J* = 3 Hz, C$_q$), 131.6 (d, *J* = 8 Hz, CH), 115.0 (d, *J* = 21 Hz, CH), 79.9 (d, *J* = 1 Hz, CH), 67.9 (CH$_2$), 41.0 (CH$_2$), 30.9 (CH$_2$), 25.6 (CH$_2$); **^{19}F NMR (282 MHz, CDCl$_3$)**: δ (ppm): −117.4; **GC-MS: t_R (50_40)**: 7.2 min; **EI-MS**: *m/z* (%): 109 (48), 83 (14), 71 (100), 43 (35), 41 (13); **HR-MS (ESI)**: *m/z* calculated for $[C_{17}H_{18}ONa]^+$ ($[M + Na]^+$): 203.0843, measured: 203.0841; **IR (ATR)**: ν (cm^{-1}): 2970, 2933, 2864, 1603, 1509, 1487, 1221, 1159, 1061, 837, 812, 762, 761, 623.

Ethyl 4-((tetrahydrofuran-2-yl)methyl)benzoate (95)
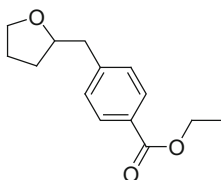
GP3: Prepared from 4-penten-1-ol (**54**) and 4-(ethoxycarbonyl)-benzene diazonium tetrafluoroborate (**88**). Pale yellow oil (39 mg, 0.17 mmol, 83 %).

R_f **(pentane:dichloromethane 1:1)**: 0.17; **^{1}H NMR (300 MHz, CDCl$_3$)**: δ (ppm): 7.97 (d, *J* = 8.2 Hz, 2H), 7.30 (d, *J* = 8.2 Hz, 1H), 4.36 (q, *J* = 7.1 Hz, 2H), 4.08 (m, 1H), 3.88 (dt, *J* = 13.3, 6.8 Hz, 1H), 3.73 (dd, *J* = 13.8, 7.4 Hz, 1H), 2.94 (dd, *J* = 13.6, 6.7 Hz, 1H), 2.82 (dd, *J* = 13.6, 6.0 Hz, 1H), 1.80–1.99 (m, 3H), 1.54 (m, 1H), 1.38 (t, *J* = 7.1 Hz, 3H); **^{13}C NMR (75.5 MHz, CDCl$_3$)**: δ (ppm): 166.1 (C = O), 144.4 (C$_q$), 129.6 (CH), 129.2 (CH), 128.5 (C$_q$), 79.5 (CH), 68.0 (CH$_2$), 60.8 (CH$_2$), 41.9 (CH$_2$), 31.0 (CH$_2$), 25.6 (CH$_2$), 14.3 (CH$_3$); **GC-MS: t_R (50_40)**: 8.9 min; **EI-MS**: *m/z* (%): 164 (29), 71 (100), 43 (21); **HR-MS (ESI)**:

m/z calculated for $[C_{14}H_{18}O_3Na]^+$ ($[M + Na]^+$): 257.1148, measured: 257.1152; **IR (ATR)**: ν (cm^{-1}): 2976, 2941, 2868, 1714, 1611, 1416, 1367, 1273, 1178, 1104, 1062, 1022, 857, 759, 708, 631.

2-(3-Methoxy-5-(trifluoromethyl)benzyl)tetrahydrofuran (99)
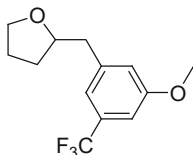
GP3: Prepared from 4-penten-1-ol (**54**) and 3-methoxy-5-(trifluoro-methyl)ben-zenediazonium tetrafluoroborate (**92**). Pale yellow oil (17 mg, 64 µmol, 32 %).

R_f **(pentane:dichloromethane 1:1)**: 0.28; **^{1}H NMR (300 MHz, CDCl$_3$)**: δ (ppm): 7.08 (s, 1H), 6.97 (s, 2H), 4.08 (m, 1H), 3.88 (m, 1H), 3.83 (s, 3H), 3.74 (m, 1H), 2.89 (dd, J = 13.8, 6.8 Hz, 1H), 2.79 (dd, J = 13.8, 5.8 Hz, 1H), 1.81– 2.02 (m, 3H), 1.55 (m, 1H); **^{13}C NMR (75.5 MHz, CDCl$_3$)**: δ (ppm): 159.7 (C$_q$), 141.6 (C$_q$), 131.6 (q, J = 32 Hz, C$_q$), 124.0 (q, J = 272 Hz, CF$_3$), 118.6 (q, J = 1 Hz, CH), 118.3 (q, J = 4 Hz, CH), 108.3 (q, J = 4 Hz, CH), 79.4 (CH), 68.0 (CH$_2$), 55.4 (CH$_3$), 41.7 (CH$_2$), 31.0 (CH$_2$), 25.6 (CH$_2$); **^{19}F NMR (282 MHz, CDCl$_3$)**: δ (ppm): −162.6; **GC-MS**: **t_R (50_40)**: 7.9 min; **EI-MS**: m/z (%): 189 (13), 71 (100), 43 (27); **HR-MS (ESI)**: m/z calculated for $[C_{13}H_{15}F_3O_2Na]^+$ ($[M + Na]^+$): 283.0916, measured: 283.0926; **IR (ATR)**: ν (cm^{-1}): 2947, 2869, 1605, 1466, 1441, 1352, 1319, 1247, 1167, 1057, 872, 704, 630.

2-(4-Bromobenzyl)tetrahydrofuran (97)
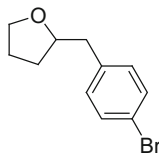
GP3: Prepared from 4-penten-1-ol (**54**) and 4-bromobenzenediazonium tetra-fluoroborate (**90**). Pale yellow oil (29 mg, 0.12 mmol, 60 %).

R_f **(pentane:dichloromethane 1:1)**: 0.28; **^{1}H NMR (300 MHz, CDCl$_3$)**: δ (ppm): 7.40 (d, J = 8.3 Hz, 2H), 7.11 (d, J = 8.3 Hz, 2H), 3.98–4.07 (m, 1H), 3.84–3.91 (m, 1H), 3.69–3.78 (m, 1H), 2.83 (dd, J = 13.7, 6.7 Hz, 1H), 2.72 (dd, J = 13.7, 6.0 Hz, 1H), 1.79–1.98 (m, 3H), 1.53 (m, 1H); **^{13}C NMR (75.5 MHz, CDCl$_3$)**: δ (ppm): 138 (C$_q$), 131.3 (CH), 131.0 (CH), 120.0 (C$_q$), 79.6 (CH), 68.0 (CH$_2$), 41.3 (CH$_2$), 31.0 (CH$_2$), 25.6 (CH$_2$); **GC-MS**: **t_R (50_40)**: 8.2 min; **EI-MS**:

m/z (%): 171 (11), 169 (12), 90 (13), 89 (11), 71 (100), 43 (26); **HR-MS (ESI)**: *m/z* calculated for $[C_{11}H_{13}BrONa]^+$ ($[M + Na]^+$): 263.0042, measured: 263.0050; **IR (ATR)**: ν (cm^{-1}): 2969, 2930, 2862, 1488, 1404, 1071, 1062, 1012, 833, 633.

### 2-(2-Bromo-4-chlorobenzyl)tetrahydrofuran (98)
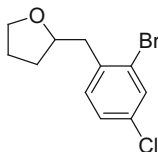
GP3: Prepared from 4-penten-1-ol (**54**) and 2-bromo-4-chlorobenzene diazonium tetrafluoroborate (**91**). Pale yellow oil (23 mg, 84 μmol, 42 %).

R_f **(pentane:dichloromethane 1:1)**: 0.44; **^{1}H NMR (300 MHz, CDCl$_3$)**: δ (ppm): 7.55 (d, *J* = 1.7 Hz, 1H), 7.19–7.27 (m, 2H), 4.12 (m, 1H), 3.90 (m, 1H), 3.74 (m, 1H), 2.93 (d, *J* = 6.4 Hz, 2H), 1.79–2.03 (m, 3H), 1.59 (m, 1H); **^{13}C NMR (75.5 MHz, CDCl$_3$)**: δ (ppm): 137.1 (C$_q$), 132.7 (C$_q$), 132.2 (CH), 132.1 (CH), 127.5 (CH), 124.9 (C$_q$), 78.1 (CH), 67.9 (CH$_2$), 41.0 (CH$_2$), 31.0 (CH$_2$), 25.6 (CH$_2$); **GC-MS**: t_R **(50_40)**: 8.5 min; **EI-MS**: *m/z* (%):89 (10), 71 (100), 43 (20); **HR-MS (ESI)**: *m/z* calculated for $[C_{11}H_{12}BrClONa]^+$ ($[M + Na]^+$): 298.9631, measured: 298.9635; **IR (ATR)**: ν (cm^{-1}): 2970, 2867, 1586, 1556, 1469, 1380, 1061, 1037, 838, 631.

(2-Methoxyoctyl)benzene (102)
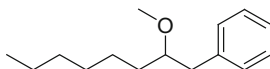
GP4: Prepared from 1-octene, benzenediazonium tetrafluoro-borate and methanol. Colorless oil (38 mg, 0.17 mmol, 86 %).

GP5: Prepared from 1-octene, diphenyliodonium tetrafluoroborate and methanol. Colorless oil (36 mg, 0.16 mmol, 82 %). The reaction was also conducted on a 2.00 mmol scale (402 mg, 1.82 mmol, 91 %).

R_f **(pentane:dichloromethane 3:1)**: 0.20; **^{1}H NMR (300 MHz, CDCl$_3$)**: δ (ppm): 7.25–7.33 (m, 2H), 7.17–7.24 (m, 3H), 3.36 (m, 1H), 3.32 (s, 3H), 2.85 (dd, *J* = 13.7, 6.2 Hz, 1H), 2.70 (dd, *J* = 13.7, 6.2 Hz, 1H), 1.37–1.49 (m, 3H), 1.19–1.36 (m, 7H), 0.88 (t, *J* = 6.8 Hz, 3H); **^{13}C NMR (75.5 MHz, CDCl$_3$)**: δ (ppm): 139.4 (C$_q$), 129.5 (CH), 128.3 (CH), 126.1 (CH), 82.5 (CH), 57.1 (CH$_3$), 40.3 (CH$_2$), 33.7 (CH$_2$), 32.0 (CH$_2$), 29.6 (CH$_2$), 25.4 (CH$_2$), 22.8 (CH$_2$), 14.2 (CH$_3$); **GC-MS**: t_R **(50_40)**: 8.1 min; **EI-MS**: *m/z* (%): 135 (11), 130 (10), 129 (100), 117 (12), 104 (10), 103 (12), 97 (79), 91 (46), 69 (11), 65 (10), 55 (54), 45 (20), 43 (11), 41 (11); **HR-MS (ESI)**: *m/z* calculated for $[C_{15}H_{24}ONa]^+$

([M + Na]$^+$): 243.1719, measured: 243.1731; **IR (ATR)**: ν (cm^{-1}): 2927, 2857, 1495, 1455, 1377, 1360, 1181, 1097, 1031, 909, 733, 699.

1-(3-Methoxy-4-phenylbutoxy)-4-nitrobenzene (112)
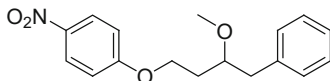
GP5: Prepared from 1-(but-3-en-1-yloxy)-4-nitrobenzene, diphenyliodonium tetrafluoroborate and methanol. Pale yellow oil (40 mg, 0.13 mmol, 66 %).

R$_f$ (pentane:ethyl acetate 9:1): 0.26; **^{1}H NMR (400 MHz, CDCl$_3$)**: δ (ppm): 8.18 (dm, J = 9.3 Hz, 2H), 7.28–7.34 (m, 2H), 7.20–7.28 (m, 3H), 6.92 (dm, J = 9.3 Hz, 2H), 4.08–4.18 (m, 2H), 3.64 (dddd, J = 9.0, 6.7, 5.6, 3.6 Hz, 1H), 3.36 (s, 3H), 2.97 (dd, J = 13.7, 5.6 Hz, 1H), 2.78 (dd, J = 13.7, 6.8 Hz, 1H), 2.01 (dddd, J = 14.5, 7.9, 6.8, 3.6 Hz, 1H), 1.87 (m, 1H); **^{13}C NMR (101 MHz, CDCl$_3$)**: δ (ppm): 164.1 (C$_q$), 141.5 (C$_q$), 138.2 (C$_q$), 129.6 (CH), 128.5 (CH), 126.5 (CH), 126.0 (CH), 114.5 (CH), 78.8 (CH), 65.6 (CH$_2$), 57.5 (CH$_3$), 40.1 (CH$_2$), 33.4 (CH$_2$); **GC-MS**: **t$_R$ (50_40)**: 10.7 min; **EI-MS**: m/z (%): 210 (34), 209 (18), 178 (100), 164 (10), 152 (53), 91 (48), 71 (14), 65 (10); **HR-MS (ESI)**: m/z calculated for [C$_{17}$H$_{19}$NO$_4$Na]$^+$ ([M + Na]$^+$): 324.1206, measured: 324.1209; **IR (ATR)**: ν (cm^{-1}): 2931, 2826, 1607, 1592, 1510, 1497, 1468, 1454, 1338, 1332, 1298, 1260, 1173, 1110, 1032, 992, 862, 845, 752, 728, 701, 658, 630.

Dimethyl 2-benzyl-2-(2-methoxy-3-phenylpropyl)malonate (114)
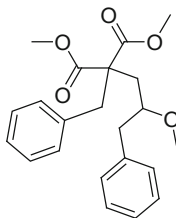
GP5: Prepared from dimethyl 2-allyl-2-benzylmalonate, diphenyl-iodonium tetrafluoroborate and methanol. Colorless oil (50 mg, 0.14 mmol, 67 %).

R$_f$ (pentane:ethyl acetate 9:1): 0.17; **^{1}H NMR (300 MHz, CDCl$_3$)**: δ (ppm): 7.23–7.34 (m, 3H), 7.13–7.20 (m, 2H), 6.98–7.12 (m, 3H), 6.61–6.66 (m, 2H), 3.66 (s, 3H), 3. 60 (s, 3H), 3.52 (tdd, J = 10.1, 4.2, 1.8 Hz, 1H), 3.28 (s, 3H), 3.28 (d, J = 13.9 Hz, 1H), 3.05 (d, J = 13.9 Hz, 1H), 2.99 (dd, J = 13.3, 4.1 Hz, 1H), 2.57 (dd, J = 13.3, 8.3 Hz, 1H), 2.04 (dd, J = 15.0, 10.3 Hz, 1H), 1.91 (dd, J = 15.0, 1.8 Hz, 1H); **^{13}C NMR (75.5 MHz, CDCl$_3$)**: δ (ppm): 172.0 (C$_q$), 171.6 (C$_q$), 138.0 (C$_q$), 135.9 (C$_q$), 129.9 (CH), 129.8 (CH), 128.7 (CH), 128.3 (CH), 126.8 (CH), 126.5 (CH), 79.4 (CH), 57.2 (CH$_3$), 57.0 (C$_q$), 52.2 (CH$_3$), 52.2 (CH$_3$), 40.4 (CH$_2$), 38.3 (CH$_2$), 36.8 (CH$_2$); **GC-MS**: **t$_R$ (50_40)**: 10.4 min; **EI-MS**: m/z (%): 279 (30), 247 (26), 219 (13), 188 (17), 187 (100), 155 (10), 143 (19), 128 (14),

117 (11), 115 (14), 91 (56); **HR-MS (ESI)**: *m/z* calculated for $[C_{22}H_{26}O_5Na]^+$ ([M + Na]⁺): 393.1672, measured: 393.1668; **IR (ATR)**: ν (cm⁻¹): 2950, 2828, 1731, 1496, 1454, 1435, 1294, 1265, 1254, 1221, 1197, 1176, 1090, 1060, 1031, 1012, 951, 927, 918, 891, 819, 736, 701, 630.

1-(3-Methoxy-4-phenylbutoxy)-4-methoxybenzene (115)
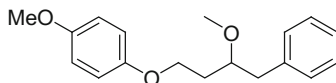
GP3: Prepared from 1-(but-3-en-1-yloxy)-4-methoxybenzene, diphenyliodonium tetrafluoroborate and methanol. Colorless oil (15 mg, 52 μmol, 26 %).

R_f **(pentane:ethyl acetate 9:1)**: 0.31; **¹H NMR (300 MHz, CDCl₃)**: δ (ppm): 7.18–7.33 (m, 5H), 6.92 (s, 4H), 3.96–4.03 (m, 2H), 3.76 (s, 3H), 3.65 (dtd, *J* = 8.3, 6.2, 3.9 Hz, 1H), 3.33 (s, 3H), 2.91 (dd, *J* = 13.7, 6.0 Hz, 1H), 2.79 (dd, *J* = 13.7, 6.3 Hz, 1H), 1.76–2.03 (m, 2H); **¹³C NMR (75.5 MHz, CDCl₃)**: δ (ppm): 153.8 (C_q), 153.3 (C_q), 138.7 (C_q), 129.7 (CH), 128.5 (CH), 126.3 (CH), 115.6 (CH), 114.7 (CH), 79.2 (CH), 65.3 (CH₂), 57.6 (CH₃), 55.9 (CH₃), 40.4 (CH₂), 33.9 (CH₂); **GC-MS**: t_R **(50_40)**: 9.8 min; **EI-MS**: *m/z* (%): 286 (54), 164 (10), 163 (100), 137 (35), 135 (11), 131 (28), 124 (65), 123 (15), 109 (30), 107 (13), 103 (14), 92 (13), 91 (71), 77 (17), 65 (14); **HR-MS (ESI)**: *m/z* calculated for $[C_{18}H_{22}O_3Na]^+$ ([M + Na]⁺): 309.1461, measured: 309.1465; **IR (ATR)**: ν (cm⁻¹): 2930, 2832, 1507, 1466, 1454, 1389, 1361, 1289, 1266, 1229, 1181, 1156, 1098, 1039, 824, 795, 735, 700, 637, 624.

2-(3-Methoxy-4-phenylbutyl)isoindoline-1,3-dione (116)
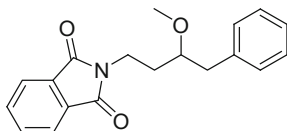
GP5: Prepared from 2-(but-3-en-1-yl)isoindoline-1,3-dione, diphenyliodonium tetrafluoroborate and methanol. Colorless oil which solidified upon standing (32 mg, 0.10 mmol, 52 %).

R_f **(pentane:ethyl acetate 9:1)**: 0.14; **¹H NMR (300 MHz, CDCl₃)**: δ (ppm): 7.85–7.91 (m, 2H), 7.72–7.79 (m, 2H), 7.28–7.36 (m, 2H), 7.19–7.28 (m, 3H), 3.84 (t, *J* = 7.1 Hz, 2H), 3.52 (dddd, *J* = 7.5, 6.6, 5.6, 4.1 Hz, 1H), 3.40 (s, 3H), 2.96 (dd, *J* = 13.7, 5.6 Hz, 1H), 2.81 (dd, *J* = 13.7, 6.7 Hz, 1H), 1.75–1.96 (m, 2H); **¹³C NMR (75.5 MHz, CDCl₃)**: δ (ppm): 168.5 (C_q), 138.3 (C_q), 134.0 (CH), 132.3 (C_q), 129.6 (CH), 128.4 (CH), 126.3 (CH), 123.3 (CH), 80.2 (CH), 57.1 (CH₃), 39.8 (CH₂), 35.0 (CH₂), 32.3 (CH₂); **GC-MS**: t_R **(50_40)**: 10.7 min; **EI-MS**: *m/z* (%): 219 (15), 218 (100), 187 (12), 186 (89), 160 (91), 133 (13), 130 (11), 104 (12), 91 (42), 77 (17), 76 (12), 71 (16), 65 (10); **HR-MS (ESI)**: *m/z* calculated for $[C_{19}H_{19}NO_3Na]^+$ ([M + Na]⁺): 332.1257, measured: 332.1254; **IR (ATR)**:

ν (cm^{-1}): 2930, 2827, 1771, 1707, 1495, 1467, 1439, 1396, 1373, 1267, 1188, 1100, 1026, 923, 866, 793, 735, 719, 700, 630, 604.

1-Methyl-4-(2-Methoxyoctyl)benzene (103)
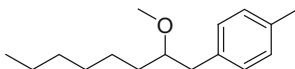
GP4: Prepared from 1-octene, *p*-toluenediazonium tetrafluoroborate and methanol. Colorless oil (29 mg, 0.12 mmol, 62 %).

R$_f$ (pentane:dichloromethane 3:1): 0.39; **^{1}H NMR (300 MHz, CDCl$_3$)**: δ (ppm): 7.08–7.15 (m, 4H), 6.96–7.07 (m, 3H), 3.27–3.46 (m, 4H), 2.82 (dd, *J* = 13.7, 6.1 Hz, 1H), 2.67 (dd, *J* = 13.7, 6.2 Hz, 1H), 2.33 (s, 3H), 1.38–1.52 (m, 3H), 1.21–1.38 (m, 7H), 0.85–0.95 (m, 3H); **^{13}C NMR (75.5 MHz, CDCl$_3$)**: δ (ppm): 136.3 (C$_q$), 135.5 (C$_q$), 129.4 (CH), 129.0 (CH), 82.6 (CH), 57.1 (CH$_3$), 39.9 (CH$_2$), 33.7 (CH$_2$), 32.0 (CH$_2$), 29.6 (CH$_2$), 25.5 (CH$_2$), 22.8 (CH$_2$), 21.2 (CH$_3$), 14.2 (CH$_3$); **GC-MS: t$_R$ (50_40)**: 8.2 min; **EI-MS**: *m/z* (%): 149 (10), 130 (11), 129 (93), 128 (28), 117 (25), 115 (24), 106 (11), 105 (81), 103 (21), 98 (10), 97 (100), 92 (21), 79 (20), 78 (12), 77 (26), 69 (11), 55 (43), 43 (12), 41 (30), 39 (12); **HR-MS (EI)**: *m/z* calculated for [C$_{16}$H$_{26}$ONa]$^+$ ([M + Na]$^+$): 257.1876, measured: 257.1878; **IR (ATR)**: ν (cm^{-1}): 2954, 2926, 2857, 2822, 1515, 1458, 1377, 1359, 1206, 1184, 1097, 1039, 1023, 909, 841, 803, 734, 648, 629.

1-Methyl-2-(2-Methoxyoctyl)benzene (104)
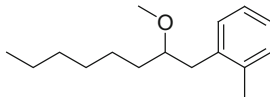
GP4: Prepared from 1-octene, *o*-toluenediazonium tetrafluoroborate and methanol. Colorless oil (13 mg, 55.46 μmol, 28 %).

GP5: Prepared from 1-octene, di(*o*-tolyl)iodonium tetrafluoroborate and methanol. Colorless oil (35 mg, 0.15 mmol, 75 %).

R$_f$ (pentane:dichloromethane 3:1): 0.31; **^{1}H NMR (300 MHz, CDCl$_3$)**: δ (ppm): 7.09–7.19 (m, 4H), 3.36 (m, 1H), 3.30 (s, 3H), 2.91 (dd, *J* = 13.8, 6.6 Hz, 1H), 2.67 (dd, *J* = 13.8, 6.4 Hz, 1H), 2.35 (s, 3H), 1.39–1.54 (m, 3H), 1.20–1.39 (m, 7H), 0.84–0.93 (m, 3H); **^{13}C NMR (75.5 MHz, CDCl$_3$)**: δ (ppm): 137.7 (C$_q$), 136.4 (C$_q$), 130.4 (CH), 130.3 (CH), 126.3 (CH), 125.9 (CH), 81.9 (CH), 57.3 (CH$_3$), 38.0 (CH$_2$), 34.2 (CH$_2$), 32.0 (CH$_2$), 29.6 (CH$_2$), 25.6 (CH$_2$), 22.8 (CH$_2$), 19.9 (CH$_3$), 14.2 (CH$_3$); **GC-MS: t$_R$ (50_40)**: 8.2 min; **EI-MS**: *m/z* (%): 130 (13), 129 (100), 128 (25), 119 (13), 117 (15), 115 (32), 106 (10), 105 (79), 104 (11), 103 (23), 97 (97), 91 (22), 79 (23), 78 (12), 77 (15), 71 (10), 69 (13), 58 (11), 55 (46), 45 (16), 43 (22), 41 (24), 39 (11); **HR-MS (EI)**: *m/z* calculated for [C$_{16}$H$_{26}$ONa]$^+$ ([M + Na]$^+$): 257.1876, measured: 257.1885; **IR (ATR)**: ν (cm^{-1}): 2954, 2927, 2857, 2822, 1493, 1459, 1378, 1360, 1186, 1129, 1096, 1013, 909, 867, 843, 824, 735, 629, 615.

1-Bromo-4-(2-methoxyoctyl)benzene (106)
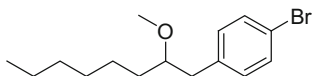
GP4: Prepared from 1-octene, *p*-bromobenzenedia-zonium tetrafluoroborate and methanol. Colorless oil (41 mg, 0.14 mmol, 69 %).

R_f **(pentane:dichloromethane 3:1)**: 0.33; ^{1}**H NMR (300 MHz, CDCl$_3$)**: δ (ppm): 7.37–7.44 (m, 2H), 7.05–7.13 (m, 2H), 3.26–3.37 (m, 4H), 2.76 (dd, J = 13.8, 6.4 Hz, 1H), 2.68 (dd, J = 13.8, 5.8 Hz, 1H), 1.37–1.51 (m, 3H), 1.17–1.37 (m, 7H), 0.82–0.95 (m, 3H); ^{13}**C NMR (75.5 MHz, CDCl$_3$)**: δ (ppm): 138.3 (C$_q$), 131.4 (CH), 131.3 (CH), 120.0 (C$_q$), 82.2 (CH), 57.2 (CH$_3$), 39.7 (CH$_2$), 33.6 (CH$_2$), 32.0 (CH$_2$), 29.5 (CH$_2$), 25.4 (CH$_2$), 22.8 (CH$_2$), 14.2 (CH$_3$); **GC-MS: t$_R$ (50_40)**: 8.8 min; **EI-MS**: *m/z* (%): 171 (39), 169 (35), 134 (29), 130 (12), 129 (100), 115 (10), 98 (10), 97 (66), 91 (17), 90 (29), 89 (23), 58 (12), 55 (42), 45 (13), 43 (11), 41 (10), 41 (12); **HR-MS (EI)**: *m/z* calculated for [C$_{15}$H$_{23}$BrONa]$^+$ ([M + Na]$^+$): 321.0824, measured: 321.0836; **IR (ATR)**: ν (cm^{-1}): 2928, 2857, 2824, 1488, 1465, 1404, 1377, 1360, 1182, 1095, 1073, 1012, 908, 838, 826, 802, 733, 648, 630.

Ethyl and Methyl 4-(2-methoxyoctyl)benzoate (109)
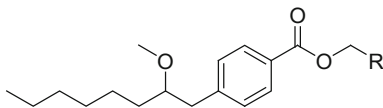
GP4: Prepared from 1-octene, *p*-(ethoxycarbonyl)benzenediazonium tetrafluoroborate and methanol. Colorless oil (37 mg, 64 %). The ethyl ester product was obtained as an inseparable 92:8 mixture with the corresponding methyl ester, which presumably results from partial transesterification with the methanol solvent. The yield reported is the calculated oxyarylation yield based on this ratio of the two compounds. The NMR data below refer to the major ethyl ester product.

R_f **(pentane:dichloromethane 1:1)**: 0.34; ^{1}**H NMR (300 MHz, CDCl$_3$)**: δ (ppm): 7.96 (dm, J = 8.3 Hz, 2H), 7.27 (dm, J = 8.3 Hz, 2H), 4.36 (q, J = 7.1 Hz, 2H), 3.36 (m, 1H), 3.29 (s, 3H), 2.85 (dd, J = 13.7, 6.5 Hz, 1H), 2.76 (dd, J = 13.7, 5.8 Hz, 1H), 1.33–1.49 (m, 6H), 1.18–1.33 (m, 7H), 0.82–0.92 (m, 3H); ^{13}**C NMR (75.5 MHz, CDCl$_3$)**: δ (ppm): 166.8 (C$_q$), 144.8 (C$_q$), 129.6 (CH), 129.5 (CH), 128.5 (C$_q$), 82.2 (CH), 60.9 (CH$_2$), 57.2 (CH$_3$), 40.4 (CH$_2$), 33.8 (CH$_2$), 31.9 (CH$_2$), 29.5 (CH$_2$), 25.4 (CH$_2$), 22.7 (CH$_2$), 14.5 (CH$_3$), 14.2 (CH$_3$); **GC-MS: t$_R$ (50_40)**: 9.3 min; **EI-MS**: *m/z* (%): 247 (20), 207 (15), 164 (37), 163 (12), 147 (10), 135 (20), 131 (10), 129 (100), 118 (18), 115 (12), 107 (19), 103 (10), 97 (88), 91 (25), 90 (23), 89 (12), 77 (10), 55 (45), 45 (19), 43 (16), 41 (19); **HR-MS (EI)**: *m/z* calculated for [C$_{18}$H$_{28}$O$_3$Na]$^+$ ([M + Na]$^+$): 315.1931, measured: 315.1938; **IR (ATR)**: ν (cm^{-1}): 2980, 2954, 2930, 2858, 2825, 1716, 1611, 1575, 1509, 1464,

1447, 1416, 1391, 1367, 1311, 1273, 1178, 1101, 1022, 910, 860, 822, 761, 732, 706, 648, 629.

1-(2-Methoxyoctyl)-4-(trifluoromethyl)benzene (108)
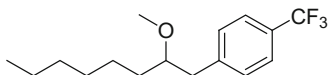
GP5: Prepared from 1-octene, di(*p*-trifluoromethyl)-phenyliodonium tetrafluoroborate and methanol. Colorless oil (21 mg, 73 μmol, 36 %).

R_f (pentane:dichloromethane 3:1): 0.41; **^{1}H NMR (300 MHz, CDCl$_3$)**: δ (ppm): 7.54 (dm, *J* = 8.1 Hz, 2H), 7.32 (dm, *J* = 8.1 Hz, 2H), 3.37 (m, 1H), 3.30 (s, 3H), 2.85 (dd, *J* = 13.8, 6.4 Hz, 1H), 2.78 (dd, *J* = 13.8, 5.8 Hz, 1H), 1.37–1.51 (m, 3H), 1.18–1.37 (m, 7H), 0.83–0.92 (m, 3H); **^{13}C NMR (151 MHz, CDCl$_3$)**: δ (ppm): 143.6 (q, *J* = 1 Hz, C$_q$), 129.9 (CH), 128.5 (q, *J* = 32 Hz, C$_q$), 125.2 (q, *J* = 4 Hz, CH), 124.5 (q, *J* = 272 Hz, C$_q$), 82.1 (CH), 57.2 (CH$_3$), 40.2 (CH$_2$), 33.7 (CH$_2$), 32.0 (CH$_2$), 29.5 (CH$_2$), 25.4 (CH$_2$), 22.8 (CH$_2$), 14.2 (CH$_3$); **^{19}F NMR (564 MHz, CDCl$_3$)**: δ (ppm): −62.4; **GC-MS: t_R (50_40)**: 7.9 min; **EI-MS**: *m/z* (%): 203 (25), 183 (11), 172 (11), 171 (11), 159 (93), 151 (16), 140 (12), 129 (100), 119 (12), 109 (32), 97 (84), 91 (10), 71 (12), 69 (15), 58 (11), 55 (53), 45 (21), 43 (20), 41 (27), 39 (10); **HR-MS (EI)**: *m/z* calculated for [C$_{16}$H$_{23}$F$_3$ONa]$^+$ ([M + Na]$^+$): 311.1593, measured: 311.1601; **IR (ATR)**: ν (cm^{-1}): 2930, 2872, 2859, 2827, 1619, 1459, 1440, 1418, 1323, 1163, 1120, 1109, 1067, 1020, 909, 849, 823, 734, 659, 640.

Ethyl and Methyl 3-(2-methoxyoctyl)benzoate (110)
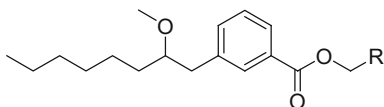
GP5: Prepared from 1-octene, di(*m*-(ethoxycarbonyl)phenyl)iodonium tetrafluoroborate and methanol. Colorless oil (29 mg, 50 %). The ethyl ester product was obtained as an inseparable 81:19 mixture with the corresponding methyl ester, which presumably results from partial transesterification with the methanol solvent. The yield reported is the calculated oxyarylation yield based on this ratio of the two compounds. The NMR data below refer to the major ethyl ester product.

R_f (pentane:dichloromethane 1:1): 0.34; **^{1}H NMR (300 MHz, CDCl$_3$)**: δ (ppm): 7.86–7.91 (m, 2H), 7.31–7.44 (m, 2H), 4.37 (q, *J* = 7.1 Hz, 2H), 3.36 (m, 1H), 3.30 (s, 3H), 2.86 (dd, *J* = 13.8, 6.5 Hz, 1H), 2.76 (dd, *J* = 13.8, 5.8 Hz, 1H), 1.35–1.51 (m, 6H), 1.18–1.35 (m, 7H), 0.82–0.92 (m, 3H); **^{13}C NMR (75.5 MHz, CDCl$_3$)**: δ (ppm): 170.6 (C$_q$), 166.9 (C$_q$), 139.7 (C$_q$), 134.2 (CH), 130.5 (CH), 128.3 (CH), 127.4 (CH), 82.3 (CH), 61.0 (CH$_2$), 57.2 (CH$_3$), 40.2 (CH$_2$), 33.7 (CH$_2$), 32.0 (CH$_2$), 29.5 (CH$_2$), 25.4 (CH$_2$), 22.7 (CH$_2$), 14.5 (CH$_3$), 14.2 (CH$_3$); **GC-MS: t_R (50_40)**: 9.2 min; **EI-MS**: *m/z* (%): 247 (38), 163 (15), 135 (15),

129 (95), 119 (18), 118 (15), 115 (12), 97 (100), 91 (11), 90 (20), 89 (15), 55 (18), 55 (11), 45 (13), 43 (12), 41 (16); **HR-MS (EI)**: *m/z* calculated for $[C_{18}H_{28}O_3Na]^+$ ($[M + Na]^+$): 315.1931, measured: 315.1932; **IR (ATR)**: ν (cm^{-1}): 2929, 2857, 1719, 1607, 1588, 1445, 1367, 1275, 1197, 1100, 1026, 912, 865, 820, 750, 697, 674, 629, 610.

2-(4-Methylbenzyl)-1-tosylpyrrolidine (120)
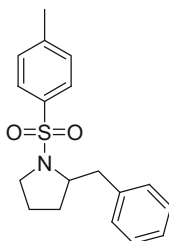
Prepared from 4-methyl-*N*-(pent-4-en-1-yl)benzenesulfonamide (**73**) and diphenyliodonium tetrafluoroborate (**101**). Viscous oil that solidified upon standing (50 mg, 0.16 mmol, 79 %).

R$_f$ (pentane:ethyl acetate 9:1): 0.20; **^{1}H NMR (400 MHz, CDCl$_3$)**: δ (ppm): 7.76 (d, *J* = 8.3 Hz, 2H), 7.19–7.34 (m, 7H), 3.83 (m, 1H), 3.40 (m, 1H), 3.25 (dd, *J* = 13.3, 4.6 Hz, 1H), 3.13 (dt, *J* = 10.1, 7.1 Hz, 1H), 2.76 (dd, *J* = 13.3, 9.6 Hz, 1H), 2.42 (s, 3H), 1.58–1.71 (m, 2H), 1.36–1.51 (m, 2H); **^{13}C NMR (101 MHz, CDCl$_3$)**: δ (ppm): 143.4 (C$_q$), 138.6 (C$_q$), 134.7 (C$_q$), 129.8 (CH), 129.7 (CH), 128.5 (CH), 127.6 (CH), 126.5 (CH), 61.7 (CH), 49.3 (CH$_2$), 42.8 (CH$_2$), 29.9 (CH$_2$), 23.9 (CH$_2$), 21.6 (CH$_3$); **GC-MS: t$_R$ (50_40)**: 11.2 min; **EI-MS**: *m/z* (%): 225 (14), 224 (100), 155 (37), 91 (60), 65 (17); **HR-MS (ESI)**: *m/z* calculated for $[C_{18}H_{21}NO_2SNa]^+$ ($[M + Na]^+$): 338.1185, measured: 338.1199; **IR (ATR)**: ν (cm^{-1}): 2974, 2927, 2873, 1598, 1595, 1453, 1339, 1305, 1289, 1267, 1196, 1156, 1092, 1033, 1017, 987, 847, 816, 802, 734, 702, 663, 631,607.

6.4 Visible Light Photoredox Catalyzed Trifluoromethylation-Ring Expansion via Semipinacol Rearrangement

6.4.1 Synthesis of (Oxa)Cycloalkanol Substrates

Substrate **156, 157,** and **158** were synthesized by Dr. Jun-Long Li (WWU Münster). The following substrates were synthesized by self according to the procedures

given in the cited references. No attempts were made to optimize yields for the synthesis of substrates.

General Procedure 6:

Y = CH$_2$, O
n = 0, 1

Br$_2$ (1.2 equiv.), P(OPh)$_3$ (1.1 equiv.)

NEt$_3$ (1.3 equiv.), DCM
-78 °C - rt, 24 - 36 h

Y = CH$_2$, O
n = 0, 1
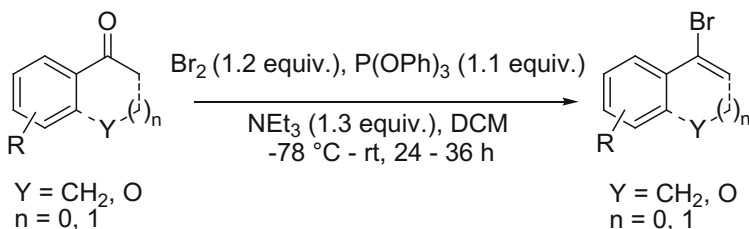
Following a modified report from Prati et al. [37], bromine (1.2 equiv.) was added dropwise to a solution of triphenyl phosphite (1.1 equiv.) in anhydrous dichloromethane (8 mL/mmol) at −78 °C under argon. Anhydrous triethylamine (1.3 equiv.) ollowed by acetophenone (1.0 equiv.) was added to the faint orange reaction mixture at −78 °C (if acetophenone is solid, then a solution in anhydrous dichloromethane was prepared and used). The reaction mixture was stirred at rt for 24–36 h. The crude reaction mixture was directly loaded on silica plug for purification by flash column chromatography (eluent:pentane: ethyl acetate 50:1 to 20:1) to afford pure vinylic bromide. vinylic bromides were directly used in next step.

General Procedure 7:

1. Mg (3 eq.), I$_2$ (0.05 equiv.)
   EtBr (0.4 equiv.)
   THF, 65 °C, 3 h

2. X$\diagup\diagdown$=O
   (1.4 equiv.), 65 °C, 9 h

X = CH$_2$, O
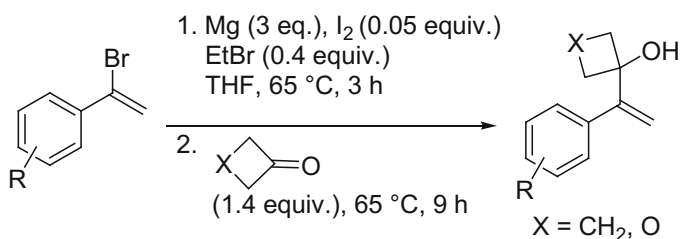
Following a modified procedure from Toste et al. [38], in a heat gun dried two necked round bottomed flask equipped with a magnetic stir bar and a reflux condenser under argon atmosphere, addition of dry THF (5 mL/mmol) to a mixture of magnesium turnings (3.0 equiv.) and iodine crystals (0.05 equiv.) resulted in an intense brown reaction mixture. Brown colour disappeared when bromoethane (0.4 equiv.) was added to the heterogeneous reaction mixture at rt. A solution of (1-bromovinyl)arene (1.0 equiv.) in THF (1.5 mL/mmol) was added dropwise to the reaction mixture. The reaction mixture was allowed to stir at 65 °C for 3 h. A solution of cyclic ketone (1.4 equiv.) in THF (1.5 mL/mmol) was added

dropwise at 65 °C and the resulted reaction mixture was allowed to stir at 65 °C for another 9 h. The reaction mixture was quenched with satd. NH_4Cl solution (aq.). The organic phase was extracted with ethyl acetate and dried over $MgSO_4$. Solvents were removed under reduced pressure and the crude reaction mixture was purified by flash column chromatography through silica gel (eluent = pentane:ethyl acetate 19:1 to 9:1) to afford pure product.

General Procedure 8:
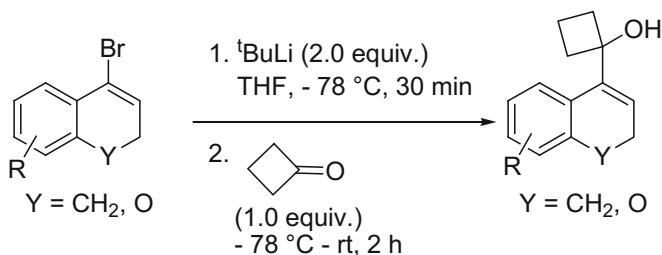
Following a modified procedure from Alexakis et al. [39], in a heat gun dried Schlenk flask equipped with a magnetic stir bar under argon atmosphere, ^{t}BuLi in heptane (1.7 M, 2.0 equiv.) was added dropwise to a solution of vinylic bromide (1.0 equiv.) in THF (2.5 mL/mmol) at −78 °C over 10 min. The resulted reaction mixture was stirred at −78 °C another 30 min. Cyclic ketone (1.0 equiv.) was added dropwise to the reaction mixture and stirred at −78 °C for 1 h. Then the reaction mixture was allowed to warm up at rt and stirred for another 1 h. The reaction was quenched with water and aqueous layer was extracted with dichloromethane. The combined organic layers was dried over $MgSO_4$, removed under reduced pressure and the crude reaction mixture was purified by flash column chromatography through silica gel (eluent = pentane:ethyl acetate 9:1) to afford pure product.

1-(1-Phenylvinyl)cyclobutan-1-ol (142)

GP7: 1-(1-Phenylvinyl)cyclobutan-1-ol was prepared from (1-bromovinyl)benzene (1.1 g, 6.0 mmol). Colourless oil (860 mg, 4.94 mmol, 82 %).
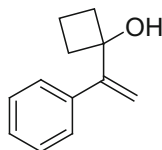
R_f (pentane:ethyl acetate 9:1): 0.20; **^{1}H NMR (300 MHz, CDCl$_3$)**: δ (ppm): 7.44–7.52 (m, 2H), 7.27–7.38 (m, 3H), 5.37 (d, J = 4.7, 2H), 2.37–2.65 (m, 2H), 2.14–2.33 (m, 2H), 1.87–2.08 (m, 2H), 1.41–1.71 (m, 1H); **^{13}C NMR (75.5 MHz, CDCl$_3$)**: δ (ppm): 152.5, 139.2, 128.3, 127.7, 127.7, 113.0, 78.2, 35.8, 13.5; **GC-MS**: t_R **(50_40)**: 7.4 min; **EI-MS**: m/z (%): 174 (17), 146 (47), 145 (70),

132 (20), 131 (55), 129 (21), 128 (27), 127 (21), 119 (10), 118 (97) 117 (100), 116 (22), 115 (43), 104 (16), 103 (82), 102 (21), 96 (12), 91 (35), 78 (25), 77 (55), 63 (10), 51 (22), 43(10); **HR-MS (ESI)**: *m/z* calculated for $[C_{12}H_{14}ONa]^+$ $([M + Na]^+)$: 197.0937, measured: 197.0933.

1-(1-(4-Fluorophenyl)vinyl)cyclobutan-1-ol (146)
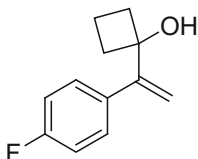
GP6: 1-(1-Bromovinyl)-4-fluorobenzene was prepared from 4′-fluoroacetophenone (829 mg, 6.00 mmol). Light yellow oil (680 mg, 3.38 mmol, 56 %).

^{1}H NMR (300 MHz, CDCl$_3$): δ (ppm): 7.53–7.61 (m, 2H), 6.96–7.09 (m, 2H), 6.05 (d, *J* = 2.1 Hz, 1H), 5.76 (d, *J* = 2.1, 1H); **GC-MS**: **t$_R$ (50_40)**: 6.4 min; **EI-MS**: *m/z* (%): 202 (10), 122 (10), 121 (100), 120 (36), 101 (52), 95 (10), 94 (13), 81 (22), 79 (14), 75 (22), 74 (19), 63 (16), 51 (11), 50 (20), 38 (10).

GP7: 1-(1-(4-Fluorophenyl)vinyl)cyclobutan-1-ol was prepared from 1-(1-bromovinyl)-4-fluorobenzene (503 mg, 2.50 mmol). Colourless oil (230 mg, 1.20 mmol, 48 %).

R$_f$ (pentane:ethyl acetate 9:1): 0.19; **^{1}H NMR (300 MHz, CDCl$_3$)**: δ (ppm): 7.37–7.56 (m, 2H), 6.93–7.06 (m, 2H), 5.34 (dd, *J* = 9.4, 0.8 Hz, 2H), 2.35–2.56 (m, 2H), 2.14–2.31 (m, 2H), 1.79–2.06 (m, 2H), 1.54–1.69 (m, 1H); **^{13}C NMR (75.5 MHz, CDCl$_3$)**: δ (ppm): 162.5 (d, *J* = 246.4 Hz), 151.5, 135.1 (d, *J* = 3.3 Hz), 129.4 (d, *J* = 7.9 Hz), 115.1 (d, *J* = 21.2 Hz), 113.0 (d, *J* = 1.2 Hz), 78.2, 35.7, 13.5; **^{19}F NMR (300 MHz, CDCl$_3$)**: −115.08; **GC-MS**: **t$_R$ (50_40)**: 7.5 min; **EI-MS**: *m/z* (%): 192 (13), 174 (11), 164 (43), 163 (76), 150 (12), 149 (54), 147 (26), 146 (47), 145 (39), 144 (17) 136 (46), 135 (88), 134 (25), 133 (63) 123 (12) 122 (14), 121 (99), 120 (47), 117 (15), 115 (39), 109 (75), 107 (23), 102 (11) 101 (100), 96 (37), 95 (47), 94 (26), 83 (18), 81 (11), 77 (14), 75 (60) 74 (28), 71 (13), 70 (15), 69 (12), 68 (12), 62 (18), 57 (12), 53 (15) 51 (27), 50 (24), 44 (11), 43 (59), 42 (33), 41 (36), 39 (67);

HR-MS (ESI): *m/z* calculated for $[C_{12}H_{13}FONa]^+$ $([M + Na]^+)$: 215.0843, measured: 215.0840.

1-(1-(4-Chlorophenyl)vinyl)cyclobutan-1-ol (147)
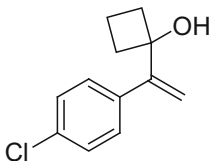
GP6:   1-(1-Bromovinyl)-4-chlorobenzene   was   prepared   from   4′-chlor-oacetophenone   (1.24 g,   8.00 mmol).   Pale   yellow   solid   (406 mg,   1.87 mmol, 23 %).

GC-MS: t_R **(50_40)**: 7.2 min; **EI-MS**: *m/z* (%): 218 (19), 216 (14), 139 (34), 138 (16), 137 (100), 136 (16), 102 (43), 101 (48), 76 (10), 75 (32), 74 (22), 63 (16), 62 (12), 51 (21), 50 (25).

GP7:   1-(1-(4-Chlorophenyl)vinyl)cyclobutan-1-ol   was   prepared   from   1-(1-bromovinyl)-4-chlorobenzene (395 mg, 1.82 mmol). Light yellow oil (130 mg, 0.623 mmol, 34 %).

R_f **(pentane:ethyl acetate 9:1)**: 0.19; **^{1}H NMR (300 MHz, CDCl$_3$)**: δ (ppm): 7.40–7.47 (m, 2H), 7.23–7.32 (m, 2H), 5.37 (dd, *J* = 6.2, 0.7 Hz, 2H), 2.35–2.53 (m, 2H), 2.11–2.29 (m, 2H), 1.80–2.10 (m, 2H), 1.53–1.69 (m, 1H); **^{13}C NMR (75.5 MHz, CDCl$_3$)**: δ (ppm): 151.4, 137.6, 133.5, 129.1, 128.4, 113.5, 78.1, 35.7, 13.5; **GC-MS**: t_R **(50_40)**: 8.1 min; **EI-MS**: *m/z* (%): 208 (10), 146 (11), 145 (100), 139 (10), 137 (19), 128 (10), 127 (20), 125 (14), 117 (58), 116 (20) 115 (46), 102 (27), 101 (29), 91 (10), 77 (14), 75 (26), 74 (11), 63 (10), 51 (14), 43 (12), 39 (15); **HR-MS (ESI)**: *m/z* calculated for $[C_{12}H_{13}ClONa]^+$ $([M + Na]^+)$: 231.0547, measured: 231.0541.

1-(1-(*p*-Tolyl)vinyl)cyclobutan-1-ol (148)
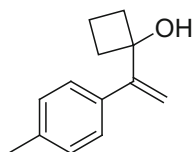
GP6: 1-(1-Bromovinyl)-4-methylbenzene was prepared from 4′-methylacetophe-none (1.07 g, 8.00 mmol). Light yellow oil (740 mg, 3.75 mmol, 47 %).

^{1}H NMR (300 MHz, CDCl$_3$): δ (ppm): 7.50 (d, *J* = 8.3 Hz, 2H), 7.16 (d, *J* = 8.3 Hz, 2H), 6.08 (d, *J* = 2.0 Hz, 1H), 5.73 (d, *J* = 2.0, 1H), 2.37 (s, 3H); **GC-MS**: t_R **(50_40)**: 6.9 min; **EI-MS**: *m/z* (%): 198 (14), 196 (13), 118 (10), 117 (100), 116 (20), 115 (87), 91 (39), 89 (23), 65 (14), 63 (32), 62 (16), 51 (19), 50 (16), 39 (19).

GP7: 1-(1-(*p*-Tolyl)vinyl)cyclobutan-1-ol was prepared from 1-(1-bromovinyl)-4-methylbenzene (591 mg, 3.00 mmol). Light yellow oil (345 mg, 1.83 mmol, 61 %).

R_f **(pentane:ethyl acetate 9:1)**: 0.22; **^{1}H NMR (300 MHz, CDCl$_3$)**: δ (ppm): 7.38 (d, *J* = 8.2 Hz, 2H), 7.14 (d, *J* = 8.2, 2H), 5.33 (s, 2H), 2.40–2.59 (m, 2H), 2.35 (s, 2H), 2.18–2.30 (m, 2H), 1.88–2.04 (m, 2H), 1.53–1.79 (m, 1H); **^{13}C NMR (75.5 MHz, CDCl$_3$)**: δ (ppm): 152.4, 137.4, 136.3, 129.0, 127.6, 112.2, 78.3, 35.9, 21.2, 13.5; **GC-MS**: t_R **(50_40)**: 7.8 min; **EI-MS**: *m/z* (%): 188 (19), 160 (14), 159 (14), 146 (21), 145 (100), 141 (11), 132 (32), 131 (23), 129 (18), 128 (19), 127 (14), 118 (14), 117 (96), 116 (26), 115 (95), 105 (28), 103 (10), 102 (12), 92 (14), 91 (52), 89 (17), 77 (19), 65 (17), 63 (17), 51 (13), 43 (14), 41 (10), 39 (22);

HR-MS (ESI): *m/z* calculated for $[C_{13}H_{16}ONa]^+$ ([M + Na]$^+$): 211.1093, measured: 211.1094.

1-(1-([1,1′-Biphenyl]-4-yl)vinyl)cyclobutan-1-ol (151)
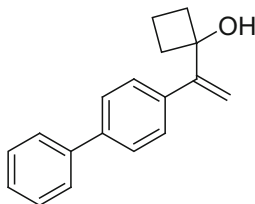
GP6: 4-(1-Bromovinyl)-1,1′-biphenyl was prepared from 4′-phenylacetophenone (1.18 g, 6.00 mmol). White solid (820 mg, 3.16 mmol, 53 %).

^{1}H NMR (300 MHz, CDCl$_3$): δ (ppm): 7.55–7.75 (m, 6H), 7.33–7.51 (m, 3H), 6.18 (d, *J* = 2.1 Hz, 1H), 5.81 (d, *J* = 2.0 Hz, 1H); **GC-MS: t$_R$ (50_40)**: 8.9 min; **EI-MS**: *m/z* (%): 260 (20.0), 258 (21.0), 180 (15.0), 179 (100.0), 178 (64.0), 177 (10.0), 176 (15.0), 152 (16.0), 151 (10.0), 89 (14.0), 76 (12.0).

GP7: 1-(1-([1,1′-Biphenyl]-4-yl)vinyl)cyclobutan-1-ol was prepared from 4-(1-bromovinyl)-1,1′-biphenyl (518 mg, 2.00 mmol). White solid (346 mg, 1.38 mmol, 69 %).

R$_f$ (pentane:ethyl acetate 9:1): 0.15; **^{1}H NMR (400 MHz, CDCl$_3$)**: δ (ppm): 7.64–7.54 (m, 6H), 7.47–7.43 (m, 2H), 7.33–7.38 (m, 1H), 5.43 (dd, *J* = 13.0, 0.8 Hz, 2H), 2.48–2.57 (m, 2H), 2.25–2.33 (m, 2H), 1.96–2.07 (m, 2H), 1.60–1.78 (m, 1H); **^{13}C NMR (100 MHz, CDCl$_3$)**: δ (ppm): 152.0, 140.9, 140.5, 138.1, 128.9, 128.1, 127.4, 127.1, 127.0, 112.9, 78.3, 35.9, 13.6; **GC-MS: t$_R$ (50_40)**: 9.6 min; **EI-MS**: *m/z* (%): 251 (16), 250 (75), 222 (24), 221 (27), 208 (11), 207 (17), 205 (14), 204 (15), 203 (24), 202 (14) 194 (56), 193 (24), 191 (17), 189 (10), 180 (23), 179 (100), 178 (99), 177 (16), 176 (19), 167 (45), 165 (35), 154 (17), 153 (12), 152 (35), 151 (15), 115 (17), 77 (15), 76 (11), 43 (11); **HR-MS (ESI)**: *m/z* calculated for $[C_{18}H_{18}ONa]^+$ ([M + Na]$^+$): 273.1250, measured: 273.1256.

1-(1-(4-Methoxyphenyl)vinyl)cyclobutan-1-ol (152)
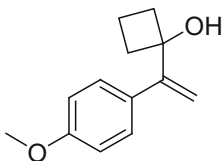
GP6: 1-(1-Bromovinyl)-4-methoxybenzene was prepared from 4′-methoxyacetophenone (1.20 g, 8.00 mmol). Light sensitive purple solid (758 mg, 3.56 mmol, 45 %).

^{1}H NMR (300 MHz, CDCl$_3$): δ (ppm): 7.53 (d, *J* = 8.8 Hz, 2H), 6.87 (d, *J* = 8.8 Hz, 2H), 6.01 (d, *J* = 1.9 Hz, 1H), 5.67 (d, *J* = 2.0, 1H), 3.82 (s, 3H); **GC-MS: t$_R$ (50_40)**: 8.2 min; **EI-MS**: *m/z* (%): 204 (62), 186 (13), 176 (37), 175

(40), 162 (15), 161 (41), 160 (14), 159 (34), 155 (11), 148 (40), 147 (36), 146 (12), 145 (77), 144 (14), 134 (20), 133 (100), 132 (11), 131 (10), 128 (15), 127 (10), 121 (50), 119 (10), 118 (19), 117 (29), 116 (10), 115 (36), 108 (13), 105 (21), 103 (18), 102 (11), 91 (28), 90 (20) 89 (29), 79 (14), 78 (11), 77 (33), 65 (17), 64 (10), 63 (21), 51 (13), 43 (11), 39 (16).

GP7: 1-(1-(4-Methoxyphenyl)vinyl)cyclobutan-1-ol was prepared from 1-(1-bromovinyl)-4-methoxybenzene (639 mg, 3.00 mmol). Light yellow oil (366 mg, 1.79 mmol, 60 %).

R_f (pentane:ethyl acetate 9:1): 0.19; **^{1}H NMR (300 MHz, CDCl$_3$)**: δ (ppm): 7.43 (d, J = 8.9 Hz, 2H), 6.87 (d, J = 8.9 Hz, 2H), 5.30 (dd, J = 3.9, 0.9 Hz, 2H), 3.81 (s, 3H), 2.38–2.55 (m, 2H), 2.15–2.32 (m, 2H), 1.89–2.07 (m, 2H), 1.53–1.70 (m, 2H); **^{13}C NMR (75.5 MHz, CDCl$_3$)**: δ (ppm): 159.2, 151.7, 131.4, 128.8, 113.7, 111.6, 78.3, 55.4, 35.8, 13.5; **GC-MS**: **t_R (50_40)**: 8.2 min; **EI-MS**: *m/z* (%): 204 (62), 186 (13), 176 (37), 175 (40), 162 (15), 161 (41), 160 (14), 159 (34), 155 (11), 148 (40) 147 (36), 146 (12), 145 (77), 144 (14), 134 (20), 133 (100), 132 (11), 131 (10), 128 (15), 127 (10), 121 (50), 119 (10), 118 (19), 117 (29), 116 (10), 115 (36), 108 (13), 105 (21), 103 (18), 102 (11), 91 (28), 90 (20), 89 (29), 79 (14), 78 (11), 77 (33), 65 (16), 64 (14), 63 (20), 51 (13), 43 (11), 39 (16); **HR-MS (ESI)**: *m/z* calculated for $[C_{13}H_{16}O_2Na]^+$ ($[M + Na]^+$): 227.1043, measured: 227.1050.

1-(1-(Benzo[*d*][1, 3]dioxol-5-yl)vinyl)cyclobutan-1-ol (153)
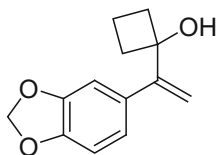
GP6: 5-(1-bromovinyl)benzo[*d*][1,3]dioxole was prepared from 1-(benzo[*d*][1,3]dioxol-5-yl)ethan-1-one (985 mg, 6.00 mmol). Light sensitive greenish oil (640 mg, 2.82 mmol, 47 %).

GC-MS: **t_R (50_40)**: 7.8 min; **EI-MS**: *m/z* (%): 228 (17), 226 (18), 148 (11), 147 (100), 145 (10), 117 (16), 89 (52), 73 (15), 63 (33), 62 (18).

GP7: 1-(1-(benzo[*d*][1,3]dioxol-5-yl)vinyl)cyclobutan-1-ol was prepared from 5-(1-bromovinyl)benzo[*d*][1,3]dioxole (668 mg, 2.50 mmol). Light yellow oil (445 mg, 2.04 mmol, 82 %).

R_f (pentane:ethyl acetate 9:1): 0.15; **^{1}H NMR (300 MHz, CDCl$_3$)**: δ (ppm): 6.95–7.02 (m, 2H), 6.77 (d, J = 8.0 Hz, 1H), 5.95 (s, 2H), 5.15–5.37 (m, 2H), 2.35–2.61 (m, 2H), 2.14–2.30 (m, 2H), 1.91–2.04 (m, 2H), 1.55–1.69 (m, 1H); **^{13}C NMR (100 MHz, CDCl$_3$)**: δ (ppm): 152.0, 147.6, 147.2, 133.2, 121.2, 112.3, 108.3, 108.1, 101.1, 78.3, 35.8, 13.5; **GC-MS**: **t_R (50_40)**: 8.5 min; **EI-MS**: *m/z* (%): 219 (10), 218 (80), 190 (26), 189 (12), 162 (57), 161 (41), 160 (100), 159 (13), 148 (18), 147 (100) 145 (12), 135 (49), 133 (10), 132 (77), 131 (49), 122 (13),

117 (20), 115 (25), 104 (28), 103 (38), 91 (14), 90 (11), 89 (75), 78 (17), 77 (31), 73 (15), 65 (13), 64 (10), 63 (54), 62 (15), 53 (13), 51 (29), 43 (17), 41 (11), 39 (29); **HR-MS (ESI)**: *m/z* calculated for $[C_{13}H_{14}O_3Na]^+$ $([M + Na]^+)$: 241.0835, measured: 241.0834.

1-(1-(Naphthalen-2-yl)vinyl)cyclobutan-1-ol (154)
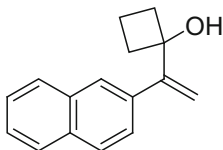
GP6: 2-(1-Bromovinyl)naphthalene was prepared from 2-acetonaphthone (1.19 g, 7.00 mmol). Pale yellow solid (900 mg, 3.86 mmol, 55 %).

^{1}H NMR (300 MHz, CDCl$_3$): δ (ppm): 8.09 (d, *J* = 1.9 Hz, 1H), 7.76–7.93 (m, 3H), 7.65–7.73 (m, 1H), 7.47–7.56 (m, 2H), 6.26 (dd, *J* = 2.1, 0.8 Hz, 1H), 5.88 (dd, *J* = 2.1, 0.8 Hz, 1H); **GC-MS**: **t_R (50_40)**: 8.4 min; **EI-MS**: *m/z* (%): 234 (17), 232 (20), 154 (11), 153 (100), 152 (75), 151 (24), 150 (11), 127 (10), 126 (13), 76 (10), 75 (10), 74 (10), 63 (13), 50 (11).

GP7: 1-(1-(Naphthalen-2-yl)vinyl)cyclobutan-1-ol was prepared from 2-(1-bromovinyl)naphthalene (700 mg, 3.00 mmol). Light yellow oil (445 mg, 1.98 mmol, 66 %).

R_f (pentane:ethyl acetate 9:1): 0.17; **^{1}H NMR (300 MHz, CDCl$_3$)**: δ (ppm): 7.81–7.91 (m, 1H), 7.71–7.78 (m, 3H), 7.54 (dd, *J* = 8.5, 1.8 Hz, 1H), 7.34–7.43 (m, 2H), 5.41 (dd, *J* = 6.2, 0.8 Hz, 2H), 2.40–2.51 (m, 2H), 2.11–2.29 (m, 2H), 1.81–2.04 (m, 2H), 2.51–2.65 (m, 1H); **^{13}C NMR (75.5 MHz, CDCl$_3$)**: δ (ppm): 152.7, 136.7, 133.4, 132.9, 128.4, 127.8, 127.7, 126.6, 126.2, 126.1, 126.1, 113.5, 78.4, 36.0, 13.6; **GC-MS**: **t_R (50_40)**: 7.1 min; **EI-MS**: *m/z* (%): 224 (32), 196 (12), 195 (23), 181 (23), 179 (15), 178 (20), 168 (54), 167 (39), 166 (12), 165 (32) 154 (12), 153 (75), 152 (100), 151 (40) 150 (15), 141 (25), 139 (12), 128 (22), 127 (17), 126 (15), 115 (15), 43 (20), 39 (16); **HR-MS (ESI)**: *m/z* calculated for $[C_{16}H_{16}ONa]^+$ $([M + Na]^+)$: 247.1093, measured: 247.1097.

1-(1-(*m*-Tolyl)vinyl)cyclobutan-1-ol (149)
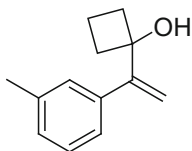
GP6: 1-(1-Bromovinyl)-3-methylbenzene was prepared from 3′-methylacetophenone (2.15 g, 16.00 mmol). Light yellow oil (715 mg, 3.63 mmol, 23 %).

¹H NMR (300 MHz, CDCl₃): δ (ppm): 7.31–7.46 (m, 1H), 7.20–7.29 (m, 1H), 7.15 (ddq, *J* = 7.5, 2.0, 0.9 Hz, 1H), 6.11 (d, *J* = 1.9 Hz, 1H), 5.77 (d, *J* = 1.9 Hz, 1H), 2.38 (s, 3H); **GC-MS: t_R (50_40)**: 6.6 min; **EI-MS**: *m/z* (%): 198 (19), 196 (19), 117 (95), 116 (21), 115 (100), 91 (40), 89 (22), 74 (13), 65 (16), 63 (30), 62 (14), 51 (20), 50 (19), 39 (23).

GP7: 1-(1-(*m*-Tolyl)vinyl)cyclobutan-1-ol was prepared from 1-(1-bromovinyl)-3-methylbenzene (296 mg, 1.50 mmol). Light yellow oil (85 mg, 0.45 mmol, 30 %).

R_f (pentane:ethyl acetate 9:1): 0.22; **¹H NMR (300 MHz, CDCl₃)**: δ (ppm): 7.18–7.36 (m, 3H), 7.11 (dtd, *J* = 7.2, 1.7, 0.8 Hz, 1H), 5.35 (dd, *J* = 7.0, 1.0 Hz, 2H), 2.41–2.54 (m, 2H), 2.36 (s, 3H), 2.17–2.31 (m, 2H), 1.89–2.07 (m, 2H), 1.56–1.73 (m, 1H); **¹³C NMR (75.5 MHz, CDCl₃)**: δ (ppm): 152.6, 139.2, 137.9, 128.4, 128.4, 128.2, 124.8, 112.8, 78.2, 35.8, 21.7, 13.5; **GC-MS: t_R (50_40)**: 7.7 min; **EI-MS**: *m/z* (%): 207 (14), 145 (47), 132 (57), 131 (14), 129 (15), 128 (10), 117 (84), 116 (21), 115 (100), 105 (11), 102 (13), 91 (46), 89 (15), 77 (19), 65 (18), 63 (20), 43 (21), 42 (20), 39 (29); **HR-MS (ESI)**: *m/z* calculated for $[C_{13}H_{16}ONa]^+$ ($[M + Na]^+$): 211.1093, measured: 211.1093.

1-(1-(*o*-Tolyl)vinyl)cyclobutan-1-ol (150)
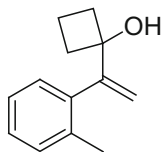
GP6: 1-(1-Bromovinyl)-2-methylbenzene was prepared from 2′-methylacetophenone (1.07 g, 8.00 mmol). Colourless oil (703 mg, 3.57 mmol, 45 %).

¹H NMR (300 MHz, CDCl₃): δ (ppm): 7.01–7.27 (m, 4H), 5.80 (d, *J* = 1.6 Hz, 1H), 5.65 (d, *J* = 1.5, 1H), 2.32 (s, 3H); **GC-MS: t_R (50_40)**: 6.6 min; **EI-MS**: *m/z* (%): 198 (13), 196 (13), 117 (85), 116 (29), 115 (100), 91 (32), 89 (17), 65 (10), 63 (23), 62 (13), 51 (14), 50 (14), 39 (17).

GP7: 1-(1-(*o*-Tolyl)vinyl)cyclobutan-1-ol was prepared from 1-(1-bromovinyl)-2-methylbenzene (591 mg, 3.00 mmol). Light yellow oil (302 mg, 1.60 mmol, 53 %).

R_f (pentane:ethyl acetate 4:1): 0.22; **¹H NMR (400 MHz, CDCl₃)**: δ (ppm): 7.10–7.24 (m, 4H), 5.54 (d, *J* = 1.4 Hz, 1H), 4.99 (d, *J* = 1.4 Hz, 1H), 2.36–2.49 (m, 2H), 2.29 (s, 3H), 2.04–2.15 (m, 2H), 1.90–2.02 (m, 1H), 1.84 (s, 1H), 1.54–1.64 (m, 1H); **¹³C NMR (100 MHz, CDCl₃)**: δ (ppm): 152.7, 140.0, 136.4, 130.3, 129.1, 127.4, 125.3, 113.7, 78.6, 35.8, 20.6, 13.7; **GC-MS: t_R (50_40)**: 7.6 min; **EI-MS**: *m/z* (%): 146 (15), 145 (40), 141 (13), 131 (12), 129 (10), 128 (14), 117 (68), 116 (34), 115 (100), 92 (10), 91 (40), 89 (14), 77 (10), 73 (21), 65 (10), 63 (10), 43 (17), 41 (10), 39 (23); **HR-MS (ESI)**: *m/z* calculated for $[C_{13}H_{16}ONa]^+$ ($[M + Na]^+$): 211.1093, measured: 211.1105.

1-(3,4-Dihydronaphthalen-1-yl)cyclobutan-1-ol (155)
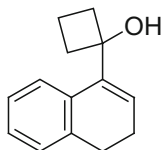
GP6: 4-Bromo-1,2-dihydronaphthalene was prepared from 3,4-dihydronaphthalen-1(2*H*)-one (910 mg, 6.40 mmol). Pale yellow oil (924 mg, 4.42 mmol, 69 %).

^{1}H NMR (300 MHz, CDCl$_3$): δ (ppm): 7.47 (dd, *J* = 7.4, 1.6 Hz, 1H), 7.06–7.21 (m, 2H), 6.96–7.05 (m, 1H), 6.37 (t, *J* = 4.8 Hz, 1H), 2.77 (t, *J* = 8.1 Hz, 2H), 2.26–2.33 (m, 2H); **GC-MS: t$_R$ (50_40)**: 7.7 min; **EI-MS**: *m/z* (%): 210 (16), 208 (18), 130 (11), 129 (100), 128 (71), 127 (30), 64 (14), 63 (11), 51 (12).

GP8: 1-(3,4-Dihydronaphthalen-1-yl)cyclobutan-1-ol was prepared from 4-bromo-1,2-dihydronaphthalene (585 mg, 2.80 mmol). White solid (421 mg, 2.10 mmol, 75 %).

^{1}H NMR (300 MHz, CDCl$_3$): δ (ppm): 7.52 (dt, *J* = 6.5, 1.6 Hz, 1H), 7.11–7.23 (m, 3H), 6.20 (t, *J* = 4.7 Hz, 1H), 2.75 (t, *J* = 7.9 Hz, 2H), 2.50–2.60 (m, 2H), 2.29–2.40 (m, 4H), 1.91–2.05 (m, 2H), 1.53–1.68 (m, 1H); **^{13}C NMR (75.5 MHz, CDCl$_3$)**: δ (ppm): 139.6, 137.5, 132.3, 128.0, 126.9, 126.2, 125.5, 125.4, 87.5, 35.9, 28.3, 23.3, 14.0; **GC-MS: t$_R$ (50_40)**: 8.5 min; **EI-MS**: *m/z* (%): 200 (34), 182 (27), 172 (40), 171 (21), 167 (22), 165 (11), 157 (40), 155 (11), 154 (22), 153 (33), 152 (24), 144 (24), 143 (13), 141 (20), 130 (26), 129 (100), 128 (82), 127 (29), 117 (12), 116 (21), 115 (30), 77 (10); **HR-MS (ESI)**: *m/z* calculated for [C$_{14}$H$_{16}$ONa]$^+$ ([M + Na]$^+$): 223.1093, measured: 223.1096.

1-(Cyclohex-1-en-1-yl)cyclobutan-1-ol (163)
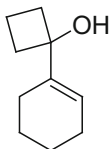
GP6: 1-Bromocyclohex-1-ene was prepared from cyclohexanone (785 mg, 8.00 mmol). Pale yellow oil (850 mg, 5.28 mmol, 66 %).

^{1}H NMR (300 MHz, CDCl$_3$): δ (ppm): 6.03 (tt, *J* = 4.0, 1.7 Hz, 1H), 2.38–2.46 (m, 2H), 2.03–2.10 (m, 2H), 1.67–1.81 (m, 2H), 1.55–1.65 (m, 2H); **GC-MS: t$_R$ (50_40)**: 5.4 min; **EI-MS**: *m/z* (%): 160 (10), 81 (100), 79 (30), 77 (12), 53 (33), 51 (12), 41 (12), 39 (15).

GP7: 1-(Cyclohex-1-en-1-yl)cyclobutan-1-ol was prepared from 1-bromocyclohex-1-ene (483 mg, 3.00 mmol). Colourless oil (200 mg, 1.31 mmol, 44 %).

¹H NMR (300 MHz, CDCl₃): δ (ppm): 5.70–5.75 (m, 1H), 2.22–2.38 (m, 2H), 1.93–2.12 (m, 6H), 1.79–1.93 (m, 1H), 1.45–1.70 (m, 6H); **¹³C NMR (75.5 MHz, CDCl₃)**: δ (ppm): 140.4, 120.7, 78.3, 34.2, 25.2, 23.0, 23.0, 22.4, 13.3; **GC-MS**: **t_R (50_40)**: 6.8 min; **EI-MS**: *m/z* (%): 134 (19), 124 (31), 123 (21), 119 (11), 110 (25), 109 (69), 106 (12), 105 (21), 96 (19), 95 (44), 93 (11), 92 (13), 91 (57), 82 (18) 81 (100), 80 (35), 79 (50), 78 (20), 77 (31), 67 (35), 66 (13), 65 (15), 55 (20), 53 (27), 51 (17), 43 (51), 41 (30), 39 (33); **HR-MS (ESI)**: *m/z* calculated for $[C_{10}H_{16}ONa]^+$ ($[M + Na]^+$): 175.1093, measured: 175.1096.

3-(1-Phenylvinyl)oxetan-3-ol (161)
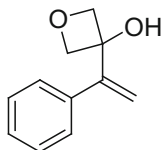
GP7: 3-(1-Phenylvinyl)oxetan-3-ol was prepared from (1-bromo-vinyl)benzene (1.1 g, 6.0 mmol). White solid (860 mg, 4.94 mmol, 82 %).

¹H NMR (300 MHz, CDCl₃): δ (ppm): 7.44–7.52 (m, 2H), 7.27–7.38 (m, 3H), 5.37 (d, *J* = 4.7, 2H), 2.37–2.65 (m, 2H), 2.14–2.33 (m, 2H), 1.87–2.08 (m, 2H), 1.41–1.71 (m, 1H); **¹³C NMR (75.5 MHz, CDCl₃)**: δ (ppm): 152.5, 139.2, 128.3, 127.7, 127.7, 113.0, 78.2, 35.8, 13.5; **GC-MS**: **t_R (50_40)**: 7.4 min; **EI-MS**: *m/z* (%): 174 (17), 146 (47), 145 (70), 132 (20), 131 (55), 129 (21), 128 (27), 127 (21), 119 (10), 118 (97) 117 (100), 116 (22), 115 (43), 104 (16), 103 (82), 102 (21), 96 (12), 91 (35), 78 (25), 77 (55), 63 (10), 51 (22), 43(10); **HR-MS (ESI)**: *m/z* calculated for $[C_{12}H_{14}ONa]^+$ ($[M + Na]^+$): 197.0937, measured: 197.0933.

3-(1-(4-Fluorophenyl)vinyl)oxetan-3-ol (162) [40]
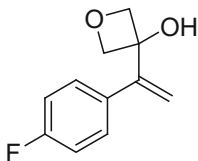
GP6: 1-(1-Bromovinyl)-4-fluorobenzene was prepared from 4′-fluoroacetophenone (829 mg, 6.00 mmol). Light yellow oil (680 mg, 3.38 mmol, 56 %).

¹H NMR (300 MHz, CDCl₃): δ (ppm): 7.53–7.61 (m, 2H), 6.96–7.09 (m, 2H), 6.05 (d, *J* = 2.1 Hz, 1H), 5.76 (d, *J* = 2.1, 1H); **GC-MS**: **t_R (50_40)**: 6.4 min; **EI-MS**: *m/z* (%): 202 (10), 122 (10), 121 (100), 120 (36), 101 (52), 95 (10), 94 (13), 81 (22), 79 (14), 75 (22), 74 (19), 63 (16), 51 (11), 50 (20), 38 (10).

GP7:   3-(1-(4-Fluorophenyl)vinyl)oxetan-3-ol   was   prepared   from   1-(1-bromovinyl)-4-fluorobenzene   (302 mg,   1.50 mmol).   White   solid   (117 mg, 1.20 mmol, 48 %).

^{1}H NMR (300 MHz, CDCl$_3$): δ (ppm): 7.30–7.46 (m, 2H), 6.82–7.10 (m, 2H), 5.55 (s, 1H), 5.39 (s, 1H), 4.89 (dd, J = 6.9, 1.0 Hz, 2H), 4.77 (dd, J = 6.9, 0.9 Hz, 2H),   2.49   (s,   1H);   **^{13}C   NMR   (75.5 MHz,   CDCl$_3$)**:   δ   (ppm):   162.8   (d, J = 247.9 Hz), 148.2, 128.7 (d, J = 8.0 Hz), 115.8, 115.5, 114.9 (d, J = 1.1 Hz), 83.2, 76.7; **^{19}F NMR (300 MHz, CDCl$_3$)**: −113.72; **GC-MS: t$_R$ (50_40)**: 7.7 min; **EI-MS**: *m/z* (%): 165 (11), 164 (100), 163 (69), 149 (39), 147 (23), 146 (22), 145 (20), 136 (34), 135 (69), 134 (21), 133 (36), 121 (46), 120 (21), 117 (14), 115 (24), 109 (32), 107 (10), 101 (51), 96 (20), 95 (17), 75 (30), 74 (10), 63 (10), 57 (10), 1 (15), 50 (11), 43 (20), 39 (11); **HR-MS (ESI)**: *m/z* calculated for $[C_{11}H_{10}FO_2Na]^+$ ([M + Na]$^+$): 217.0635, measured: 217.0647.

1-(1-Phenylvinyl)cyclopentan-1-ol (160)
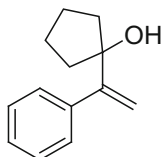
GP7: 1-(1-Phenylvinyl)cyclopentan-1-ol was prepared from (1-bromovinyl)benzene (732 mg, 4.00 mmol). Colourless oil (300 mg, 1.59 mmol, 40 %).

R$_f$ (pentane:ethyl acetate 9:1): 0.25; **^{1}H NMR (300 MHz, CDCl$_3$)**: δ (ppm): 7.39–7.45   (m,   2H),   7.27–7.38   (m,   3H),   5.47   (d, J = 1.4 Hz,   1H),   5.11   (d, J = 1.5 Hz, 1H), 1.77–1.99 (m, 6H), 1.64–1.75 (m, 2H), 1.48 (s, 1H); **^{13}C NMR (75.5 MHz, CDCl$_3$)**: δ (ppm): 155.1, 141.9, 128.6, 128.0, 127.2, 113.3, 84.2, 39.4, 23.4; **GC-MS: t$_R$ (50_40)**: 7.7 min; **EI-MS**: *m/z* (%): 189 (10), 188 (63), 170 (28), 160 (10), 159 (36), 155 (17), 146 (12), 145 (28), 142 (33), 141 (43) 131 (37), 129 (36), 128 (29), 127 (15), 118 (20), 117 (40), 116 (16), 115 (45), 105 (24), 104 (94), 103 (100), 102 (23), 97(34), 92 (14), 91 (75), 85 (30), 79 (12), 78 (33), 77 (79), 76 (13), 67 (34), 65 (14), 63 (16), 57 (17), 55 (20), 53 (11), 52 (11), 51 (36), 50 (12), 43   (17),   41   (28),   39   (27);   **HR-MS   (ESI)**:   *m/z*   calculated   for $[C_{13}H_{16}ONa]^+$ ([M + Na]$^+$): 211.1093, measured: 211.1093.

1-(1H-inden-3-yl)cyclobutan-1-ol (159) [39]
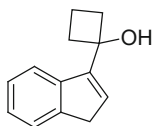
Following a procedure from Alexakis et al. [39], n-BuLi (3.36 mL, 5.37 mmol, 1.6 M in hexane, 1.5 equiv.) was added to a solution of indene (631 μL, 5.37 mmol, 1.5 equiv.) in diethylether (10 mL) at −78 °C. The reaction mixture was   stirred   at   rt   for   3 h.   After   cooling   to   −78 °C,   cyclobutanone

(270 μL, 3.58 mmol, 1.00 equiv.) was added dropwise to the reaction mixture. The resulting reaction mixture was warmed up slowly and continued the stirring for 4 h. After cooling to 0 °C, the reaction mixture was quenched with glacial acetic acid (360 μL). The quenched reaction mixture was then diluted with water and extracted with diethyl ether. The organic layer was washed with brine, dried over $MgSO_4$ and concentrated under reduced pressure. The crude mixture was purified by flash column chromatography through silica (eluent:pentane:ethyl acetate 9:1 to 4:1) to deliver pure product (614 mg, 3.29 mmol, 92 %) as white solid.

^{1}H NMR (400 MHz, CDCl$_3$): δ (ppm): 7.59 (dt, $J = 7.7, 1.0$ Hz, 1H), 7.49 (dt, $J = 7.4, 1.0$ Hz, 1H), 7.30 (td, $J = 7.6, 1.2$ Hz, 1H), 7.23 (td, $J = 7.4, 1.2$ Hz, 1H), 6.46 (t, $J = 2.1$ Hz, 1H), 3.41 (d, $J = 2.0$ Hz, 2H), 2.51–2.63 (m, 2H), 2.30–2.46 (m, 2H), 1.86–1.97 (m, 1H), 1.57–1.69 (m, 2H); **^{13}C NMR (75.5 MHz, CDCl$_3$):** δ (ppm): 147.4, 145.2, 142.8, 128.3, 126.1, 125.0, 124.2, 121.7, 74.1, 37.7, 35.7, 13.4; **GC-MS: t_R (50_40):** 8.2 min; **EI-MS:** m/z (%): 186 (41), 168 (22), 167 (20), 159 (13), 158 (97), 157 (33), 153 (13), 142 (18), 141 (19), 140 (28) 139 (30), 130 (22), 129 (42), 128 (27), 127 (12), 116 (63), 115 (100), 114 (10), 89 (14), 71 (17), 65 (11), 64 (12), 63 (17), 51 (10), 43 (28), 39 (10); **HR-MS (ESI):** m/z calculated for $[C_{13}H_{14}ONa]^+$ ($[M + Na]^+$): 209.0937, measured: 209.0948.

6.4.2   Synthesis and Characterization of Trifluoromethylated Cycloalkanone Compounds

General Procedure 9:
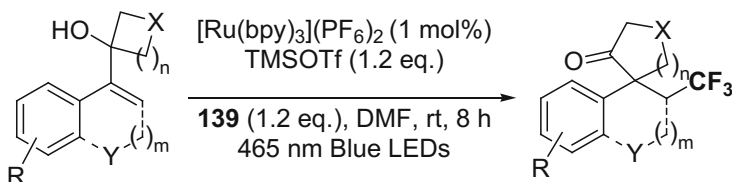
In a heat gun dried Schlenk tube equipped with a magnetic stirring bar, substrate (**142, 146–163**, 0.2 mmol, 1.0 equiv.) followed by trimethylsilyl trifluoromethanesulfonate (43 μL, 0.24 mmol, 1.2 equiv.) was dissolved in anhydrous DMF (2 mL). The reaction mixture was stirred for 2 h. [Ru(bpy)$_3$](PF$_6$)$_2$ (1.70 mg, 0.002 mmol, 0.010 equiv.) and 5-(trifluoromethyl)dibenzothio-phenium trifluoromethanesulfonate (**139**, 97 mg, 0.24 mmol, 1.2 equiv.) were then added to the reaction mixture and the mixture was allowed to stir for 6 h under irradiation of visible light from 5 W blue LEDs ($\lambda_{max} = 465$ nm, situated ~5 cm away from the reaction vessel in a custom-made "light box", see Fig. 6.2). The reaction mixture was quenched with aq. saturated Na$_2$SO$_3$ solution (5 mL) and extracted with ethyl

acetate (3 × 10 mL). The combined organic layers were washed with water (15 mL), brine solution (15 mL), dried over MgSO$_4$ and concentrated under reduced pressure. The crude reaction mixture was purified by flash column chromatography through silica gel (pentane:dichloromethane 9:1 to 3:2 for **143, 164–172**, **178–180** and pentane:ethyl acetate 99:1 to 19:1 for **173–177**) to afford pure product (**143**, **164–180**).

2-Phenyl-2-(2,2,2-trifluoroethyl)cyclopentan-1-one (143)
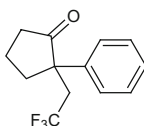
GP9: Prepared from 1-(1-phenylvinyl)cyclobutan-1-ol (**142**, 35 mg, 0.20 mmol). Colourless oil (36 mg, 0.15 mmol, 74 %).

R$_f$ (pentane:dichloromethane 3:2): 0.31; **^{1}H NMR (300 MHz, CDCl$_3$)**: δ (ppm): 7.25–7.36 (m, 4H), 7.18–7.24 (m, 1H), 2.86 (dd, J = 13.2, 6.3 Hz, 1H), 2.74 (dq, J = 15.5, 11.2 Hz, 1H), 2.42 (dq, J = 15.5, 11.0 Hz, 1H), 1.86–2.32 (m, 4H), 1.62–1.83 (m, 1H); **^{13}C NMR (75.5 MHz, CDCl$_3$)**: δ (ppm): 216.3 (C$_q$), 136.1 (C$_q$), 129.1 (CH), 127.8 (CH), 126.9 (CH), 126.3 (q, J = 277.7 Hz, CF$_3$), 53.4 (q, J = 1.9 Hz, C$_q$), 42.1 (q, J = 27.4 Hz, CH$_2$), 35.6 (CH$_2$), 32.5 (q, J = 1.3 Hz, CH$_2$), 18.4 (CH$_2$); **^{19}F NMR (300 MHz, CDCl$_3$)**: δ (ppm): −60.40 (t, J = 11.1 Hz); **GC-MS: t$_R$ (50_40)**: 7.4 min; **EI-MS**: m/z (%): 242 (44), 187 (11), 186 (100), 153 (13), 131 (38), 129 (14), 128 (11), 117 (37), 115 (35), 104 (22), 103 (48), 102 (10), 91 (24), 78 (18), 77 (28), 65 (10), 51 (16), 39 (11); **HR-MS (ESI)**: m/z calculated for [C$_{13}$H$_{13}$F$_3$ONa]$^+$ ([M + Na]$^+$): 265.0811, measured: 265.0817; **IR (ATR)**: ν (cm^{-1}): 2976, 1739, 1497, 1447, 1432, 1372, 1301, 1258, 1213, 1155, 1116, 1083, 1036, 981, 842, 753, 699, 636.

2-Phenyl-2-(2,2,2-trifluoroethyl)-1-oxaspiro[2.3]hexane (144)
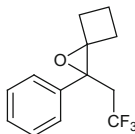
Obtained as colourless oil.

R$_f$ (pentane:dichloromethane 3:2): 0.60; **^{1}H NMR (600 MHz, CDCl$_3$)**: δ (ppm): 7.34–7.36 (m, 2H), 7.27–7.30 (m, 3H), 3.01 (dq, J = 15.3, 10.1 Hz, 1H), 2.52–2.57 (m, 1H), 2.41–2.47 (m, 1H), 2.29 (dq, J = 15.0, 10.2 Hz, 1H), 2.20–2.25 (m, 1H), 1.87–1.94 (m, 1H), 1.76–1.81 (m, 1H), 1.67–1.74 (m, 1H); **^{13}C NMR (150 MHz, CDCl$_3$)**: δ (ppm): 136.7 (C$_q$), 128.3 (CH), 127.8 (CH), 126.3 (CH), 126.0 (q, J = 278.7 Hz, CF$_3$), 69.3 (C$_q$), 61.7 (q, J = 2.6 Hz, C$_q$), 38.8 (q, J = 28.2 Hz, CH$_2$), 29.3 (CH$_2$), 28.8 (CH$_2$), 12.5 (CH$_2$); **^{19}F NMR (600 MHz, CDCl$_3$)**: δ (ppm): −60.98 (t, J = 10.2 Hz); **GC-MS: t$_R$ (50_40)**: 7.1 min; **EI-MS**: m/z (%): 242 (21), 214 (50), 213 (57), 186 (46), 173 (12), 172 (62), 171 (64),

159 (11), 153 (12), 152 (19), 151 (33), 145 (13), 143 (32), 133 (13), 131 (52), 129 (20), 128 (31), 127 (13),), 122 (36), 117 (27), 115 (41), 105 (40), 104 (13), 103 (100), 102 (19), 91 (29), 78 (27), 77 (93), 71 (12), 63 (13), 54 (15), 53 (20), 51 (42), 43 (17), 42 (26), 39 (48); **HR-MS (ESI)**: m/z calculated for $[C_{13}H_{13}F_3ONa]^+$ ($[M + Na]^+$): 265.0811, measured: 265.0815; **IR (ATR)**: ν (cm^{-1}): 2933, 1426, 1364, 1306, 1358, 1139, 1123, 1112, 1063, 832, 730, 701, 663, 632, 610.

2-(4-Fluorophenyl)-2-(2,2,2-trifluoroethyl)cyclopentan-1-one (164)
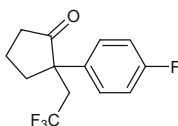
GP9: Prepared from 1-(1-(4-fluorophenyl)vinyl)cyclobutan-1-ol (**146**, 38 mg, 0.20 mmol). Colourless oil (38 mg, 0.15 mmol, 73 %).

R_f **(pentane:dichloromethane 3:2)**: 0.57; **¹H NMR (300 MHz, CDCl₃)**: δ (ppm): 7.32–7.42 (m, 2H), 6.97–7.09 (m, 2H), 2.90 (dd, J = 13.2, 6.3 Hz, 1H), 2.79 (dq, J = 15.5, 11.2 Hz, 1H), 2.43 (dq, J = 15.5, 11.2 Hz, 1H), 2.17–2.35 (m, 2H), 1.92–2.16 (m, 2H), 1.67–1.89 (m, 1H); **¹³C NMR (75.5 MHz, CDCl₃)**: δ (ppm): 216.1 (C_q), 162.3 (d, J = 247.5 Hz, C_q), 131.6 (d, J = 3.3 Hz, C_q), 128.8 (d, J = 8.1 Hz, CH), 126.3 (q, J = 278.3 Hz, CF₃), 116.0 (d, J = 21.4 Hz, CH), 52.8 (q, J = 1.9 Hz, C_q), 42.2 (q, J = 27.5 Hz, CH₂), 35.6 (CH₂), 32.9 (q, J = 1.4 Hz, CH₂), 18.4 (CH₂); **¹⁹F NMR (300 MHz, CDCl₃)**: δ (ppm): −60.42 (t, J = 11.0 Hz),–114.66 (s); **GC-MS**: t_R **(50_40)**: 7.4 min; **EI-MS**: m/z (%): 260 (37), 205 (11), 204 (100), 171 (11), 149 (23), 135 (15), 133 (16), 121 (41), 109 (12), 101 (18); **HR-MS (ESI)**: m/z calculated for $[C_{13}H_{12}F_4OAg]^+$ ($[M + Ag]^+$): 366.9870, measured: 366.9876; **IR (ATR)**: ν (cm^{-1}): 2975, 2893, 1740, 1604, 1510, 1472, 1461, 1434, 1408, 1373, 1302, 1258, 1236, 1215, 1166, 1156, 1119, 1075, 1014, 982, 850, 837, 821, 721, 662, 628.

### 2-(4-Chlorophenyl)-2-(2,2,2-trifluoroethyl)cyclopentan-1-one (165)
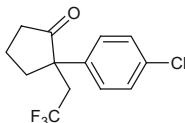
GP9: Prepared from 1-(1-(4-chlorophenyl)vinyl)cyclobutan-1-ol (**147**, 42 mg, 0.20 mmol). Colourless oil solidified upon cooling (33 mg, 0.12 mmol, 60 %).

R_f **(pentane:dichloromethane 3:2)**: 0.51; **¹H NMR (300 MHz, CDCl₃)**: δ (ppm): 7.29–7.36 (m, 4H), 2.85–2.92 (m, 1H), 2.71–2.83 (m, 1H), 2.36–2.53 (m, 1H), 1.96–2.34 (m, 4H), 1.67–1.88 (m, 1H); **¹³C NMR (75.5 MHz, CDCl₃)**: δ (ppm): 215.9 (C_q), 134.5 (C_q), 134.0 (C_q), 129.2 (CH), 128.5 (CH), 126.3 (q, J = 278.2 Hz, CF₃), 53.0 (q, J = 1.8 Hz, C_q), 42.1 (q, J = 27.5 Hz, CH₂), 35.6 (CH₂), 32.7 (q, J = 1.5 Hz, CH₂), 18.5 (CH₂); **¹⁹F NMR (300 MHz, CDCl₃)**:

δ (ppm): −60.39 (t, J = 11.0 Hz); **GC-MS: t_R (50_40)**: 8.0 min; **EI-MS**: m/z (%): 278 (12), 276 (37), 222 (32), 221 (12), 220 (100), 213 (26), 185 (10), 165 (16), 151 (12), 139 (11), 137 (32), 129 (11), 128 (11), 116 (10), 115 (24), 102 (18), 101 (20), 75 (14), 51 (11); **HR-MS (ESI)**: m/z calculated for $[C_{13}H_{12}ClF_3ONa]^+$ ($[M + Na]^+$): 299.0421, measured: 299.0391; **IR (ATR)**: ν (cm^{-1}): 2977, 2890, 1741, 1493, 1473, 1433, 1372, 1301, 1258, 1213, 1199, 1172, 1154, 1117, 1075, 1013, 982, 848, 809, 742, 703, 662, 631.

2-(*p*-Tolyl)-2-(2,2,2-trifluoroethyl)cyclopentan-1-one (166)
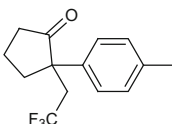
GP9: Prepared from 1-(1-(*p*-tolyl)vinyl)cyclobutan-1-ol (**148**, 38 mg, 0.20 mmol). Colourless oil upon cooling solidified (40 mg, 0.16 mmol, 78 %).

R_f (pentane:dichloromethane 3:2): 0.34; **^{1}H NMR (300 MHz, CDCl$_3$)**: δ (ppm): 7.28 (d, J = 8.3 Hz, 2H), 7.17 (d, J = 8.3 Hz, 2H), 2.91 (dd, J = 13.2, 6.3 Hz, 1H), 2.80 (dq, J = 15.5, 11.3 Hz, 1H), 2.48 (dq, J = 15.4, 11.1 Hz, 1H), 1.92–2.39 (m, 4H), 2.34 (s, 3H), 1.72–1.89 (m, 1H); **^{13}C NMR (75.5 MHz, CDCl$_3$)**: δ (ppm): 216.4 (C$_q$), 137.6 (C$_q$), 133.0 (C$_q$), 129.8 (CH), 126.8 (CH), 126.4 (q, J = 278.4 Hz, CF$_3$), 53.1 (q, J = 1.7 Hz, C$_q$), 42.1 (q, J = 27.2 Hz, CH$_2$), 35.6 (CH$_2$), 32.6 (q, J = 1.4 Hz, CH$_2$), 21.1 (CH$_3$), 18.4 (CH$_2$); **^{19}F NMR (300 MHz, CDCl$_3$)**: δ (ppm): −60.38 (t, J = 11.2 Hz); **GC-MS: t_R (50_40)**: 7.7 min; **EI-MS**: m/z (%): 256 (38), 201 (12), 200 (100), 145 (33), 131 (11), 129 (12), 128 (12), 118 (11), 117 (34), 116 (11), 115 (35), 91 (27); **HR-MS (ESI)**: m/z calculated for $[C_{14}H_{15}F_3ONa]^+$ ($[M + Na]^+$): 279.0967, measured: 279.0980; **IR (ATR)**: ν (cm^{-1}): 2975, 1739, 1513, 1459, 1432, 1407, 1371, 1301, 1258, 1211, 1197, 1156, 1116, 1075, 1032, 1022, 981, 876, 846, 807, 738, 721, 658, 653, 625.

2-([1,1′-Biphenyl]-4-yl)-2-(2,2,2-trifluoroethyl)cyclopentan-1-one (169)
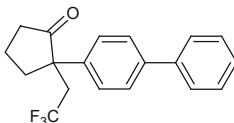
GP9: Prepared from 1-(1-([1,1′-biphenyl]-4-yl)vinyl)cyclobutan-1-ol (**151**, 50 mg, 0.20 mmol). Colourless oil (52 mg, 0.16 mmol, 82 %).

R_f (pentane:dichloromethane 3:2): 0.40; **^{1}H NMR (300 MHz, CDCl$_3$)**: δ (ppm): 7.54–7.64 (m, 4H), 7.41–7.48 (m, 4H), 7.32–7.38 (m, 1H), 2.96 (dd, J = 13.4, 6.3 Hz, 1H), 2.85 (dq, J = 15.4, 11.2 Hz, 1H), 2.53 (dq, J = 15.5, 11.0 Hz, 1H), 1.98–2.43 (m, 4H), 1.76–1.95 (m, 1H); **^{13}C NMR (75.5 MHz, CDCl$_3$)**: δ (ppm): 216.3 (C$_q$), 140.6 (C$_q$), 140.3 (C$_q$), 135.1 (C$_q$), 129.0 (CH), 127.7 (CH), 127.7 (CH), 127.4 (CH), 127.2 (CH), 126.4 (q, J = 278.4 Hz, CF$_3$),

53.3 (q, J = 1.4 Hz, C_q), 42.1 (q, J = 27.4 Hz, CH_2), 35.7 (CH_2), 32.6 (q, J = 1.6 Hz, CH_2), 18.5 (CH_2); **^{19}F NMR (300 MHz, CDCl$_3$)**: δ (ppm): −60.30 (t, J = 11.1 Hz); **GC-MS: t_R (50_40)**: 9.5 min; **EI-MS**: m/z (%): 319 (12), 318 (50), 263 (18), 262 (100), 207 (19), 179 (26), 178 (35), 165 (10), 152 (11); **HR-MS (ESI)**: m/z calculated for $[C_{19}H_{17}F_3ONa]^+$ ($[M + Na]^+$): 341.1124, measured: 341.1145; **IR (ATR)**: ν (cm^{-1}): 2974, 1739, 1488, 1474, 1432, 1406, 1371, 1315, 1301, 1258, 1214, 1198, 1155, 1116, 1074, 1034, 1007, 982, 919, 875, 851, 817, 761, 731, 698, 661, 632.

2-(4-Methoxyphenyl)-2-(2,2,2-trifluoroethyl)cyclopentan-1-one (170)
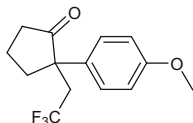
GP9: Prepared from 1-(1-(4-methoxyphenyl)vinyl)cyclobutan-1-ol (**152**, 41 mg, 0.20 mmol). Colourless oil (49 mg, 0.18 mmol, 90 %).

R_f (pentane:dichloromethane 3:2): 0.54; **^{1}H NMR (300 MHz, CDCl$_3$)**: δ (ppm): 7.27–7.32 (m, 2H), 6.85–6.90 (m, 2H), 3.79 (s, 3H), 2.87 (dd, J = 13.2, 6.2 Hz, 1H), 2.69–2.86 (m, 1H), 2.39–2.51 (m, 1H), 1.93–2.36 (m, 4H), 1.70–1.88 (m, 1H); **^{13}C NMR (100 MHz, CDCl$_3$)**: δ (ppm): 216.3 (C_q), 159.2 (C_q), 128.2 (CH), 127.6 (C_q), 126.4 (q, J = 278.3 Hz, CF_3), 114.4 (CH), 55.3 (CH_3), 52.7 (q, J = 1.9 Hz, C_q), 42.1 (q, J = 27.1 Hz, CH_2), 35.5 (CH_2), 32.7 (q, J = 1.6 Hz, CH_2), 18.4 (CH_2); **^{19}F NMR (300 MHz, CDCl$_3$)**: δ (ppm): −60.40 (t, J = 11.1 Hz); **GC-MS: t_R (50_40)**: 8.1 min; **EI-MS**: m/z (%): 272 (31), 217 (12), 216 (100), 161 (30), 133 (32); **HR-MS (ESI)**: m/z calculated for $[C_{14}H_{15}F_3O_2Na]^+$ ($[M + Na]^+$): 295.0916, measured: 295.0921; **IR (ATR)**: ν (cm^{-1}): 2962, 2841, 1738, 1609, 1581, 1512, 1463, 1442, 1407, 1372, 1294, 1254, 1214, 1187, 1156, 1116, 1074, 1034, 981, 875, 847, 811, 661, 641, 625.

2-(Benzo[*d*][1,3]dioxol-5-yl)-2-(2,2,2-trifluoroethyl)cyclopentan-1-one (171)
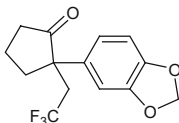
GP9: Prepared from 1-(1-(benzo[*d*][1,3]dioxol-5-yl)vinyl)cyclobutan-1-ol (**153**, 44 mg, 0.20 mmol). Colourless oil (49 mg, 0.17 mmol, 86 %).

R_f (pentane:dichloromethane 3:2): 0.41; **^{1}H NMR (300 MHz, CDCl$_3$)**: δ (ppm): 6.88 (d, J = 1.9 Hz, 1H), 6.83 (dd, J = 8.2, 2.0 Hz, 1H), 6.77 (d, J = 8.2 Hz, 1H), 5.95–5.96 (m, 2H), 2.79–2.86 (m, 1H), 2.75 (dq, J = 15.5, 11.2 Hz, 1H), 2.11–2.51 (m, 3H), 1.93–2.11 (m, 2H), 1.71–1.88 (m, 1H); **^{13}C NMR (75.5 MHz, CDCl$_3$)**: δ (ppm): 216.0 (C_q), 148.5 (C_q), 147.2 (C_q), 129.5 (C_q), 126.4 (q, J = 278.3 Hz, CF_3), 120.5 (CH), 108.6 (CH), 107.5 (CH), 101.4

(CH$_2$), 53.0 (q, J = 1.7 Hz, C$_q$), 42.2 (q, J = 27.2 Hz, CH$_2$), 35.5 (CH$_2$), 33.0 (q, J = 1.6 Hz, CH$_2$), 18.4 (CH$_2$); **^{19}F NMR (300 MHz, CDCl$_3$)**: δ (ppm): −60.44 (t, J = 11.1 Hz); **GC-MS: t$_R$ (50_40)**: 8.5 min; **EI-MS**: m/z (%): 286 (37), 231 (11), 230 (100), 229 (26), 175 (19), 147 (14), 89 (11), 63 (10); **HR-MS (ESI)**: m/z calculated for [C$_{14}$H$_{13}$F$_3$O$_3$Na]$^+$ ([M + Na]$^+$): 309.0709, measured: 309.0717; **IR (ATR)**: ν (cm^{-1}): 2974, 2894, 1737, 1504, 1489, 1437, 1373, 1301, 1238, 1199, 1171, 1149, 1116, 1074, 1038, 984, 898, 879, 841, 807, 729, 700, 651, 631.

2-(Naphthalen-2-yl)-2-(2,2,2-trifluoroethyl)cyclopentan-1-one (172)
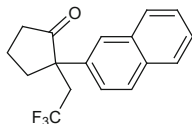
GP9: Prepared from 1-(1-(naphthalen-2-yl)vinyl)cyclobutan-1-ol (**154**, 45 mg, 0.20 mmol). Colourless oil (47 mg, 0.16 mmol, 80 %).

R$_f$ (pentane:ethyl acetate 9:1): 0.49; **^{1}H NMR (300 MHz, CDCl$_3$)**: δ (ppm): 7.70–7.98 (m, 4H), 7.39–7.67 (m, 3H), 3.06 (dd, J = 13.8, 5.8 Hz, 1H), 2.92 (dq, J = 15.5, 11.2 Hz, 1H), 2.58 (dq, J = 15.5, 11.1 Hz, 1H), 2.11–2.43 (m, 3H), 1.99–2.09 (m, 1H), 1.76–1.93 (m, 1H); **^{13}C NMR (75.5 MHz, CDCl$_3$)**: δ (ppm): 216.2 (C$_q$), 133.5 (C$_q$), 133.4 (C$_q$), 132.7 (C$_q$), 129.0 (CH), 128.3 (CH), 127.6 (CH), 126.6 (CH), 126.6 (CH), 126.4 (q, J = 278.2 Hz, CF$_3$), 126.3 (CH), 124.4 (CH), 53.7 (q, J = 1.7 Hz, C$_q$), 42.0 (q, J = 27.5 Hz, CH$_2$), 35.7 (CH$_2$), 32.7 (q, J = 1.4 Hz, CH$_2$), 18.5 (CH$_2$); **^{19}F NMR (300 MHz, CDCl$_3$)**: δ (ppm): −60.29 (t, J = 11.1 Hz); **GC-MS: t$_R$ (50_40)**: 9.0 min; **EI-MS**: m/z (%): 293 (10), 292 (56), 237 (16), 236 (100), 181 (33), 167 (13), 166 (11), 165 (25), 154 (15), 153 (33), 151 (39), 128 (20); **HR-MS (ESI)**: m/z calculated for [C$_{17}$H$_{15}$F$_3$ONa]$^+$ ([M + Na]$^+$): 315.0967, measured: 315.0960; **IR (ATR)**: ν (cm^{-1}): 2976, 1738, 1598, 1506, 1459, 1432, 1371, 1300, 1257, 1197, 1152, 1120, 1074, 986, 864, 812, 747, 648, 615.

### 2-(*m*-Tolyl)-2-(2,2,2-trifluoroethyl)cyclopentan-1-one (167)
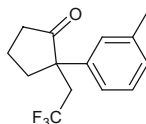
GP9: Prepared from 1-(1-(*m*-tolyl)vinyl)cyclobutan-1-ol (**149**, 38 mg, 0.2 mmol). Colourless oil (26 mg, 0.10 mmol, 51 %).

R$_f$ (pentane:dichloromethane 3:2): 0.34; **^{1}H NMR (300 MHz, CDCl$_3$)**: δ (ppm): 7.16–7.31 (m, 3H), 7.07–7.14 (m, 1H), 2.86 (dd, J = 13.3, 6.4 Hz, 1H), 2.79 (dq, J = 15.5, 11.3 Hz, 1H), 2.51 (dq, J = 15.5, 11.1 Hz, 1H), 1.91–2.22 (m, 4H), 2.36 (s, 3H), 1.69–1.91 (m, 1H); **^{13}C NMR (75.5 MHz, CDCl$_3$)**: δ (ppm): 216.4 (C$_q$), 138.7 (C$_q$), 136.1 (C$_q$), 128.9 (CH), 128.6 (CH), 127.6 (CH), 126.4 (q,

J = 278.4 Hz, CF$_3$), 123.7 (CH), 53.4 (q, J = 1.7 Hz, C$_q$), 42.1 (q, J = 27.3 Hz, CH$_2$), 35.6 (CH$_2$), 32.5 (q, J = 1.4 Hz, CH$_2$), 21.7 (CH$_3$), 18.4 (CH$_2$); **^{19}F NMR (300 MHz, CDCl$_3$)**: δ (ppm): −60.37 (t, J = 11.3 Hz); **GC-MS**: **t$_R$ (50_40)**: 7.6 min; **EI-MS**: m/z (%): 256 (46), 213 (12), 201 (12), 200 (100), 145 (40), 131 (18), 129 (18), 128 (17), 118 (29), 117 (36), 116 (15), 115 (45), 105 (10), 92 (15), 91 (34), 65 (12), 39 (11); **HR-MS (ESI)**: m/z calculated for [C$_{14}$H$_{15}$F$_3$ONa]$^+$ ([M + Na]$^+$): 279.0967, measured: 279.0977; **IR (ATR)**: ν (cm^{-1}): 2976, 2965, 2892, 1741, 1605, 1491, 1471, 1459, 1432, 1407, 1372, 1301, 1259, 1196, 1153, 1121, 1096, 1075, 984, 776, 706, 662, 640.

2-(*o*-Tolyl)-2-(2,2,2-trifluoroethyl)cyclopentan-1-one (168)
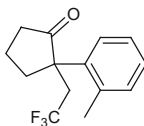
GP9: Prepared from 1-(1-(*o*-tolyl)vinyl)cyclobutan-1-ol (**150**, 38 mg, 0.20 mmol). Colourless oil (20 mg, 0.08 mmol, 39 %).

R$_f$ (pentane:dichloromethane 3:2): 0.46; **^{1}H NMR (300 MHz, CDCl$_3$)**: δ (ppm): 7.15–7.25 (m, 2H), 7.08–7.13 (m, 1H), 7.00–7.03 (m, 1H), 2.73–3.00 (m, 3H), 2.37–2.49 (m, 1H), 2.46 (s, 3H), 2.15–2.33 (m, 2H), 1.86–1.98 (m, 1H), 1.57–1.73 (m, 1H); **^{13}C NMR (75.5 MHz, CDCl$_3$)**: δ (ppm): 217.4 (C$_q$), 136.8 (C$_q$), 136.4 (C$_q$), 133.7 (CH), 127.9 (CH), 127.3 (CH), 126.3 (q, J = 278.4 Hz, CF$_3$), 126.2 (CH), 54.7 (q, J = 1.5 Hz, C$_q$), 38.7 (q, J = 27.3 Hz, CH$_2$), 36.3 (CH$_2$), 33.4 (q, J = 1.5 Hz, CH$_2$), 21.4 (CH$_3$), 18.3 (CH$_2$); **^{19}F NMR (300 MHz, CDCl$_3$)**: δ (ppm): −60.44 (t, J = 11.5 Hz); **GC-MS**: **t$_R$ (50_40)**: 7.7 min; **EI-MS**: m/z (%): 257 (11), 256 (73), 225 (10), 214 (12), 213 (22), 201 (10), 200 (79), 199 (11), 185 (19), 173 (15), 165 (15), 155 (18), 146 (14), 145 (81), 143 (13), 131 (42), 130 (13), 129 (49), 128 (36), 127 (12), 118 (37), 117 (86), 116 (32), 115 (100), 105 (19), 92 (19), 91 (68), 89 (14), 77 (20), 71 (13), 69 (10), 65 (23), 63 (16), 55 (14), 51 (18), 39 (25); **HR-MS (ESI)**: m/z calculated for [C$_{14}$H$_{15}$F$_3$ONa]$^+$ ([M + Na]$^+$): 279.0967, measured: 279.0972; **IR (ATR)**: ν (cm^{-1}): 2962, 1745, 1490, 1456, 1433, 1370, 1298, 1259, 1138, 1118, 1074, 982, 633.

2′-(Trifluoromethyl)-3′,4′-dihydro-2′H-spiro[cyclopentane-1,1′-naphthalen]-2-one (173)
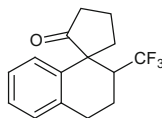
GP9: Prepared from 1-(3,4-dihydronaphthalen-1-yl)cyclobutan-1-ol (**155**, 40 mg, 0.20 mmol). White solids (28 mg, 0.10 mmol, 52 %, 1:1 dr).

Diastereomer A:

R_f (pentane:ethyl acetate 19:1): 0.21; **^{1}H NMR (600 MHz, CDCl$_3$)**: δ (ppm): 7.11–7.17 (m, 2H), 7.07–7.10 (m, 1H), 6.76–6.79 (m, 1H), 2.92–3.01 (m, 3H), 2.53–2.68 (m, 3H), 2.04–2.19 (m, 4H), 1.84–1.95 (m, 1H); **^{13}C NMR (150 MHz, CDCl$_3$)**: δ (ppm): 222.3 (C$_q$), 141.3 (C$_q$), 134.9 (C$_q$), 129.3 (CH), 127.5 (q, J = 280.6 Hz, CF$_3$), 127.2 (CH), 127.0 (CH), 126.9 (CH), 53.8 (q, J = 1.4 Hz, C$_q$), 45.9 (q, J = 25.4 Hz, CH), 40.0 (q, J = 1.1 Hz, CH$_2$), 35.8 (q, J = 1.5 Hz, CH$_2$), 28.7 (CH$_2$), 20.3 (q, J = 2.8 Hz, CH$_2$), 18.9 (q, J = 1.1 Hz, CH$_2$); **^{19}F NMR (600 MHz, CDCl$_3$)**: δ (ppm): −65.38 (d, J = 9.6 Hz); **GC-MS: t$_R$ (50_40)**: 8.4 min; **EI-MS**: m/z (%): 268 (38), 213 (13), 212 (100), 144 (10), 143 (28), 141 (14), 129 (16), 128 (30), 115 (21); **HR-MS (ESI)**: m/z calculated for [C$_{15}$H$_{16}$F$_3$O]$^+$ ([M + H]$^+$): 269.1148, measured: 269.1146; **IR (ATR)**: ν (cm^{-1}): 2962, 2904, 1742, 1493, 1451, 1407, 1385, 1342, 1317, 1269, 1229, 1151, 1124, 1101, 1074, 1012, 976, 945, 888, 822, 755, 725, 687, 629.

Diastereomer B:

R_f (pentane:ethyl acetate 19:1): 0.15; **^{1}H NMR (600 MHz, CDCl$_3$)**: δ (ppm): 7.13–7.18 (m, 2H), 7.08–7.12 (m, 1H), 6.95–6.98 (m, 1H), 2.97–3.02 (m, 1H), 2.77–2.84 (m, 1H), 2.64–2.73 (m, 2H), 2.54–2.60 (m, 1H), 2.47–2.54 (m, 1H), 2.36–2.45 (m, 2H), 2.13–2.19 (m, 2H), 2.04–2.09 (m, 1H); **^{13}C NMR (150 MHz, CDCl$_3$)**: δ (ppm): 218.6 (C$_q$), 138.9 (C$_q$), 136.3 (C$_q$), 129.1 (CH), 128.0 (CH), 127.2 (q, J = 282.3 Hz, CF$_3$), 126.8 (CH), 126.8 (CH), 53.0 (C$_q$), 46.6 (q, J = 25.1 Hz, CH), 41.5 (q, J = 1.2 Hz, CH$_2$), 38.3 (q, J = 1.2 Hz, CH$_2$), 27.2 (CH$_2$), 20.1 (q, J = 3.0 Hz, CH$_2$), 18.7 (CH$_2$); **^{19}F NMR (600 MHz, CDCl$_3$)**: δ (ppm): −63.42 (d, J = 9.8 Hz); **GC-MS: t$_R$ (50_40)**: 8.5 min; **EI-MS**: m/z (%): 268 (37), 213 (13), 212 (100), 144 (11), 143 (28), 141 (15), 129 (17), 128 (31), 116 (10), 115 (23); **HR-MS (ESI)**: m/z calculated for [C$_{15}$H$_{16}$F$_3$O]$^+$ ([M + H]$^+$): 269.1148, measured: 269.1146; **IR (ATR)**: ν (cm^{-1}): 3025, 2968, 2927, 2908, 2851, 1740, 1493, 1450, 1446, 1407, 1384, 1350, 1302, 1272, 1229, 1188, 1140, 1117, 1081, 1048, 1020, 984, 921, 873, 846, 820, 784, 760, 683.

3-(Trifluoromethyl)spiro[chromane-4,1′-cyclopentan]-2′-one (176)
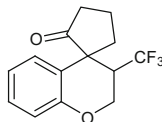
GP9: Prepared from 1-(2H-chromen-4-yl)cyclobutan-1-ol (**158**, 46 mg, 0.22 mmol). White solid (24 mg, 0.09 mmol, 41 %, 10:1 dr).

Major diastereomer:

R_f (pentane:ethyl acetate 19:1): 0.12; **^{1}H NMR (300 MHz, CDCl$_3$)**: δ (ppm): 7.08–7.21 (m, 1H), 6.92–6.97 (m, 2H), 6.87–6.91 (m, 1H), 4.70 (dd, J = 11.7, 6.1 Hz, 1H), 4.24 (ddq, J = 11.7, 2.8, 1.4 Hz, 1H), 2.71–2.83 (m, 1H), 2.63–2.71

(m, 1H), 2.39–2.57 (m, 3H), 2.09–2.24 (m, 2H); **^{13}C NMR (100 MHz, CDCl$_3$)**: δ (ppm): 216.8 (C$_q$), 154.4 (C$_q$), 128.6 (CH), 128.1 (CH), 125.8 (q, J = 281.9 Hz, CF$_3$), 124.2 (C$_q$), 121.8 (CH), 117.4 (CH), 61.4 (q, J = 3.9 Hz, CH$_2$), 49.8 (C$_q$), 45.0 (q, J = 26.0 Hz, CH), 40.7 (CH$_2$), 38.1 (CH$_2$), 18.2 (CH$_2$); **^{19}F NMR (300 MHz, CDCl$_3$)**: δ (ppm): −63.14 (d, J = 9.3 Hz); **GC-MS: t$_R$ (50_40)**: 8.3 min; **EI-MS**: m/z (%): 270 (30), 215 (12), 214 (100), 145 (26), 131 (10), 115 (16), 77 (10); **HR-MS (ESI)**: m/z calculated for [C$_{14}$H$_{13}$F$_3$O$_2$Na]$^+$ ([M + Na]$^+$): 293.0760, measured: 293.0762; **IR (ATR)**: ν (cm^{-1}): 2998, 2971, 2916, 1737, 1609, 1585, 1492, 1466, 1453, 1397, 1369, 1313, 1282, 1247, 1223, 1136, 1108, 1075, 1055, 1008, 946, 918, 862, 829, 796, 761, 736, 703, 689, 637, 606.

5′,7′-Dimethyl-2′-(trifluoromethyl)-3′,4′-dihydro-2′H-spiro[cyclopentane-1,1′-naphthalen]-2-one (174)
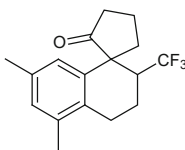

GP9: Prepared from 1-(5,7-dimethyl-3,4-dihydronaphthalen-1-yl)cyclobutan-1-ol (**156**, 46 mg, 0.20 mmol). White solids (17 mg, 0.06 mmol, 29 %, 1.1:1 dr).

Major diastereomer:

R$_f$ **(pentane:ethyl acetate 19:1)**: 0.26; **^{1}H NMR (300 MHz, CDCl$_3$)**: δ (ppm): 6.86 (s, 1H), 6.41 (s, 1H), 2.78–2.97 (m, 2H), 2.59–2.71 (m, 4H), 1.96–2.26 (m, 4H), 2.23 (s, 3H), 2.17 (s, 3H), 1.78–1.93 (m, 1H); **^{13}C NMR (75.5 MHz, CDCl$_3$)**: δ (ppm): 223.0 (C$_q$), 141.4 (C$_q$), 136.5 (C$_q$), 136.0 (C$_q$), 130.3 (C$_q$), 129.6 (CH), 127.5 (q, J = 280.7 Hz, CF$_3$), 125.5 (CH), 53.9 (C$_q$), 45.7 (q, J = 25.5 Hz, CH), 40.3 (CH$_2$), 35.9 (CH$_2$), 26.0 (CH$_2$), 21.2 (CH$_3$), 20.2 (q, J = 2.6 Hz, CH$_2$), 19.9 (CH$_3$), 18.9 (CH$_2$); **^{19}F NMR (300 MHz, CDCl$_3$)**: δ (ppm): −60.43 (d, J = 9.5 Hz); **GC-MS: t$_R$ (50_40)**: 8.9 min; **EI-MS**: m/z 297 (12), 296 (60), 254 (14), 253 (76), 241 (15), 240 (96), 226 (15), 225 (100), 157 (10), 156 (13), 155 (14), 142 (12), 141 (20), 128 (16), 115 (11); **HR-MS (ESI)**: m/z calculated for [C$_{17}$H$_{19}$F$_3$ONa]$^+$ ([M + Na]$^+$): 319.1280, measured: 319.1286; **IR (ATR)**: ν (cm^{-1}): 2951, 1743, 1613, 1480, 1457, 1407, 1384, 1345, 1317, 1297, 1268, 1228, 1150, 1120, 1074, 1036, 1036, 1015, 981, 942, 902, 853, 713, 656, 631.

Minor diastereomer:

R$_f$ **(pentane:ethyl acetate 19:1)**: 0.21; **^{1}H NMR (300 MHz, CDCl$_3$)**:: δ (ppm): 6.87 (s, 1H), 6.59 (s, 1H), 2.32–2.85 (m, 8H), 2.25 (s, 3H), 2.20 (s, 3H), 2.20–2.28 (m, 3H); **^{13}C NMR (75.5 MHz, CDCl$_3$)**: δ (ppm): 219.2 (C$_q$), 138.5 (C$_q$), 136.1 (C$_q$), 135.6 (C$_q$), 132.0 (C$_q$), 129.5 (CH), 127.2 (q, J = 282.2 Hz, CF$_3$), 126.4 (CH), 53.4 (C$_q$), 45.7 (q, J = 25.3 Hz, CH), 41.9 (CH$_2$), 38.4 (CH$_2$), 23.9 (CH$_2$), 21.3 (CH$_3$), 20.0 (q, J = 2.9 Hz, CH$_2$), 19.8 (CH$_3$), 18.6 (CH$_2$); **^{19}F NMR (300 MHz, CDCl$_3$)**: δ (ppm): −63.35 (d, J = 9.9 Hz); **GC-MS: t$_R$ (50_40)**:

9.0 min; **EI-MS**: *m/z* (%): 297 (11), 296 (57), 268 (11), 254 (14), 253 (77), 241 (17), 240 (92), 226 (17), 225 (100), 157 (11), 156 (14), 155 (12), 153 (10), 142 (12), 141 (21), 129 (12), 128 (16), 115 (13); **HR-MS (ESI)**: *m/z* calculated for $[C_{17}H_{19}F_3ONa]^+$ ($[M + Na]^+$): 319.1280, measured: 319.1283; **IR (ATR)**: ν (cm^{-1}): 2966, 2916, 1741, 1482, 1459, 1381, 1272, 1199, 1181, 1142, 1128, 1113, 1087, 1043, 1015, 854, 792, 656, 644, 609.

6′-Methoxy-2′-(trifluoromethyl)-3′,4′-dihydro-2′H-spiro[cyclopentane-1,1′-naphthalen]-2-one (175)
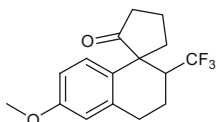
GP9: Prepared from 1-(6-methoxy-3,4-dihydronaphthalen-1-yl)cyclobutan-1-ol (**157**, 46 mg, 0.20 mmol). White solid upon cooling (28 mg, 0.09 mmol, 47 %, > 25:1 dr).

Major diastereomer:

R$_f$ (pentane:ethyl acetate 19:1): 0.10; **^{1}H NMR (300 MHz, CDCl$_3$)**: δ (ppm): 6.87 (d, *J* = 8.7 Hz, 1H), 6.74 (dd, *J* = 8.8, 2.8 Hz, 1H), 6.62 (d, *J* = 2.7 Hz, 1H), 3.77 (s, 3H), 2.92–3.02 (m, 1H), 2.26–2.83 (m, 7H), 1.99–2.20 (m, 3H); **^{13}C NMR (75.5 MHz, CDCl$_3$)**: δ (ppm): 219.0 (C$_q$), 158.0 (C$_q$), 137.7 (C$_q$), 130.9 (C$_q$), 129.1 (CH), 127.2 (q, *J* = 282.3 Hz, CF$_3$), 113.4 (CH), 113.2 (CH), 55.3 (CH$_3$), 52.5 ((C$_q$), 46.4 (q, *J* = 25.2 Hz, CH), 41.3 (CH$_2$), 38.1 (CH$_2$), 27.3 (CH$_2$), 20.1 (q, *J* = 3.1 Hz, CH$_2$), 18.5 (CH$_2$); **^{19}F NMR (300 MHz, CDCl$_3$)**: δ (ppm): −63.35 (d, *J* = 9.9 Hz); **GC-MS**: **t$_R$ (50_40)**: 9.2 min; **EI-MS**: *m/z* (%): 298 (18), 270 (11), 243 (15), 242 (100), 174 (11), 115 (13); **HR-MS (ESI)**: *m/z* calculated for $[C_{16}H_{17}F_3O_2Na]^+$ ($[M + Na]^+$): 321.1073, measured: 321.1078; **IR (ATR)**: ν (cm^{-1}): 2964, 1740, 1612, 1578, 1503, 1462, 1381, 1347, 1320, 1302, 1264, 1244, 1229, 1189, 1142, 1123, 1083, 1066, 1047, 945, 896, 869, 851, 819, 735, 703, 627.

2′-(Trifluoromethyl)-2′,3′-dihydrospiro[cyclopentane-1,1′-inden]-2-one (177)
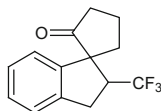
Prepared from 1-(1H-inden-3-yl)cyclobutan-1-ol (**159**, 37 mg, 0.20 mmol). White solids (27 mg, 0.11 mmol, 53 %, 1.5:1 dr). The starting material 1-(1H-inden-3-yl)cyclobutan-1-ol (**159**, 8.0 g, 0.04 mmol, 22 %) was recovered.

The reaction was repeated with **139** (2.0 equiv.) under similar conditions. White solids (33 mg, 0.13 mmol, 65 %, 1.5:1 dr).

Major diastereomer:

R_f **(pentane:ethyl acetate 19:1)**: 0.18; **^{1}H NMR (400 MHz, CDCl$_3$)**: δ (ppm): 7.19–7.32 (m, 3H), 7.03–7.10 (m, 1H), 3.35–3.54 (m, 1H), 3.04–3.24 (m, 2H), 2.35–2.67 (m, 4H), 2.05–2.29 (m, 2H); **^{13}C NMR (100 MHz, CDCl$_3$)**: δ (ppm): 216.4 (C$_q$), 145.2 (C$_q$), 141.1 (C$_q$), 128.1 (CH), 127.6 (CH), 126.8 (q, $J = 279.4$ Hz, CF$_3$), 125.0 (CH), 122.5 (CH), 60.7 (q, $J = 1.5$ Hz, C$_q$), 54.4 (q, $J = 27.1$ Hz, CH), 38.4 (CH$_2$), 37.3 (CH$_2$), 32.1 (q, $J = 1.3$ Hz, CH$_2$), 20.0 (CH$_2$); **^{19}F NMR (300 MHz, CDCl$_3$)**: δ (ppm): −64.68 (d, $J = 9.0$ Hz); **GC-MS**: t_R **(50_40)**: 8.0 min; **EI-MS**: m/z (%): 254 (31), 199 (12), 198 (100), 129 (41), 128 (25), 115 (10); **HR-MS (ESI)**: m/z calculated for [C$_{14}$H$_{13}$F$_3$ONa]$^+$ ([M + Na]$^+$): 277.0811, measured: 277.0823; **IR (ATR)**: ν (cm^{-1}): 2967, 2921, 1736, 1481, 1464, 1448, 1408, 1378, 1321, 1273, 1251, 1229, 1194, 1167, 1131, 1103, 1070, 1039, 1101, 950, 921, 875, 818, 771, 757, 727, 705, 665, 645, 620, 600.

Minor diastereomer:

R_f **(pentane:ethyl acetate 19:1)**: 0.21; **^{1}H NMR (400 MHz, CDCl$_3$)**: δ (ppm): 7.13–7.31 (m, 3H), 6.96 (dd, $J = 6.7$, 1.6 Hz, 1H), 3.43–3.67 (m, 1H), 3.11–3.29 (m, 2H), 2.57–2.68 (m, 1H), 2.38–2.52 (m, 2H), 2.04–2.26 (m, 3H); **^{13}C NMR (100 MHz, CDCl$_3$)**: δ (ppm): 218.5 (C$_q$), 145.6 (C$_q$), 139.7 (C$_q$), 128.1 (CH), 127.6 (CH), 127.0 (q, $J = 278.1$ Hz, CF$_3$), 125.0 (CH), 122.7 (CH), 61.5 (q, $J = 1.5$ Hz, C$_q$), 48.9 (q, $J = 27.2$ Hz, CH), 37.4 (CH$_2$), 32.3 (q, $J = 1.7$ Hz, CH$_2$), 31.8 (q, $J = 2.7$ Hz, CH$_2$), 18.8 (CH$_2$); **^{19}F NMR (300 MHz, CDCl$_3$)**: δ (ppm): −65.58 (d, $J = 9.9$ Hz); **GC-MS**: t_R **(50_40)**: 7.9 min; **EI-MS**: m/z (%): 254 (30), 199 (12), 198 (100), 129 (41), 128 (24), 115 (11); **HR-MS (ESI)**: m/z calculated for [C$_{14}$H$_{13}$F$_3$ONa]$^+$ ([M + Na]$^+$): 277.0811, measured: 277.0817; **IR (ATR)**: ν (cm^{-1}): 2975, 2922, 2902, 1737, 1477, 1443, 1396, 1327, 1276, 1253, 1196, 1164, 1146, 1117, 1077, 1045, 1008, 965, 933, 875, 837, 816, 765, 733, 707, 690, 648, 632.

4-Phenyl-4-(2,2,2-trifluoroethyl)dihydrofuran-3(2H)-one (179)
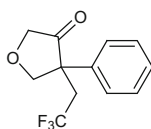
GP9: Prepared from 3-(1-phenylvinyl)oxetan-3-ol (**161**, 35 mg, 0.20 mmol). Colourless oil (13.0 mg, 0.05 mmol, 27 %).

R_f **(pentane:dichloromethane 3:2)**: 0.46; **^{1}H NMR (400 MHz, CDCl$_3$)**: δ (ppm): 7.49 (t, $J = 7.6$ Hz, 2H), 7.39 (t, $J = 7.6$ Hz, 2H), 7.32 (t, $J = 7.6$ Hz, 1H), 5.05 (d, $J = 10.7$ Hz, 1H), 4.22 (d, $J = 10.7$ Hz, 1H), 4.11 (d, $J = 17.5$ Hz, 1H), 3.92 (d, $J = 17.5$ Hz, 1H), 3.03 (dq, $J = 15.5$, 11.0 Hz, 1H), 2.53 (dq, $J = 15.5$, 10.5 Hz, 1H); **^{13}C NMR (100 MHz, CDCl$_3$)**: δ (ppm): 211.7 (C$_q$), 134.2 (C$_q$), 129.2 (CH), 128.4 (CH), 126.7 (CH), 126.0 (q, $J = 278.1$ Hz, CF$_3$), 74.1 (q, $J = 2.4$ Hz, CH$_2$), 69.6 (CH$_2$), 52.1 (C$_q$), 38.9 (q, $J = 28.8$ Hz, CH$_2$); **^{19}F NMR (300 MHz, CDCl$_3$)**: δ (ppm): −60.86 (t, $J = 10.8$ Hz); **GC-MS**: t_R **(50_40)**:

7.2 min; **EI-MS**: *m/z* (%): 187 (11), 186 (100), 153 (11), 117 (21), 115 (17), 103 (45), 78 (16), 77 (18), 51 (11); **HR-MS (ESI)**: *m/z* calculated for $[C_{12}H_{11}F_3O_2Na]^+$ ($[M + Na]^+$): 267.0603, measured: 267.0610; **IR (ATR)**: ν (cm^{-1}): 1728, 1600, 1499, 1449, 1418, 1373, 1309, 1258, 1229, 1130, 1111, 1056, 1033, 1002, 929, 854, 738, 699, 638, 621.

4-(4-Fluorophenyl)-4-(2,2,2-trifluoroethyl)dihydrofuran-3(2H)-one (180)
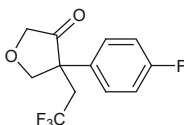
GP9: Prepared from 3-(1-(4-fluorophenyl)vinyl)oxetan-3-ol (**162**, 39 mg, 0.20 mmol). Colourless oil (15 mg, 0.06 mmol, 29 %).

R_f (pentane:dichloromethane 3:2): 0.43; **^{1}H NMR (300 MHz, CDCl$_3$)**: δ (ppm): 7.39–7.57 (m, 2H), 7.00–7.15 (m, 2H), 5.01 (d, *J* = 10.9 Hz, 1H), 4.21 (d, *J* = 10.9 Hz, 1H), 4.11 (d, *J* = 17.6 Hz, 1H), 3.92 (d, *J* = 17.6 Hz, 1H), 3.01 (dq, *J* = 15.6, 11.0 Hz, 1H), 2.48 (dq, *J* = 15.7, 10.5 Hz, 1H); **^{13}C NMR (100 MHz, CDCl$_3$)**: δ (ppm): 211.4 (C$_q$), 162.6 (d, *J* = 248.4 Hz, C$_q$), 129.7 (d, *J* = 3.3 Hz, C$_q$), 128.7 (d, *J* = 8.3 Hz, CH), 125.9 (q, *J* = 278.1 Hz, CF$_3$), 116.2 (d, *J* = 21.6 Hz, CH), 74.3 (q, *J* = 2.3 Hz, CH$_2$), 69.5 (CH$_2$), 51.6 (q, *J* = 1.5 Hz, C$_q$), 38.9 (q, *J* = 28.8 Hz, CH$_2$); **^{19}F NMR (300 MHz, CDCl$_3$)**: δ (ppm): −60.83,−113.70; **GC-MS**: **t_R (50_40)**: 7.2 min; **EI-MS**: *m/z* (%): 205 (11), 204 (100), 171 (12), 133 (13), 121 (68), 101 (24), 96 (10); **HR-MS (ESI)**: *m/z* calculated for $[C_{12}H_{10}F_4O_2Na]^+$ ($[M + Na]^+$): 285.0509, measured: 285.0516; **IR (ATR)**: ν (cm^{-1}): 2920, 1728, 1605, 1513, 1435, 1415, 1374, 1310, 1259, 1238, 1163, 1134, 1110, 1056, 931, 835, 639.

2-Phenyl-2-(2,2,2-trifluoroethyl)cyclohexan-1-one (178)
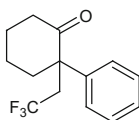
GP9: Prepared from 1-(1-phenylvinyl)cyclopentan-1-ol (**160**, 38 mg, 0.20 mmol). Colourless oil (17 mg, 0.07 mmol, 33 %).

R_f (pentane:dichloromethane 3:2): 0.54; **^{1}H NMR (300 MHz, CDCl$_3$)**: δ (ppm): 7.30–7.39 (m, 2H), 7.24–7.30 (m, 1H), 7.16–7.22 (m, 2H), 2.99–3.04 (m, 1H), 2.45–2.79 (m, 2H), 2.18–2.39 (m, 2H), 1.89–2.03 (m, 1H), 1.60–1.89 (m, 4H); **^{13}C NMR (75.5 MHz, CDCl$_3$)**: δ (ppm): 210.6 (C$_q$), 138.4 (C$_q$), 129.3 (CH), 127.6 (CH), 127.1 (CH), 126.7 (q, *J* = 278.2 Hz, CF$_3$), 54.6 (q, *J* = 1.8 Hz, C$_q$), 43.1 (q, *J* = 26.7 Hz, CH$_2$), 39.3 (CH$_2$), 34.3 (q, *J* = 1.8 Hz, CH$_2$), 28.2 (CH$_2$), 21.5 (CH$_2$); **^{19}F NMR (300 MHz, CDCl$_3$)**: δ (ppm): −58.75 (t, *J* = 11.5 Hz); **GC-MS**: **t_R (50_40)**: 7.7 min; **EI-MS**: *m/z* (%): 256 (18), 213 (12), 212 (77), 186 (18), 145 (14), 130 (11), 129 (100), 128 (12), 117 (30), 116 (11), 115 (39), 109 (14),

103 (26), 91 (41), 78 (12), 77 (22), 51 (12), 42 (11), 39 (10); **HR-MS (ESI)**: *m/z* calculated for $[C_{14}H_{15}F_3ONa]^+$ $([M + Na]^+)$: 279.0967, measured: 165.0971; **IR (ATR)**: ν (cm^{-1}): 2949, 1709, 1497, 1451, 1427, 1373, 1305, 1264, 1233, 1164, 1125, 1099, 1038, 906, 843, 727, 651, 628.

6.4.3   Synthetic Manipulations of Trifluoromethylated Cycloalkanone Product

Synthesis of (*E*)-2-Phenyl-2-(2,2,2-trifluoroethyl)cyclopentan-1-one oxime (184)
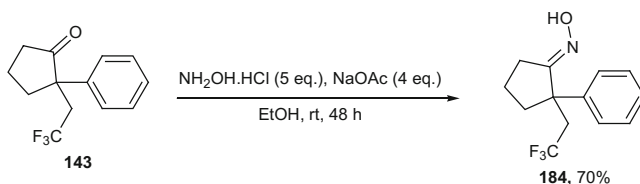
Hydroxylamine hydrochloride (63 mg, 0.91 mmol, 5.0 equiv.) and sodium acetate (60 mg, 0.73 mmol, 4.0 equiv.) were added to a solution of 2-phenyl-2-(2,2,2-trifluoroethyl)cyclopentan-1-one (**143**, 44 mg, 0.18 mmol, 1.0 equiv.) in ethanol (1.8 mL) and the resulting reaction mixture was stirred at rt for 48 h. Water (2 mL) was then added to quench the reaction. The organic layer was extracted with ethyl acetate (3×10 mL), washed with brine, dried over $MgSO_4$ and concentrated under reduced pressure. The crude reaction mixture was purified by flash column chromatography through silica gel (pentane: ethyl acetate 19:1) to afford pure (*E*)-2-phenyl-2-(2,2,2-trifluoroethyl)cyclopentan-1-one oxime (**184**, 33 mg, 0.13 mmol, 70 %) as a white solid.

(*E*)-2-Phenyl-2-(2,2,2-trifluoroethyl)cyclopentan-1-one oxime (184)
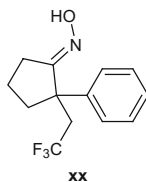
R$_f$ (pentane:ethyl acetate 19:1): 0.18; **^{1}H NMR (300 MHz, CDCl$_3$)**: δ (ppm): 7.42–7.50 (m, 2H), 7.29–7.38 (m, 2H), 7.22–7.28 (m, 1H), 2.75–3.03 (m, 2H), 2.47–2.68 (m, 2H), 2.39 (ddt, *J* = 19.2, 9.4, 2.0 Hz, 1H), 1.77–2.01 (m, 2H), 1.48–1.72 (m, 1H); **^{13}C NMR (75.5 MHz, CDCl$_3$)**: δ (ppm): 168.6 (C$_q$), 139.3 (C$_q$), 128.7 (CH), 127.4 (CH), 127.2 (CH), 126.4 (q, *J* = 278.5 Hz, CF$_3$), 50.3 (q, *J* = 1.7 Hz, C$_q$), 43.6 (q, *J* = 26.8 Hz, CH$_2$), 35.3 (q, *J* = 1.5 Hz, CH$_2$), 25.7 (CH$_2$), 20.6 (q, *J* = 0.7 Hz, CH$_2$); **^{19}F NMR (300 MHz, CDCl$_3$)**: δ (ppm): −60.10

(t, J = 11.2 Hz); **GC-MS**: **t$_R$ (50_40)**: 8.1 min; **EI-MS**: m/z (%): 258 (14), 257 (93), 241 (22), 240 (94), 225 (10), 215 (10), 212 (47), 200 (46), 199 (28), 188 (15), 186 (23), 179 (12), 175 (12), 174 (95), 173 (35), 170 (10), 164 (13), 160 (14), 159 (87), 158 (16), 157 (11), 156 (18), 151 (17), 147 (11), 146 (26), 143 (14), 141 (10), 135 (18), 134 (10), 133 (21), 131 (10), 130 (25), 129 (41), 128 (47), 127 (22), 117 (32), 116 (30), 115 (100), 109 (61), 104 (23), 103 (54), 102 (22), 101 (11), 91 (73), 89 (15), 78 (27), 77 (63), 76 (12), 75 (11), 73 (12), 69 (12), 65 (17), 64 (11), 63 (16), 54 (19), 52 (12), 51 (39), 50 (13), 41 (20), 39 (23); **HR-MS (ESI)**: m/z calculated for $[C_{13}H_{14}F_3NONa]^+$ ($[M + Na]^+$): 280.0920, measured: 280.0911; **IR (ATR)**: ν (cm^{-1}): 3299, 2995, 1497, 1457, 1448, 1426, 1370, 1295, 1260, 1240, 1209, 1160, 1120, 1083, 1042, 998, 958, 917, 830, 733, 700, 649.

Synthesis of 2-Phenyl-2-(2,2,2-trifluoroethyl)cyclopentan-1-ol (182)

NaBH$_4$ (1.5 equiv.)

MeOH, 0 °C, 45 min

143　　　　　　　　　**182**, 91%, dr = 25:1
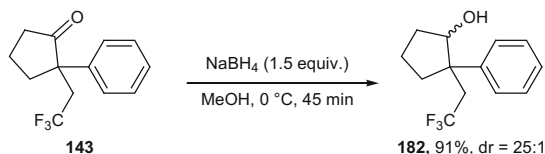
Sodium borohydride (17 mg, 0.45 mmol, 1.5 equiv.) was added to a solution of 2-phenyl-2-(2,2,2-trifluoroethyl)cyclopentan-1-one (**143**, 70 mg, 0.29 mmol, 1.0 equiv.) in methanol (2 mL) at 0 °C and the resulting reaction mixture was stirred at same temperature for 45 min. Water (2 mL) was then added to quench the reaction. The organic layer was extracted with ethyl acetate (3×15 mL), washed with brine, dried over MgSO$_4$ and concentrated under reduced pressure. The crude reaction mixture was purified by flash column chromatography through silica gel (pentane: ethyl acetate 19:1 to 17:3) to afford pure 2-phenyl-2-(2,2,2-trifluoroethyl) cyclopentan-1-ol (**182**, 64 mg, 0.26 mmol, 91 %, dr = 25:1) as a colourless oil.

2-Phenyl-2-(2,2,2-trifluoroethyl)cyclopentan-1-ol (182)
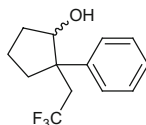
Major diastereomer: R$_f$ (pentane:ethyl acetate 4:1): 0.54; **^{1}H NMR (300 MHz, CDCl$_3$)**: δ (ppm): 7.43–7.56 (m, 4H), 7.36–7.42 (m, 1H), 4.24–4.30 (m, 1H), 2.68 (dqd, J = 15.3, 11.2, 1.0 Hz, 1H), 2.24–2.53 (m, 3H), 2.06–2.22 (m, 2H), 1.89–2.03 (m, 1H), 1.71–1.87 (m, 1H), 1.52 (s, 1H); **^{13}C NMR (75.5 MHz, CDCl$_3$)**: δ (ppm): 140.8 (C$_q$), 132.0 (C$_q$), 128.9 (CH), 128.0 (CH), 127.2 (CH), 126.5 (q, J = 278.8 Hz, CF$_3$), 79.8 (q, J = 1.3 Hz, CH), 52.8 (q, J = 1.4 Hz, C$_q$), 41.3 (q, J = 23.6 Hz, CH$_2$), 30.6 (CH$_2$), 30.3 (q, J = 1.6 Hz, CH$_2$), 20.0 (CH$_2$); **^{19}F NMR (300 MHz, CDCl$_3$)**: δ (ppm): −59.61 (t, J = 10.9 Hz); **GC-MS**: **t$_R$ (50_40)**: 7.6 min; **EI-MS**: m/z (%): 245 (10), 244 (75), 226 (30), 211 (22), 200 (23), 198 (10), 187 (11), 186 (26), 174 (35), 173 (63), 161 (10), 153 (12), 147 (15), 144 (10), 143 (78), 133 (41), 129 (26), 128 (28), 127 (16), 118 (12), 117 (100), 116 (17), 115 (65), 109 (58), 105 (17), 104 (11), 103 (52), 102 (12), 92 (11), 91 (78), 79 (12), 78

(27), 77 (44), 71 (33), 65 (11), 57 (32), 51 (21), 43 (17), 39 (15); **HR-MS (ESI)**: *m/z* calculated for $[C_{13}H_{15}F_3ONa]^+$ ($[M + Na]^+$): 267.0967, measured: 267.0968; **IR (ATR)**: ν (cm^{-1}): 2966, 2888, 1498, 1447, 1371, 1287, 1259, 1118, 1082, 1062, 1036, 983, 973, 875, 766, 704, 652, 621.

Synthesis of 6-Phenyl-6-(2,2,2-trifluoroethyl)tetrahydro-2H-pyran-2-one (183)

143 → **183**, 81%

Reagents: MMPP (3.3 equiv.), DMF/H₂O (3:1), 45 °C, 48h
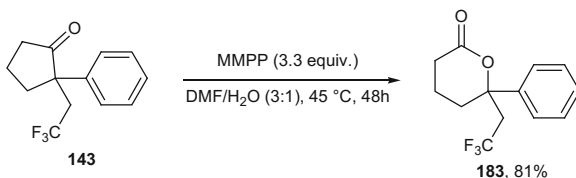
Magnesium monoperoxyphthalate hexahydrate (MMPP, 243 mg, 0.492 mmol, 3.30 equiv.) was added to a solution of 2-phenyl-2-(2,2,2-trifluoroethyl) cyclopentan-1-one (**143**, 36 mg, 0.15 mmol, 1.0 equiv.) in DMF/H$_2$O (375 µL/125 µL) and the resulting reaction mixture was stirred at 45 °C for 48 h. After cooling to rt, the reaction mixture was treated with saturated aqueous Na$_2$S$_2$O$_3$ solution (2 mL) followed by saturated aqueous NaHCO$_3$ (2 mL). The organic layer was extracted with ethyl acetate (3 × 10 mL), washed with brine, dried over MgSO$_4$ and concentrated under reduced pressure. The crude reaction mixture was purified by flash column chromatography through silica gel (pentane: ethyl acetate 9:1 to 4:1) to afford pure product (**183,** 31 mg, 0.12 mmol, 81 %) as a white solid.

6-Phenyl-6-(2,2,2-trifluoroethyl)tetrahydro-2H-pyran-2-one (183)

7
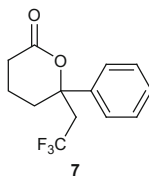
R$_f$ (pentane:ethyl acetate 4:1): 0.15; **^{1}H NMR (300 MHz, CDCl$_3$)**: δ (ppm): 7.30–7.44 (m, 5H), 2.64–2.87 (m, 2H), 2.32–2.57 (m, 3H), 2.22 (td, *J* = 13.8, 13.4, 4.3 Hz, 1H), 1.74–1.85 (m, 1H), 1.47–1.63 (m, 1H); **^{13}C NMR (75.5 MHz, CDCl$_3$)**: δ (ppm): 170.3 (C$_q$), 141.4 (C$_q$), 129.1 (CH), 128.4 (CH), 125.1 (CH), 126.8 (q, *J* = 278.7 Hz, CF$_3$), 83.6 (q, *J* = 2.0 Hz, C$_q$), 46.9 (q, *J* = 27.4 Hz, CH$_2$), 31.2 (q, *J* = 1.5 Hz, CH$_2$), 29.0 (CH$_2$), 16.1 (CH$_2$); **^{19}F NMR (300 MHz, CDCl$_3$)**: δ (ppm): −59.80 (t, *J* = 10.5 Hz); **GC-MS: t$_R$ (50_40)**: 8.1 min; **EI-MS**: *m/z* (%): 186 (33), 176 (13), 175 (100), 147 (47), 117 (12), 115 (17), 111 (21), 105 (90), 103 (26), 91 (16), 78 (13), 77 (52), 70 (44), 55 (24), 51 (23), 42 (65), 41 (10), 39 (14); **HR-MS (ESI)**: *m/z* calculated for $[C_{13}H_{13}F_3O_2Na]^+$ ($[M + Na]^+$): 281.0760, measured: 281.0768; **IR (ATR)**: ν (cm^{-1}): 2945, 1733, 1496, 1448, 1383, 1354, 1321, 1122, 1083, 1047, 1000, 971, 937, 916, 862, 833, 766, 736, 703, 683, 658, 610.

6.4.4 Mechanistic Investigations

6.4.4.1 Intermediate Trapping Experiments

Radical Trapping Experiment
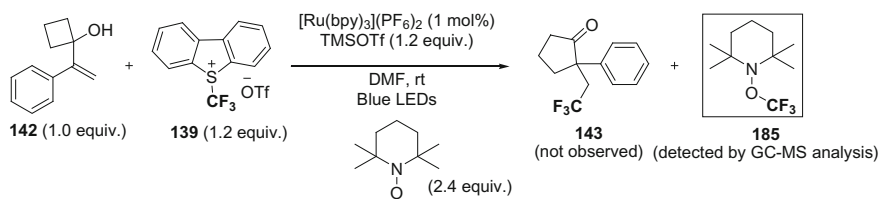
142 (1.0 equiv.)   **139** (1.2 equiv.)

143 (not observed)   **185** (detected by GC-MS analysis)

In a flame dried Schlenk tube equipped with a magnetic stirring bar, 1-(1-phenylvinyl)cyclobutan-1-ol (**142**, 17.4 mg, 0.10 mmol, 1.00 equiv.) followed by trimethylsilyl trifluoromethanesulfonate (22 µL, 0.12 mmol, 1.2 equiv.) was dissolved in anhydrous DMF (1 mL). The reaction mixture was stirred for 2 h. [Ru(bpy)$_3$](PF$_6$)$_2$ (0.90 mg, 0.001 mmol, 0.010 equiv.), 5-(trifluoromethyl)dibenzothiophenium trifluoromethanesulfonate (**139**, 49 mg, 0.12 mmol, 1.2 equiv.) and 2,2,6,6-tetramethyl-1-piperidinyloxyl (TEMPO, 38 mg, 0.24 mmol, 2.4 equiv.) were then added to the reaction tube and the mixture was allowed to stir for 10 h under irradiation of visible light from 5 W blue LEDs (λ_{max} = 465 nm, situated $\sim$5 cm away from the reaction vessel in a custom-made "light box", see Fig. 6.2). The product 2-phenyl-2-(2,2,2-trifluoroethyl)cyclopentan-1-one (**143**) was not observed by GC-MS analysis (applied method has been mentioned in general information), but an adduct **185** between radical scavenger TEMPO radical and trifluoromethyl radical was observed (see Fig. 6.6).

Carbocation Trapping Experiment
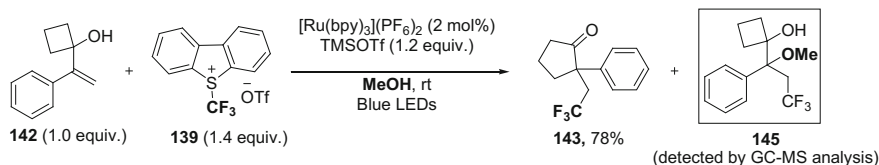
142 (1.0 equiv.)   **139** (1.4 equiv.)

143, 78%   **145** (detected by GC-MS analysis)

In a heat gun dried Schlenk tube equipped with a magnetic stirring bar, 1-(1-phenylvinyl)cyclobutan-1-ol (**142**, 17.4 mg, 0.10 mmol, 1.00 equiv.) followed by trimethylsilyl trifluoromethanesulfonate (22 µL, 0.12 mmol, 1.2 equiv.) was dissolved in anhydrous MeOH (1 mL). The reaction mixture was stirred for 2 h.
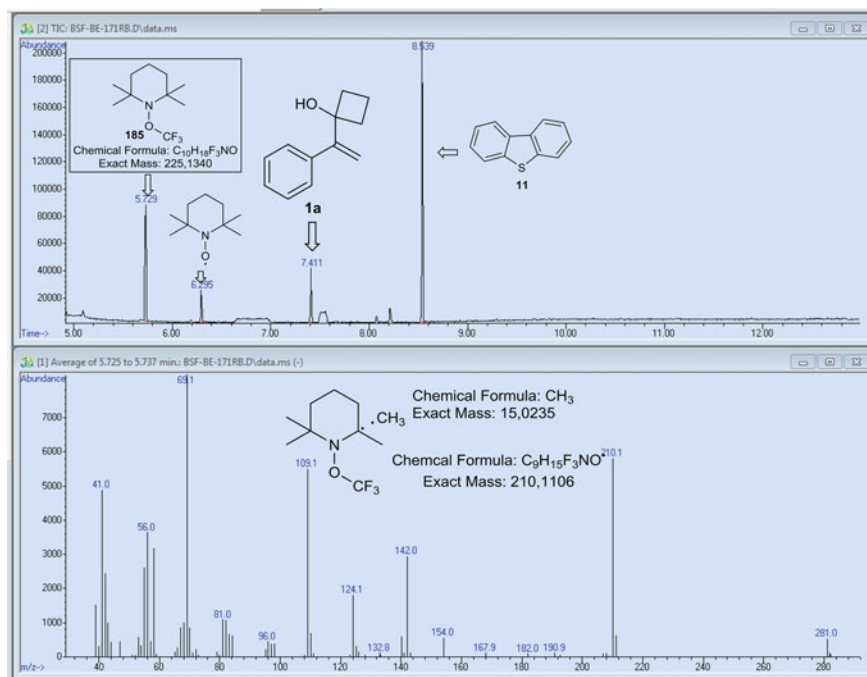
Fig. 6.6 Radical inhibition experiment in presence of radical scavenger TEMPO: an adduct (**185**, t_R = 5.73 min) between radical scavenger TEMPO radical and trifluoromethyl radical was detected in GC-MS analysis (*above*) and fragmentation pattern of the adduct (**185**, t_R = 5.73 min) in mass spectrum was shown (*below*). Sahoo et al. [56]. Copyright Wiley-VCH Verlag GmbH & Co. KGaA. Reproduced with permission

$[Ru(bpy)_3](PF_6)_2$ (1.8 mg, 0.002 mmol, 0.020 equiv.) and 5-(trifluoromethyl) dibenzothiophenium trifluoromethane-sulfonate (**139**, 57 mg, 0.14 mmol, 1.4 equiv.) were then added to the reaction tube. The mixture was allowed to stir for 6 h under irradiation of visible light from 5 W blue LEDs (λ_{max} = 465 nm, situated ∼ 5 cm away from the reaction vessel in a custom-made "light box", see Fig. 6.2). The product 2-phenyl-2-(2,2,2-trifluoroethyl)cyclopentan-1-one (3aa) was obtained in 78 % GC yield as major product along with the formation of methanol trapped adduct **145** (detected by GC-MS analysis, applied method has been mentioned in general information) (see Fig. 6.7).

6.4.4.2 Quantum Yield Measurement

Following a modified procedure reported by Melchiorre et al. [41], an aq. ferrioxalate actinometer solution was prepared and stored in dark. The actinometer solution measures the photodecomposition of ferric oxalate anions to ferrous
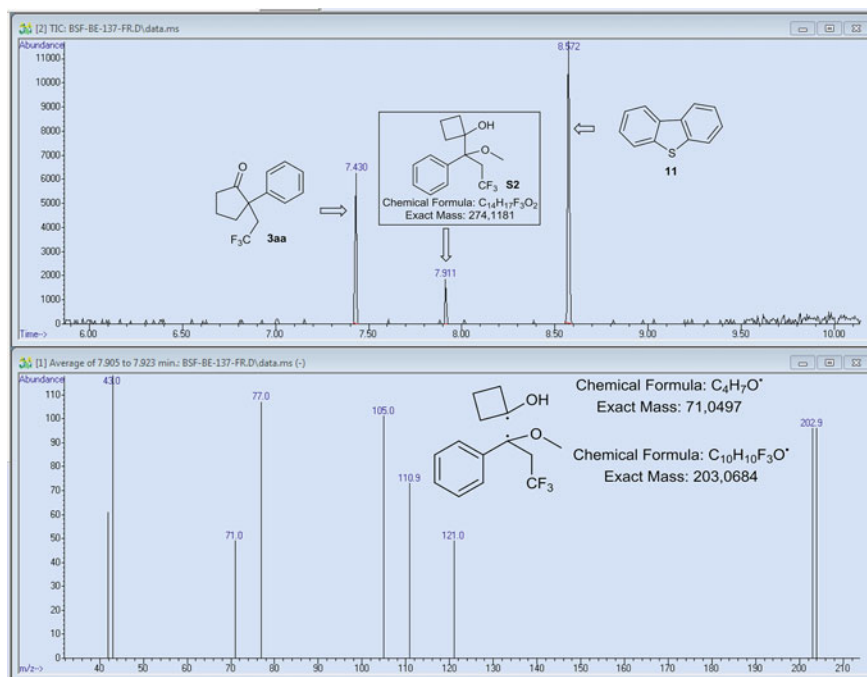
Fig. 6.7 Carbocation Trapping experiment: an adduct (**145**, t_R = 7.91 min) between methanol and intermediate C was detected in GC-MS analysis (*above*) and fragmentation pattern of the adduct (**145**, t_R = 7.91 min) in mass spectrum was shown (*below*). Sahoo et al. [56]. Copyright Wiley-VCH Verlag GmbH & Co. KGaA. Reproduced with permission

oxalate anions, which are reacted with 1,10-phenanthroline to form $Fe(Phen)_3^{2+}$ and estimated by monitoring UV/Vis absorbance at wavelength 510 nm. The numbers of $Fe(Phen)_3^{2+}$ complex formed are related to the numbers of photons absorbed by the actinometer solution.

Preparation of the solutions used for the studies:

1. Potassium ferrioxalate solution: Potassium ferrioxalte trihydrate (295 mg) and 95–98 % H_2SO_4 (140 μL) were added to a 50 mL volumetric flask and filled to the mark with distilled water.
2. Buffer solution: Sodium acetate (4.94 g) and 95–98 % H_2SO_4 (1.0 mL) were added to a 100 mL volumetric flask and filled to the mark with distilled water.
3. The reaction solution: 1-(1-phenylvinyl)cyclobutanol (**142**, 87 mg, 0.50 mmol, 1.0 equiv.), Umemoto's reagent (**139**, 241 mg, 0.60 mmol, 1.2 equiv.) and [Ru (bpy)₃](PF₆)₂ (4.3 mg, 0.005 mmol, 0.01 equiv.) were dissolved in 2 mL of DMF in a 5 mL volumetric flask followed by addition of TMSOTf (108 μL, 0.60 mmol, 1.2 equiv.). Finally the flask was filled to the mark with DMF.

The actinometry measurements:

(a) 1 mL of the actinometer solution was taken in a quartz cuvette (l = 1 cm). 1 mL of the reaction solution was also taken in a quartz cuvette (l = 1 cm). Both the cuvettes of actinometer solution and reaction solution were placed next to each other at a distance of 5 cm away from a 5 W blue LED (λ_{max} = 465 nm) and irradiated for 6 min. The same process was repeated for different time intervals 7.5 min, 9 min and 10.5 min.

(b) After irradiation, the actinometer solution was transferred to a 10 mL volumetric flask containing 1.0 mg of 1,10-phenanthroline in 2 ml of buffer solution. The flask was filled to the mark with distilled water. In a similar manner, a blank solution (10 mL) was also prepared using the actinometer solution stored in dark.

(c) Absorbance of the actinometer solution after complexation with 1,10-phenanthroline at λ = 510 nm was measured by UV/Vis spectrophotometer (Fig. 6.8).

(d) According to the Beer's law, the number of moles of Fe^{2+} formed (x) for each sample was determined.

$$Fe^{2+} = \frac{v_1 v_3 \Delta A(510 \text{ nm})}{10^3 v_2 l \varepsilon(510 \text{ nm})}$$

v_1	Irradiated volume (1 mL).
v_2	The aliquot of the irradiated solution taken for the estimation of Fe^+ ions (1 mL).
v_3	Final volume of the solution after complexation with 1,10-phenanthroline (10 mL).
$\varepsilon(510 \text{ nm})$	Molar extinction coefficient of $Fe(Phen)_3^{2+}$ complex (11,100 L mol^{-1} cm^{-1}).

Fig. 6.8 Absorption spectra of actinometer solutions and blank solution
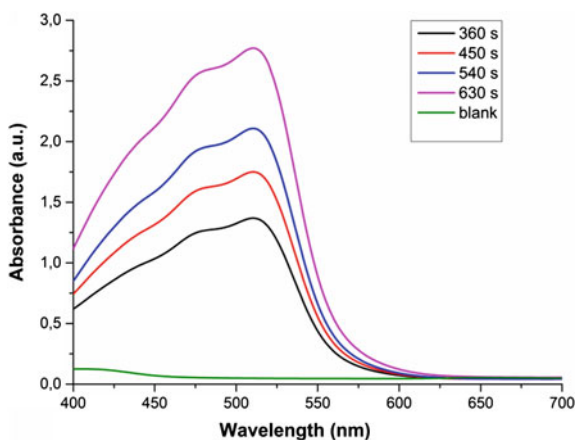
l   Optical path-length of the cuvette (1 cm).

ΔA(510 nm)   Difference in absorbance between the irradiated solution and the solution stored in dark (blank).

(e) The number of moles of Fe^{2+} formed (x) was plotted as a function of time (t) (Fig. 6.9). The slope (dx/dt) of the line is equal to the number of moles of Fe^{2+} formed per unit time.

(f) This slope (dx/dt) was correlated to the number of moles of incident photons per unit time (F = photon flux) by using following equation:

$$\Phi(\lambda) = \frac{\frac{dx}{dt}}{F(1 - 10^{-A(\lambda)})}$$

$\Phi(\lambda)$ The quantum yield for Fe^{2+} formation, which is 0.9 at 450 nm [41].

$A(\lambda)$ Absorbance of the ferrioxalate actinometer solution at a wavelength of 450 nm, which was measured placing 1 mL of the solution in a cuvette of pathlength 1 cm by UV/Vis spectrophotometer. We obtained an absorbance value of 0.289.

The determined incident photon per unit time (F) is 9.145×10^{-9} einstein sec^{-1}.

(g) The number of moles of the product **143** formed was determined by GC (FID) analysis using mesitylene as internal standard reference. The measured absorbance of the reaction solution at 450 nm by UV/Vis spectrophotometer is greater than 3. Thus the number of moles of photons absorbed by reaction sample per unit time $\{F \times (1 - 10^{-A(\lambda)})\}$ is roughly equal to the number of moles of incident photon per unit time (F). The number of moles of product **143** formed was plotted against the number of moles of photon absorbed by the reaction (Table 6.1 and Fig. 6.10). The slope of the line is equal to the quantum yield of the reaction. The calculated apparent **quantum yield** (Φ) of the reaction is **3.8**.

Fig. 6.9 Formation of Fe^{2+} upon photodecomposition of ferrioxalate in different time intervals. Sahoo et al. [56]. Copyright Wiley-VCH Verlag GmbH & Co. KGaA. Reproduced with permission
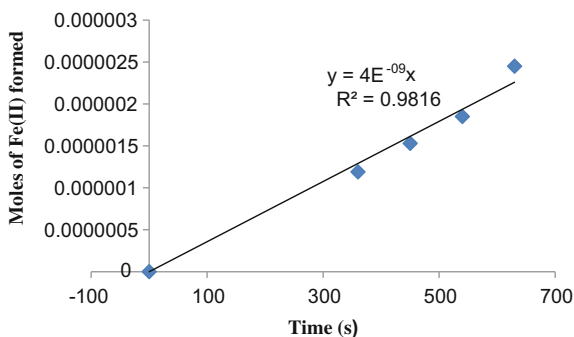
Table 6.1 The formation of the product **143** in different time intervals upon absorbing photons

Time interval (s)	The amount of **143** formed (mol)	The photon absorbed (mol)
0	0	0
360	1.18×10^{-5}	3.292×10^{-6}
450	1.56×10^{-5}	4.115×10^{-6}
540	1.92×10^{-5}	4.938×10^{-6}
630	2.26×10^{-5}	5.761×10^{-6}

Sahoo et al. [56]. Copyright Wiley-VCH Verlag GmbH & Co. KGaA. Reproduced with permission

Fig. 6.10 The plot of moles of product **143** formed against moles of photon absorbed. Sahoo et al. [56]. Copyright Wiley-VCH Verlag GmbH & Co. KGaA. Reproduced with permission

$y = 3.8439x$
$R^2 = 0.9966$
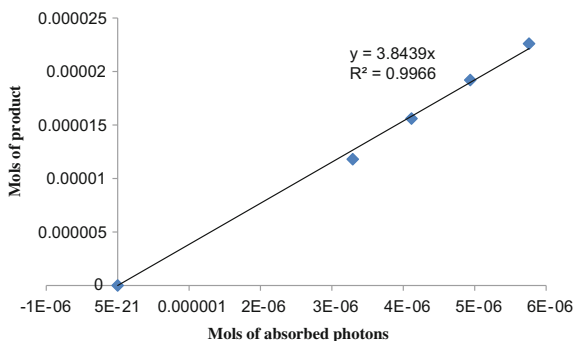
6.5   Transition Metal Free Visible Light Mediated Synthesis of Polycyclic Indolizines

6.5.1   Synthesis of Substrates

6.5.1.1   Synthesis of Bromopyridine Substrates

Synthesis of 2-bromo-5-phenylpyridine

Pd(PPh$_3$)$_4$ (1 mol%), K$_2$CO$_3$ (29 equiv.)
toluene:H$_2$O (1:1), 120 °C, 4 d

1 equiv.   1 equiv.   88%
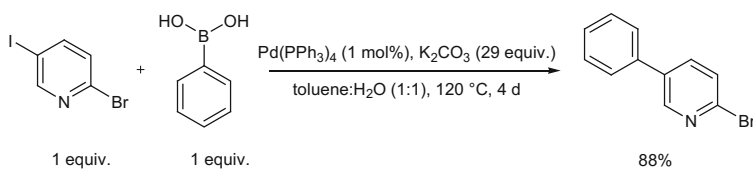
Following a modified procedure from von Zelewsky et al. [42], a mixture of 2-bromo-5-iodopyridine (5.11 g, 18 mmol), phenylboronic acid (2.19 g, 18 mmol), Pd(PPh$_3$)$_4$ (20.8 mg, 0.02 mmol) in toluene (72 mL) and K$_2$CO$_3$ (72 g, 522 mmol) in water (72 mL) in a round bottomed flask equipped with a condenser was allowed

to heat at 120 °C for 4 d. After cooling to rt, the layers were separated and aqueous layer was extracted with dichloromethane (3 × 15 mL). The combined organic layers were washed with water until the pH was brought to 7, dried with MgSO$_4$ and concentrated under reduced pressure. The crude mixture was purified by flash column chromatography through silica using pentane:ethyl acetate:triethylamine (6:5:0.1) to afford (3.72 g, 15.8 mmol, 88 %) as a white solid.

R$_f$ (pentane:ethyl acetate:NEt$_3$ 6:5:0.1): 0.69; **^{1}H NMR (400 MHz, CDCl$_3$)**: δ (ppm): 8.59 (d, J = 2.3, 1H), 7.73 (dd, J = 8.3, 2.6 Hz, 1H), 7.53–7.60 (m, 3H), 7.40–7.51 (m, 3H); **^{13}C NMR (101 MHz, CDCl$_3$)**: δ (ppm): 148.6, 141.0, 137.1, 136.6, 136.2, 129.4, 128.7, 128.1, 127.1; **GC-MS**: t$_R$ (50_40): 8.6 min; **EI-MS**: m/z (%): 236 (12), 235 (93), 234 (12), 233 (93), 155 (14), 154 (100), 153 (21), 128 (28), 127 (68), 126 (23) 77 (19), 63 (15), 51 (12); **HR-MS (ESI)**: m/z calculated for [C$_{11}$H$_8$BrNNa]$^+$ ([M + Na]$^+$): 255.9732, measured: 255.9719; **IR (ATR)**: ν (cm^{-1}): 3090, 3057, 3020, 1575, 1546, 1439, 1390, 1364, 1353, 1318, 1278, 1228, 1139, 1082, 1041, 1027, 994, 946, 914, 831, 756, 653, 635, 615.

Synthesis of *tert*-butyl 2-(pyridin-2-yl)acetate and benzyl 2-(pyridin-2-yl) acetate
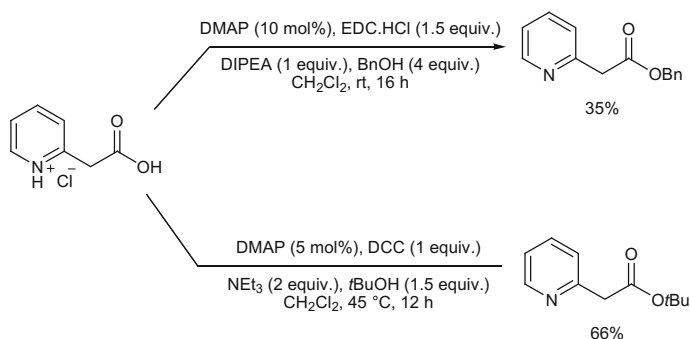
***tert*-Butyl 2-(pyridin-2-yl)acetate**
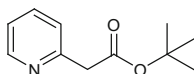
Following a modified procedure from Fuchs et al. [43], triethyl amine (2.24 mL, 16.1 mmol) and 1,3-dicyclohexylcarbodiimide (DCC) (1.66 g, 8.03 mmol), 4-(dimethylamino)pyridine (DMAP) (49 mg, 0.40 mmol) were added to a suspension of 2-pyridylacetic acid hydrochloride (1.39 g, 8.03 mmol) and *tert* butanol (1.15 mL, 12.1 mmol) in dichloromethane (40 mL) at rt. The reaction mixture was stirred overnight at 45 °C. The reaction mixture was filtered to remove 1,3-dicyclohexylurea. The filtrate was washed with water (3 × 10 mL), dried with MgSO$_4$ and concentrated under reduced pressure. The crude product was purified

by flash column chromatography through silica gel (eluent = pentane:ethyl acetate, 5:1 to 2:1) to afford (1.02 g, 5.28 mmol, 66 %) as a light yellow oil.

R_f (pentane:ethyl acetate 3:2): 0.48; **^{1}H NMR (300 MHz, CDCl$_3$)**: δ (ppm): 8.54 (ddd, J = 4.9, 1.8, 0.9 Hz, 1H), 7.64 (td, J = 7.6, 1.8 Hz, 1H), 7.22–7.33 (m, 1H), 7.16 (dt, J = 7.5, 4.9, 1.2 Hz, 1H), 3.75 (s, 2H), 1.44 (s, 9H); **^{13}C NMR (75.5 MHz, CDCl$_3$)**: δ (ppm): 170.1, 155.1, 149.4, 136.6, 124.0, 122.0, 81.3, 45.2, 28.2; **GC-MS**: t_R (50_40): 7.2 min; **EI-MS**: m/z (%): 120 (31), 93 (26), 92 (38), 65 (19), 57 (100), 41 (31), 39 (17); **HR-MS (ESI)**: m/z calculated for $[C_{11}H_{15}NO_2Na]^+$ ($[M + Na]^+$): 216.0995, measured: 216.1014; **IR (ATR)**: ν (cm^{-1}): 2979, 2933, 1728, 1592, 1572, 1475, 1436, 1393, 1368, 1339, 1254, 1141, 1092, 1050, 996, 952, 873, 834, 752, 666, 621.

Benzyl 2-(pyridin-2-yl)acetate
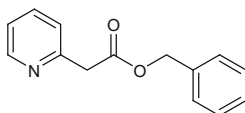
N,N-diisopropyl ethyl amine (DIPEA) (0.87 mL, 5.01 mmol), *N*-(3-dimethylaminopropyl)-*N'*-ethylcarbodiimide hydrochloride (EDC.HCl) (1.42 g, 7.52 mmol) and 4-(dimethylamino)pyridine (DMAP) (61 mg, 0.5 mmol) were added to a suspension of 2-pyridylacetic acid hydrochloride (0.87 g, 5.01 mmol) and benzyl alcohol (2.07 mL, 20.0 mmol) in dichloromethane (16.3 mL). The reaction mixture was allowed to stir at rt for 16 h. The reaction mixture was diluted with ethyl acetate (10 mL) and extracted with 2 M HCl (3 × 10 mL). The combined aqueous layers were neutralized with solid NaHCO$_3$ (6.3 g) and extracted with ethyl acetate (3 × 15 mL). The organic layers were dried over MgSO$_4$ and concentrated under reduced pressure. The crude mixture was purified by flash column chromatography through silica gel (eluent = pentane:ethyl acetate, 2:1) to afford (393 mg, 1.73 mmol, 35 %) as a light yellow oil.

R_f (pentane:ethyl acetate 3:2): 0.36; **^{1}H NMR (300 MHz, CDCl$_3$)**: δ (ppm): 8.57 (d, J = 4.4 Hz, 1H), 7.67 (td, J = 7.7, 1.8 Hz, 1H), 7.27–7.39 (m, 6H), 7.21 (ddd, J = 7.5, 4.9, 1.1 Hz, 1H), 5.17 (s, 2H), 3.92 (s, 2H); **^{13}C NMR (75.5 MHz, CDCl$_3$)**: δ (ppm): 170.6, 154.3, 149.4, 137.0, 135.8, 128.7, 128.4, 128.3, 124.2, 122.4, 66.9, 43.9; **GC-MS**: t_R (50_40): 8.8 min; **EI-MS**: m/z (%): 93 (100), 92 (21), 91 (68), 65 (23); **HR-MS (ESI)**: m/z calculated for $[C_{14}H_{13}NO_2Na]^+$ ($[M + Na]^+$): 250.0849, measured: 250.0837; **IR (ATR)**: ν (cm^{-1}): 3065, 3035, 2955, 1734, 1592, 1572, 1498, 1475, 1456, 1436, 1378, 1337, 1258, 1237, 1213, 1148, 1091, 1050, 996, 911, 831, 748, 699, 645, 619, 598.

Synthesis of methyl esters of pyridyl-2-yl acetic acid
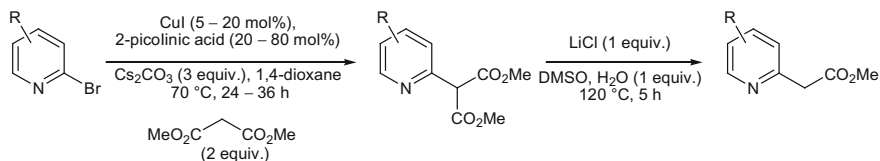
General Procedure 10:

Following a modified procedure from Kwong et al. [44], a flame dried Schlenk flask equipped with a magnetic stir bar was charged with CuI (0.050–0.20 equiv.), 2-picolinic acid (0.20–0.80 equiv.), Cs_2CO_3 (3.0 equiv.) and, if solid, the pyridyl iodide (1.0 equiv.) under argon. Dry 1,4-dioxane followed dimethyl malonate (2.0 equiv.) and, if liquid, the pyridyl iodide (1.0 equiv.) was added to the reaction vessel. The Schlenk flask was sealed tightly and placed in a preheated oil bath at 70 °C for 36 h. After cooling to rt, the reaction mixture was quenched with satd. aq. NH_4Cl solution and extracted with ethyl acetate. The combined organic layers were dried over $MgSO_4$, filtered and concentrated under reduced pressure. The crude reaction mixture was purified by flash column chromatography through silica gel (eluent = pentane:ethyl   acetate)   to   afford   the   pure   dimethyl   2-(pyridin-2-yl)malonates.

General Procedure 11:

Dimethyl 2-(pyridin-2-yl)malonate (1.0 equiv.) in DMSO was treated with lithium chloride (2.0–2.5 equiv.) and water (1.0 equiv.). The resulting mixture was heated at 120 °C for 5 h. After cooling to rt, the reaction mixture was quenched with brine and extracted with ethyl acetate. The organic layers were dried over $MgSO_4$, filtered and concentrated under reduced pressure. The crude reaction mixture was purified by flash column chromatography through silica gel (eluent = pentane:ethyl acetate) to afford the pure methyl 2-(pyridin-2-yl)acetates.

Dimethyl 2-(5-fluoropyridin-2-yl)malonate
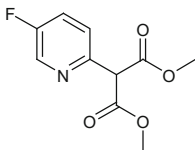
Prepared following **GP10** on a 5.7 mmol scale from 2-bromo-5-fluoropyridine (1.0 g, 5.7 mmol, 1.0 equiv.), CuI (163 mg, 0.856 mmol, 15 mol%), 2-picolinic acid (420 mg, 3.41 mmol, 0.600 equiv.), Cs_2CO_3 (5.51 g, 16.9 mmol, 3.00 equiv.) and dimethyl malonate (1.30 mL, 11.4 mmol, 2.00 equiv.) in 1,4-dioxane

(11.5 mL). Purification via flash column chromatography through silica gel (eluent = pentane:ethyl acetate, 9:1) afforded methyl 2-(5-fluoropyridin-2-yl)malonate (253 mg, 1.11 mmol, 20 %) as a greenish yellow oil.

R_f **(pentane:ethyl acetate 4:1)**: 0.32; **^{1}H NMR (300 MHz, CDCl$_3$)**: δ (ppm): 8.42 (dt, J = 2.9, 0.6 Hz, 1H), 7.53 (ddd, J = 8.7, 4.4, 0.7 Hz, 1H), 7.44 (ddd, J = 8.7, 7.9, 2.9 Hz, 1H), 4.98 (s, 1H), 3.79 (s, 6H); **^{13}C NMR (75 MHz, CDCl$_3$)**: δ (ppm): 167.9, 159.3 (d, J = 257.1 Hz), 148.8 (d, J = 4.1 Hz), 137.8 (d, J = 24.1 Hz), 125.1 (d, J = 4.6 Hz), 123.9 (d, J = 18.6 Hz), 59.5 (d, J = 1.3 Hz), 53.3; **^{19}F NMR (282 MHz, CDCl$_3$)**: −127.46; **GC-MS**: t_R (50_40): 7.5 min; **EI-MS**: m/z (%): 281 (18), 227 (27), 196 (25), 195 (10), 169 (12), 168 (45), 152 (38), 151 (11), 147 (12), 140 (100), 138 (10), 137 (47), 125 (58), 124 (27), 112 (18), 111 (25), 110 (27), 109 (36), 97 (12), 96 (25), 82 (24), 81 (15), 73 (22), 59 (34); **HR-MS (ESI)**: m/z calculated for $[C_{10}H_{10}FNO_4Na]^+$ ($[M + Na]^+$): 250.0486, measured: 250.0492; **IR (ATR)**: ν (cm^{-1}): 2958, 2361, 1734, 1588, 1482, 1436, 1391, 1318, 1255, 1225, 1203, 1148, 1021, 936, 917, 840, 775, 731, 717, 666, 625, 596.

Methyl 2-(5-fluoropyridin-2-yl)acetate

Prepared following **GP11** on a 2.36 mmol scale from dimethyl 2-(5-fluoropyridin-2-yl)malonate (470 mg, 2.36 mmol, 1.00 equiv.), lithium chloride (250 mg, 5.90 mmol, 2.50 equiv.) and water (32 μL, 2.4 mmol, 1.0 equiv.) in DMSO (4.2 mL). Purification via flash column chromatography through silica gel (eluent = pentane:ethyl acetate, 3:2) afforded methyl 2-(5-fluoropyridin-2-yl)acetate (162 mg, 0.958 mmol, 41 %) as a pale yellow oil.

R_f **(pentane:ethyl acetate 3:2)**: 0.48; **^{1}H NMR (300 MHz, CDCl$_3$)**: δ (ppm): 8.41 (d, J = 2.8 Hz, 1H), 7.39 (td, J = 8.3, 2.8 Hz, 1H), 7.31 (d, J = 8.6, 4.4 Hz, 1H), 3.85 (s, 2H), 3.72 (s, 3H), 3.33 (s, 3H); **^{13}C NMR (75 MHz, CDCl$_3$)**: δ (ppm): 171.0, 158.8 (d, J = 255.5 Hz), 150.3, 137.7 (d, J = 23.9 Hz), 125.0 (d, J = 4.3 Hz), 123.8 (d, J = 18.6 Hz), 52.4, 42.9; **^{19}F NMR (282 MHz, CDCl$_3$)**: −129.16; **GC-MS**: t_R (50_40): 6.6 min; **EI-MS**: m/z (%): 169 (27), 154 (20), 138 (14), 137 (13), 124 (11), 111 (43), 110 (100), 84 (10), 83 (34), 59 (19), 57 (16); **HR-MS (ESI)**: m/z calculated for $[C_8H_8FNO_2Na]^+$ ($[M + Na]^+$): 192.0431, measured: 192.0432; **IR (ATR)**: ν (cm^{-1}): 2956, 1736, 1587, 1485, 1437, 1391, 1342, 1254, 1226, 1195, 1160, 1018, 914, 834, 667, 617, 610.

Methyl 2-(5-(trifluoromethyl)pyridin-2-yl)acetate
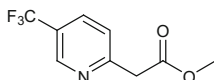
Prepared following **GP10** on a 14.0 mmol scale from 2-bromo-5-(trifluoromethyl) pyridine (3.16 g, 14.0 mmol, 1.00 equiv.), CuI (400 mg, 2.10 mmol, 15 mol%),

2-picolinic acid (1.03 g, 8.40 mmol, 0.600 equiv.), Cs_2CO_3 (13.7 g, 42.1 mmol, 3.00 equiv.) and dimethyl malonate (3.2 mL, 28 mmol, 2.0 equiv.) in 1,4-dioxane (14 mL). Purification via flash column chromatography through silica gel (eluent = pentane:ethyl acetate, 9:1) afforded an inseparable yellow mixture (3.8 g) of dimethyl 2-(5-(trifluoromethyl)pyridin-2-yl)malonate ($\sim$2.2 g, $\sim$7.9 mmol, $\sim$57 % (NMR)) and dimethyl malonate ($\sim$1.6 g, 12 mmol) in the ratio of 1:1.5. This mixture was used directly in the next step.

Prepared following **GP11** on a $\sim$7.05 mmol scale from dimethyl 2-(5-(trifluoromethyl)pyridin-2-yl)malonate ($\sim$1.95 g, $\sim$7.05 mmol, 1.00 equiv.), lithium chloride (747 mg, 17.6 mmol, 2.50 equiv.) and water (96 µL, 7.1 mmol, 1.0 equiv.) in DMSO (12.6 mL). Purification via flash column chromatography through silica gel (eluent = pentane:ethyl acetate, 3:1) afforded methyl 2-(5-(trifluoromethyl)pyridin-2-yl)acetate (473 mg, 2.16 mmol, 15 % over two steps) as a yellow oil.

R_f **(pentane:ethyl acetate 3:2)**: 0.55; **^{1}H NMR (400 MHz, CDCl$_3$)**: δ (ppm): 8.83 (dt, J = 2.0, 1.0 Hz, 1H), 7.88 –7.93 (m, 1H), 7.46 (d, J = 8.2 Hz, 1H), 3.74 (s, 2H), 3.74 (s, 3H); **^{13}C NMR (101 MHz, CDCl$_3$)**: δ (ppm): 170.2, 158.1, 146.3 (q, J = 3.9 Hz), 133.9 (q, J = 3.4 Hz), 125.3 (q, J = 33.2 Hz), 123.8, 123.5 (q, J = 272.5 Hz), 52.4, 43.5; **^{19}F NMR (300 MHz, CDCl$_3$)**: −62.44; **GC-MS**: t_R (50_40): 6.5 min; **EI-MS**: m/z (%): 219 (21), 204 (26), 200 (10), 188 (24), 187 (12), 174 (11), 161 (53), 160 (100), 140 (20), 133 (15), 113 (15), 63 (11), 59 (35); **HR-MS (ESI)**: m/z calculated for $[C_9H_8F_3NO_2Na]^+$ ($[M + Na]^+$): 242.0399, measured: 242.0407; **IR (ATR)**: ν (cm^{-1}): 2958, 2861, 2341, 1738, 1610, 1577, 1438, 1395, 1327, 1260, 1246, 1162, 1126, 1080, 1048, 1018, 943, 838, 751, 695, 661, 629.

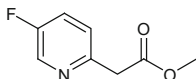### Dimethyl 2-(5-methylpyridin-2-yl)malonate
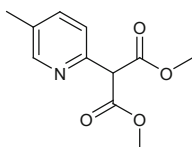
Prepared following **GP10** on a 5.00 mmol scale from 2-bromo-5-methylpyridine (860 mg, 5.00 mmol, 1.00 equiv.), CuI (48 mg, 0.25 mmol, 5 mol%), 2-picolinic acid (123 mg, 1.00 mmol, 20 mol%), Cs_2CO_3 (4.89 g, 15.0 mmol, 3.00 equiv.) and dimethyl malonate (1.14 mL, 10.0 bmmol, 2.00 equiv.) in 1,4-dioxane (10 mL). Purification via flash column chromatography through silica gel (eluent = pentane:ethyl acetate, 2:1 to 1:1) afforded dimethyl 2-(5-methylpyridin-2-yl) malonate (225 mg, 1.23 mmol, 25 %) as a light yellow oil.

R_f **(pentane:ethyl acetate 4:1)**: 0.13; **^{1}H NMR (400 MHz, CDCl$_3$)**: δ (ppm): 8.39 (dt, J = 2.4, 0.9 Hz, 1H), 7.52 (ddd, J = 8.1, 2.3, 0.9 Hz, 1H), 7.37 (dd, J = 8.0, 0.9 Hz, 1H), 4.94 (s, 1H), 3.77 (s, 6H), 2.33 (d, J = 0.8 Hz, 3H); **^{13}C NMR (101 MHz, CDCl$_3$)**: δ (ppm): 168.2, 150.0, 149.9, 137.6, 133.0, 123.3, 5b9.9, 53.1, 18.3; **GC-MS**: t_R (50_40): 8.1 min; **EI-MS**: m/z (%): 223 (38), 192

(27),191 (25), 165 (37), 164 (25), 148 (30), 137 (10), 136 (100), 134 (12), 133 (57), 132 (10), 122 (34), 121 (33), 120 (22), 108 (14), 107 (30), 106 (21), 105 (10), 104 (24), 93 (13), 92 (18), 79 (12), 78 (15), 77 (22), 65 (14), 59 (15), 51 (12); **HR-MS (ESI)**: *m/z* calculated for $[C_{11}H_{13}NO_4Na]^+$ $([M + Na]^+)$: 246.0737, measured: 246.0735; **IR (ATR)**: ν (cm^{-1}): 3006, 2956, 1735, 1574, 1486, 1435, 1383, 1319, 1300, 1239, 1220, 1203, 1148, 1030, 937, 911, 835, 773, 720, 650, 621, 601.

Methyl 2-(5-methylpyridin-2-yl)acetate

Prepared following **GP11** on a 2.464 mmol scale from dimethyl 2-(5-methylpyridin-2-yl)malonate (550 mg, 2.464 mmol, 1.00 equiv.), lithium chloride (261 mg, 6.16 mmol, 2.50 equiv.) and water (33 μL, 2.5 mmol, 1.0 equiv.) in DMSO (4.4 mL). Purification via flash column chromatography through silica gel (eluent = pentane:ethyl acetate, 2:1) afforded methyl 2-(5-methylpyridin-2-yl)acetate (126 mg, 0.763 mmol, 31 %) as a light yellow oil.

R_f **(pentane:ethyl acetate 2:1)**: 0.19; **^{1}H NMR (400 MHz, CDCl$_3$)**: δ (ppm): 8.39 (d, *J* = 2.2 Hz, 1H), 7.51 (dd, *J* = 7.9, 1.8 Hz, 1H), 7.22 (d, *J* = 7.9 Hz, 1H), 3.86 (s, 2H), 3.72 (s, 3H), 3.33 (s, 3H); **^{13}C NMR (101 MHz, CDCl$_3$)**: δ (ppm): 171.2, 151.1, 149.3, 138.0, 132.1, 123.8, 52.4, 43.0, 18.3; **GC-MS**: t_R (50_40): 7.1 min; **EI-MS**: *m/z* (%): 165 (39), 134 (12), 133 (17), 120 (10), 107 (83), 106 (100), 79 (28), 78 (12), 77 (31); **HR-MS (ESI)**: *m/z* calculated for $[C_9H_{11}NO_2Na]^+$ $([M + Na]^+)$: 188.0682, measured: 188.0690; **IR (ATR)**: ν (cm^{-1}): 3005, 2954, 1737, 1602, 1572, 1488, 1436, 1383, 1341, 1260, 1218, 1194, 1157, 1032, 1015, 827, 693, 647, 629.

Dimethyl 2-(5-phenylpyridin-2-yl)malonate
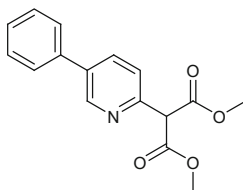
Prepared following **GP10** on a 6.4 mmol scale from 2-bromo-5-phenylpyridine (1.5 g, 6.4 mmol, 1.0b equiv.), CuI (183 mg, 0.961 mmol, 0.15 equiv.), 2-picolinic acid (473 mg, 3.85 mmol, 0.600 equiv.), Cs$_2$CO$_3$ (6.30 g, 19.2 mmol, 3.00 equiv.) and dimethyl malonate (1.47 mL, 12.8 mmol, 2.00 equiv.) in 1,4-dioxane (6.5 mL). Purification via flash column chromatography through silica gel (eluent = pentane:ethyl acetate, 4:1) afforded dimethyl 2-(5-phenylpyridin-2-yl) malonate (1.04 g, 3.65 mmol, 57 %) as a pale yellow oil.

R$_f$ (pentane:ethyl acetate 4:1): 0.19; **^{1}H NMR (400 MHz, CDCl$_3$)**: δ (ppm): 8.79 (dd, J = 2.4, 0.8 Hz, 1H), 7.81 (dd, J = 8.2, 2.4 Hz, 1H), 7.57 (dt, J = 8.0, 1.0 Hz, 3H), 7.44–7.52 (m, 2H), 7.37–7.44 (m, 2H), 5.05 (s, 1H), 3.81 (s, 6H); **^{13}C NMR (101 MHz, CDCl$_3$)**: δ (ppm): 168.0, 151.5, 147.8, 137.3, 136.4, 135.6, 129.3, 128.4, 127.3, 123.8, 59.9, 53.2; **GC-MS**: t$_R$ (50_40): 9.8 min; **EI-MS**: m/z (%): 285 (100), 281 (31), 254 (15), 253 (30), 253 (11), 209 (25), 207 (18), 198 (33), 198 (56), 195 (68), 191 (12), 184 (12), 183 (13), 169 (13), 168 (15), 139 (16), 115 (15); **HR-MS (ESI)**: m/z calculated for [C$_{16}$H$_{15}$NO$_4$Na]$^+$ ([M + Na]$^+$): 308.0893, measured: 308.0892; **IR (AbTR)**: ν (cm^{-1}): 3060, 2955, 1736, 1596, 1581, 1564, 1475, 1436, 1374, 1307, 1267, 1246, 1200, 1150, 1029, 1008, 939, 913, 846, 756, 735, 699, 622, 599.

Methyl 2-(5-phenylpyridin-2-yl)acetate

Prepared following **GP11** on a 5.92 mmol scale from dimethyl 2-(5-phenylpyridin-2-yl)malonate (1.69 g, 5.92 mmol, 1.00 equiv.), lithium chloride (774 mg, 18.3 mmol, 3.00 equiv.) and water (99 μL, 7.3 mmol, 1.2 equiv.) in DMSO (13 mL). Purification via flash column chromatography through silica gel (eluent = pentane:ethyl acetate, 3:2) afforded methyl 2-(5-phenylpyridin-2-yl)acetate (607 mg, 2.67 mmol, 45 %) as a yellowish brown solid.

R$_f$ (pentane:ethyl acetate 3:2): 0.39; **^{1}H NMR (300 MHz, CDCl$_3$)**: δ (ppm): 8.79 (dd, J = 2.4, 0.9 Hz, 1H), 7.86 (dd, J = 8.0, 2b.4 Hz, 1H), 7.54–7.60 (m, 2H), 7.43–7.52 (m, 2H), 7.34–7.43 (m, 2H), 3.91 (s, 2H), 3.75 (s, 3H); **^{13}C NMR (75.5 MHz, CDCl$_3$)**: δ (ppm): 171.2, 153.2, 148.0, 137.7, 135.4, 135.3, 129.2, 128.2, 127.2, 123.9, 52.3, 43.5; **GC-MS**: t$_R$ (50_40): 9.0 min; **EI-MS**: m/z (%): 227 (59), 195 (20), 170 (14), 169 (100), 168 (76), 167 (26), 141 (32), 139 (14), 115 (26); **HR-MS (ESI)**: m/z calculated for [C$_{14}$H$_{13}$NO$_2$Na]$^+$ ([M + Na]$^+$): 250.0838, measured: 250.0850; **IR (ATR)**: ν (cm^{-1}): 3028, 3012, 2956, 2928, 1737, 1596, 1583, 1563, 1481, 1450, 1434, 1404, 1376, 1345, 1260, 1221, 1189, 1147, 1035, 1003, 898, 839, 775, 755, 721, 695, 647, 610, 576.
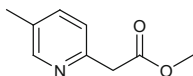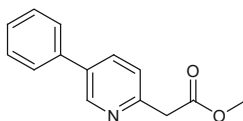
Dimethyl 2-(4-chloropyridin-2-yl)malonate

Prepared following **GP10** on a 5.00 mmol scale from 2-bromo-4-chloropyridine (962 mg, 5.00 mmol, 1.00 equiv.), CuI (48 mg, 0.25 mmol, 5 mol%), 2-picolinic

acid (123 mg, 1.00 mmol,20 mol%), Cs_2CO_3 (4.89 g, 15.0 mmol, 3.00 equiv.) and dimethyl malonate (0.86 mL, 7.5 mmol, 1.5 equiv.) in 1,4-dioxane (10 mL). Purification via flash column chromatography through silica gel (eluent = pentane: ethyl acetate, 17:3 to 3:2) afforded dimethyl 2-(4-chloropyridin-2-yl)malonate (430 mg, 1.77 mmol, 24 %) as a light yellow oil.

R$_f$ (pentane:ethyl acetate 4:1): 0.23; **^{1}H NMR (600 MHz, CDCl$_3$)**: δ (ppm): 8.47 (d, J = 5.4 Hz, 1H), 7.54 (d, J = 1.8 Hz, 1H), 7.29 (dd, J = 5.4, 2.0 Hz, 1H), 4.97 (s, 1H), 3.80 (s, 6H); **^{13}C NMR (150 MHz, CDCl$_3$)**: δ (ppm): 167.4, 154.3, 150.2, 145.2, 124.5, 123.9, 59.9, 53.3; **GC-MS**: t$_R$ (50_40): 8.1 min; **EI-MS**: m/z (%): 244 (11), 243 (31), 214 (19), 213 (12), 212 (60), 211 (19), 187 (13), 186 (13), 185 (39), 184 (32), 180 (11), 170 (19), 168 (50), 158 (31), 156 (100), 155 (24), 154 (23), 153 (67), 143 (25), 142 (30), 141 (58), 140 (33), 129 (10), 128 (31), 127 (35), 126 (29), 125 (28), 114 (14), 113 (15), 112 (31), 99 (11), 93 (10), 91 (11), 90 (45), 89 (11), 78 (18), 77 (12), 76 (15), 73 (11), 65 (15), 64 (13), 63 (60), 62 (27), 61 (10), 59 (92), 51 (21), 50 (13), 39 (13); **HR-MbS (ESI)**: m/z calculated for $[C_{10}H_{10}ClNO_4Na]^+$ ($[M + Na]^+$): 266.0191, measured: 266.0193; **IR (ATR)**: ν (cm^{-1}): 3008, 2956, 2361, 2341, 1736, 1621, 1575, 1558, 1464, 1435, 1393, 1312, 1272, 1234, 1200, 1151, 1103, 1026, 992, 939, 913, 835, 702, 629.
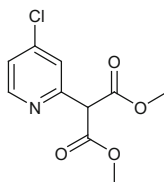
Methyl 2-(4-chloropyridin-2-yl)acetate

Prepared following **GP11** on a 1.71 mmol scale from dimethyl 2-(4-chloropyridin-2-yl)malonate (417 mg, 1.71 mmol, 1.00 equiv.), lithium chloride (145 mg, 3.42 mmol, 2.00 equiv.) and water (23 μL,b 1.7 mmol, 1.0 equiv.) in DMSO (3 mL). Purification via flash column chromatography through silica gel (eluent = pentane:ethyl acetate, 3:1) afforded methyl 2-(4-chloropyridin-2-yl)acetate (122 mg, 0.657 mmol, 38 %) as a yellow oil.

R$_f$ (pentane:ethyl acetate 3:2): 0.39; **^{1}H NMR (400 MHz, CDCl$_3$)**: δ (ppm): 8.45 (d, J = 5.4 Hz, 1H), 7.34 (d, J = 1.9 Hz, 1H), 7.23 (dd, J = 5.4, 1.9 Hz, 1H), 3.85 (s, 2H), 3.73 (s, 3H); **^{13}C NMR (101 MHz, CDCl$_3$)**: δ (ppm): 170.5, 155.8, 150.3, 145.0, 124.5, 122.9, 52.5, 43.4; **GC-MS**: t$_R$ (50_40): 7.2 min; **EI-MS**: m/z (%): 185 (23), 170 (12), 156 (11), 154 (34), 153 (16), 140 (11), 129 (26), 128 (38), 127 (81), 126 (100), 99 (25), 91 (12), 90 (27), 73 (12), 64 (16), 63 (25), 59 (28), 51 (10); **HR-MS (ESI)**: m/z calculated for $[C_{10}H_8ClNO_2Na]^+$ ($[M + Na]^+$): 208.0136, measured: 208.0137; **IR (ATR)**: ν (cm^{-1}): 3055, 3007, 2954, 1736, 1576, 1556, 1468, 1436, 1395, 1337, 1293, 1257, 1239, 1196, 1159, 1103, 1010, 936, 905, 882, 829, 763, 752, 709, 648, 626.

Dimethyl 2-(4-methylpyridin-2-yl)malonate
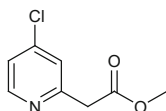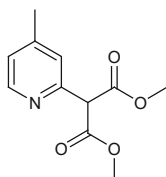

Prepared following **GP10** on a 1.8 mmol scale from 2-bromo-4-methylpyridine (0.20 mL, 1.8 mmol, 1.0 equiv.), CuI (17 mg, 89 µmol, 5 mol%), 2-picolinic acid (44 mg, 0.36 mmol, 0.20 equiv.), Cs_2CO_3 (1.76 g, 5.40 mmol, 3.00 equiv.) and dimethyl malonate (0.41 mL, 3.6 mmol, 2.0 bequiv.) in 1,4-dioxane (7.2 mL). Purification via flash column chromatography through silica gel (eluent = pentane: ethyl acetate, 7:3) afforded dimethyl 2-(4-methylpyridin-2-yl)malonate (191 mg, 0.856 mmol, 48 %) as a pale yellow oil.

R_f **(pentane:ethyl acetate 4:1)**: 0.16; **^{1}H NMR (300 MHz, CDCl$_3$)**: δ (ppm): 8.37 (dd, *J* = 5.1, 0.8 Hz, 1H), 7.22–7.40 (m, 1H), 7.03 (ddd, *J* = 5.1, 1.6, 0.8 Hz, 1H), 4.90 (s, 1H), 3.73 (s, 6H), 2.32 (s, 3H); **^{13}C NMR (75.5 MHz, CDCl$_3$)**: δ (ppm): 167.9, 152.5, 149.1, 148.2, 124.5, 124.2, 60.0, 53.0, 21.1; **GC-MS**: t_R (50_40): 8.0 min; **EI-MS**: *m/z* (%): 223 (39), 192 (45), 191 (29), 165 (62), 164 (18), 148 (43), 137 (10), 136 (100), 134 (18), 133 (76), 122 (42), 121 (37), 120 (24), 108 (18), 107 (40), 106 (23), 105 (10), 104 (24), 93 (15), 92 (26), 79 (13), 78 (18), 77 (21), 65 (18), 59 (18), 52 (10), 51 (11), 39 (11); **HR-MS (ESI)**: *m/z* calculated for $[C_{11}H_{13}NO_4Na]^+$ ($[M + Na]^+$): 246.0737, measured: 246.0741; **IR (ATR)**: ν (cm^{-1}): 3012, 2955, 1736, 1606, 1563, 1436, 1299, 1256, 1196, 1150, 1031, 996, 945, 929, 834, 794, 773, 728, 622.

Methyl 2-(4-methylpyridin-2-yl)acetate
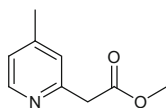
Prepared following **GP11** on a 2.73 mmol scale from dimethyl 2-(4-methylpyridin-2-yl)malonate (610 mg, 2.73 mmol, 1.00 equiv.), lithium chloride (290 mg, 6.85 mmol, 2.50 equiv.) and water (37 µL, 2.7 mmol, 1.0 equiv.) in DMSO (4.9 mL). Purification via flash column chromatography through silica gel (eluent = pentane:ethyl acetate, 2:1 to 1:1) afforded methyl 2-(4-methylpyridin-2-yl) acetate (200 mg, 1.21 mmol, 44 %) as a pale yellow oil.

R_f **(pentane:ethyl acetate 3:2)**: 0.43; **^{1}H NMR (300 MHz, CDCl$_3$)**: δ (ppm): 8.41 (d, *J* = 8.2, 0.8 Hz, 1H), 7.10–7.16 (m, 1H), 7.05 (dt, *J* = 5.2, 1.1 Hz, 1H), 3.85 (s, 2H), 3.73 (s, 3H), 2.36 (s, 3H); **^{13}C NMR (75.5 MHz, CDCl$_3$)**: δ (ppm): 171.2, 153.9, 148.8, 148.7, 125.1, 123.5, 52.4, 43.4, 21.2; **GC-MS**: t_R (50_40): 7.1 min; **EI-MS**: *m/z* (%): 165 (26), 134 (19), 133 (16), 120 (11), 107 (100), 106 (92), 79 (30), 78 (10), 77 (30), 39 (10); **HR-MS (ESI)**: *m/z* calculated for

$[C_9H_{11}NO_2Na]^+$ ($[M + Na]^+$): 188.0682, measured: 188.0687; **IR (ATR)**: ν (cm^{-1}): 2953, 1735, 1605, 1562, 1435, 1337, 1265, 1247, 1200, 1154, 1016, 998, 918, 829, 652, 620, 601.

Synthesis of methyl 2-(isoquinolin-1-yl)acetate

59%

mCPBA (1.0 equiv.)
CH$_2$Cl$_2$, rt, 4 h

Ac$_2$O/DMF
0 °C - rt, 15 h

(1.2 equiv.)

25%
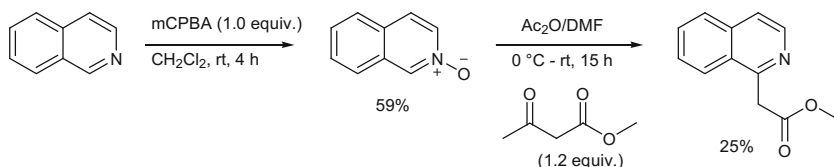
Isoquinoline 2-oxide
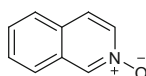
Following a modified procedure from Lakshman et al. [45], *meta*-chloroperbenzoic acid (mCPBA, 4.77 g, 19.4 mmol, 70 wt%) was added portion wise to a stirred solution of isoquinoline (2.28 mL, 19.4 mmol) in chloroform (7 mL) at 0 °C. The resulting mixture was allowed to stir at rt for 4 h. The reaction mixture was diluted with chloroform (8 mL), solid K$_2$CO$_3$ (10.1 g, 77.4 mmol) was added and the resulting mixture was stirred for another 10 min. After filtration to remove solid by-products, the filtrate was dried over MgSO$_4$ and concentrated under reduced pressure. Purification by flash column chromatography through neutral alumina (eluent = dichloromethane:methanol, 100:0 to 50:1) afforded isoquinoline 2-oxide (1.66 g, 11.4 mmol, 59 %) as a white solid.

R$_f$ (on neutral alumina, dichloromethane:methanol 50:1): 0.14; **^{1}H NMR (300 MHz, CDCl$_3$)**: δ (ppm): 8.74 (s, 1H), 8.10 (dd, J = 7.1, 1.6 Hz, 1H), 7.73–7.81 (m, 1H), 7.51–7.81 (m, 5H); **^{13}C NMR (75.5 MHz, CDCl$_3$)**: δ (ppm): 136.8, 136.3, 129.6, 129.5, 129.2, 128.9, 126.7, 125.1, 124.4; **GC-MS**: t$_R$ (50_40): 6.9 min; **EI-MS**: *m/z* (%): 130 (11), 129 (100), 128 (19), 102 (29), 51 (10); **HR-MS (ESI)**: *m/z* calculated for $[C_9H_7NONa]^+$ ($[M + Na]^+$): 168.0420, measured: 168.0420; **IR (ATR)**: ν (cm^{-1}): 3049, 3033, 1640, 1624, 1598, 1567, 1492, 1449, 1370, 1324, 1280, 1255, 1205, 1179, 1144, 1119, 1015, 961, 913, 868, 815, 751, 731, 622.

Methyl 2-(isoquinolin-1-yl)acetate
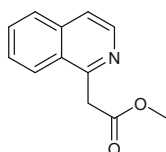
Following a modified procedure from Funakoshi et al. [46], methyl acetoacetate (1.29 mL, 12.0 mmol) was added to a solution of isoquinoline 2-oxide (1.45 g, 10.0 mmol) in acetic anhydride (2.27 mL)/DMF (10 mL) in a NaCl:ice (1:3) bath. The resulting mixture was stirred at the same temperature for 3 h and then at rt for 12 h. The reaction mixture was diluted with ethyl acetate (80 mL) and washed with 10 % aq. Na_2CO_3 solution (2 × 50 mL) and brine (5 × 80 mL). The organic layers were extracted with 10 % HCl (5 × 30 mL) and the HCl layer was made alkaline with 1 M NaOH solution (200 mL). The alkaline aqueous layers were finally extracted with dichloromethane, dried over $MgSO_4$ and concentrated under reduced pressure. Purification via flash column chromatography through silica gel (eluent = pentane:ethyl acetate 4:1) followed by recrystallization (2×) from hexane afforded Methyl 2-(isoquinolin-1-yl)acetate (510 mg, 2.53 mmol, 25 %) as a pale yellow semi-solid compound.

R_f (pentane:ethyl acetate 3:2): 0.30; **^{1}H NMR (400 MHz, CDCl$_3$)**: δ (ppm): 8.48 (d, J = 5.8 Hz, 1H), 8.09 (dt, J = 8.5, 1.0 Hz, 1H), 7.87 (dt, J = 8.2, 1.0 Hz, 1H), 7.71 (ddd, J = 8.2, 6.9, 1.2 Hz, 1H), 7.60–7.67 (m, 2H), 4.39 (s, 2H), 3.72 (s, 2H); **^{13}C NMR (101 MHz, CDCl$_3$)**: δ (ppm): 170.9, 154.5, 141.7, 136.6, 130.6, 127.9, 127.6, 127.5, 125.3, 120.8, 52.5, 41.9; **GC-MS**: t_R (50_40): 8.4 min; **EI-MS**: m/z (%): 201 (52), 170 (13), 169 (24), 158 (12), 144 (11), 143 (100), 142 (58), 140 (14), 116 (15), 115 (91), 114 (10), 89 (11); **HR-MS (ESI)**: m/z calculated for $[C_{12}H_{11}NO_2Na]^+$ ($[M + Na]^+$): 224.0682, measured: 224.0682; **IR (ATR)**: ν (cm^{-1}): 3066, 3006, 2955, 2362, 2339, 1740, 1706, 1624, 1588, 1563, 1501, 1452, 1435, 1386, 1330, 1291, 1260, 1227, 1210, 1171, 1088, 1012, 978, 831, 800, 753, 673.

Synthesis of methyl 2-bromo-(5-bromopyridin-2-yl)acetate
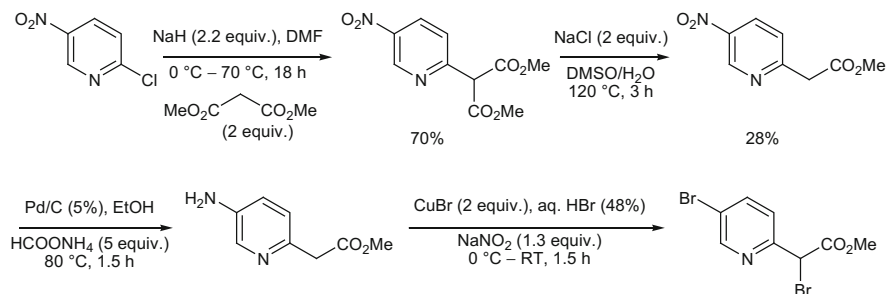
Dimethyl 2-(5-nitropyridin-2-yl)malonate
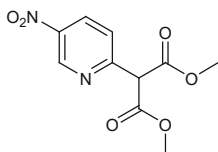
Dimethyl malonate (7.21 ml, 63.1 mmol) was added dropwise to a suspension of sodium hydride (2.67 g, 66.7 mmol, 60 % wt. in mineral oil) in dry DMF (26 ml) with vigorous stirring at 0 °C for 15 min. The stirring was continued at 0 °C for another 45 min. To the stirred reaction mixture, a solution of 2-chloro-5-nitropyridine (5.00 g, 31.5 mmol) in dry DMF (52 ml) was added dropwise and then the stirring was continued at 70 °C for 18 h. After cooling to rt, the reaction mixture was quenched with saturated aq. NH$_4$Cl solution. Filtration followed by drying under vacuum afforded dimethyl 2-(5-nitropyridin-2-yl)malonate (5.6 g, 22 mmol, 70 %) as an orange solid.

R$_f$ (pentane:ethyl acetate 3:2): 0.51; **^{1}H NMR (300 MHz, CDCl$_3$)**: δ (ppm): 9.38 (dd, J = 2.7, 0.7 Hz, 1H), 8.51 (dd, J = 8.7, 2.7 Hz, 1H), 7.76 (dd, J = 8.6, 0.7 Hz, 1H), 5.10 (s, 1H), 3.81 (s, 6H); **^{13}C NMR (75.5 MHz, CDCl$_3$)**: δ (ppm): 166.9, 158.7, 144.8, 143.9, 132.0, 124.5, 60.1, 53.6; **GC-MS**: t$_R$ (50_40): 8.6 min; **EI-MS**: m/z (%): 254 (28), 223 (70), 222 (15), 196 (18), 195 (100), 179 (50), 178 (12), 168 (10), 167 (52), 165 (16) 164 (38), 153 (10), 152 (91), 151 (19), 149 (15) 148 (24), 147 (12), 137 (12), 134 (14), 133 (21), 122 (10), 121 (74), 106 (16), 105 (16), 104 (13), 93 (19), 92 (39), 91 (25), 90 (13), 79 (17), 78 (17), 77 (16), 64 (12), 63 (46), 62 (17), 59 (94) 51 (15), 50 (12), 39 (11); **HR-MS (ESI)**: m/z calculated for [C$_{10}$H$_{10}$N$_2$O$_6$Na]$^+$ ([M + Na]$^+$): 277.0431, measured: 277.0434; **IR (ATR)** ν (cm^{-1}): 3077, 2958, 2923, 2854, 2361, 2341, 1729, 1663, 1638, 1599, 1579, 1522, 1438, 1378, 1352, 1329, 1308, 1278, 1239, 1201, 1161, 1119, 1089, 1038, 1018, 991, 947, 936, 913, 843, 795, 744, 729, 705, 688, 655, 641, 605.

Methyl 2-(5-nitropyridin-2-yl)acetate
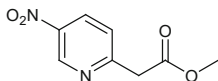
A solution of NaCl (2.53 g, 43.3 mmol) in water (15 mL) was added to dimethyl 2-(5-nitropyridin-2-yl)malonate (5.50 g, 21.6 mmol) in DMSO (15 mL) in a round-bottomed flask equipped with a condenser. The reaction mixture was heated at 120 °C for 3 h. After cooling to rt, the mixture was diluted with water, extracted with ethyl acetate, dried with MgSO$_4$ and concentrated under reduced pressure. The crude reaction mixture was purified by flash column chromatography through silica gel using (eluent = pentane:ethyl acetate, 4:1) to afford methyl 2-(5-nitropyridin-2-yl) acetate (2.38 g, 12.1 mmol, 28 %) as a yellow oil.

R$_f$ (pentane:ethyl acetate 3:2): 0.42; **^{1}H NMR (400 MHz, CDCl$_3$)**: δ (ppm): 9.38 (d, J = 2.6, 1H), 8.46 (dd, J = 8.5, 2.6 Hz, 1H), 7.54 (d, J = 8.5, 1H), 4.00 (s, 2H), 3.75 (s, 3H); **^{13}C NMR (101 MHz, CDCl$_3$)**: δ (ppm): 169.9, 160.7, 145.0, 143.4, 131.8, 124.4, 52.7, 43.7; **GC-MS**: t$_R$ (50_40): 7.9 min; **EI-MS**: m/z (%): 196 (56), 181 (71), 165 (63), 164 (23), 150 (13), 138 (84), 137 (62), 122 (37), 107 (10), 106 (23) 94 (12), 93 (10), 92 (34), 91 (21) 90 (16) 80 (41), 79 (16), 78 (16), 77 (21), 66 (30), 65 (27), 64 (75), 63 (67), 62 (14), 59 (100), 53 (12), 52 (30), 51 (24), 50 (20), 39 (21), 38 (14); **HR-MS (ESI)**: m/z calculated for [C$_8$H$_8$N$_2$O$_4$Na]$^+$ ([M + Na]$^+$): 219.0376, measured: 219.0378; **IR (ATR)**: ν (cm^{-1}): 3102, 3078,

2962, 2361, 2340, 1730, 1600, 1580, 1508, 1476, 1434, 1411, 1362, 1261, 1237, 1187, 1169, 1118, 1022, 991, 944, 903, 865, 848, 827, 725, 684, 630.

Methyl 2-(5-aminopyridin-2-yl)acetate
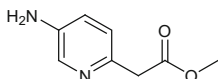
A suspension of methyl 2-(5-nitropyridin-2-yl)acetate (1.17 g, 5.96 mmol) in ethanol (5.5 ml) was added to 5 % Pd/C (235 mg) in ethanol (3.7 mL). Ammonium formate (1.88 g, 29.8 mmol) was added to the heterogeneous reaction mixture and refluxed under argon for 1.5 h. The reaction mixture was filtered through Celite and the solvents were removed under reduced pressure. The residue was purified by flash column chromatography through silica gel (eluent = dichloromethane: methanol, 24:1) to afford methyl 2-(5-aminopyridin-2-yl)acetate (798 mg, 4.76 mmol, 80 %) as a pale yellow oil.

R_f **(dichloromethane:methanol 19:1)**: 0.19; **^{1}H NMR (300 MHz, CDCl$_3$)**: δ (ppm): 8.05 (dd, J = 2.8, 0.8 Hz, 1H), 7.14–7.03 (m, 1H), 6.98 (dd, J = 8.3, 2.8 Hz, 1H), 3.75 (s, 2H), 3.70 (s, 3H), 3.24 (s, 2H, broad); **^{13}C NMR (75.5 MHz, CDCl$_3$)**: δ (ppm): 171.7, 143.7, 141.6, 136.6, 124.2, 122.9, 52.3, 42.6; **GC-MS**: t_R (50_40): 8.0 min; **EI-MS**: m/z (%): 166 (38), 108 (14), 107 (100), 80 (21); **HR-MS (ESI)**: m/z calculated for $[C_8H_{10}N_2O_2Na]^+$ ([M + Na]$^+$): 189.0634, measured: 189.0635; **IR (ATR)**: ν (cm^{-1}): 3436, 3341, 3213, 2954, 2361, 2340, 1728, 1629, 1602, 1575, 1493, 1436, 1340, 1297, 1267, 1247, 1197, 1161, 1016, 902, 838, 735, 697, 647, 609.

Methyl 2-bromo-(5-bromopyridin-2-yl)acetate
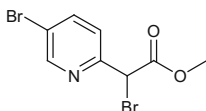
Following a modified procedure reported from Morgentin et al. [47], NaNO$_2$ (117 mg, 1.70 mmol) was added portionwise to a solution of methyl 2-(5-aminopyridin-2-yl)acetate (218 mg, 1.31 mmol) and CuBr (375 mg, 2.61 mmol) in 48 % aq. HBr (6 mL) at 0 °C and the mixture was stirred at rt for 1.5 h. Aq. NaOH solution (1 N) was added to adjust the pH to 5. The reaction mixture was extracted with ethyl acetate (3 × 10 mL). The combined organic phases were dried over MgSO$_4$, filtered and concentrated under reduced pressure. The crude mixture was purified by flash column chromatography through silica gel (eluent = pentane: ethyl acetate, 19:1) to afford methyl 2-bromo-(5-bromopyridin-2-yl)acetate (47 mg, 0.15 mmol, 12 %) as a white solid upon cooling.

R_f **(pentane:ethyl acetate 4:1)**: 0.53; **^{1}H NMR (300 MHz, CDCl$_3$)**: δ (ppm): 8.60 (dd, J = 2.4, 0.8 Hz, 1H), 7.88 (dd, J = 8.4, 2.3 Hz, 1H), 7.62 (dd, J = 8.4, 0.7 Hz, 1H), 5.48 (s, 1H), 3.82 (s, 3H); **^{13}C NMR (75.5 MHz, CDCl$_3$)**: δ (ppm):

168.0, 153.9, 150.4, 140.1, 125.2, 121.1, 53.8, 46.4; **GC-MS**: t_R (50_40): 8.3 min; **EI-MS**: m/z (%): 311 (13),309 (25), 307 (14), 252 (29), 250 (59), 248 (31), 231 (14), 230 (100), 229 (14), 228 (99), 202 (67), 200 (75), 199 (10), 197 (11), 186 (16), 184 (16), 173 (17), 172 (19), 171 (29), 170 (18), 169 (14), 145 (13), 143 (17), 93 (22), 91 (11), 90 (54), 64 (13), 63 (51), 62 (20), 59 (26), 50 (12), 39 (10); **HR-MS (ESI)**: m/z calculated for $[C_8H_7Br_2NO_2Na]$ + ([M + Na] +): 329.8736, measured: 329.8722; **IR (ATR)**: ν (cm^{-1}): 3009, 2980, 2955, 1747, 1575, 1558, 1459, 1438, 1371, 1324, 1278, 1249, 1220, 1172, 1149, 1135, 1092, 1001, 973, 920, 903, 865, 844, 775, 704, 628.

Bromination of 2-pyridine acetic acid esters to form brominated pyridines
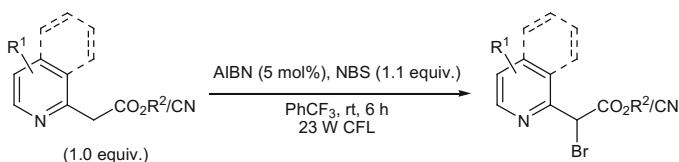
General Procedure 12:

   In an oven dried round bottomed flask equipped with a magnetic stir bar, *N*-bromosuccinimide (NBS, 1.1 equiv.) and azobisisobutyronitrile (AIBN, 5 mol%) were added to a solution of the pyridine substrate (1.0 equiv.) in α,α,α-trifluorotoluene. The reaction mixture was allowed to stir at rt for 6 h under irradiation of visible light from a household 23 W CFL. The solvent was removed under reduced pressure and the crude reaction mixture was purified by flash column chromatography through silica gel (eluent = pentane:ethyl acetate 9:1) to afford the pure brominated pyridines.

Methyl 2-bromo-2-(pyridin-2-yl)acetate
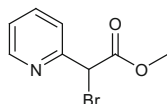
Prepared following **GP12** on a 10.6 mmol scale from methyl 2-(pyridin-2-yl)ac-etate (1.60 g, 10.6 mmol, 1.00 equiv.), *N*-bromosuccinimide (NBS, 2.08 g, 11.6 mmol, 1.10 equiv.) and azobisisobutyronitrile (AIBN, 80 mg, 0.49 mmol, 5 mol%) in α,α,α-trifluorotoluene (16 mL, 0.66 M). Purification via flash column chromatography through silica gel (eluent = pentane:ethyl acetate, 9:1) afforded Methyl 2-bromo-2-(pyridin-2-yl)acetate (1.69 g, 7.35 mmol, 70 %) as a yellow oil.

   R_f (pentane:ethyl acetate 4:1): 0.29; **^{1}H NMR (400 MHz, CDCl$_3$)**: δ (ppm): 8.55 (ddd, *J* = 4.9, 1.8, 1.0 Hz, 1H), 7.75 (td, *J* = 7.7, 1.8 Hz, 1H),

7.69 (dt, J = 8.0, 1.2 Hz, 1H), 7.21–7.32 (m, 1H), 5.53 (s, 1H), 3.81 (s, 3H); **^{13}C NMR (101 MHz, CDCl$_3$)**: δ (ppm): 168.3, 155.4, 149.4, 137.5, 123.8, 123.8, 53.7, 47.4; **GC-MS**: t_R (50_40): 7.5 min; **EI-MS**: *m/z* (%): 231 (13), 229 (14), 172 (42), 170 (43), 151 (10), 150 (100), 122 (46), 120 (11), 119 (23), 106 (17) 122 (46), 94 (15), 93 (19), 92 (14) 91 (47) 79 (10), 78 (17), 65 (21), 64 (26), 63 (34), 62 (12), 51 (11); **HR-MS (ESI)**: *m/z* calculated for $[C_8H_8BrNO_2Na]^+$ $([M + Na]^+)$: 251.9631, measured: 251.9623; **IR (ATR)**: ν (cm^{-1}): 3056, 3009, 2955, 1742, 1589, 1573, 1469, 1435, 1332, 1281, 1253, 1228, 1191, 1146, 1093, 1051, 999, 903, 862, 748, 706, 616.

Ethyl 2-bromo-2-(pyridin-2-yl)acetate

Prepared following **GP12** on a 3.02 mmol scale from ethyl 2-(pyridin-2-yl)acetate (500 mg, 3.02 mmol, 1.00 equiv.), *N*-bromosuccinimide (NBS, 592 g, 3.33 mmol, 1.10 equiv.) and azobisisobutyronitrile (AIBN, 30 mg, 0.18 mmol, 5 mol%) in α,α,α-trifluorotoluene (6.0 mL, 0.50 M). Purification via flash column chromatography through silica gel (eluent = pentane:ethyl acetate, 9:1) afforded ethyl 2-bromo-2-(pyridin-2-yl)acetate (615 mg, 2.52 mmol, 83 %) as a yellow oil.

    R_f (pentane:ethyl acetate 3:1): 0.48; **^{1}H NMR (300 MHz, CDCl$_3$)**: δ (ppm): 8.49 (ddd, J = 4.9, 1.8, 1.0 Hz, 1H), 7.62–7.72 (m, 2H), 7.19 (ddd, J = 7.1, 4.9, 1.6 Hz, 1H), 5.47 (s, 1H), 4.15– 4.26 (m, 2H), 1.22(t, J = 7.1 Hz, 3H); **^{13}C NMR (75.5 MHz, CDCl$_3$)**: δ (ppm): 167.6, 155.3, 149.2, 137.2, 123.6, 123.6, 62.7, 47.7, 13.1; **GC-MS**: t_R (50_40): 7.7 min; **EI-MS**: *m/z* (%): 243 (14), 200 (12), 198 (11), 191 (53), 173 (59), 172 (100), 171 (65), 170 (100), 164 (40), 120 (55), 119 (35), 108 (31), 93 (15), 92 (53), 91 (57), 90 (10), 80 (10), 78 (13), 65 (36), 64 (37), 63 (40), 62 (13), 51 (11); **HR-MS (ESI)**: *m/z* calculated for $[C_9H_{10}BrNO_2Na]^+$ $([M + Na]^+)$: 265.9787, measured: 265.9788; **IR (ATR)**: ν (cm^{-1}): 3056, 2983, 2939, 2905, 1741, 1589, 1573, 1469, 1436, 1392, 1369, 1328, 1291, 1256, 1229, 1146, 1095, 1025, 996, 633, 616.

tert-Butyl 2-bromo-2-(pyridin-2-yl)acetate

Prepared following **GP12** on a 3.1 mmol scale from *tert*-butyl 2-(pyridin-2-yl) acetate (0.60 g, 3.1 mmol, 1.0 equiv.), *N*-bromosuccinimide (608 mg, 3.42 mmol, 1.10 equiv.) and azobisisobutyronitrile (AIBN, 26 mg, 0.16 mmol, 5 mol%) in α,α,α-trifluorotoluene (5 mL, 0.6 M). Purification via flash column chromatography through silica gel (eluent = pentane:ethyl acetate, 9:1) afforded *tert*-butyl

2-bromo-2-(pyridin-2-yl)acetate (0.71 g, 2.6 mmol, 94 %) as a light greenish yellow solid.

R$_f$ (pentane:ethyl acetate 4:1): 0.43; **^{1}H NMR (300 MHz, CDCl$_3$)**: δ (ppm): 8.53 (ddd, J = 4.9, 1.8, 1.0 Hz, 1H), 7.78–7.63 (m, 2H), 7.61–7.79 (m, 2H), 7.23 (ddd, J = 7.1, 4.9, 1.5 Hz, 1H), 5.41 (s, 1H), 1.46 (s, 9H); **^{13}C NMR (75.5 MHz, CDCl$_3$)**: δ (ppm): 166.6, 155.9, 149.2, 137.2, 123.7, 123.5, 83.5, 49.1, 27.9; **GC-MS**: t$_R$ (50_40): 7.9 min; **EI-MS**: m/z (%): 173 (12), 171 (12), 91 (10), 57 (100), 41 (22); **HR-MS (ESI)**: m/z calculated for $[C_{11}H_{14}BrNO_2Na]^+$ ([M + Na]$^+$): 294.0100, measured: 294.0099; **IR (ATR)**: ν (cm^{-1}): 3003, 2978, 2936, 2880, 1741, 1586, 1574, 1472, 1459, 1438, 1394, 1370, 1331, 1283, 1283, 1258, 1157, 1133, 1093, 1049, 995, 954, 871, 843, 761, 748, 670, 614.
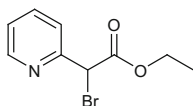
Benzyl 2-bromo-2-(pyridin-2-yl)acetate
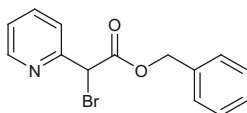
Prepared following **GP12** on a 0.83 mmol scale from benzyl 2-(pyridin-2-yl)acetate (230 mg, 0.830 mmol, 1.00 equiv.), *N*-bromosuccinimide (NBS, 163 mg, 0.916 mmol, 1.10 equiv.) and azobisisobutyronitrile (AIBN, 6.8 mg, 0.04 mmol, 0.05 equiv.) in α,α,α-trifluorotoluene (1.6 mL, 0.52 M). Purification via flash column chromatography through silica gel (eluent = pentane:ethyl acetate, 9:1) afforded benzyl 2-bromo-2-(pyridin-2-yl)acetate (250 mg, 0.817 mmol, 98 %) as a light yellow oil.

R$_f$ (pentane:ethyl acetate 4:1): 0.33; **^{1}H NMR (300 MHz, CDCl$_3$)**: δ (ppm): 8.55 (ddd, J = 4.9, 1.8, 1.0 Hz, 1H), 7.74 (td, J = 7.6, 1.8 Hz, 1H), 7.19 (dt, J = 8.0, 1.2 Hz, 1H), 7.31–7.38 (m, 5H), 7.27 (td, J = 4.9, 1.4 Hz, 1H), 5.59 (s, 1H), 5.25 (d, J = 3.8 Hz, 2H); **^{13}C NMR (75 MHz, CDCl$_3$)**: δ (ppm): 167.6, 155.3, 149.2, 137.6, 135.1, 128.7, 128.6, 128.3, 123.9, 123.8, 68.4, 47.4; **GC-MS**: t$_R$ (50_40): 9.4 min; **EI-MS**: m/z (%): 120 (93), 93 (13), 92 (20), 91 (100), 65 (20); **HR-MS (ESI)**: m/z calculated for $[C_{14}H_{12}BrNO_2Na]^+$ ([M + Na]$^+$): 327.9944, measured: 327.9940; **IR (ATR)**: ν (cm^{-1}): 3063, 3034, 3010, 2959, 1743, 1589, 1574, 1498, 1468, 1457, 1436, 1377, 1329, 1258, 1225, 1141, 1093, 1050, 996, 972, 972, 908, 746, 699, 631.
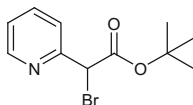
2-Bromo-2-(pyridin-2-yl)acetonitrile
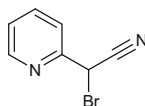
Prepared following **GP12** on a 4.23 mmol scale from 2-(pyridin-2-yl)acetonitrile (500 mg, 4.23 mmol, 1.00 equiv.), *N*-bromosuccinimide (NBS, 829 mg, 4.66 mmol, 1.10 equiv.) and azobisisobutyronitrile (AIBN, 35 mg, 0.21 mmol, 5 mol%) in α,α,α-trifluorotoluene (6.0 mL, 0.70 M). Purification via flash column

chromatography through silica gel (eluent = pentane:ethyl acetate, 9:1) afforded 2-bromo-2-(pyridin-2-yl)acetonitrile (811 mg, 4.12 mmol, 97 %) as a pink solid.

R_f **(pentane:ethyl acetate 3:1)**: 0.35; **^{1}H NMR (300 MHz, CDCl$_3$)**: δ (ppm): 8.63–8.65 (m, 1H), 7.82 (td, J = 7.7, 1.8, 1H), 7.67 (dt, J = 7.9, 1.0, 1H), 7.35 (ddd, J = 7.6, 4.9, 1.1 Hz, 1H), 5.58 (s, 1H); **^{13}C NMR (75.5 MHz, CDCl$_3$)**: δ (ppm): 152.5 (C$_q$), 150.3 (CH), 138.1 (CH), 124.7 (CH), 122.4 (CH), 115.8 (C$_q$), 28.9(CH); **GC-MS**: t$_R$ (50_40): 7.2 min; **EI-MS**: m/z (%): 118 (21), 117 (100), 90 (28), 78 (11), 63 (12); **HR-MS (ESI)**: m/z calculated for [C$_7$H$_5$BrN$_2$Na]$^+$ ([M + Na]$^+$): 218.9528, measured: 218.9526; **IR (ATR)**: ν (cm^{-1}): 2974, 2249, 1588, 1471, 1440, 1284, 1240, 1190, 1150, 1099, 1053, 993, 967, 905, 836, 792, 749, 663, 616.

## Methyl 2-bromo-2-(5-fluoropyridin-2-yl)acetate
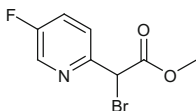
Prepared following **GP12** on a 0.76 mmol scale from methyl 2-(5-fluoropyridin-2-yl) acetate (162 mg, 0.958 mmol, 1.00 equiv.), *N*-bromosuccinimide (NBS, 174 mg, 0.975 mmol, 1.10 equiv.) and azobisisobutyronitrile (AIBN, 7.3 mg, 0.04 mmol, 5 mol%) in α,α,α-trifluorotoluene (1.8 mL, 0.42 M). Purification via flash column chromatography through silica gel (eluent = pentane:ethyl acetate, 9:1) afforded methyl 2-bromo-2-(5-fluoropyridin-2-yl)acetate (206 mg, 0.830 mmol, 87 %) as a light yellow oil.

R_f **(pentane:ethyl acetate 4:1)**: 0.45; **^{1}H NMR (300 MHz, CDCl$_3$)**: δ (ppm): 8.33 (d, J = 2.9 Hz, 1H), 7.70 (ddd, J = 8.8, 4.3, 0.6 Hz, 1H), 7.41 (ddd, J = 8.7, 7.9, 2.9 Hz, 1H), 5.50 (s, 1H), 3.76 (s, 3H); **^{13}C NMR (75.5 MHz, CDCl$_3$)**: δ (ppm): 168.0 (d, J = 0.8 Hz), 159.0 (d, J = 258.6 Hz), 151.2 (d, J = 4.0 Hz), 137.4 (d, J = 24.3 Hz), 125.1 (d, J = 4.9 Hz), 124.1 (d, J = 18.9 Hz), 53.6, 46.2 (d, J = 1.7 Hz); **^{19}F NMR (282 MHz, CDCl$_3$)**: −125.96; **GC-MS**: t$_R$ (50_40): 7.3 min; **EI-MS**: m/z (%): 190 (33), 188 (33), 169 (11), 168 (100), 140 (52), 137 (20), 124 (16), 111 (12), 110 (14), 109 (38) 96 (10), 83 (14), 82 (22), 81 (17), 59 (14); **HR-MS (ESI)**: m/z calculated for [C$_8$H$_7$BrFNO$_2$Na]$^+$ ([M + Na]$^+$): 269.9536, measured: 269.9539; **IR (ATR)**: ν (cm^{-1}): 2956, 1743, 1587, 1478, 1437, 1390, 1324, 1258, 1224, 1146, 1118, 1004, 915, 871, 842, 816, 788, 769, 701, 658, 620.

Methyl 2-bromo-2-(5-(trifluoromethyl)pyridin-2-yl)acetate

Prepared following **GP12** on a 0.80 mmol scale from methyl 2-(5-(trifluoromethyl)pyridin-2-yl)acetate (176 mg, 0.803 mmol, 1.00 equiv.), *N*-bromosuccinimide (NBS, 157 mg, 0.882 mmol, 1.10 equiv.) and azobisisobutyronitrile (AIBN, 6.6 mg, 40 μmol, 5 mol%) in α,α,α-trifluorotoluene (1.6 mL, 0.50 M). Purification via flash column chromatography through silica gel (eluent = pentane:ethyl acetate, 9:1) afforded methyl 2-bromo-2-(5-(trifluoromethyl)pyridin-2-yl)acetate (151 mg, 0.507 mmol, 63 %) as a pale yellow oil.

R$_f$ (pentane:ethyl acetate 4:1): 0.61;**^{1}H NMR (300 MHz, CDCl$_3$)**: δ (ppm): 8.66–8.90 (m, 1H), 7.94–8.05 (m, 1H), 7.86 (dt, *J* = 8.3, 0.8 Hz, 1H), 5.56 (s, 1H), 3.83 (s, 3H); **^{13}C NMR (75.5 MHz, CDCl$_3$)**: δ (ppm): 167.8, 159.1, 146.2 (q, *J* = 4.0 Hz), 134.7 (q, *J* = 3.4 Hz), 126.7 (q, *J* = 33.3 Hz), 123.8, 123.2 (q, *J* = 272.6 Hz), 53.9, 46.2; **^{19}F NMR (282 MHz, CDCl$_3$)**: −62.56; **GC-MS**: t$_R$ (50_40): 7.2 min; **EI-MS**: *m/z* (%): 240 (28), 238 (29), 219 (14), 218 (100), 190 (16), 187 (19), 174 (36), 161 (12), 160 (17), 159 (22) 139 (10), 132 (10), 63.(15), 59 (28); **HR-MS (ESI)**: *m/z* calculated for [C$_9$H$_7$BrF$_3$NO$_2$Na]$^+$ ([M + Na]$^+$): 319.9504, measured: 319.9499; **IR (ATR)**: ν (cm^{-1}): 2959, 1747, 1606, 1579, 1438, 1396, 1329, 1296, 1257, 1131, 1080, 1017, 1027, 631.

Methyl 2-bromo-2-(5-methylpyridin-2-yl)acetate

Prepared following **GP12** on a 0.76 mmol scale from methyl 2-(5-methylpyridin-2-yl)acetate (125 mg, 0.757 mmol, 1.00 equiv.), *N*-bromosuccinimide (NBS, 148 mg, 0.830 mmol, 1.10 equiv.) and azobisisobutyronitrile (AIBN, 6.2 mg, 38 μmol, 5 mol%) in α,α,α-trifluorotoluene (1.5 mL, 0.5 M). Purification via flash column chromatography through silica gel (eluent = pentane:ethyl acetate, 9:1) afforded methyl 2-bromo-2-(5-methylpyridin-2-yl)acetate (149 mg, 0.610 mmol, 80 %) as a yellow oil.

R$_f$ (pentane:ethyl acetate 4:1): 0.33; **^{1}H NMR (400 MHz, CDCl$_3$)**: δ (ppm): 8.38 (dt, *J* = 1.9, 0.8 Hz, 1H), 7.37–7.77 (m, 2H), 5.55 (s, 1H), 3.81 (s, 3H), 2.35 (s, 1H); **^{13}C NMR (101 MHz, CDCl$_3$)**: δ (ppm): 168.4, 152.4, 149.4, 138.3, 123.4, 53.7, 47.0, 18.4; **GC-MS**: t$_R$ (50_40): 10.9 min; **EI-MS**: *m/z* (%): 245 (11), 243 (11), 186 (31), 184 (32), 165 (14), 164 (100), 136 (96), 134 (10), 133 (16), 120 (11) 108 (10), 107 (29), 106 (23), 105 (13) 104 (31) 92 (13), 79 (26), 78 (32), 77 (43), 65 (14), 59 (13), 52 (17), 51 (25), 50 (13), 39 (19); **HR-MS (ESI)**: *m/z* calculated for [C$_9$H$_{11}$BrNO$_2$Na]$^+$ ([M + Na]$^+$): 265.9787, measured: 265.9795; **IR (ATR)**: ν (cm^{-1}): 3006, 2954, 1743, 1574, 1482, 1436, 1383, 1329, 1288, 1253, 1217, 1147, 1031, 1004, 905, 839, 703, 632.
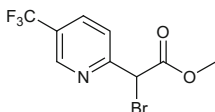
Methyl 2-bromo-2-(5-phenylpyridin-2-yl)acetate

Prepared following **GP12** on a 0.801 mmol scale from methyl 2-(5-phenylpyridin-2-yl)acetate (182 mg, 0.801 mmol, 1.00 equiv.), *N*-bromosuccinimide (NBS, 157 mg, 0.882 mmol, 1.10 equiv.) and azobisisobutyronitrile (AIBN, 6.6 mg, 40 μmol, 5 mol%) in α,α,α-trifluorotoluene (1.6 mL, 0.50 M). Purification via column chromatography through silica gel (eluent = pentane:ethyl acetate, 9:1) afforded methyl 2-bromo-2-(5-phenylpyridin-2-yl)acetate (209 mg, 0.701 mmol, 88 %) as a pale yellow solid.

R_f **(pentane:ethyl acetate 4:1)**: 0.42; **^{1}H NMR (300 MHz, CDCl$_3$)**: δ (ppm): 8.77 (dd, *J* = 2.4, 0.8 Hz, 1H), 7.93 (dd, *J* = 8.1, 2.4 Hz, 1H), 7.76 (dd, *J* = 8.2, 0.8 Hz, 1H), 7.54–7.61 (m, 2H), 7.37–7.52 (m, 3H), 5.60 (s, 1H), 3.84 (s, 3H); **^{13}C NMR (75.5 MHz, CDCl$_3$)**: δ (ppm): 168.3, 153.9, 147.7, 137.0, 136.8, 135.8, 129.3, 128.6, 127.3, 123.7, 53.7, 47.2; **GC-MS**: t_R (50_40): 9.7 min; **EI-MS**: *m/z* (%): 307 (10), 305 (10), 248 (10), 246 (11), 227 (21), 226 (70), 199 (15), 198 (100), 169 (29), 168 (19), 167 (21), 166 (20), 141 (15), 140 (14), 139 (27), 115 (13); **HR-MS (ESI)**: *m/z* calculated for [C$_{14}$H$_{12}$BrNO$_2$Na]$^+$ ([M + Na]$^+$): 327.9944, measured: 327.9934; **IR (ATR)**: ν (cm^{-1}): 3009, 2978, 2956, 2361, 2340, 1747, 1588, 1564, 1473, 1450, 1435, 1375, 1349, 1327, 1306, 1279, 1249, 1220, 1185, 1170, 1141, 997, 897, 871, 851, 749, 727, 701, 691, 661, 626, 613.

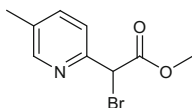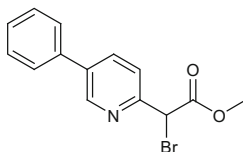**Methyl 2-bromo-2-(4-chloropyridin-2-yl)acetate**

Prepared following **GP12** on a 0.620 mmol scale from methyl 2-(4-chloropyridin-2-yl)acetate (115 mg, 0.620 mmol, 1.00 equiv.), *N*-bromosuccinimide (NBS, 121 mg, 0.680 mmol, 1.10 equiv.) and azobisisobutyronitrile (AIBN, 5.1 mg, 31 μmol, 5 mol%) in α,α,α-trifluorotoluene (1.2 mL, 0.5 M). Purification via column chromatography through silica gel (eluent = pentane:ethyl acetate, 9:1) afforded methyl 2-bromo-2-(4-chloropyridin-2-yl)acetate (108 mg, 0.408 mmol, 66 %) as a white solid.

R_f **(pentane:ethyl acetate 4:1)**: 0.45; **^{1}H NMR (300 MHz, CDCl$_3$)**: δ (ppm): 8.44 (dd, *J* = 5.3, 0.6 Hz, 1H), 7.72 (dd, *J* = 1.9, 0.6 Hz, 1H), 7.27 (dd, *J* = 5.3, 1.9 Hz, 1H), 5.48 (s, 1H), 3.82 (s, 3H); **^{13}C NMR (75.5 MHz, CDCl$_3$)**: δ (ppm): 167.9, 156.8, 150.1, 146.4, 124.3, 124.2, 53.8, 46.4; **GC-MS**: t_R (50_40): 7.9 min; **EI-MS**: *m/z* (%): 206 (36), 204 (26), 186 (33), 185 (12), 184 (100), 156 (24), 153

(16), 140 (25), 128 (11), 127 (20) 126 (14), 125 (20), 112 (10), 99 (12), 90 (21), 63 (30), 62 (15), 59 (23); **HR-MS (ESI)**: *m/z* calculated for $[C_8H_7BrClNO_2Na]^+$ ($[M + Na]^+$): 287.9220, measured: 287.9228; **IR (ATR)**: ν (cm^{-1}): 2955, 1754, 1574, 1558, 1479, 1464, 1449, 1433, 1397, 1327, 1288, 1245, 1227, 1189, 1157, 1106, 994, 921, 892, 875, 843, 760, 702, 679.
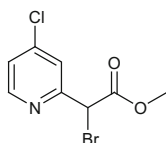
Methyl 2-bromo-2-(4-methylpyridin-2-yl)acetate
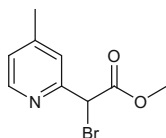
Prepared following **GP12** on a 1.00 mmol scale from methyl 2-(4-methylpyridin-2-yl)acetate (165 mg, 1.00 mmol, 1.00 equiv.), *N*-bromosuccinimide (NBS, 196 mg, 1.10 mmol, 1.10 equiv.) and azobisisobutyronitrile (AIBN, 8.2 mg, 50 μmol, 5 mol%) in α,α,α-trifluorotoluene (2.0 mL, 0.50 M). Purification via flash column chromatography through silica gel (eluent = pentane:ethyl acetate, 9:1) afforded methyl 2-bromo-2-(4-methylpyridin-2-yl)acetate (185 mg, 0.758 mmol, 76 %) as a light yellow solid.

R$_f$ (pentane:ethyl acetate 4:1): 0.42; **^{1}H NMR (300 MHz, CDCl$_3$)**: δ (ppm): 8.40 (d, *J* = 5.1, 0.8 Hz, 1H), 7.50 (dt, *J* = 1.6, 0.8 Hz, 1H), 7.07 (ddd, *J* = 5.1, 1.6, 0.8 Hz, 1H), 5.51 (s, 1H), 3.81 (s, 3H), 2.38 (s, 3H); **^{13}C NMR (75 MHz, CDCl$_3$)**: δ (ppm): 168.4, 155.0, 149.0, 149.0, 124.8, 124.5, 53.7, 47.5, 21.3; **GC-MS**: t$_R$ (50_40): 7.8 min; **EI-MS**: *m/z* (%): 245 (10), 243 (10), 186 (33), 184 (33), 165 (13), 164 (100), 149 (14), 136 (65), 134 (24), 133 (14) 120 (16), 108 (10), 107 (23), 106 (16) 105 (12) 104 (25), 92 (13), 79 (19), 78 (23), 77 (26), 65 (10), 52 (10), 51 (12), 39 (10); **HR-MS (ESI)**: *m/z* calculated for $[C_9H_{10}BrNO_2Na]^+$ ($[M + Na]^+$): 265.9787, measured: 265.9787; **IR (ATR)**: ν (cm^{-1}): 2951, 1751, 1605, 1559, 1489, 1434, 1410, 1337, 1291, 1260, 1247, 1210, 1186, 1156, 1110, 994, 943, 885, 840, 823, 768, 744, 706, 681.

Methyl 2-bromo-2-(isoquinolin-1-yl)acetate
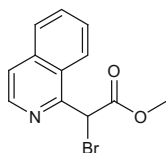
Prepared following **GP12** on a 1.12 mmol scale from methyl 2-(isoquinolin-1-yl) acetate (223 mg, 1.12 mmol, 1.00 equiv.), *N*-bromosuccinimide (NBS, 213 mg, 1.22 mmol, 1.10 equiv.) and azobisisobutyronitrile (9.2 mg, 56 μmol, 5 mol%) in α,α,α-trifluorotoluene (2.0 mL, 0.56 M). Purification via column chromatography through silica gel (eluent = pentane:ethyl acetate, 9:1) afforded methyl 2-bromo-2-(isoquinolin-1-yl)acetate (177 mg, 0.63 mmol, 56 %) as a light yellow solid.

R$_f$ (pentane:ethyl acetate 4:1): 0.30; **^{1}H NMR (400 MHz, CDCl$_3$)**: δ (ppm): 8.48 (d, *J* = 5.6 Hz, 1H), 8.21 (dq, *J* = 8.0, 0.9 Hz, 1H), 7.80–7.96 (m, 1H), 7.52–7.76 (m, 3H), 6.31 (s, 1H), 3.85 (s, 3H); **^{13}C NMR (101 MHz, CDCl$_3$)**: δ (ppm): 167.7, 154.8, 142.0, 137.0, 130.7, 128.0, 127.8, 125.9, 124.7, 122.1, 53.9, 47.1; **GC-MS**: t$_R$ (50_40): 9.1 min; **EI-MS**: *m/z* (%): 281 (24), 279 (26), 222 (13), 220 (13), 201 (14), 200 (57), 173 (12), 172 (100), 170 (13), 169 (17) 144 (17), 143 (35), 142 (15), 141 (29), 140 (42), 129 (10), 128 (12), 115 (29), 114 (27), 113 (17); **HR-MS (ESI)**: *m/z* calculated for $[C_{12}H_{10}BrNO_2Na]^+$ $([M + Na]^+)$: 301.9787, measured: 301.9784; **IR (ATR)**: ν (cm^{-1}): 3056, 3014, 2996, 2963, 2950, 1741, 1624, 1585, 1562, 1500, 1438, 1386, 1353, 1297, 1272, 1213, 1192, 1166, 1137, 1083, 1044, 1023, 995, 966, 907, 882, 830, 798, 752, 723, 667, 643, 579.

6.5.1.2   Synthesis of Enol Carbamate Substrates
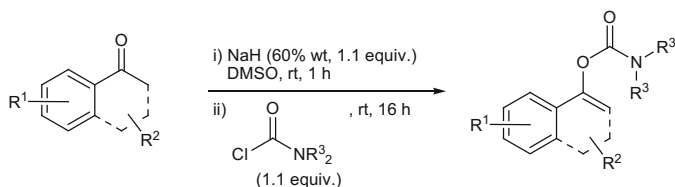
General Procedure 13:

Following a modified procedure from Feringa et al. [48], sodium hydride (60 % wt in mineral oil, 1.1 equiv.) was added to anhydrous DMSO (0.5 M) and the suspension was stirred at 50 °C for 2 h under an argon atmosphere. The mixture was cooled to rt, a solution of the ketone (1.0 equiv.) in anhydrous DMSO (2.0 M) was added dropwise over 15 min and stirring was continued at rt for an additional 1 h. The dialkyl carbamyl chloride (1.1 equiv.) was then added dropwise over 15 min and the mixture was stirred for 16 h at rt. Water was added to quench the reaction and the mixture was then extracted with ethyl acetate (2 × 15 mL). The combined organic fractions were washed with brine, dried over anhydrous Na$_2$SO$_4$, filtered and concentrated under reduced pressure. The crude products were purified by column chromatography through silica gel to afford the pure enol carbamates.

3,4-Dihydronaphthalen-1-yl dimethylcarbamate [49]
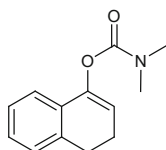
Prepared following **GP13** on a 25.0 mmol scale from 1-tetralone (3.66 g, 25.0 mmol, 1.00 equiv.), NaH (60 % wt in mineral oil, 1.20 g, 30.0 mmol, 1.20 equiv.) and dimethylcarbamoyl chloride (2.77 mL, 30.0 mmol, 1.20 equiv.). Purification via flash column chromatography through silica gel (eluent = pentane: ethyl acetate, 4:1) afforded 3,4-dihydronaphthalen-1-yl dimethylcarbamate (2.81 g, 12.9 mmol, 52 %) as a pink solid.

R$_f$ (pentane:ethyl acetate 2:1): 0.38; **^{1}H NMR (300 MHz, CDCl$_3$)**: δ (ppm): 7.09–7.20 (m, 4H), 5.71 (t, J = 4.7 Hz, 1H), 3.13 (s, 3H), 3.00 (s, 3H), 2.86 (t, J = 8.1 Hz, 2H), 2.44 (ddd, J = 9.0, 7.4, 4.7 Hz, 2H); **^{13}C NMR (75.5 MHz, CDCl$_3$)**: δ (ppm): 154.9, 146.1, 136.6, 131.3, 127.8, 127.6, 126.5, 120.8, 115.2, 36.8, 36.5, 27.7, 22.2; **GC-MS**: t$_R$ (50_40): 8.8 min; **EI-MS**: m/z (%): 217 (21), 115 (11), 72 (100); **HR-MS (ESI)**: m/z calculated for $[C_{13}H_{15}NO_2Na]^+$ ($[M + Na]^+$): 240.0995, measured: 240.0999; **IR (ATR)**: ν (cm^{-1}): 2939, 1716, 1660, 1487, 1452, 1386, 1357, 1334, 1279, 1228, 1179, 1167, 1128, 1080, 1038, 1000, 915, 872, 766, 737, 678.

3,4-Dihydronaphthalen-1-yl diethylcarbamate

Prepared following **GP13** on a 5.00 mmol scale from 1-tetralone (731 mg, 5.00 mmol, 1.00 equiv.), NaH (60 % wt in mineral oil, 220 mg, 5.50 mmol, 1.10 equiv.) and diethylcarbamoyl chloride (697 μL, 5.50 mmol, 1.10 equiv.). Purification via flash column chromatography through silica gel (eluent = pentane: ethyl acetate, 9:1) afforded 3,4-dihydronaphthalen-1-yl diethylcarbamate (992 mg, 4.04 mmol, 81 %) as a colorless oil.

R$_f$ (pentane:ethyl acetate 9:1): 0.22; **^{1}H NMR (400 MHz, CDCl$_3$)**: δ (ppm): 7.07–7.21 (m, 4H), 5.73 (t, J = 4.7 Hz, 1H), 3.47 (q, J = 7.1 Hz, 2H), 3.38 (q, J = 7.1 Hz, 2H), 2.87 (t, J = 8.1 Hz, 2H), 2.44 (ddd, J = 9.1, 7.5, 4.7 Hz, 2H), 1.29 (t, J = 7.1 Hz, 3H), 1.20 (t, J = 7.2 Hz, 3H); **^{13}C NMR (101 MHz, CDCl$_3$)**: δ (ppm): 154.1, 146.1, 136.5, 131.4, 127.7, 127.5, 126.4, 120.7, 115.0, 42.2, 41.9, 27.6, 22.2, 14.4, 13.4; **GC-MS**: t$_R$ (50_40): 9.1 min; **EI-MS**: m/z (%): 245 (16), 128 (7), 127 (5), 117 (5), 115 (16), 101 (6), 100 (100), 91 (6), 72 (47), 44 (8); **HR-MS (ESI)**: m/z calculated for $[C_{15}H_{19}NO_2Na]^+$ ($[M + Na]^+$): 268.1308, measured: 268.1308; **IR (ATR)**: ν (cm^{-1}): 2936, 2832, 1714, 1658, 1488, 1473, 1458, 1419, 1379, 1361, 1337, 1316, 1270, 1230, 1223, 1184, 1154, 1131, 1078, 1019, 957, 936, 917, 856, 782, 758, 735, 631.

3,4-Dihydronaphthalen-1-yl pyrrolidine-1-carboxylate

Prepared following **GP13** on a 5.00 mmol scale from 1-tetralone (731 mg, 5.00 mmol, 1.00 equiv.), NaH (60 % wt in mineral oil, 220 mg, 5.50 mmol, 1.10 equiv.) and 1-pyrrolidine carbamyl chloride (608 µL, 5.50 mmol, 1.10 equiv.). Purification via flash column chromatography through silica gel (eluent = pentane: ethyl acetate, 4:1) afforded 3,4-dihydronaphthalen-1-yl pyrrolidine-1-carboxylate (1.04 g, 4.27 mmol, 85 %) as a white solid.

R_f (pentane:ethyl acetate 4:1): 0.20; **^{1}H NMR (300 MHz, CDCl$_3$)**: δ (ppm): 7.09–7.22 (m, 4H), 5.75 (t, J = 4.7 Hz, 1H), 3.59 (d, J = 6.6 Hz, 2H), 3.46 (t, J = 6.6 Hz, 2H), 2.86 (t, J = 8.1 Hz, 2H), 2.08 (ddd, J = 9.0, 7.4, 4.7 Hz, 2H), 1.82–2.04 (m, 4H); **^{13}C NMR (75.5 MHz, CDCl$_3$)**: δ (ppm): 153.1, 145.8, 136.5, 131.4, 127.7, 127.4, 126.4, 120.8, 115.0, 46.5, 46.4, 27.6, 25.9, 25.0, 22.2; **GC-MS**: t_R (50_40): 9.8 min; **EI-MS**: m/z (%): 243 (12), 128 (6), 115 (14), 99 (6), 98 (100), 91 (5), 56 (18), 55 (48); **HR-MS (ESI)**: m/z calculated for [C$_{15}$H$_{17}$NO$_2$Na]$^+$ ([M + Na]$^+$): 266.1151, measured: 2661151; **IR (ATR)**: ν (cm^{-1}): 2939, 2879, 1710, 1676, 1659, 1487, 1464, 1442, 1427, 1401, 1357, 1332, 1323, 1277, 1230, 1220, 1181, 1126, 1094, 1050, 1033, 1021, 1012, 966, 913, 873, 848, 769, 752, 747, 704, 658, 608.
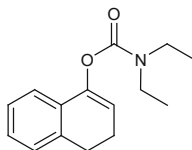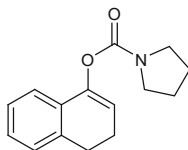
3,4-Dihydronaphthalen-1-yl morpholine-4-carboxylate
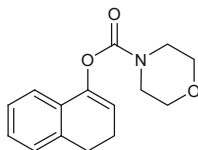
Prepared following **GP13** on a 5.00 mmol scale from 1-tetralone (731 mg, 5.00 mmol, 1.00 equiv.), NaH (60 % wt in mineral oil, 220 mg, 5.50 mmol, 1.10 equiv.) and 4-morpholine carbonyl chloride (643 µL, 5.50 mmol, 1.10 equiv.). Purification via flash column chromatography through silica gel (eluent = pentane: ethyl acetate, 2:1) afforded 3,4-dihydronaphthalen-1-yl morpholine-4-carboxylate (1.19 g, 4.59 mmol, 92 %) as a white solid.

R_f (pentane:ethyl acetate 2:1): 0.33; **^{1}H NMR (300 MHz, CDCl$_3$)**: δ (ppm): 7.12–7.22 (m, 3H), 7.09 (m, 1H), 5.73 (t, J = 4.7 Hz, 1H), 3.63 − 3.81 (m, 6H), 3.56 (br s, 2H), 2.87 (t, J = 8.1 Hz, 2H), 2.45 (ddd, J = 9.0, 7.5, 4.7 Hz, 2H); **^{13}C NMR (101 MHz, CDCl$_3$)**: δ (ppm): 153.7, 145.9, 136.6, 131.1, 128.0, 127.7, 126.5, 120.6, 115.5, 66.8, 66.8, 45.0, 44.3, 27.6, 22.2; **GC-MS**: t_R (50_40): 9.8 min; **EI-MS**: m/z (%): 193 (9), 115 (32), 114 (100), 91 (14), 70 (77), 45 (10), 42 (21), 40 (7); **HR-MS (ESI)**: m/z calculated for [C$_{15}$H$_{17}$NO$_3$Na]$^+$ ([M + Na]$^+$):

282.1101, measured: 282.1107; **IR (ATR)**: ν (cm^{-1}): 3024, 2979, 2965, 2913, 2890, 2848, 2926, 1708, 1657, 1485, 1452, 1422, 1370, 1358, 1333, 1296, 1277, 1241, 1220, 1178, 1159, 1133, 1114, 1086, 1067, 1049, 1033, 982, 942, 914, 887, 865, 840, 789, 761, 756, 738, 723, 677, 641.

Cyclohex-1-en-1-yl dimethylcarbamate [49]
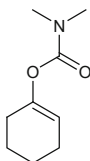
Prepared following **GP13** on a 25.0 mmol scale from cyclohexanone (2.45 g, 25.0 mmol, 1.00 equiv.), NaH (60 % wt in mineral oil, 1.20 g, 30.0 mmol, 1.20 equiv.) and dimethylcarbamyl chloride (2.77 mL, 30.0 mmol, 1.20 equiv.). Purification via flash column chromatography through silica gel (eluent = pentane: ethyl acetate, 6:1) afforded cyclohex-1-en-1-yl dimethylcarbamate (1.21 g, 7.15 mmol, 29 %) as a colorless oil.

R_f **(pentane:ethyl acetate 2:1)**: 0.45; **^{1}H NMR (300 MHz, CDCl$_3$)**: δ (ppm): 5.32–5.35 (m, 1H), 2.92 (s, 3H), 2.91 (s, 3H), 2.05–2.16 (m, 4H), 1.67–1.75 (m, 2H), 1.52–1.60 (m, 2H); **^{13}C NMR (75.5 MHz, CDCl$_3$)**: δ (ppm): 155.1, 148.8, 113.6, 36.5, 36.4, 27.3, 23.8, 22.8, 21.9; **GC-MS**: t_R (50_40): 7.2 min; **EI-MS**: *m/z* (%): 169 (13), 72 (100); **HR-MS (ESI)**: *m/z* calculated for [C$_9$H$_{15}$NO$_2$Na]$^+$ ([M + Na]$^+$): 192.0995, measured: 192.1003; **IR (ATR)**: ν (cm^{-1}): 2931, 1712, 1491, 1447, 1390, 1363, 1272, 1169, 1132, 1071, 1045, 1014, 924, 875, 760, 668, 629.

3,4-Dihydronaphthalen-1-yl methyl carbonate
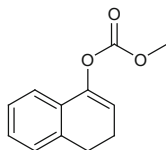
Prepared following a modified procedure from Stoltz et al. [50] 1-Tetralone (439 mg, 3.00 mmol, 1.00 equiv.) was added dropwise over 15 min to a solution of lithium hexamethyldisilazide (LiHMDS, 552 mg, 3.30 mmol, 1.10 equiv.) in THF (7.0 mL) at 0 °C. The mixture was stirred for an additional 1.5 h at 0 °C before being added dropwise to a solution of methyl chloroformate (278 μL, 3.60 mmol, 1.2 equiv.) in THF (17.0 mL) at −78 °C over 15 min. The mixture was allowed to warm to rt and stirred for 16 h before being quenched by pouring into a mixture of dichloromethane (20 mL), water (10 mL) and sat. aq. NH$_4$Cl solution (10 mL). The crude product was extracted into dichloromethane (2 × 20 mL), washed with brine

(40 mL), dried over anhydrous $MgSO_4$, filtered and concentrated under reduced pressure. Purification via flash column chromatography (eluent = pentane:ethyl acetate, 98:2 to 97:3) afforded 3,4-Dihydronaphthalen-1-yl methyl carbonate (310 mg, 1.52 mmol, 51 %) as a colorless viscous oil.

R_f (pentane:ethyl acetate 97:3): 0.16; **^{1}H NMR (300 MHz, CDCl$_3$)**: δ (ppm): 7.13–7.21 (m, 4H), 5.81 (t, J = 4.7 Hz, 1H), 3.88 (s, 3H), 2.87 (t, J = 8.1 Hz, 2H), 2.45 (ddd, J = 8.9, 7.5, 4.7 Hz, 2H); **^{13}C NMR (75.5 MHz, CDCl$_3$)**: δ (ppm): 154.3, 146.3, 136.5, 130.3, 128.2, 127.7, 126.6, 120.8, 115.2, 55.5, 27.5, 22.1; **GC-MS**: t_R (50_40): 8.1 min; **EI-MS**: m/z (%): 205 (11), 204 (86), 159 (38), 146 (11), 145 (94), 144 (29), 129 (148), 128 (72), 127 (18), 117 (54), 116 (24), 115 (100), 105 (11), 91 (31), 90 (12), 89 (17), 63 (10), 59 (14); **HR-MS (ESI)**: m/z calculated for $[C_{12}H_{12}O_3Na]^+$ ($[M + Na]^+$): 227.0679, measured: 227.0681; **IR (ATR)**: ν (cm^{-1}): 2954, 2889, 2836, 1760, 1658, 1489, 1440, 1332, 1249, 1223, 1185, 1135, 1049, 1014, 941, 916, 883, 828, 770, 742, 629, 610.

6.5.2   *Photocatalytic Synthesis of Indolizines*
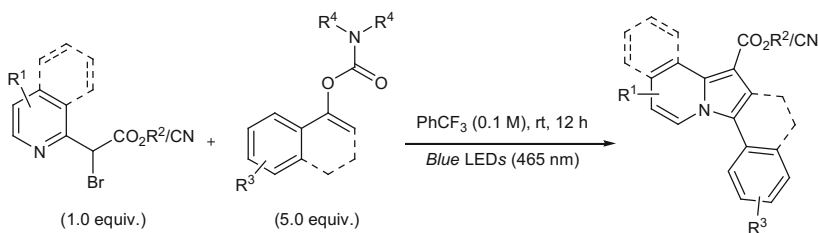
General Procedure 14:

In a flame dried screw capped Schlenk tube equipped with a magnetic stir bar, the enol carbamate (5.0 equiv.) was dissolved in α,α,α-trifluorotoluene (0.10 M) and then the 2-bromopyridine substrate (1.0 equiv.) and hexamethyldisilazane (1.0 equiv.) were added via syringe. The resulting mixture was degassed using three freeze-pump-thaw cycles and the tube was finally backfilled with argon. The reaction mixture was allowed to stir at rt for 12 h under irradiation of visible light from 5 W blue LEDs (λ_{max} = 465 nm). The solvent was removed under reduced pressure and the crude reaction mixture was purified by flash column chromatography through silica gel to afford the pure indolizine products **195**, **205–222**.

Methyl 5,6-dihydrobenzo[*g*]pyrido[1,2-*a*]indole-7-carboxylate (195)
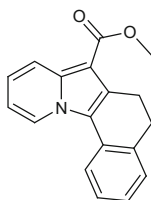
Prepared following **GP14** on a 0.30 mmol scale from methyl 2-bromo-2-(pyridin-2-yl)acetate (69 mg, 0.30 mmol, 1.0 equiv.), 3,4-dihydronaphthalen-1-yl dimethylcarbamate (324 mg, 1.50 mmol, 5.00 equiv.) and hexamethyldisilazane (63 μL, 0.30 mmol, 1.0 equiv.) in α,α,α-trifluorotoluene (3.0 mL, 0.10 M). Purification via flash column chromatography through silica gel (eluent = pentane: ethyl acetate, 20:1) afforded **195** (52 mg, 0.19 mmol, 63 %) as a white solid. Unreacted enol carbamate (262 mg, 1.21 mmol, 4.02 equiv.) was also recovered.

   R_f (pentane:ethyl acetate 9:1): 0.27; **^{1}H NMR (600 MHz, CDCl$_3$)**: δ (ppm): 8.69 (dt, *J* = 7.0, 1.1 Hz, 1H), 8.32 (dt, *J* = 9.0, 1.2 Hz, 1H), 7.74 (d, *J* = 7.7 Hz, 1H), 7.35 (dd, *J* = 7.3, 0.8 Hz, 1H), 7.32 (d, *J* = 7.7, 1.5 Hz, 1H), 7.17 (td, *J* = 7.4, 1.2 Hz, 1H), 7.08 (ddd, *J* = 9.0, 6.7, 1.1 Hz, 1H), 6.83 (td, *J* = 6.8, 1.4 Hz, 1H) 3.93 (s, 3H), 3.20–3.24 (m, 2H), 2.92 (t, *J* = 7.3 Hz, 2H); **^{13}C NMR (150 MHz, CDCl$_3$)**: δ (ppm): 166.0 (C$_q$), 137.5 (C$_q$), 136.7 (C$_q$), 131.1 (C$_q$), 128.8 (CH), 128.7 (C$_q$), 126.7 (CH), 125.8 (CH), 124.0 (CH), 122.6 (C$_q$), 122.1 (CH), 120.4 (CH), 119.3 (CH), 113.2 (CH), 101.5 (C$_q$), 50.9 (CH$_3$), 30.2 (CH$_2$), 22.4 (CH$_2$); **GC-MS**: **t_R (50_40)**: 12.0 min; **EI-MS**: *m/z* (%): 278 (19), 277 (100), 276 (13), 246 (13), 244 (30), 218 (24), 217 (54), 216 (23), 215 (12), 189 (10), 109 (20), 108 (10); **HR-MS (ESI)**: *m/z* calculated for $[C_{18}H_{15}NO_2]^+$ ($[M]^+$): 277.1103, measured: 277.1093; calculated for $[C_{18}H_{15}NO_2Na]^+$ ($[M + Na]^+$): 300.0995, measured: 300.0994; **IR (ATR)**: ν (cm^{-1}): 3055, 3012, 2945, 2902, 2843, 1681, 1632, 1600, 1507, 1488, 1457, 1434, 1395, 1357, 1321, 1283, 1234, 1203, 1146, 1124, 1108, 1069, 1026, 914, 822, 778, 750, 740, 710, 688, 660, 646, 621.

Ethyl 5,6-dihydrobenzo[*g*]pyrido[1,2-*a*]indole-7-carboxylate (205)
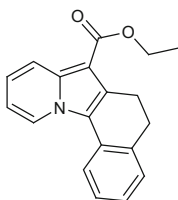
Prepared following **GP14** on a 0.30 mmol scale from ethyl 2-bromo-2-(pyridin-2-yl)acetate (73 mg, 0.30 mmol, 1.0 equiv.), 3,4-dihydronaphthalen-1-yl dimethylcarbamate (324 mg, 1.50 mmol, 5.00 equiv.) and hexamethyldisilazane (63 μL, 0.30 mmol, 1.0 equiv.) in α,α,α-trifluorotoluene (3.0 mL, 0.10 M). Purification via flask column chromatography through silica gel (eluent = pentane:

ethyl acetate, 20:1) afforded **205** (53 mg, 0.18 mmol, 61 %) as a pale yellow oil which solidified upon cooling. Unreacted enol carbamate (260 mg, 1.20 mmol, 3.99 equiv.) was also recovered.

R$_f$ (pentane:ethyl acetate 9:1): 0.45; **^{1}H NMR (300 MHz, CDCl$_3$)**: δ (ppm): 8.67 (d, J = 6.9 Hz, 1H), 8.33 (dt, J = 9.0, 1.2 Hz, 1H), 7.73 (d, J = 7.9 Hz, 1H), 7.32 (td, J = 7.4, 1.4 Hz, 2H), 7.17 (td, J = 7.4, 1.1 Hz, 1H), 7.07 (ddd, J = 9.0, 6.7, 1.0 Hz, 1H), 6.81 (td, J = 6.9, 1.4 Hz, 1H), 4.41 (q, J = 7.1 Hz, 2H), 3.24 (dd, J = 8.2, 6.4 Hz, 2H), 2.92 (t, J = 7.3 Hz, 2H), 1.45 (t, J = 7.1 Hz, 3H); **^{13}C NMR (75.5 MHz, CDCl$_3$)**: δ (ppm): 165.5 (C$_q$), 137.4 (C$_q$), 136.6 (C$_q$), 131.1 (C$_q$), 128.8 (CH), 128.7 (C$_q$), 126.7 (CH), 125.7 (CH), 123.9 (CH),122.5 (C$_q$), 121.9 (CH), 120.4 (CH), 119.3 (CH), 113.0 (CH), 101.7 (CH$_2$), 59.5 (CH$_2$), 30.2 (CH$_2$), 22.3 (CH$_2$), 14.8 (CH$_3$); **GC-MS**: **t$_R$ (50_40)**:11.3 min; **EI-MS**: m/z (%): 292 (21), 291 (100), 263 (25), 262 (21), 246 (12), 244 (25), 219 (10), 218 (36), 217 (58), 216 (21), 215 (11), 92109 (18); **HR-MS (ESI)**: m/z calculated for $[C_{19}H_{17}NO_2Na]^+$ ($[M + Na]^+$): 314.1151, measured: 314.1152; **IR (ATR)**: ν (cm^{-1}): 3056, 2980, 2927, 2905, 1677, 1631, 1599, 1509, 1479, 1453, 1408, 1384, 1357, 1322, 1283, 1232, 1201, 1147, 1124, 1108, 1071, 1031, 985, 949, 837, 823, 778, 751, 742, 722, 717, 687, 656, 650, 624.

tert-Butyl 5,6-dihydrobenzo[_g_]pyrido[1,2-_a_]indole-7-carboxylate (206)
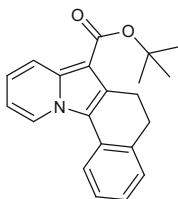
Prepared following **GP14** on a 0.30 mmol scale from _tert_-Butyl 2-bromo-2-(pyridin-2-yl)acetate (82 mg, 0.30 mmol, 1.0 equiv.), 3,4-dihydronaphthalen-1-yl dimethylcarbamate (324 mg, 1.50 mmol, 5.00 equiv.) and hexamethyldisilazane (63 μL, 0.30 mmol, 1.0 equiv.) in α,α,α-trifluorotoluene (3.0 mL, 0.10 M). Purification via flash column chromatography through silica gel (eluent = pentane: ethyl acetate, 20:1) afforded **206** (43 mg, 0.13 mmol, 45 %) as a yellow oil. Unreacted enol carbamate (274 mg, 1.26 mmol, 4.20 equiv.) was also recovered.

R$_f$ (pentane:ethyl acetate 9:1): 0.47; **^{1}H NMR (300 MHz, CDCl$_3$)**: δ (ppm): 8.67 (dt, J = 7.1, 1.1 Hz, 1H), 8.31 (dt, J = 9.0, 1.3 Hz, 1H), 7.72–7.75 (m, 1H), 7.28–7.36 (m, 2H), 7.16 (td, J = 7.5, 1.2 Hz, 1H), 7.05 (ddd, J = 9.1, 6.7, 1.1 Hz, 1H), 6.79 (td, J = 6.9, 1.5 Hz, 1H), 3.23 (dd, J = 8.2, 6.4 Hz, 2H), 2.92 (t, J = 7.3 Hz, 1H), 1.67 (s, 9H); **^{13}C NMR (75.5 MHz, CDCl$_3$)**: δ (ppm): 165.0 (C$_q$), 137.2 (C$_q$), 136.6 (C$_q$), 131.1 (C$_q$), 128.8 (CH), 126.7 (CH), 125.6 (CH), 123.8 (CH), 122.3 (C$_q$), 121.6 (CH), 120.3 (CH), 119.2 (CH), 112.9 (CH), 103.1 (C$_q$), 79.9 (C$_q$), 30.3 (CH$_2$), 28.9 (CH$_3$), 22.3 (CH$_2$); **GC-MS**: **t$_R$ (50_40)**: 9.8 min;

EI-MS: *m/z* (%): 220 (12), 219 (100), 218 (70), 217 (41), 207 (11); **HR-MS (ESI)**: *m/z* calculated for $[C_{21}H_{21}NO_2Na]^+$ ($[M + Na]^+$): 342.1465, measured: 342.1464; **IR (ATR)**: ν (cm^{-1}): 3059, 2974, 2932, 2893, 2838, 2360, 2340, 1678, 1631, 1602, 1530, 1505, 1488, 1453, 1440, 1399, 1365, 1322, 1281, 1243, 1223, 1203, 1168, 1155, 1122, 1107, 1069, 1016, 988, 947, 880, 837, 784, 755, 732, 702, 687, 659, 638, 622.

Benzyl 5,6-dihydrobenzo[*g*]pyrido[1,2-*a*]indole-7-carboxylate (207)
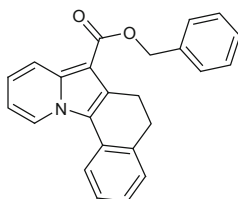
Prepared following **GP14** on a 0.20 mmol scale from benzyl 2-bromo-2-(pyridin-2-yl)acetate (61 mg, 0.20 mmol, 1.0 equiv.), 3,4-dihydronaphthalen-1-yl dimethylcarbamate (217 mg, 1.00 mmol, 5.00 equiv.) and hexamethyldisilazane (42 μL, 0.20 mmol, 1.0 equiv.) in α,α,α-trifluorotoluene (2.0 mL, 0.10 M). Purification via flash column chromatography through silica gel (eluent = pentane: ethyl acetate, 20:1) afforded **207** (34 mg, 96 μmol, 48 %) as a light yellow oil. Unreacted enol carbamate (180 mg, 829 μmol, 4.14 equiv.) was also recovered.

R_f **(pentane:ethyl acetate 9:1)**: 0.54; **^{1}H NMR (300 MHz, C$_6$D$_6$)**: δ (ppm): 8.68 (dt, *J* = 9.0, 1.3 Hz, 1H), 8.18 (dd, *J* = 7.1, 1.2 Hz, 1H), 7.34–7.49 (m, 3H), 7.18–7.27 (m, 5H), 7.06–7.15 (m, 1H), 6.69 (ddd, *J* = 9.0, 6.7, 1.0 Hz, 1H), 6.26 (td, *J* = 6.9, 1.4 Hz, 1H), 5.47 (s, 2H), 3.37 (dd, *J* = 8.1, 6.6 Hz, 2H), 2.73 (t, *J* = 7.3 Hz, 2H); **^{13}C NMR (75 MHz, C$_6$D$_6$)**: δ (ppm): 164.8 (C$_q$), 137.9 (C$_q$), 137.8 (C$_q$), 137.7 (C$_q$), 131.3 (C$_q$), 128.9 (C$_q$), 128.9 (CH), 128.7 (CH), 128.4 (CH), 126.7 (CH), 125.8 (CH), 123.8 (CH), 122.7 (C$_q$), 121.8 (CH), 120.6 (CH), 119.5 (CH), 112.9 (CH), 102.1 (C$_q$), 65.4 (CH$_2$), 30.3 (CH$_2$), 22.8 (CH$_2$) [Note: one peak at δ (ppm) = 128.0 (CH) overlaps with the benzene carbon peak, but is observed in the DEPT spectrum]; **GC-MS: t$_R$ (50_40)**: 15.0 min; **EI-MS**: *m/z* (%): 354 (27), 353 (100), 263 (10), 262 (43), 246 (13), 244 (29), 219 (28), 218 (72), 217 (100), 216 (29), 215 (12), 203 (10), 190 (10), 189 (11), 116 (15), 91 (47), 73 (10), 65 (15); **HR-MS (ESI)**: *m/z* calculated for $[C_{24}H_{19}NO_2]^+$ ($[M]^+$): 353.1410, measured: 353.1439, *m/z* calculated for $[C_{24}H_{19}NO_2Na]^+$ ($[M + Na]^+$): 376.1308, measured: 376.1302; **IR (ATR)**: ν (cm^{-1}): 3032, 2941, 2890, 2834, 1736, 1683, 1631, 1602, 1504, 1454, 1439, 1403, 1368, 1322, 1280, 1228, 1202, 1184, 1159, 1123, 1107, 1066, 1019, 780, 755, 739, 697, 631.

**5,6-Dihydrobenzo[*g*]pyrido[1,2-*a*]indole-7-carbonitrile (208)**
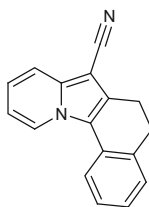
Prepared following **GP14** on a 0.30 mmol scale from 2-bromo-2-(pyridin-2-yl) acetonitrile (59 mg, 0.30 mmol, 1.0 equiv.), 3,4-dihydronaphthalen-1-yl diethyl-carbamate (368 mg, 1.50 mmol, 5.00 equiv.) and hexamethyldisilazane (63 μL, 0.30 mmol, 1.0 equiv.) in α,α,α-trifluorotoluene (3.0 mL, 0.10 M). Purification via flash column chromatography through silica gel (eluent = pentane:ethyl acetate, 20:1) afforded **208** (12 mg, 49 μmol, 16 %) as a white solid. Unreacted enol car-bamate (280 mg, 1.14 mmol, 3.80 equiv.) was also recovered.

  R$_f$ (pentane:ethyl acetate 9:1): 0.24; **^{1}H NMR (400 MHz, CDCl$_3$)**: δ (ppm): 8.67 (dt, *J* = 7.1, 1.1 Hz, 1H), 7.60–7.78 (m, 2H), 7.30–7.40 (m, 2H), 7.20 (td, *J* = 7.5, 1.2 Hz, 1H), 7.09 (ddd, *J* = 8.9, 6.7, 1.0 Hz, 1H), 6.87 (td, *J* = 6.9, 1.4 Hz, 1H), 2.90–3.03 (m, 4H); **^{13}C NMR (101 MHz, CDCl$_3$)**: δ (ppm): 138.6 (C$_q$), 136.3 (C$_q$), 131.0 (C$_q$), 129.2 (CH), 128.1 (C$_q$), 127.0 (CH), 126.5 (CH), 124.5 (CH), 122.3 (C$_q$), 122.0 (CH), 119.6 (CH), 118.2 (CH), 116.4 (C$_q$), 113.7 (CH), 81.8 (C$_q$), 29.9 (CH$_2$), 21.7 (CH$_2$); **GC-MS**: **t$_R$ (50_40)**: 11.6 min; **EI-MS**: *m/z* (%): 245 (17), 244 (100), 243 (50), 242 (39); **HR-MS (EI)**: *m/z* calculated for [C$_{17}$H$_{12}$N$_2$Na]$^+$ ([M + Na]$^+$): 267.0893, measured: 267.0891; **IR (ATR)**: ν (cm^{-1}): 2209, 1511, 1487, 1438, 1396, 1207, 1144, 1023, 744, 721, 687.

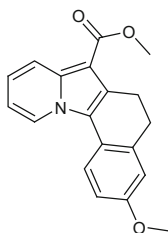**Methyl 3-methoxy-5,6-dihydrobenzo[*g*]pyrido[1,2-*a*]indole-7-carboxylate (209)**

Prepared following **GP14** on a 0.30 mmol scale from methyl 2-bromo-2-(pyridin-2-yl)acetate (69 mg, 0.30 mmol, 1.0 equiv.), 6-methoxy-3,4-dihydronaphthalen-1-yl dimethylcarbamate (371 mg, 1.50 mmol, 5.00 equiv.) and hexamethyldisilazane (63 μL, 0.30 mmol, 1.0 equiv.) in α,α,α-trifluorotoluene (3.0 mL, 0.10 M). Purification via flash column chromatography through silica gel (eluent = pentane:ethyl acetate, 20:1 to 5:1) afforded **209** (62 mg, 0.20 mmol, 67 %) as a pale yellow solid. Unreacted enol carbamate (298 mg, 1.21 mmol, 4.02 equiv.) was also recovered.

R$_f$ (pentane:ethyl acetate 20:1): 0.22; **^{1}H NMR (300 MHz, CDCl$_3$)**: δ (ppm): 8.61 (dt, J = 7.1 Hz, 1H), 8.29 (dd, J = 9.1, 1.2 Hz, 1H), 7.66 (d, J = 8.5 Hz, 1H), 7.04 (ddd, J = 9.0, 6.7, 1.0 Hz, 1H), 6.94 (d, J = 2.6 Hz, 1H), 6.76–6.88 (m, 2H), 3.92 (s, 3H), 3.85 (s, 3H), 3.21 (dd, J = 8.2, 6.4 Hz, 2H), 2.90 (dd, J = 8.3, 6.2 Hz, 2H); **^{13}C NMR (75.5 MHz, CDCl$_3$)**: δ (ppm): 166.0 (C$_q$), 157.6 (C$_q$), 138.8 (C$_q$), 136.9 (C$_q$), 129.4 (C$_q$), 123.6 (CH), 122.5 (C$_q$), 121.8 (C$_q$), 121.5 (CH), 120.5 (CH), 120.3 (CH), 115.2 (CH), 113.0 (CH), 111.2 (CH), 101.2 (C$_q$), 55.4 (CH$_3$), 50.8 (CH$_3$), 30.7 (CH$_2$), 22.3 (CH$_2$); **GC-MS: t$_R$ (50_40)**: 14.4 min; **EI-MS**: m/z (%): 308 (20), 307 (100), 293 (10), 292 (55), 276 (7), 274 (5), 253 (5), 249 (6), 232 (12), 205 (8), 204 (29), 203 (11), 177 (8), 137 (5), 135 (6), 102 (8), 75 (5), 73 (12), 59 (6); **HR-MS (ESI)**: m/z calculated for [C$_{19}$H$_{17}$NO$_3$]$^+$ ([M]$^+$): 307.1203, measured: 307.1195, m/z calculated for [C$_{19}$H$_{17}$NO$_3$Na]$^+$ ([M + Na]$^+$): 330.1101, measured: 330.1098; **IR (ATR)**: ν (cm^{-1}): 3079, 3056, 3013, 2977, 2945, 2902, 2840, 1680, 1632, 1600, 1506, 1490, 1457, 1434, 1395, 1355, 1321, 1282, 1232, 1201, 1192, 1100, 1145, 1123, 1108, 1068, 1025, 1006, 968, 821, 778, 748, 740, 722, 710, 687, 660, 644, 622.

Methyl   10-bromo-3-methoxy-5,6-dihydrobenzo[g]pyrido[1,2-a]indole-7-carboxylate (218)

Prepared following **GP14** on a 0.20 mmol scale from methyl 2-bromo-2-(5-bromopyridin-2-yl)acetate   (62 mg,   0.20 mmol,   1.0   equiv.), 6-methoxy-3,4-dihydronaphthalen-1-yl dimethylcarbamate (247 mg, 1.00 mmol, 5.00 equiv.) and hexamethyldisilazane (42 μL, 0.20 mmol, 1.0 equiv.) in α,α,α-trifluorotoluene (2.0 mL, 0.10 M). Purification via flash column chromatography through silica gel (eluent = pentane:ethyl acetate, 20:1) afforded **218** (57 mg, 0.15 mmol, 74 %) as a yellow solid. Unreacted enol carbamate (203 mg, 821 μmol, 4.10 equiv.) was also recovered.
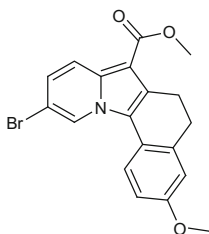
R$_f$ (pentane:ethyl acetate 9:1): 0.36; **^{1}H NMR (400 MHz, C$_6$D$_6$)**: δ (ppm): 8.31–8.34 (m, 1H), 8.30 (dd, J = 9.5, 0.8 Hz, 1H), 8.14 (d, J = 8.5 Hz, 1H), 6.79 (d, J = 2.7 Hz, 1H), 6.72 (dd, J = 9.5, 1.6 Hz, 1H), 6.50 (dd, J = 8.5, 2.7 Hz, 1H), 3.65 (s, 3H), 3.38 (s, 3H), 3.10–3.31 (m, 2H), 2.64 (t, J = 7.3 Hz, 2H); **^{13}C NMR (101 MHz, C$_6$D$_6$)**: δ (ppm): 165.2 (C$_q$), 158.4 (C$_q$), 139.0 (C$_q$), 135.0 (C$_q$), 129.8 (C$_q$), 123.7 (CH), 123.5 (CH), 123.2 (C$_q$), 121.4 (C$_q$), 121.1 (CH), 121.0 (CH), 115.5 (CH), 111.5 (CH), 108.1 (C$_q$), 103.2 (C$_q$), 54.9 (CH$_3$), 50.5 (CH$_3$), 30.6 (CH$_2$), 22.7 (CH$_2$); **GC-MS: t$_R$ (50_40)**: 13.4 min; **EI-MS**: m/z (%): 388 (21), 387 (95), 386 (22), 385 (100), 373 (10), 372 (45), 371 (11), 370 (44), 354 (11), 312

(11), 310 (10), 284 (13), 204 (17), 203 (21), 202 (19), 177 (10), 176 (12), 102 (13), 101 (12); **HR-MS (ESI)**: m/z calculated for $[C_{19}H_{16}Br^{79}NO_3]^+$ ($[M]^+$): 385.0308, measured: 385.0309, m/z calculated for $[C_{19}H_{16}Br^{79}NO_3Na]^+$ ($[M + Na]^+$): 408.0206, measured: 408.0209; **IR (ATR)**: ν (cm^{-1}): 3009, 2944, 2906, 2834, 1694, 1616, 1577, 1520, 1437, 1414,1391, 1332, 1312, 1298, 1281, 1265, 1253, 1235, 1167, 1125, 1076, 1057, 1045, 984, 966, 917, 896, 874, 813, 792, 765, 730, 717, 702, 685, 648, 590.

Methyl 10-fluoro-3-methoxy-5,6-dihydrobenzo[g]pyrido[1,2-a]indole-7-carboxylate (219)
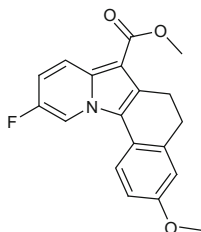

Prepared following **GP14** on a 0.20 mmol scale from methyl 2-bromo-2-(5-fluoropyridin-2-yl)acetate (50 mg, 0.20 mmol, 1.0 equiv.), 6-methoxy-3,4-dihydronaphthalen-1-yl dimethylcarbamate (247 mg, 1.00 mmol, 5.00 equiv.) and hexamethyldisilazane (42 μL, 0.20 mmol, 1.0 equiv.) in α,α,α-trifluorotoluene (2.0 mL, 0.10 M). Purification via flash column chromatography through silica gel (eluent = pentane:ethyl acetate, 20:1) afforded **219** (36 mg, 0.11 mmol, 55 %) as a yellowish brown solid. Unreacted enol carbamate (198 mg, 801 μmol, 4.01 equiv.) was also recovered.

R$_f$ (pentane:ethyl acetate 9:1): 0.25; **^{1}H NMR (300 MHz, C$_6$D$_6$)**: δ (ppm): 8.38 (ddd, J = 9.8, 6.1, 0.7 Hz, 1H), 8.07 (ddd, J = 5.8, 2.4, 0.7 Hz, 1H), 7.12 (d, J = 8.5 Hz, 1H), 6.79 (d, J = 2.6 Hz, 1H), 6.62 (dd, J = 8.5, 2.7 Hz, 1H), 6.51 (ddd, J = 9.9, 7.7, 2.1 Hz, 1H), 3.66 (s, 3H), 3.39 (s, 3H), 3.23–3.28 (m, 2H), 2.64 (t, J = 7.3 Hz, 2H); **^{13}C NMR (75.5 MHz, C$_6$D$_6$)**: δ (ppm): 165.2 (C$_q$), 158.3 (C$_q$), 154.3 (d, J = 235.0 Hz, C$_q$), 138.9 (C$_q$), 134.4 (C$_q$), 130.2 (d, J = 235.0 Hz, C$_q$), 123.7 (d, J = 1.8 Hz, C$_q$), 121.5 (C$_q$), 121.1 (d, J = 235.0 Hz, CH), 120.8 (CH), 115.3 (CH), 112.2 (d, J = 24.6 Hz, CH), 111.7 (CH), 110.2 (d, J = 41.30 Hz, CH), 103.0 (C$_q$), 54.9 (CH$_3$), 50.5 (CH$_3$), 30.7 (CH$_2$), 22.8 (CH$_2$); **^{19}F NMR (282 MHz, CDCl$_3$)**: −139.74; **GC-MS: t$_R$ (50_40)**: 13.4 min; **EI-MS**: m/z (%): 326 (21), 325 (100), 311 (10), 310 (51), 250 (13), 222 (26); **HR-MS (ESI)**: m/z calculated for $[C_{19}H_{16}FNO_3]^+$ ($[M]^+$): 325.1114, measured: 325.1110, m/z calculated for $[C_{19}H_{16}FNO_3Na]^+$ ($[M + Na]^+$): 348.1006, measured: 348.1006; **IR (ATR)**: ν (cm^{-1}): 3090, 2990, 2954, 2939, 2909, 2835, 1697, 1646, 1601, 1580, 1534, 1498, 1470,1437, 1425, 1397, 1351, 1334, 1306, 1287, 1248, 1202, 1186, 1153, 1108, 1071, 1036, 996, 947, 942, 898, 862, 847, 791, 742, 719, 696, 650, 614.

Methyl   3-methoxy-10-(trifluoromethyl)-5,6-dihydrobenzo[*g*]pyrido[1,2-*a*] indole-7-carboxylate (220)
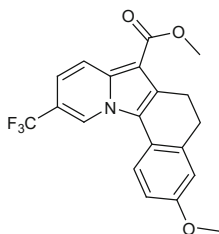
Prepared following **GP14** on a 0.20 mmol scale from methyl 2-bromo-2-(5-(tri-fluoromethyl)pyridin-2-yl)acetate   (60 mg,   0.20 mmol,   1.0   equiv.), 6-methoxy-3,4-dihydronaphthalen-1-yl dimethylcarbamate (247 mg, 1.00 mmol, 5.00 equiv.) and hexamethyldisilazane (42 μL, 0.20 mmol, 1.0 equiv.) in α,α,α-trifluorotoluene (2.0 mL, 0.10 M). Purification via flash column chromatography through silica gel (eluent = pentane:ethyl acetate, 20:1) afforded **220** (49 mg, 0.13 mmol, 65 %) as a yellow solid. Unreacted enol carbamate (198 mg, 801 μmol, 4.01 equiv.) was also recovered.

R$_f$ (pentane:ethyl acetate 9:1): 0.29; **^{1}H NMR (400 MHz, C$_6$D$_6$)**: δ (ppm): 8.49 (q, *J* = 1.4 Hz, 1H), 8.41 (dt, *J* = 9.4, 0.9 Hz, 1H), 6.82 (d, *J* = 2.6 Hz, 1H), 6.75 (dd, *J* = 9.4, 1.6 Hz, 1H), 6.50 (dd, *J* = 8.5, 2.7 Hz, 1H), 3.65 (s, 3H), 3.37 (s, 3H), 3.25 (dd, *J* = 8.1, 6.5 Hz, 2H), 2.64 (t, *J* = 7.3 Hz, 2H) [*one proton peak partially overlaps with benzene proton peak at* δ (ppm) = 7.16]; **^{13}C NMR (101 MHz, C$_6$D$_6$)**: δ (ppm): 165.1 (C$_q$), 158.6 (C$_q$), 139.1 (C$_q$), 136.3 (C$_q$), 130.7 (C$_q$), 124.6 (q, *J* = 271.2 Hz, C$_q$), 124.2 (C$_q$), 122.0 (q, *J* = 6.2 Hz, CH), 121.2 (CH), 121.1 (CH), 121.0 (C$_q$), 116.7 (q, *J* = 33.5 Hz, C$_q$), 116.0 (q, *J* = 2.5 Hz, CH), 115.8 (CH), 111.5 (CH), 103.9 (C$_q$), 54.9 (CH$_3$), 50.7 (CH$_3$), 30.5 (CH$_2$), 22.6 (CH$_2$); **^{19}F NMR (282 MHz, CDCl$_3$)**: −62.05; **GC-MS**: t$_R$ (50_40): 12.3 min; **EI-MS**: *m/z* (%): 376 (22), 375 (100), 360 (44), 300 (11), 272 (16); **HR-MS (ESI)**: *m/z* calculated for [C$_{20}$H$_{16}$F$_3$NO$_3$Na]$^+$ ([M + Na]$^+$): 398.0974, measured: 398.0984; **IR (ATR)**: ν (cm^{-1}): 2944, 2837, 2358, 1690, 1645, 1617, 1579, 1516, 1498, 1432,1406, 1363, 1341, 1325, 1307, 1250, 1214, 1162, 1120, 1077, 1053, 1037, 983, 955, 888, 865, 831, 817, 805, 773, 716, 702, 682, 651, 637, 599.

Methyl   3-methoxy-10-methyl-5,6-dihydrobenzo[*g*]pyrido[1,2-*a*]indole-7-carboxylate (217)
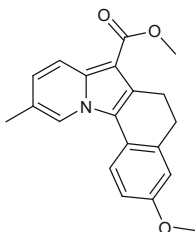
Prepared following **GP14** on a 0.20 mmol scale from methyl 2-bromo-2-(5-methylpyridin-2-yl)acetate (49 mg, 0.20 mmol, 1.0 equiv.), 6-methoxy-3,4-dihydronaphthalen-1-yl dimethylcarbamate (247 mg, 1.00 mmol, 5.00 equiv.) and hexamethyldisilazane (42 μL, 0.20 mmol, 1.0 equiv.) in α,α,α-trifluorotoluene (2.0 mL, 0.10 M). Purification via flash column chromatography through silica gel (eluent = pentane:ethyl acetate, 20:1) afforded **217** (42 mg, 0.13 mmol, 65 %) as a pale yellow solid. Unreacted enol carbamate (198 mg, 801 μmol, 4.01 equiv.) was also recovered.

R$_f$ (pentane:ethyl acetate 9:1): 0.29; **^{1}H NMR (600 MHz, C$_6$D$_6$)**: δ (ppm): 8.57 (d, *J* = 9.1 Hz, 1H), 8.06 (d, *J* = 1.2 Hz, 1H), 7.46 (d, *J* = 8.5 Hz, 1H), 6.85 (d, *J* = 2.7 Hz, 1H), 6.74 (dd, *J* = 8.4, 2.7 Hz, 1H), 6.54 (dd, *J* = 9.1, 1.4 Hz, 1H), 3.71 (s, 3H), 3.41 (s, 3H), 3.34–3.38 (m, 2H), 2.72 (t, *J* = 7.3 Hz, 2H), 1.82 (s, 3H); **^{13}C NMR (150 MHz, C$_6$D$_6$)**: δ (ppm): 165.6 (C$_q$), 158.1 (C$_q$), 139.1 (C$_q$), 136.2 (C$_q$), 129.4 (C$_q$), 128.4 (CH), 124.2 (CH), 122.4 (C$_q$), 122.2 (C$_q$), 121.5 (CH), 121.0 (CH), 120.2 (C$_q$), 115.4 (CH), 111.7 (CH), 102.0 (C$_q$), 54.9 (CH$_3$), 50.4 (CH$_3$), 31.0 (CH$_2$), 23.0 (CH$_2$), 18.3 (CH$_3$); **GC-MS: t$_R$ (50_40)**: 15.4 min; **EI-MS**: *m/z* (%): 322 (21), 321 (100), 307 (11), 306 (59), 246 (10), 218 (21); **HR-MS (ESI)**: *m/z* calculated for [C$_{20}$H$_{19}$NO$_3$]$^+$ ([M]$^+$): 321.1359, measured: 321.1359, *m/z* calculated for [C$_{20}$H$_{19}$NO$_3$Na]$^+$ ([M + Na]$^+$): 344.1257, measured: 344.1254; **IR (ATR)**: ν (cm^{-1}): 3023, 2978, 2948, 2899, 2830, 1682, 1609, 1581, 1540, 1512, 1495, 1465, 1436, 1399, 1342, 1308, 1301, 1274, 1246, 1219, 1185, 1172, 1129, 1101, 1069, 1031, 981, 958, 920, 903, 847, 797, 779, 695, 655, 621, 597.

Methyl   3-methoxy-10-phenyl-5,6-dihydrobenzo[*g*]pyrido[1,2-*a*]indole-7-carboxylate (216)
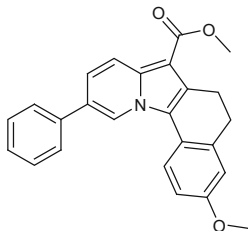
Prepared following **GP14** on a 0.20 mmol scale from methyl 2-bromo-2-(5-phenylpyridin-2-yl)acetate (61 mg, 0.20 mmol, 1.0 equiv.), 6-methoxy-3,4-dihydronaphthalen-1-yl dimethylcarbamate (247 mg, 1.00 mmol, 5.00 equiv.) and hexamethyldisilazane (42 μL, 0.20 mmol, 1.0 equiv.) in α,α,α-trifluorotoluene (2.0 mL, 0.10 M). Purification via flash column chromatography through silica gel (eluent = pentane:ethyl acetate, 20:1) afforded **216** (47 mg, 0.12 mmol, 61 %) as a yellow solid. Unreacted enol carbamate (203 mg, 821 μmol, 4.10 equiv.) was also recovered.

R$_f$ (pentane:ethyl acetate 9:1): 0.26; **^{1}H NMR (300 MHz, CD$_2$Cl$_2$)**: δ (ppm): 8.74 (t, *J* = 1.5 Hz, 1H), 8.24 (dd, *J* = 9.3, 0.9 Hz, 1H), 7.47 (d, *J* = 8.5 Hz, 1H),

7.51–7.59 (m, 2H), 7.36–7.47 (m, 2H), 7.29–7.36 (m, 1H), 7.25 (dd, J = 9.3, 1.6 Hz, 1H), 6.87 (d, J = 2.6 Hz, 1H), 6.78 (dd, J = 8.5, 2.8 Hz, 1H), 3.81 (s, 3H), 3.75 (s, 3H), 3.06–3.15 (m, 2H), 2.82 (t, J = 7.3 Hz, 2H); **^{13}C NMR (75.5 MHz, CD$_2$Cl$_2$)**: δ (ppm): 166.0 (C$_q$), 158.3 (C$_q$), 139.4 (C$_q$), 138.5 (C$_q$), 136.2 (C$_q$), 130.2 (C$_q$), 129.6 (CH), 128.3 (CH), 127.6 (C$_q$), 127.5 (CH), 123.4 (C$_q$), 122.2 (CH), 122.1 (C$_q$), 121.7 (CH), 121.1 (CH), 120.3 (CH), 115.6 (CH), 111.7 (CH), 101.8 (C$_q$), 55.8 (CH$_3$), 51.1 (CH$_3$), 31.1 (CH$_2$), 27.8 (CH$_2$); **GC-MS**: t_R (50_40): 14.6 min; **EI-MS**: m/z (%): 384 (30), 383 (100), 368 (36), 323 (18), 308 (10), 281 (19), 280 (16), 265 (11), 165 (13), 145 (10), 139 (11), 73 (16); **HR-MS (ESI)**: m/z calculated for $[C_{25}H_{21}NO_3]^+$ ($[M]^+$): 383.1516, measured: 383.1510, m/z calculated for $[C_{25}H_{21}NO_3Na]^+$ ($[M + Na]^+$): 406.1414, measured: 406.1406; **IR (ATR)**: ν (cm^{-1}): 3074, 3032, 2958, 2934, 2906, 2836, 2362, 1676, 1607, 1582, 1540, 1508, 1489, 1433,1397, 1350, 1339, 1315, 1289, 1248, 1214, 1200, 1177, 1143, 1107, 1072, 1033, 996, 982, 955, 899, 879, 806, 779, 753, 699, 655, 637, 606, 591.

Methyl 9-chloro-3-methoxy-5,6-dihydrobenzo[*g*]pyrido[1,2-*a*]indole-7-carboxylate (214)
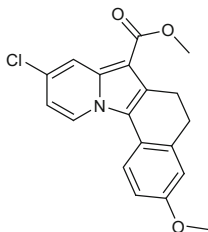

Prepared following **GP14** on a 0.20 mmol scale from methyl 2-bromo-2-(4-chloropyridin-2-yl)acetate (53 mg, 0.20 mmol, 1.0 equiv.), 6-methoxy-3,4-dihydronaphthalen-1-yl dimethylcarbamate (247 mg, 1.00 mmol, 5.00 equiv.) and hexamethyldisilazane (42 μL, 0.20 mmol, 1.0 equiv.) in α,α,α-trifluorotoluene (2.0 mL, 0.10 M). Purification via flash column chromatography through silica gel (eluent = pentane:ethyl acetate, 20:1) afforded **214** (51 mg, 0.15 mmol, 75 %) as a yellow solid. Unreacted enol carbamate (197 mg, 797 μmol, 3.98 equiv.) was also recovered.

R$_f$ (pentane:ethyl acetate 9:1): 0.25; **^{1}H NMR (400 MHz, C$_6$D$_6$)**: δ (ppm): 8.63 (dd, J = 2.4, 0.8 Hz, 1H), 7.76 (d, J = 7.2 Hz, 1H), 7.13 (d, J = 8.5 Hz, 1H), 6.79 (d, J = 2.7 Hz, 1H), 6.73 (dd, J = 8.5, 2.7 Hz, 1H), 6.23 (dd, J = 7.4, 2.4 Hz, 1H), 3.60 (s, 3H), 3.40 (s, 3H), 3.27 (dd, J = 8.1, 6.6 Hz, 2H), 2.64 (t, J = 7.3 Hz, 2H); **^{13}C NMR (101 MHz, C$_6$D$_6$)**: δ (ppm): 165.1 (C$_q$), 158.4 (C$_q$), 139.0 (C$_q$), 136.7 (C$_q$), 130.2 (C$_q$), 124.0 (CH), 123.0 (C$_q$), 121.6 (C$_q$), 120.9 (CH), 119.5 (CH), 115.3 (CH), 113.8 (CH), 111.8 (CH), 102.4 (C$_q$), 54.9 (CH$_3$), 50.5 (CH$_3$), 30.7 (CH$_2$), 22.6 (CH$_2$) [*Note: one C$_q$ peak overlaps with the benzene carbon*

peak]; **GC-MS**: **t$_R$ (50_40)**: 16.6 min; **EI-MS**: *m/z* (%): 343 (35), 342 (22), 341 (100), 328 (19), 327 (11), 326 (51), 266 (10), 238 (15); **HR-MS (ESI)**: *m/z* calculated for $[C_{19}H_{16}ClNO_3Na]^+$ ($[M + Na]^+$): 364.0711, measured: 364.0710; **IR (ATR)**: ν (cm^{-1}): 3076, 2990, 2953, 2932, 2895, 2832, 1687, 1607, 1582, 1527, 1503, 1498, 1462, 1439, 1424, 1381, 1364, 1332, 1310, 1246, 1203, 1180, 1119, 1091, 1051, 1029, 994, 965, 894, 881, 863, 806, 761, 739, 711, 679, 660, 624, 594.

Methyl 3-methoxy-9-methyl-5,6-dihydrobenzo[*g*]pyrido[1,2-*a*]indole-7-carboxylate (213)
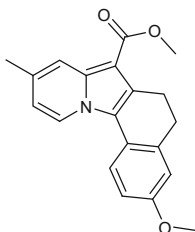

Prepared following **GP14** on a 0.20 mmol scale from methyl 2-bromo-2-(4-methylpyridin-2-yl)acetate (49 mg, 0.20 mmol, 1.0 equiv.), 6-methoxy-3,4-dihydronaphthalen-1-yl dimethylcarbamate (247 mg, 1.00 mmol, 5.00 equiv.) and hexamethyldisilazane (42 µL, 0.20 mmol, 1.0 equiv.) in α,α,α-trifluorotoluene (2.0 mL, 0.10 M). Purification via flash column chromatography through silica gel (eluent = pentane:ethyl acetate, 20:1) afforded **213** (44 mg, 0.14 mmol, 68 %) as a greenish yellow solid. Unreacted enol carbamate (192 mg, 776 µmol, 3.88 equiv.) was also recovered.

R$_f$ (pentane:ethyl acetate 9:1): 0.17; **^{1}H NMR (400 MHz, C$_6$D$_6$)**: δ (ppm): 8.47 (dt, *J* = 2.2, 1.1 Hz, 1H), 8.08 (d, *J* = 7.1 Hz, 1H), 7.33 (d, *J* = 8.5 Hz, 1H), 6.83 (d, *J* = 2.5 Hz, 1H), 6.75 (dd, *J* = 8.4, 2.8 Hz, 1H), 6.11 (dd, *J* = 7.2, 2.0 Hz, 1H), 3.72 (s, 3H), 3.42 (s, 3H), 3.31–3.37 (m, 2H), 2.71 (t, *J* = 7.3 Hz, 2H) 2.01 (s, 3H); **^{13}C NMR (101 MHz, C$_6$D$_6$)**: δ (ppm): 165.7 (C$_q$), 158.0 (C$_q$), 138.8 (C$_q$), 137.9 (C$_q$), 132.0 (C$_q$), 129.3 (C$_q$), 123.1 (CH), 122.4 (C$_q$), 122.2 (C$_q$), 120.7 (CH), 119.5 (CH), 115.3 (CH), 115.2 (CH), 111.7 (CH), 100.9 (C$_q$), 54.9 (CH$_3$), 50.4 (CH$_3$), 31.0 (CH$_2$), 22.9 (CH$_2$), 21.0 (CH$_3$); **GC-MS**: **t$_R$ (50_40)**: 15.6 min; **EI-MS**: *m/z* (%): 322 (24), 321 (100), 307 (13), 306 (63), 246 (11), 218 (17), 217 (10); **HR-MS (ESI)**: *m/z* calculated for $[C_{20}H_{19}NO_3]^+$ ($[M]^+$): 321.1359, measured: 321.1359, *m/z* calculated for $[C_{20}H_{19}NO_3Na]^+$ ($[M + Na]^+$): 344.1257, measured: 344.1253; **IR (ATR)**: ν (cm^{-1}): 3069, 3001, 2978, 2942, 2910, 2836, 1674, 1639, 1604, 1578, 1522, 1499, 1454, 1426, 1382, 1348, 1318, 1278, 1241, 1203, 1180, 1160, 1132, 1103, 1060, 1034, 983, 937, 902, 876, 845, 808, 771, 710, 669, 632, 604.

Methyl   10-methoxy-12,13-dihydrobenzo[6,7]indolo[2,1-*a*]isoquinoline-14-carboxylate (215)
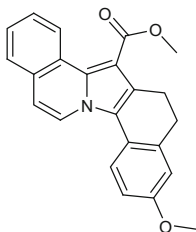
Prepared following **GP14** on a 0.20 mmol scale from methyl 2-bromo-2-(isoquinolin-1-yl)acetate   (56 mg,   0.20 mmol,   1.0   equiv.),   6-methoxy-3,4-dihydronaphthalen-1-yl dimethylcarbamate (247 mg, 1.00 mmol, 5.00 equiv.) and hexamethyldisilazane (42 μL, 0.20 mmol, 1.0 equiv.) in α,α,α-trifluorotoluene (2.0 mL, 0.10 M). Purification via flash column chromatography through silica gel (eluent = pentane:ethyl acetate, 20:1) afforded **213** (30.0 mg, 0.084 mmol, 42 %) as a pale yellow solid. Unreacted enol carbamate (208 mg, 841 μmol, 4.21 equiv.) was also recovered.

R_f (pentane:ethyl acetate 9:1): 0.18; **^{1}H NMR (300 MHz, CDCl$_3$)**: δ (ppm): 9.22 (ddt, *J* = 8.5, 1.4, 0.7 Hz, 1H), 8.41 (d, *J* = 7.4 Hz, 1H), 7.58–7.70 (m, 2H), 7.54 (ddd, *J* = 8.5, 7.1, 1.6 Hz, 1H), 7.45 (ddd, *J* = 7.7, 7.1, 1.3 Hz, 1H), 6.91–7.02 (m, 2H), 6.85 (dd, *J* = 8.5, 2.7 Hz, 1H), 3.99 (s, 3H), 3.85 (s, 3H), 3.00–3.14 (m, 2H), 2.90 (dd, *J* = 8.4, 5.9 Hz, 2H); **^{13}C NMR (75.5 MHz, CDCl$_3$)**: δ (ppm): 167.2 (C_q), 157.9 (C_q), 139.2 (C_q), 131.8 (C_q), 128.5 (C_q), 127.5 (CH), 127.0 (C_q), 127.0 (CH), 126.8 (CH), 126.1 (CH), 125.9 (C_q), 124.1 (C_q), 122.2 (CH), 121.3 (CH), 115.1 (CH), 113.3 (CH), 111.3 (CH), 107.0 (C_q), 55.5 (CH$_3$), 51.5 (C_q), 31.0 (CH$_2$), 22.8 (CH$_2$); **GC-MS**: **t_R (50_40)**: 16.2 min; **EI-MS** *m/z* (%): 358 (26), 357 (100), 342 (35), 254 (18), 253 (10); **HR-MS (ESI)**: *m/z* calculated for [C$_{23}$H$_{19}$NO$_3$]$^+$ ([M]$^+$): 357.1359, measured: 357.1359, *m/z* calculated for [C$_{23}$H$_{19}$NO$_3$Na]$^+$ ([M + Na]$^+$): 380.1257, measured: 380.1253; **IR (ATR)**: ν (cm^{-1}): 2995, 2947, 2929, 2899, 2837, 2359, 1695, 1608, 1579, 1536, 1497, 1457, 1434, 1353, 1335, 1300, 1265, 1247, 1195, 1160, 1143, 1100, 1066, 1046, 1036, 996, 971, 872, 856, 817, 789, 761, 716, 676, 644, 601.

Methyl 2-fluoro-5,6-dihydrobenzo[*g*]pyrido[1,2-*a*]indole-7-carboxylate (212)
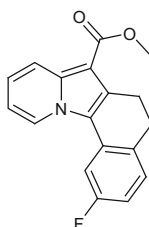
Prepared following **GP14** on a 0.30 mmol scale from methyl 2-bromo-2-(pyridin-2-yl)acetate (69 mg, 0.30 mmol, 1.0 equiv.), 7-fluoro-3,4-dihydronaphthalen-1-yl diethylcarbamate (395 mg, 1.50 mmol, 5.00 equiv.) and hexamethyldisilazane (63 μL, 0.30 mmol, 1.0 equiv.) in α,α,α-trifluorotoluene (3.0 mL, 0.10 M). Purification via flash column chromatography through silica gel (eluent = pentane:ethyl acetate, 20:1) afforded **212** (34 mg, 0.12 mmol, 38 %) as a colorless solid. Unreacted enol carbamate (331 mg, 1.26 mmol, 4.19 equiv.) was also recovered.

^{1}H NMR (300 MHz, CDCl$_3$): δ (ppm): 8.59 (d, J = 7.1 Hz, 1H), 8.31 (dt, J = 9.1, 1.3 Hz, 1H), 7.41 (dd, J = 10.3, 2.5, 1H), 7.27 (dd, J = 8.2, 6.1 Hz, 1H), 7.11 (ddd, J = 9.1, 6.7, 1.1 Hz, 1H), 6.80 − 6.89 (m, 2H), 3.92 (s, 3H), 3.20 (dd, J = 8.2, 6.5 Hz, 2H), 2.87 (t, J = 7.3 Hz, 2H); **^{13}C NMR (101 MHz, CDCl$_3$)**: δ (ppm): 165.8 (C$_q$), 161.9 (d, J = 243 Hz, C$_q$), 137.8 (C$_q$), 131.8 (C$_q$), 131.8 (d, J = 3 Hz, C$_q$), 129.9 (d, J = 8 Hz, C$_q$), 129.8 (d, J = 9 Hz, CH), 123.8 (CH), 122.5 (CH), 121.8 (d, J = 2 Hz, C$_q$), 120.4 (CH), 113.5 (CH), 111.8 (d, J = 21 Hz, CH), 106.6 (d, J = 24 Hz, CH), 101.7 (C$_q$), 50.9 (CH$_3$), 29.4 (CH$_2$), 22.5 (CH$_2$); **^{19}F NMR (282 MHz, CDCl$_3$)**: −115.4; **R$_f$ (pentane:ethyl acetate 20:1)**: 0.22; **GC-MS: t$_R$ (50_40)**: 11.8 min; **EI-MS**: m/z (%): 296 (20), 295 (100), 294 (13), 279 (8), 265 (7), 264 (15), 263 (5), 262 (34), 236 (23), 235 (39), 234 (21), 233 (8), 208 (5), 134 (11), 131 (11), 117 (21); **HR-MS (ESI)**: m/z calculated for [C$_{18}$H$_{14}$FNO$_2$Na]$^+$ ([M + Na]$^+$): 318.0901, measured: 318.0904; **IR (ATR)**: ν (cm^{-1}): 3078, 3022, 2939, 2838, 1698, 1610, 1589, 1508, 1485, 1408,1445, 1427, 1386, 1345, 1320, 1258, 1206, 1157, 1100, 1072, 1021, 976, 942, 879, 852, 831, 807, 777, 735, 712, 688, 668, 629, 585.

Methyl 2,4-dimethyl-5,6-dihydrobenzo[*g*]pyrido[1,2-*a*]indole-7-carboxylate (211)
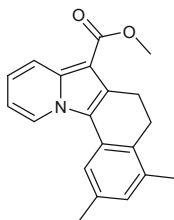
Prepared following **GP14** on a 0.30 mmol scale from methyl 2-bromo-2-(pyridin-2-yl)acetate (69 mg, 0.30 mmol, 1.0 equiv.), 5,7-dimethyl-3,4-dihydronaphthalen-1-yl diethylcarbamate (410 mg, 1.50 mmol, 5.00 equiv.) and hexamethyldisilazane (63 μL, 0.30 mmol, 1.0 equiv.) in α,α,α-trifluorotoluene (3.0 mL, 0.10 M). Purification via flash column chromatography through silica gel (eluent = pentane:ethyl acetate, 20:1) afforded **211** (61 mg, 0.20 mmol, 67 %) as a pale yellow solid. Unreacted enol carbamate (296 mg, 1.08 mmol, 3.61 equiv.) was also recovered.

R$_f$ (pentane:ethyl acetate 20:1): 0.25; **^{1}H NMR (400 MHz, C$_6$D$_6$)**: δ (ppm): 8.59 (dt, J = 9.0, 1.3 Hz, 1H), 8.31 (dt, J = 7.0, 1.2 Hz, 1H), 7.23 (s, 1H),

6.75 (s, 1H), 6.63 (ddd, *J* = 9.0, 6.7, 1.1 Hz, 1H), 6.17 (td, *J* = 6.9, 1.5 Hz, 1H), 3.69 (s, 3H), 3.29–3.35 (m, 2H), 2.67 (t, *J* = 7.4 Hz, 2H), 2.20 (s, 3H), 2.12 (s, 3H); **^{13}C NMR (101 MHz, C$_6$D$_6$)**: δ (ppm): 165.5 (C$_q$), 137.7 (C$_q$), 135.9 (C$_q$), 135.0 (C$_q$), 132.1 (C$_q$), 130.9 (C$_q$), 129.1 (CH), 128.8 (C$_q$), 123.9 (CH), 123.3 (C$_q$), 121.5 (CH), 120.7 (CH), 118.6 (CH), 112.8 (CH), 102.1 (C$_q$), 50.4 (CH$_3$), 25.4 (CH$_2$), 22.7 (CH$_2$), 21.5 (CH$_3$), 20.3 (CH$_3$); **GC-MS: t$_R$ (50_40_320)**: 11.8 min; **EI-MS**: *m/z* (%): 306 (23), 305 (100), 304 (9), 274 (8), 273 (5), 272 (21), 246 (10), 245 (19), 244 (6), 231 (6), 230 (7), 228 (6), 129 (5); **HR-MS (ESI)**: *m/z* calculated for [C$_{20}$H$_{19}$NO$_2$]$^+$ ([M]$^+$): 305.1410, measured: 305.1401, *m/z* calculated for [C$_{20}$H$_{19}$NO$_2$Na]$^+$ ([M + Na]$^+$): 328.1308, measured: 328.1300; **IR (ATR)**: ν (cm^{-1}): 2949, 2898, 2877, 2832, 1696, 1679, 1632, 1610, 1577, 1536, 1505, 1479, 1431, 1392, 1378, 1342, 1312, 1291, 1231, 1199, 1100, 1157, 1134, 1087, 1024, 984, 959, 939, 912, 857, 835, 777, 732, 725, 707, 694, 671, 655.

Methyl 2,3-dimethoxy-5,6-dihydrobenzo[*g*]pyrido[1,2-*a*]indole-7-carboxylate (210)
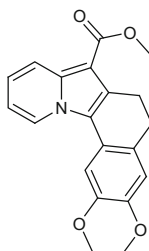

Prepared following **GP14** on a 0.30 mmol scale from methyl 2-bromo-2-(pyridin-2-yl)acetate (69 mg, 0.30 mmol, 1.0 equiv.), 6,7-dimethoxy-3,4-dihydronaphthalen-1-yl diethylcarbamate (458 mg, 1.50 mmol, 5.00 equiv.) and hexamethyldisilazane (63 μL, 0.30 mmol, 1.0 equiv.) in α,α,α-trifluorotoluene (3.0 mL, 0.10 M). Purification via flash column chromatography through silica gel (eluent = toluene:ethyl acetate, 2:1) afforded **210** (62 mg, 0.18 mmol, 61 %) as a yellow solid. Unreacted enol carbamate (293 mg, 959 μmol, 3.20 equiv.) was also recovered.

R$_f$ (toluene:ethyl acetate 2:1): 0.48; **^{1}H NMR (400 MHz, C$_6$D$_6$)**: δ (ppm): 8.62 (dt, *J* = 9.0, 1.3 Hz, 1H), 8.19 (d, *J* = 7.1 Hz, 1H), 7.11 (s, 1H), 6.66 (s, 1H), 6.64 (ddd, *J* = 9.0, 6.7, 1.0 Hz, 1H), 6.22 (td, *J* = 6.8, 1.5 Hz, 1H), 3.71 (s, 3H), 3.53 (s, 3H), 3.47 (s, 3H), 3.38–3.43 (m, 2H), 2.72 (t, *J* = 7.5 Hz, 2H); **^{13}C NMR (101 MHz, C$_6$D$_6$)**: δ (ppm): 165.6 (C$_q$), 148.5 (C$_q$), 148.4 (C$_q$), 137.2 (C$_q$), 130.3 (C$_q$), 129.8 (C$_q$), 123.2 (CH), 123.1 (C$_q$), 121.8 (C$_q$), 121.1 (CH), 120.8 (CH), 114.0 (CH), 112.9 (CH), 107.0 (CH), 102.3 (C$_q$), 56.7 (CH$_3$), 55.8 (CH$_3$), 50.5 (CH$_3$), 30.1 (CH$_2$), 23.2 (CH$_2$); **GC-MS: t$_R$ (50_40)**: 16.0 min; **EI-MS**: *m/z* (%): 338 (19), 337 (100), 323 (6), 322 (41), 293 (10), 208 (8), 191 (10), 44 (5), 40 (6); **HR-MS (ESI)**: *m/z* calculated for [C$_{20}$H$_{19}$NO$_4$]$^+$ ([M]$^+$): 337.1309, measured: 337.1312, *m/z* calculated for [C$_{20}$H$_{19}$NO$_4$Na]$^+$ ([M + Na]$^+$): 360.1206, measured: 360.1208; **IR (ATR)**: ν (cm^{-1}): 3016, 2933, 2832, 1681, 1631, 1608, 1581, 1505,

1466, 1452, 1433, 1405, 1389, 1363, 1335, 1321, 1310, 1277, 1256, 1239, 1214, 1189, 1183, 1150, 1127, 1109, 1065, 1038, 1027, 1010, 982, 935, 919, 880, 853, 813, 791, 779, 740, 725, 718, 691, 676, 664, 615, 605.

Methyl   5-(3,4-dichlorophenyl)-5,6-dihydrobenzo[*g*]pyrido[1,2-*a*]indole-7-carboxylate (221)

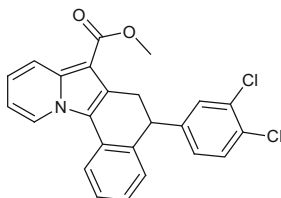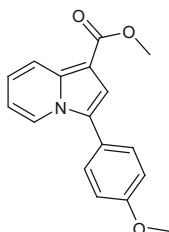Prepared following **GP14** on a 0.30 mmol scale from methyl 2-bromo-2-(pyridin-2-yl)acetate (69 mg, 0.30 mmol, 1.0 equiv.), 4-(3,4-dichlorophenyl)-3,4-dihydronaphthalen-1-yl diethylcarba-mate (584 mg, 1.50 mmol, 5.00 equiv.) and hexamethyldisilazane (63 μL, 0.30 mmol, 1.0 equiv.) in α,α,α-trifluorotoluene (3.0 mL, 0.10 M). Purification via flash column chromatography through silica gel (eluent = pentane:toluene, 1:1 to pentane:ethyl acetate, 4:1) afforded **221** (42 mg, 0.10 mmol, 33 %) as a yellow solid. Unreacted enol carbamate (494 mg, 1.27 mmol, 4.23 equiv.) was also recovered.

R$_f$ (pentane:toluene 1:1): 0.35; **^{1}H NMR (400 MHz, C$_6$D$_6$)**: δ (ppm): 8.55 (dt, *J* = 9.0, 1.3 Hz, 1H), 8.11 (dm, *J* = 7.1 Hz, 1H), 7.39 (dd, *J* = 7.9, 1.2 Hz, 1H), 7.16 (s, 1H), 7.10 (tm, *J* = 7.7 Hz, 1H), 6.94 (td, *J* = 7.5, 1.2 Hz, 1H), 6.90 (d, *J* = 8.3 Hz, 1H), 6.75 (dt, *J* = 7.6, 1.1 Hz, 1H), 6.59–6.66 (m, 2H), 6.19 (td, *J* = 6.9, 1.5 Hz, 1H), 3.75 (dd, *J* = 10.2, 5.8 Hz, 1H), 3.61 (s, 3H), 3.61 (dd, *J* = 16.4, 5.8 Hz, 1H), 3.41 (dd, *J* = 16.4, 10.2 Hz, 1H); **^{13}C NMR (101 MHz, C$_6$D$_6$)**: δ (ppm): 165.3 (C$_q$), 144.0 (C$_q$), 138.1 (C$_q$), 138.0 (C$_q$), 132.9 (C$_q$), 131.0 (CH), 130.9 (C$_q$), 130.7 (CH), 129.1 (C$_q$), 129.1 (CH), 128.7 (C$_q$), 128.1 (CH), 127.2 (CH), 126.2 (CH), 123.8 (CH), 122.0 (CH), 120.8 (CH), 119.9 (CH), 113.2 (CH), 102.5 (C$_q$), 50.5 (CH$_3$), 45.2 (CH), 30.1 (CH$_2$) [*Note: One quaternary carbon peak was not detected due to overlapping with the signal for C$_6$D$_6$*]; **GC-MS: t$_R$ (50_40_320)**: 16.3 min; **EI-MS**: *m/z* (%): 424 (15), 423 (80), 422 (29), 421 (100), 415 (13), 405 (9), 355 (5), 343 (5), 342 (9), 332 (16), 329 (10), 328 (10), 327 (12), 325 (7), 282 (16), 276 (21), 269 (9), 268 (12), 265 (5), 261 (22), 254 (7), 251 (12), 244 (28), 221 (12), 217 (27), 216 (17), 195 (8), 194 (16), 159 (19), 149 (14), 147 (16), 145 (19), 135 (22), 119 (7), 73 (8); **HR-MS (ESI)**: *m/z* calculated for [C$_{24}$H$_{17}$NO$_2$Cl$_2$]$^+$ ([M]$^+$): 421.0631, measured: 421.0634, *m/z* calculated for [C$_{24}$H$_{17}$NO$_2$Cl$_2$Na]$^+$ ([M + Na]$^+$): 444.0529, measured: 444.0530; **IR (ATR)**: ν (cm^{-1}): 3101, 3081, 3057, 2975, 2949, 2910, 2851, 1682, 1634, 1597, 1561, 1531, 1518, 1508, 1473, 1455, 1436, 1396, 1357, 1327, 1319, 1303, 1295, 1236, 1228, 1197, 1167, 1146, 1128, 1103, 1072, 1054, 1030, 998, 971, 947, 921, 911, 895, 870, 834, 820, 778, 761, 752, 737, 723, 710, 704, 690, 681, 666, 650, 617.

Methyl 3-(4-methoxyphenyl)indolizine-1-carboxylate (222) [51]

Prepared following **GP14** on a 0.20 mmol scale from methyl 2-bromo-2-(pyridin-2-yl)acetate (46 mg, 0.20 mmol, 1.0 equiv.), 1-(4-methoxyphenyl)vinyl dimethylcarbamate (221 mg, 1.00 mmol, 5.00 equiv.) and hexamethyldisilazane (42 μL, 0.20 mmol, 1.0 equiv.) in α,α,α-trifluorotoluene (2.0 mL, 0.10 M). Purification via flash column chromatography through silica gel (eluent = pentane:ethyl acetate, 20:1) afforded **222** (16 mg, 55 μmol, 28 %) as a white solid. Unreacted enol carbamate (170 mg, 768 μmol, 3.84 equiv.) was also recovered.

R_f **(pentane:ethyl acetate 9:1)**: 0.21; **^{1}H NMR (400 MHz, C$_6$D$_6$)**: δ (ppm): 8.71 (dt, J = 9.1, 1.3 Hz, 1H), 7.87 (dt, J = 7.1, 1.1 Hz, 1H), 7.60 (s, 1H), 7.14–7.23 (m, 2H), 6.76–6.90 (m, 2H), 6.71 (ddd, J = 9.1, 6.6, 1.1 Hz, 1H), 6.16 (td, J = 6.9, 1.4 Hz, 1H), 3.81 (s, 3H), 3.40 (s, 3H); **^{13}C NMR (101 MHz, C$_6$D$_6$)**: δ (ppm): 165.1 (C$_q$), 159.9 (C$_q$), 136.6 (C$_q$), 130.4 (CH), 126.5 (C$_q$), 124.0 (C$_q$), 123.3 (CH), 121.8 (CH), 120.6 (CH), 116.2 (CH), 114.8 (CH), 112.4 (CH), 104.8 (C$_q$), 54.9 (CH$_3$), 50.6 (CH$_3$); **GC-MS: t$_R$ (50_40)**: 11.3 min; **EI-MS**: m/z (%): 282 (19), 281 (100), 267 (11), 266 (61), 250 (27), 179 (13), 178 (17), 89 (11); **HR-MS (ESI)**: m/z calculated for [C$_{17}$H$_{15}$NO$_3$Na]$^+$ ([M + Na]$^+$): 304.0944, measured: 304.0943; **IR (ATR)**: ν (cm^{-1}): 3003, 2964, 2839, 2361, 2340, 1686, 1635, 1613, 1573, 1551, 1528, 1510, 1492, 1440, 1409, 1370, 1331, 1305, 1287, 1260, 1243, 1214, 1173, 1147, 1106, 1046, 1030, 1009, 949, 919, 861, 834, 807, 776, 746, 660, 624, 608, 593, 576.

6.5.3   Structural Manipulations of Indolizine
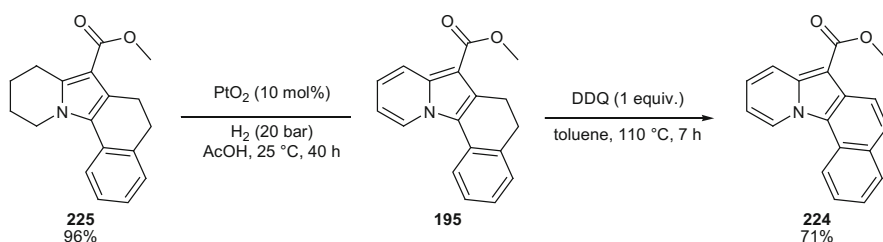
Oxidation of Methyl 5,6-dihydrobenzo[*g*]pyrido[1,2-*a*]indole-7-carboxylate (195)

Methyl benzo[*g*]pyrido[1,2-*a*]indole-7-carboxylate (224)
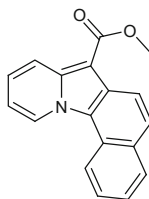
In a screw capped Schlenk tube, 2,3-dichloro-5,6-dicyano-1,4-benzoquinone (DDQ, 57 mg, 0.25 mmol, 1.0 equiv.) was added to a solution of **195** (70 mg, 0.25 mmol, 1.0 equiv.) in dry toluene (2.5 mL). The reaction vessel was sealed tightly and heated at 110 °C for 7 h. After cooling to rt, the reaction mixture was concentrated under reduced pressure. The crude reaction mixture was purified via flash column chromatography through silica gel (eluent = pentane:ethyl acetate, 19:1 to 17:3) to afford methyl benzo[*g*]pyrido[1,2-*a*]indole-7-carboxylate (**224**, 49 mg, 0.18 mmol, 71 %) as a yellow solid.

R_f (pentane:ethyl acetate 9:1): 0.12; **^{1}H NMR (300 MHz, CDCl$_3$)**: δ (ppm): 9.28 (dt, *J* = 7.3, 1.1 Hz, 1H), 8.46–8.73 (m, 3H), 8.08 (dd, *J* = 8.0, 1.4 Hz, 1H), 7.87 (d, *J* = 8.9 Hz, 1H), 7.72 (ddd, *J* = 8.5, 7.0, 1.4 Hz, 1H), 7.55 (ddd, *J* = 8.0, 7.0, 1.0 Hz, 1H), 7.36 (ddd, *J* = 9.2, 6.6, 1.0 Hz, 1H), 7.01 (ddd, *J* = 7.3, 6.6, 1.5 Hz, 1H), 4.05 (s, 3H); **^{13}C NMR (75.5 MHz, CDCl$_3$)**: δ (ppm): 166.3 (C$_q$), 140.1 (C$_q$), 131.0 (C$_q$), 130.1 (CH), 127.7 (C$_q$), 127.2 (CH), 127.1 (CH), 127.1 (CH), 124.9 (CH), 123.9 (CH), 123.2 (C$_q$), 123.2 (C$_q$), 121.2 (CH), 120.8 (CH), 119.7 (CH), 112.6 (CH), 97.1 (C$_q$), 51.0 (CH$_3$); **GC-MS: t_R (50_40)**: 13.0 min; **EI-MS**: *m/z* (%): 276 (20), 275 (100), 245 (11), 244 (60), 217 (33), 216 (30), 215 (22), 214 (13); **HR-MS (ESI)**: *m/z* calculated for [C$_{18}$H$_{13}$NO$_2$Na]$^+$ ([M + Na]$^+$): 298.0838, measured: 298.00841; **IR (ATR)**: ν (cm^{-1}): 3177, 2946, 2846, 1680, 1618, 1598, 1529, 1503, 1474, 1439, 1415, 1380, 1351, 1288, 1257, 1199, 1161, 1127, 1113, 1081, 1016, 965, 848, 812, 728, 678, 616.

Reduction of Methyl 5,6-dihydrobenzo[*g*]pyrido[1,2-*a*]indole-7-carboxylate (195)

Methyl 5,6,8,9,10,11-hexahydrobenzo[*g*]pyrido[1,2-*a*]indole-7-carboxylate (225)
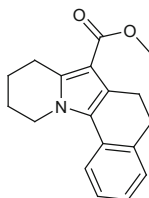
In a glass vial equipped with a magnetic stiring bar, Platinum (IV) oxide (PtO$_2$, 4.4 mg, 0.020 mmol, 10 mol%) was added to a solution of **195** (55 mg, 0.20 mmol, 1.0 equiv.) in glacial acetic acid (1 mL). The reaction vessel was placed in a stainless-steel reactor. The autoclave was purged three times with hydrogen gas before setting up the reaction pressure at 20 bar. The reaction mixture was allowed to stir at 25 °C for 40 h. The reaction mixture was diluted with water, neutralized with NaHCO$_3$ and extracted with ethyl acetate. The organic phase was washed with brine solution, dried over MgSO$_4$ and concentrated under reduced pressure. The crude reaction mixture was purified via flash column chromatography through neutral alumina (eluent = pentane:ethyl acetate, 19:1 to 9:1) to afford Methyl 5,6,8,9,10,11-hexahydrobenzo[*g*]pyrido[1,2-*a*]indole-7-carboxylate (**225**, 54 mg, 0.19 mmol, 96 %) as a white solid upon cooling.

R$_f$ (on neutral alumina, pentane:ethyl acetate 9:1): 0.33; **^{1}H NMR (300 MHz, CDCl$_3$)**: δ (ppm): 7.40 (dd, *J* = 7.7, 1.3 Hz, 1H), 7.17–7.26 (m, 2H), 7.07 (td, *J* = 7.4, 1.2 Hz, 1H), 4.26 (t, *J* = 5.8 Hz, 2H), 3.81 (s, 3H), 3.18 (t, *J* = 6.4 Hz, 2H), 2.96 (ddd, *J* = 8.3, 6.5, 1.7 Hz, 2H), 2.84 (dd, *J* = 8.6, 5.5 Hz, 2H), 1.85–2.05 (m, 4H); **^{13}C NMR (75.5 MHz, CDCl$_3$)**: δ (ppm): 166.4 (C$_q$), 138.4 (C$_q$), 136.6 (C$_q$), 129.5 (C$_q$), 128.6 (CH), 128.0 (C$_q$), 126.5 (CH), 125.0 (CH), 123.5 (C$_q$), 120.9 (CH), 108.2 (C$_q$), 50.5 (CH$_3$), 46.8 (CH$_2$), 30.9 (CH$_2$), 24.9 (CH$_2$), 23.7 (CH$_2$), 21.7 (CH$_2$), 19.8 (CH$_2$); **GC-MS**: t$_R$ (50_40): 11.8 min; **EI-MS**: *m/z* (%): 282 (20), 281 (100), 280 (12), 266 (43), 250 (13), 248 (12), 222 (31), 221 (26), 220 (20), 180 (18); **HR-MS (ESI)**: *m/z* calculated for [C$_{18}$H$_{19}$NO$_2$Na]$^+$ ([M + Na]$^+$): 304.1308, measured: 304.1311; **IR (ATR)**: ν (cm^{-1}): 2950, 2899, 2869, 2843, 1682, 1603, 1541, 1499, 1437, 1424, 1386, 1354, 1330, 1274, 1245, 1232, 1184, 1169, 1130, 1099, 1073, 1062, 1003, 771, 715, 668, 643, 600.

6.5.4 Mechanistic Experiments

6.5.4.1 Radical Trapping Experiments
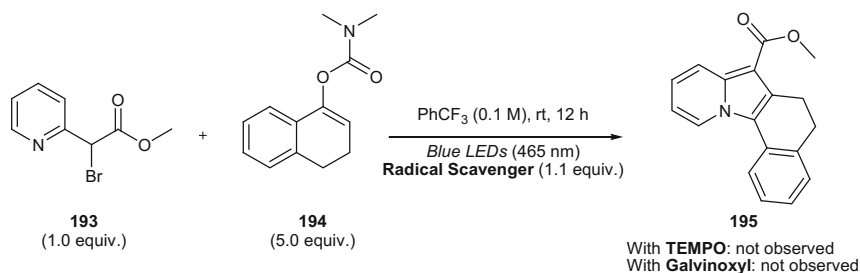
In a flame dried screw capped Schlenk tube equipped with a magnetic stir bar, 3,4-dihydronaphthalen-1-yl dimethylcarbamate (**194**, 109 mg, 0.500 mmol, 5.00 equiv.) was dissolved in α,α,α-trifluorotoluene (1.0 mL) and then 2-bromo-2-(pyridin-2-yl)acetate (**193**, 23 mg, 0.10 mmol, 1.0 equiv.), hexamethyldisilazane (21 μL, 0.10 mmol, 1.0 equiv.) and 2,2,6,6-tetramethyl-1-piperidinyloxyl (TEMPO, 17 mg, 0.11 mmol, 1.1 equiv.) or 2,6-di-*tert*-butyl-α-(3,5-di-*tert*-butyl-4-oxo-2,5-cyclohexadien-1-ylidene)-*p*-tolyloxyl   (galvinoxyl,   46 mg, 0.11 mmol, 1.1 equiv.) were added. The resulting mixture was degassed using three freeze-pump-thaw cycles and the tube was finally backfilled with argon. The reaction mixture was allowed to stir at rt for 12 h under irradiation of visible light from 5 W blue LEDs (λ_{max} = 465 nm). The reaction mixture was analyzed by nanospray ESI mass spectrometry. In both cases, methyl 5,6-dihydrobenzo[*g*]pyrido[1,2-*a*]indole-7-carboxylate (**195**) was not observed. For the reaction with TEMPO, peaks consistent with adducts (**226** and **227**) between the radical scavenger and two different proposed radical intermediates **B** and **C** (see Scheme 4.11) were detected (Fig. 4.10).

6.5.4.2   Cyclic Voltammetry Measurements of Indolizine Compound

The cell used for cyclic voltametry measurement consisted of an Ag/AgCl reference electrode, a Pt counter electrode and a Pt working electrode. The measurement was conducted on a degassed solution of **195** (0.05 mM) prepared in 0.1 M tetrabutylammonium tetrafluoroborate (TBA.BF$_4$) solution in CH$_3$CN. The data was recorded using an Autolab potentiostat (Eco chemie, Netherlands) running GPES software and was plotted with Origin software (see Fig. 4.8 in Chap. 4).

6.5.4.3   Determination of the Luminescence Lifetime of Indolizine Compound

The luminescence lifetime of indolizine **195** was recorded on a FluoTime300 spectrometer from PicoQuant equipped with a 300 W ozone-free Xe lamp (250–900 nm), a 10 W Xe flash-lamp (250–900 nm, pulse width < 10 μs) with repetition rates of 0.1–300 Hz, an excitation monochromator (Czerny-Turner 2.7 nm/mm dispersion, 1200 grooves/mm, blazed at 300 nm), diode lasers (pulse width < 80 ps) operated by a computer-controlled laser driver PDL-820 (repetition rate up to 80 MHz, burst mode for slow and weak decays), two emission monochromators (Czerny-Turner, selectable gratings blazed at 500 nm with 2.7 nm/mm dispersion and 1200 grooves/mm, or blazed at 1250 nm with 5.4 nm/mm dispersion and 600 grooves/mm), Glan-Thompson polarizers for excitation (Xe-lamps) and emission, a Peltier-thermostatized sample holder from Quantum Northwest (−40 to 105 °C), and two detectors, namely a PMA Hybrid 40 (transit time spread FWHM < 120 ps, 300–720 nm) and a R5509-42 NIR-photomultiplier tube (transit time spread FWHM 1.5 ns, 300–1400 nm) with external cooling (−80 °C) from
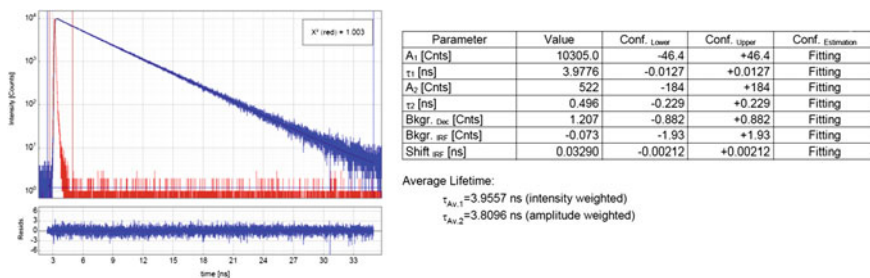
Fig. 6.11 Determination of the luminescence lifetime of indolizine **195**. A graph showing the excited state decay and the mathematical fitting is given on the *left* and a table displaying the obtained data is given on the *right*. Sahoo et al. [56]. Copyright Wiley-VCH Verlag GmbH & Co. KGaA. Reproduced with permission

Hamamatsu. Steady-state and fluorescence lifetime was recorded in TCSPC mode by a PicoHarp 300 (minimum base resolution 4 ps). Lifetime analysis was performed using the commercial FluoFit software. The quality of the fit was assessed by minimizing the reduced chi squared function (χ^2) and visual inspection of the weighted residuals and their autocorrelation (see Fig. 6.11). The luminescence lifetime of indolizine **195** thus measure was 4 ns (Fig. 6.11).

6.5.4.4   Stern-Volmer Luminescence Quenching Experiments

In a quartz cuvette, an appropriate amount of quencher **X** (**193**, **194** or HMDS) was added to a solution of **195** in $PhCF_3$ (1.0 mM). The intensity of the emission peak at 442 nm (λ_{ex} = 372 nm) expressed as the ratio I_0/I, where I_0 is the emission intensity of **195** at 442 nm in the absence of a quencher and I is the observed intensity, as a function of the quencher concentration was measured. Stern-Volmer plots for each component are given in Fig. 4.6 in Chap. 4.

6.5.4.5   Effect of Suspending Visible Light Irradiation

In a flame dried screw capped Schlenk tube equipped with a magnetic stir bar, 3,4-dihydronaphthalen-1-yl dimethylcarbamate (**194**, 109 mg, 0.500 mmol, 5.00 equiv.) was dissolved in α,α,α-trifluorotoluene (1.0 mL) and then 2-bromo-2-(pyridin-2-yl)acetate (**193**, 23 mg, 0.10 mmol, 1.0 equiv.) and hexamethyldisilazane (21 μL, 0.10 mmol, 1.0 equiv.) were added. The resulting mixture was degassed using three freeze-pump-thaw cycles and the tube was finally backfilled with argon. The reaction mixture was allowed to stir at rt with alternating periods of visible light irradiation (5 W blue LEDs, λ_{max} = 465 nm) followed by periods in darkness. Aliquots were taken under a flow of argon and the yield of indolizine **195** was monitored by GC analysis using mesitylene as an internal standard.

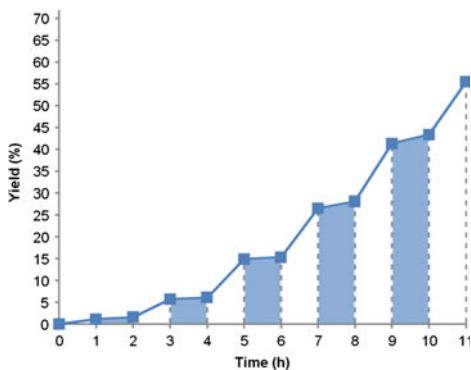| Time (h)	Phase	Yield (%)[b]
0	Dark	0%
1	Light	1.1%
2	Dark	1.6%
3	Light	5.7%
4	Dark	6.1%
5	Light	14.9%
6	Dark	15.3%
7	Light	26.6%
8	Dark	28.1%
9	Light	41.3%
10	Dark	43.3%
11	Light	55.5%

[b] GC yield using mesitylene as internal standard.

Fig. 6.12 Yield of **195** measured at different times after periods of visible light irradiation and periods of darkness. On the graph on the right, the blue shaded areas represent periods in the dark while the unshaded regions show periods under light irradiation. Sahoo et al. [56]. Copyright Wiley-VCH Verlag GmbH & Co. KGaA. Reproduced with permission

The measured yields of **195** at different time points are shown in the table and graph in Fig. 6.12. A significant dropping off of the reaction efficiency was observed during periods of darkness, which could be restarted upon applying light irradiation.

6.5.4.6 Visible Light-Mediated Indolizine-Catalyzed Alkylation of N-Methylindole
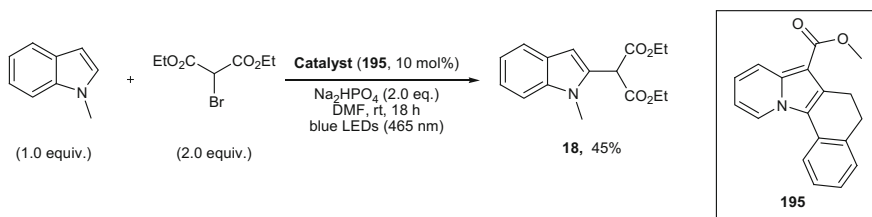
Diethyl 2-(1-methyl-1H-indol-2-yl)malonate (18)

In a flame dried screw capped Schlenk tube equipped with a magnetic stir bar, diethyl 2-bromomalonate (68 μL, 0.40 mmol, 2.0 equiv.) was added to a solution of N-methylindole (25 μL, 0.20 mmol, 1.0 equiv.), methyl 5,6-dihydrobenzo[g]pyrido [1,2-a]indole-7-carboxylate (**195**, 5.6 mg, 20 μmol, 10 mol%), Na_2HPO_4 (57 mg, 0.40 mmol, 2.0 equiv.) in anhydrous DMF (2.0 mL) under argon. The resulting mixture was degassed using three freeze-pump-thaw cycles and the tube was backfilled with argon. The degassed reaction mixture was allowed to stir at rt for 18 h under irradiation of visible light from 5 W blue LEDs (λ_{max} = 465 nm).

The reaction mixture was diluted with water (3 mL) and extracted with ethyl acetate (3 × 5 mL). The combined organic layers were dried over $MgSO_4$ and concentrated under reduced pressure. The crude reaction mixture was purified via flash column chromatography through silica gel (eluent = pentane:ethyl acetate 19:1 to 9:1) to afford diethyl 2-(1-methyl-1H-indol-2-yl)malonate (**18**, 26 mg, 90 μmol, 45 %) as a yellowish orange oil.
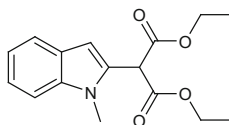
R_f (pentane:ethyl acetate 4:1): 0.41; **^{1}H NMR (400 MHz, CDCl$_3$)**: δ (ppm): 7.78 (d, *J* = 7.9 Hz, 1H), 7.47–7.55 (m, 2H), 7.42 (ddd, *J* = 8.3, 7.0, 1.3 Hz, 1H), 7.30 (ddd, *J* = 8.0, 7.0, 1.1 Hz, 1H), 6.78 (s, 1H), 5.12 (s, 1H), 4.41–4.52 (m, 4H), 3.91 (s, 3H), 1.49 (t, *J* = 7.1 Hz, 6H); **^{13}C NMR (101 MHz, CDCl$_3$)**: δ (ppm): 167.1, 158.4, 138.0, 131.0, 127.4, 122.1, 120.9, 119.8, 109.4, 103.1, 62.3, 51.4, 30.4, 14.2; **GC-MS**: t_R (50_40): 9.5 min; **EI-MS**: *m/z* (%): 290 (10), 289 (55), 217 (15), 216 (100), 188 (15), 171 (13), 146 (32), 144 (41), 143 (18), 115 (19); **HR-MS (ESI)**: *m/z* calculated for $[C_{16}H_{19}NO_4Na]^+$ ([M + Na]$^+$): 312.1206, measured: 312.1202; **IR (ATR)**: ν (cm^{-1}): 3057, 2982, 2937, 2361, 2340, 1732, 1541, 1468, 1401, 1368, 1342, 1303, 1265, 1236, 1207, 1150, 1097, 1030, 743, 632.

6.5.4.7   Single Crystal X-ray Analysis of Indolizine Compound (214)

Tables 6.2, 6.3, 6.4 and 6.5

Parameters	Compound 214
Empirical formula	$C_{19}H_{16}ClNO_3$
Molecular weight	341.78 gmol^{-1}
Crystal system, space group	Monoclinic, P 2 l/c (14)
Unit cell dimensions	a = 9.2567(2) Å, α = 90.000°
	b = 7.6968(2) Å, β = 98.1490(10)°
	c = 21.6732(5) Å, γ = 90.000°
Volume	1528.56(6) Å^3
Z, calculated density	4, 1.485 g cm^{-3}
Absorption coefficient	2.367 mm^{-1}
F(000)	712.0
θ Range	4.1212–68.2644°
Limiting indices	−11 ≤ h ≤ 11
	−9 ≤ k ≤ 9
	−26 ≤ l ≤ 26
Reflections collected/unique	32,320/2801 [R(int) = 0.0532]
Data/restraints/parameters	2801/0/219

(continued)

(continued)

Goodness-of-fit on F^2	1.054
Final R indices [I > 2σ(I)]	R1 = 0.0317, wR^2 = 0.0828
R indices (all data)	R1 = 0.0362, wR^2 = 0.0861
Largest diff. peak and hole	0.264 and −0.298 eÅ^{-3}

Table 6.2 Bond lengths (Å) for compound 214

Cl1–C6	1.7392(15)	O1–C17	1.2128(18)
O2–C17	1.3534(18)	O2–C18	1.4434(18)
O3–C15	1.3731(18)	O3–C19	1.4285(18)
N1–C8	1.3804(19)	N1–C4	1.3922(19)
N1–C1	1.4052(19)	C1–C2	1.405(2)
C1–C5	1.412(2)	C2–C3	1.414(2)
C2–C17	1.456(2)	C3–C4	1.378(2)
C3–C9	1.4997(19)	C4–C12	1.460(2)
C5–C6	1.360(2)	C5–H5	0.95
C6–C7	1.414(2)	C7–C8	1.354(2)
C7–H7	0.95	C8–H8	0.95
C9–C10	1.533(2)	C9–H9A	0.99
C9–H9B	0.99	C10–C11	1.513(2)
C10–H10A	0.99	C10–H10B	0.99
C11–C16	1.391(2)	C11–C12	1.412(2)
C12–C13	1.399(2)	C13–C14	1.385(2)
C13–H13	0.95	C14–C15	1.393(2)
C14–H14	0.95	C15–C16	1.391(2)
C16–H16	0.95	C18–H18A	0.98
C18–H18B	0.98	C18–H18C	0.98
C19–H19A	0.98	C19–H19B	0.98
C19–H19C	0.98		

Table 6.3 Bond angles (°) for compound 214

C17–O2–C18	114.89(11)	C15–O3–C19	116.76(12)
C8–N1–C4	129.83(13)	C8–N1–C1	120.90(12)
C4–N1–C1	108.93(12)	C2–C1–N1	107.31(12)
C2–C1–C5	134.21(14)	N1–C1–C5	118.42(13)
C1–C2–C3	106.98(13)	C1–C2–C17	127.57(13)
C3–C2–C17	125.45(13)	C4–C3–C2	109.11(13)
C4–C3–C9	119.98(13)	C2–C3–C9	130.91(13)
C3–C4–N1	107.60(13)	C3–C4–C12	123.46(13)
N1–C4–C12	128.85(13)	C6–C5–C1	119.18(14)
C6–C5–H5	120.4	C1–C5–H5	120.4

(continued)

Table 6.3 (continued)

C5–C6–C7	121.67(14)	C5–C6–Cl1	119.74(12)
C7–C6–Cl1	118.58(11)	C8–C7–C6	119.18(14)
C8–C7–H7	120.4	C6–C7–H7	120.4
C7–C8–N1	120.52(14)	C7–C8–H8	119.7
N1–C8–H8	119.7	C3–C9–C10	108.91(12)
C3–C9–H9A	109.9	C10–C9–H9A	109.9
C3–C9–H9B	109.9	C10–C9–H9B	109.9
H9A–C9–H9B	108.3	C11–C10–C9	112.81(12)
C11–C10–H10A	109.0	C9–C10–H10A	109.0
C11–C10–H10B	109.0	C9–C10–H10B	109.0
H10A–C10–H10B	107.8	C16–C11–C12	120.48(14)
C16–C11–C10	120.56(13)	C12–C11–C10	118.87(13)
C13–C12–C11	118.10(13)	C13–C12–C4	126.16(13)
C11–C12–C4	115.65(13)	C14–C13–C12	121.33(13)
C14–C13–H13	119.3	C12–C13–H13	119.3
C13–C14–C15	119.93(14)	C13–C14–H14	120.0
C15–C14–H14	120.0	O3–C15–C16	124.41(13)
O3–C15–C14	115.69(13)	C16–C15–C14	119.90(13)
C15–C16–C11	120.21(13)	C15–C16–H16	119.9
C11–C16–H16	119.9	O1–C17–O2	122.20(13)
O1–C17–C2	125.18(14)	O2–C17–C2	112.62(12)
O2–C18–H18A	109.5	O2–C18–H18B	109.5
H18A–C18–H18B	109.5	O2–C18–H18C	109.5
H18A–C18–H18C	109.5	H18B–C18–H18C	109.5
O3–C19–H19A	109.5	O3–C19–H19B	109.5
H19A–C19–H19B	109.5	O3–C19–H19C	109.5
H19A–C19–H19C	109.5	H19B–C19–H19C	109.5

Table 6.4 Torsion angles (°) for compound 214

C8–N1–C1–C2	−173.20(12)	C4–N1–C1–C2	0.74(15)
C8–N1–C1–C5	4.4(2)	C4–N1–C1–C5	178.37(12)
N1–C1–C2–C3	0.96(16)	C5–C1–C2–C3	−176.13(16)
N1–C1–C2–C17	−179.37(14)	C5–C1–C2–C17	3.5(3)
C1–C2–C3–C4	−2.35(16)	C17–C2–C3–C4	177.97(14)
C1–C2–C3–C9	177.74(14)	C17–C2–C3–C9	−1.9(2)
C2–C3–C4–N1	2.80(16)	C9–C3–C4–N1	−177.27(12)
C2–C3–C4–C12	−174.07(13)	C9–C3–C4–C12	5.8(2)
C8–N1–C4–C3	171.03(14)	C1–N1–C4–C3	−2.19(15)
C8–N1–C4–C12	−12.3(2)	C1–N1–C4–C12	174.46(14)
C2–C1–C5–C6	174.23(15)	N1–C1–C5–C6	−2.6(2)

Table 6.4 (continued)

C1–C5–C6–C7	−0.2(2)	C1–C5–C6–Cl1	−179.20(11)
C5–C6–C7–C8	1.3(2)	Cl1–C6–C7–C8	−179.67(11)
C6–C7–C8–N1	0.5(2)	C4–N1–C8–C7	−175.92(14)
C1–N1–C8–C7	−3.4(2)	C4–C3–C9–C10	28.99(18)
C2–C3–C9–C10	−151.11(15)	C3–C9–C10–C11	−49.94(16)
C9–C10–C11–C16	−143.43(14)	C9–C10–C11–C12	39.94(18)
C16–C11–C12–C13	1.8(2)	C10–C11–C12–C13	178.39(13)
C16–C11–C12–C4	178.56(13)	C10–C11–C12–C4	−4.8(2)
C3–C4–C12–C13	157.00(15)	N1–C4–C12–C13	−19.2(2)
C3–C4–C12–C11	−19.5(2)	N1–C4–C12–C11	164.31(14)
C11–C12–C13–C14	−2.4(2)	C4–C12–C13–C14	−178.83(14)
C12–C13–C14–C15	1.1(2)	C19–O3–C15–C16	9.1(2)
C19–O3–C15–C14	−171.05(13)	C13–C14–C15–O3	−178.86(13)
C13–C14–C15–C16	1.0(2)	O3–C15–C16–C11	178.22(13)
C14–C15–C16–C11	−1.6(2)	C12–C11–C16–C15	0.2(2)
C10–C11–C16–C15	−176.35(13)	C18–O2–C17–O1	3.5(2)
C18–O2–C17–C2	−177.03(13)	C1–C2–C17–O1	−173.31(15)
C3–C2–C17–O1	6.3(2)	C1–C2–C17–O2	7.2(2)
C3–C2–C17–O2	−173.17(13)		

Table 6.5 Hydrogen bond distances (Å) and angles (°) for compound 214

	Donor-H	Acceptor-H	Donor-acceptor	Angle
C5–H5⋯O2	0.95	2.40	2.9315(18)	114.7
C16–H16⋯O1	0.95	2.47	3.3219(18)	149.6

6.6 Synthesis and Characterizations of Novel Metal-Organic Frameworks (MOFs)

The following compounds were synthesized by self according to the procedures given in the cited references. DUT-6 (Boron) **234** and chiral DUT-6 (Boron) **235** were synthesized and characterized by Stella Helten, Dr. Volodymyr Bon (all Technical University of Dresden, Dresden).

6.6.1   Synthesis of 4,4',4''-Boranetriyltris (3,5-Dimethylbenzoic Acid) (H₃TPB)

Tris(4-bromo-2,6-dimethylphenyl)borane(230)
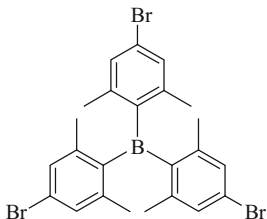
Following a modified procedure by Zhang et al. [52], a flame dried Schlenk tube was charged with 5-bromo-2-iodo-1,3-dimethyl benzene (**229**, 1.0 g, 3.216 mmol) in a glovebox. Dry diethyl ether (20 ml) was added to the flask and the mixture was cooled to −78 °C. To the reaction mixture at −78 °C, a solution of n-BuLi (1.6 M, 2 ml, 3.216 mmol) in hexane was added dropwise. The reaction mixture was allowed to warm up to 0 °C and stirred for 30 min. The reaction mixture was again cooled down to −78 °C and BF₃·Et₂O (0.1 ml, 0.8 mmol) was added dropwise. The whole reaction mixture was slowly allowed to warm up to rt and stirred overnight. Water was added to quench the reaction and the mixture was extracted with diethyl ether. The organic layers were washed with brine, dried over anhydrous MgSO₄ and the solvents were removed under reduced pressure. The crude reaction mixture was purified by column chromatography (eluent:pentane) to give tris(4-bromo-2,6-dimethylphenyl)borane (**230**) as a white solid (189.2 mg, 42 %).

R_f **(pentane)**: 0.36; **¹H NMR (300 MHz, CDCl₃)**: δ (ppm): 7.11 (s, 6H), 1.97 (s, 18H); **¹³C NMR (75.5 MHz, CDCl₃)**: δ (ppm): 144.7, 142.6, 130.9, 124.5, 22.9; **HR-MS (ESI)**: m/z calculated for $[C_{24}H_{24}B_1Br_3HCOO]^-$ ([M + HCOO]⁻): 604.9504, measured: 604.9491; **IR (ATR)**: ν (cm⁻¹): 2966, 2923, 1565, 1437, 1240, 1201, 1118, 1030, 938, 881, 850, 712, 662.

Trimethyl 4,4′,4″-boranetriyltris(3,5-dimethylbenzoate)(231)
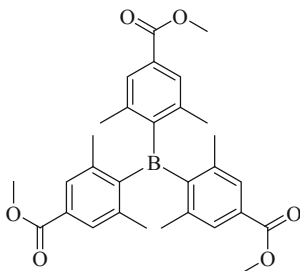

Tris(4-bromo-2,6-dimethylphenyl)borane (**230**, 100 mg, 0.178 mmol) and tetrakis (triphenylphosphine)palladium(0) (62.4 mg, 0.054 mmol) were added to an

oven-dried screw-capped 3 ml glass vial equipped with a magnetic stirring bar under argon. Dry toluene (0.6 ml), distilled triethylamine (0.3 ml) and dry methanol (0.6 ml) were added to the vial. The vial was placed in a 150 ml stainless-steel reactor (*Note: four vials were placed in a reactor at a time*). The autoclave was carefully purged with carbon monoxide gas three times before the pressure was adjusted 40 bar. The reaction mixture was stirred at 125 °C for 36 h. Then the mixture was allowed to cool down to rt and the autoclave was carefully depressurized. The crude mixture was filtered through a plug of Celite using ethyl acetate as eluent and the solvents were removed under reduced pressure. The residue was purified by column chromatography (eluent:pentane:ethyl acetate = 10:1) to give trimethyl 4,4′,4″boranetriyltris(3,5-dimethylbenzoate)(**231**) as a light brown foamy solid (41.9 mg, 47 %).

R_f **(pentane:ethyl acetate 10:1)**: 0.15; **^{1}H NMR (300 MHz, CDCl$_3$)**: δ (ppm): 7.61 (s, 6H), 3.90 (s, 9H), 2.05 (s, 18H); **^{13}C NMR (75.5 MHz, CDCl$_3$)**: δ (ppm): 167.3, 150.6, 140.8, 131.4, 128.9, 52.2, 23.0; **HR-MS (ESI)**: *m/z* calculated for $[C_{30}H_{33}B_1O_6Na]^+$ ([M + Na]$^+$): 523.2262, measured: 523.2263; **IR (ATR)**: ν (cm^{-1}): 2953, 2360, 1719, 1553, 1435, 1410, 1301, 1208, 1142, 1115, 1016, 984, 898, 837, 768, 746, 711, 666.

4,4′,4″-Boranetriyltris(3,5-dimethylbenzoic acid)(228)
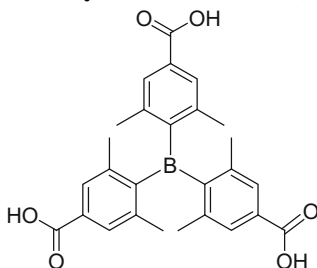
In a 250 ml round bottom flask, trimethyl 4,4′,4″-boranetriyltris (3,5-dimethylbenzoate) (**231**, 694 mg, 1.387 mmol) was dissolved in 28 ml methanol. To this methanol solution, sodium hydroxide (277.4 mg, 6.935 mmol) in 28 ml water was added and the reaction mixture was refluxed at 70 °C for 15 h (turbid reaction mixture turned to clear solution). After cooling the reaction mixture down to rt, it was diluted with water and filtered through Büchner funnel equipped with a sinter disc. The filtrate was acidified with aq. H_2SO_4 solution (1 M) at pH 5–6 to precipitate out the product. The precipitate was filtered and dried under vacuum to give 4,4′,4″-boranetriyltris(3,5-dimethylbenzoic acid) (**228**) as a white solid (604 mg, 95 %).

^{1}H NMR (300 MHz, DMSO-d$_6$): δ (ppm): 12.96 (broad signal, 3H), 7.55 (s, 6H), 2.02 (s, 18H); **^{13}C NMR (75.5 MHz, DMSO-d$_6$)**: δ (ppm): 167.2, 149.7, 140.2, 131.9, 128.4, 22.2; **HR-MS (ESI)**: *m/z* calculated for $[C_{27}H_{26}B_1O_6]^-$ ([M–H]$^-$): 457.1828, measured: 457.1812; **IR (ATR)**: ν (cm^{-1}): 2963, 2925, 1686, 1549, 1418, 1295, 1228, 1199, 1119, 1031, 899, 834, 771, 719, 665.

6.6.2   Synthesis of (S)-2-(4-Benzyl-2-Oxooxazolidin-3-yl) Terephthalic Acid

(*S*)-4-benzyloxazolidin-2-one was synthesized in practical courses and used as received.

Dimethyl 2-bromoterephthalate
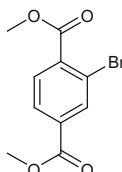
Following our previous procedure [53], in a two necked round bottomed flask eqquiped with a magnetic stir bar and connected with a reflux condenser, 2-bromoterephthalic acid (3.65 g, 14.9 mmol, 1 equiv.) was suspended in MeOH (125 mL) and heated at 70 °C for 15 min. $SOCl_2$ (22.4 mL, 298 mmol, 20 equiv.) was then added to the solution and refluxed for another 12 h. After cooling the reaction mixture to rt, MeOH was removed under reduced pressure. The residue was extracted with diethyl ether and the organic phase was washed with aq. 10 % KOH followed by brine. The organic layer was dried over $MgSO_4$ and concentrated under reduced pressure. The crude reaction mixture was purified by flash column chromatography (eluent:pentane:ethyl acetate 9:1) to afford pure dimethyl 2-bromoterephthalate (3.21 g, 11.8 mmol, 79 %) as a white solid.

¹H NMR (300 MHz, CDCl₃): δ (ppm): 8.31 (d, *J* = 1.6 Hz, 1H), 8.00 (dd, *J* = 8.1, 1.6 Hz, 1H), 7.81 (d, *J* = 8.1 Hz, 1H), 3.96 (s, 3H), 3.94 (s, 3H).

Dimethyl (*S*)-2-(4-benzyl-2-oxooxazolidin-3-yl)terephthalate
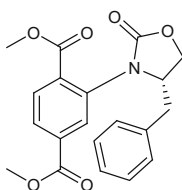
Following our previous procedure [53], in a Schlenk tube under argon, *N,N'*-dimethylethylenediamine (310 μL, 2.88 mmol, 0.31 equiv.) was added to a mixture of dimethyl 2-bromoterephthalate (2.56 g, 9.37 mmol, 1.00 equiv.), (*S*)-4-benzyloxazolidin-2-one (1.83 g, 10.1 mmol, 1.10 equiv.), CuI (268 mg, 1.41 mmol, 0.15 equiv.) and K_2CO_3 (2.60 g, 18.8 mmol, 2.01 equiv.) in dry toluene (15.4 mL) and heated at 110 °C for 48 h. After cooling to rt, the reaction mixture was filtered through a short silica plug (eluent: ethyl acetate). The solvent was removed under reduced pressure and purified by flash column chromatography

(eluent:pentane:ethyl acetate 1:1) to deliver pure dimethyl (*S*)-2-(4-benzyl-2-oxooxazolidin-3-yl)terephthalate (1.70 g, 4.60 mmol, 49 %) as yellowish foamy solid.

¹H NMR (300 MHz, CDCl₃): δ (ppm): 8.02 (d, *J* = 1.0 Hz, 2H), 7.93 (s, 1H), 7.06–7.30 (m, 5H), 4.58–4.77 (m, 1H), 4.46 (t, *J* = 8.5 Hz, 1H), 4.25 (dd, *J* = 8.7, 6.6 Hz, 1H), 3.96 (s, 3H), 3.94 (s, 3H), 3.11 (dd, *J* = 13.6, 4.7 Hz, 1H), 2.91 (dd, *J* = 13.6, 9.8 Hz, 1H); **HR-MS (ESI)**: *m/z* calculated for $[C_{20}H_{19}NO_6Na]^+$ ([M + Na]⁺): 392.1105, measured: 392.1106.

(*S*)-2-(4-Benzyl-2-oxooxazolidin-3-yl)terephthalic acid
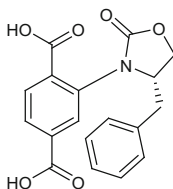
Following our previous procedure [53], in a two necked round bottomed flask eqquiped with a magnetic stir bar and connected with a reflux condenser, dimethyl (*S*)-2-(4-benzyl-2-oxooxazolidin-3-yl)terephthalate (1.69 g, 4.59 mmol, 1.00 equiv.) was dissolved in a mixture of MeOH (179 mL) and THF (179 mL). After adding aq. 1 N NaOH (152 mL), the resulting reaction mixture was allowed to stir for 16 h. The reaction mixture was acidified with conc. HCl to pH: 5–6 and the organic solvents were removed under reduced pressure. The aqueous phase was extracted with CHCl₃/^{i}PrOH (5/1) mixture. The combined organic layers were dried over MgSO₄ and concentrated under reduced pressure. The crude residue was dissolved in acetone and precipitated out by adding pentane. The solid was filtered off and dried to give pure (*S*)-2-(4-Benzyl-2-oxooxazolidin-3-yl)terephthalic acid (**233**, 1.50 g, 4.41 mmol, 96 %) as a white solid.

¹H NMR (300 MHz, CDCl₃): δ (ppm): 13.38 (s, 2H), 7.83–7.95 (m, 3H), 7.09–7.23 (m, 5H), 4.68–4.85 (m, 1H), 4.44 (t, *J* = 8.5 Hz, 1H), 4.20 (dd, *J* = 8.5, 6.7 Hz, 1H), 2.93 (s, 1H), 2.91 (d, *J* = 2.8 Hz, 1H); **HR-MS (ESI)**: *m/z* calculated for $[C_{18}H_{14}NO_6]^-$ ([M–H]⁻): 340.0816, measured: 340.0839.

6.6.3 Synthesis of DUT-6 (Boron) (234)

Zn(NO₃)₂·4H₂O (56 mg, 0.20 mmol, 11.1 equiv.), terephthalic acid (9.00 mg, 0.054 mmol, 3.00 equiv.) and 4,4′,4″-boranetriyltris(3,5-dimethylbenzoic acid) (8.10 mg, 0.018 mmol, 1.00 equiv.) were dissolved in *N,N*-diethylformamide (10 mL) by ultrasonication. The solution was placed in a glass Pyrex tube with a size of 100 × 16 mm. The vial was sealed tightly with a screw cap and heated at 80 °C in an oven for 48 h. After cooling down to room temperature, the mother liquor was pipetted off and the colourless crystals were washed with fresh DEF five

times. The solvent was then exchanged with ethanol five times. 24 h were left between consecutive washing and solvent exchange steps.

For physisorption measurements, the ethanol was removed from the pores by drying in supercritical CO_2.

Elemental Analysis: calculated values for $Zn_4O(C_8H_4O_4)(C_{27}H_{24}BO_6)_{4/3}$: C, 50.39 %; H, 3.46 %; measured: C, 49.92 %; H, 3.73 %.

6.6.4   Synthesis of Chiral DUT-6 (Boron) (235)

$Zn(NO_3)_2\cdot4H_2O$ (60 mg, 0.20 mmol, 7.14 equiv.), (*S*)-2-(4-Benzyl-2-oxazilidin-3-yl)terephthalic acid (0.028 mg, 0.048 mmol, 1.71 equiv.) and 4,4′,4″-borane-triyltris(3,5-dimethylbenzoic acid) (13.0 mg, 0.028 mmol, 1.00 equiv.) were dissolved in *N,N*-diethylformamide (10 mL) by ultrasonication. The vial was sealed tightly with a screw cap and heated at 80 °C in an oven for 48 h. After cooling down to room temperature, the mother liquor was pipetted off and replaced by fresh DEF five times. The solvent was then exchanged with ethanol five times. 24 h were left between consecutive washing and exchange steps.

6.6.5   Single Crystal X-Ray Analysis of DUT-6 (Boron)

Parameters	DUT-6 (boron) $Zn_4O(C_{27}H_{24}BO_6)_{4/3}(C_8H_4O_4)$ (234)
Empirical formula	$C_{121.5}H_{206.5}B_{1.33}N_{15.5}O_{28.5}Zn_4$
Molecular weight	2616.4 gmol^{-1}
Crystal system, space group	Cubic, $Pm\bar{3}n$ (223)
Unit cell dimensions	a = 26.510(3) Å
Volume	18,631(6) Å^3
Z, calculated density	6, 1.399 g cm^{-3}
Absorption coefficient	1.513 mm^{-1}
F(000)	8392.0
θ Range	1.354–25.391°
Limiting indices	$-12 \leq h \leq 25$ $-25 \leq k \leq 24$ $-25 \leq l \leq 16$
Reflections collected/unique	11,962/1506 [R(int) = 0.0497]
Data/restraints/parameters	1506/11/82
Goodness-of-fit on F^2	1.109
Final R indices [I > 2σ(I)]	R1 = 0.1167, wR^2 = 0.3864
Largest diff. peak and hole	0.183 and -0.774 eÅ^{-3}

CCDC-1009603 contains the supplementary crystallographic data for this compound. This data can be obtained free of charge from the Cambridge Crystallographic Data Centre via www.ccdc.cam.ac.uk/data_request/cif

6.6.6   Determination of BET Area

Rouquerol and Llewellyn [54] suggested three consistency criteria when using the BET method to determine the surface area of metal-organic frameworks. We chose the area of the adsorption branch for BET area determination accordingly.

The first criterion states that the analysis should be limited to the range in which the term $n\left(1 - \frac{p}{p_0}\right)$ increases continuously as a function of the relative pressure which can be well seen in Fig. 6.13 depicting this function with the chosen pressure range of $7.7 \times 10^{-4} \leq p/p_0 \leq 9.8 \times 10^{-2}$.

The second criterion states that the BET constant resulting from the linear fit should be positive and have a minimum value of $C = 10$ which is also met as the resulting BET constant is $C = 343.12$.

According to the third consistency criterion, the relative pressure that corresponds to the calculated BET monolayer capacity applying equation $\left(\frac{p}{p_0}\right)_{n_m} = \frac{1}{\sqrt{C}+1}$ should be located in the chosen pressure range. Inserting the determined BET constant into this equation gives $\left(\frac{p}{p_0}\right)_{n_m} = 0.05122$ which is located in the above mentioned chosen pressure range and therefore all three consistency criteria are met.

6.6.7   CO₂ Physisorption Isotherms for DUT-6

Figures 6.14 and 6.15.

Fig. 6.13 BET plot of the p/p_0 range chosen for the determination of the BET surface area. Ref. [55]—reproduced by permission of The Royal Society of Chemistry
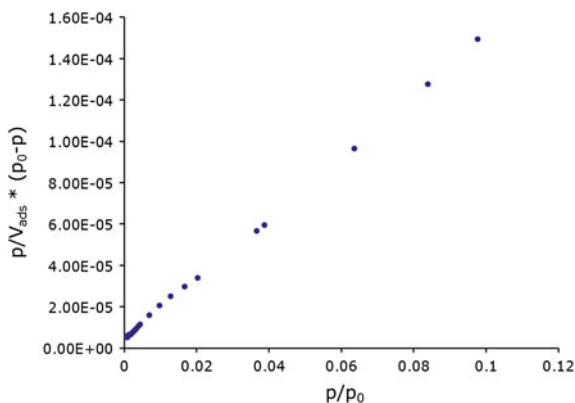
Fig. 6.14 CO$_2$ physisorption isotherm at 194 K of DUT-6; *solid symbols* represent adsorption, *empty symbols* represent desorption. Ref. [55]—reproduced by permission of The Royal Society of Chemistry

Fig. 6.15 CO$_2$ physisorption isotherm at 273 K of DUT-6 (*solid symbols* represent adsorption, *empty symbols* represent desorption. Ref. [55]—reproduced by permission of The Royal Society of Chemistry
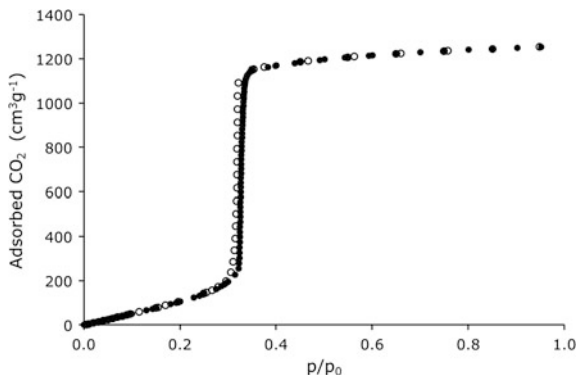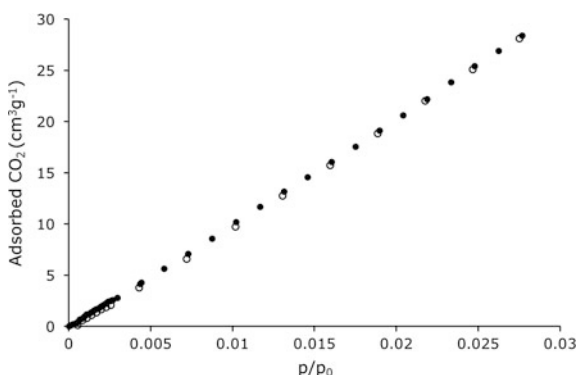

References

1. G.R. Fulmer, A.J.M. Miller, N.H. Sherden, H.E. Gottlieb, A. Nudelman, B.M. Stoltz, J.E. Bercaw, K.I. Goldberg, Organometallics **29**, 2176–2179 (2010)
2. M. Bandini, Chem. Soc. Rev. **40**, 1358–1367 (2011)
3. Z. Otwinowski, W. Minor, Methods Enzymol. **276**, 307–326 (1997)
4. Z. Otwinowski, D. Borek, W. Majewski, W. Minor, Acta Crystallogr. **A59**, 228–234 (2003)
5. G.M. Sheldrick, Acta Crystallogr. **A46**, 467–473 (1990)
6. G.M. Sheldrick, Acta Crystallogr. **A64**, 112–122 (2008)
7. U. Mueller, N. Darowski, M.R. Fuchs, R. Förster, M. Hellmig, K.S. Paithankar, S. Pühringer, M. Steffien, G. Zocher, M.S. Weiss, J. Synchrotron Radiat. **19**, 442–449 (2012)
8. M. Krug, M.S. Weiss, U. Heinemann, U. Mueller, J. Appl. Crystallogr. **45**, 568–572 (2012)
9. W. Kabsch, Acta Crystallogr. D Biol. Crystallogr. **66**, 125–132 (2010)
10. G.M. Sheldrick, Acta Crystallogr. A **64**, 112–122 (2008)
11. A.L. Spek, Acta Crystallogr. D Biol. Crystallogr. **65**, 148–155 (2009)
12. M.A. Ischay, Z. Lu, T.P. Yoon, J. Am. Chem. Soc. **132**, 8572–8574 (2010)
13. C. Bronner, O.S. Wenger, Phys. Chem. Chem. Phys. **16**, 3617–3622 (2014)
14. D.P. Rillema, G. Allen, T.J. Meyer, D. Conrad, Inorg. Chem. **22**, 1617–1622 (1983)
15. S. Sprouse, K.A. King, P.J. Spellane, R.J. Watts, J. Am. Chem. Soc. **106**, 6647–6653 (1984)
16. A.B. Tamayo, B.D. Alleyne, P.I. Djurovich, S. Lamansky, I. Tsyba, N.N. Ho, R. Bau, M.E. Thompson, J. Am. Chem. Soc. **125**, 7377–7387 (2003)

17. J.D. Slinker, A.A. Gorodetsky, M.S. Lowry, J. Wang, S. Parker, R. Rohl, S. Bernhard, G.G. Malliaras, J. Am. Chem. Soc. **126**, 2763–2767 (2004)
18. D. Hanss, J.C. Freys, G. Bernardinelli, O.S. Wenger, Eur. J. Inorg. Chem. **2009**, 4850–4859 (2009)
19. P. de Frémont, N.M. Scott, E.D. Stevens, S.P. Nolan, Organometallics **24**, 2411–2418 (2005)
20. A.S.K. Hashmi, I. Braun, M. Rudolph, F. Rominger, Organometallics **31**, 644–661 (2012)
21. N. Mézailles, L. Ricard, F. Gagosz, Org. Lett. **7**, 4133–4136 (2005)
22. W.F. Gabrielli, S.D. Nogai, J.M. McKenzie, S. Cronje, H.G. Raubenheimer, New J. Chem. **33**, 2208–2218 (2009)
23. P.G. Jones, A.G. Maddock, M.J. Mays, M.M. Muir, A.F. Williams, J. Chem. Soc. Dalton Trans. 1434–1439 (1977)
24. S. Nicolai, J. Waser, Org. Lett. **13**, 6324–6327 (2011)
25. G. Zhang, L. Cui, Y. Wang, L. Zhang, J. Am. Chem. Soc. **132**, 1474–1475 (2010)
26. I.M. Pastor, I. Peñafiel, M. Yus, Tetrahedron Lett. **49**, 6870–6872 (2008)
27. A. Fernández-Mateos, P. Herrero Teijón, L. Mateos Burón, R. Rabanedo Clemente, R. Rubio González, J. Org. Chem. **72**, 9973–9982 (2007)
28. Z. Cai, N. Yongpruksa, M. Harmata, Org. Lett. **14**, 1661–1663 (2012)
29. M.C. Marcotullio, V. Campagna, S. Sternativo, F. Costantino, M. Curini, Synthesis **2006**, 2760–2766 (2006)
30. H. Teller, M. Corbet, L. Mantilli, G. Gopakumar, R. Goddard, W. Thiel, A. Fürstner, J. Am. Chem. Soc. **134**, 15331–15342 (2012)
31. D.P. Curran, N. Fairweather, J. Org. Chem. **68**, 2972–2974 (2003)
32. P. Hanson, J.R. Jones, A.B. Taylor, P.H. Walton, A.W. Timms, J. Chem. Soc. Perkin Trans. **2**, 1135–1150 (2002)
33. M. Bielawski, D. Aili, B. Olofsson, J. Org. Chem. **73**, 4602–4607 (2008)
34. Y. Senda, H. Kanto, H. Itoh, J. Chem. Soc. Perkin Trans. **2**, 1143–1146 (1997)
35. S. Nagumo, Y. Ishii, Y.-I. Kakimoto, N. Kawahara, Tetrahedron Lett. **43**, 5333–5337 (2002)
36. J.P. Wolfe, M.A. Rossi, J. Am. Chem. Soc. **126**, 1620–1621 (2004)
37. A. Spaggiari, D. Vaccari, P. Davoli, G. Torre, F. Prati, J. Org. Chem. **72**, 2216–2219 (2007)
38. X.-Z. Shu, M. Zhang, Y. He, H. Frei, F.D. Toste, J. Am. Chem. Soc. **136**, 5844–5847 (2014)
39. F. Romanov-Michailidis, L. Guénée, A. Alexakis, Angew. Chem. Int. Ed. **52**, 9266–9270 (2013)
40. Q. Yin, S.-L. You, Org. Lett. **16**, 1810–1813 (2014)
41. S.R. Kandukuri, A. Bahamonde, I. Chatterjee, I.D. Jurberg, E.C. Escudero-Adán, P. Melchiorre, Angew. Chem. Int. Ed. **54**, 1485–1489 (2015)
42. M. Duggeli, C. Goujon-Ginglinger, S.R. Ducotterd, D. Mauron, C. Bonte, A.v. Zelewsky, H. Stoeckli-Evans, A. Neels, Org. Biomol. Chem. **1**, 1894–1899 (2003)
43. H.Y. Kim, D.A. Lantrip, P.L. Fuchs, Org. Lett. **3**, 2137–2140 (2001)
44. S.F. Yip, H.Y. Cheung, Z. Zhou, F.Y. Kwong, Org. Lett. **9**, 3469–3472 (2007)
45. H.P. Kokatla, P.F. Thomson, S. Bae, V.R. Doddi, M.K. Lakshman, J. Org. Chem. **76**, 7842–7848 (2011)
46. K. Funakoshi, H. Inada, M. Hamana, Chem. Pharm. Bull. **32**, 4731–4739 (1984)
47. R. Morgentin, F. Jung, M. Lamorlette, M. Maudet, M. Ménard, P. Plé, G. Pasquet, F. Renaud, Tetrahedron **65**, 757–764 (2009)
48. L. Panella, B.L. Feringa, J.G. de Vries, A.J. Minnaard, Org. Lett. **7**, 4177–4180 (2005)
49. M. Boultadakis-Arapinis, M.N. Hopkinson, F. Glorius, Org. Lett. **16**, 1630–1633 (2014)
50. D.C. Behenna, J.T. Mohr, N.H. Sherden, S.C. Marinescu, A.M. Harned, K. Tani, M. Seto, S. Ma, Z. Novák, M.R. Krout, R.M. McFadden, J.L. Roizen, J.A. Enquist, D.E. White, S.R. Levine, K.V. Petrova, A. Iwashita, S.C. Virgil, B.M. Stoltz, Chem. Eur. J. **17**, 14199–14223 (2011)
51. L. Xiang, Y. Yang, X. Zhou, X. Liu, X. Li, X. Kang, R. Yan, G. Huang, J. Org. Chem. **79**, 10641–10647 (2014)
52. J. Li, G. Zhang, D. Zhang, R. Zheng, Q. Shi, D. Zhu, J. Org. Chem. **75**, 5330–5333 (2010)

53. M. Padmanaban, P. Muller, C. Lieder, K. Gedrich, R. Grunker, V. Bon, I. Senkovska, S. Baumgartner, S. Opelt, S. Paasch, E. Brunner, F. Glorius, E. Klemm, S. Kaskel, Chem. Commun. **47**, 12089–12091 (2011)
54. J. Rouquerol, P. Llewellyn, F. Rouquerol, in *Characterization of Porous Solids VII Proceedings of the 7th International Symposium on the Characterization of Porous Solids (COPS-VII)*, Aix-en-Provence, France, 26–28 May 2005, Vol. 160. ed. by J.R.P.L. Llewellyn, F. Rodriquez-Reinoso, N. Seaton (Elsevier, 2007), pp. 49–56
55. S. Helten, B. Sahoo, V. Bon, I. Senkovska, S. Kaskel, F. Glorius, CrystEngComm **17**, 307–312 (2015)
56. B. Sahoo, J.-L. Li, F. Glorius, visible-light photoredox-catlyzed semipinacol-type rearrangement: trifluoromethylation/ring expansion via a radical-polar mechanism. Angew. Chem. Int. Ed. **54**, 11577–11580 (2015)

Curriculum Vitae

Dr. Basudev Sahoo

Personal Informations:

> **Date of Birth:** 04/04/1987
> **Nationality:** Indian

Professional Experience

10/2015–Present	Postdoctoral Fellow at **Leibniz-Institut für Katalyse e.V. an der Universität Rostock** (**LIKAT Rostock**), Rostock, Germany (**Advisor: Prof. Dr. Matthias Beller**).

Education

10/2011–08/2015	PhD Thesis under the supervision of **Prof. Dr. Frank Glorius** at the **Westfälische Wilhelms-Universität Münster**, Germany. **Grade:** Summa Cum Laude (highest distinction). **Thesis**: *Visible Light Photocatalyzed Redox Neutral Organic Reactions and Synthesis of Novel Metal-Organic Frameworks (MOFs).*
05/2010–06/2010	Summer Research Internship under the supervision of **Prof. Dr. Munna Sarkar** at the **Saha Institute of Nuclear Physics (SINP), Kolkata**, India. **Project**: *The Binding Ability of Copper Complexes of Non-Steroidal Anti-Inflammatory Drugs (NSAIDs) with DNA to Investigate Anticancer Activity through DNA Backbone Distortion.*
08/2009–05/2011	M.Sc. in Chemistry from the **Indian Institute of Technology (IIT) Kanpur**, India (Master Thesis under the supervision of **Prof. Dr. Manas K. Ghorai**). **CGPA:** 9.2 out of 10.

	Thesis: *Lewis Acid Catalyzed Regioselective Ring Opening of Small Azacyclic Compounds with Active Methylene Compounds to Construct γ-Amino Butyric Acid Analogues.*
07/2006–07/2009	B.Sc. in Chemistry (Honours), Mathematics, and Physics from the **Ramakrishna Mission Residential College (Narendrapur), University of Calcutta,** Kolkata, India. Cumulative percentage (Honours): 71.9 % (1st class).
07/2004–06/2006	Higher Secondary (10+2) from the **Satmile High School** under the **West Bengal Council of Higher Secondary Education (WBCHSE)**, India. Marks obtained 85.4 % (1st division).
05/1994–05/2004	Secondary (10) from the **North Junbani Brajamal Primary School** and **Chandanpur Birendra Siksha Sadan** under the **West Bengal Board of Secondary Education (WBBSE)**, India. Marks obtained 85.9 % (1st division).

Publications

11. "*Accelerated Discovery in Photocatalysis using a Mechanism-Based Screening Method*" Matthew N. Hopkinson, Adrián Gómez-Suárez, Michael Teders, **Basudev Sahoo**, Frank Glorius,* *Angew. Chem.* **2016**, *128*, 4434-4439; *Angew. Chem. Int. Ed.* **2016**, *55*, 4361–4366.

10. "*Dual Gold/Photoredox-Catalyzed C(sp)–H Arylation of Terminal Alkynes with Diazonium Salts*" Adrian Tlahuext Aca,[†] Matthew N. Hopkinson,[†] **Basudev Sahoo**, Frank Glorius,* *Chem. Sci.* **2016**, *7*, 89–93. ([†]These authors contributed equally to this work).

9. "*External Photocatalyst-Free Visible Light-Mediated Synthesis of Indolizines*" **Basudev Sahoo**,[†] Matthew N. Hopkinson,[†] Frank Glorius,* *Angew. Chem.* **2015**, *127,* 15766–15770; *Angew. Chem. Int. Ed.* **2015**, *54*, 15545–15549. ([†]These authors contributed equally to this work)

8. "*Visible Light Photoredox-Catalyzed Semipinacol-Type Rearrangement: Trifluoromethylation/Ring Expansion via a Radical-Polar Mechanism*" **Basudev Sahoo**, Jun-Long Li, Frank Glorius,* *Angew. Chem.* **2015**, *127*, 11740−11744; *Angew. Chem. Int. Ed.* **2015**, *54*, 11577–11580.

7. "*Functional group tolerance in BTB-based Metal-Organic Frameworks (BTB—benzene-1,3,5-tribenzoate)*" Stella Helten, **Basudev Sahoo**, Philipp Müller, Daniel Janßen-Müller, Nicole Klein, Ronny Grünker, Volodymyr Bon, Frank Glorius, Stefan Kaskel, Irena Senkovska,* *Microporous Mesoporous Mater.* **2015**, *216*, 42–50.

6. "*Copolymerisation at work: the first example of a highly porous MOF comprising a triarylborane-based linker*" Stella Helten,[†] **Basudev Sahoo**,[†] Volodymyr Bon, Irena Senkovska, Stefan Kaskel,* Frank Glorius,* *CrystEngComm.* **2015**, *17*, 307–312. ([†]These authors contributed equally to this work)

5. "*N-Heterocyclic Carbene Catalyzed Switchable Reactions of Enals with Azoalkenes: Formal [4+3] and [4+1] Annulations for the Synthesis of 1,2-Diazepines and Pyrazoles*" Chang Guo, **Basudev Sahoo**, Constantin G. Daniliuc, Frank Glorius,* *J. Am. Chem. Soc.* **2014**, *136,* 17402−17405.

4. "*Dual Photoredox and Gold Catalysis: Intermolecular Multicomponent Oxyarylation of Alkenes*" Matthew N. Hopkinson, **Basudev Sahoo**, Frank Glorius,* *Adv. Synth. Catal.* **2014**, *356,* 2794–2800.

3. "*Conjugate Umpolung of β,β-Disubstituted Enals by Dual Catalysis with an N-Heterocyclic Carbene and a Brønsted Acid: Facile Construction of Contiguous Quaternary Stereocenters*" Jun-Long Li, **Basudev Sahoo**, Constantin G. Daniliuc, Frank Glorius,* *Angew. Chem.* **2014**, *126*, 10683 −10687; *Angew. Chem. Int. Ed.* **2014**, *53*, 10515–10519.

2. "*Dual Catalysis sees the Light: Combining Photoredox with Organo-, Acid and Transition Metal Catalysis*" Matthew N. Hopkinson,[†] **Basudev Sahoo**,[†] Jun-Long Li, Frank Glorius,* *Chem. Eur. J.* **2014**, *20*, 3874–3886. ([†]These authors contributed equally to this work)

1. "*Combining Gold and Photoredox Catalysis: Visible Light-Mediated Oxy- and Amino-arylation of Alkenes*" **Basudev Sahoo**, Matthew N. Hopkinson, Frank Glorius,* *J. Am. Chem. Soc.* **2013**, *135,* 5505–5508.

Conferences and Presentations

4. "*Photoredox Catalysis Meets Gold Catalysis: Visible Light Mediated Difunctionalization of Alkenes*" 8th Asian–European Symposium on Metal Mediated Efficient Organic Synthesis (AES-MMEOS), Izmir, Turkey, September 7–10, 2014 (poster presentation).

3. "*Pd Catalyzed C-H Functionalization of a Metal-Organic Framework (MOF): Mild, Selective, and Efficient*" International MOF Symposium 2013, Dresden, Germany, September 16–17, 2013 (poster presentation).

2. "*Difunctionalization of Alkenes Using a Dual Gold and Photoredox Catalytic System*" 14th Tetrahedron Symposium: Challenges in Organic and Bioorganic Chemistry, Vienna, Austria, June 25–28, 2013 (poster presentation).

1. "*Synthesis of a Novel Organic Linker and its Metal-Organic Frameworks Towards Heterogeneous Catalysis*" 13th Belgian Organic Synthesis Symposium (BOSS XIII), Leuven, Belgium, July 15-20, 2012 (poster presentation).

Academic Achievements/Awards

- Recipient of **Springer Thesis Prize** from the **Springer**, Germany (2016) for recognizing outstanding PhD research.
- Awarded with a special certificate by the Rector of **Westfälische Wilhelms-Universität Münster**, Germany (December, 2015) for obtaining **Summa Cum Laude** (highest distinction) in PhD.

- Recipient of a competitive Doctoral Research Fellowship from the **NRW International Graduate School of Chemistry**, Münster, Germany to pursue doctoral research (2011–2014).
- Recipient of a competitive Summer Research Internship Fellowship with a certificate from the **Saha Institute of Nuclear Physics (SINP), Kolkata** (5/2010–6/2010).
- Recipient of a Merit Scholarship from the **Department of Chemistry, Indian Institute of Technology (IIT) Kanpur** (2009–2011).
- Selected for an interview for prestigious "**Shyama Prasad Mukherjee (SPM) Fellowship**" (a fellowship by **CSIR, India**), 2011 for doctoral studies in India.
- Qualified for a doctoral research fellowship upon passing the **Graduate Aptitude Test (GATE)** conducted by IITs in February 2011 (All India Rank 1 among 10608 chemical science candidates).
- Qualified for a **Junior Research Fellowship (JRF)** upon passing the **National Eligibility Test (NET)** conducted by the Joint **CSIR (Council of Scientific & Industrial Research)—UGC (University Grant Commission)**, **India** in December, 2010 (All India Rank 14 among 1067 chemical science candidates).
- Secured All India Rank 22 among 2585 chemistry candidates appeared in the **Joint Admission Test for M.Sc. (IIT-JAM)** conducted by IITs (2009).

Teaching Experience

- Supervision of two Master and one Bachelor students for their projects at the **Westfälische Wilhelms-Universität Münster**, Germany.